# PENGANTAR KIMIA MEDISINAL

Oleh :
apt. Dian Purwita Sari, M.Biotech.

PRODI FARMASI
STIKES NOTOKUSUMO

# Kontrak pembelajaran

Pertemuan : 14 kali pertemuan

Dosen : apt. Dian Purwita Sari. M.Biotech.

Arief Kusuma Wardani, S.Si., M.Pharm.Sci

Penilaian : UTS: 30 %

UAS: 40%

Tugas: 30%

Bu Dian

- Pendahuluan kimia medisinal
- Hubungan sifat fisika kimia obat dengan aktifitas dan interaksi obat dengan reseptor
- Hubungan stereokimia dengan aktifitas obat
- Hubungan struktur kimia obat dengan proses adsorpsi dan distribusi

Pak Arief

- Hubungan struktur kimia obat dengan proses metabolisme dan ekskresi
- Hubungan kuantitatif antara struktur dan aktivitas obat
- Konsep pengembangan dan penemuan obat baru sintetik dan bahan alam
- Obat Antibiotika, Obat Antiinfeksi, Obat Adrenergik dan Obat Kolinergik
- Obat Antiulcer, Obat Antikanker, Obat Diuretik, Obat Analgetik Opioid

# PENUGASAN KIMIA MEDISINAL

**Tugas kelompok (per kelompok 5 mahasiswa, 8@5, 2@4):**

- Tugas 1 (dengan bu Ipung): Mengumpulkan referensi mengenai hubungan struktur dan aktifitas obat.
- Tugas 2 (dengan pak Arief): Presentasi mengenai hubungan struktur dan aktifitas obat (membuat ppt dan presentasi).

- Pilihan golongan obat: antibiotik, antiinfeksi (virus, jamur, protozoa, antelmintik, dll), adrenergik/kolinergik (agonis, antagonis), antikanker, antidiabetes, psikotropik, antihistamin, dll.

- Presentasi: (silakan berdiskusi dengan pak Arief)
  - di kelas, atau
  - dengan membuat rekaman yang diupload di youtube, publikasikan tayangan kepada rekan-rekan dan publik untuk disimak dan mendapat respon/tanggapan (komen, like).

- Batas waktu:
  - **kumpulan referensi: sebelum UTS, maks. 23 Oktober 2024**
  - **presentasi: silakan bersepakat dengan pak Arief.**

# Referensi

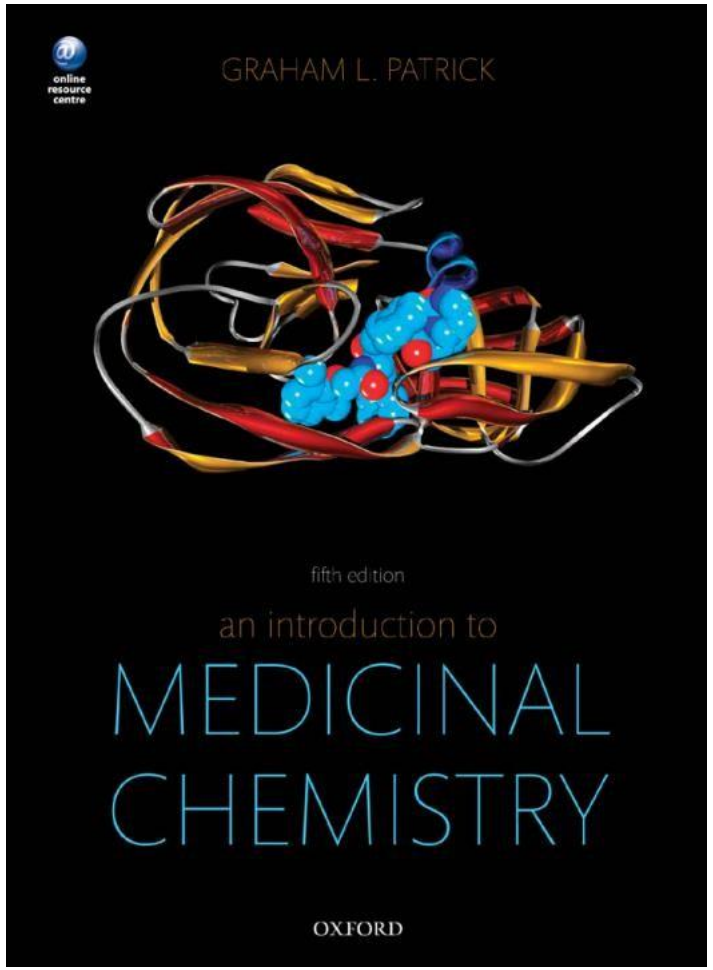
online resource centre
GRAHAM L. PATRICK
fifth edition
an introduction to
MEDICINAL CHEMISTRY
OXFORD

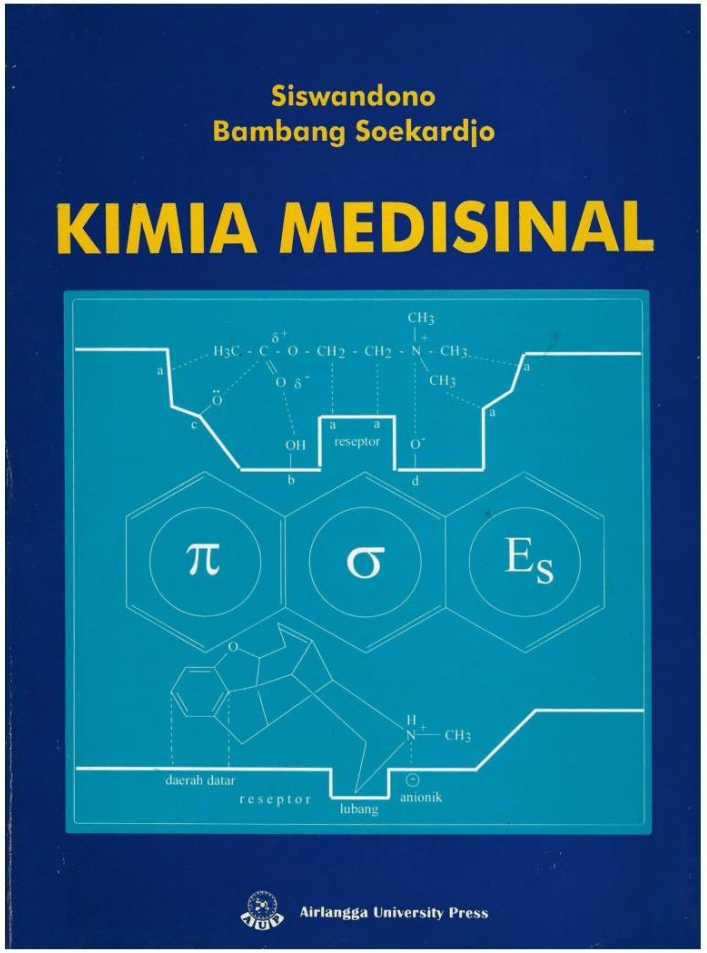
Siswandono
Bambang Soekardjo
KIMIA MEDISINAL
reseptor
daerah datar
reseptor
lubang
anionik
Airlangga University Press

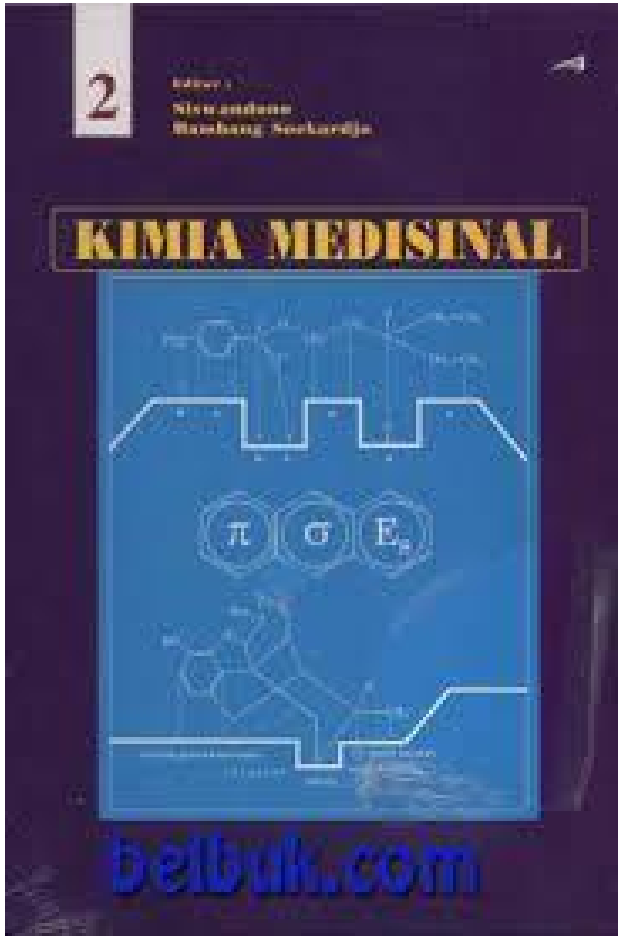
2
KIMIA MEDISINAL
belbuk.com

# PENGANTAR KIMIA MEDISINAL

Oleh :
apt. Dian Purwita Sari, M.Biotech.

PRODI FARMASI
STIKES NOTOKUSUMO

# MEDICINAL CHEMISTRY

## Why It's Important?

Drug Design
Drug Development

Create and refined molecules

Improve human health and reduce suffering

Interdisciplinary subject

# Materi

- Definisi
- Ruang Lingkup
- Keterkaitan dengan Bidang Ilmu Lainnya
- Pengembangan Obat Baru
- Peran Kimed dalam Pengembangan Obat

# Definisi

- **Kimia Medisinal (Burger, 1970)**

ılmu pengetahuan yang merupakan cabang dari ilmu kimia dan biologi, yang digunakan untuk memahami dan menjelaskan mekanisme kerja obat. Sebagai dasar adalah mencoba menetapkan **hubungan struktur kimia dan aktivitas biologis obat**, serta menghubungkan **perilaku biodinamik melalui sifat-sifat fisik dan reaktifitas kimia senyawa**.

# Definisi

- **IUPAC (1974)** International Union of Pure and Applied Chemistry

Ilmu pengetahuan yang mempelajari penemuan, pengembangan, identifikasi dan interpretasi cara kerja senyawa biologis aktif (obat) pada tingkat molekul.

# Definisi

- **Kimia Medisinal menurut Taylor dan Kennewell (1981)**

Studi kimiawi senyawa atau obat yang dapat memberikan efek menguntungkan dalam sistem kehidupan dan melibatkan studi hubungan **struktur kimia senyawa dengan aktivitas biologis serta mekanisme cara kerja senyawa pada sistem biologis,** dalam usaha mendapatkan efek pengobatan yang maksimal dan memperkecil efek samping yang tidak menguntungkan.

# Definisi

**Disimpulkan**

**Kimia medisinal**

**Ilmu yang mempelajari hubungan struktur kimia suatu senyawa atau obat dengan aktivitas biologisnya**

# Ruang Lingkup

Isolasi & Identifikasi senyawa aktif dalam tanaman yang secara empirik telah digunakan untuk pengobatan

Sintesis struktur analog dari bentuk dasar senyawa yang mempunyai aktivitas pengobatan yang potensial

Mencari struktur induk baru dengan cara sintesis senyawa organik, dengan atau tanpa berhubungan dengan zat aktif alamiah

Menghubungkan struktur kimia dengan cara kerja obat

Mengembangkan rancangan obat

Mengembangkan hubungan struktur dan aktivitas biologis melalui sifat kimia fisika dengan bantuan statistik

# Kimia Medisinal

Biologi

Fisika

Matematika

Kimia

Biokimia

Farmakologi

Kimia Organik

Statistika, komputer

Multi disiplin yang melibatkan banyak disiplin ilmu lainnya

**Sintesis, Kimia Organik**

Sintesis kimia dan kimia organic adalah dasar kimia medisinal karena tugas utama dari med chemist's adalah menggabungkan molekul kecil untuk menciptakan senyawa baru

**Farmakologi**

Merupakan ilmu yang mempelajari aksi obat dalam tubuh dan nasib obat dalam tubuh.

**FARMAKOKINETIK**
Mempelajari pergerakan obat sepanjang tubuh

**FARMAKODINAMIK**
Mempelajari bagaimana obat akan berikatan dengan target dan efek apa yang akan di timbulkan

# Sejarah Kimia Medisinal

## Obat pada Zaman Kuno

Obat telah dikenal pada masyarakat : Cina, Hindus, Mayans dan Medetarinia diantaranya :

- Chang sang (alkaloid antimalarial)
- Ma Huang (didalamnya terdapat efedrin)
- Ipecacuanha (ada emetin sebagai anti disentri)

## Abad Pertengahan

Paraceius menggunakan antimony dan garamnya dalam semua ramuan untuk menyembuhkan penyakit

## Abad 19

- Ilmu kimia berkembang pesat
- Mulai disusun herbal pharmacopoeia
- Sintesis mulai berkembang. Misal : Asam asetat dari metana
- Penelitian obat banyak mengeksplorasi sumber tanaman
- Banyak dilakukan isolasi misal: morfin, emetin, kafein
- Mulai digunakan obat dari senyawa tunggal
- Industri farmasi berkembang pada akhir abad 19

## Abad 20

Kimia sintetik berkembang pesat, penemuan obat baru dengan pencetakan moderen

# Sejarah Kimia Medisinal

Asam asetat disintesis dari metana melalui dua tahap. Tahap pertama, gas metan, bromina dalam bentuk hidrogen bromida (40 wt% $HBr/H_2O$) dan oksigen direaksikan dengan menggunakan katalis $Ru/SiO_2$ menghasilkan $CH_3Br$ dan CO. Tahap kedua $CH_3Br$ dan CO direaksikan lagi dengan $H_2O$ dengan bantuan katalis $RhCl_3$ menghasilkan asam asetat dan asam bromida. Mekanisme reaksinya dapat ditunjukkan:

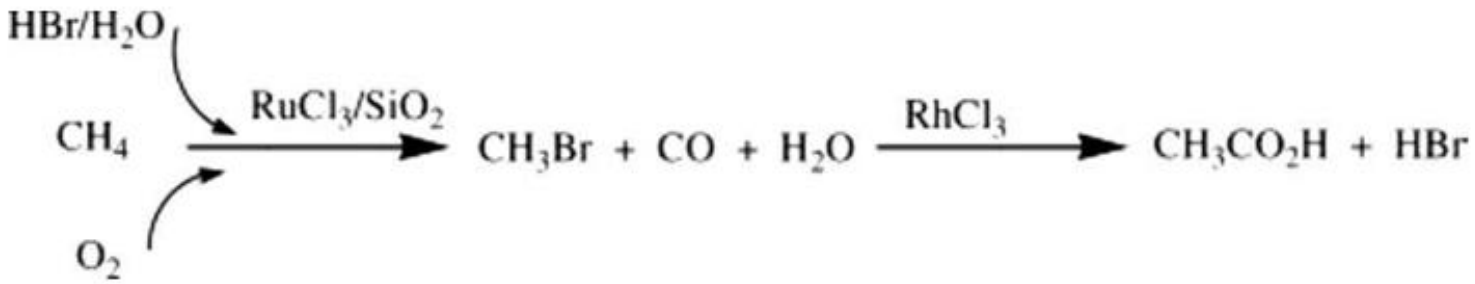



# OBAT

**Definisi Obat**

Obat adalah setiap molekul yang berinteraksi dengan system biologis dan menghasilkan respon biologis

**Drug Vs Medicine**

Para ahli kimia medisinal tidak menyukai istilah drug, karena punya konotasi negative. Mereka lebih suka ,menggunakan istilah medicine

**Bad Drug Vs Good drug**

Obat yang baik adalah obat yang digunakan dalam pengobatan suatu penyakit

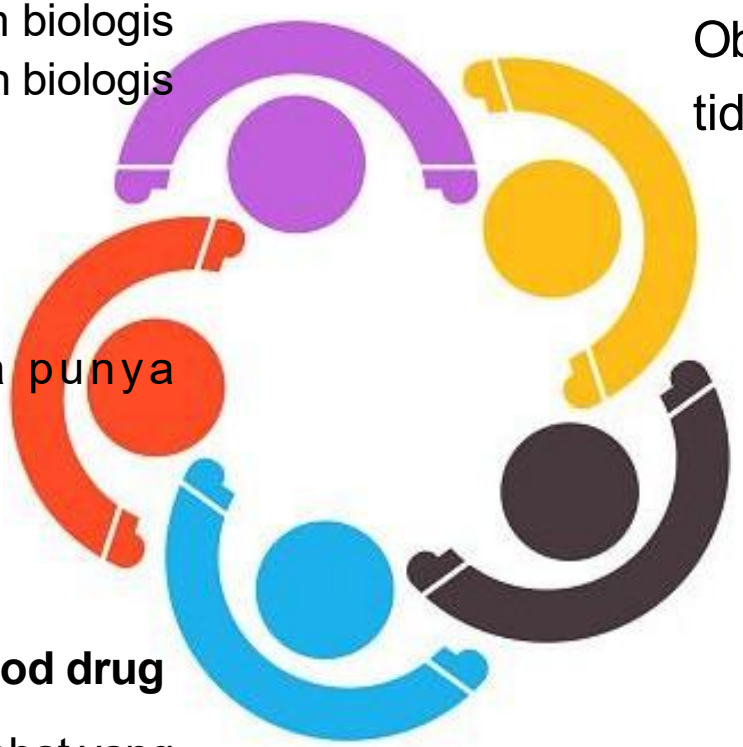

**Safe Drug Vs Unsafe drug**

Obat yang aman adalah obat yang tidak menimbulkan efek samping

**kesimpulan**

Adakah obat yang benar-benar aman dan baik?

# OBAT Vs RACUN

Definisi obat disini juga mencakup molekul-molekul lain yang tidak digunakan sebagai obat, seperti toksin dan racun.

Kedua kelompok senyawa tersebut umumnya tidak digunakan sebagai obat, namun dapat berinteraksi dengan tubuh dan menghasilkan respon biologis sehingga disebut pula “obat”.

**Toksin** adalah zat beracun yang dihasilkan oleh sel atau organisme hidup

**Racun (poison)** adalah setiap zat baik padat, cair maupun gas yang dapat mengganggu sel atau organisme

Apakah obat dapat menjadi racun?

Apakah racun dapat menjadi obat?

# Apakah Obat Benar-Benar Aman?

**Morfin**

Analgesik yang sangat kuat, namun efek sampingnya sangat serius, seperti toleransi, depresi pernafasan dan ketergantungan

## Alkohol

Alkohol merupakan obat yang banyak digunakan. Dosis terapinya sangat sulit ditentukan

## Kafein

Kafein hadir dalam teh dan kopi sebagai minuman sehari hari. Kenyataan kafein dapat memberikan efek stimulan dan menimbulkan ketergantungan. Kafein adalah obat

## Arsenik

Arsen adalah zat yang sangat beracun, namun, turunan senyawanya berguna sebagai anticancer dan anti protozoa

## Bisa ular

Bisa ular sangat beracun, namun dapat menjadi titik awal penemuan ACE inhibitor

**Penisilin**

Pada awal penemuannya, penisilin dianggap sebagai obat yang paling efektif dan aman. Tapi sekarang, penisilin telah neyebabkan resistensi beberapa bakteri

# KERJA OBAT

Obat dapat menghasilkan efek jika terjadi interaksi dengan target kerjanya. Target kerja obat dalam kimia medisinal dikaji pada level molekul. Interaksi ini terjadi melalui ikatan intermolekuler

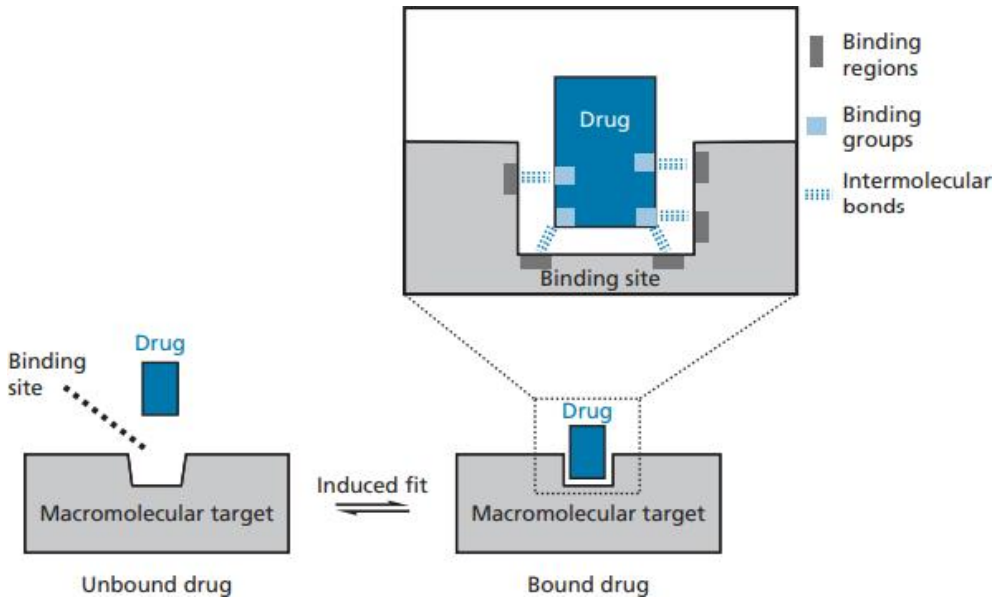


Target kerja obat dikaji pada level molekul, karena dengan begitu kita akan benar-benar mengerti bagaimana obat bekerja. Target kerja obat umumnya berupa molekul protein (enzim, reseptor, protein transport, dll)

### Ikatan intermolekuler

Berupa ikatan yang lemah antara molekul target dan obat ikatan ini dapat berupa ikatan ionic, ikatan hydrogen, interaksi dipol-dipol, interaksi ion-dipol, interaksi vanderwals

# KLASIFIKASI OBAT

**Berdasarkan efek farmakologisnya**

- Analgetik
- Antipsikotik
- Antihipertensi
- Antibiotik

**Berdasarkan Sistem Targetnya**

Obat dapat diklasifikasikan berdasarkan apakah obat tersebut mempengaruhi system target tertentu, misalkan:

- Obat system kardiovasekular
- Obat system pernafasan
- Obat system endokrin

**Berdasarkan Srtuktur molekulmya**

Dikelompokkan berdasarkan kemiripan rangka strukturnya, misal:

- Antibiotik beta lactam
- Barbiturat
- Steroid

**Berdasarkan Molekul Targetnya**

Berdasarkan molekul yang menjadi target kerjanya, misalkan:

Antikolinesterase

- **Agonis** dopamine
- **Antagonis** dopamin

# Pengembangan Obat Baru

Pada awal pengembangan obat, usaha penemuan obat baru pada umumnya bersifat trial and error sehingga biaya pengembangan obat baru sangat mahal.

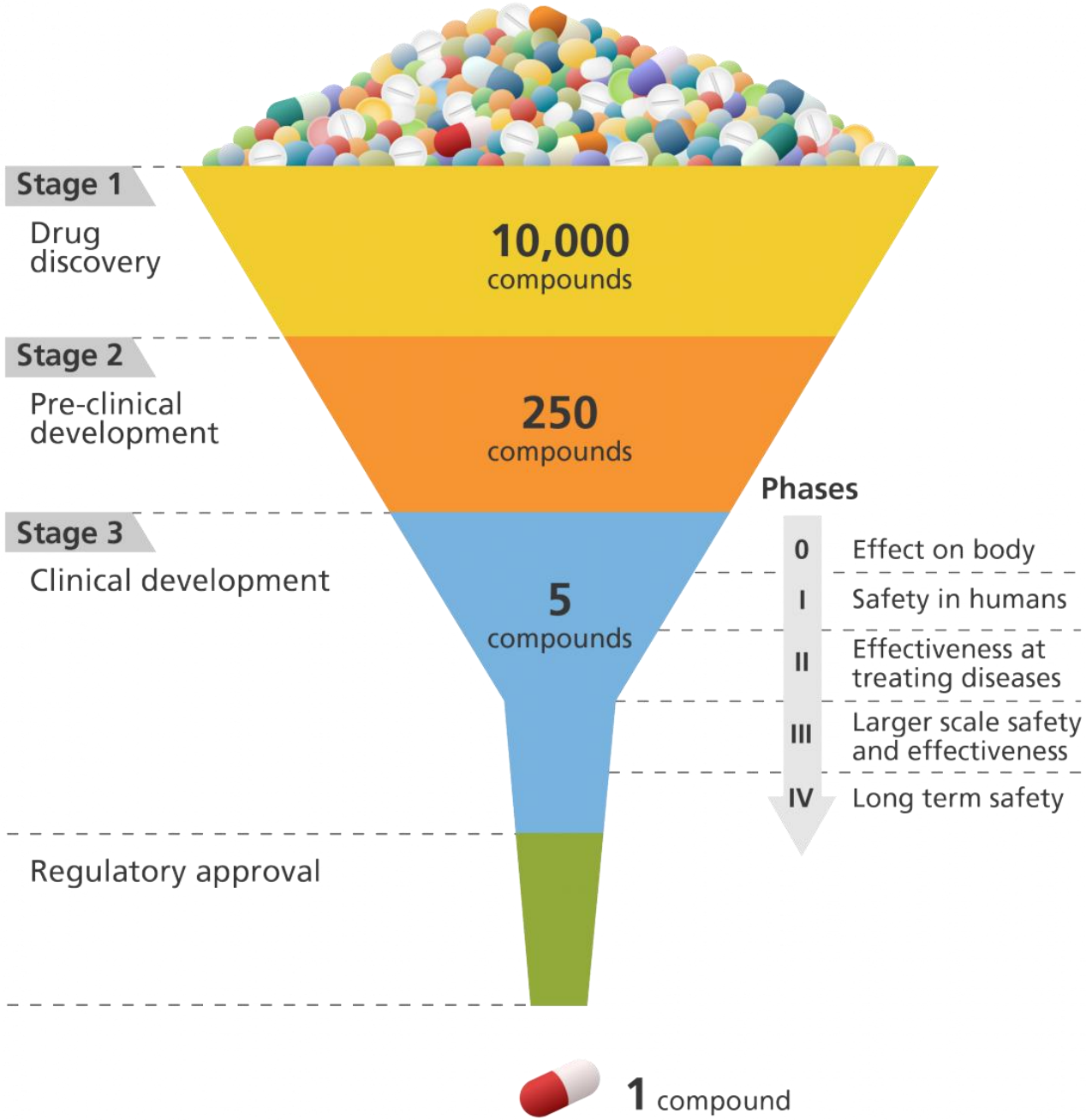

# Pengembangan Obat Baru

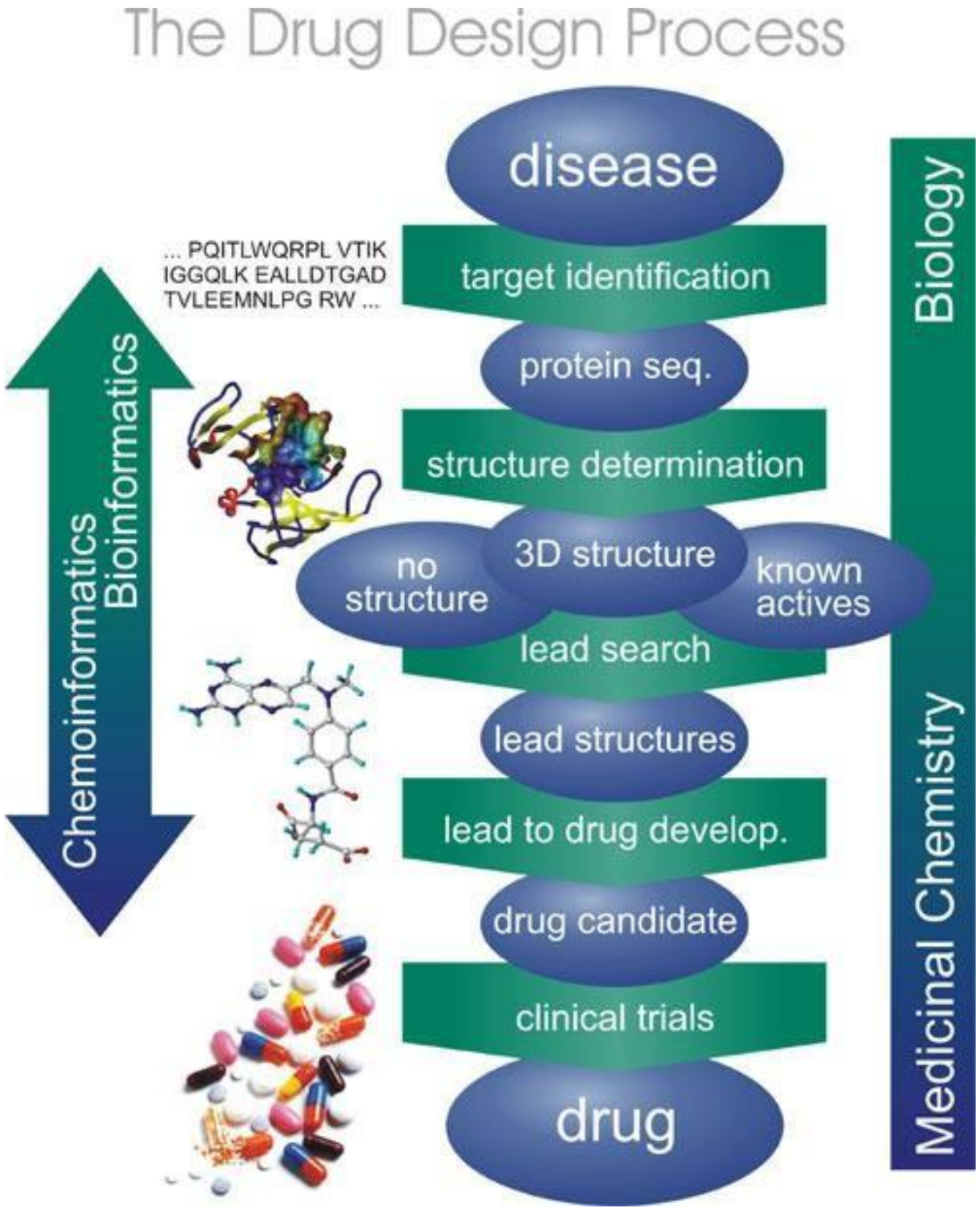

# RANCANGAN OBAT

Usaha mengembangkan obat yang telah ada, yang telah diketahui struktur molekul dan aktivitas biologinya, atas dasar penalaran yang sistematik dan rasional, dengan mengurangi trial and error seminimal mungkin

- **Elaborasi sistematik**
- **Mengembangkan obat yang sudah ada**
- **Aktivitas optimal & efek samping minimal**
- **Manipulasi molekul**

# PENCARIAN SENYAWA AKTIF

**Pencarian senyawa penuntun**

- Senyawa yang diguakan sebagai pangkal tolak modifikasi molekul..
- Senyawa yang dapat menimbulkan aktivitas biologis

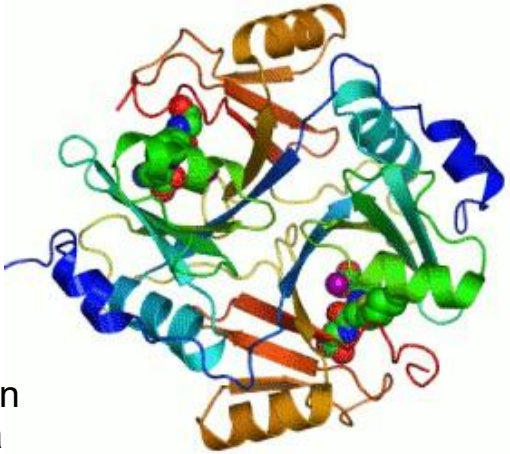

**Modifikasi struktur**

- Mensintesis sejjumlah senyawa penuntun, melakukan identifikasi struntur danmenguji aktivitas biologisnya

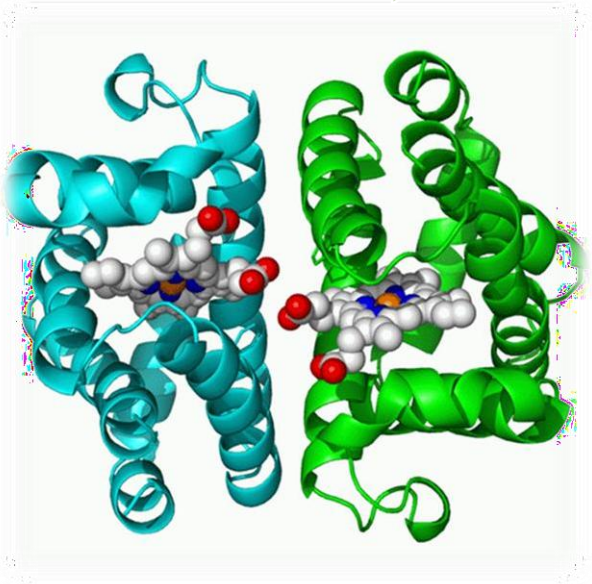

**HKSA**

- membahas tentang hubungan antara struktur molekul dengan aktivitas biologisnya yang dinyatakan secara kuantitatif

**Statistik**

- Statistik analisis regresi, pilih senyawa “terbaik” secara hipotesis

# Computer-aided drug design

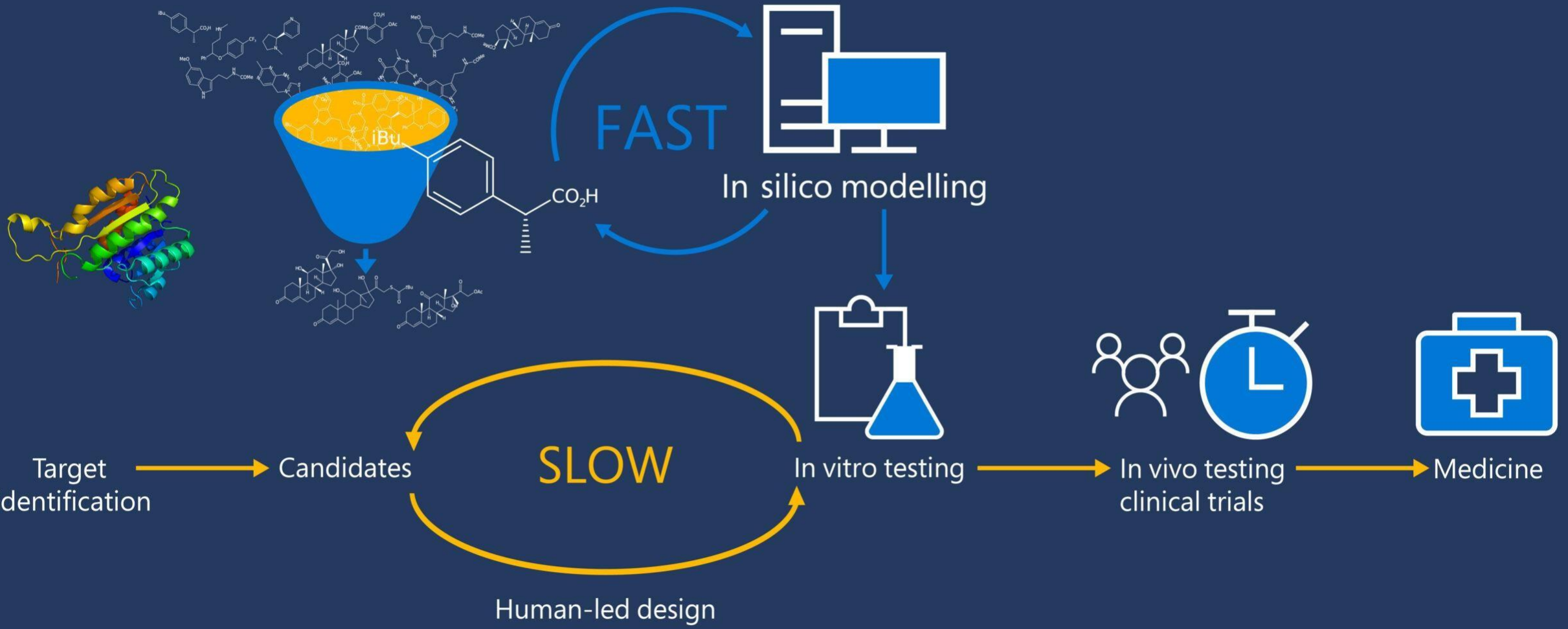

Penapisan Farmakologis

Uji Toksisitas Akut

Uji Stabilitas

Uji Farmakologis Lanjut

Uji Toksisitas Sub Akut

Uji Farmakokinetik pada Hewan

Uji Teratogenik & Mutagenik

Uji Klinis Fase I (Keamanan)

Pengembangan & Uji Stabilitas Bentuk Sediaan

Uji Klinis Fase II (Efikasi)

Studi Toksisitas Klinik

Uji Farmakokinetik Pada Manusia

Uji Klinis Fase III (Efikasi Multi Centre)

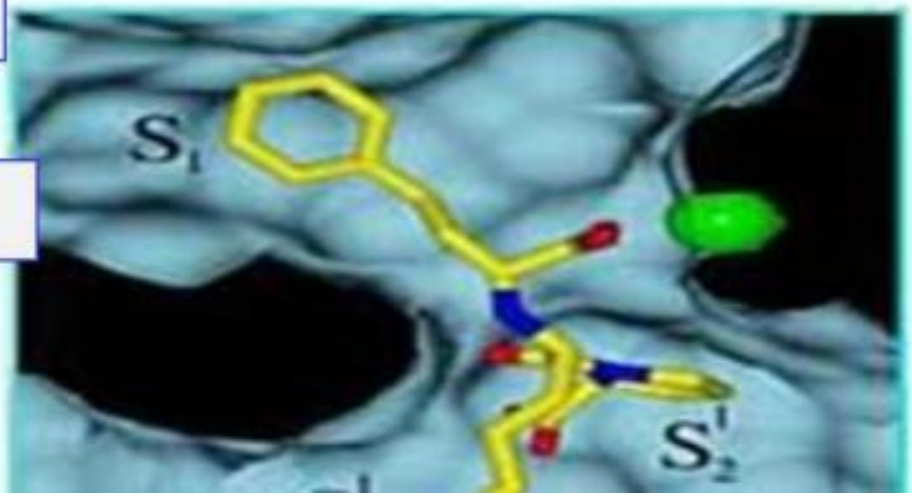


Pemasaran Obat Baru

Uji Klinis Fase IV (MESO)

# Mencari Senyawa Penuntun

1. **Penapisan Acak Senyawa Produk Alam** → ekstrak alam atau orga binatang untuk pengobatan
2. **Penemuan Secara Kebetulan**→ ditemukan secara kebetulan dalam lab atau klinik oleh ahli farmasi, ahli kimia, dokter atau peneliti
3. **Hasil Uji Metabolit Obat** → ada obat yang baru menimbulkan aktivitas setelah mengalami proses metabolism (Pro-drug)
4. **Studi Biomolekul dan Endokrinologi**→ senyawa antara proses metabolism dan biokatalisis
5. **Studi Perbandingan Biokimia** → perbedaan proses biokimia antar spesies-aksi selektif pada spesies tertentu

# Examples used natural product (NP) resources in drug discovery

(a) Aspirin was developed from natural product salicin.

(b) Codeine was prepared using morphine as the lead compound.

(c) The anticancer drug paclitaxel was isolated from yew.

(d) and (e) Penicillin G and quinine were isolated from Penicillium and Cinchona respectively.

(e) (f) The strategy of developing dual-active agents using a natural product lead compound 1-methylhydantoin.

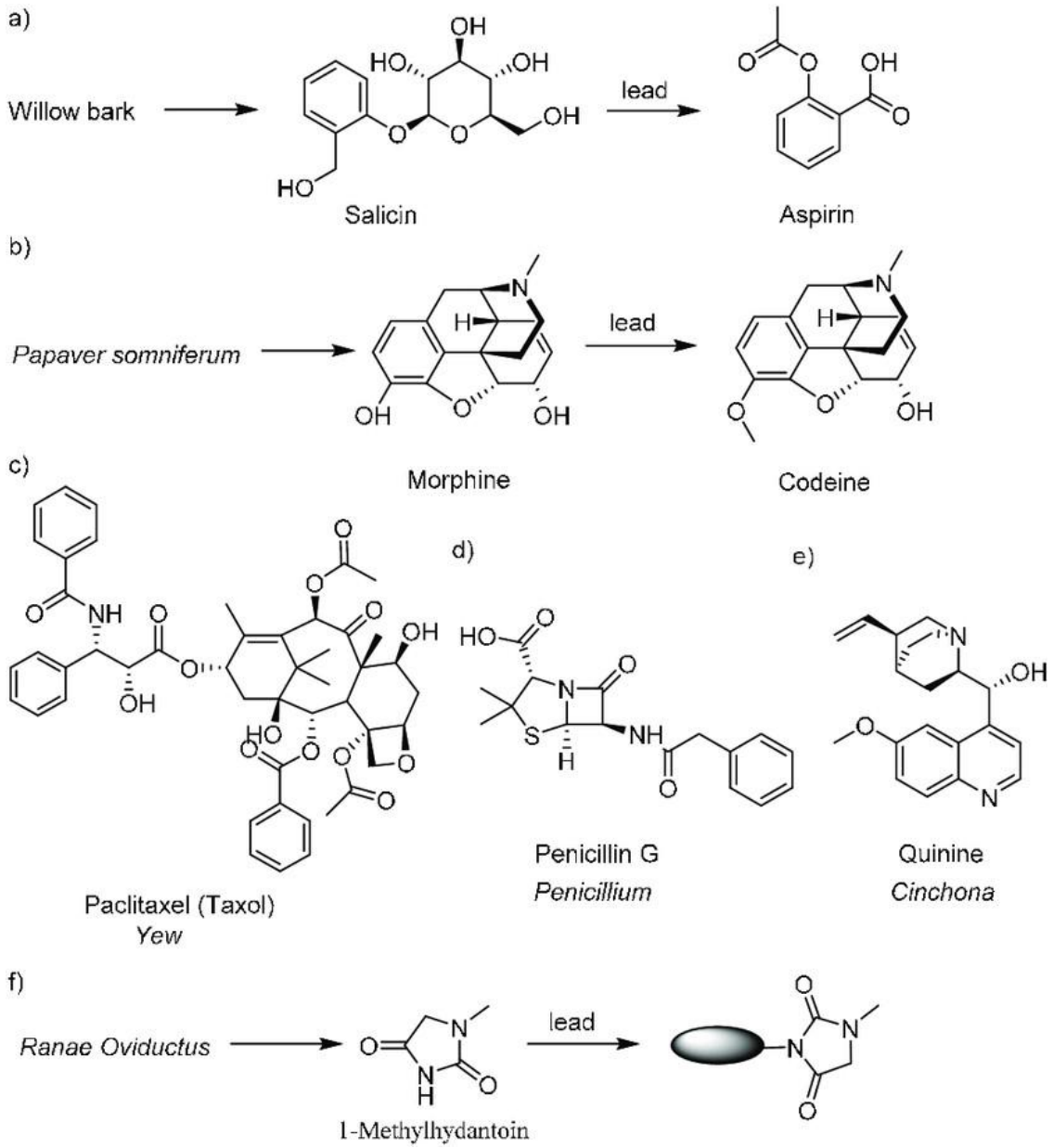

# Mencari Senyawa Penuntun

1. **Analisis Aktivitas senyawa Multi Poten**→ senyawa yang mempunyai kemampuan untuk menyebabkan dua atau lebih tipe aktivitas yang berbeda – beda reseptor
2. **Efek Samping Obat** → efek samping dipandang sebagai efek yang tidak diinginkan karena mempengaruhi Kesehatan individu.
3. **Hasil antara Sintesis Obat** → senyawa lain disamping produk yang terjadi pada reaksi sintesis
4. **Merancang struktur baru dan penapisan biologis**→ melakukan sistesis senyawa kimia murni kemudian dilakukan penapisan aktivitas biologis secara acak

# Thankyrase → enzim polymerase as lead compound

**22a**
cLogP: 3.9
TPSA: 136
TNKS2: 0.73
HEK293: 0.81

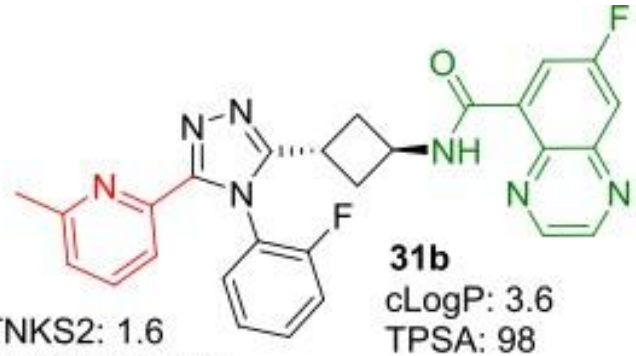

**31b**
cLogP: 3.6
TPSA: 98
TNKS2: 1.6
HEK293: 0.169

**31a**
cLogP: 3.5
TPSA: 98
TNKS2: 1.7
HEK293: 1.5

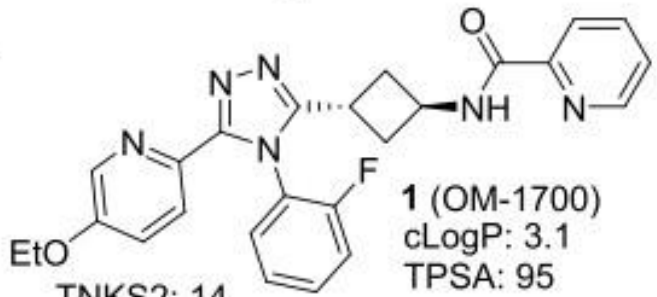

**1** (OM-1700)
cLogP: 3.1
TPSA: 95
TNKS2: 14
HEK293: 19

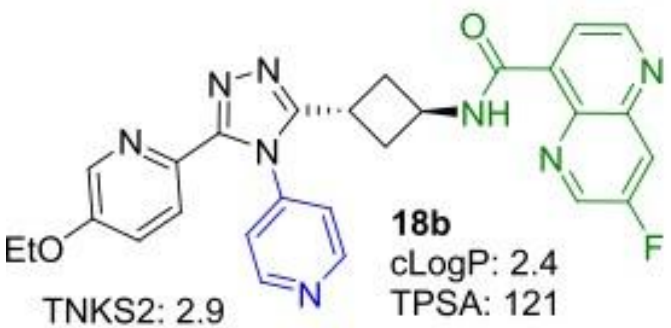

**18b**
cLogP: 2.4
TPSA: 121
TNKS2: 2.9
HEK293: 6

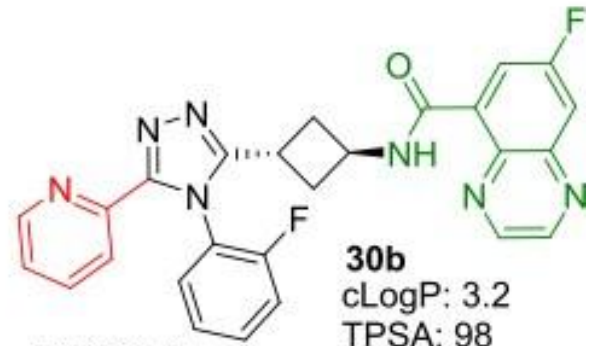

**30b**
cLogP: 3.2
TPSA: 98
TNKS2: 2
HEK293: 0.794

**24** (OM-153)
cLogP: 3.4
TPSA: 108
TNKS2: 2.0
HEK293: 0.63

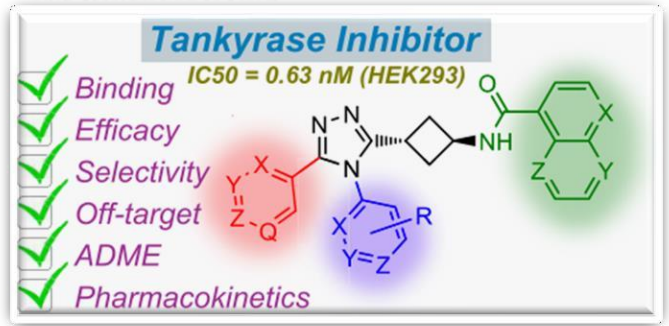

# Struktur Vs Aktivitas

**Struktur kimia obat ternyata dapat menjelaskan sifat obat dan terlihat bahwa gugus molekul obat berkaitan dengan aktivitas biologisnya**

- Senyawa dengan gugus fungsional yang sama dan mempunyai aktivitas biologis yang sama → bekerja pada reseptor yang sama atau mempengaruhi proses biokimia yang sama pula

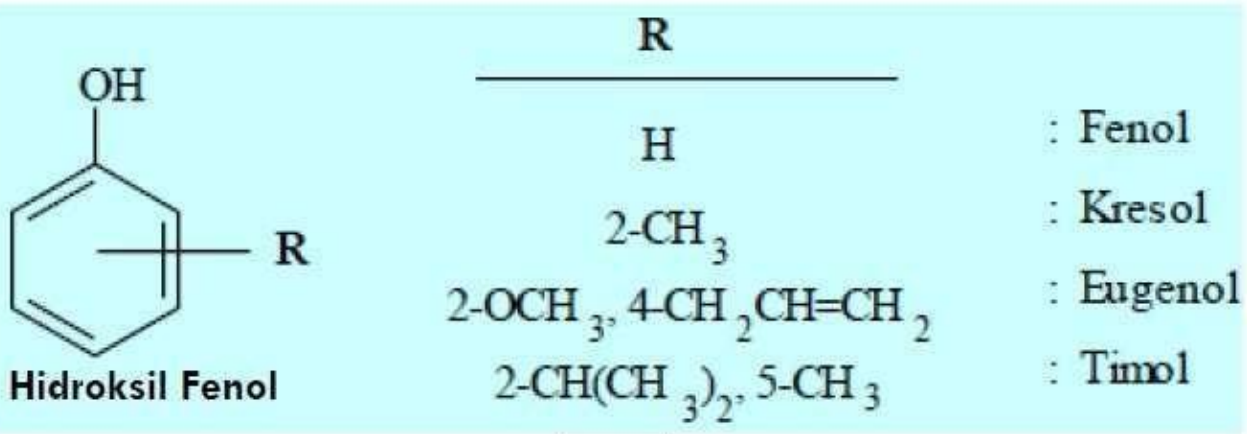


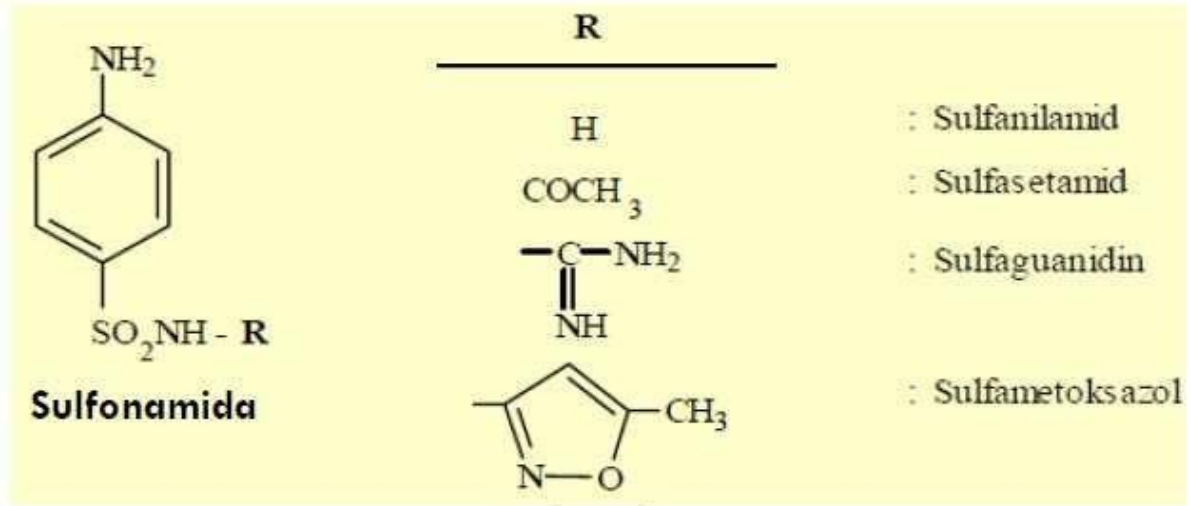

# Struktur Vs Aktivitas

- senyawa dengan gugus fungsional yang berbeda dan mempunyai aktivitas biologis yang sama → aktivitas turunan tersebut tidak tergantung pada struktur kimia spesifik, tetapi lebih tergantung pada sifat kimia fisik, seperti kelarutan dan aktivitas termodinamika

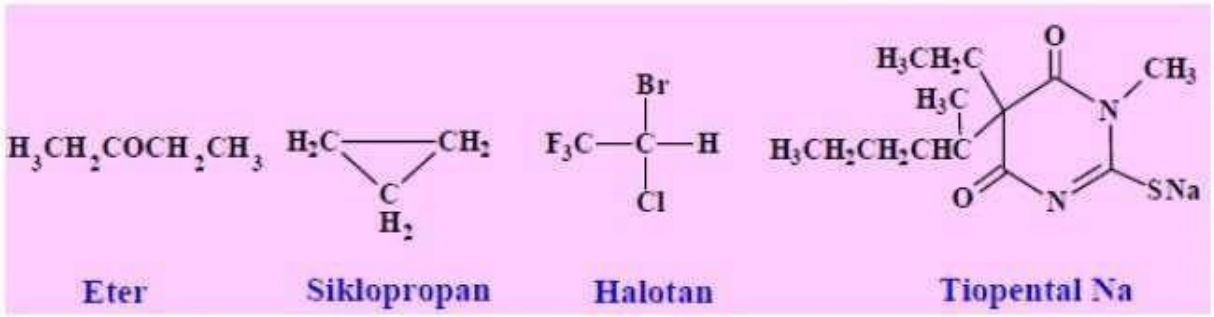


Lebih tergantung pada sifat kimia fisika (kelarutan dan aktivitas termodinamika)

**ANESTESI SISTEMIK**

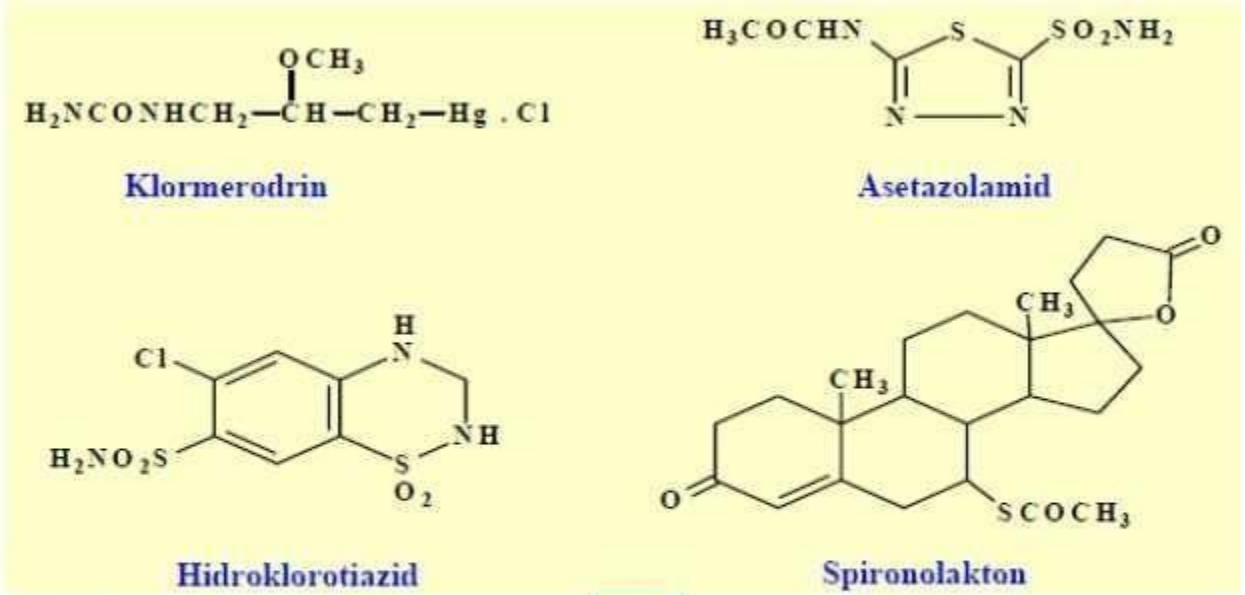


Proses biokimia BEDA (mekanisme kerjanya beda), efek biologisnya SAMA

**DIURETIK**

2015

# Struktur Vs Aktivitas

- Senyawa dengan unit struktur yang sama tetapi dapat memberikan aktivitas biologi yang bermacam-macam → dengan sedikit perubahan struktur akan berinteaksi dengan reseptor yang berbeda sehingga menimbulkan respon biologis yang berbeda pula

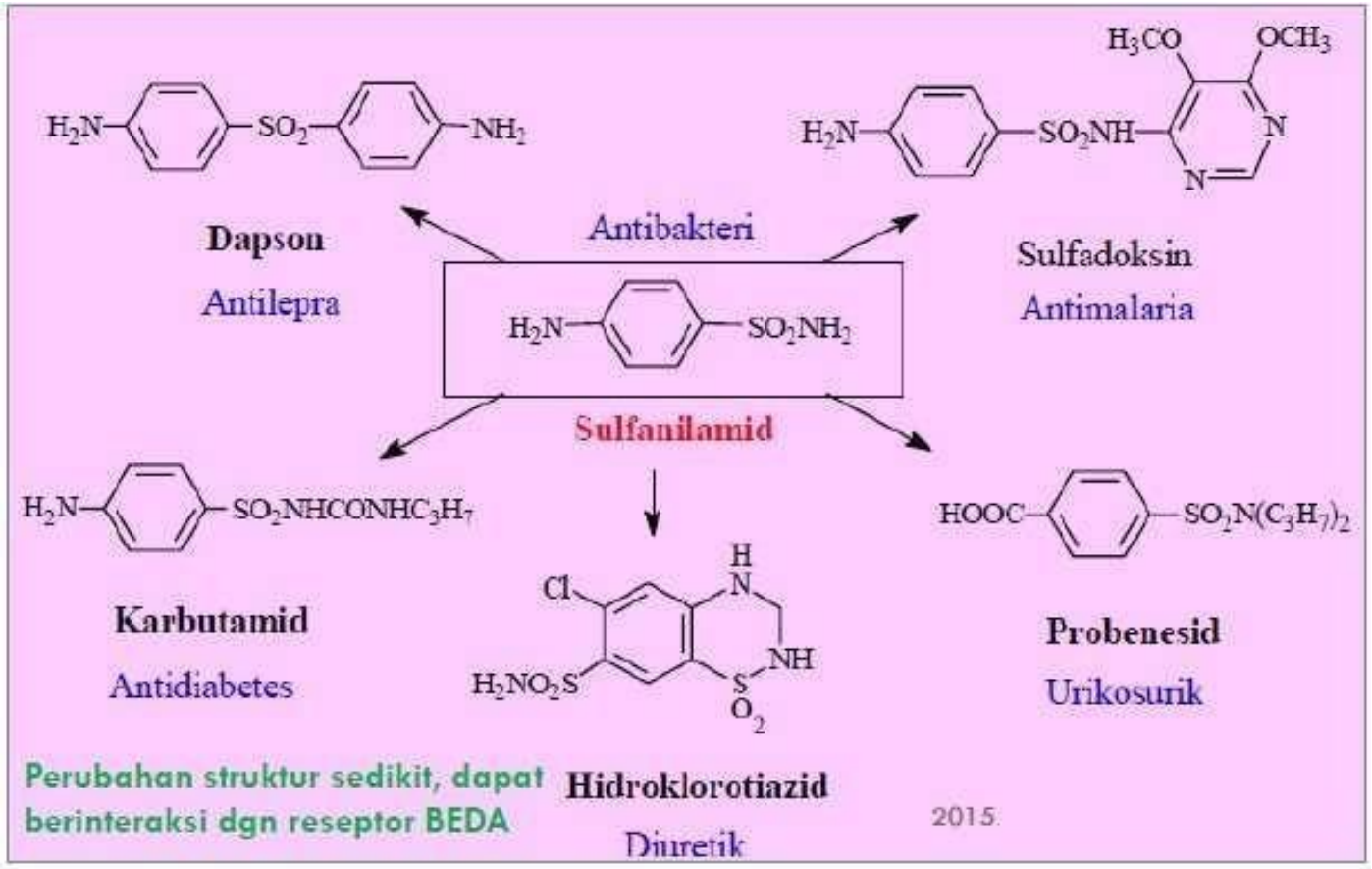

# Key Point

- Drugs are compounds that interact with a biological system to produce a biological response.
- No drug is totally safe. Drugs vary in the side effects they might have.
- The dose level of a compound determines whether it will act as a medicine or as a poison.
- The principle of selective toxicity means that useful drugs show toxicity against foreign or abnormal cells but not against normal host cells.
- Drug targets are macromolecules that have a binding site into which the drug fits and binds.

# THE END

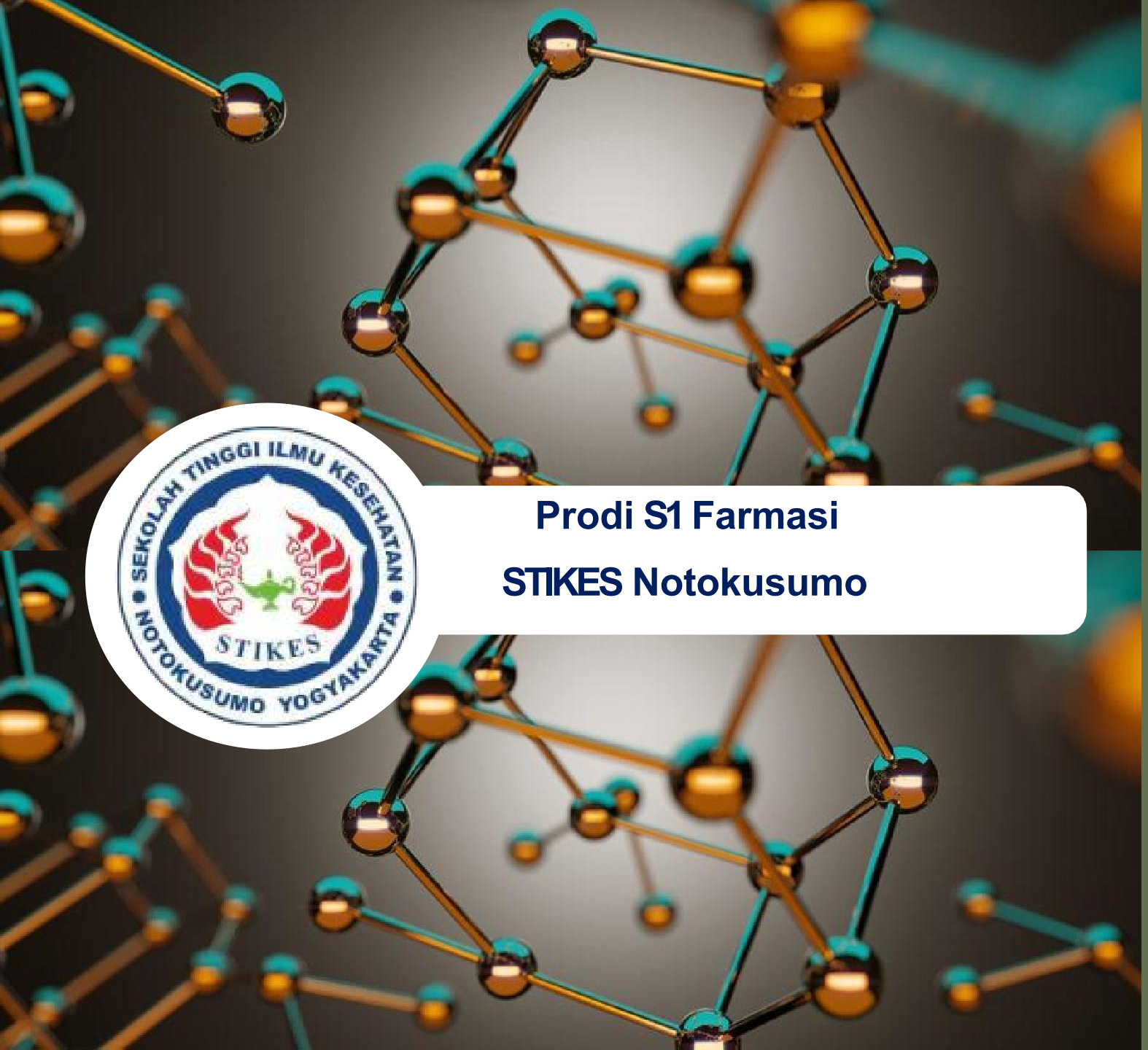

Prodi S1 Farmasi

STIKES Notokusumo

# Hubungan sifat fisika kimia obat dengan aktivitas dan Interaksi obat dengan reseptor

apt. Dian Purwita Sari, M.Biotech.

# Hubungan Sifat Fisika Kimia Obat dengan Aktivitas Biologis Obat

- Sifat kimia fisika dapat mempengaruhi aktivitas biologis obat oleh karena dapat mempengaruhi distribusi obat dalam tubuh dan proses interaksi obat-reseptor
- Beberapa sifat kimia fisika penting yang berhubungan dengan aktivitas biologis :

**IONISASI**

**PEMBENTUKAN KHELAT**

**POTENSIAL REDOKS**

**TEGANGAN PERMUKAAN**

# 1. IONISASI DAN AKTIVITAS BIOLOGIS

## OBAT AKTIF DALAM BENTUK TIDAK TERION

Sebagian besar obat bersifat **asam atau basa lemah,** bentuk **tidak terionnya** dapat memberikan **efek biologis**. Hal ini dimungkinkan jika kerja obat terjadi di membran sel atau di dalam sel.

**Fenobarbital –** asam lemah

Turunan asam barbiturat, dapat menembus sawar darah otak dan menimbulkan efek penekanan fungsi SSP dan pernafasaan dalam bentuk tidak terion

**Bagaimana pengaruh pH pada obat bersifat asam dan basa lemah?**

- pH dapat berpengaruh terhadap sifat kelarutan dan koefisien partisi obat
- Bentuk molekul obat – mudah larut dalam lemak – mudah menembus membrane biologis – jumlah yang berinteraksi dengan reseptor besar – aktivitas biologis besar

# IONISASI DAN AKTIVITAS BIOLOGIS

## Bagaimana pengaruh pH pada obat bersifat asam dan basa lemah?

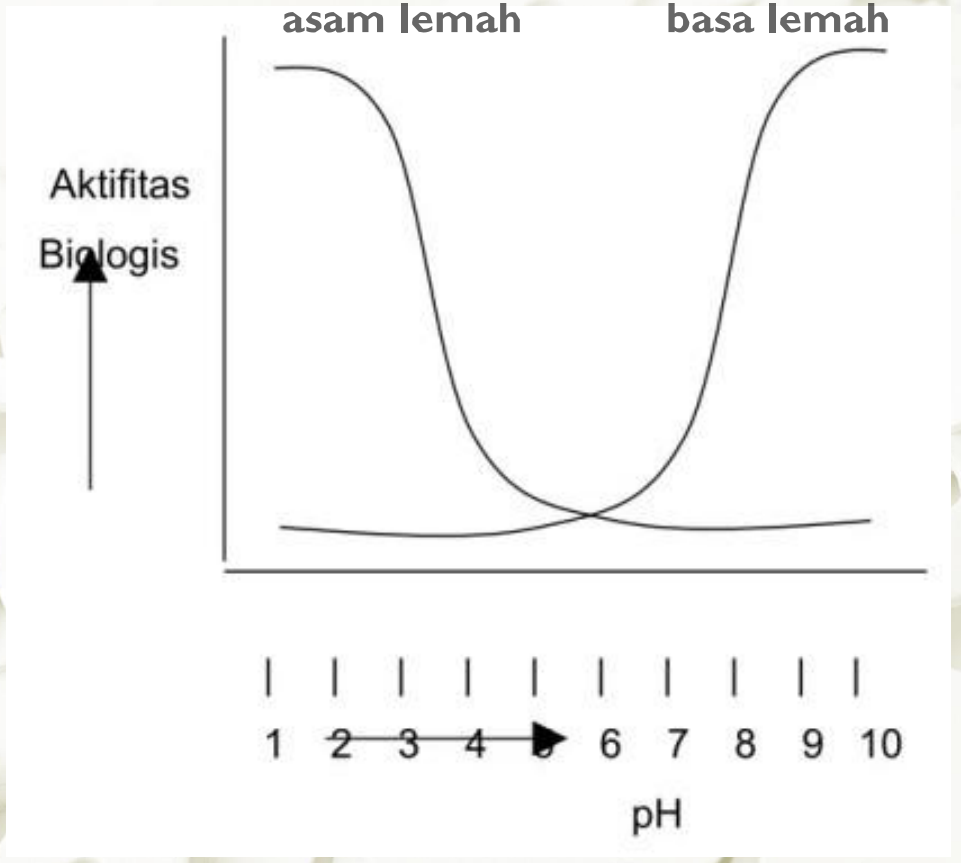


Contoh :

Asam benzoate, asam salisilat dan asam mandelate

Aktivitas antibakteri bertambah besar pada suasanan asam. pH = 3 aktivitas antibakteri 100 kali lebih besar disbanding pada suasana netral

Fenobartital. pKa = 7,4??

# IONISASI DAN AKTIVITAS BIOLOGIS

## OBAT AKTIF DALAM BENTUK ION

Beberapa senyawa obat menunjukkan aktivitas biologis yang meningkat bila derajad ionisasinya meningkat. Senyawa ion – sulit menembus membran biologis – efek biologis diluar sel

Postulat Bell dan Robin (1942) mengenai sulfonamida :

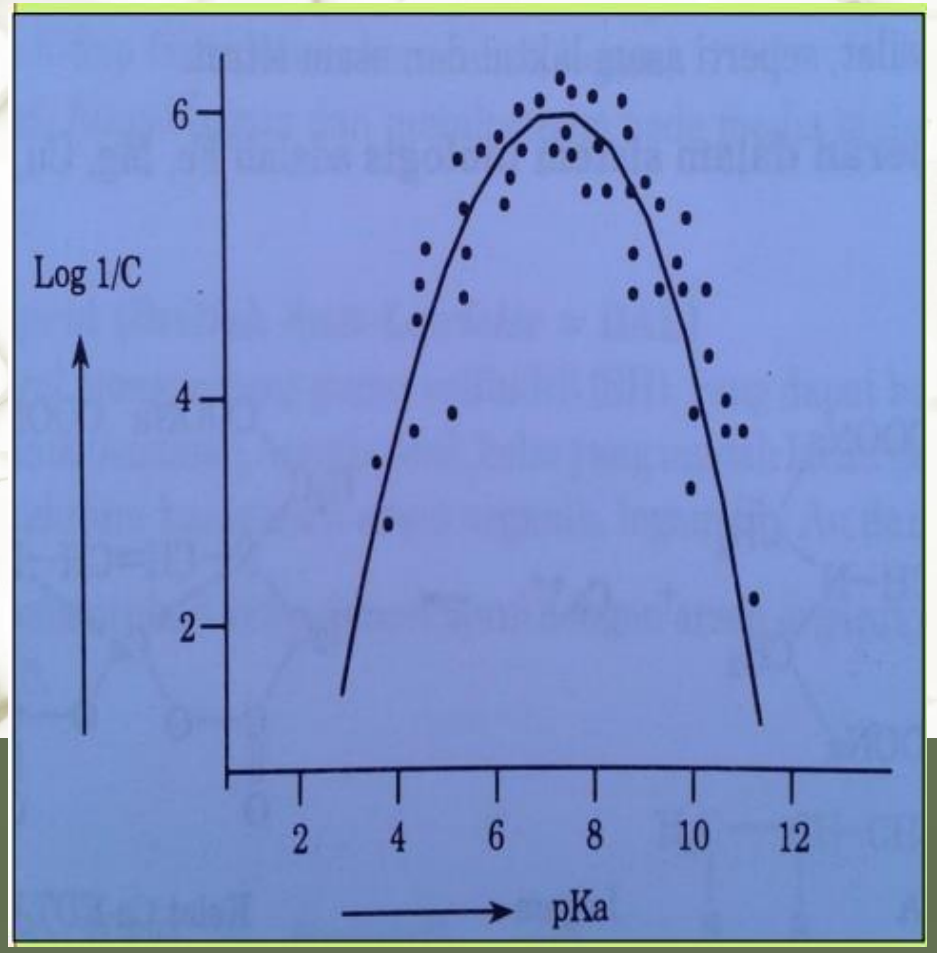

# 2. Pembentukan Khelat dan Aktivitas Biologis

- **Khelat** adalah senyawa yang dihasilkan oleh kombinasi senyawa yang mengandung gugus electron donor dengan ion logam, membentuk suatu struktur cincin.

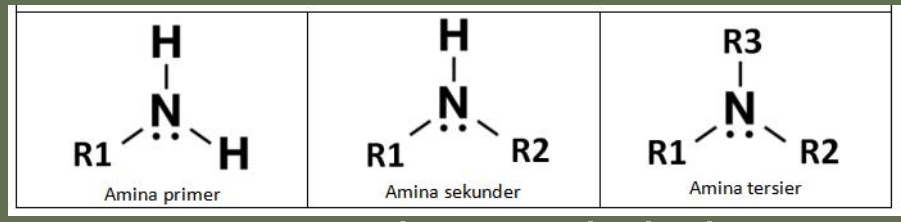


- Gugus yang dapat membentuk kelat a.l:

  Gugus amin primer, sekunder dan tersier, Oksim, Imin, Imin tersubtitusi, Tioter, Keto, Tioketo, Hidroksil, Tioalkohol, Karboksilat, fosfonat dan Sulfonat.

  Contoh :

  kelat antara etilen diamin tetra asetat dengan Ca

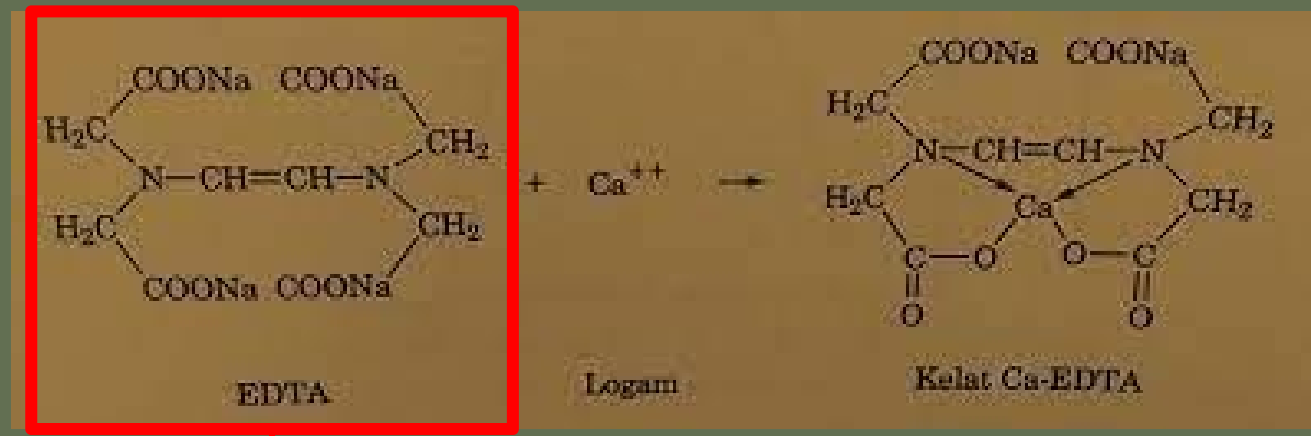


**Ligan** = senyawa yang dapat membentuk Struktur cincin dengan ion logam karena Mengandung atom yang bersifat electron Donor, seperti N, S, dan O

# Penggunaan Ligan di Bidang Farmasi

1. Membunuh MO dengan cara membentuk kelat dengan logam esensial yang diperlukan untuk pertumbuhan sel (bakterisida, fungisida dan virisida)
2. Untuk menghilangkan logam yang tidak diinginkan atau membahayakan (antidotum keracunan logam)
3. Untuk studi logam dan metaloenzim pada media biologis

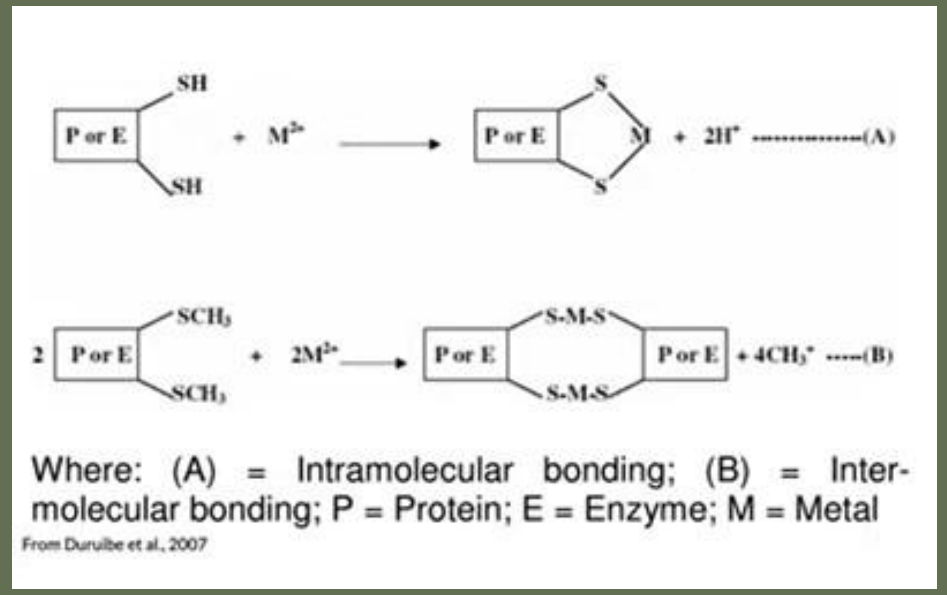


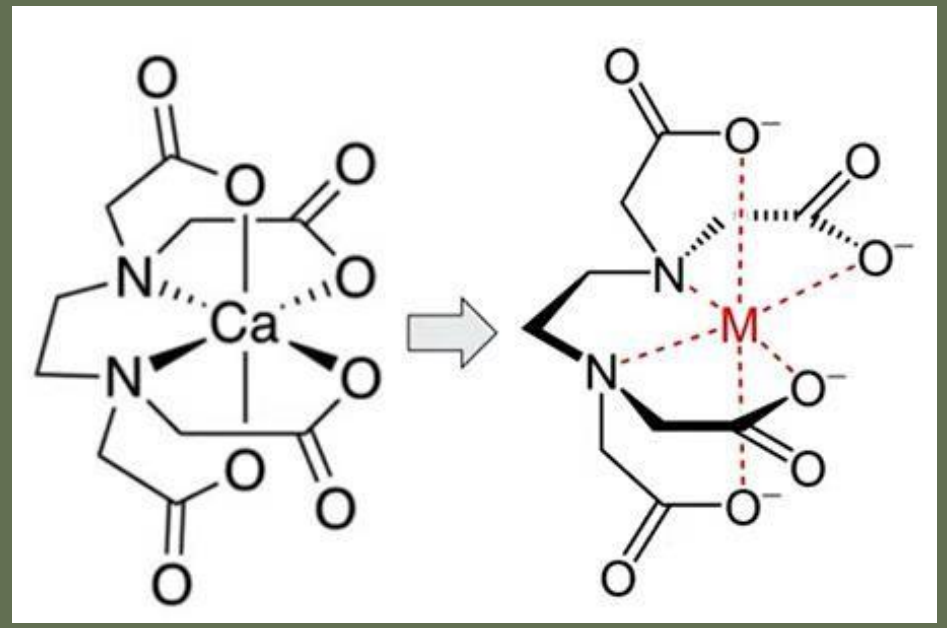

# Antidotum keracunan logam

## Dimerkaprol

Dimerkaprol mengandung gugus sulfhidril (SH) yang dapat berinteraksi dengan arsen organik (lewisite), membentuk kelat yang mudah larut. Spesifik untuk antidotum keracunan arsen organik, logam Sb, Au dan Hg.

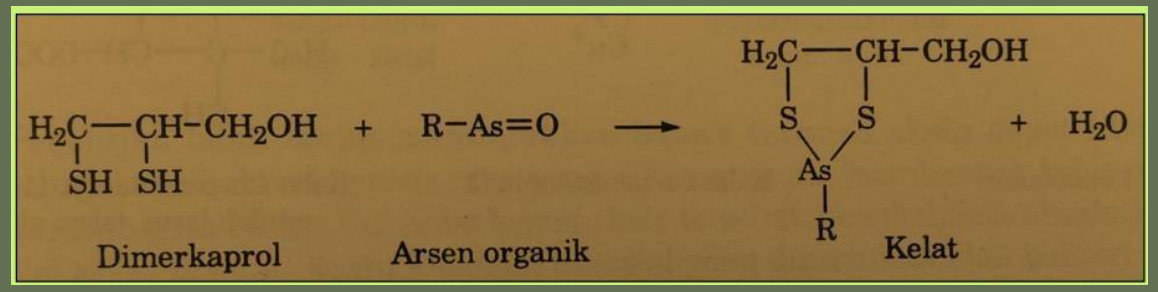


## Penisilamin

Merupakan senyawa hasil hidrolisis penisilin dalam suasana asam, digunakan untuk antidotum keracunan logam Cu, Au dan Pb. Digunakan juga untuk pengobatan penyakit wilson, penyakit genetik yang menyebabkan gangguan ekskresi Cu → kadar Cu di dalam darah >> Penisilamin+Cu++ → kelat yang mudah larut air

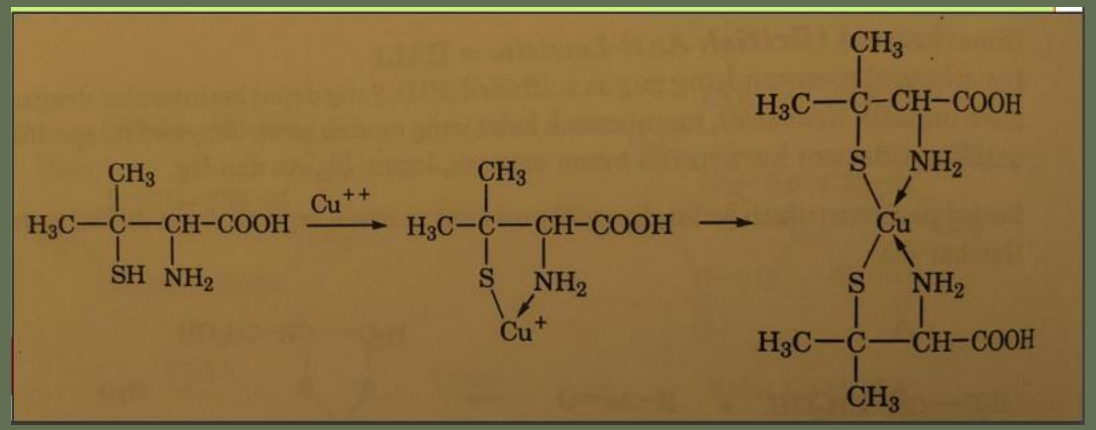

# Antimikroba

## Isoniazid, Tiosetazon dan Etambutol

Ketiganya dapat berinteraksi dengan ion Cu++ membentuk kelat yang larut dalam lemak sehingga mudah menembus membran sel bakteri Mycobacterium tuberculosis.

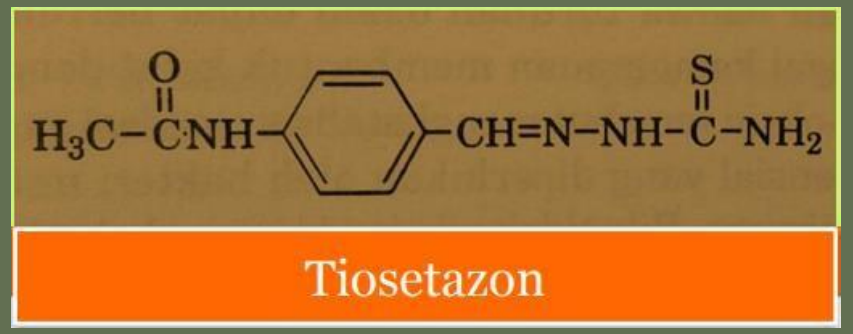


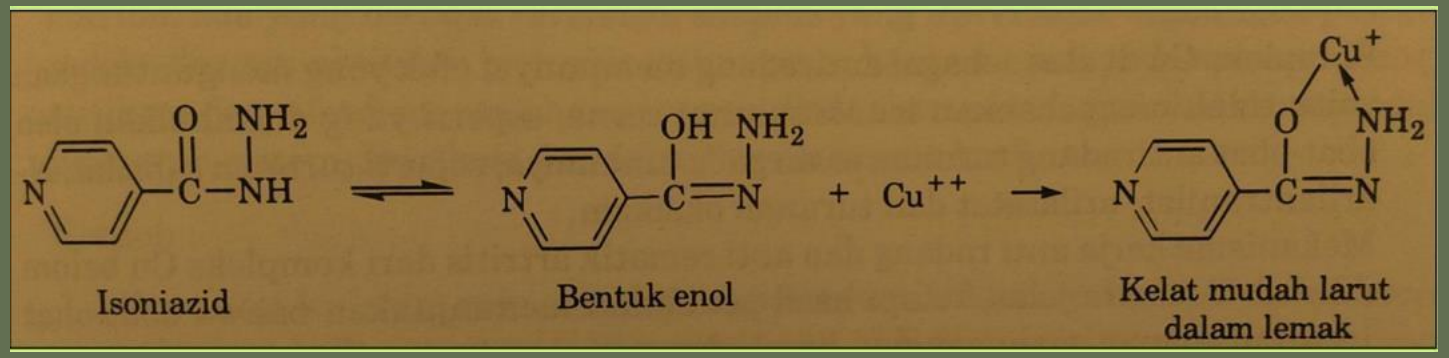


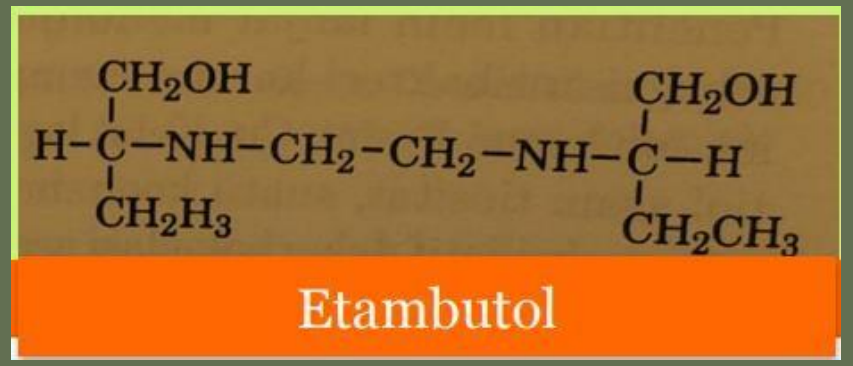

# Antimikroba

## Tetrasiklin

AB spektrum luas mengandung gugus hidroksil (C3) yang bersifat asam dan amin tersier (C4) yang bersifat basa dapat membentuk kelat dengan ion Mg++ bakteri. → Tetrasiklin juga dapat membentuk kelat dengan logam-logam lain → aktivitas menurun bila diberikan bersama susu yang mengandung Ca++, antasida yang ion mengandung Ca, Mg dan Al, atau sediaan yang mengandung Fe → Tetrasiklin dapat menyebabkan gigi berwarna kuning pada anak

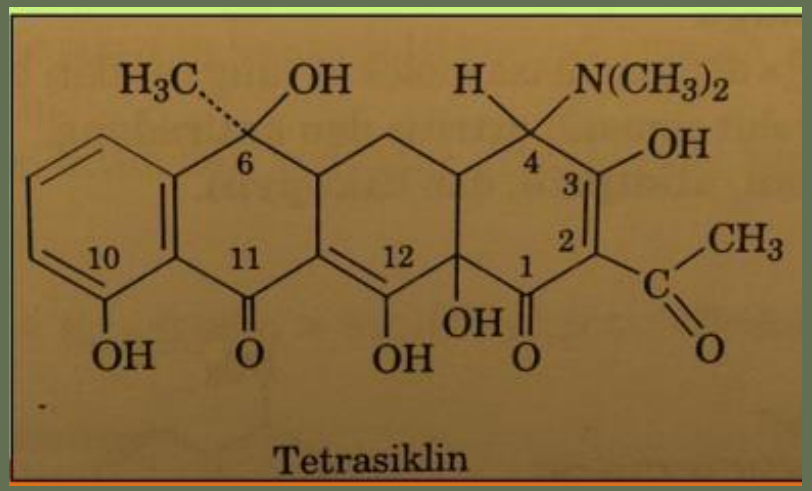

# Anticancer

## Sisplatin

Cis-dikloroetilendiaminplatinum (II) → Adalah senyawa kompleks turunan platinum yang digunakan sebagai antikanker. Isomer trans tidak menunjukkan aktivitas. → Bekerja dengan membentuk ligan reaktif kemudian Pt membentuk crosslink diantara atom N dari 2 buah guanin DNA → hambatan sintesis DNA sel kanker

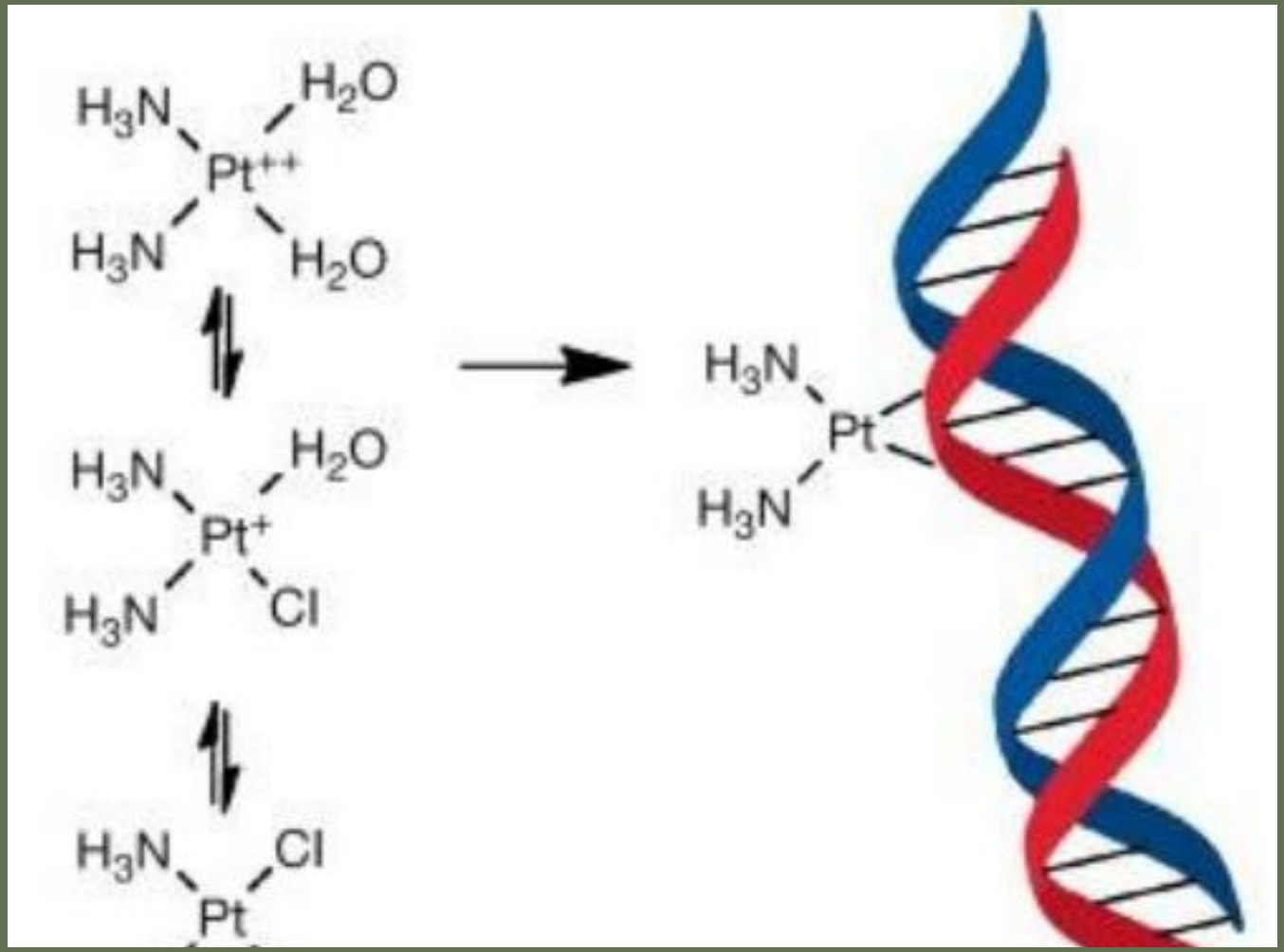

# Cautions!!!!

**Ligan-ligan yang digunakan pengobatan dapat menimbulkan toksisitas yang besar karena mengikat logam lain yang diperlukan untuk fungsi fisiologis, contoh:**

- Tiasetazon, difeniltiokarbazon, oksin dan aloksan dapat menimbulkan awal penyakit DM karena obat-obat tsb dapat membentuk kelat dengan Zn pada sel beta pankreas sehingga menghambat produksi insulin.
- Hidralazin (apresolin) penurun TD dapat menyebabkan anemia karena dapat berikatan dengan Fe darah.
- Dimerkaprol dan INH cenderung menimbulkan efek seperti histamin karena membentuk kelat dengan logam Cu yang berfungsi sebagai katalisator enzim perusak histamin (histaminase)

# 3.
# POTENSIAL REDOKS DAN AKTIVITAS BIOLOGIS

**Potensial redoks** merupakan kecenderungan senyawa untuk memberi dan menerima electron

**Reaksi redoks** adalah perpindahan electron dari satu atom ke atom molekul yang lain.

Tiap reaksi pada organisme hidup terjadi pada **potensial redoks yang optimum**, dengan kisaran yang bervariasi, sehingga diperkirakan bahawa **potensial redoks senyawa tertentu berhubungan dengan aktivitas biologisnya.**

Pengaruh potensial redoks **tidak dapat diamati secara langsung** karena hanya berlaku untuk system keseimbangan ion tunggal yang bersifat reversivel.

# Riboflavin

Merupakan koenzim faktor vitamin, aktivitas biologisnya berdasar pada kemampuan untuk menerima elektron sehingga tereduksi menjadi bentuk dihidronya

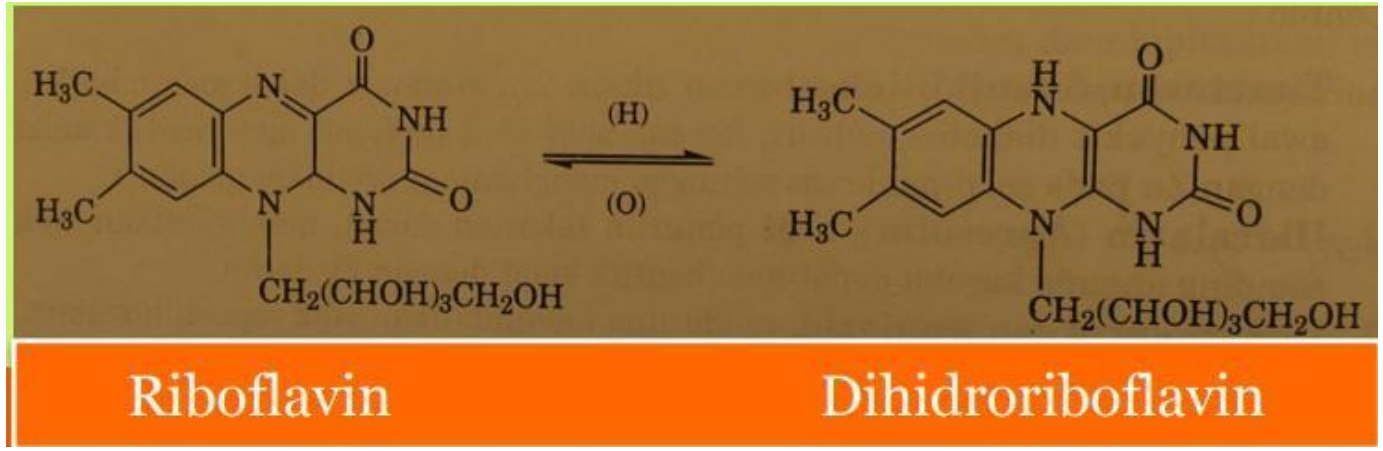

# 4. AKTIVITAS PERMUKAAN DAN AKTIVITAS BIOLOGIS

**Senyawa untuk menurunkan tegangan permukaan → surfaktan**

**Surfaktan mempengaruhi absorbsi obat. Aktivitasnya terhadap absorbsi obat tergantung pada:**

- ✓ Kadar surfaktan
- ✓ Struktur kimia surfaktan
- ✓ Efek surfaktan terhadap membran biologis
- ✓ Efek farmakologis surfaktan
- ✓ Adanya interaksi antara surfaktan dengan bahan-bahan pembawa atau bahan obat

# Pengaruh surfaktan polisorbat 80 terhadap absorbsi sekobarbital

**Pada kadar rendah** surfaktan akan meningkatkan absorbsi secobarbital karena mempengaruhi membran biologis sehingga penetrasi sekobarbital >>

**Pada kadar tinggi**, surfaktan menyebabkan partisi obat ke dalam fasa air dan misel. Obat yang berada dalam fasa misel sukar menembus membran → kecepatan absorbsi menurun

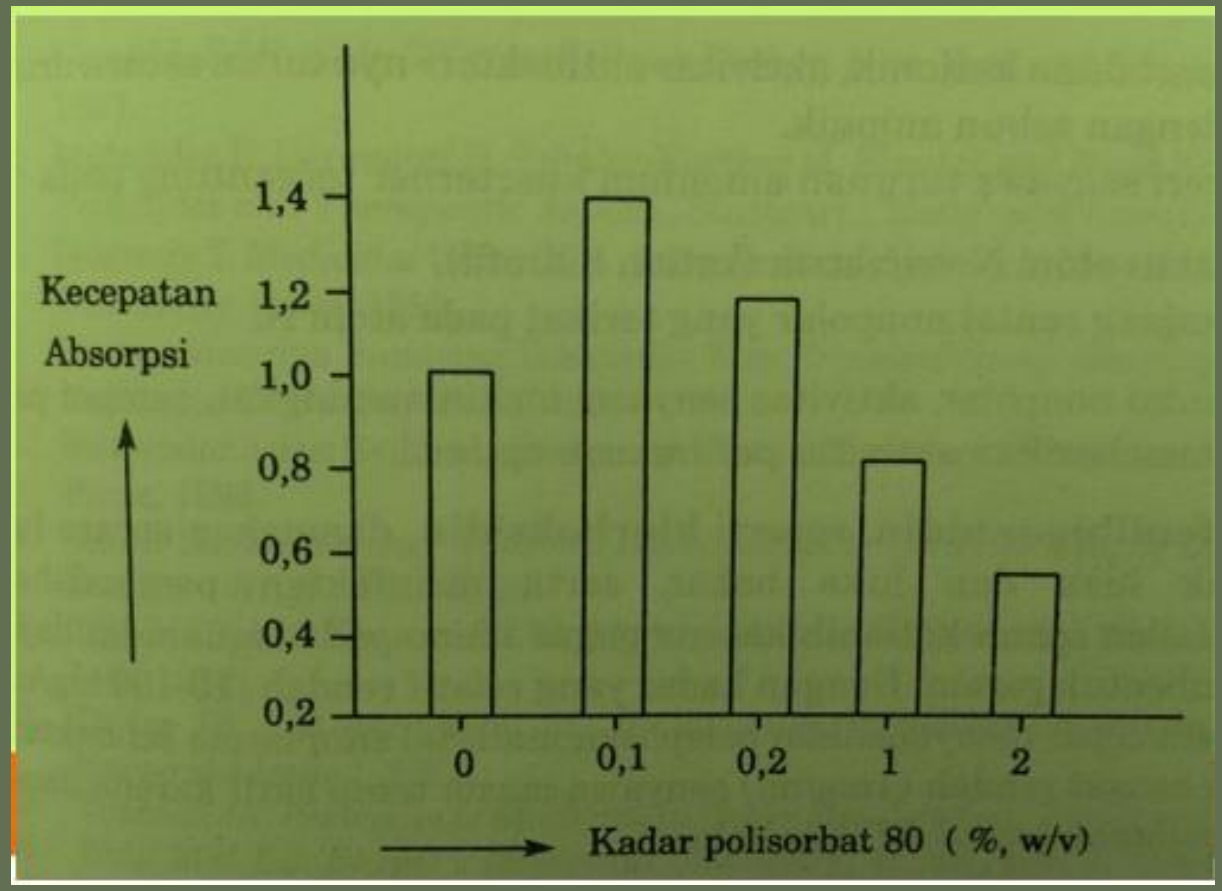

# Surfaktan pada antibakteri

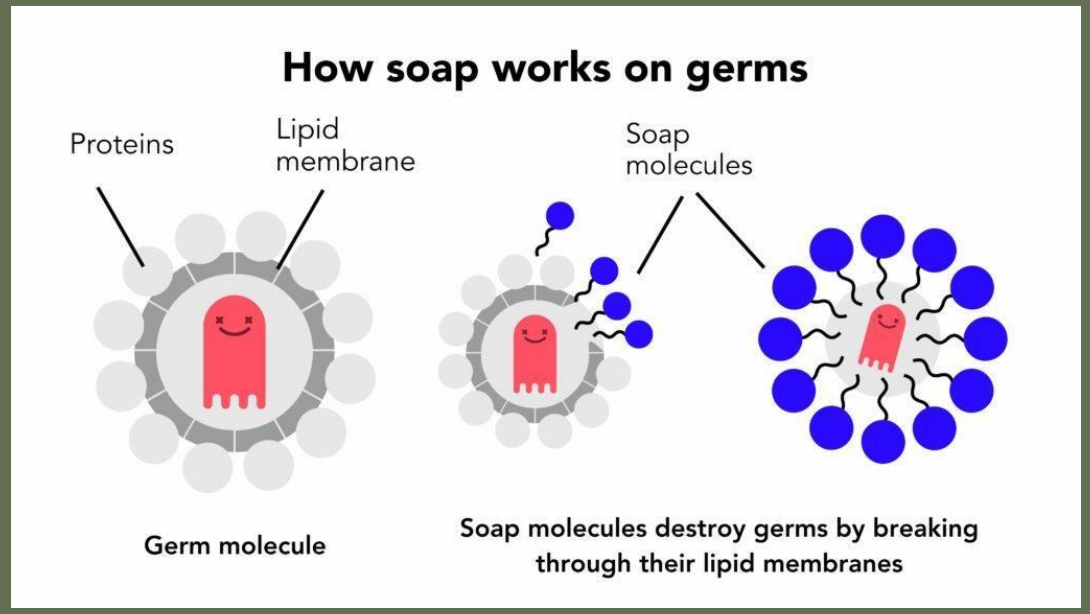


**Surfaktan memiliki aktivitas yang nyata terhadap permeabilitas membran sel bakteri**

- **Surfaktan dengan aktivitas ringan** → diabsorbsi 1 lapis pada permukaan membran sel bakteri sehingga menghalangi absorbs bahan-bahan yang dibutuhkan oleh sel.
- **Surfaktan dengan aktivitas kuat** → dapat mengubah struktur dan fungsi membran, menyebabkan denaturasi protein membran sel bakteri → lisis sel

**Karena dapat menyebabkan ketidakteraturan membrane sel, umumnya tidak digunakan secara invivo → biasanya untuk pemakaian lokal atau sterilisasi alat.**

# Contoh

- **Turunan amonium kuarterner, ex: benzalkonium klorida dan dekualinium klorida**
- **Memiliki kation hidrofil dan gugus nonpolar yang panjang**
- **Termasuk golongan antibakteri yang bersifat tidak spesifik, aktivitasnya tergantung pada:**
  - ☐ Kerapatan muatan atom N asimetrik (kation hidrofil)
  - ☐ Ukuran dan panjang rantai nonpolar
  - ☐ makin panjang rantai makin Besar aktivitas sampai titik optimalnya.

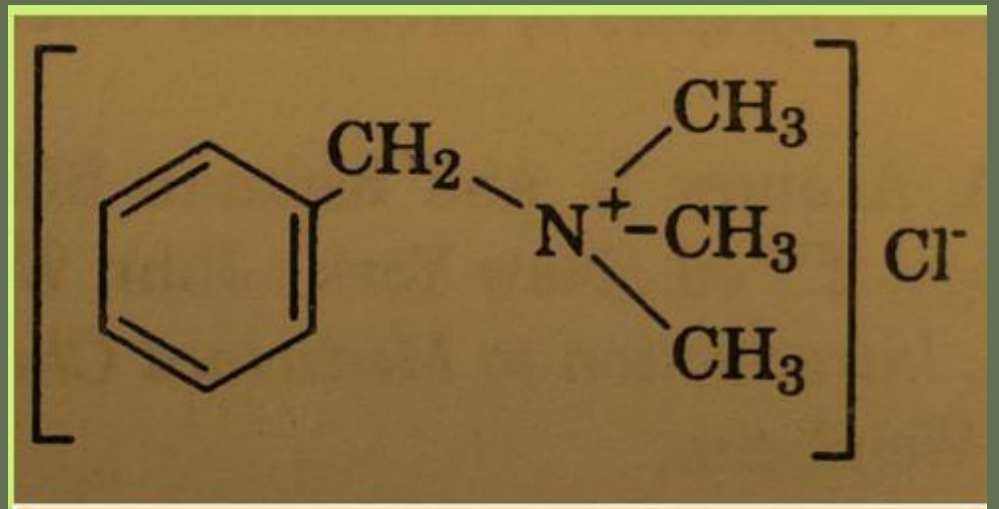


Benzalkonium klorida

# INTERAKSI OBAT DENGAN RESEPTOR

# Drug-Target Interaction

- Obat akan bekerja pada target kerja pada level molekul
- Molekul target umumnya berupa protein (enzim, reseptor, dan protein transport), atau asam nukleat (DNA, RNA)
- Target kerja biasanya disebut makromolekul, karena molekul berukuran besar tersebut terdiri atas ratusan atom dan jauh lebih besar dibandingkan molekul obat.
- Obat berinteraksi dengan target melalui pengikatan (*binding*) pada situs pengikatan (*binding site*)
- Ikatan obat dengan target umumnya terbentuk oleh ikatan ikatan yang lemah dalam *intermolekuler bonds*.

# Ikatan Intermolekuler

- **katan Kovalen**

Ikatan kovalen merupakan ikatan yang paling kuat. Ikatan kovalen jarang terlibat dalam pembentukkan ikatan antara obat dengan reseptor, kecuali dengan enzim dan D N A

- **Ikatan ionic**

Adalah ikatan yang dihasilkan oleh daya tarik menarik antar ion-ion yang muatannya berlawanan.

# Ikatan Intermolekuler

- **Interaksi dipol-dipol dan ion-dipol**

  Sifat elektronegatifitas dari atom-atom seperti O, N, S, dan halogen yang lebih besar dibandingkan elektronegatifitas dari atom karbon akan berpengaruh terhadap ikatan obat dengan reseptor. Ikatan C-X (X adalah atom-atom elektronegatif) yang terdapat pada obat maupun yang terdapat pada reseptor akan mengakibatkan distribusi elektron yang tidak simetris.

  Hal ini akan menghasilkan suatu dipol elektronik. Suatu dipol yang terbentuk di dalam molekul obat dapat berinteraksi dengan ion (interaksi ion-dipol) atau dipol lain (interaksi dipoldipol) yang bermuatan berlawan yang terdapat pada reseptor

# Interaksi dipol-dipol dan ion-dipol

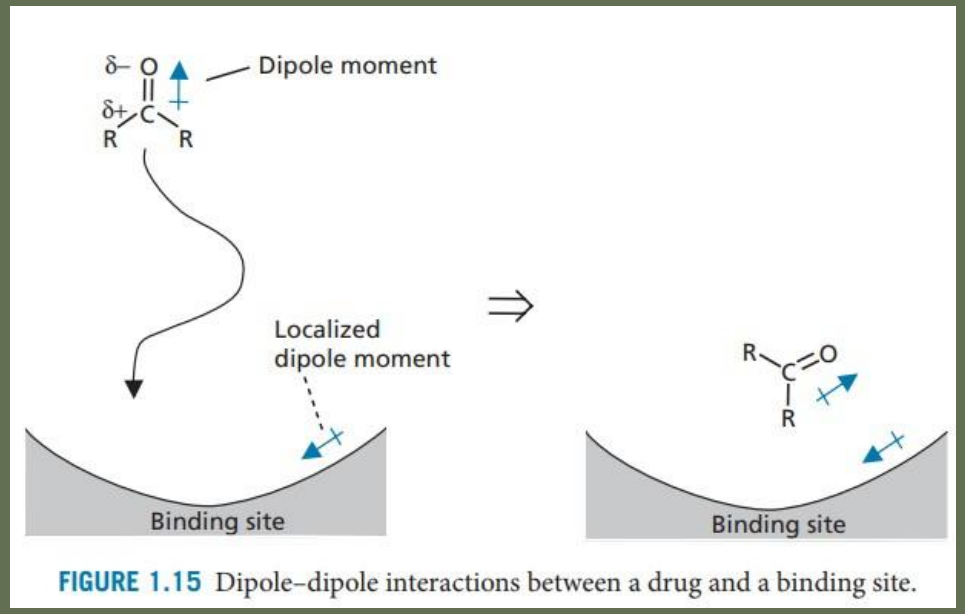


**FIGURE 1.15** Dipole–dipole interactions between a drug and a binding site.

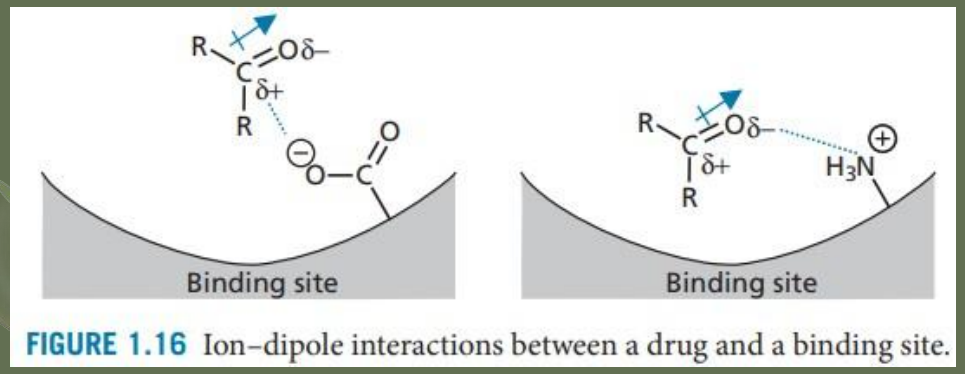


**FIGURE 1.16** Ion–dipole interactions between a drug and a binding site.

- Momen dipol adalah jumlah vector dari momen ikatan dan momen pasangan electron bebas dalam suatu molekul. Momen dipol pada beberapa molekul bersifat permanen seperti keton, akibat adanya perbedaan elektronegativitas

# Ikatan Intermolekuler

- **Ikatan Hidrogen**

Adalah suatu ikatan antara atom H yang memiliki muatan parsial positif dengan atom lain yang bersifat elektronegatif dan memiliki sepasang electron bebas dengan octet lengkap seperti, O, N, F


**FIGURE 1.6** Hydrogen bonding shown by a dashed line between a drug and a binding site (X, Y = oxygen or nitrogen; HBD = hydrogen bond donor, HBA = hydrogen bond acceptor).

# Ikatan Hidrogen

- Ikatan H terbentuk antara H yang miskin electron yang terikat secara kovalen pada atom yang elektronegatif. HBD → Hidrogen bond donor. HBA → Hidrogen bond acceptor
- Beberapa gugus fungsi dapat berperan sebagai HBD atau HBA = --OH, --NH, gugus tersebut disebut hydrogen flip-flop
- Ikatan hydrogen dapat dipandang sebagai interaksi elektrostatik lemah antara heteroatom yang sedikit negative dan atom H yang sedikit positif
- Kekuatan ikatan H sangat bervariasi antara 16-60 kj/mol
- Jarak ikatan H antara 1,5 – 2,2 Å
- Kekuatan ikatan H tergantung kekuatan HBD dan HBA

# Ikatan Intermolekuler

- **Interaksi Van der Waals**

Atom-atom pada molekul nonpolar secara temporal mempunyai distribusi kerapatan elektron nonsimetris yang merupakan akibat dari pembentukan dipol sementara. Ketika atom dari molekul lain (seperti molekul obat atau reseptor) saling mendekat, dipol sementara dari suatu molekul menginduksi dipol yang berlawanan dari molekul yang mendekat

“

Interaksi van der Walls adalah interaksi yang sangat lemah ”

# Interaksi Van der Waals

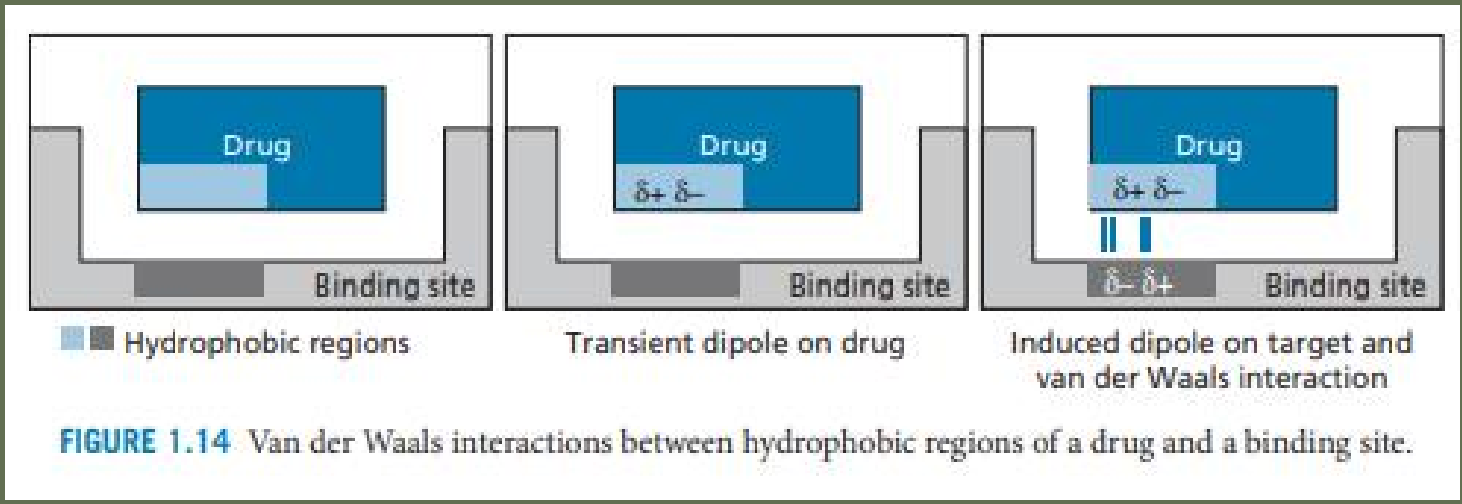


FIGURE 1.14 Van der Waals interactions between hydrophobic regions of a drug and a binding site.

- Interaksi ini melibatkan daerah-daerah hidrofobik antar 2 molekul.
- Interaksi ini deisebut juga gaya London
- Meski kekuatan interaksinya sangat lemah, namun kontribusi total dari seluruh interaksi cukup penting dalam interaksi obat-target

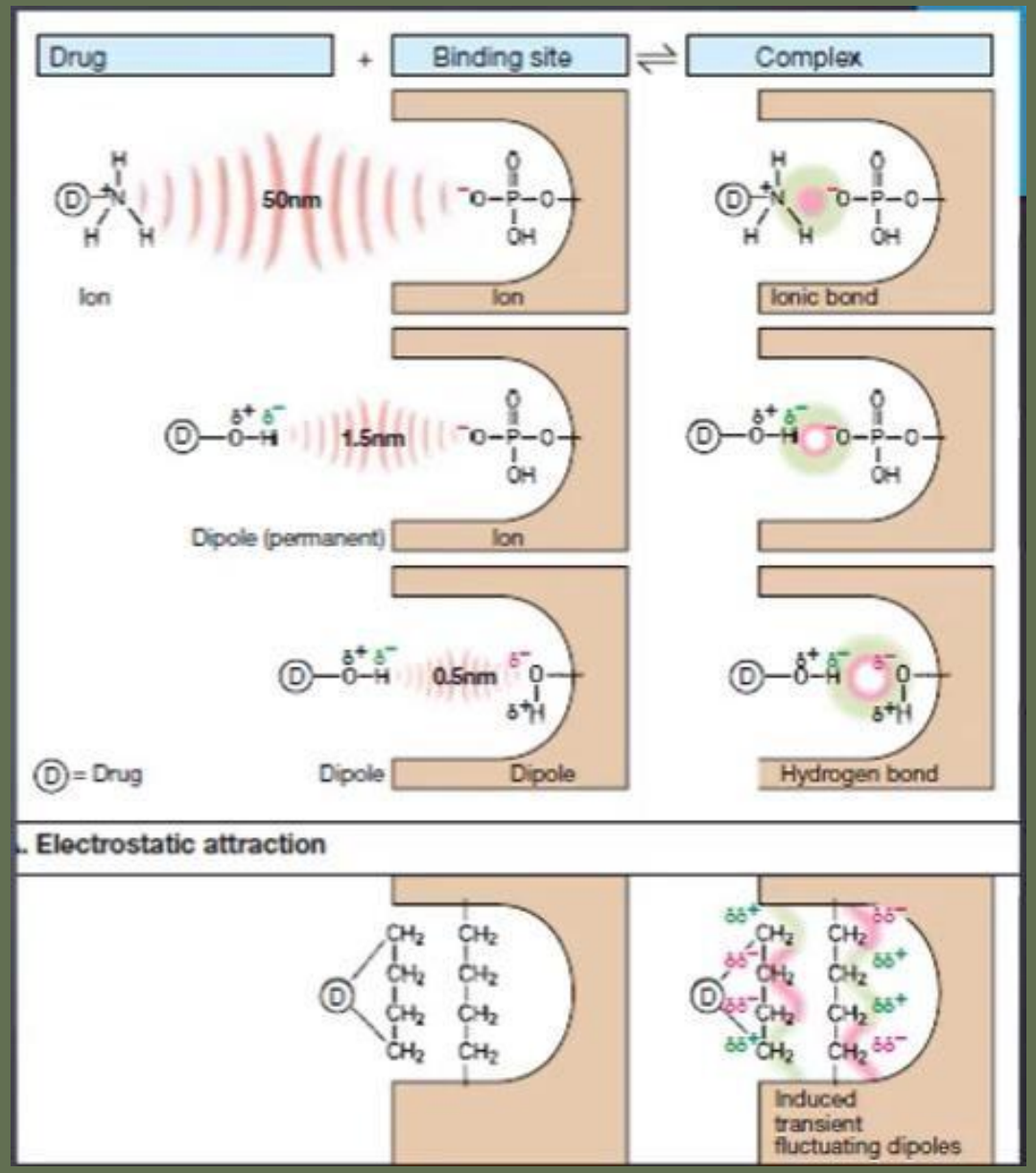


- Pada umumnya ikatan obat-reseptor bersifat reversibel sehingga obat akan segera meninggalkan reseptor jika kadar obat dalam cairan luar sel menurun
- Pada interaksi obat reseptor, senyawa dapat menggabungkan beberapa ikatan yang lemah → secara total menghasilkan ikatan yang kuat dan stabil (untuk obat antikanker dan AB)

- Senyawa dengan derajad spesifitas tinggi dapat memadukan beberapa ikatan lemah, seperti ikatan ikayan hydrogen, ion, ion dipol, dipol dipol dan ikatan vanderwals, pada interaksinya dengan reseptor sehingga secara total akan menghasilkan ikatan yang kuat dan stabil

Contoh :

1. Ikatan asetilkolin dengan enzim asetilkolin esterase
2. Ikatan prokain dengan reseptor

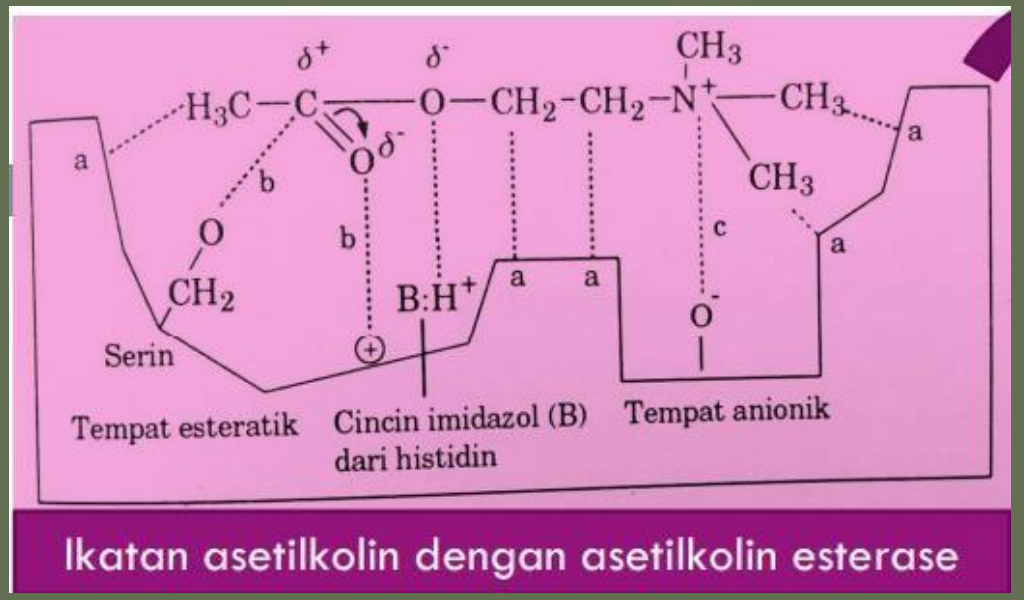

Ikatan asetilkolin dengan asetilkolin esterase

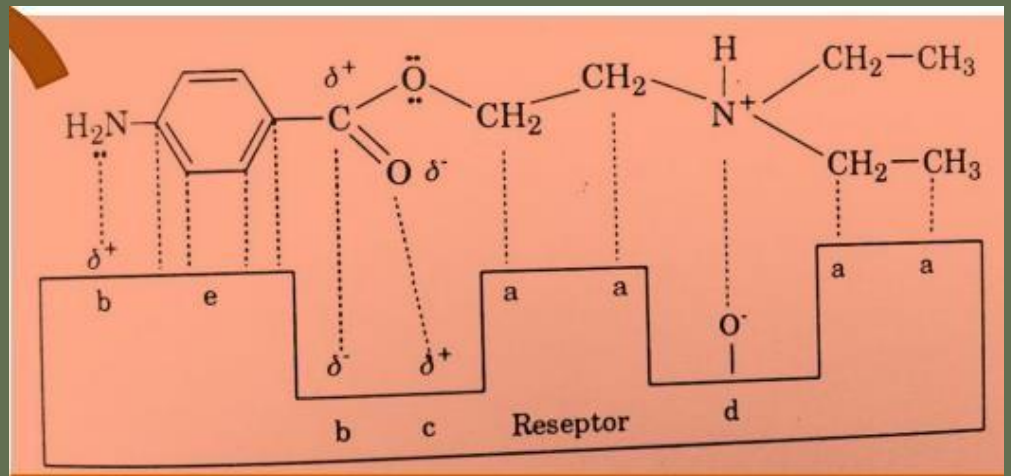

Ikatan prokain dengan reseptor

# Latihan

Perhatikan struktur adrenalin, estron dan kolesterol berikut ini!

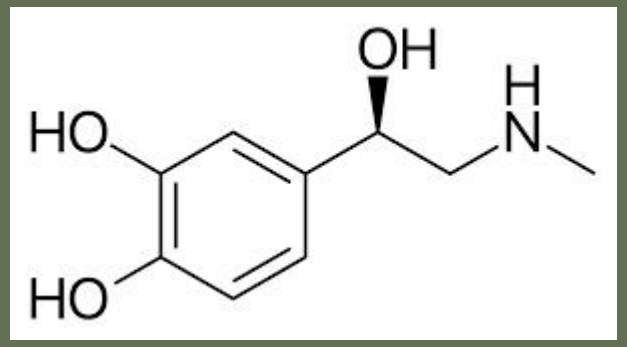


**Adrenalin**

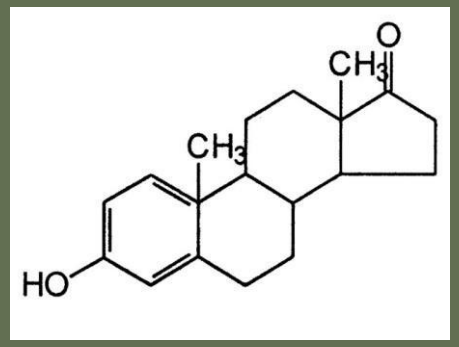


**estron**

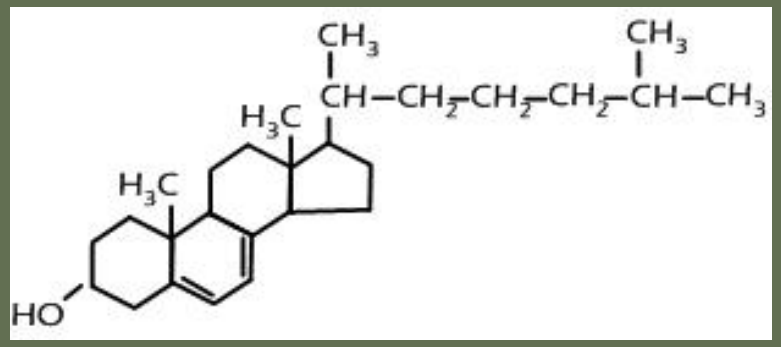


**kolesterol**

- Jenis ikatan antarmolekuler apa yang mungkin terjadi pada molekul tersebut dan dimana letaknya?

# Adrenalin

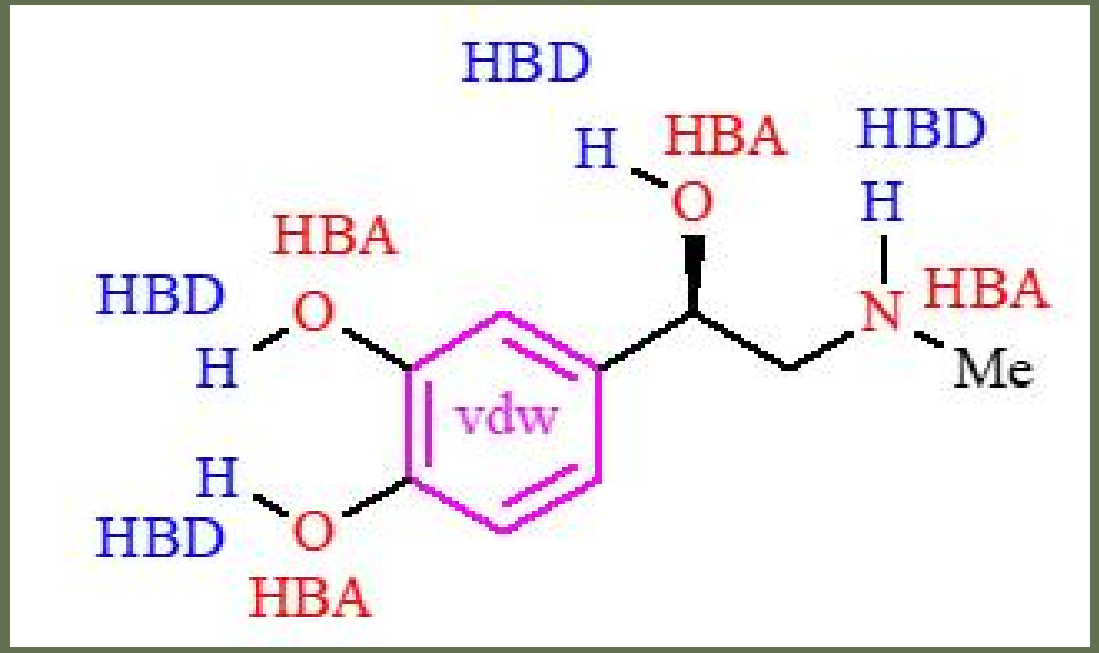


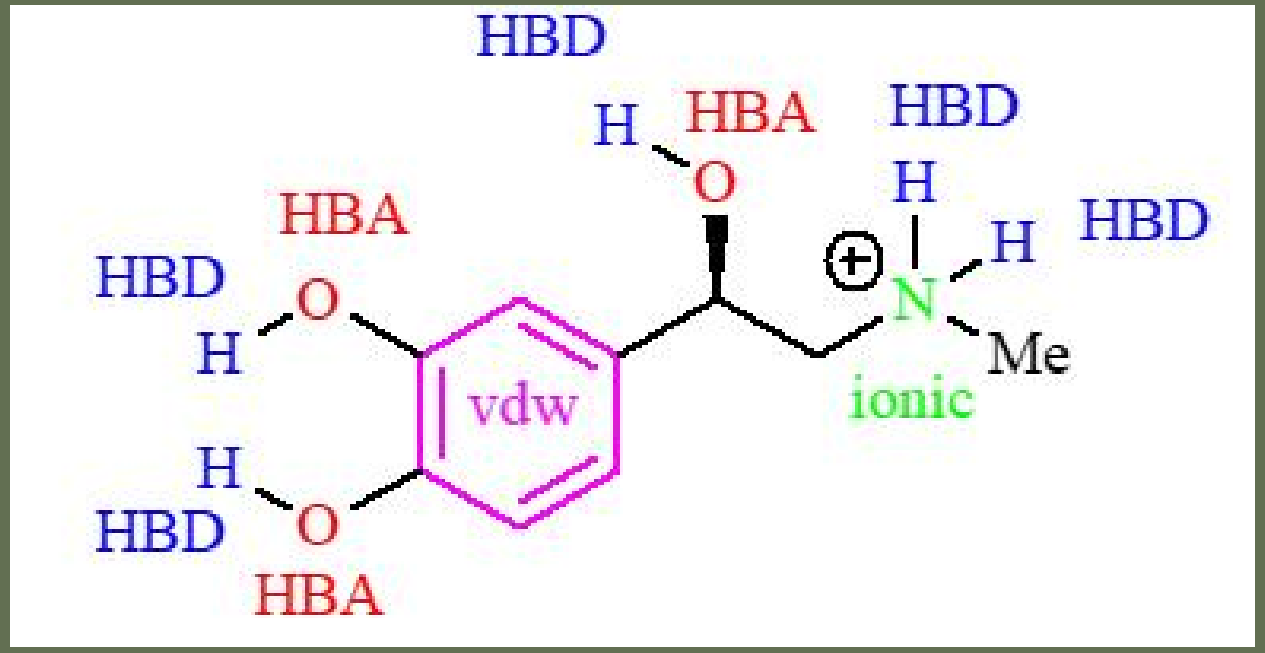


Adrenalin juga bisa ada dalam bentuk terionisasi, menghasilkan interaksi potensial yang ditunjukkan
Sisa kerangka karbon pada setiap molekul berpotensi untuk berinteraksi dengan molekul hidrofobik lainnya melalui interaksi van der Waals.

# HUBUNGAN STRUKTUR DAN INTERAKSI OBAT - RESEPTOR

# Reseptor

1. Suatu makromolekul jaringan sel hidup, mengandung gugus fungsional atau atom-atom terorganisasi, reaktif secara kimia dan bersifat spesifik, dapat berinteraksi secara reversible dengan molekul obat yang mengandung gugus fungsional spesifik, menghasilkan respon biologis yang spesifik pula.
2. Titik tangkap obat yang tersusun atas kumpulan asam amino.
3. Protein spesifik yang terdapat dalam tubuh yang akan berinteraksi dengan obat atau metabolit obat.
4. Tempat molekul obat berinteraksi membentuk suatu kompeks yang reversibel sehingga pada akhirnya menimbulkan respon.

Reseptor

- Reseptor
  - Ligan gate
  - G-Protein couple
  - Enzim linked protein
  - Steroid binding protein
- Enzim

Ligan gate, G-Protein couple, Enzim linked protein → Berada di permukaan

Steroid binding protein → Berada di inti sel

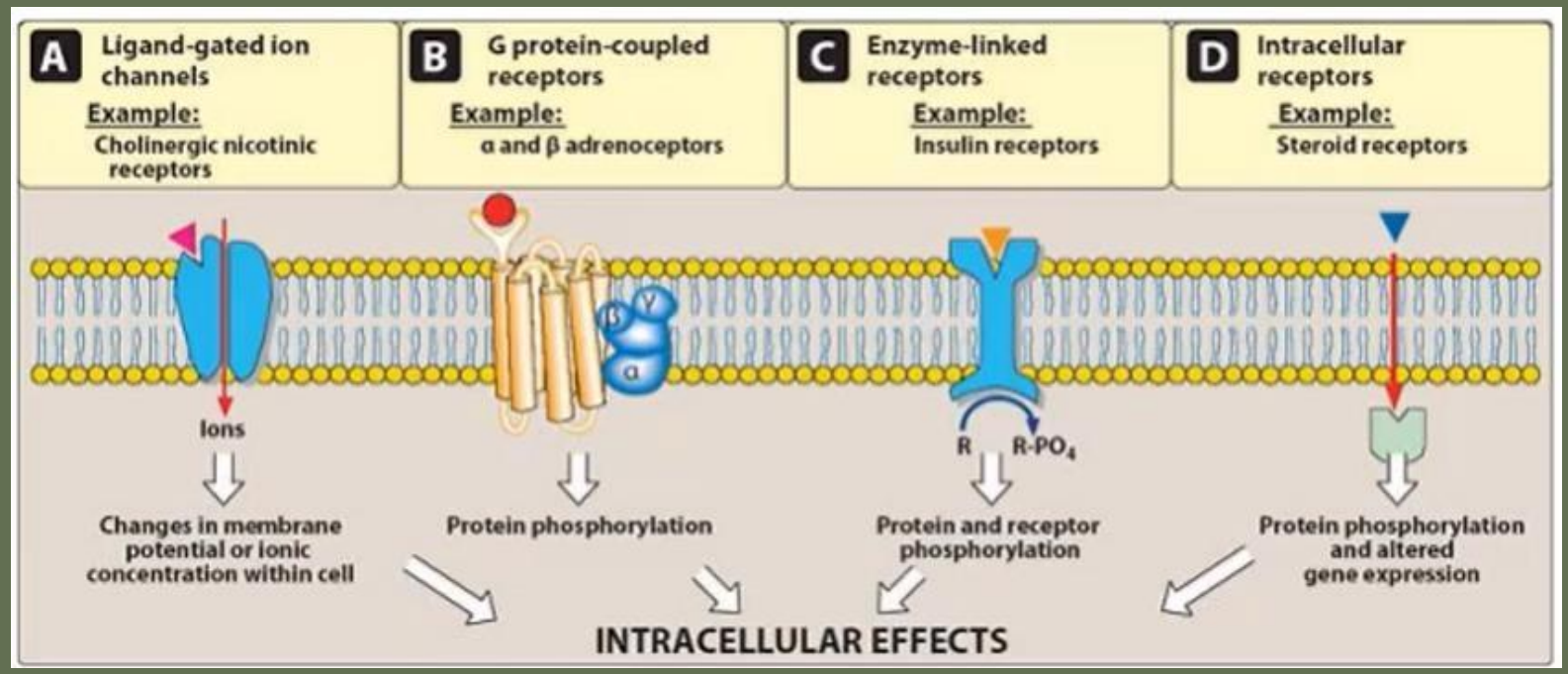

# Dimana obat akan berikatan dengan reseptor?

Hampir kebanyakan obat berikatan dengan active site dari reseptor

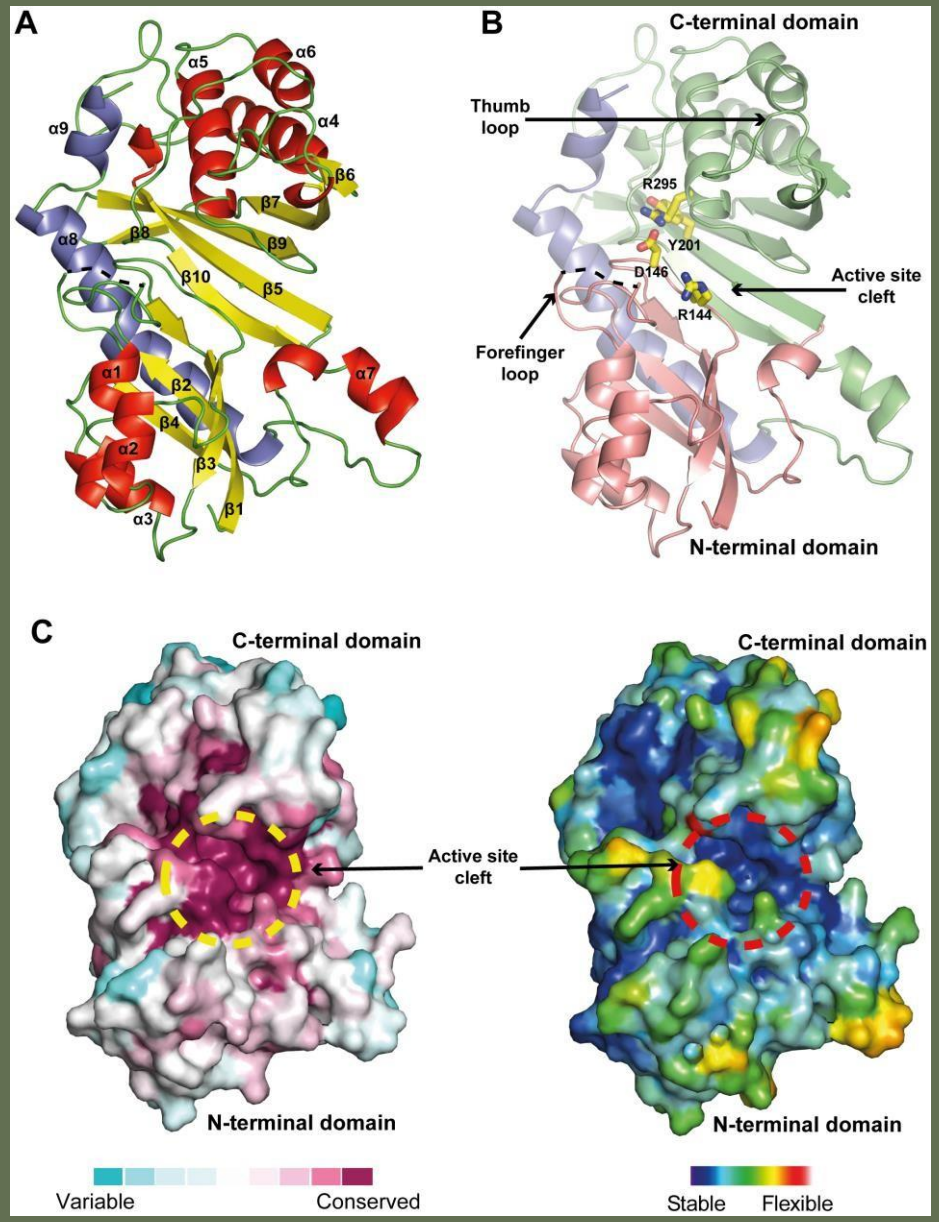

# Apa yang dimaksud dengan sisi alosterik?

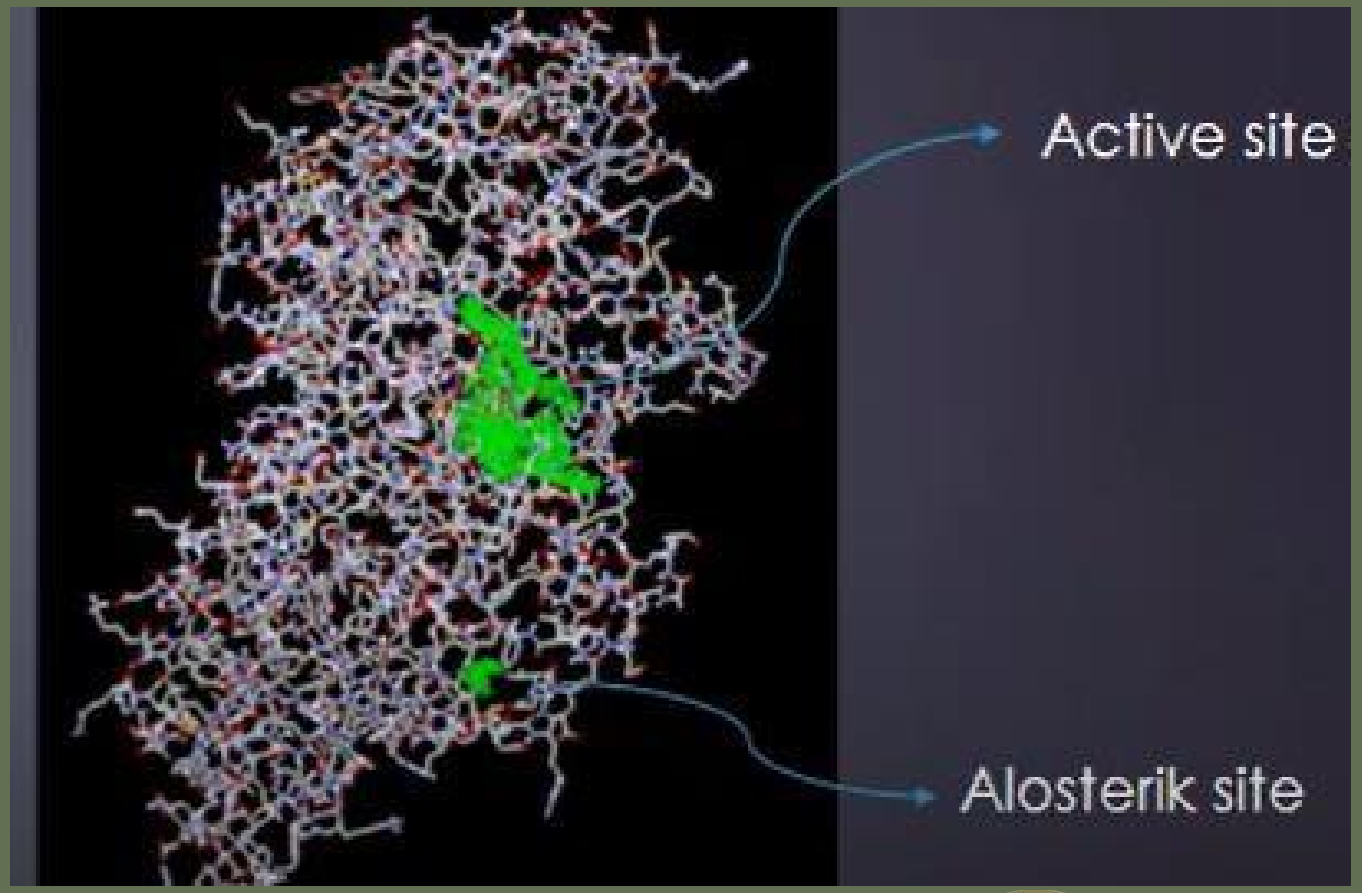


- Bukan merupakan suatu active sute. Alosterik ditempati oleh co factor/co enzim sehingga dapat mengubah sisi aktif menjadi lebih aktif (bersifat activator) atau kurang aktif (inhibitor)
- Co faktor adalah senyawa logam yang menempati sisi alosterik
- Co enzim adalah senyawa organic yang menempati sisi alosterik

# Apa efek yang ditimbulkan saat obat berikatan dengan reseptor?

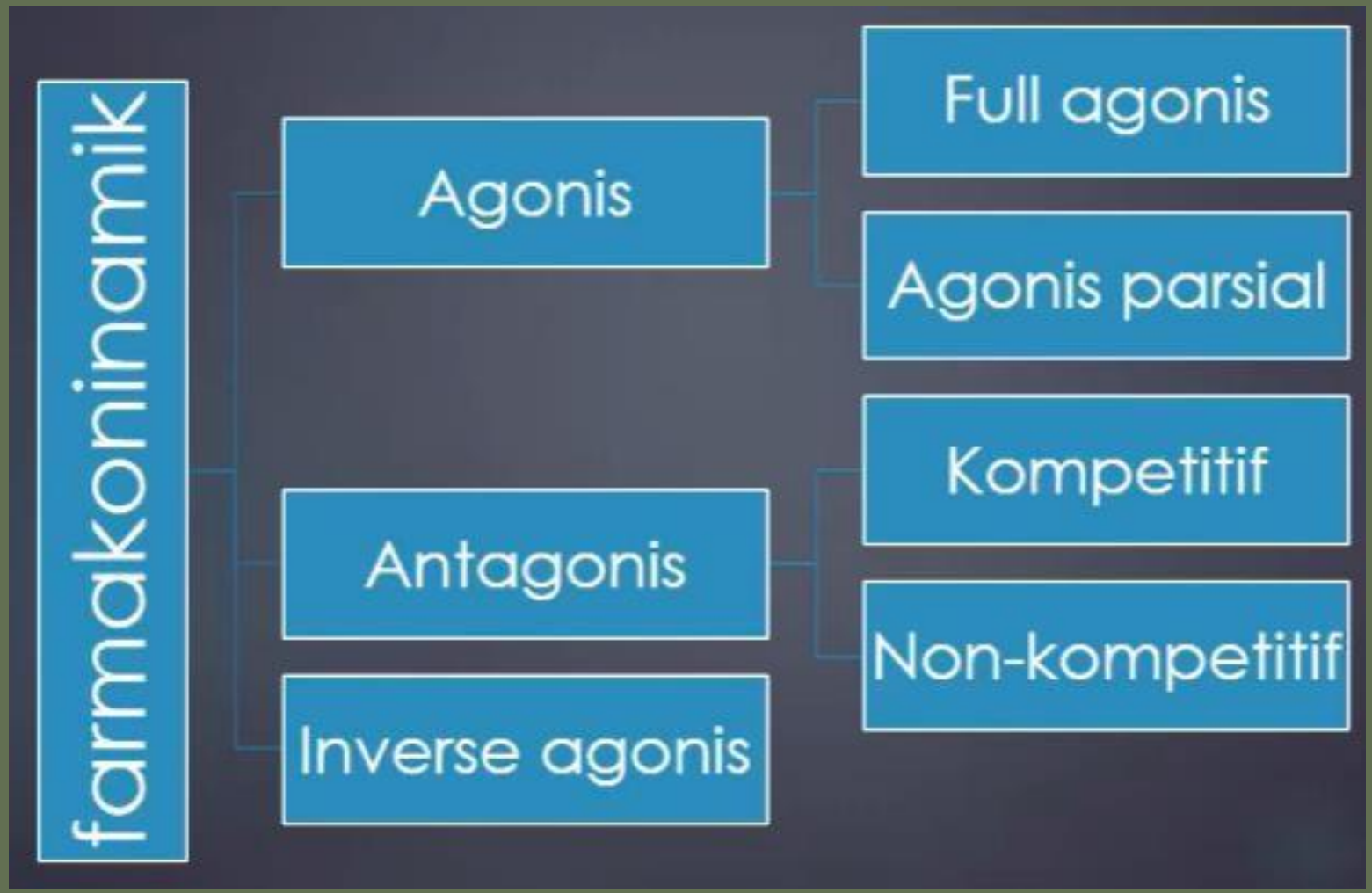


Obat (O) akan berinteraksi dengan reseptor (R) membentuk kompleks obat-reseptor (OR). Proses interaksi ini dijelaskan sebagai berikut:

$$(O) + (R) \underset{K2}{\overset{K1}{\rightleftharpoons}} (OR) \longrightarrow E$$

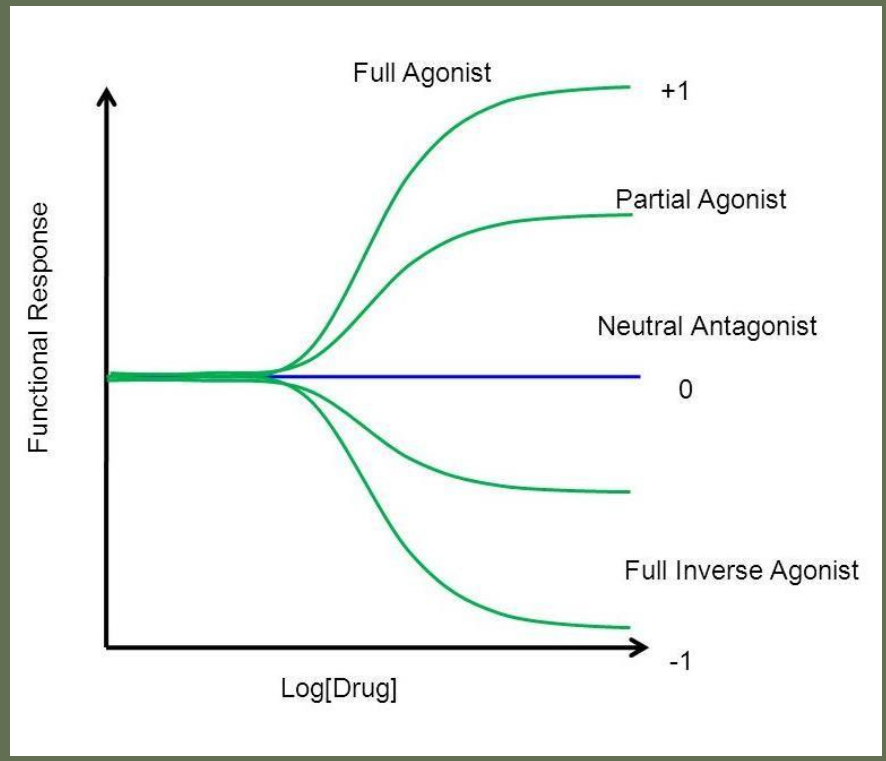


Respon biologis yang terjadi setelah pengikatan OR:

1. Rangsangan aktivitas (efek agonis)
   a) Full Agonis → menghasilkan respon maksimal
   b) Agonis parsial → menghasilkan respon yang kurang dari 100%
2. Pengurangan aktivitas (efek antagonis)
   a) Kompetitif →Ketika konsentrasi antagonis meningkat dan menghambat respon agonis secara progresif
   a) Non kompetitif → agonis berikatan secara ireversibel dengan reseptor
3. Inverse agonis → berikatan pada lokasi yang sama dengan agonis (dan biasanya berkompetisi), tetapi menghasilkan efek yang berlawanan dengan agonis

# Agonis

- Obat berikatan dengan reseptor, memiliki aktivitas intrinsik positif

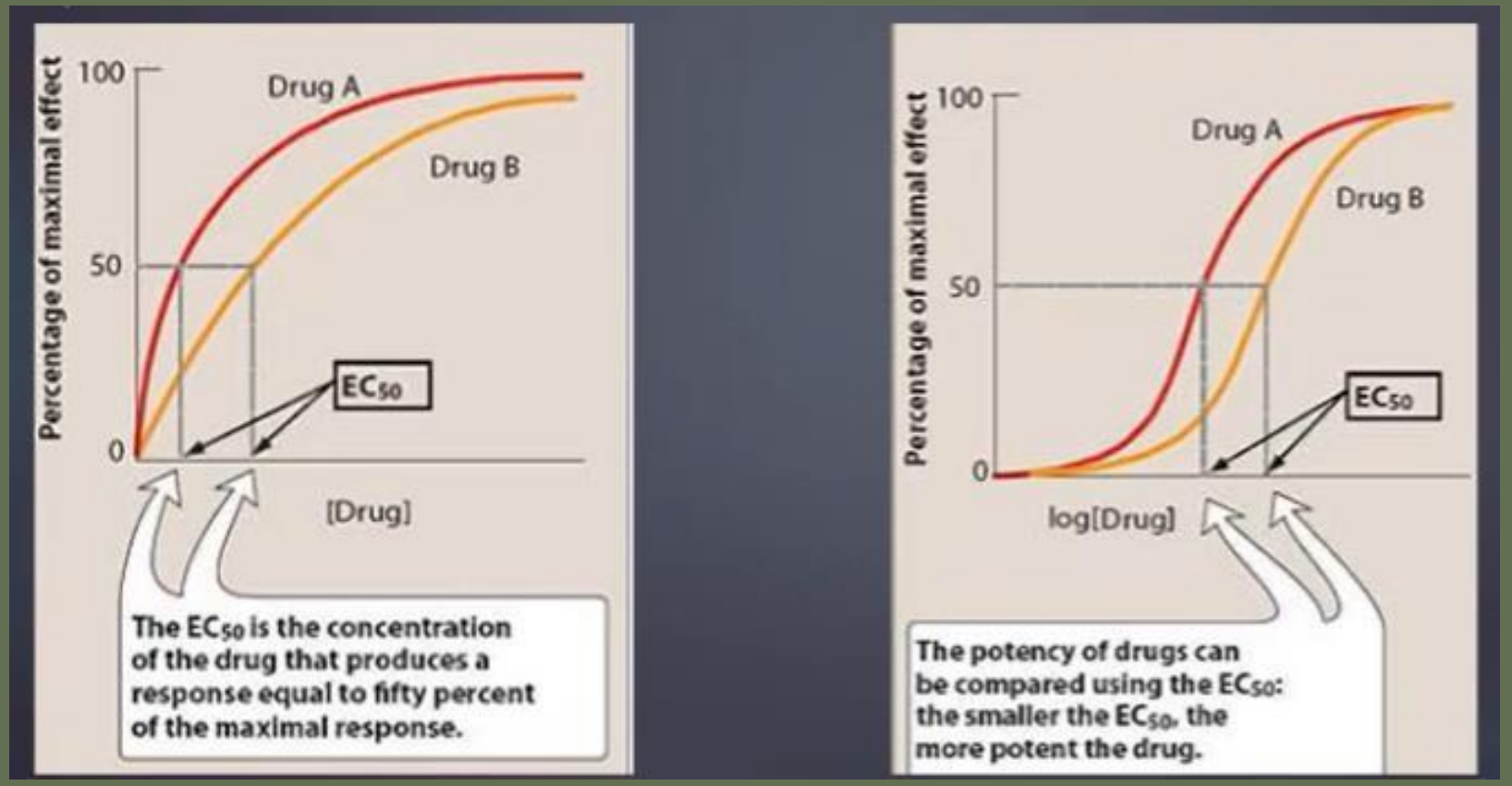

# Parsial agonis

Obat berikatan dengan reseptor, memiliki aktivitas intrinsic positif namun tidak penuh 100%

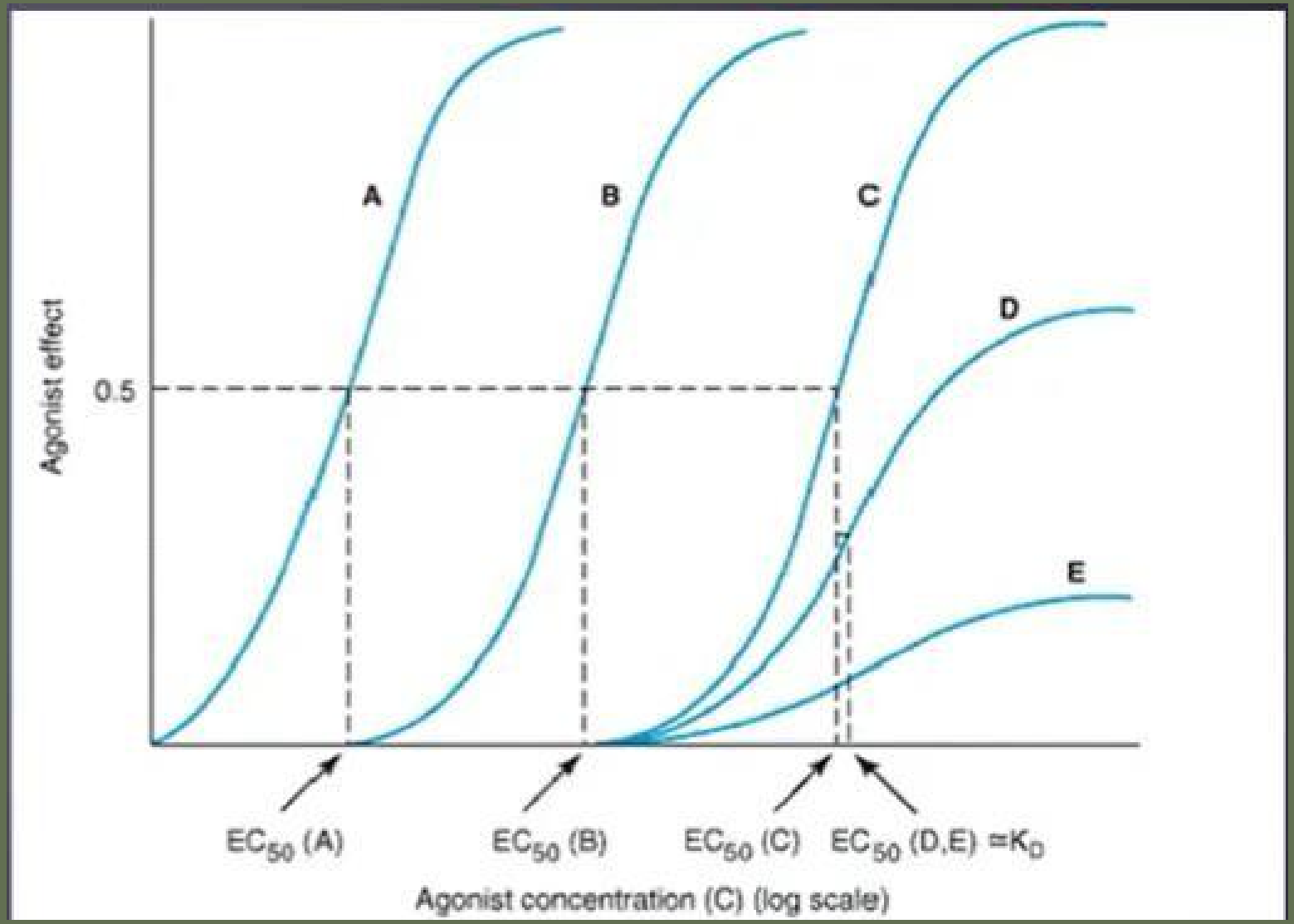

# Antagonis kompetitif

- Obat berikatan dengan reseptor memiliki aktivitas intrinsic 0 (basal condition)
- Bersaing dengan agonisnya
- Ikatan obat dan reseptor yang terbentuk adalah ikatan selain kovalen
- Menggeser kurva agonis

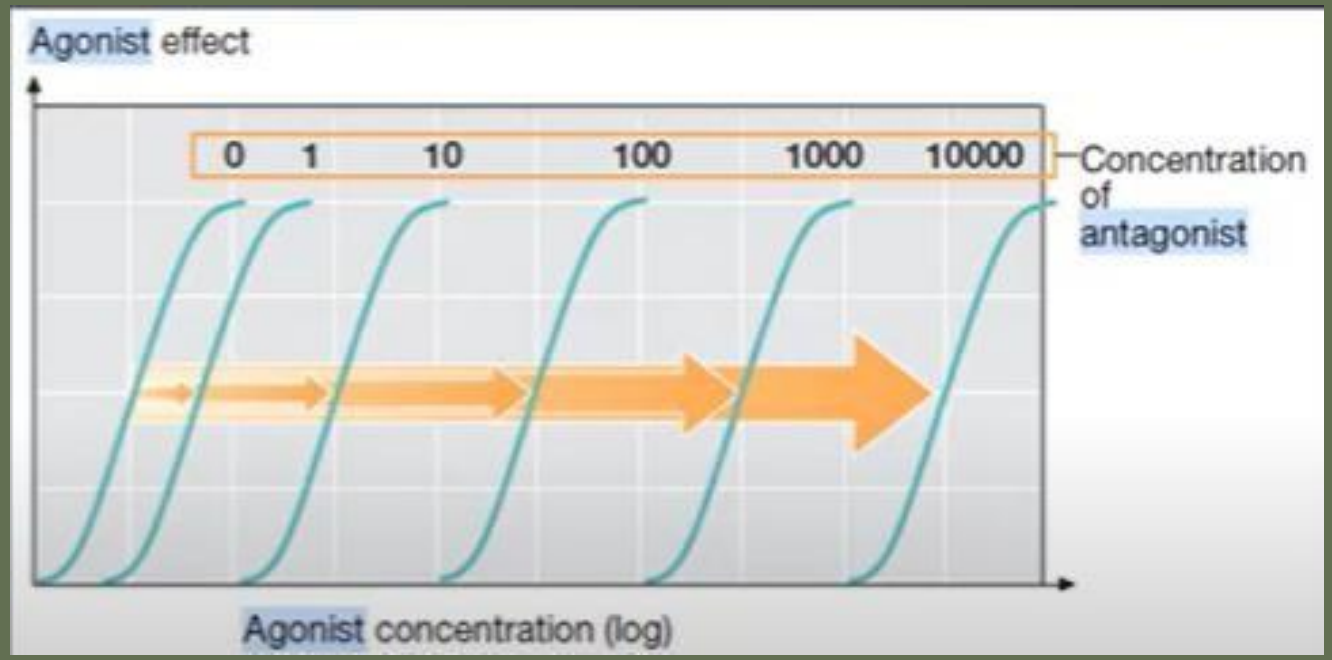

# Antagonis non kompetitif

- Obat akan berikatan dengan reseptor memiliki aktivitas intrinsic 0 (basal condition)
- Ikatan obat dannreseptor yang terbentuk adalah ikatan kovalen
- Tidak menggeser kurva agonis, namun menurunkan efektivitas obat

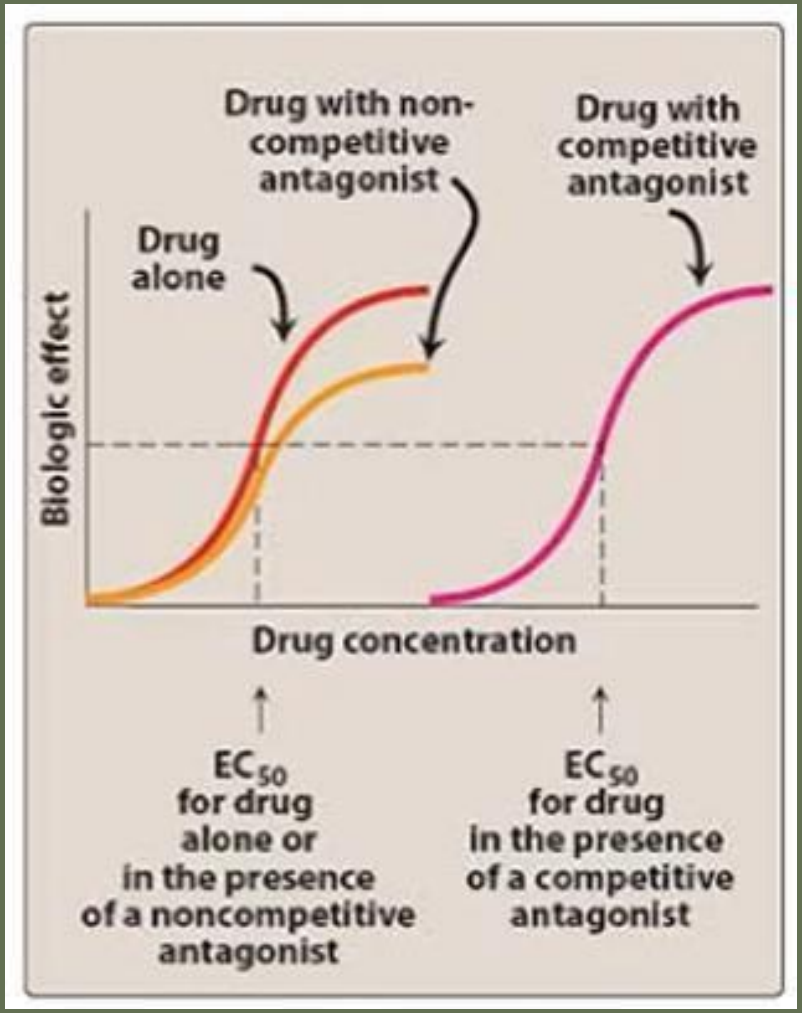

# Inverse agonis

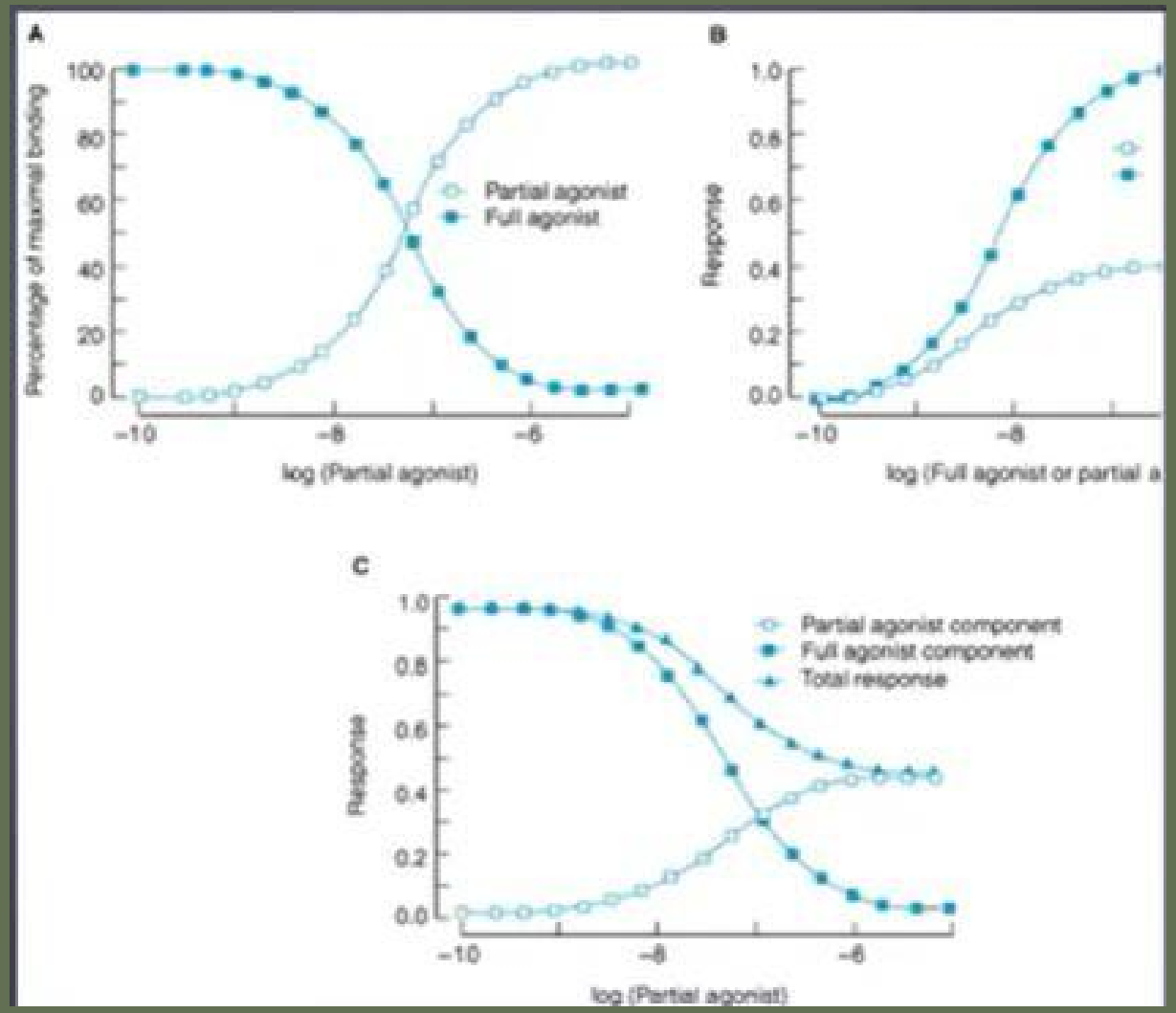


- Obat berikatan dengan reseptornya memiliki aktivitas intrinsic negative (berlawanan dengan agonisnya)

# Thank You

# Hubungan stereokimia dengan aktivitas obat

**apt. Dian Purwita Sari, M.Biotech.**

# Stereokimia :

**Studi mengenai molekul-molekul dalam ruang tiga dimensi, yakni bagaimana atom-atom dalam sebuah molekul ditata dalam ruangan satu relatif terhadap yang lain**

**Aspek stereokimia:**

1. **Isosterisme** → kemiripan sifat kimia atau fisika kelompok atom-atom dalam molekul, karena mempunyai persamaan ukuran, keelektronegatifan atau stereokimia
2. **Isomer** → "iso" yang berarti "sama" dan "meros" yang berarti "bagian". Maksudnya, senyawa-senyawa ini memiliki bagian yang sama, meskipun penyusunan atom-atomnya berbeda.

# Modifikasi Isosterisme

**Prinsip isosterisme banyak digunakan untuk memodifikasi senyawa biologis aktif**

**Contoh :**

**pergantian gugus –S- pada cincin fenotiazin dan cincin tioxanten, dengan gugus etilen –CH2CH2 - menghasilkan cincin dihidrobenzazepin dan dibenzosiklo-heptadin yang berkhasiat berlawanan**

antipsikotik, sedatif

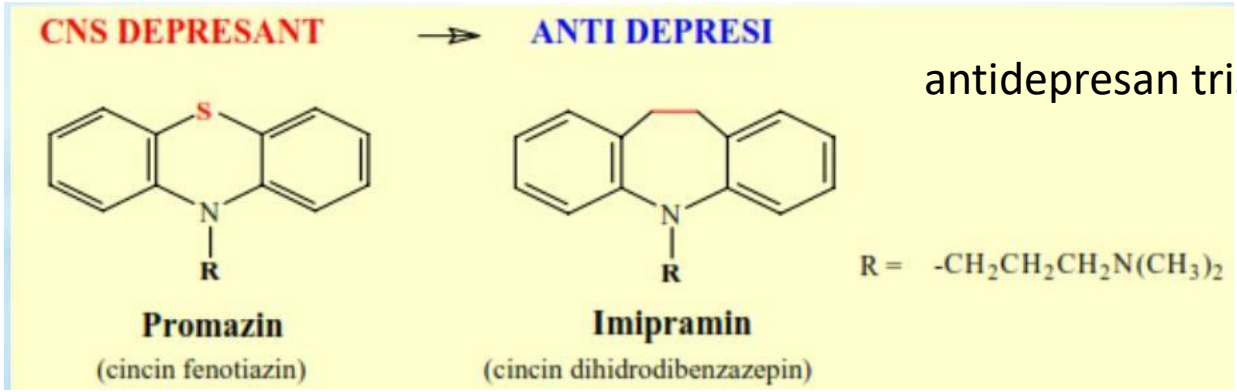


antidepresan trisiklik

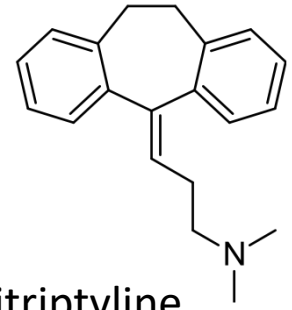


Amitriptyline

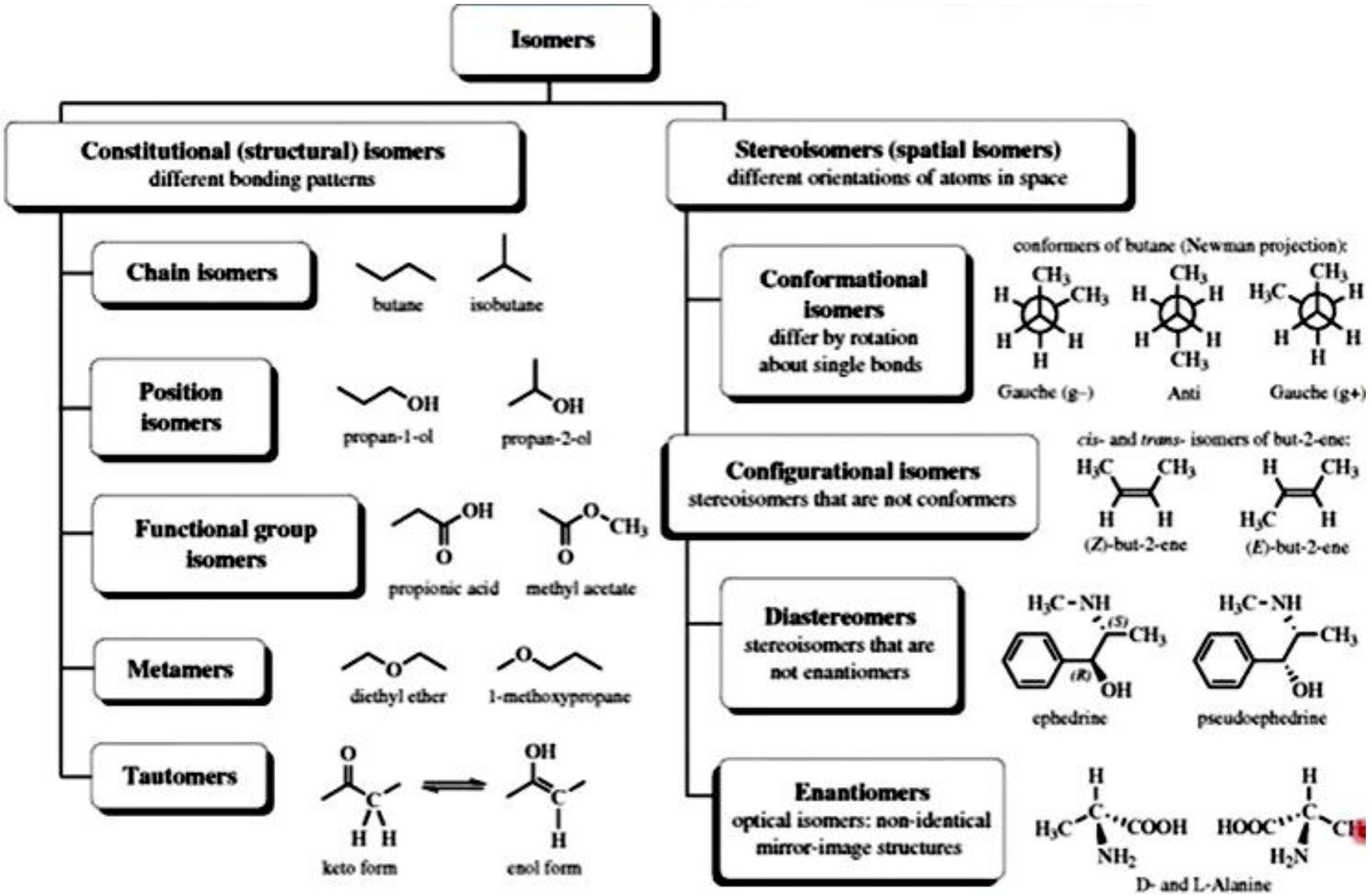
Isomers
Constitutional (structural) isomers
different bonding patterns
Stereoisomers (spatial isomers)
different orientations of atoms in space
Chain isomers
butane
isobutane
Position isomers
propan-1-ol
propan-2-ol
Functional group isomers
propionic acid
methyl acetate
Metamers
diethyl ether
1-methoxypropane
Tautomers
keto form
enol form
Conformational isomers
differ by rotation about single bonds
conformers of butane (Newman projection):
Gauche (g−)
Anti
Gauche (g+)
Configurational isomers
stereoisomers that are not conformers
cis- and trans- isomers of but-2-ene:
(Z)-but-2-ene
(E)-but-2-ene
Diastereomers
stereoisomers that are not enantiomers
ephedrine
pseudoephedrine
Enantiomers
optical isomers: non-identical mirror-image structures
D- and L-Alanine

# Isomer konformasi

Adalah isomer yang terjadi karena ada perbedaan pengaturan ruang dari atom atau gugus dalam struktur molekul obat.

Contoh: sikloheksan dapat membentuk tiga konfomer, yaitu kursi, perahu dan melipat

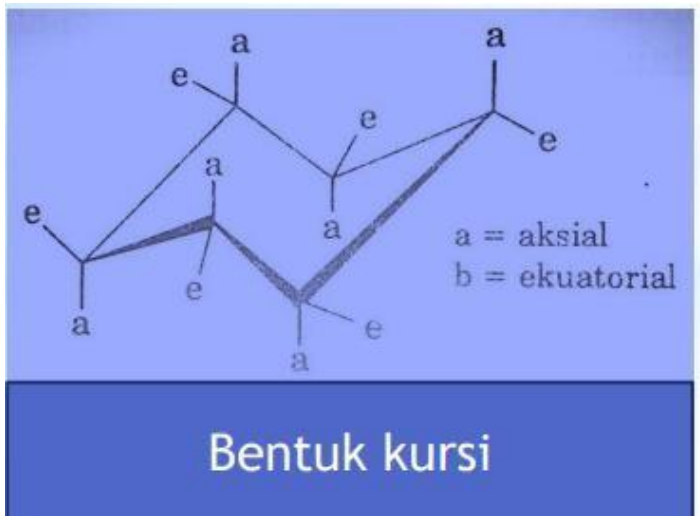



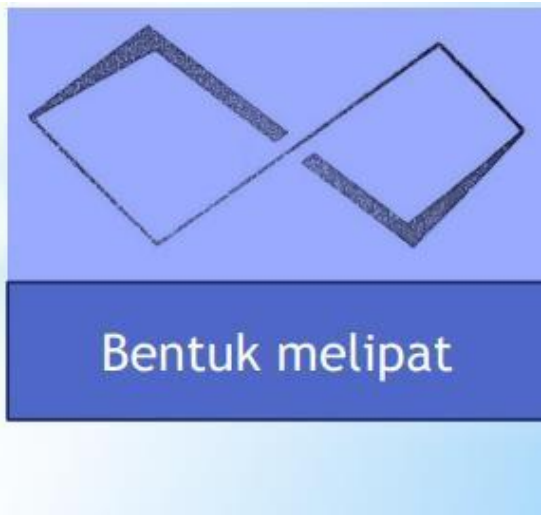

# Isomer geometrik

Atau isomer cis-trans adalah isomer yang disebabkan karena adanya atom-atom atau gugus-gugus yang terikat pada ikatan rangkap atau pada sistem alisiklik. Ikatan rangkap dan sistem alisiklik tsb membatasi gerakan atom dalam mencapai kedudukan yang stabil sehingga membentuk isomer cis-trans

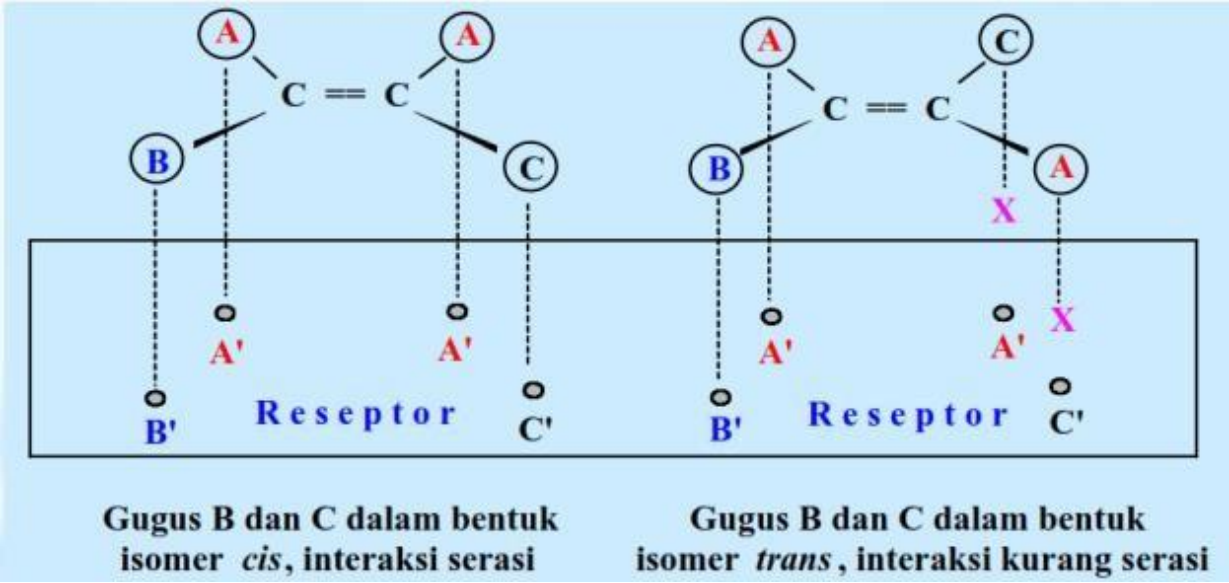

# Diastereoisomer

Adalah isomer yang disebabkan oleh senyawa yang mempunyai dua atau lebih pusat atom asimetrik, mempunyai gugus fungsional sama dan memberikan tipe reaksi yang sama pula.

* Contoh:

Efedrin, mempunyai 2 atom C asimetrik dengan 4 bentuk aktif optis

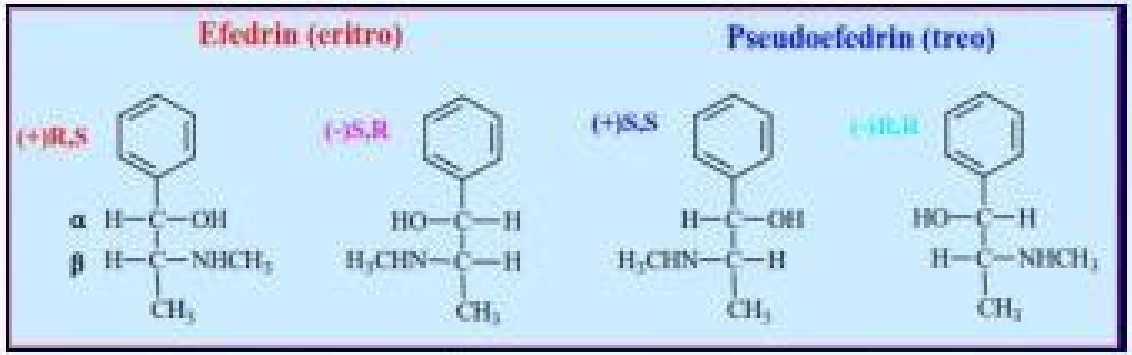


| Isomer | APR (aktivitas presor relatif) |
|---|---|
| D(-) efedrin | 36 |
| L(+) efedrin | 11 |
| D(-) pseudoefedrin | 7 |
| L(+) pseudoefedrin | 1 |
| DL(±) efedrin | 26 |
| DL(±) pseudoefedrin | 4 |

* Aktivitas optimal pada Cα posisi (S) dan CB posisi (R) → hanya bentuk D(-)efedrin yang secara nyata dapat memblok reseptor β adrenergik dan menurunkan tekanan darah

# Isomer optik

Adalah isomer yang disebabkan oleh senyawa yang mempunyai atom C asimetrik

Isomer optik memiliki sifat fisika kimia sama, hanya berbeda pada kemampuannya memutar bidan polarisasi, masing-masing hanya bisa memutar bidang polarisasi ke kiri atau ke kanan dengan sudut yang sama

Contoh:

*D-(-)-adrenalin memiliki aktivitas vasokonstriksi 12-15 kali > isomer (+)

*(-)-α-metildopa memiliki efek antihipertensi sedang isomer (+) tidak

# Kiral

Kiralitas adalah suatu **keadaan yang menyebabkan dua molekul dengan struktur yang sama tetapi berbeda susunan ruang dan konfigurasinya**. Atom yang menjadi pusat kiralitas dikenal dengan istilah atom kiral.

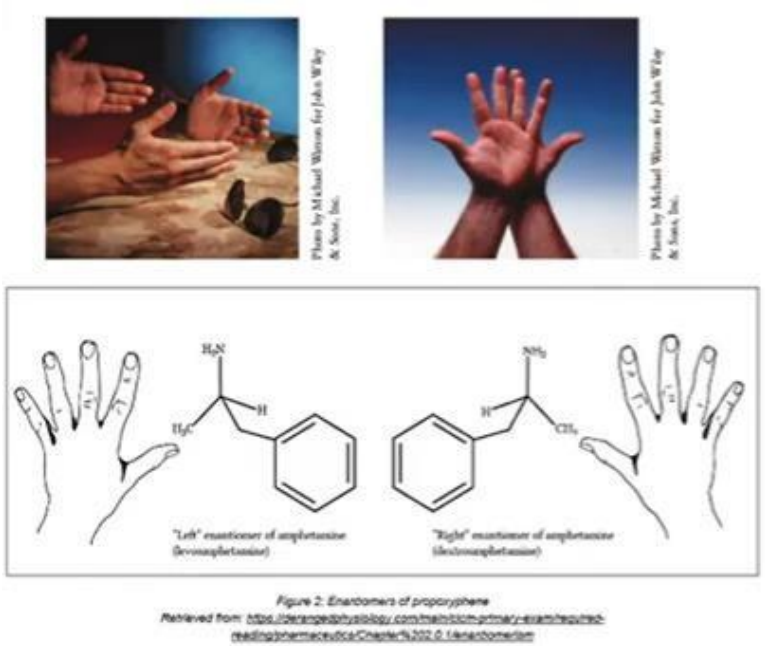

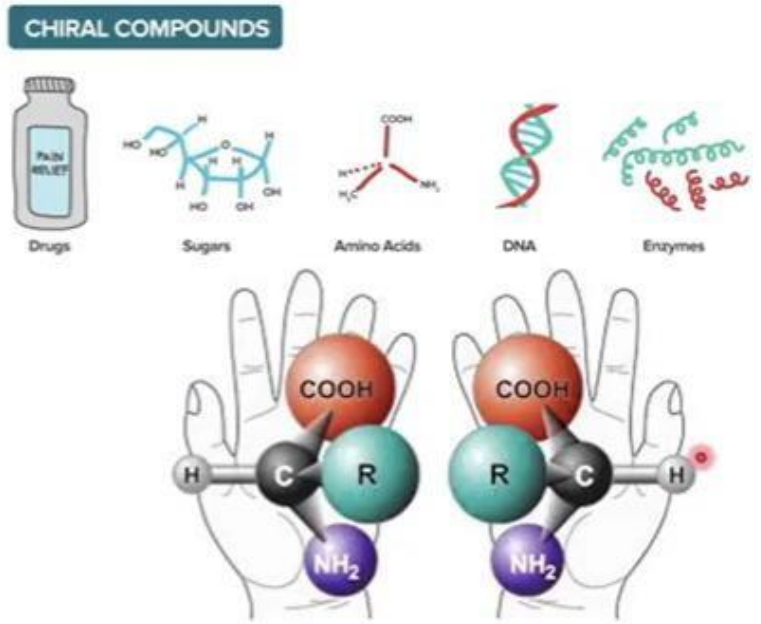

# Contoh:

half of all pharmaceuticals are chiral compounds!

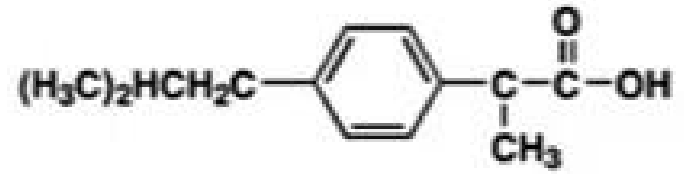


(*S*)-Ibuprofen (responsible for pain relief)

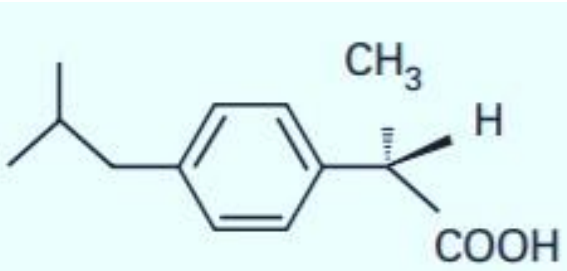


(+)-(S)-ibuprofen

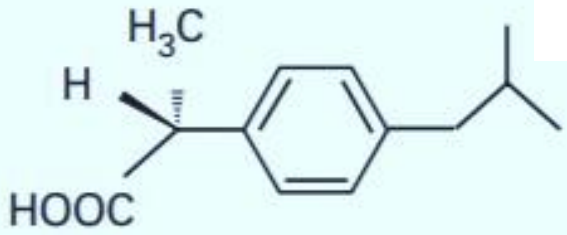


(–)-(R)-ibuprofen

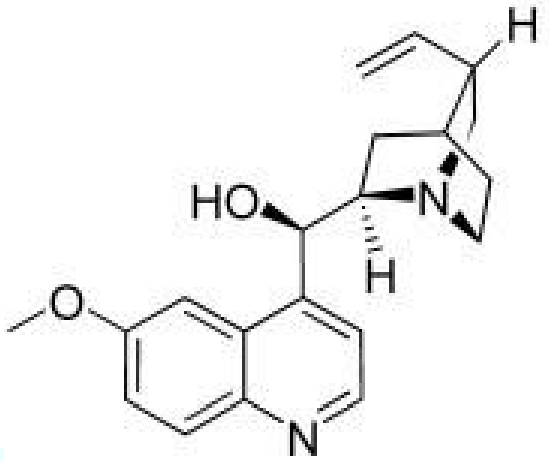


quinine **1**

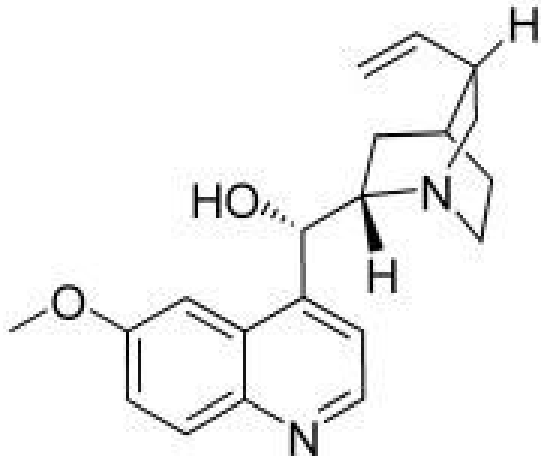


quinidine **2**

# Chirality for Improved Druggability

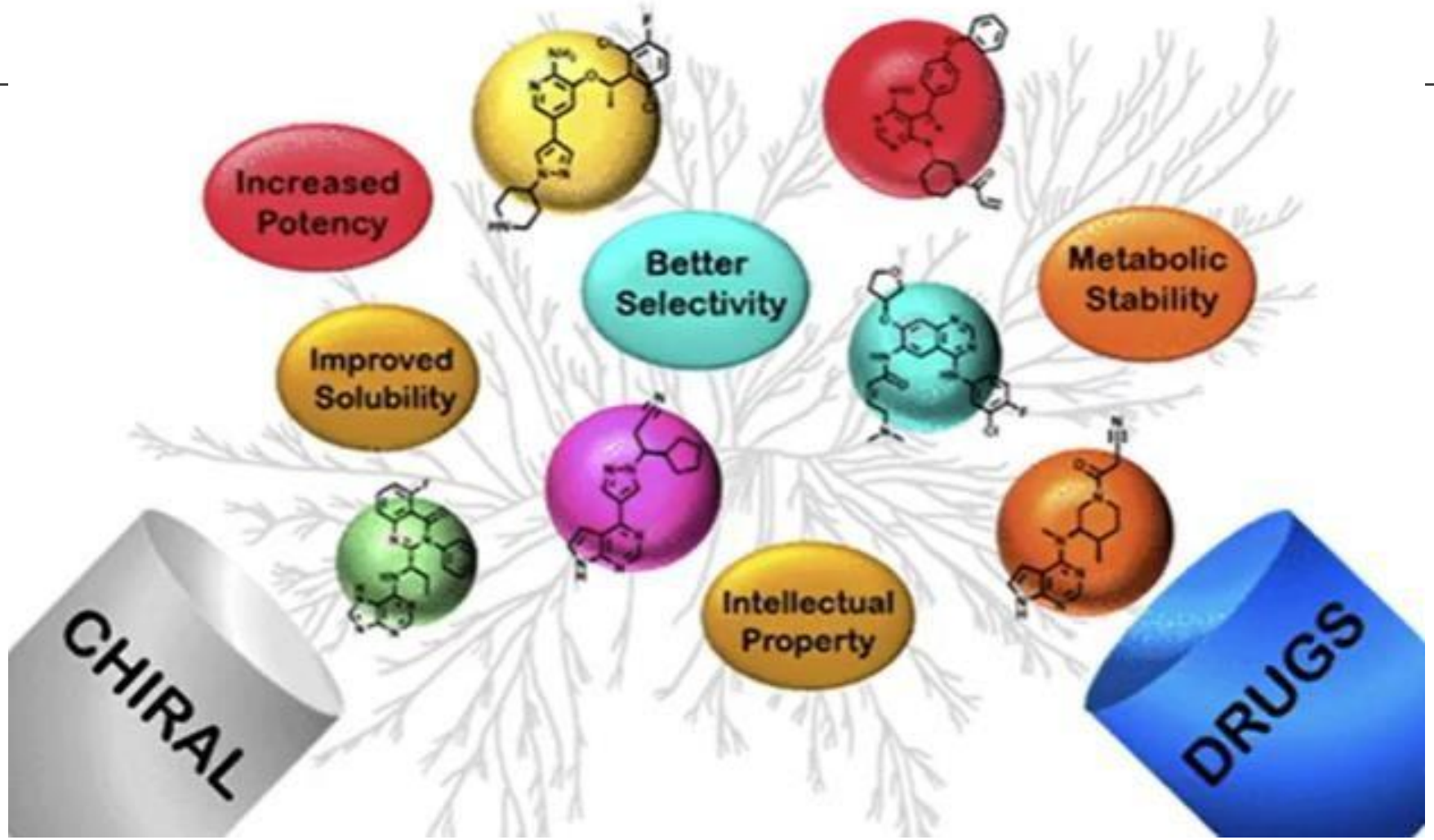

# Hubungan stereokimia dengan aktivitas obat

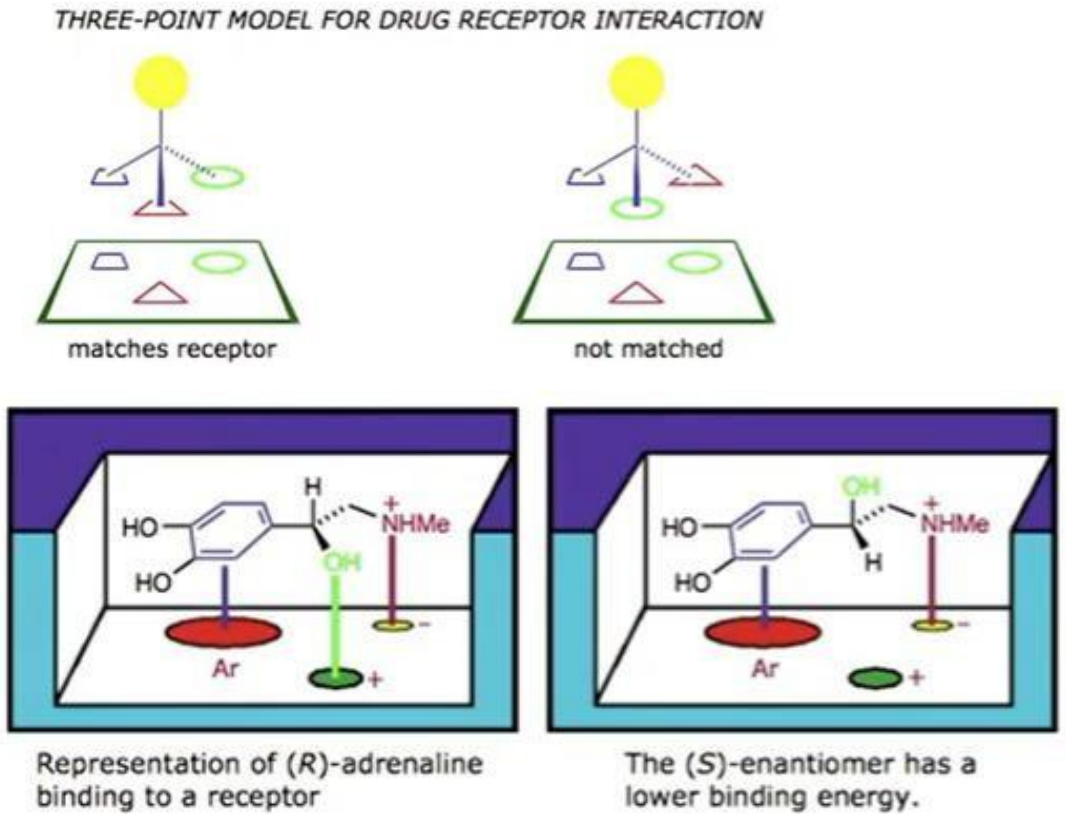


Representation of (*R*)-adrenaline binding to a receptor

The (*S*)-enantiomer has a lower binding energy.

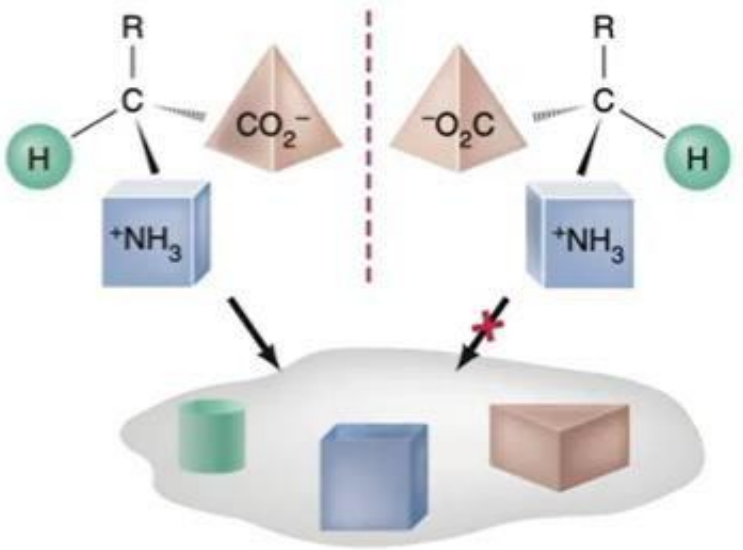


Only one of the two amino acid enantiomers shown (the left-hand one) can achieve three-point binding with the hypothetical binding site (e.g., in an enzyme).

# Contoh:

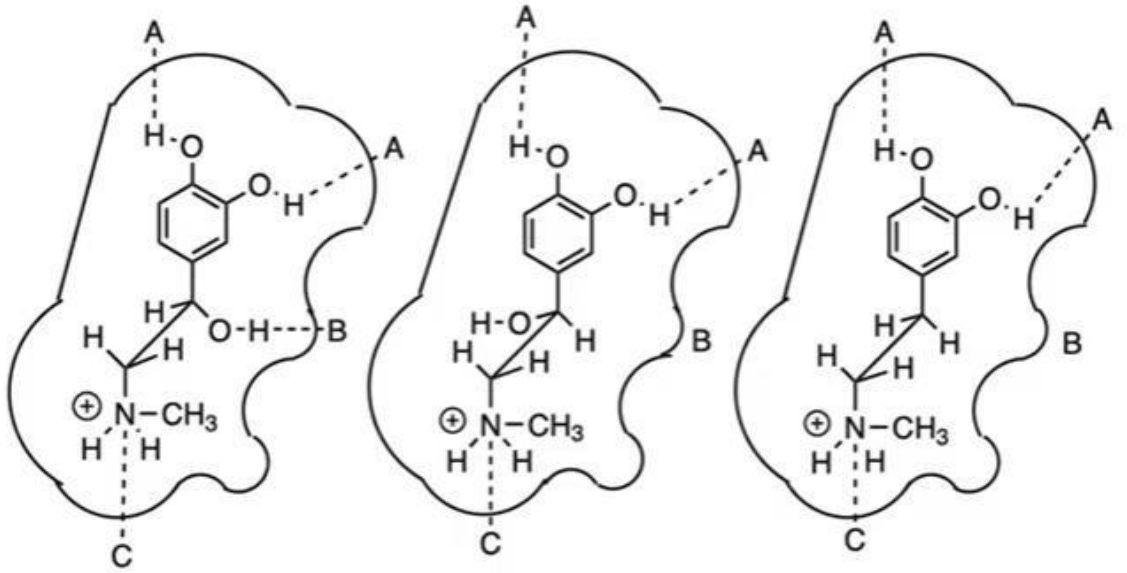


*R*-(-)-Epinephrine *S*-(+)-Epinephrine *N*-Methyldopamine

**Drug receptor interaction of R-(−)-epinephrine, S-(+)-epinephrine, and N-methyldopamine.**

# Terkadang obat dengan stereoisomer yang berbeda menghasilkan efek terapi yang berbeda. Contohnya :

dextropropoxyphene is a narcotic (opioid) analgesic drug class prescribed to treat mild to moderate pain.

Levopropoxyphene was used as an antitussive. An antitussive is a medication often recommended for the treatment of cough and associated respiratory tract

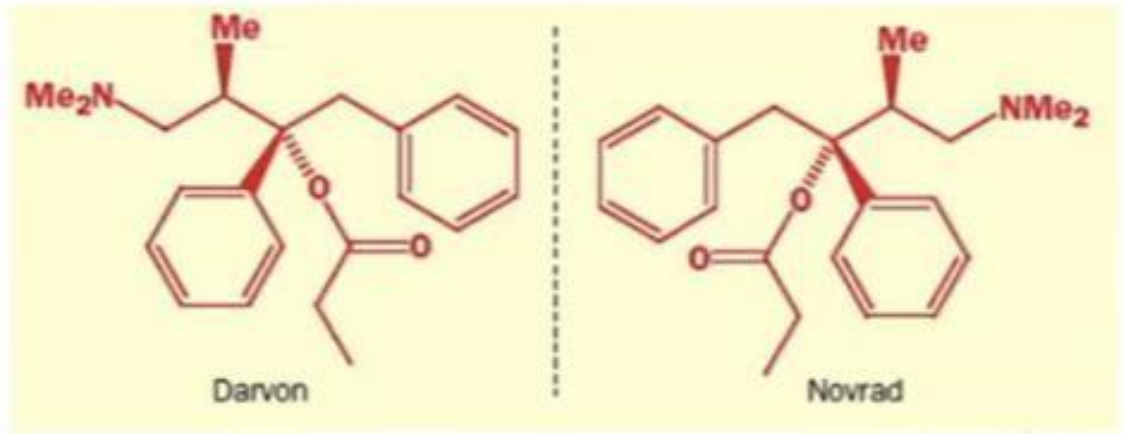

Prodi Farmasi

STIKES Notokusumo

# Hubungan struktur kimia obat dengan proses adsorpsi dan distribusi

apt. Dian Purwita Sari, M.Biotech.

Toxicol Sci. 2011 Oct; 123(2): 305–332. Published online 2011 Jul 12.
doi: 10.1093/toxsci/kfr184

PMCID: PMC3179678 | PMID: 21750349

# Arsenic Exposure and Toxicology: A Historical Perspective

Michael F. Hughes,[*,1] Barbara D. Beck,[†] Yu Chen,[‡] Ari S. Lewis,[†] and David J. Thomas[*]

Although arsenic has been used throughout history, m
detailed documentation of its use began in the late 18
century. Fowler's solution, which was discovered in 1
1% solution of potassium arsenite that was used in th
treatment of various diseases, including malaria, syphilis,
asthma, chorea, eczema, and psoriasis (Rohe, 1896; Scheindlin,
2005). In 1910, Paul Ehrlich introduced a new arsenic-based
drug called Salvarsan, which became known as the "magic
bullet" for treating syphilis and was used until the use of
penicillin became more prevalent in the 1940s (Riethmiller,
2005; Yarnell, 2005).

Arsenic also has a rich history as a cancer chemotherapeutic. As reported by Antman (2001), pharmacology texts from the 1880s described the use of arsenical pastes for the treatment of skin and breast cancer. In 1878, it was found that Fowler's solution could be effective in lowering the white blood cell count in leukemia patients (Antman, 2001, 210-9361). Although the use of Fowler's solution eventually declined over time due to its overt toxicity, a more detailed understanding of arsenic mechanism of action has allowed arsenic trioxide to emerge as an effective chemotherapeutic drug for treating acute promyelocytic leukemia (Rust and Soignet, 2001; Zhang *et al.*, 2001). With the success of this drug, the treatment of other cancers with arsenic trioxide is also being investigated (Murgo, 2001; Sekeres, 2007).

https://www.ncbi.nlm.nih.gov/pmc/articles/PMC3179678/

# pendahuluan

Obat masuk kedalam tubuh, Obat akan mengalami absorpsi

Kemungkinan obat mengalami

perubahan **fisika** → bentuk sediaan atau formulasi obat

modifikasi **kimia** → struktur molekul obat.

→ **mempengaruhi respon biologis**

Setelah diabsorbsi, obat masuk ke cairan tubuh dan didistribusikan ke organ dan jaringan.

Sebelum mencapai reseptor, obat melalui bermacam-macam sawar membrane, pengikatan protein plasma, penyimpanan dan metabolisme.

# Strategy for Cancer targeted DDS

- Hydrophilic in blood vessel → $t_{1/2}$ ↑↑
- Karakter yang disukai sel di jaringan

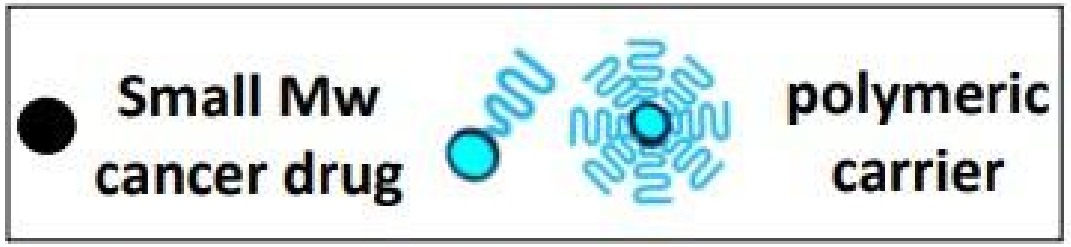


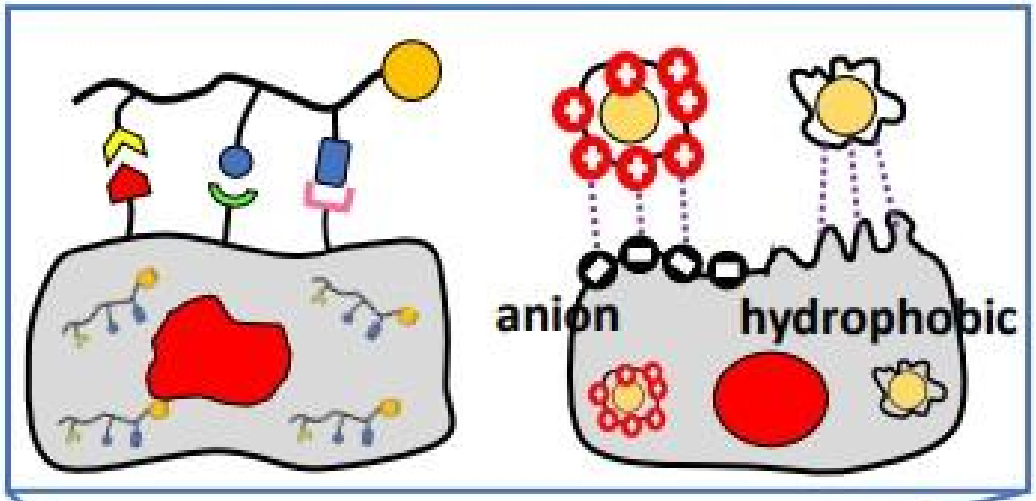


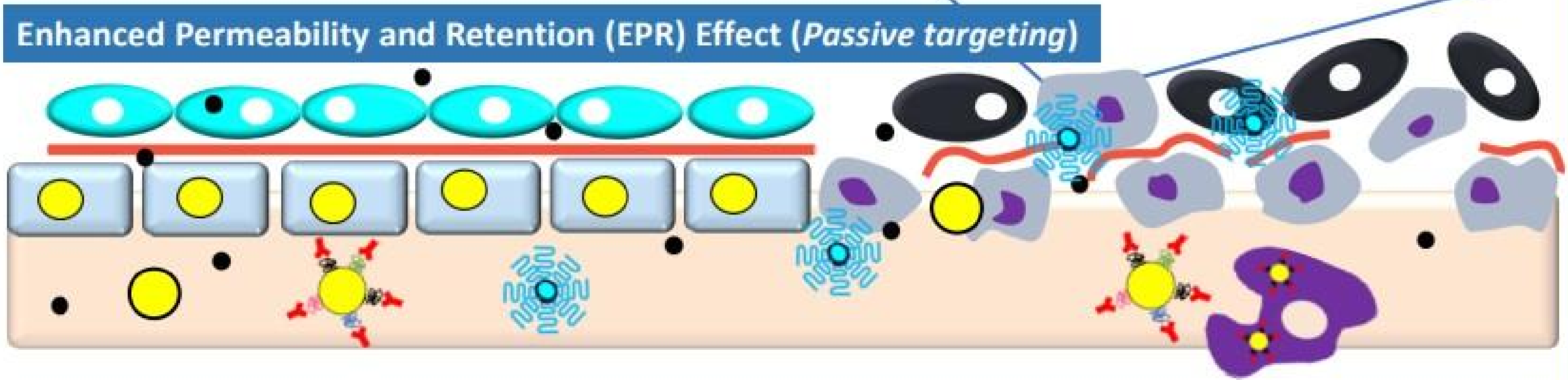

Polymeric NPs can be optimized by the coupling of targeting/responsive ligands, thereby **increasing the selectivity for cancer cells while improving the intracellular drug delivery**, reducing off-target effects, side effects, and drug toxicity.

https://www.mdpi.com › ...

Polymer-Based Drug Delivery Systems for Cancer Therapeutics - MDPI

About featured snippets  Feedback

# Proses absorbs dan distribusi obat

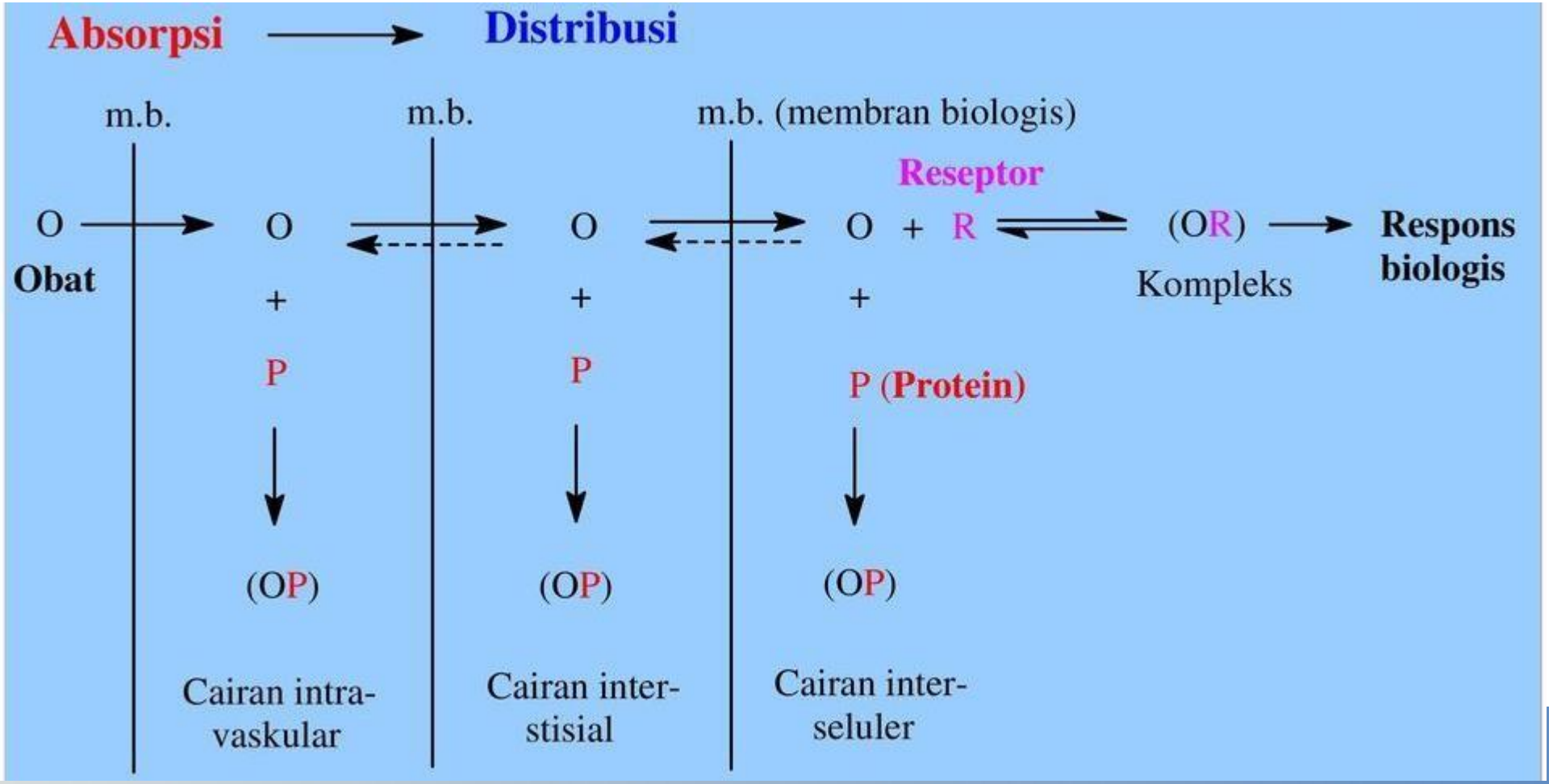

# FASA PENENTU AKTIVITAS BIOLOGIS

**FASA FARMASETIK**, meliputi:

- Proses pabrikasi, pengaturan dosis, formulasi, bentuk sediaan dan terlarutnya obat aktif
- Berperan dalam: ketersediaan obat untuk dapat diabsorbsi

**FASA FARMAKOKINETIK**, meliputi:

- Absorbsi, Distribusi, Metabolisme dan Ekskresi (ADME)
- Berperan dalam: ketersediaan obat untuk dapat mencapai jaringan sasaran (target)/reseptor →timbul respon biologis

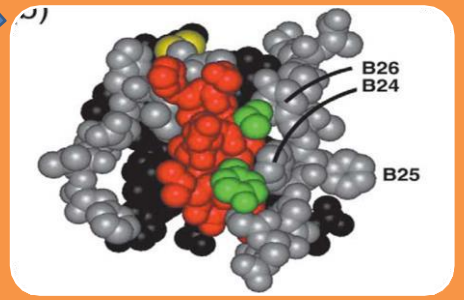


**FASA FARMAKODINAMIK**

- Adalah fasa terjadinya interaksi obat-reseptor dalam jaringan target
- Berperan dalam: timbulnya respon biologis obat

# Fasa-fasa penting dalam kerja obat

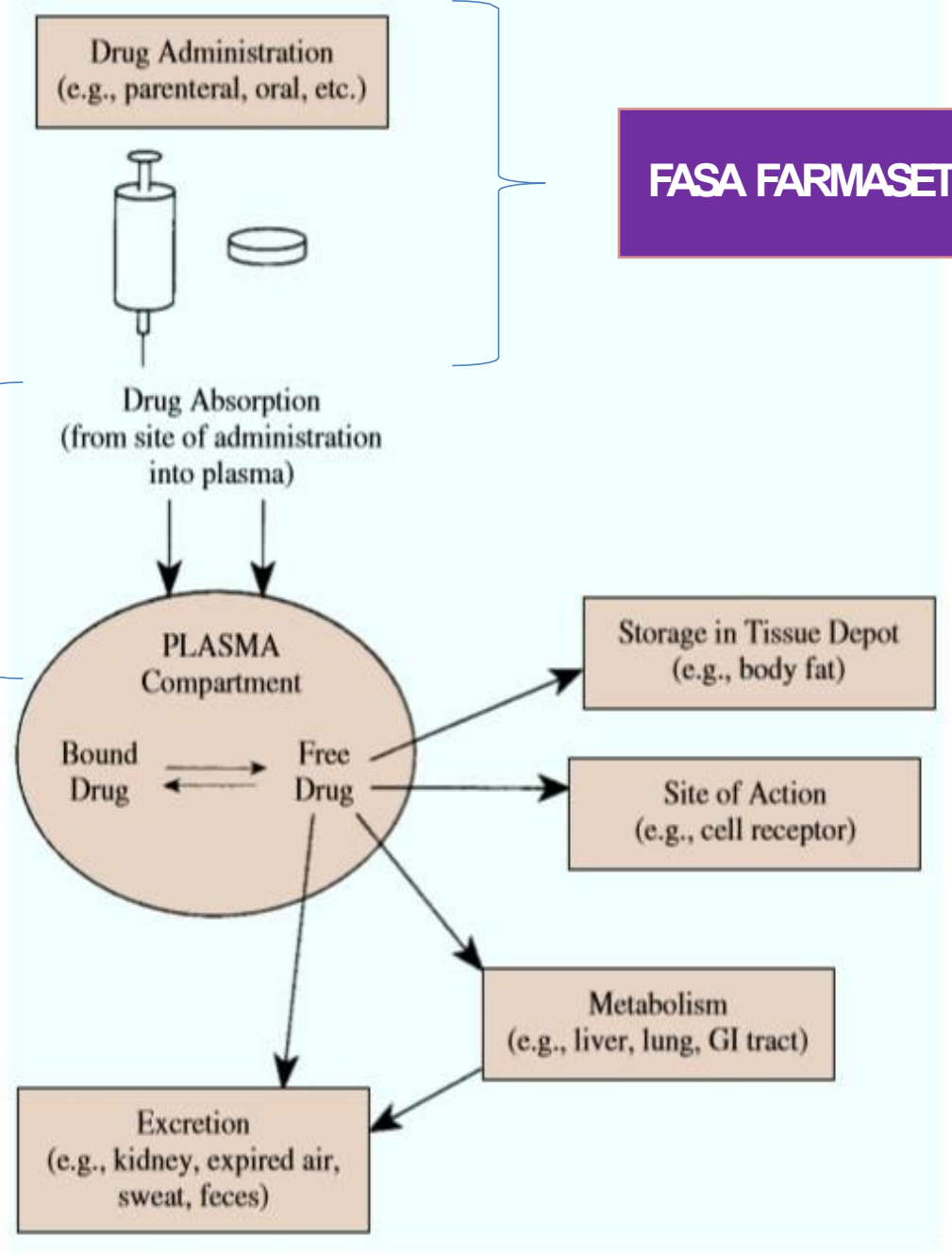


**FASA FARMASETIK**

**FASA FARMAKOKINETIK**

**FASA FARMAKODINAMIK**

## Metabolism

- Bioaktivasi
- Bioinaktivasi
- biotoksifikasi

# HUBUNGAN STRUKTUR, SIFAT FISIKA KIMIA DENGAN PROSES ABSORBSI

Proses absorpsi merupakan dasar penting dalam menentukan aktivitas farmakologi obat. Kegagalan atau kehilangan obat selama proses absorpsi akan mempengaruhi efek obat dan menyebabkan kegagalan pengobatan

Pemberian obat → melibatkan proses absorpsi yang berbeda

Pemberian secara parenteral → tidak mengalami proses absorpsi

# HUBUNGAN STRUKTUR, SIFAT FISIKA KIMIA DENGAN PROSES ABSORBSI

# 1. ABSORBSI MELALUI SALURAN CERNA

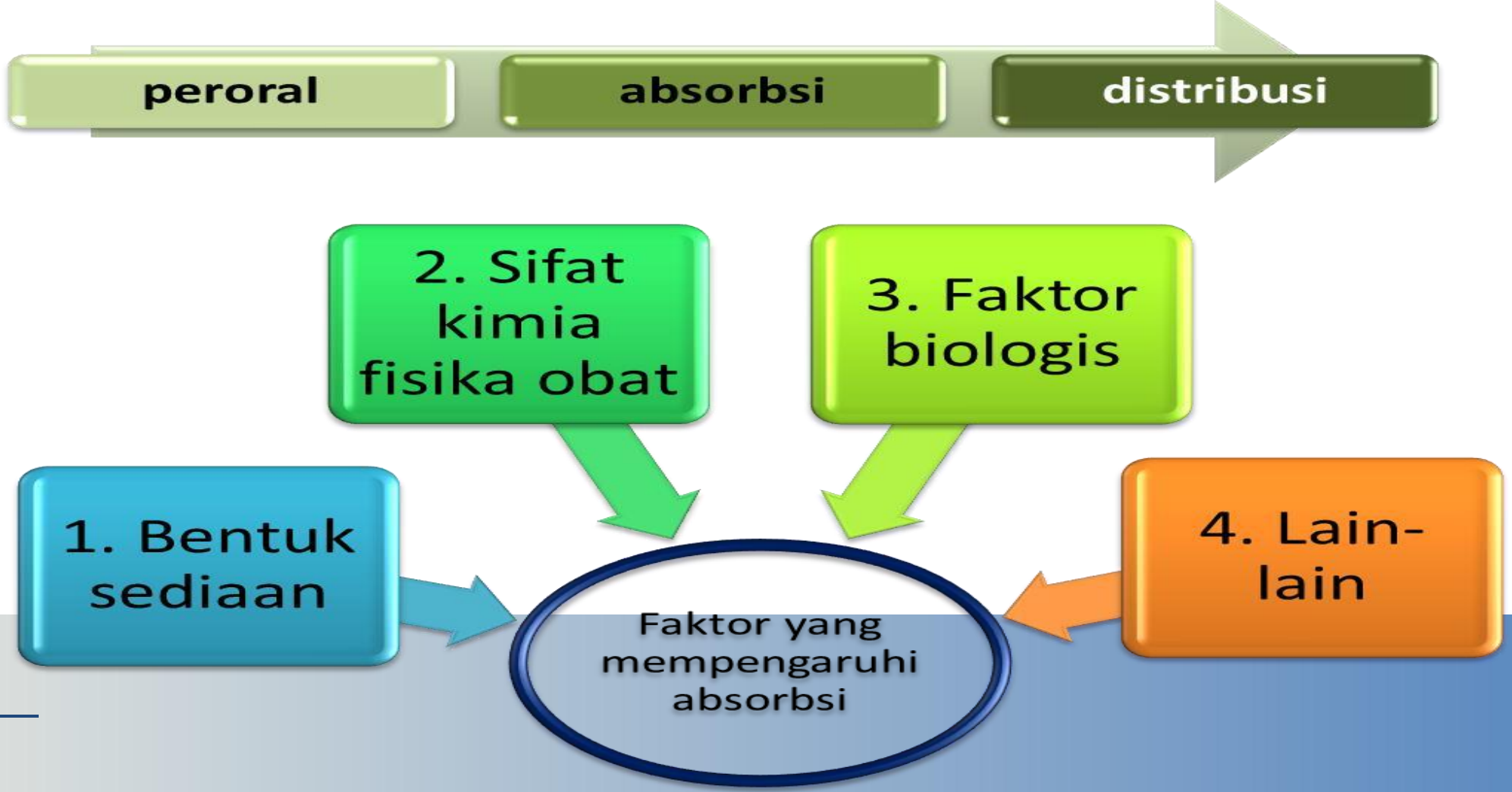

# 1. BENTUK SEDIAAN

- Berpengaruh terhadap kecepatan absorbsi obat → secara tidak langsung dapat mempengaruhi intensitas respon biologis
- Pil, tablet, kapsul, suspensi, emulsi, serbuk dan larutan→proses absorbsi obat memerlukan waktu yang berbeda-beda dan ketersediaan hayati kemungkinan juga berbeda
- Makin kecil ukuran partikel→luas permukaan yang bersinggungan dengan pelarut >> →kecepatan melarut semakin besar
- Bahan tambahan: pengisi, pelicin, penghancur, pembasah dan emulgator dapat mempengaruhi waktu hancur dan melarut obat→berpengaruh pada kecepatan absorbsi

# 2. SIFAT KIMIA FISIKA OBAT

- *Yang berpengaruh terhadap absorbsi a.l.:*
  - Bentuk asam atau Basa
  - Ester atau garam
  - kompleks atau hidrat
  - kristal atau polimorf
  - kelarutan dalam lemak atau air
  - derajat ionisasi
- *Contoh:*
  - penisilin V (bentuk garam K) lebih mudah larut daripada penisilin G (bentuk basa)
  - Novobiosin bentuk amorf lebih cepat larut daripada bentuk kristalnya

# 3. FAKTOR BIOLOGIS

*Yang berpengaruh terhadap absorbsi a.l.:*

- Variasi keasaman (pH) saluran cerna
- Sekresi cairan lambung
- Gerakan saluran cerna
- Luas permukaan saluran cerna
- Waktu pengosongan lambung dan waktu transit dalam usus
- Jumlah pembuluh darah pada tempat absorbsi

# 4. LAIN-LAIN

**Yang berpengaruh terhadap absorbsi a.l.:**

- **Umur**
- **Diet (makanan)**
- **Interaksi obat dengan senyawa lain**
- **Penyakit tertentu**

# Derajat ionisasi

- *Obat BASA LEMAH*
  - Seperti: amin aromatik [Ar-NH2], aminopirin, asetanilid, kafein dan kuinin→bila diberikan secara oral, di dalam lambung yang asam (pH 1-3,5)→ sebagian besar akan menjadi bentuk ionnya [Ar-$NH3^+$]→ kelarutan pada lemak sangat kecil→ sukar menembus membran lambung
  - Bentuk ion [Ar-$NH3^+$] masuk ke usus halus yang agak basa (pH 5-8)→ berubah menjadi bentuk tak terion kembali [Ar-NH2]→kelarutan dalam lemak besar.
- *Obat ASAM LEMAH*
  - Seperti: asam salisilat, asetosal, fenobarbital, dan asam benzoat→ pada lambung yang bersifat asam akan terdapat dalam bentuk tidak terionisasi→mudah larut dalam lemak→mudah menembus membran lambung

Saluran cerna bersifat permeabel selektif terhadap bentuk tidak terdisosiasi obat yang bersifat mudah larut dalam lemak

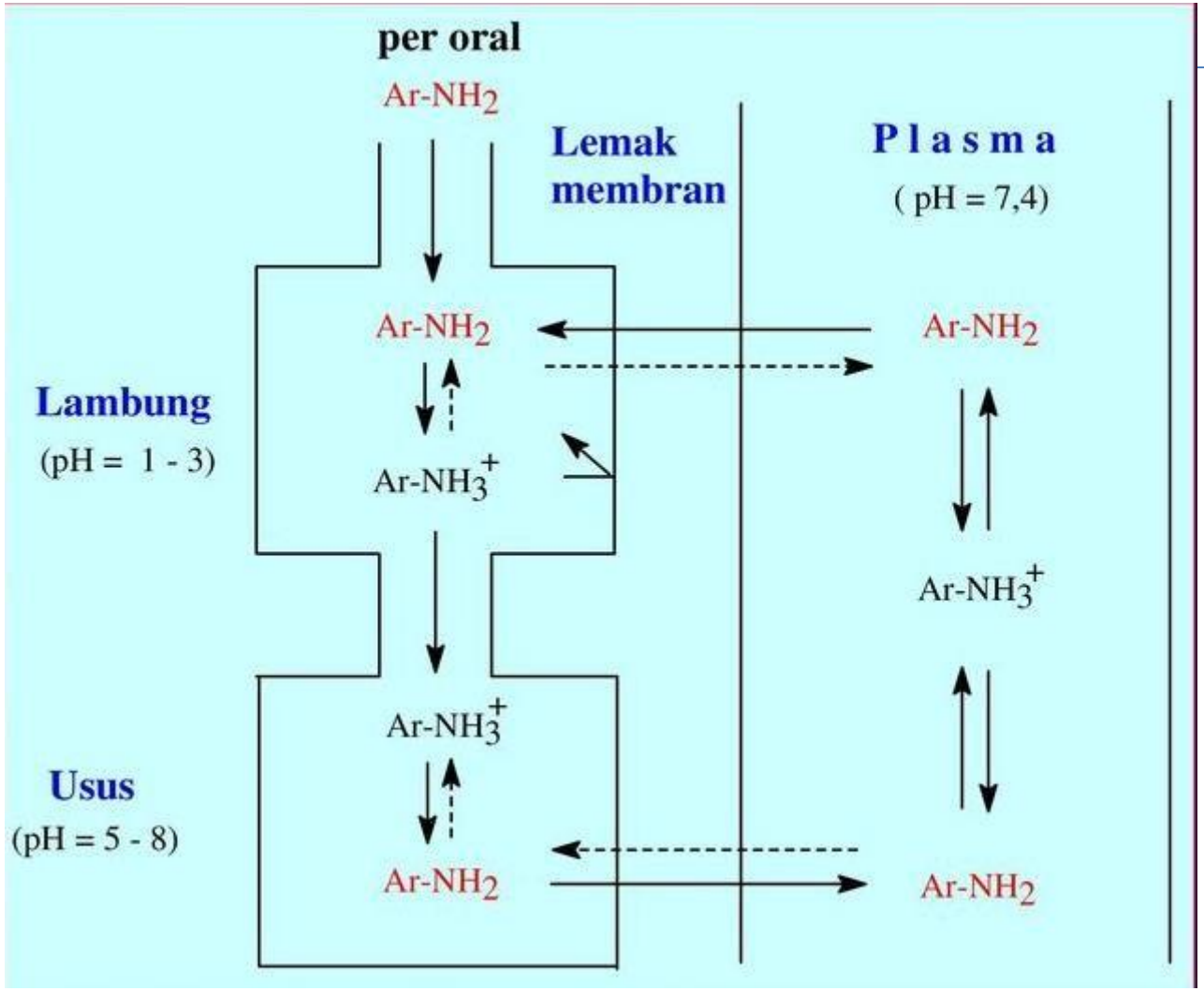

# Derajat ionisasi… con't

- *Senyawa yang TERIONISASI SEMPURNA*
  - Umumnya bersifat asam atau basa kuat, mempunyai kelarutan pada lemak yang sangat rendah→sukar menembus saluran cerna
  - Contoh: asam sulfonat, turunan amonium kuarterner
- *Senyawa yang SANGAT SUKAR LARUT DALAM AIR*
  - Tidak diabsorbsi oleh saluran cerna
  - Contoh: $BaSO_4$, MgO dan $Al(OH)_3$

# Studi tentang masalah yang berhubungan dengan absorbsi turunan amonium kuartener pada saluran cerna

- **Contoh :**

**Pemberian secara oral anthelmintic pyrvinium pamoat (Povan) dan ditiazanin iodide, ternyata obat tidak diabsorbsi oleh saluran cerna dan bersifat toksik terhadap cacing usus. Bila diserap, senyawa menimbulkan toksisitas sistemik yang tidak diharapkan**

# HUBUNGAN STRUKTUR, SIFAT FISIKA KIMIA DENGAN PROSES ABSORBSI

# 2. ABSORBSI MELALUI MATA

- Bila obat diberikan secara lokal pada mata, obat diabsorbsi melalui konjungtiva dan kornea
- Kecepatan penetrasi dipengaruhi oleh: derajat ionisasi dan koefisien partisi
- Bentuk yang tidak terion akan lebih cepat diabsorbsi oleh membran mata

# HUBUNGAN STRUKTUR, SIFAT FISIKA KIMIA DENGAN PROSES ABSORBSI

# 3. ABSORBSI MELALUI PARU

- Anestesi sistemik yang Diberikan secara inhalasi akan diabsorbsi melalui epitel paru dan membran mukosa saluran nafas, karena luas permukaan yang besar → absorbsi melalui pembuluh darah paru berjalan dengan cepat
- Absorbsi obat melalui paru tergantung pada:
  - Kadar obat dalam alveoli
  - Koefisien pasrtisi gas/darah
  - Kecepatan aliran darah paru
  - Ukuran partikel obat, hanya obat dengan ukuran < 10µm yang dapat masuk peredaran aliran paru

## HUBUNGAN STRUKTUR, SIFAT FISIKA KIMIA DENGAN PROSES ABSORBSI

# 4. ABSORBSI MELALUI KULIT

- Absorbsi obat melalui kulit sangat tergantung pada kelarutan obat dalam lemak karena epidermis berperan sebagai membran lemak biologis

# DISTRIBUSI

**Faktor-faktor yang mempengaruhi kecepatan distribusi obat di dalam tubuh:**

1. **Sifat fisika kimia obat, terutama kelarutan dalam lemak**
2. **Sifat membran biologis**
3. **Kecepatan distribusi aliran darah pada jaringan dan organ tubuh**
4. **Ikatan obat dengan sisi kehilangan**
5. **Adanya pengangkutan aktif dari bbrp obat**
6. **Masa atau volume jaringan**

Site of Loss:
tempat di mana obat berubah atau terikat sehingga tidak dapat mencapai reseptor.
Contoh: protein darah (albumin), depo penyimpanan, enzim pengurai.

# Struktur membran biologis

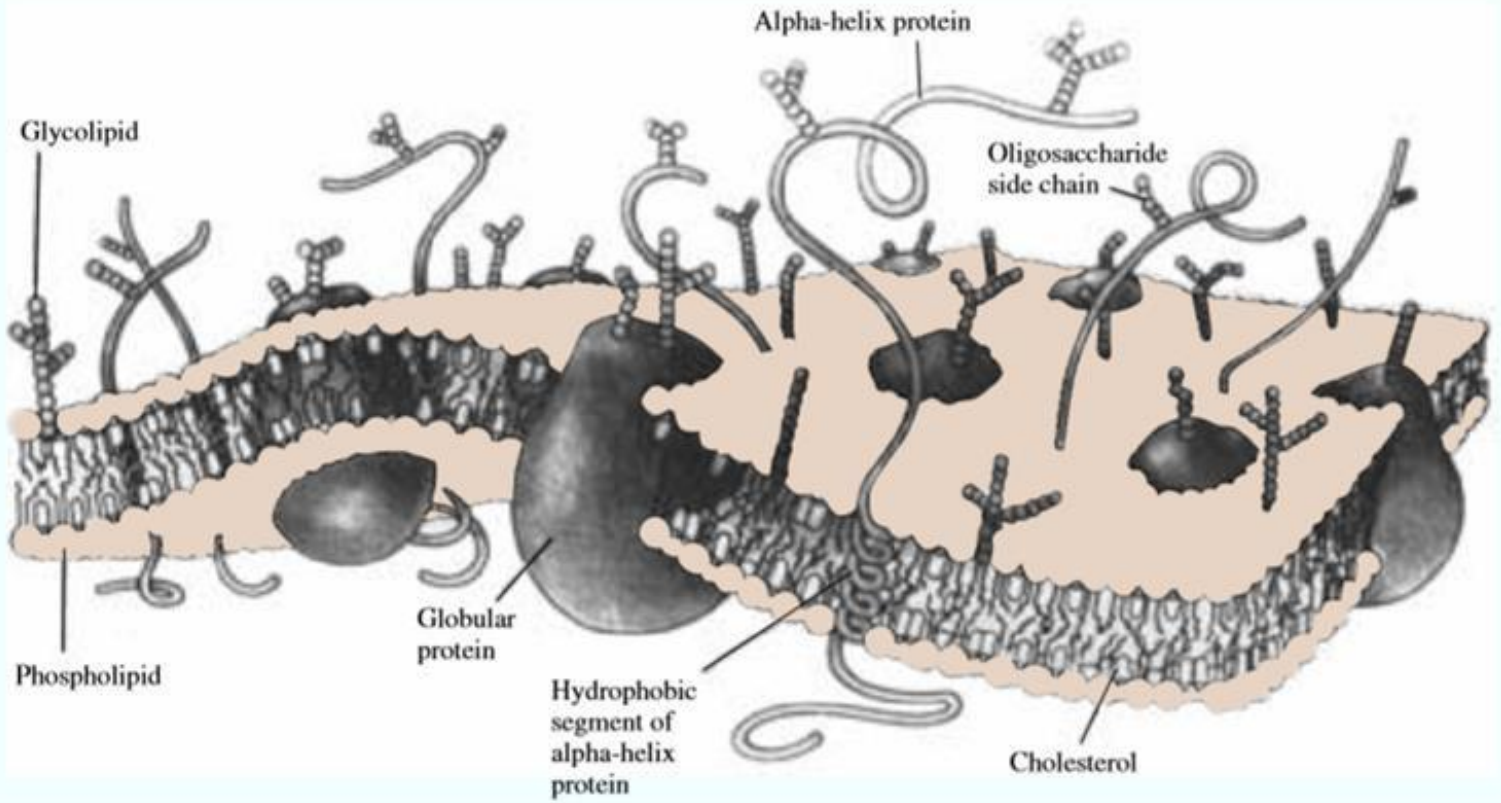


- Fungsi utama:
  - Sebagai penghalang dengan sifat semipermeabel
  - Sebagai tempat reaksi biotransformasi energi

- Contoh menbran biologis:
  - Sel epitel saluran cerna, sel epitel paru, sel endotel pembuluh darah kapiler, sawar darah otak, sawar darah cairan serecrospinal, plasenta, membrane glomerulus, membrane tubulus renalis, sel epidermis kulit

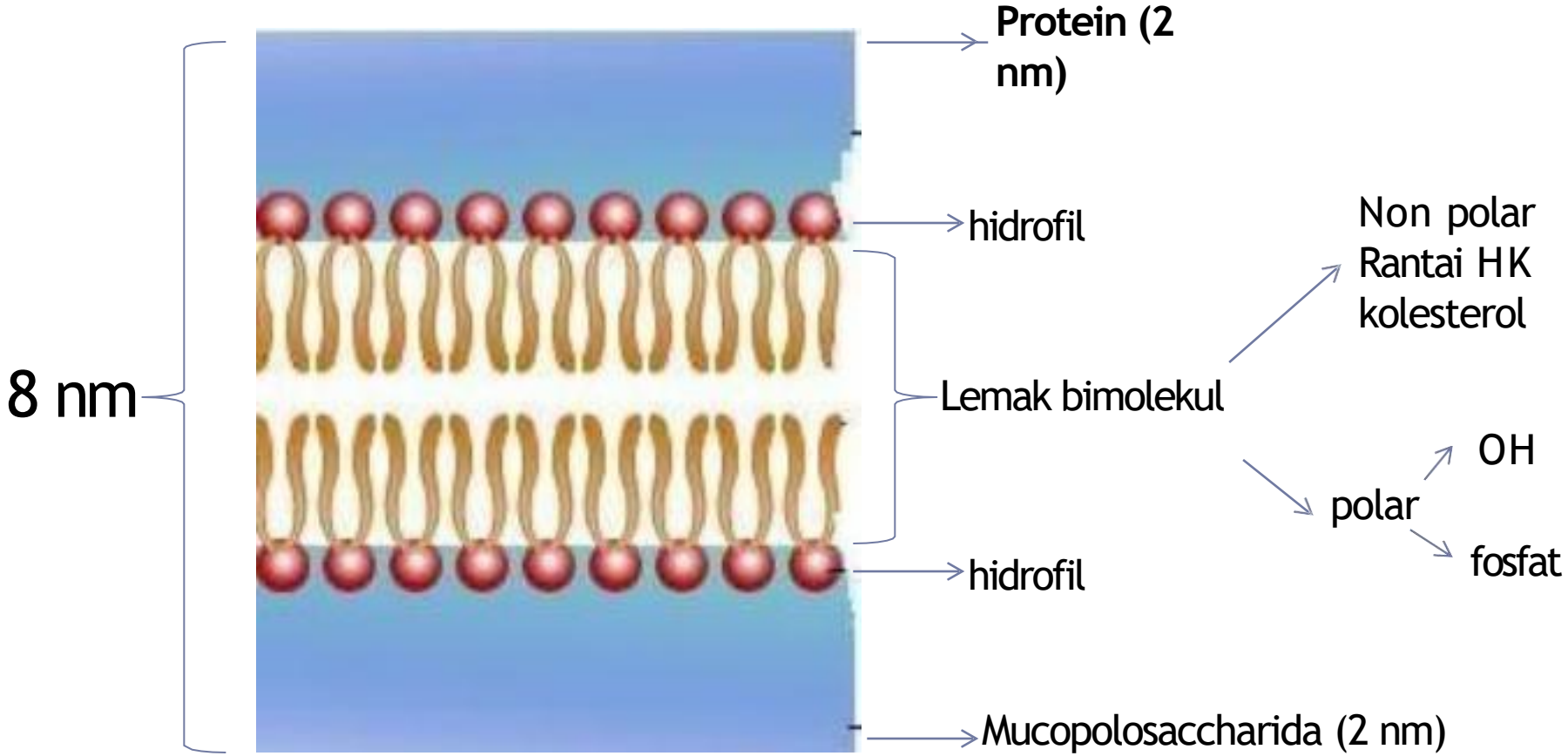
8 nm
Protein (2 nm)
hidrofil
Lemak bimolekul
Non polar
Rantai HK
kolesterol
polar
OH
fosfat
hidrofil
Mucopolosaccharida (2 nm)

# Komponen membran sel terdiri atas:

- Lapisan lemak biomolekul
  - Berdasarkan kepolarannya, lapisan ini terdiri atas bagian non polar (hidrokarbon) dan bagian polar (gugus hidroksil kolesterol dan gugus gliserilfosfat fosfolipid)
- Protein
  - Protein bersifat ampifil karena mengandung gugus hidrofil dan hidrofob
- Mukopolisakarida
  - Jumlahnya kecil dan strukturnya tidak dalam keadaan bebas tetapi dalam bentuk kombinasi dengan lemak. Berperan dalam pengenalan sel dan interaksi antigen-antibodi

# HUBUNGAN STRUKTUR, SIFAT FISIKA KIMIA DENGAN PROSES DISTRIBUSI

- Umumnya distribusi obat terjadi dengan cara menembus membran biologis melalui proses difusi. Mekanisme difusi dipengaruhi oleh: struktur kimia, sifat fisika kimia obat, dan membran biologis

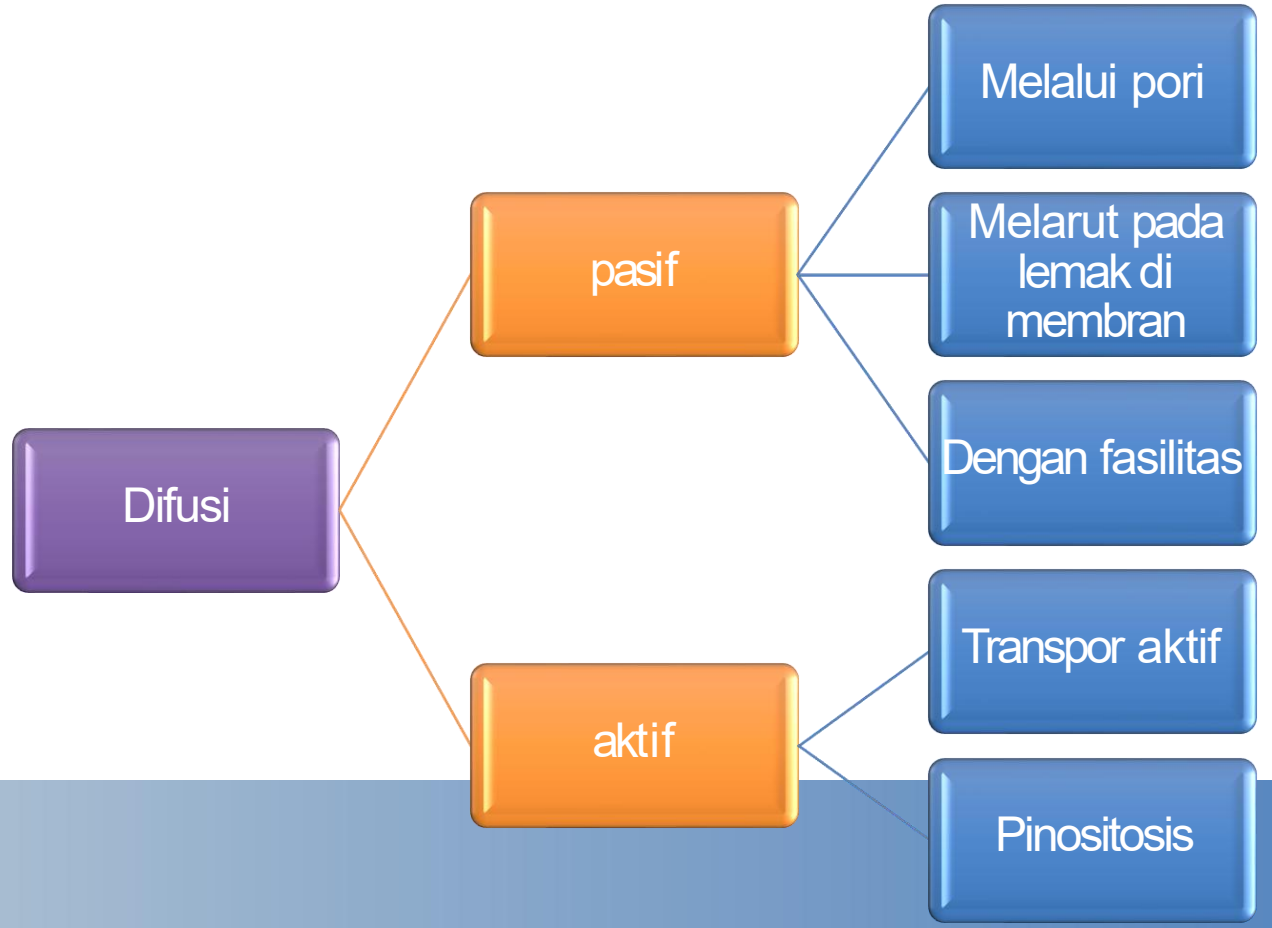

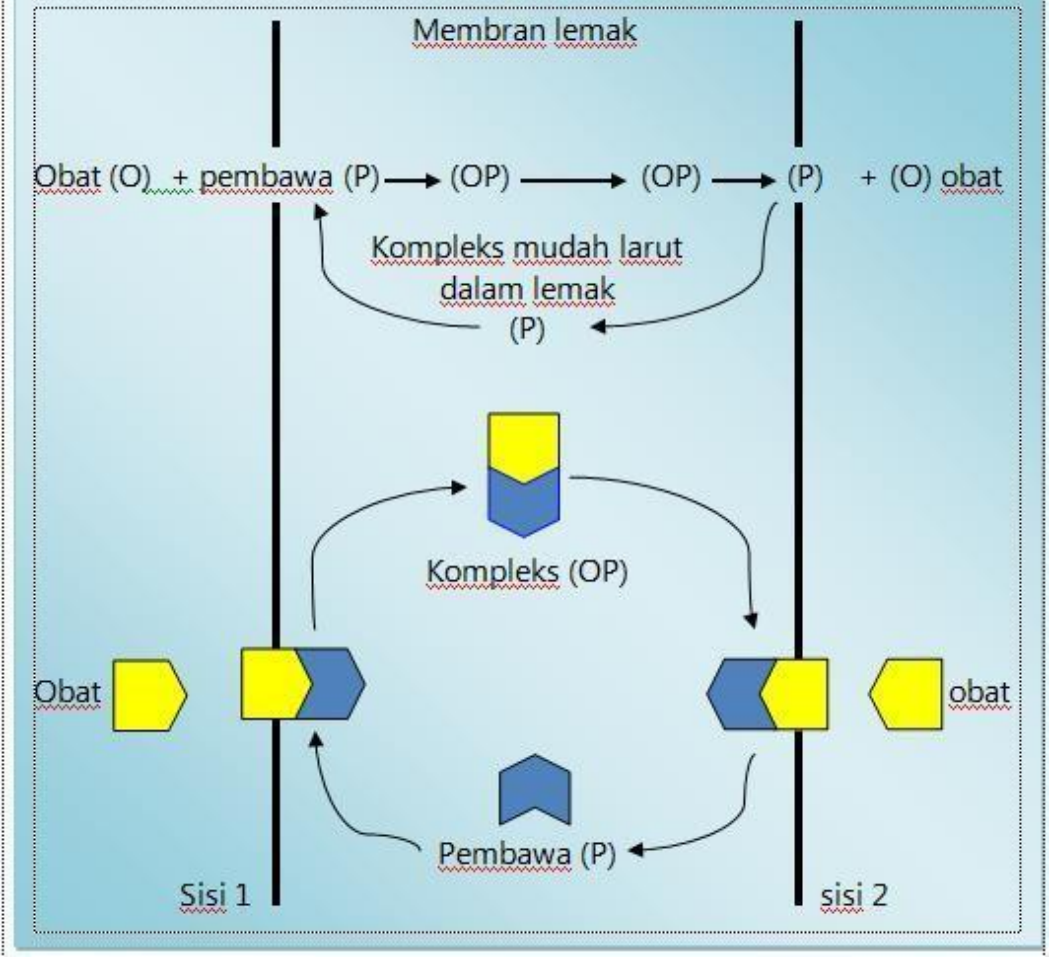


*Proses penetrasi molekul obat yang bersifat hidrofil ke membrane biologis dengan bantuan pembawa*

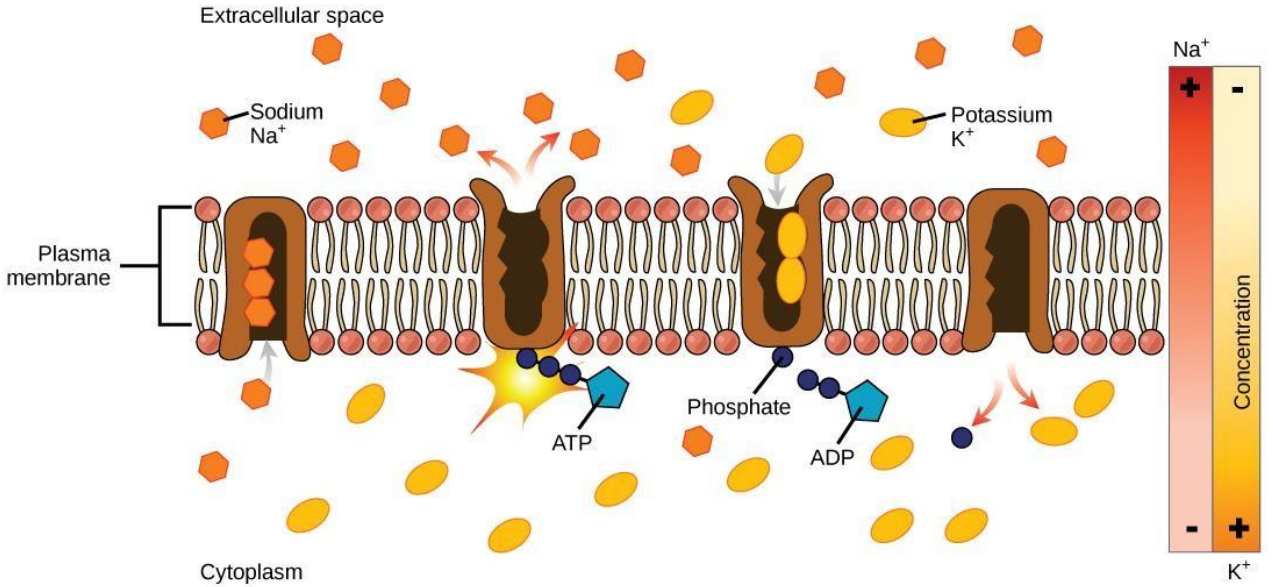


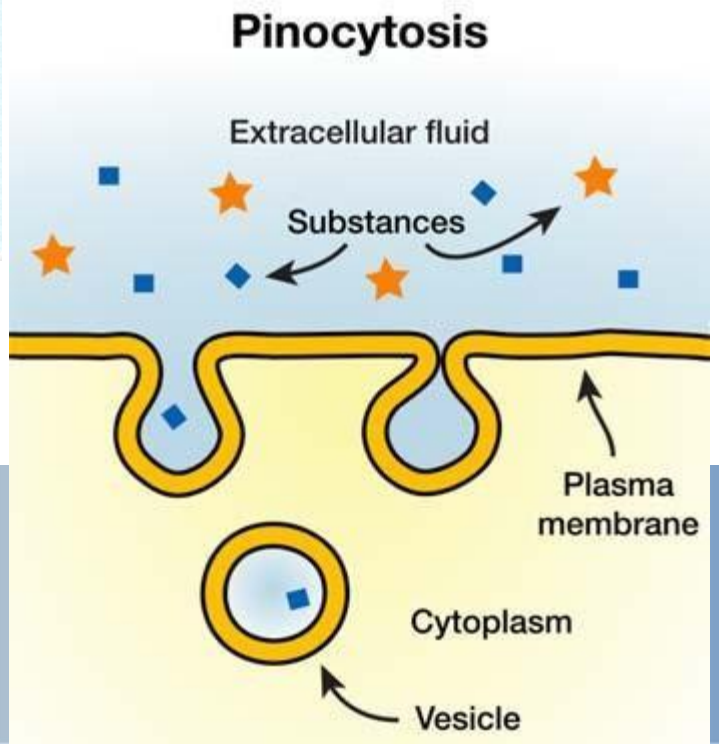


*Difusi aktif. Pengangkutan obat berjalan dari daerah berkadar rendah ke tinggi. Pengangkutan memerlukan energi yang berasal dari ATP. Reaksi pembentukan kompleks obat pembawa memerlukan efinitas*

# Interaksi obat dengan biopolymer?

# Hubungan Struktur Aktivitas Obat dengan proses Metabolisme dan Ekskresi

Arief Kusuma Wardani, S.Si., M.Pharm.Sci
Universitas Muhammadiyah Magelang

# Drug Discovery Pathway

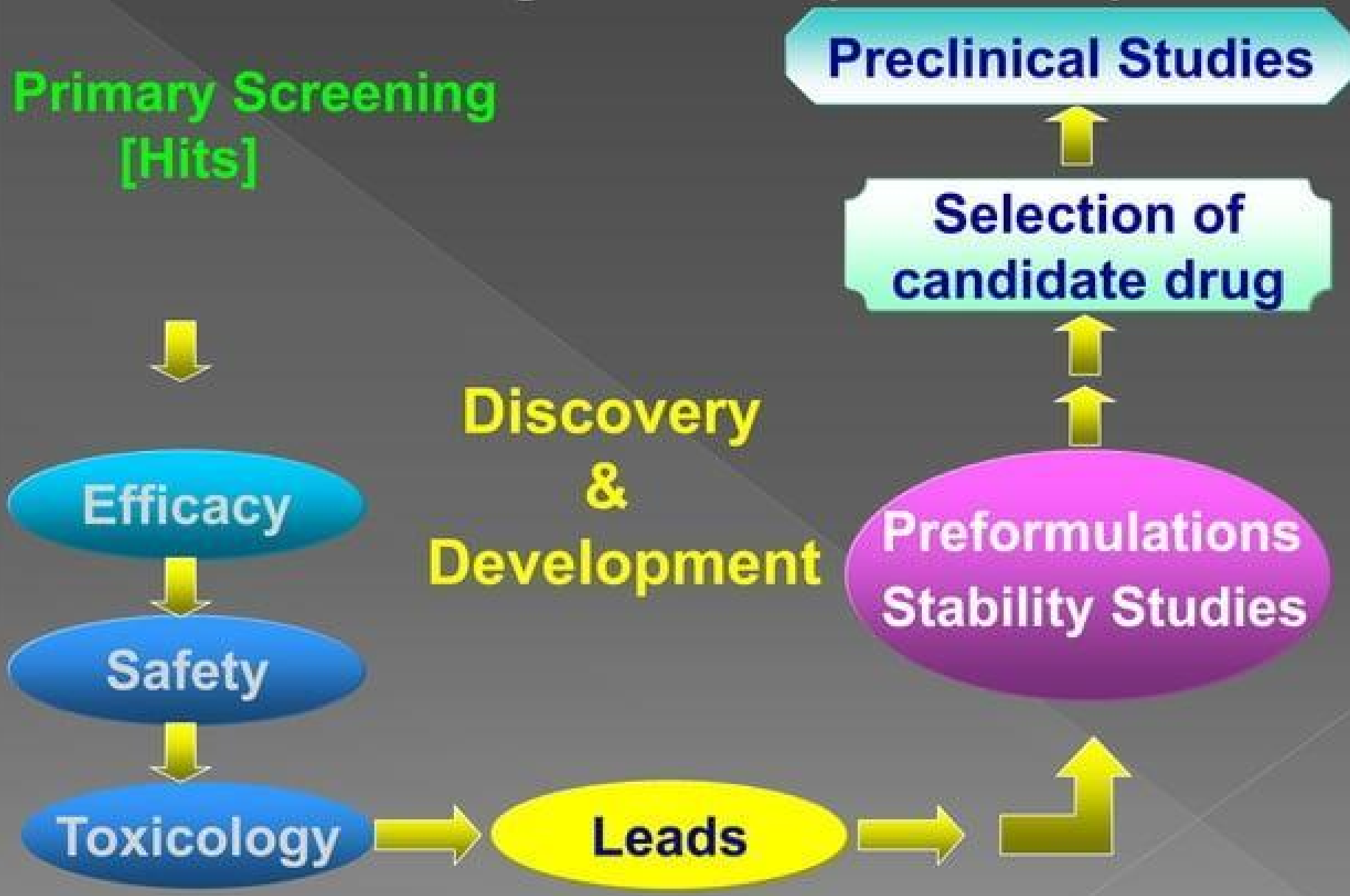

# DISCOVERY OF DRUG (LIBRIUM)

- Study of biological properties may lead to discovery of new drug.
- Some drugs are directly discovered like "LIBRIUM" (Tranquilizers).
- Another e.g. of direct discovery of drug is penicillin(antibacterial) discovered by Alexander Fleming.
- The average time require to bring a drug to market range is 12-15 years.

# Clinical trials consist of three phases:

- Phase I : Evaluate the tolerability, safety pharmacological effects in 20-100 healthy volunteers.
- Phase II : Assesses the effectiveness of the drug, determine side effects and check dosage in few 100 patients.
- Phase III : it is large trial with sevaral thousand patient in hospitals that establish efficiency of drug.

# Discovery of lead compound

- The lead compound is one which has number of attractive characteristics such as desirable biological activity but may have other undesirable characteristics such as high toxicity, insolubility, metabolic problems.
- The ideal lead compound is modified by altering the structure to get desired activity and to eliminate side effects.

# Steps involved in selection of lead compound

A) Screening:

- First step is to assay compound for particular biological activity and potency

  (i.e. antibacterial activity).

- There are two methods of screening:

  1) Random screening : in this type synthetic compound and natural products were randomly screened for activity irrespective of their structure. e.g.streptomycin

2) Non random screening: also called as targeted or focused screening, is more narrow approach than in random screening. Compound having not clear resemblance to weakly active compound uncovered in random screen.

OR

The compound containing different functional group than lead, may be tested selectively. The non-random screening is found to be more economical and less man power intensive compared to random screen.

## B) Drug metabolism studies:

During drug metabolism studies, metabolites are isolated and screened to determine the activity observed is derived from the drug molecule.

Eg. Anti-inflammatory drug sulindac is not active but on metabolic reduction it get activity.

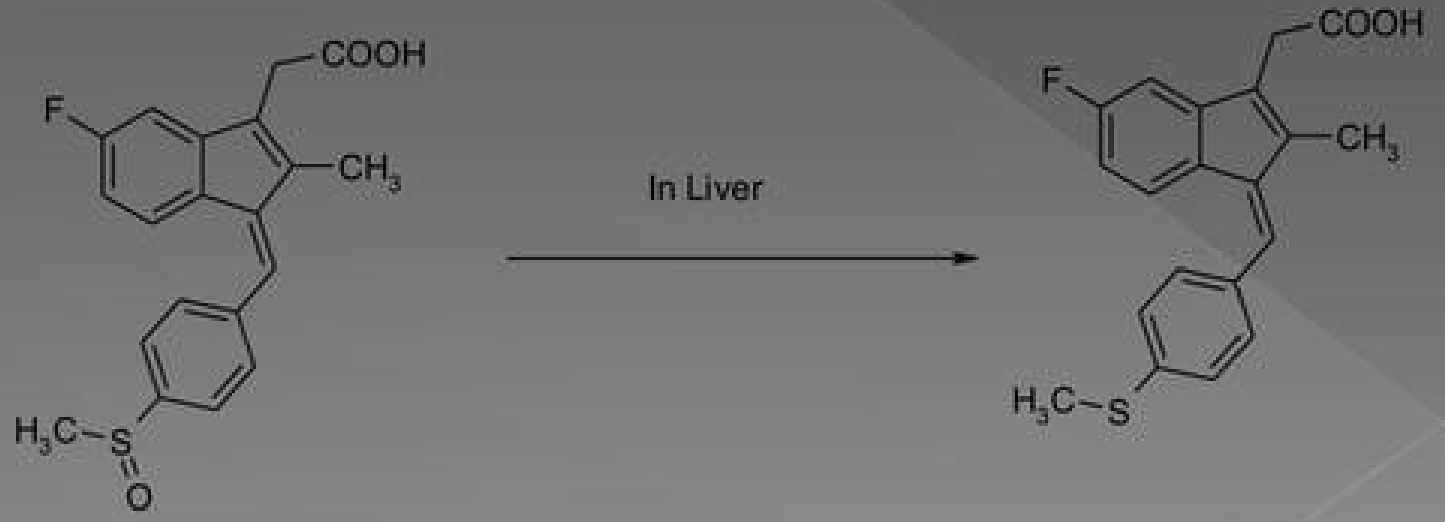


Sulindac

Metabolic product

## C) Clinical observation :

The last step in selection of lead compound is clinical observation. Sometimes compound may exhibits more than one pharmacological activity during clinical trials that is it may produce a side-effect. Then this compound can be used for secondary activity. Eg.Dimenhydrinate is used as drug for car sickness but further study shows it also effective in seasickness and airsickness.

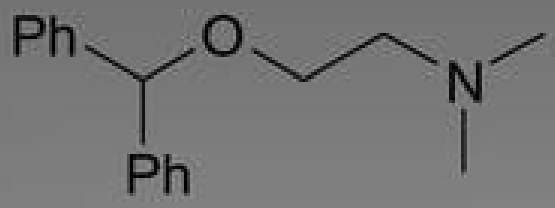


Dimenhydrinate

# Development of drug:

- After the lead compound is identified, its structure is modified in order to improve the desired pharmacological activity.

a) Pharmacophore identification : some groups are essential to hold the drug in appropriate position on the receptor. However those groups which interfere in the pharmacophore binding need to be removed.

b) Functional group modification : when functional group in a drug molecule is modified or its position changed, there is marked effect on the pharmacological effect. For Eg.


Dazoxide

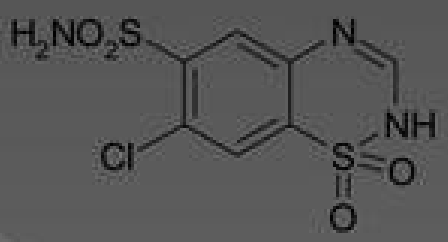


Chlorothiazine

Chlorothiazine is an anti hypertensive agent that has a strong diuretic effect as well.

Where as diazoxide shows only as antihypertensive drug without diuretic activity.

C) Structure activity relationships: From various observations it has been concluded that the physiological action of molecule was a function of its chemical constitution are the basis for structure-activity relationships(SAR).

i) **SAR in sulphonamides : (Antibacterial)**

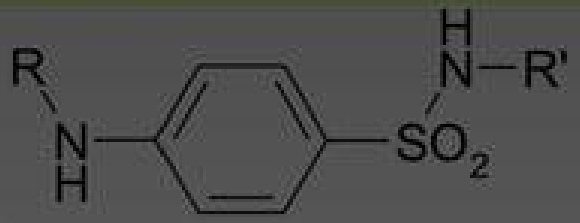


Sulphonamide

- The amino and sulfonyl group on the benzene ring should be at Para positions

- Presence of free amino group at N1 is essential for antibacterial action.
- The replacement of benzene ring by other ring system decrease the activity of compound.
- Monosubstitution at N4 ($SO_2NH$-R) increases the potency where as disubtitution at N4 (So2NR2) leads to inactive compound.
- Heterocyclic substituent at N4 result in increase of potency of the compound.

ii) SAR in Benzodiazepine: (Anticonvulsant and muscle relaxants i.e.CNS depressant)

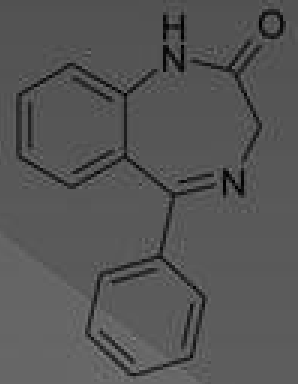


Benzodiazepine

- They must have following general structure to show CNS depressant action.

- The presence of methyl group at 1 position increases the activity .
- Replacement of O by sulphur at C2 position decreases the potency.
- The presence of hydroxyl group at 3rd position found to decrease the activity.
- The saturqation of double bond at C4-C5 reduce the activity.
- Electron withdrawing group like -Cl,-Br,-NO2.etc. at 7 position increases the activity.

# Computer-assisted Drug Design (CADD)

- Drug design is a three-dimensional puzzle where small drug molecules, ligands, are adjusted to the binding site of a protein.

- The factors which affect the protein-ligand interaction can be characterized by using molecular docking and different quantitative structure-activity relationships (QSAR) methods

# Applications

1. Find interesting lead molecules quickly
2. Predicting properties and activities of untested molecules
3. Propose compounds for synthesis
4. Validate models of receptor binding sites
5. Optimize pharmacokinetic properties of compound

# Thanks for your .....

# Quantitative Structure Activity Relationships (QSAR)

Arief Kusuma Wardani, S.Si., M.Pharm.Sci
Prodi Farmasi
Fakultas Ilmu Kesehatan
Universitas Muhamadiyah Magelang

# Modern drug discovery process

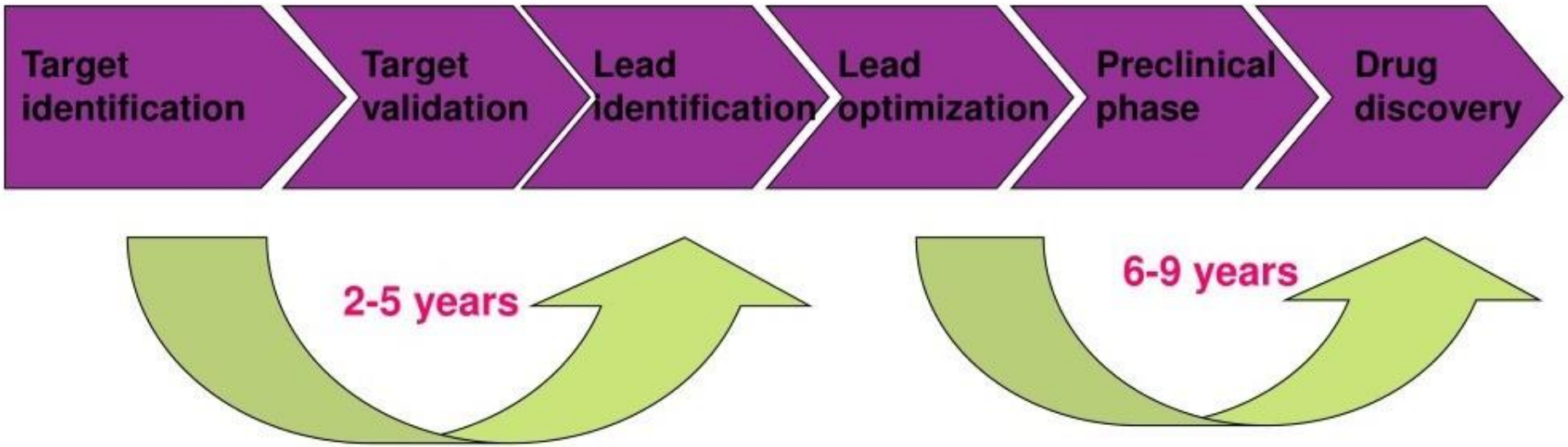


- Drug discovery is an expensive process involving high R & D cost and extensive clinical testing
- A typical development time is estimated to be 10-15 years.

# QSAR AND DRUG DESIGN

*Correlate chemical structure with activity using statistical approach*

**Compounds + biological activity**


**New compounds with improved biological activity**

# Introduction

- **Aims**
- To relate the biological activity of a series of compounds to their physicochemical parameters in a quantitative fashion using a mathematical formula
- **Requirements**
- Quantitative measurements for biological and physicochemical properties

- **Physicochemical Properties**

- Hydrophobicity of the molecule
- Hydrophobicity of substituents
- Electronic properties of substituents
- Steric properties of substituents

} Most common properties studied

# Hydrophobicity of the Molecule

$$\text{Partition Coefficient } P = \frac{[\text{Drug in octanol}]}{[\text{Drug in water}]}$$

High *P* → High hydrophobicity

# Hydrophobicity of the Molecule

- Activity of drugs is often related to *P*
  e.g. binding of drugs to serum albumin
  (straight line - limited range of log *P*)

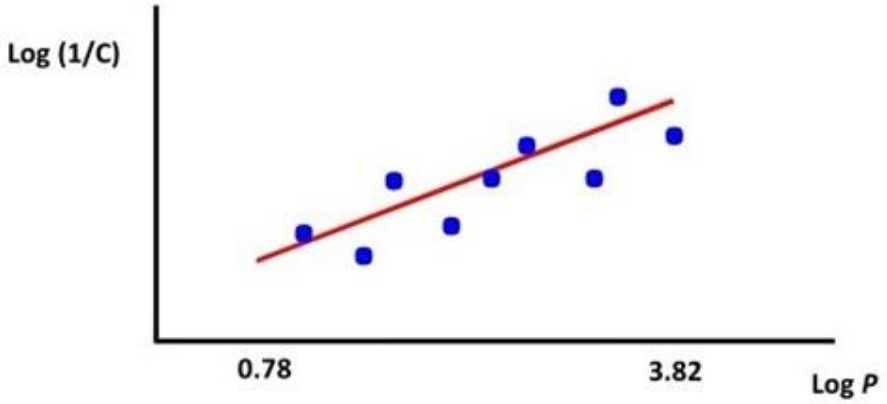


$$\text{Log } \frac{1}{C} = 0.75 \log P + 2.30$$

- Binding increases as log *P* increases
- Binding is greater for hydrophobic drugs

# Hydrophobicity of the Molecule

**Example 2** General anaesthetic activity of ethers

(parabolic curve - larger range of log *P* values)

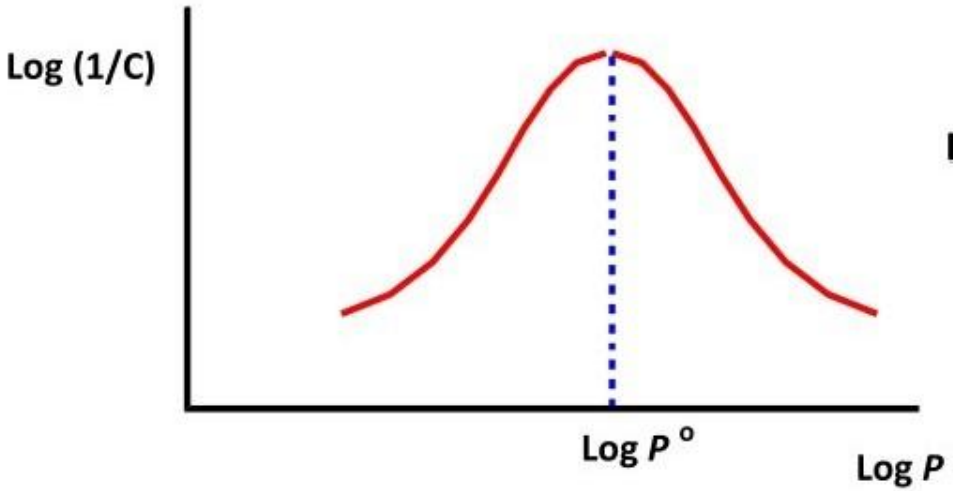


$$\text{Log}\left(\frac{1}{C}\right) = -0.22(\log P)^2 + 1.04 \log P + 2.16$$

Optimum value of log *P* for anaesthetic activity = log $P^o$

# Hydrophobicity of the Molecule

## Notes:

QSAR equations are only applicable to compounds in the same structural class (e.g. ethers)

- However, log $P^o$ is similar for anaesthetics of different structural classes

- Structures with log $P$ 2.3 enter the CNS easily
  (e.g. potent barbiturates have a log $P$ of approximately 2.0)

- Can alter log $P$ value of drugs away from 2.0 to avoid CNS side effects

# Hydrophobicity of Substituents

- the substituent hydrophobicity constant (p)

## Notes:

- A measure of a substituent's hydrophobicity relative to hydrogen
- Tabulated values exist for aliphatic and aromatic substituents
- Measured experimentally by comparison of log *P* values with log P of parent structure

**Example:**

Benzene
(Log *P* = 2.13)


Chlorobenzene
(Log *P* = 2.84)

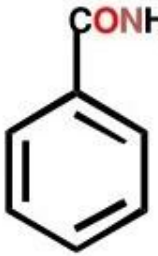


Benzamide
(Log *P* = 0.64)

$p_{Cl} = 0.71$ $p_{CONH_2} = -1.49$

- Positive values imply substituents are more hydrophobic than H
- Negative values imply substituents are less hydrophobic than H

# Hydrophobicity of Substituents

## - the substituent hydrophobicity constant (p)

**Notes:**

- The value of p is only valid for parent structures
- It is possible to calculate log *P* using p values

**Example:**

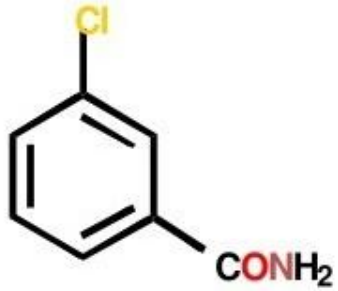


*meta*-Chlorobenzamide

$\text{Log } P_{(\text{theory})} = \log P_{(\text{benzene})} + p_{Cl} + p_{CONH_2}$

$= 2.13 + 0.71 - 1.49$

$= 1.35$

$\text{Log } P_{(\text{observed})} = 1.51$

- A QSAR equation may include both *P* and p.
- *P* measures the importance of a molecule's overall hydrophobicity (relevant to absorption, binding etc)
- p identifies specific regions of the molecule which might interact with hydrophobic regions in the binding site

# Electronic Effects

## Hammett Substituent Constant (s)

**Notes:**

- The constant (s) is a measure of the e-withdrawing or e-donating influence of substituents
- It can be measured experimentally and tabulated

(e.g. s for aromatic substituents is measured by comparing the dissociation constants of substituted benzoic acids with benzoic acid)

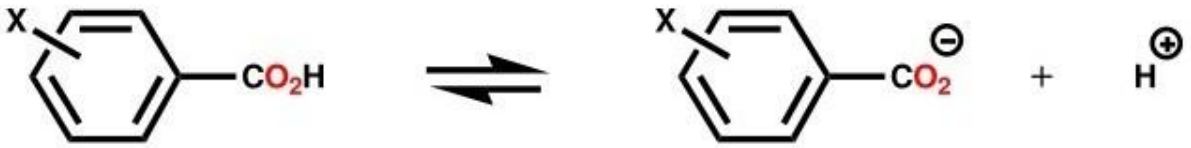


X=H $K_H$ = Dissociation constant = $\frac{[PhCO_2^-]}{[PhCO_2H]}$

## Hammett Substituent Constant (s)

### X= electron withdrawing group (e.g. $NO_2$)

X = electron withdrawing group


**Charge is stabilised by X**
**Equilibrium shifts to right**
**$K_X > K_H$**

$$s_x = \log \frac{K_X}{K_H} = \log K_X - \log K_H$$

**Positive value**

## Hammett Substituent Constant (s)

### X= electron donating group (e.g. $CH_3$)

X = electron withdrawing group

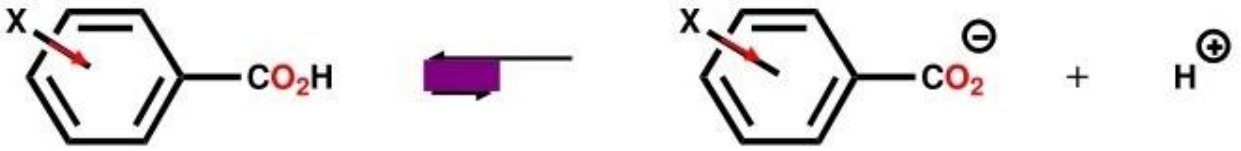


**Charge destabilised**
**Equilibrium shifts to left**
**$K_X < K_H$**

$$s_x = \log \frac{K_X}{K_H} = \log K_X - \log K_H$$

**Negative value**

# Hammett Substituent Constant (s)

**NOTES:**

**s value depends on inductive and resonance effects**

**s value depends on whether the substituent is *meta* or *para***

***ortho* values are invalid due to steric factors**

## Hammett Substituent Constant (s)

**EXAMPLES:** $s_p\ (NO_2) = 0.78$ $s_m\ (NO_2) = 0.71$

*meta*-Substitution

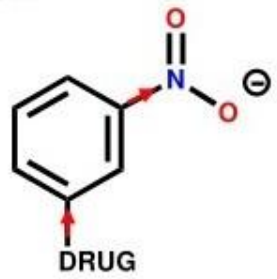


e-withdrawing (inductive effect only)

*para*-Substitution

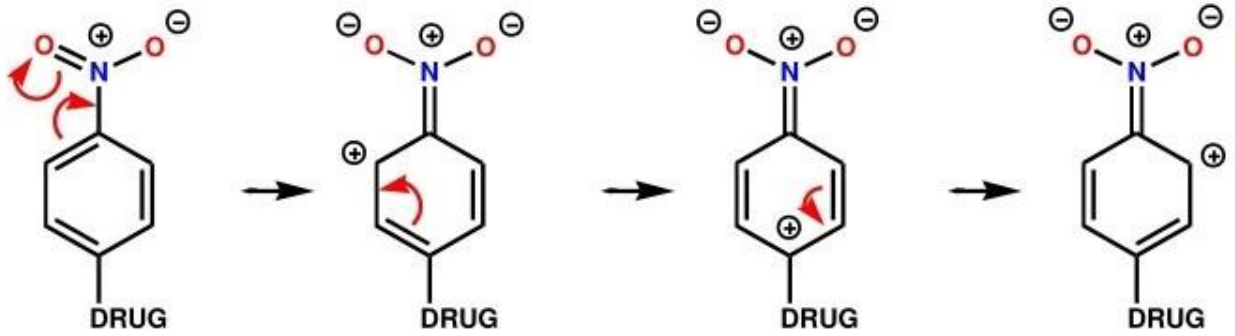


e-withdrawing (inductive + resonance effects)

## Hammett Substituent Constant (s)

**EXAMPLES:** $s_m$ (OH) = 0.12 $s_p$ (OH) = −0.37

*meta*-Substitution

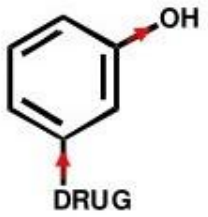


e-withdrawing (inductive effect only)

*para*-Substitution

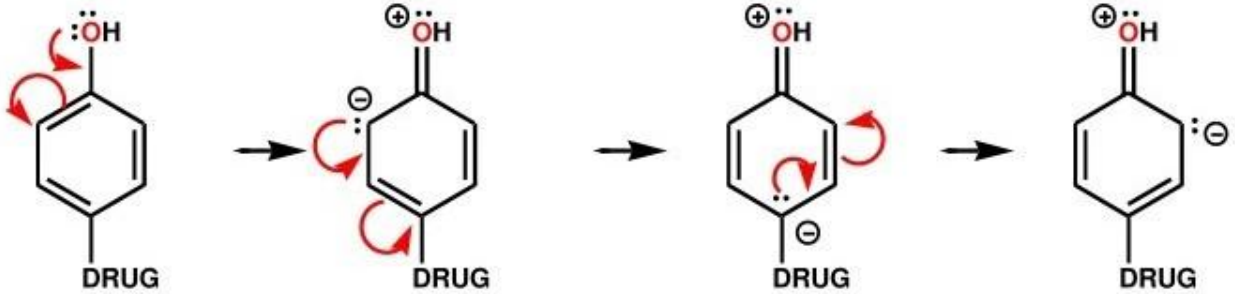


e-donating by resonance more important than inductive effect

## Hammett Substituent Constant (s)

**QSAR Equation:**

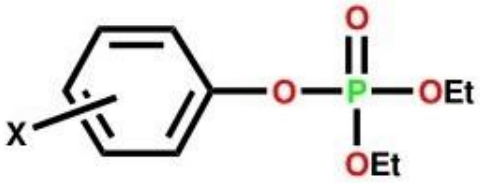


$$\log\left(\frac{1}{C}\right) = 2.282\sigma - 0.348$$

**Diethylphenylphosphates**
**(Insecticides)**

**Conclusion**: e-withdrawing substituents increase activity

## Electronic Factors *R* & *F*

- ***R*** **- Quantifies a substituent's resonance effects**
- ***F*** **- Quantifies a substituent's inductive effects**

## Aliphatic electronic substituents

- Defined by $s_I$
- Purely inductive effects
- Obtained experimentally by measuring the rates of hydrolyses of aliphatic esters
- Hydrolysis rates measured under basic and acidic conditions

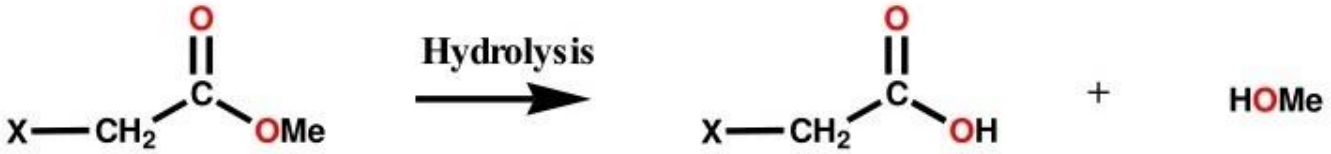


X= electron donating  Rate ↓  $s_I$ = -ve

X= electron withdrawing  Rate ↑  $s_I$ = +ve

**Basic conditions:** Rate affected by steric + electronic factors
Gives $s_I$ after correction for steric effect

**Acidic conditions:** Rate affected by steric factors only (see $E_s$)

# Steric Factors

## Taft's Steric Factor ($E_s$)

- Measured by comparing the rates of hydrolysis of substituted aliphatic esters against a standard ester under acidic conditions

$E_s = \log k_x - \log k_o$

$k_x$ represents the rate of hydrolysis of a substituted ester

$k_o$ represents the rate of hydrolysis of the parent ester

- Limited to substituents which interact sterically with the tetrahedral transition state for the reaction
- Cannot be used for substituents which interact with the transition state by resonance or hydrogen bonding
- May undervalue the steric effect of groups in an intermolecular process (i.e. a drug binding to a receptor)

# HUBUNGAN STRUKTUR AKTIVITAS OBAT DENGAN METABOLISME

Arief Kusuma Wardani, S.Si., M.Pharm.Sci

Universitas Muhammadiyah Magelang

# Metabolisme Obat

- Metabolisme obat penting karena proses2 transformasi obat mjd metabolitnya sangat mempengaruhi lama kerja (durasi) suatu aksi/efek farmakologis suatu obat.

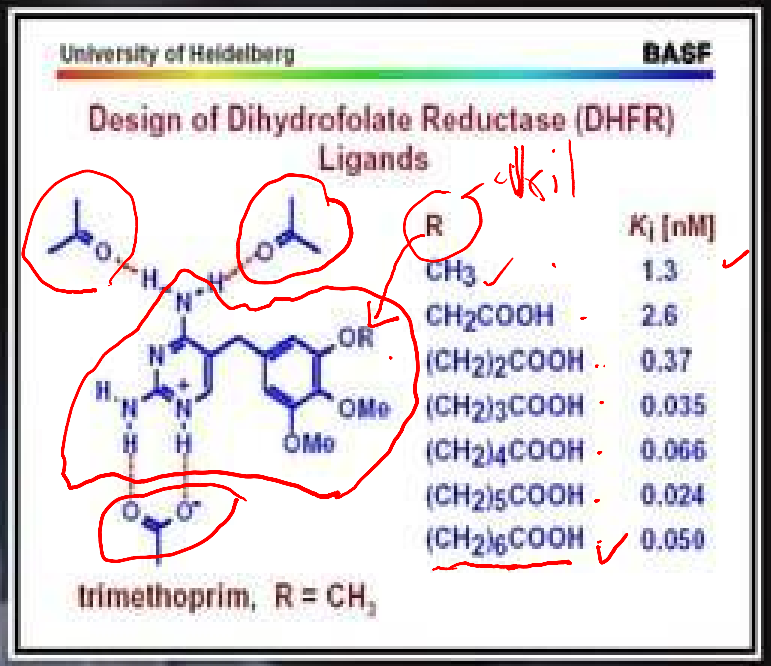


- Juga dpt melihat kemungkinan terbentuknya metabolit yg aktif (farmakologis aktif) dan mengetahui tentang bagaimana bentuk metabolit yg akan dieliminasi

# PROSES METABOLISME OBAT

I. Tujuan Umum

a. Mengubah obat mjd metabolit :

- aktif (bioaktivasi)
- tidak aktif (bioinaktivasi)
- toksik (biotoksifikasi)

b. Mudah diekskresikan

# II. Manfaat Metabolisme Obat

a. Efikasi dan keamanan
b. Pengaturan dosis
c. Bahaya zat pengotor
d. Evaluasi toksisitas
e. Pengembangan proses metabolisme
f. Dasar penjelasan proses toksik

# III. Jalur Respon Obat

a. Langsung ke “site of action” → respon biologis
b. Tidak aktif → metabolisme → aktif → “site of action” → respon biologis

# Contoh bioaktivasi & bioinaktivasi

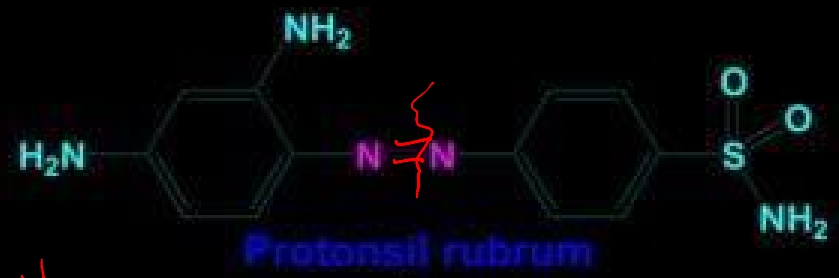


Protonsil rubrum

*in vitro* : tidak aktif
*in vivo* : aktif

reduksi : bioaktivasi


Benzene-1,2,4-triamine

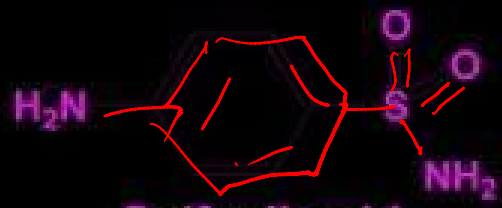


Sulfanilamid

*in vitro* : aktif
*in vivo* : aktif

Asetilasi : bioinaktivasi

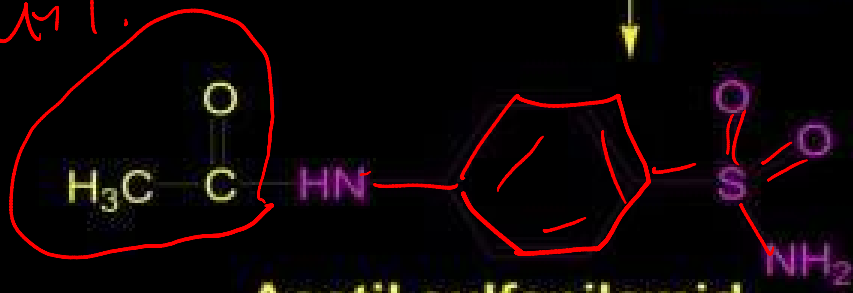


Asetil sulfanilamid

*in vitro* : tidak aktif
*in vivo* : tidak aktif

# Contoh bioaktivasi & biotoksifikasi

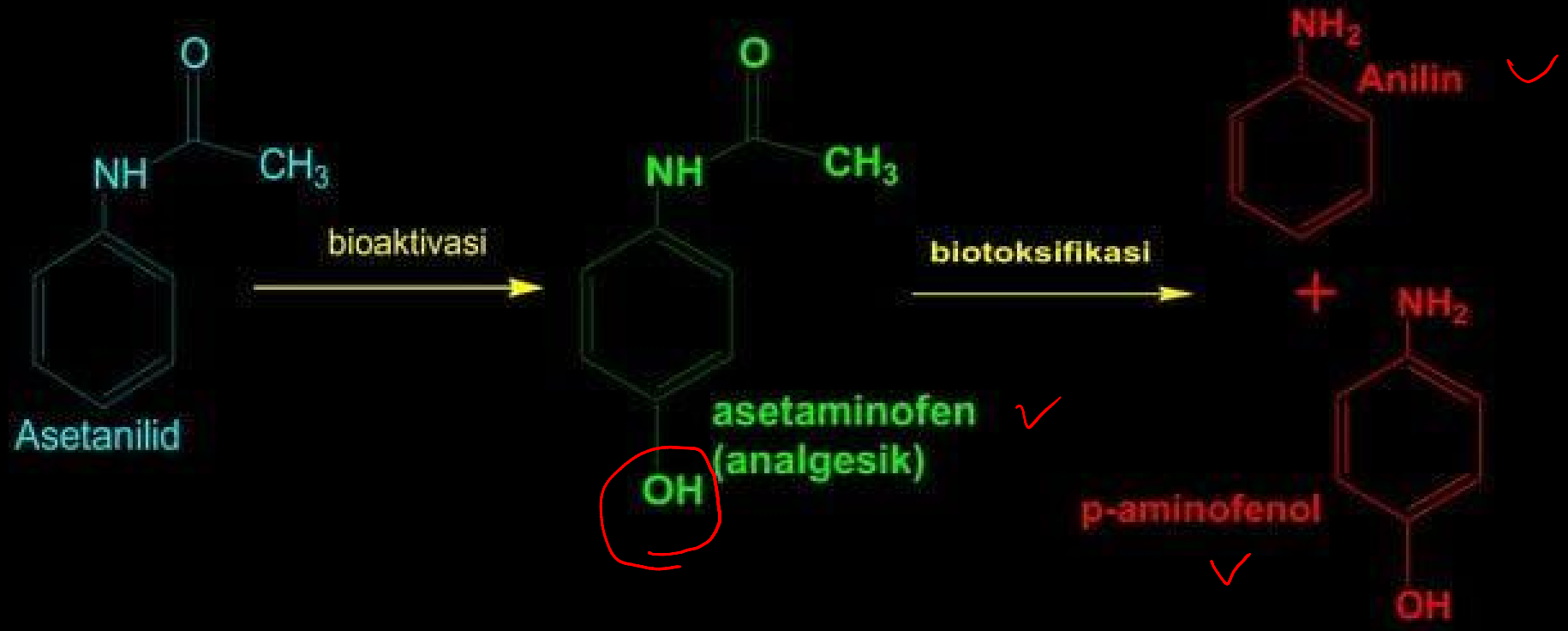

# Contoh Obat yang Hasil Metabolismenya mempunyai :

- Efek farmakologis berbeda dgn senyawa induk


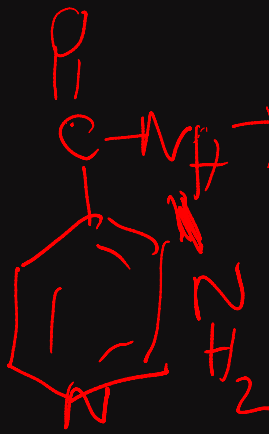

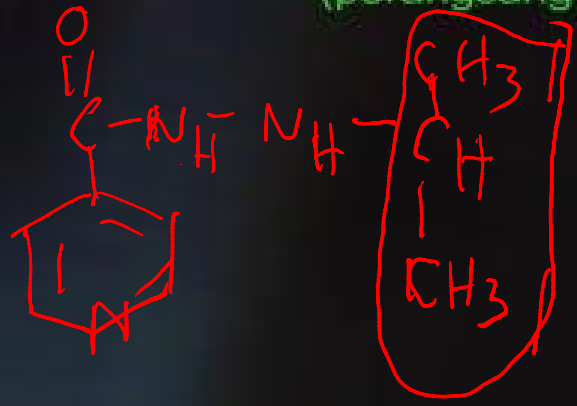

N = penghilangan gugs alkil

# Contoh hasil metabolisme

- Bbrp syw tdk mengalami proses metabolisme dan diekskresikan dari tubuh dlm bentuk tdk berubah

  a. Syw yg tdk larut dlm cairan tubuh, tdk diserap ole saluran cerna dan tahan thd pengaruh kimiawi dan enzimatik saluran cerna. Syw ini lgs dikeluarkan melalui tinja. Contoh : $BaSO_4$ dan oleum ricini

  b. Syw yg mdh larut dlm cairan tubuh dan tahan thd pengaruh kimiawi dan enzimatik. Syw ini relatif tdk toksik dan cepat dikeluarkan melalui urin. Contoh : Asam mandelat, asam sulfonat alifatik, dan aromatik

# Tempat Metabolisme

A. Jaringan
B. Organ : hati, usus

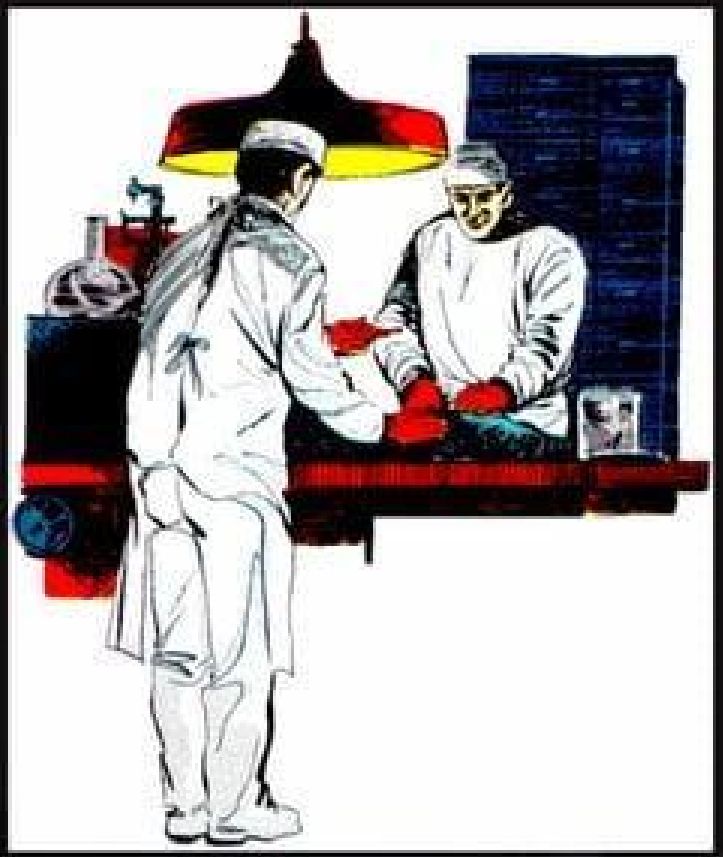

# Faktor2 yg mempengaruhi metabolisme Obat

a. Genetik/Keturunan
b. Perbedaan spesies dan galur
c. Perbedaan jenis kelamin
d. Perbedaan Umur
e. Penghambatan enzim metabolisme
f. Induksi enzim metabolisme
g. Faktor lain

# Cytochrome P450

Enzim yang ditemukan berada di hati

Cytochrome P450 meiliki peran yang luas, dalam metabolisme

-hormon steroid mengalami biosintesis dari kolesterol

-metabolisme **xenobiotics**-senyawa-senyawa yg tdk umum ditemukan dalam tubuh

-obat-obatan

-senyawa yang dihasilkan dalam produksi makanan, melalui proses pemasakan (hidrokarbon poliaromatik, juga asap tembakau) atau mikroorganisme

-umumnya utk senyawa-senyawa organik yang kurang larut dalam air

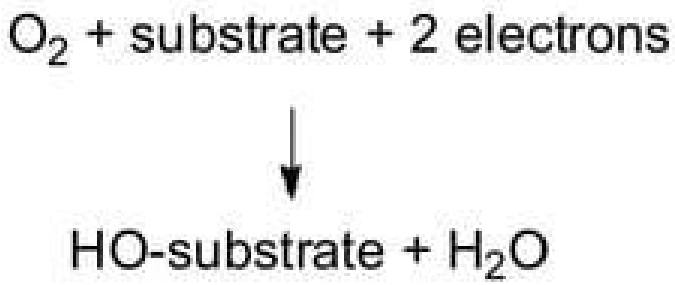


**monooxygenase**

## Cytochrome P450 contains heme.

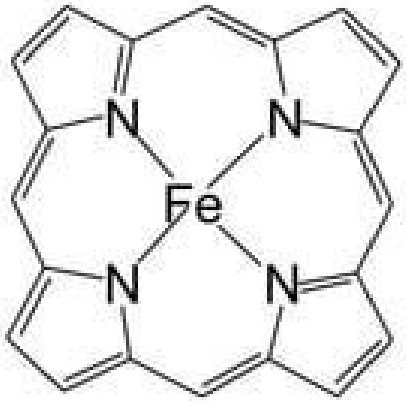


Heme

# Cytochrome P450

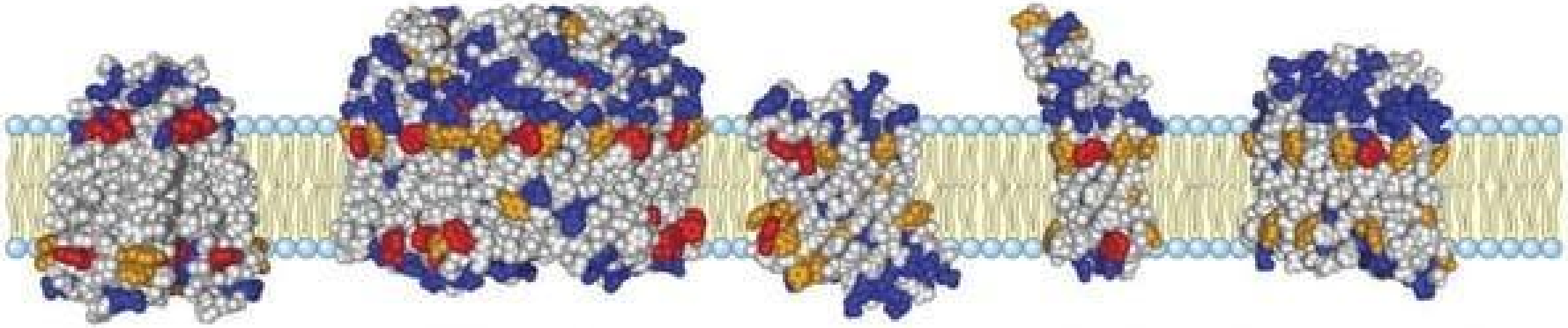

$K^+$ channel | Maltoporin | Outer membrane phospholipase A | OmpX | Phosphoporin E

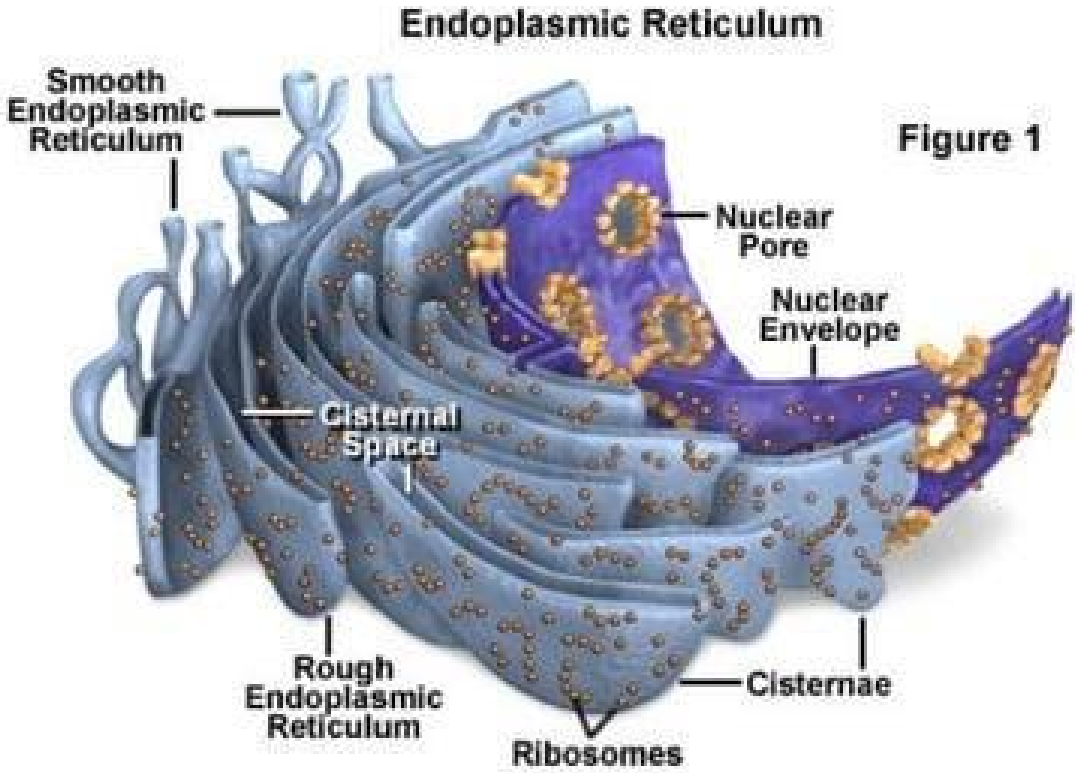


http://micro.magnet.fsu.edu/cells/endoplasmicreticulum/endoplasmicreticulum.html

# Tugas Belajar Mandiri

- Metabolisme Obat
- Contoh-contoh reaksi pada fase 1 dan 2
- Dikumpulkan minggu depan
- Bisa ditanyakan pada UTS
- Bobot: 5-10 % dari nilai akhir

# HUBUNGAN STRUKTUR AKTIVITAS

# ANTIBIOTICS

Arief Kusuma Wardani, S.Si., M.Pharm.Sci

Universitas Muhammadiyah Magelang

2024

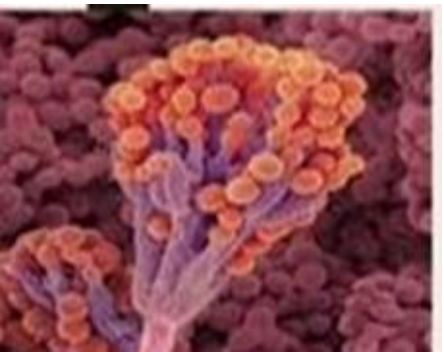

# HISTORICAL BACKGROUND

- In 1877 Louis Pasteur discovered inhibition of some microbes by other microbes during research on anthrax.
- 1908 Gelmo synthesized sulfanilamide (1st sulfonamide)
- 1910 –Paul Ehrlich for selective stains of microbes coined the terms a 'magic bullets' , "chemotherapy" or "chemical knife".
- 1913 – Eisenberg studied bactericidal properties of azo dyes with sulfonamide group.
- 1928 – Penicillin was discovered by Alexander Fleming
- 1932 – Ehrlich discovered antimicrobial activity of sulphonamides.
- 1943 – Drug companies started production of penicillins.

- 1948 – Cephalosporins were synthesized by Oxford university
- 1952 – Erythromycin derived from Streptomyces erythreus
- 1956– Vancomycin introduced for penicillin resistant species.
- 1962 – Quinolone antibiotics were first discovered.
- 1980 – Fluoro quinolones were discovered and become clinically useful

  Eg: Ciprofloxacin
- 2000 – Macrolide antibiotics introduced into clinical practice.

# HISTORY OF PENCILLINS

- Penicillin was discovered by Alexander Fleming in 1928 ,who noticed that one of his experimental cultures of staphylococcus was contaminated with mold or fungi(yeast).
- This mold caused the bacteria to lyse. Since mold belongs to the family penicillium.Fleming named the compound as penicillin.
- Penicillin is obtained from "Penicillium notatum".
- Alexander Fleming got nobel prize for explaining 'Penicillin is a chemical extract obtained from Penicillium notatum which stops the growth of other microbes'.
- Few years later,group of researchers in oxford university discovered Penicillin V,F,G,K,O,X.

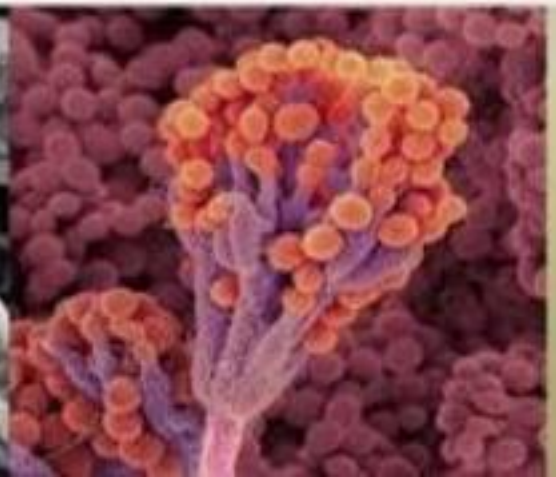

- Florey & Chain – introduced the penicillins for chemotherapy.
- Waksman - In 1942 given definition for antibiotics.

## ANTIBIOTICS –DEFINITION:

- These are the chemical substanes produced by microorganisms which has the capacity of inhibiting the growth or even destoying other microorganisms (Waksman definition).
- Antibiotics are the chemical substances or drugs produced by living organisms or marine sources which will inhibit the growth of other microorganisms in small concentrations and kill the microorganisms in high concentration.
- Antibiotics are not effective against viral infections.
- Antibiotics also includes synthetic and semisynthetic antimicrobial compounds.

  Eg: Chloramphenicol and sulphonamides.

# CLASSIFICATION

Antibiotics are classified into :

1. Based on spectrum of activity.
2. Based on the source of origin.
3. Based on mechanism of action.
4. Based on chemical structure.

- BASED ON SPECTRUM OF ACTIVITY & DEGREE OF SELECTIVITY:

1. Narrow spectrum antibiotics: High degree of selectivity towards single species of microorganism.

Eg: Nystatin ,Bacitracin.

2. Broad Spectrum antibiotics: They inhibit the growth of gram +ve and gram –ve bacteria including different species of microorganisms.

Eg: Tetracyclines and chloramphenicol

- Based on the source from which antibiotics are obtained they are classified as:

1. NATURAL ANTIBIOTICS: They are obtained from the fermentation of microorganisms.

Eg: Bacitracin ,Polymixin-B

2.SEMISYNTHETIC ANTIBIOTICS: They are produced commercially by addition of chemical agent to produce final products.

Eg: Penicillin G or V

3.SYNTHETIC ANTIBIOTICS: Antibiotics which have purely synthetic origin.

Eg: Chloramphenicol

- BASED ON MECHANISM OF ACTION

1. Drugs that interfere with biosynthesis of bacterial cellwall.

   Eg: Cephalosporins,Penicillins,Viomycin,Cycloserin

2. Drugs that interfere with the functioning of cytoplasmic membrane.

   Eg: Nystatin,Amphoterecin-B,Polymixin

3.Drugs that interfere with the protein synthesis of bacteria.

   Eg: Chloramphenicol,Erythromycin,Aminoglycosides,Tetracyclines.

4.Drugs that interfere with the nucleic acid biosynthesis.

   Eg: Actinomycin,Griseofulvin,Rifamycin,Mitomycin

- BASED ON CHEMICAL STRUCTURE:

1. Beta-lactam antibiotics: Drugs that contain β lactam ring in the structure.

   Eg: Pencillins,Cephalosporins,Monobactams, β –lactamase inhibitors.

2. Aminoglycoside antibiotics : Drugs that contain sugar moieties with aminogroups.

   Eg: Streptomycin , Gentamycin,Neomycin,Kanamycin

3. Tetracyclines: Drugs that contain four cyclic compounds.

   Eg: Chlortetracycline and oxytetracycline ,doxycycline

4. Peptide antibiotics: Drugs that contain amino acid groups.

   Eg: Bacitracin,Amphoterecin

5. Macrolides: Drugs that contain macrocyclic ring with lactone groups.

   Eg: Erythromycin, Azithromycin

6. Licomycins: Drugs that contain more than 16 atoms

   Eg: Licomycin and clindamycin

7. Antifungal antibiotics: Drugs used to treat fungal infections.

   Eg: Griseofulvin

8. Miscellaneous: Eg: Chloramphenicol

# PENICILLINS

Penicillium notatum

- Penicillin is a secondary metabolite produced by various bacteria.
- Penicillins are β-lactam antibiotics.
- A bacterial infection is caused by millions of tiny bacteria that are trying to survive by multiplying in the host.Antibiotic attacks and kill this bacteria.
- Penicillin is used as an antibiotic.It was obtained from "Penicillium notatum",now it is extracted from "Penicillium chrysogenum".
- Before the development of penicillin,many people suffered and died from bacterial infections.
- Alexander fleming discovered Penicillin in 1928.
- Penicillin G is the first antibiotic (penicillin)introduced into chemotherapy.

Penicillium chrysogenum

# Nomenclature of penicillins

- Penicillins are called as β-lactam antibiotics
- The basic structure of penicillins is:

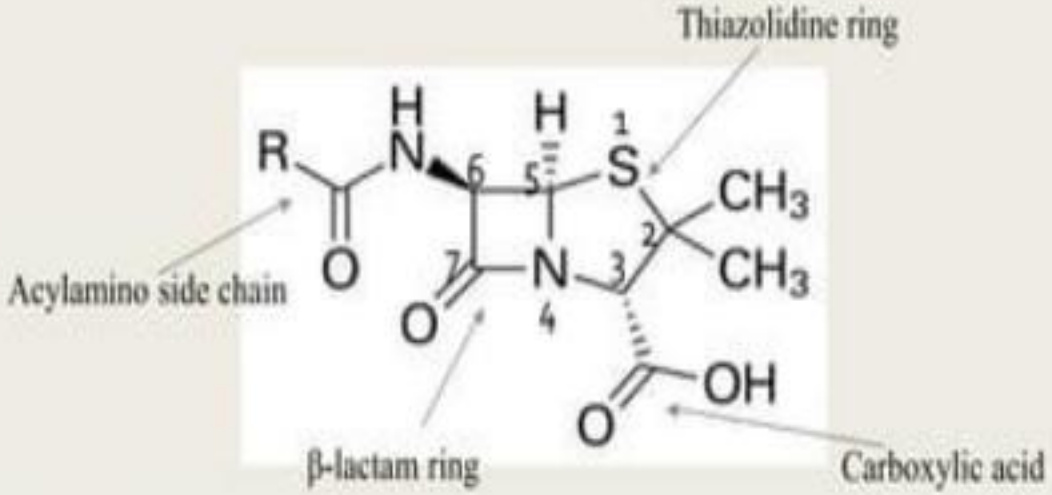


- According to chemical abstract system numbering starts 'S' atom and assigned as 1 &N is assigned as 4.
- Name of penicillin is 6-Acyl amino -2,2-dimethyl 3-carboxylic acid penam.

# Stereochemistry of penicillins

- Penicillin structure contains three chiral carbons at $C_3$ , $C_5$ &$C_6$.

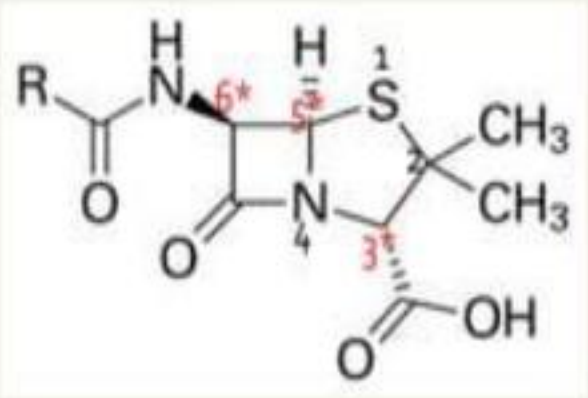


- $C_6$ -is showing L configuration, $C_3$ and $C_6$ chiral centers are trans to each other (facing opposite to each other).
- All synthetic and semi synthetic penicillin have same absolute configuration that of natural. 3S:5S:6R

# SAR of penicillins

- At position 1 ,if sulfur atom is oxidized to sulphone or sulphoxide decreases the activity of the compound.
- Methyl groups are necessary for activity at position 2 .
- Replacement of methyl groups decreases the activity.
- At 3rd position, carboxylic group of the thiazolidine ring

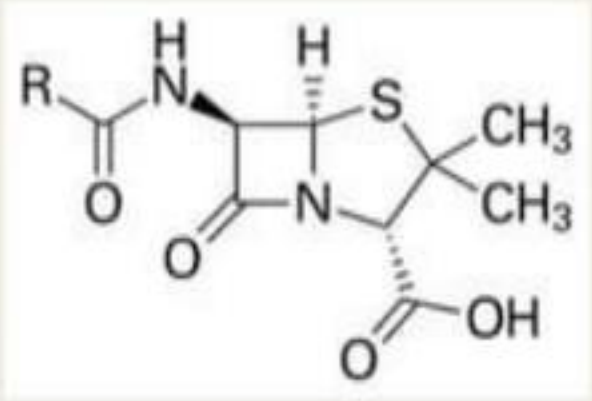


is required for the antibacterial activity.

- Replacement of carboxylic group with ether or alcohol group decreases the activity.
- β-lactam ring is required for the antibiotic activity.
- N atom is must for penicillins.
- No substitution is allowed at 5th position.
- Amide side chain with R group(either alkyl or aryl group) is essential for antibiotic activity.

# Penicillin structures and its uses

BENZYL PENICILLIN (Penicillin G)

Structure:

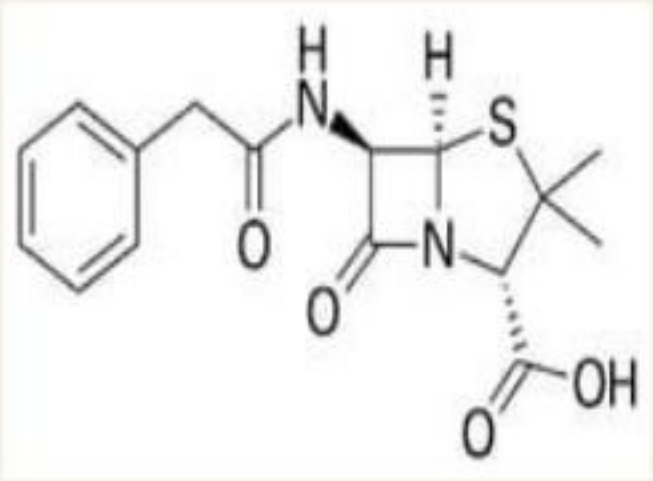


Uses: 1.Narrow spectrum antibiotic

2.Used to treat various bacterial infections caused by streptococci, meningococci, gram+ve bacilli and spirochetes species.

3. strains of Staphylococcus and Nesseiria gonnorhoea species are shows resistant by releasing β – lactamase enzyme.

## PHENOXY METHYL PENICILLIN (PENICILLIN V)

Structure:

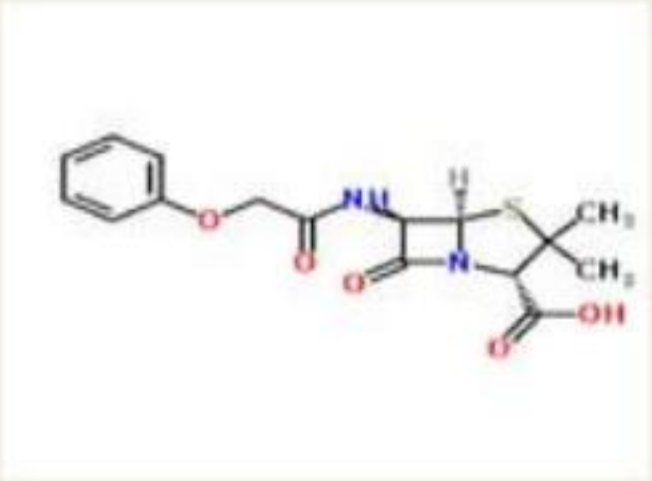

Uses: 1.Penicillin V is effective for the treatment of laryngitis,bronchitis,pneumonia,soft tissue and skin infections caused by susceptible bacteria.

2. To treat reoccurance of rheumatic fever

3.It is effective to treat oral cavity infections.

## AMOXYCILLIN

Structure:

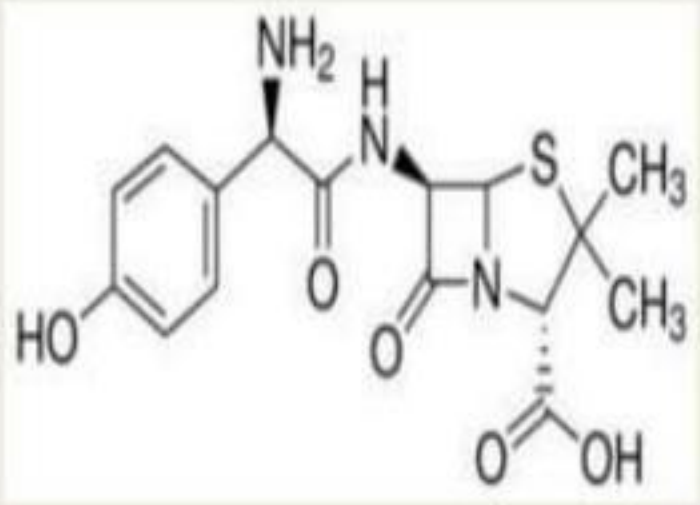


Uses: 1.To treat sinusitis and other upper respiratory tract infections

2.To treat urinary tract infections.

3.Prophylaxis treatment of bacterial endocarditis.

4.Amoxycillin is effective to treat bacterial infections of ear,nose,throat and tonsillitis.

## CLOXACILLIN

Structure:


Uses: 1.Cloxacillin is active against gram-ve bacterial infections as well.

2.It is used to treat bacterial infections of bone,heart valve,lungs,skin,blood.

3.To treat staphylococcal infections ,which are resistant to benzyl penicillin.Cloxacillin is less active than Penicillin G.

AMPICILLIN

Structure:

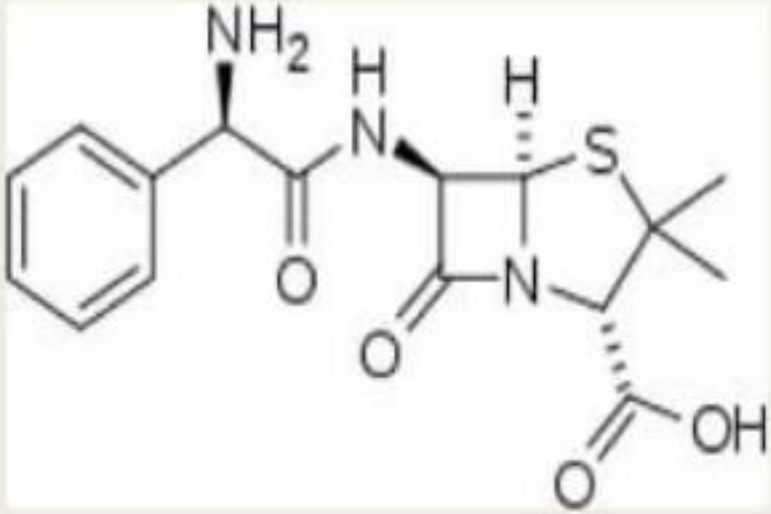


Uses: 1. Ampicillin is used in the therapy of meningitis along with 3rd generation cephalosporins.

2.Ampicillin + Gentamycin can be given to treat pneumonia,gram- ve infection.

3.To treat hepatic encephalopathy.

4.To treat biliary tract infection.

# SIDE EFFECTS &TOXICITY

- Allergy
- Hypersensitivity reactions
- Bleeding
- Degenerative changes in the spinal cord
- Convulsions
- Rashes,itching,urticaria &fever
- Wheezing
- Angioneurotic edema
- Serum sickness
- Exfoliative dermatitis
- Anaphylaxis is rare

Angioneurotic edema

Disc degeneration

Exfoliative dermatitis

# MECHANISM OF ACTION

- Penicillins interferes withthe synthesis of bacterial cellwall.
- Cellwall is composed of peptidoglycan layer,which consists of two amino sugars

  1.N-Acetyl muramic acid(NAcM)

  2.N-acetylglucosamine(NAcG)
- Peptidoglycan residues are linked together forming long strands &UDP is split off.
- Then the cleavage of terminal-D alanine of the petide occurs by transpeptidase enzyme.This process is called transpeptidation.
- The cross brindging provides necessary strength to bacterial cell wall.

- β- lactam antibiotics inhibit the transpeptidase enzyme so that cross-linking does not takes place.
- This leads to formation of cellwall deficient bacteria and causes shrinkage of the bacterial cell.
- Penicillins shows bactericidal action.

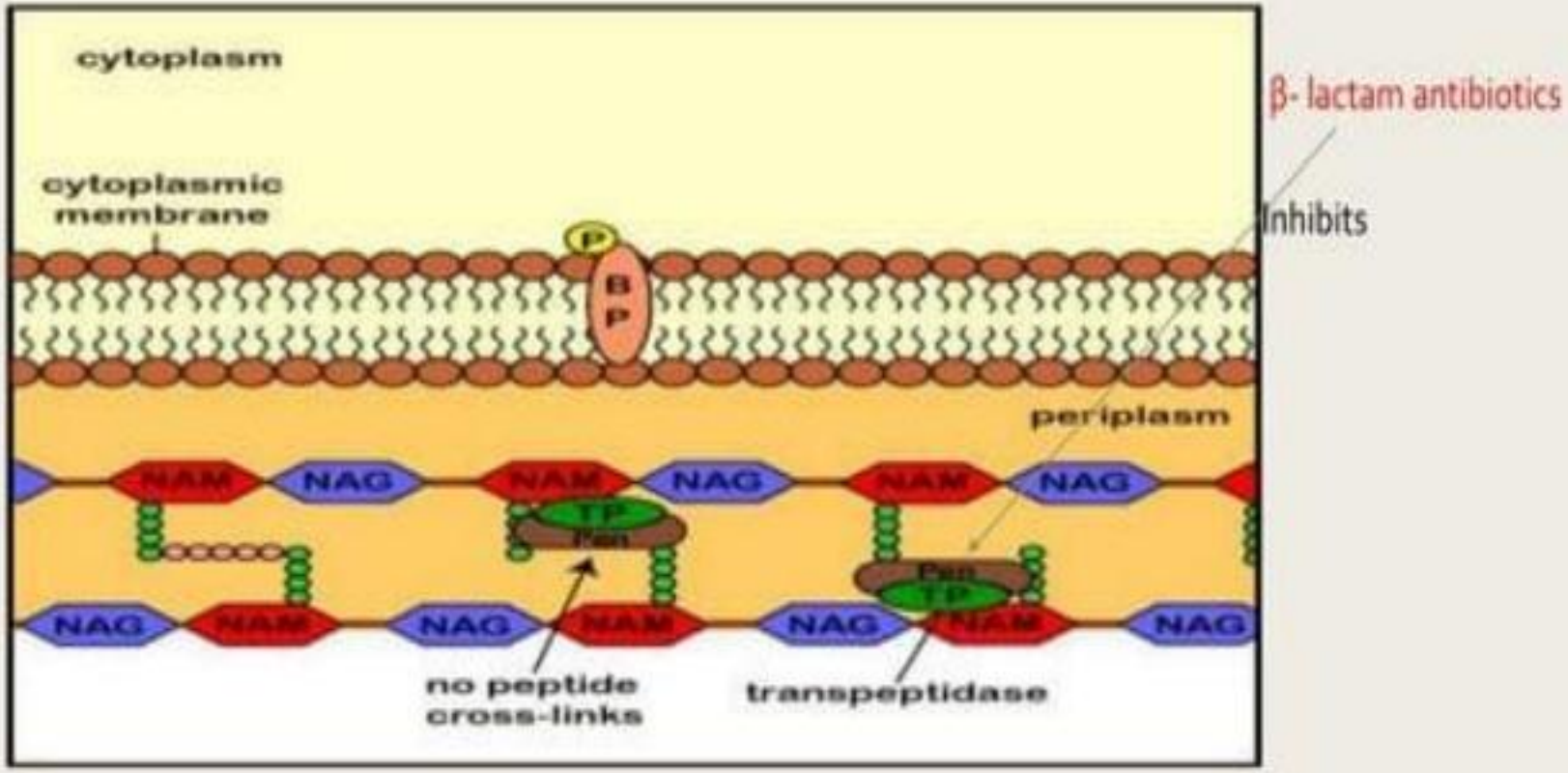

# CHEMICAL DEGRADATION OF PENICILLINS

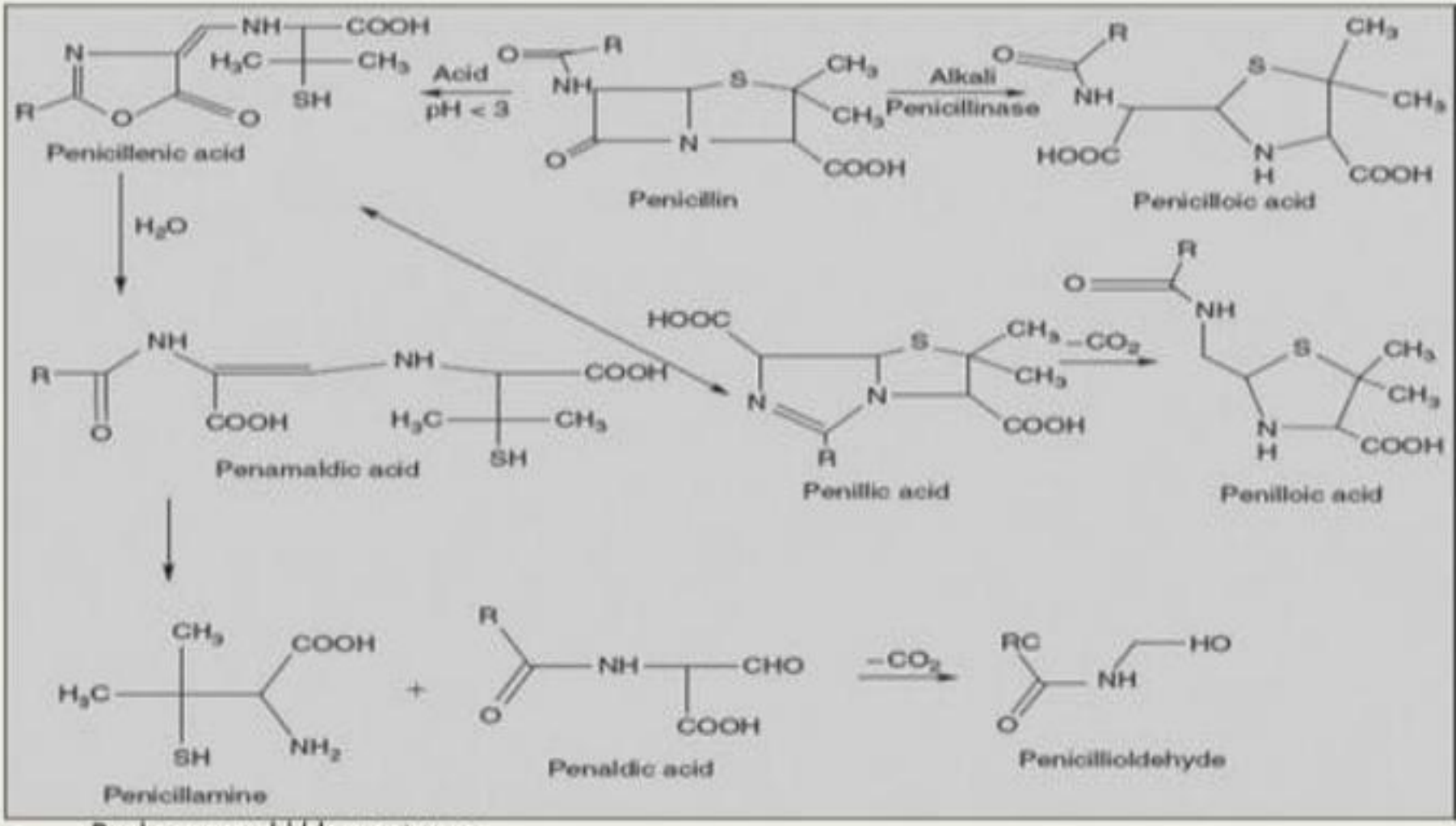

- Degradation of penicillins takes place in alkaline ,acidic conditions,in the presence of enzyme-β-lactamase and in the presence of nucleophiles like $H_2O$ and metal ions.
- Chemical degradation of penicillins gives: Penicilloic acid
  Penicillenic acid
  Penamaldic acid
  Penillic acid
  Penilloic acid
  Penicillamine
  Penaldic acid
  Penicillioldehyde

# CEPHALOSPORINS

- Cephalosporin-C was isolated by Guy Newton &Edward Abraham.
- Cephalosporins are β- lactam antibiotics containing β- lactam ring fuse with thiazine heterocyclic group.
- Cephalosporins were isolatedby an Italian scientist 'Giuseppe Brotzu' from cultures of "Cephalosporium acremonium",a fungus .
- He noticed that they are effective against Salmonella typhi (typhoid fever),which had β- lactamases.


# SAR of Cephalosporins

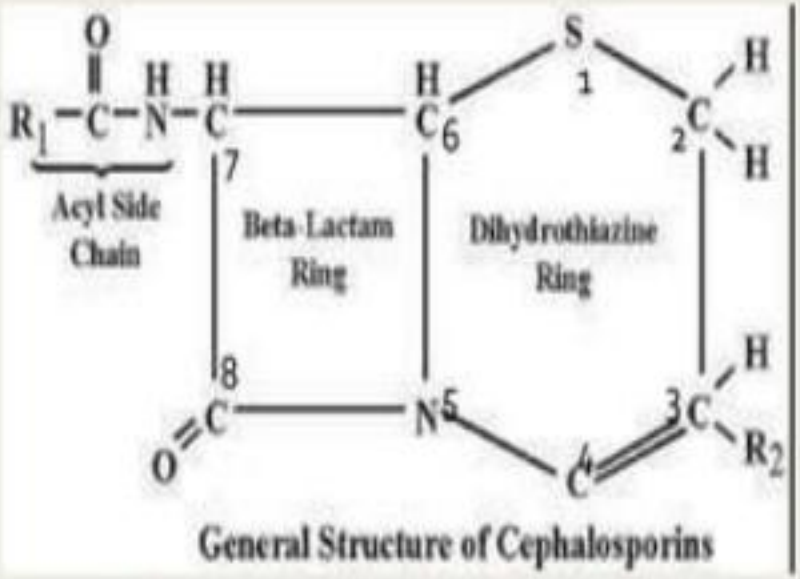


General Structure of Cephalosporins

1.β-lactam ring is fused with dihydrothiazine ring is required for the antibiotic activity.The entire ring is called as Cepham.

2.Substitution at 7th position of β-lactam ring alters the spectrum of activity of various cephalosporins.

3.At 3rd position of dihydrothiazine ring ,substitution with various groups shows pharmacokinetic properties of cephalosporins.

# Classification of cephalosporins

- Cephalosporins are classified into five generations.

1.First generation cephalosporins:

Cephalexin,Cephradine,Cefadroxil,Cephalothin,cefapirin

2.Second generation cephalosporins:

Cefuroxime,Cefoxitin,Cefaclor

3.Third generation cephalosporins:

Cefixime,Cefpodoxime,Ceftriaxone,Cefoperazone

4.Fourth generation cephalosporins:

Cefepime,Cefpirome,cefquinome

5.Fifth generation cephalosporins:

Ceftobiprole,ceftaroline,ceftolozane

- First generation cephalosporins are active against gram+ve bacterial strains,with succeeding generations progressively more active against gram –ve bacterial strains
- Fourth generation cephalosporins are extended spectrum antibiotics.

# Structures and its uses


CEPHALEXIN

Structure:

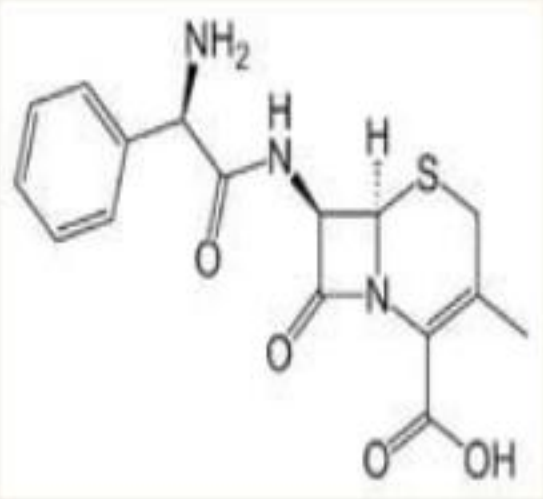


Uses: 1.First generation cephalosporin

2.To treat infections caused by gram+ve bacteria .

3.To treat upper respiratory tract infections,ear,skin,urinary tract and bone infections.


## CEFADROXIL

Structure:

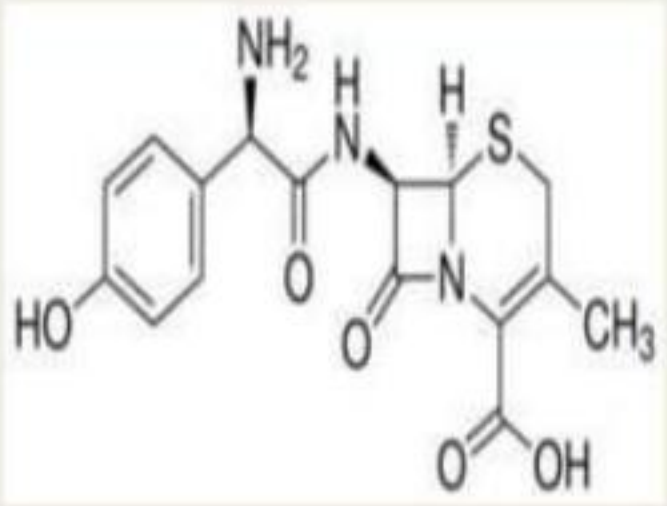


Uses: 1.First generation cephalosporin used to treat bacterial infections

2.To treat infections of throat,skin and urinary tract.

3.Used to treat gram+ve bacterial infections.

## CEFIXIME

Structure:

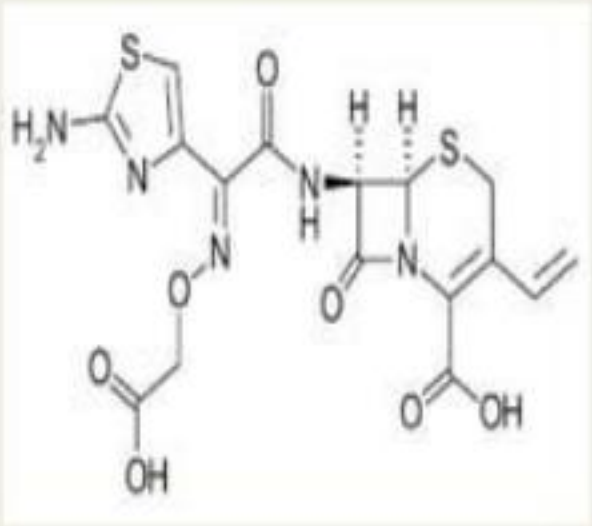


Cefixime capsules

Uses: 1.Cefixime is a third generation cephalosporin.

2.It is effective against both gram +ve and gram-ve bacterial infections.

3.Cefixime is resistant towards β-lactamase enzyme.

4.Used to treat typhoid fever and biliary tract infections.

CEFAPIRIN(CEFAPYRIDINE)

Structure:

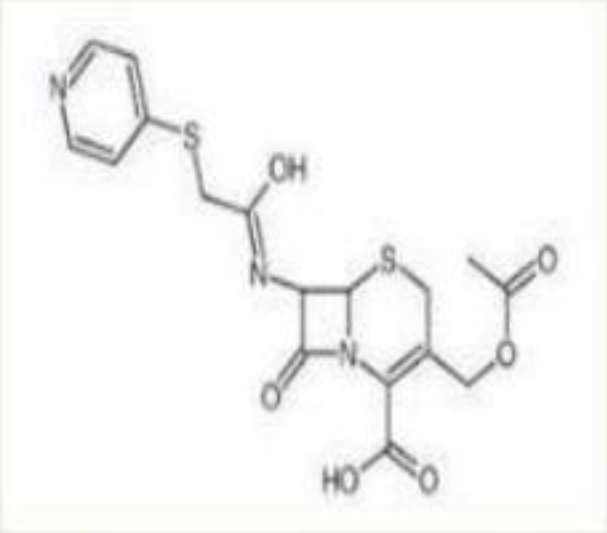


Uses: 1.Cefapirin is a first generation cephalosporin .

2.Cefapirin is combined with prednisolone to use in cattle for maintainig intramammary glands and its production of milk.

3.Cefapirin acts as a intrauterine preparation in cattle.

4.Cefapirin has been banned for usuage on human beings.

## CEFUROXIME(CEFUTROXIME)

Structure:

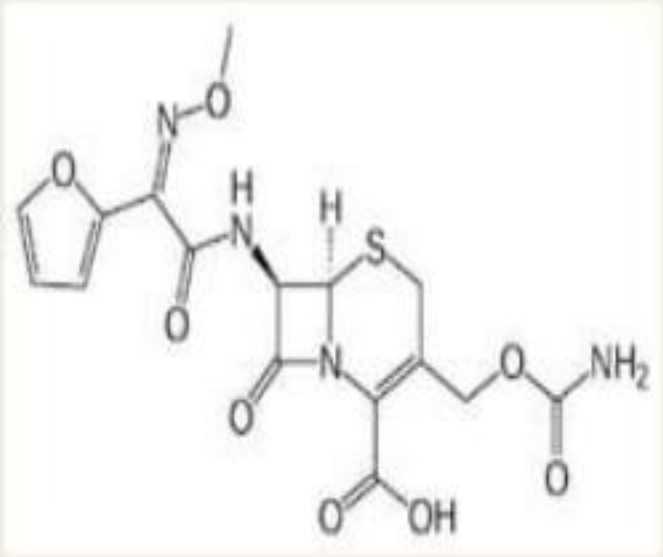



Uses: 1.Cefuroxime is a second generation cephalosporin used to treat gram-ve bacterial infections.

2.Cefuroxime is the safest antibiotic during pregnancy.

3. Used to treat tonsillitis, laryngitis, bronchitis, throat infections, pneumonia, gonorrhea, urinary tract infection caused by susceptible bacteria

# MECHANISM OF ACTION

- Cephalosporins interferes with the synthesis of bacterial cellwall.
- Cellwall is composed of peptidoglycan layer,which consists of two amino sugars

  1.N-Acetyl muramic acid(NAcM)

  2.N-acetylglucosamine(NAcG)
- Peptidoglycan residues are linked together forming long strands &UDP is split off.
- Then the cleavage of terminal-D alanine of the petide occurs by transpeptidase enzyme.This process is called transpeptidation.
- The cross bridging provides necessary strength to bacterial cell wall.

- β- lactam antibiotics inhibit the transpeptidase enzyme so that cross-linking does not takes place.
- This leads to formation of cellwall deficient bacteria and causes shrinkage of the bacterial cell.
- Cephalosporins shows bactericidal action.

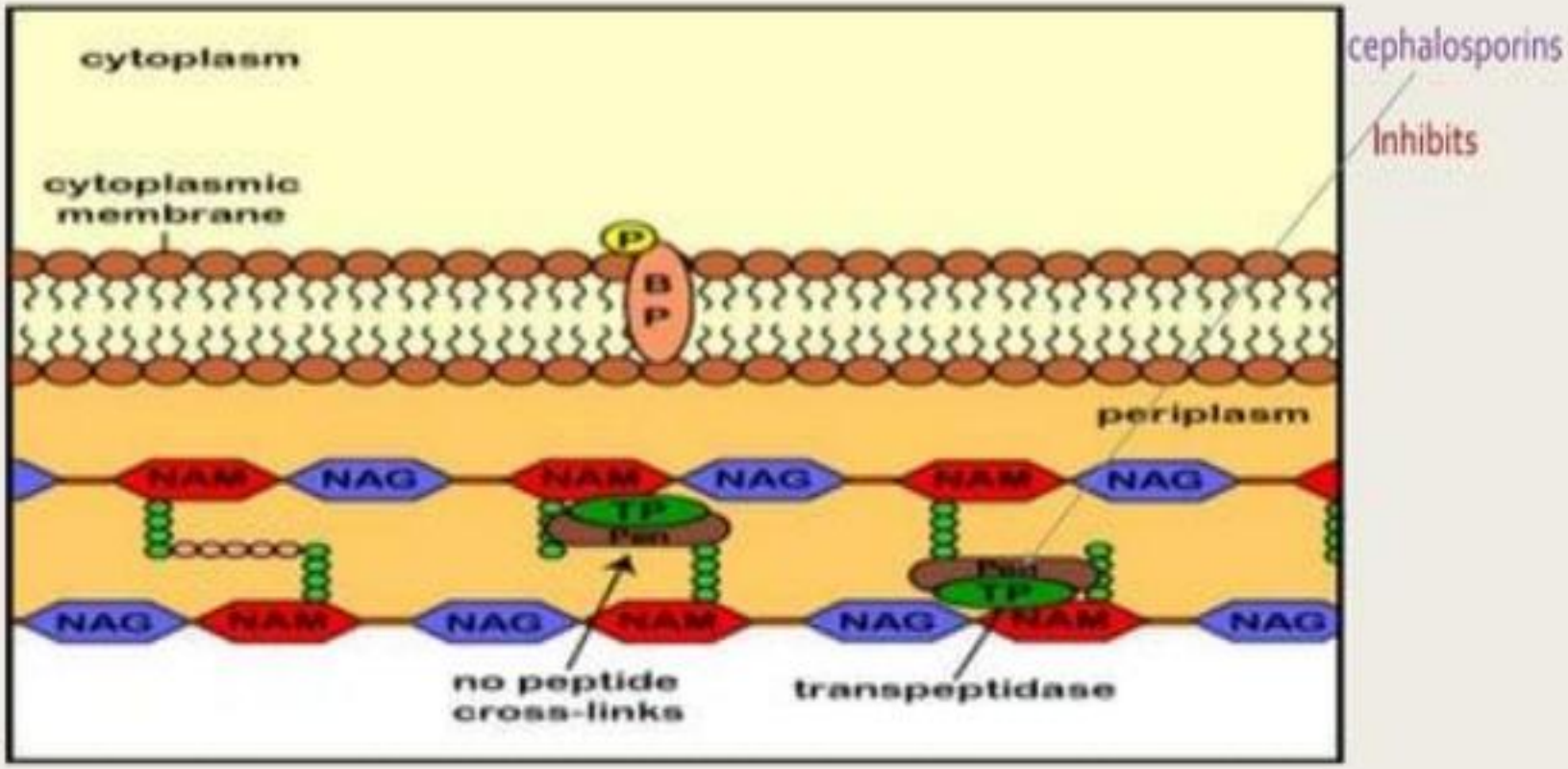

# SIDE EFFECTS AND TOXICITY

- Pain and inflammation at injection site
- Diarrhoea
- Hypersensitivity reactions
- Nephrotoxicity
- Neutropenia and thrombocytopenia
- Bleeding
- Pain on IM injection Eg:Cefalothin
- Nausea and vomiting
- Colitis
- Disulfiram like effects

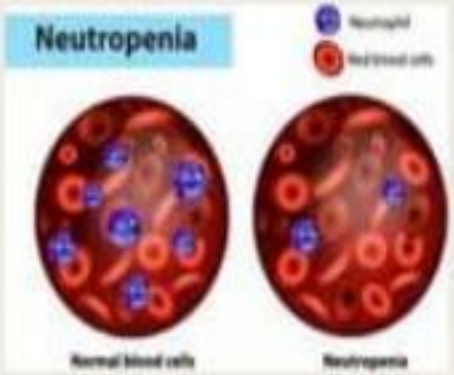


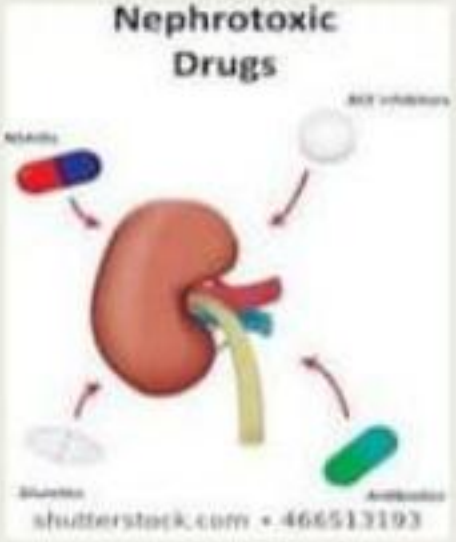

# β- LACTAMASE INHIBITORS

- β- lactamase inhibitors are a class of antibiotic drugs that blocks the activity

of β- lactamase enzyme ,which is responsible for degradation of β- lactam antibiotics.

- β- lactamase inhibitors prevents the degradation of β- lactam antibiotics by acting on bacterial microorganisms.

Eg: Clavulanic acid

Thienamycin

# CLAVULANIC ACID

- Structure:

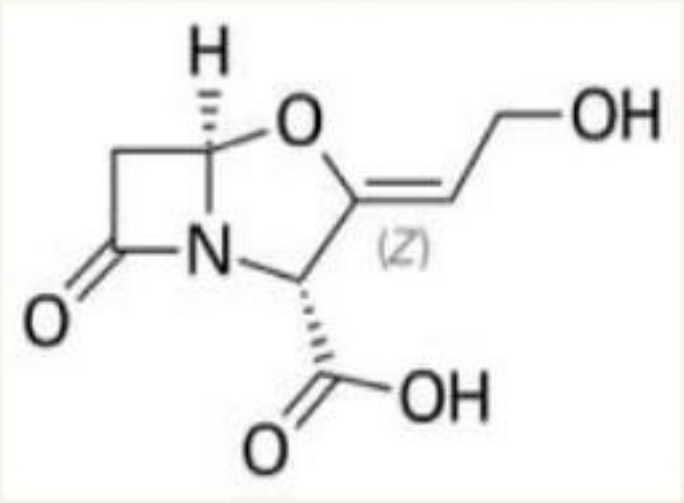


- Uses: 1.Amoxycillin – clavulanic acid is a combination used to treat variety of bacterial infections.

  2. It stops the growth of bacteria.

# THIENAMYCIN

- Structure:

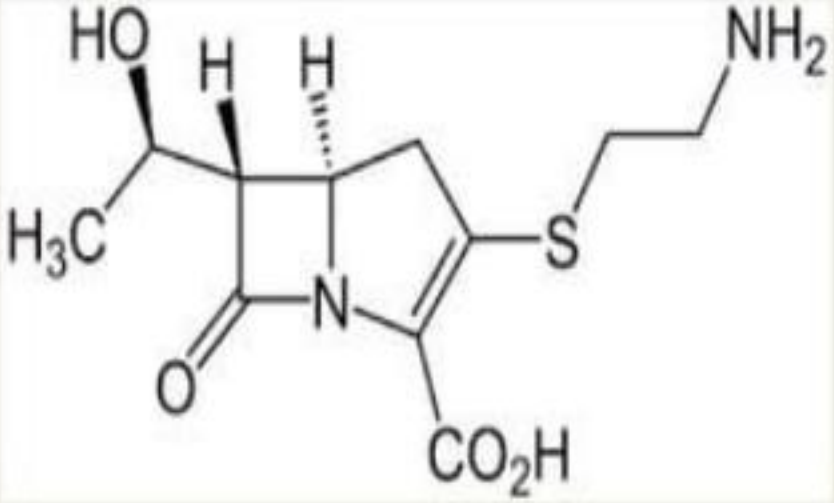


- Uses: 1.It is a naturally produced β- lactamase inhibitor.

  2.Thienamycin antibiotic is produced from "streptomyces cattleya" .

  3.Used to treat gram positive and gram negative bacterial infections.

# MECHANISM OF ACTION

- All β- lactam antibiotics interfere with the synthesis of bacterial cell wall peptidoglycan.
- After attachment to penicillin binding proteins on bacteria,they inhibit the transpeptidation enzyme that crosslinks the peptide chains attached to the backbone of the peptidoglycan.
- The final bactericidal action is the inactivation and inhibition of autolytic enzymes(β-lactamase)in the cellwall ,leading to lyse of the bacterium.
- Some tolerable microorganisms have defective autolytic enzymes in which lysis does not occur.

# MONOLACTAMS

- Monolactams are monocyclic and bacterially produced β- lactam antibiotics.
- The β- lactam ring is not fuse to another ring.
- Monolactams are effective only against aerobic gram negative bacteria.
- Monolactams are also called as monobactams.

  Eg: Sulfazecin

  Aztreonam

  Tigmonam

- Mechanism:Monolactams inhibit bacterial growth by interfering with the transpeptidation reaction of bacterial cell wall synthesis.Monolactams covalently bind to penicillin binding protein (PBP) to prevent growth of the cellwall via peptidoglycan synthesis.

# SULFAZECIN

- Structure:

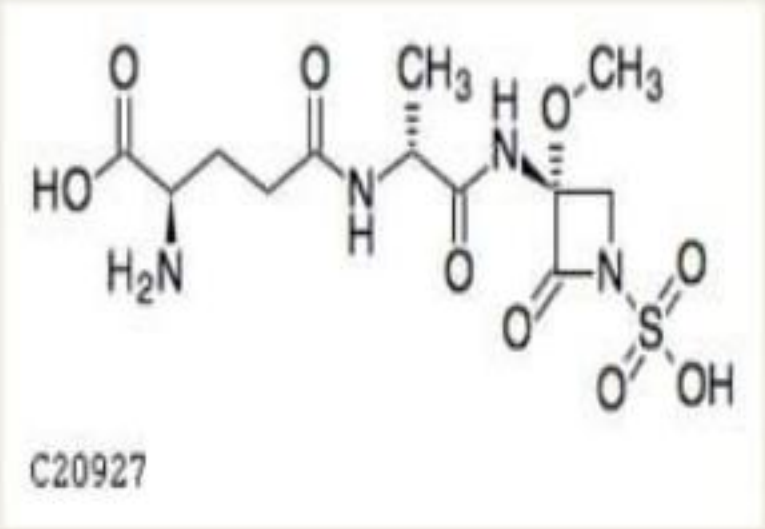


- Uses: It is active against gram negative bacteria and its infections.

# AZTREONAM

- Structure:

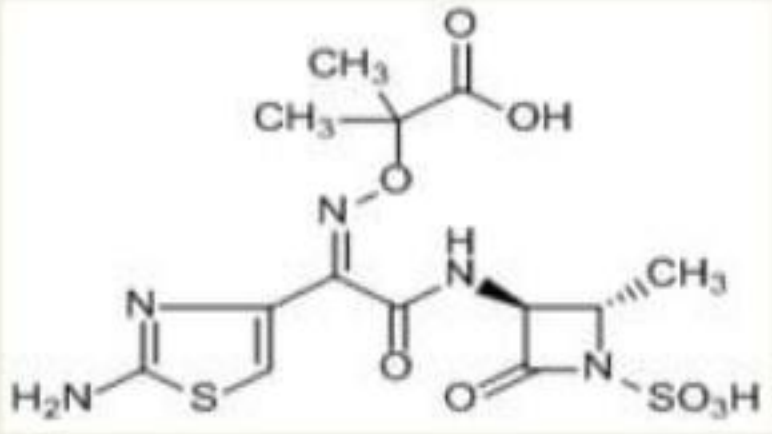


- Uses: 1.To treat sepsis

2.To treat respiratory,urinary,biliary ,gastrointestinal and female genital tract infections.

3.Aztreonam is active against aerobic gram negative bacteria.

# TIGMONAM

- Structure:

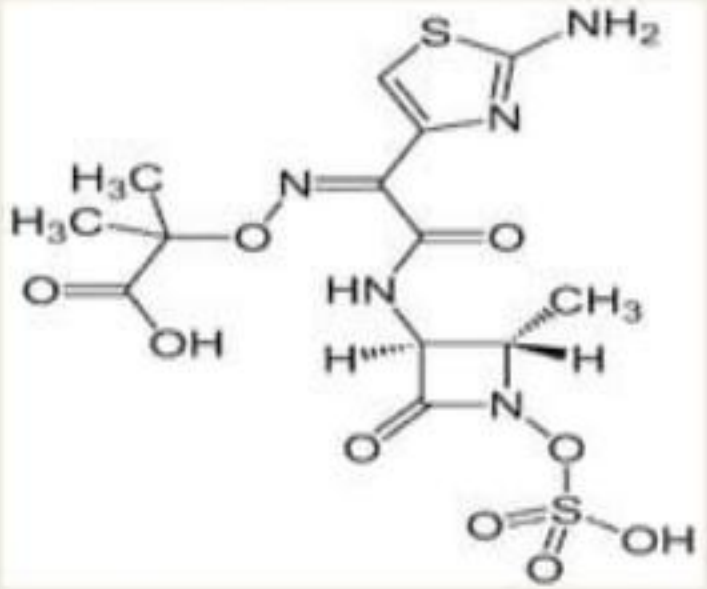


- Uses: 1. Orally active monobactam

  2.Highly resistant to β- lactamase enzyme.

  3.Tigmonam is active against Enterobacter, E.coli, Klebsiella, Proteus infections.

# AMINOGLYCOSIDES

DEFINITION:

- Aminoglycosides are a group of natural and semisynthetic antibiotics having polybasic amino groups linked glycosidically with two or more aminosugars.
- Aminoglycosides are used to treat various bacterial infections caused by gram negative bacteria.
- Aminoglycosides can be combined with penicillins or cephalosporins to show prolonged attack on gram –ve bacterial infections.
- They shows antibiotic action by inhibiting the bacterial protein synthesis.
- The drug will break down in the stomach without showing antibiotic activity through oral route but it shows better activity through parentral route.
- Examples of aminoglycosides are:

  Streptomycin,Amikacin,Neomycin,

  Kanamycin,Gentamycin,Netilmycin

- The above drugs are various aminoglycosides used to treat gram –ve bacterial infections.

# STREPTOMYCIN

Structure:

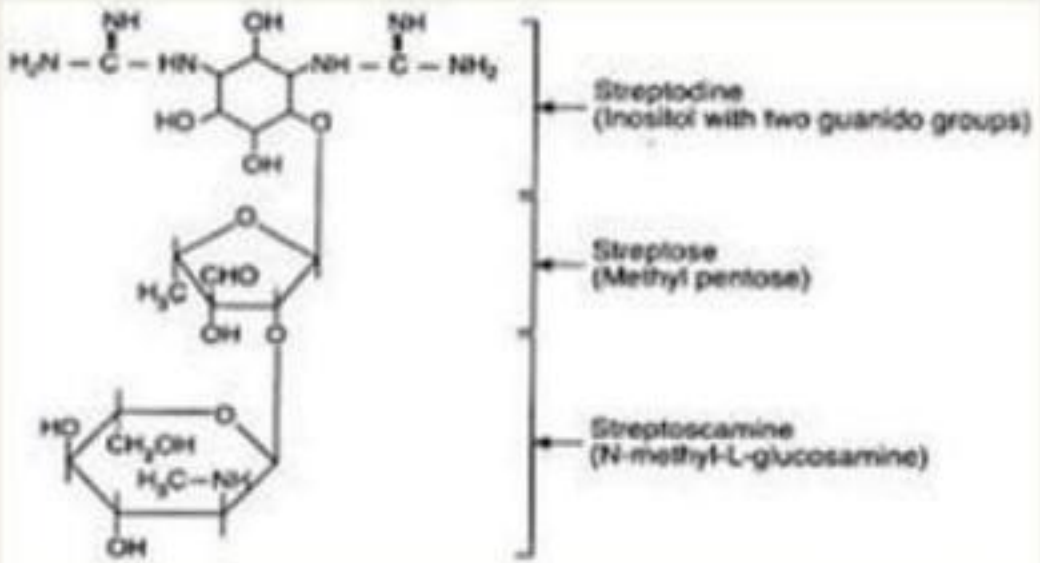


FIG. 45.9. Chemical structure of streptomycin.

Uses: 1. Streptomycin is a first line drug in the treatment of tuberculosis.

2.To treat plague and brucellosis (disease caused by unpasteurized milk or half cooked meat)

in combination with tetracycline.

3.To treat Enterococcal and streptococcal infections

# NEOMYCIN

Structure:

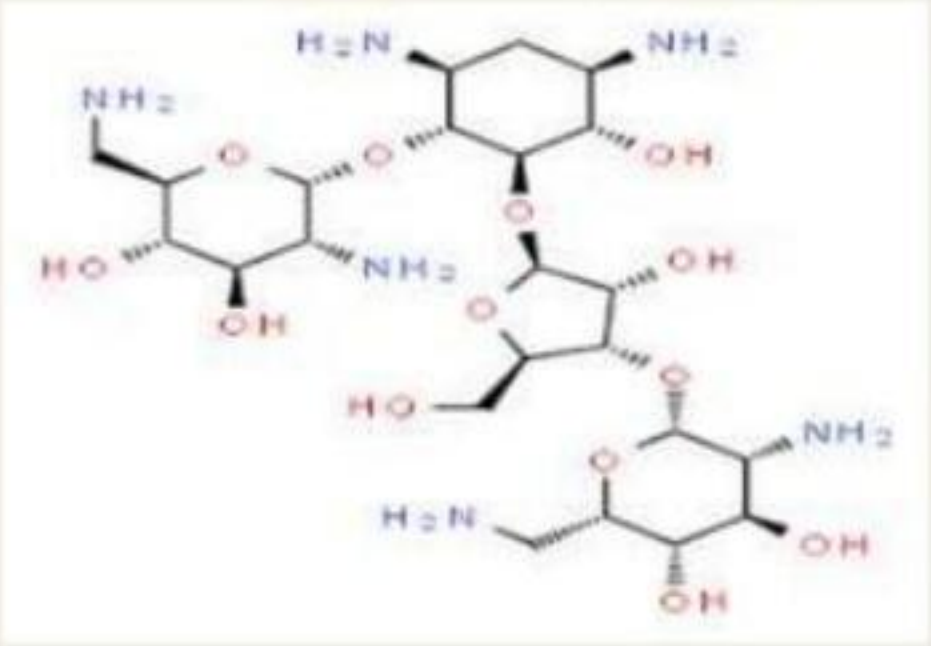

Uses: 1.To treat a variety of skin and mucous membrane infections

2.To treat gram –ve bacilli infections and gram +ve cocci infections.

# KANAMYCIN

Structure:


Uses: 1. Kanamycin is a narrow spectrum antibiotic.

2. To treat serious bacterial infections in body .

3. Used in plants transgenic resistance.

# MECHANISM OF ACTION

- Aminoglycosides inhibits protein synthesis by binding to the 30s ribosomal subunits.
- 30s ribosomal subunits interfere with the initiation complex.
- Aminoglycoside -30s ribosomal complex induce misreading of genetic code on mRNA.
- Misreading mutation of the genetic code and the synthesis of nonsense proteins occurs.
- Nonsense proteins are not normal proteins.
- So Nonsense proteins cannot take a part in bacterial cellular activities.
- Nonsense proteins will disturb the permeabitlity of bacterial cell in to the host cell.
- Finally the growth and development of bacterial cell affects and leads to bacterial cell death.

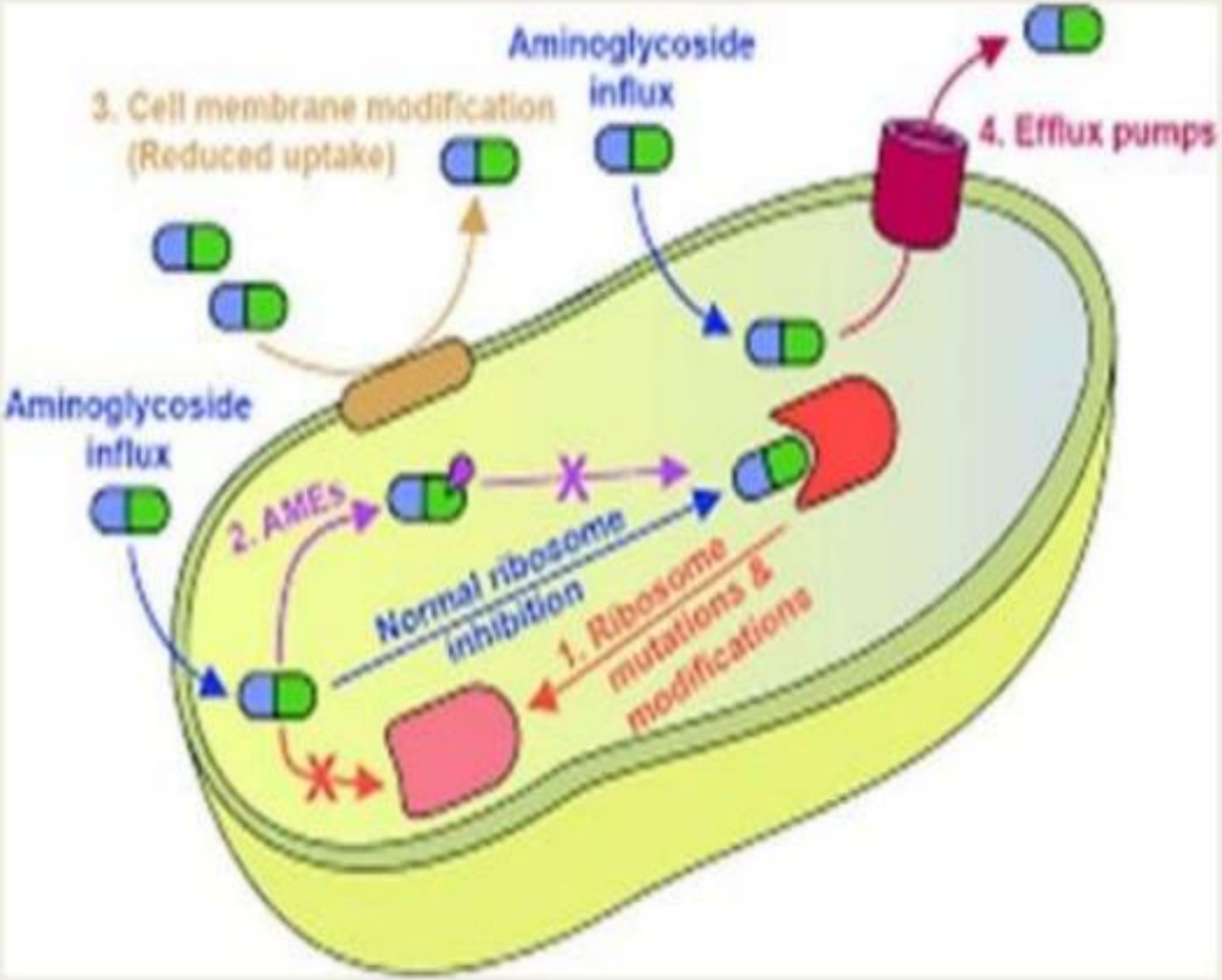
Aminoglycoside influx
3. Cell membrane modification (Reduced uptake)
4. Efflux pumps
Aminoglycoside influx
2. AMEs
Normal ribosome inhibition
1. Ribosome mutations & modifications

# SIDE EFFECTS & TOXICITY

- Nephrotoxicity
- Ototoxicity
- Headache
- Neuromuscular blockade
- Dizziness
- Vertigo
- Fever
- Skin rashes

Ototoxicity

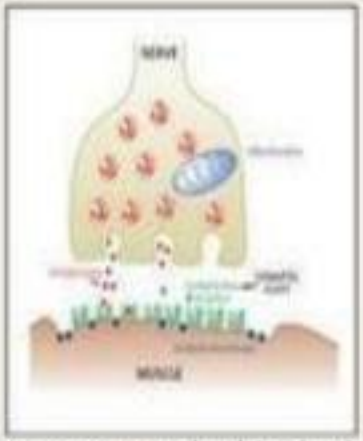

Neuromuscular blockade

Skin rashes

# TETRACYCLINES

- Tetracyclines are octahydro napthacene derivatives which are bacteriostatic and broad spectrum antibiotics that kills various types of infections caused by both gram +ve and gram –ve microorganisms.
- TETRA =four ,CYCLINES = cyclic compounds
- Tetracyclines have been introduced 50 years ago as broad spectrum antibiotics.
- They are biosynthesized from $CH_3COOH$ AND $C_3H_7COOH$ units in the microorganisms.
- They are active against both gram +ve and gram –ve bacteria.
- Tetracyclines are available for oral route and parentral route.

# SAR OF TETRACYCLINES

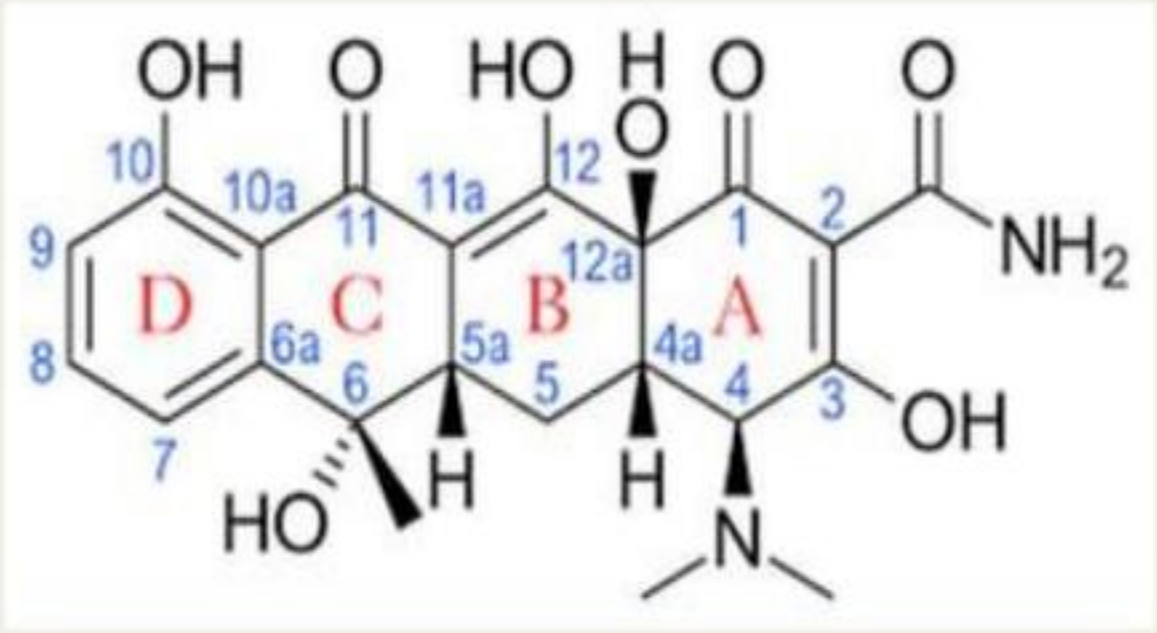


- Tetracyclines containing less than or more than four rings are inactive.

- Conversion of amide group at 2nd position decreases the activity.
- Keto-enol tautomerism between $C_2$ and $C_3$ is very important for biological activity.
- Modification of –OH group at 3rd position leads to no activity.
- Dehydration at 5a position leads to no activity.
- Epimerisation at 4th position shows no activity.
- Substitution at 5th position gives hydrophilic nature of the drug.
- Dimethyl aminogroup at 4th position shows good activity.
- $=CH_2$ group at 6th position increases antibacterial activity.
- Elimination of –OH group at 6th position increases lipophilicity Eg:Doxycycline
- Electron donating or electron withdrawing group at 7th position increases antibacterial activity.
- D ring should be always aromatic
- Changes in D ring leads to biological inactivation.
- Addition of any amino group substitution at 9th position leads to new class of antibiotics.
- Tetracycline ring is most important for antibacterial activity.

# CLASSIFICATION

According to duration of action:

1. Long acting tetracyclines (12 -16 hrs)

   Doxycline, minocycline, Meclocycline

2. Intermediate acting tetracyclines (8 -12 hrs)

   Demeclocycline, methacycline

3. Short acting tetracyclines (6-8 hrs)

   Tetracycline, chlortetracycline, Oxytetracycline

Tetracyclines are obtained from various species of streptomyces bacteria by fermentation technology.

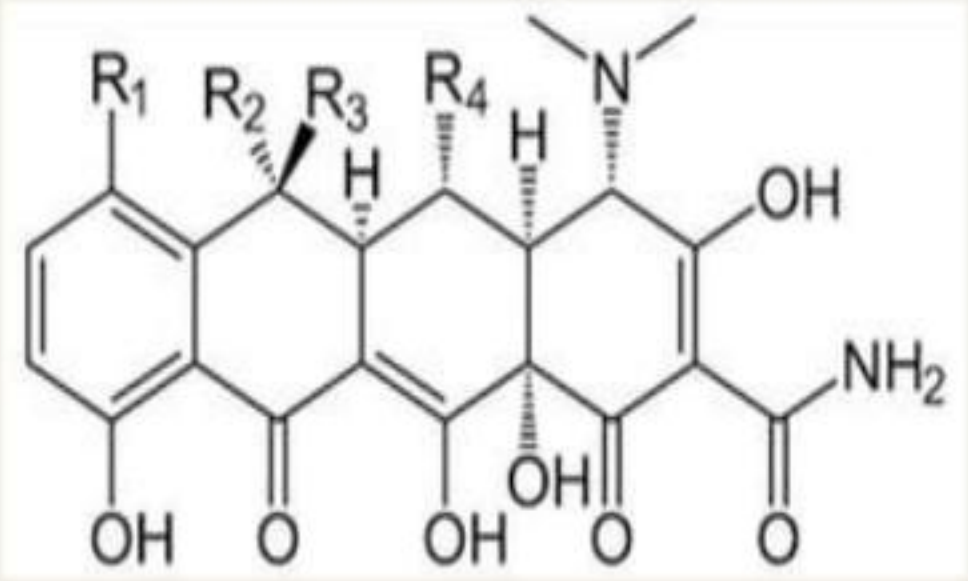


- General structure of tetracyclines

| Name of the drug | R1 | R2 | R3 | R4 |
|---|---|---|---|---|
| TETRACYCLINE | H | OH | $CH_3$ | H |
| CHLORTETRACYCLINE | Cl | OH | $CH_3$ | H |
| OXYTETRACYCLINE | H | OH | $CH_3$ | OH |
| MINOCYCLINE | $N(CH_3)_2$ | H | H | H |
| DOXYCYCLINE | H | $CH_3$ | H | OH |

# MECHANISM OF ACTION

- Tetracyclines inhibit protein syntesis by binding to the bacterial ribosome involved in the translation(protein synthesis) process and shows bacteriostatic activity.
- They bind to the 30s ribosome and inhibit the protein synthesis.
- The 70s bacterial ribosome particle is made of 30s and 50s subunits.
- The 50s subunit combines with the 30s subunit-mRNA complex and binds to t-RNA for building the protein chain.
- t-RNA contains two binding sites . a. P-site (peptidyl site) b. A-site(Acceptor aminoacyl site).
- Tetracyclines reversibly bind to the 30s subunit at the A –site to prevent attachment of the aminoacyl tRNA ,terminating the translation process.

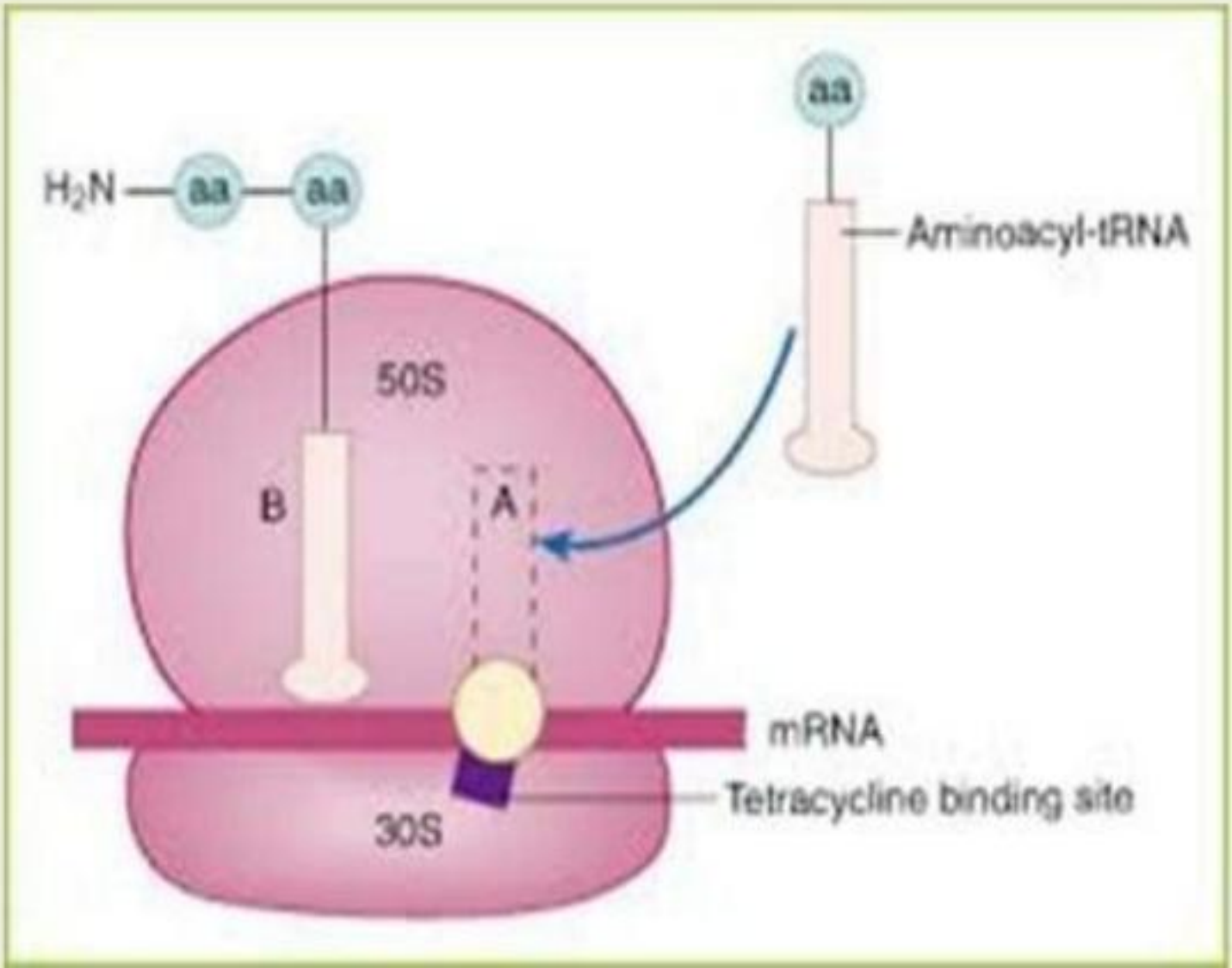
aa
$H_2N$
aa
aa
Aminoacyl-tRNA
50S
B
A
mRNA
Tetracycline binding site
30S

# TETRACYCLINES -USES

- Tetracyclines are broad spectrum antibiotics used to treat various types of infections.
- To treat eye infections.
- Tetracyclines are low cost alternative antibiotics.
- Recently, tetracyclines are used to treat cancer patients.
- To treat respiratory infections,ear,intestine and sinus
- To treat gonorrhea
- Tetracyclines are not used to treat viral infections.

# SIDE EFFECTS

- Nausea
- Vomiting
- Diarrhoea
- Teeth staining or teeth colouring
- White patches on skin
- Vaginal itching or discharge
- Trouble in swallowing(Dysphagia)
- Loss of appetite
- jaundice

Teeth staining or colouring

White patches

Jaundice

Dysphagia

# Precautions to be taken while using tetracyclines

- Complete the course of prescription
- Pregnant women should avoid tetracyclines
- Take on empty stomach with plenty of water
- Tetracyclines should not taken with milk, antacids and iron.
- Avoid exposure to sun
- Tetracyclines should not be given to Children below 8 years
- Tetracyclines passes through breast milk and affect the bones and teeth in babies.

# MACROLIDES

- Macrolides are a group of antibiotics which contains macrocyclic lactone ring (usually containing 14 or 16 atoms) to which deoxysugars are attached.
- Macrolides are obtained from streptomyces species.

Eg: Erythromycin

Azithromycin

Clarithromycin

# ERYTHROMYCIN

- Structure:

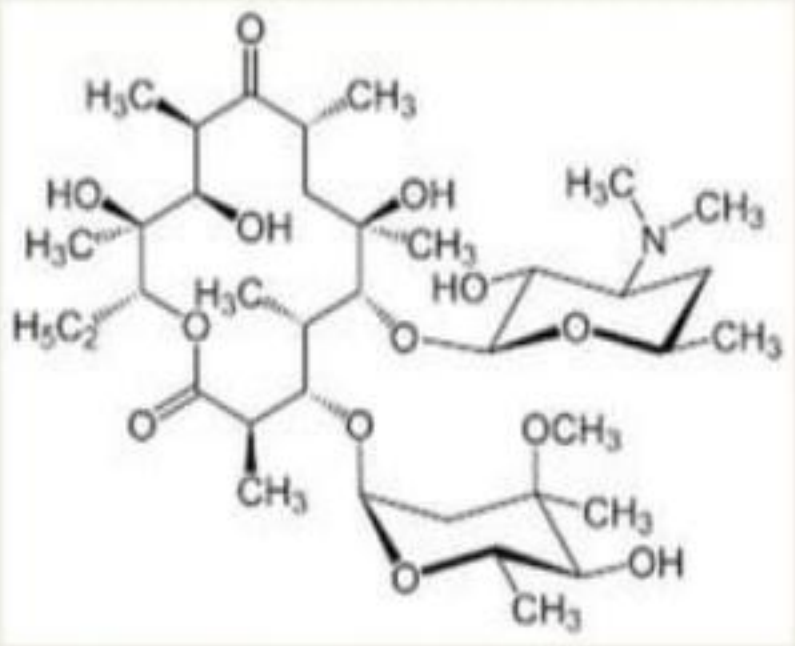


- Uses: 1.Used against gram positive & gram negative bacterial infections

  2.To treat syphilis,diptheria.

  3. To treat Pertussis (whooping cough that can cause severe coughing)

# AZITHROMYCIN


- Structure:

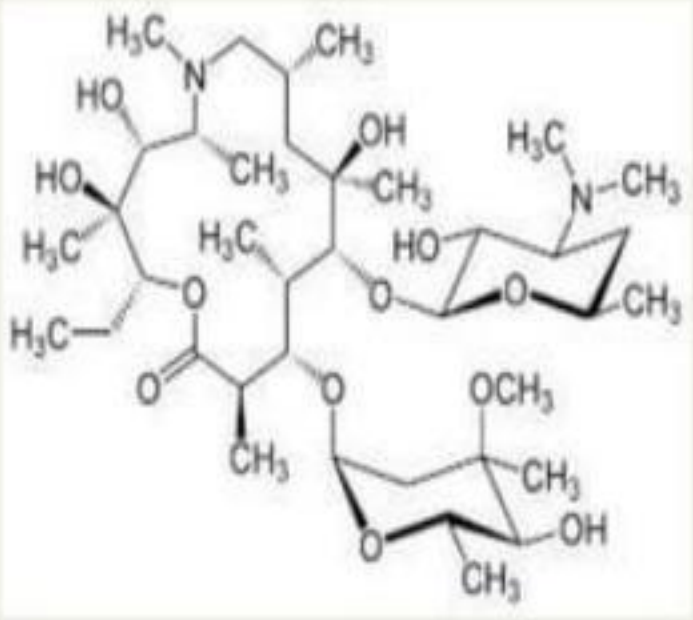

- Uses: 1. Azithromycin is active against many respiratory tract pathogens including pneumococci,mycoplasma and chlamydia species.

  2.To treat throat infections & non - gonococcal urethritis.

  3.It is expensive drug

  4.Used to prevent bacterial complications in AIDS.

# CLARITHROMYCIN

- Structure:

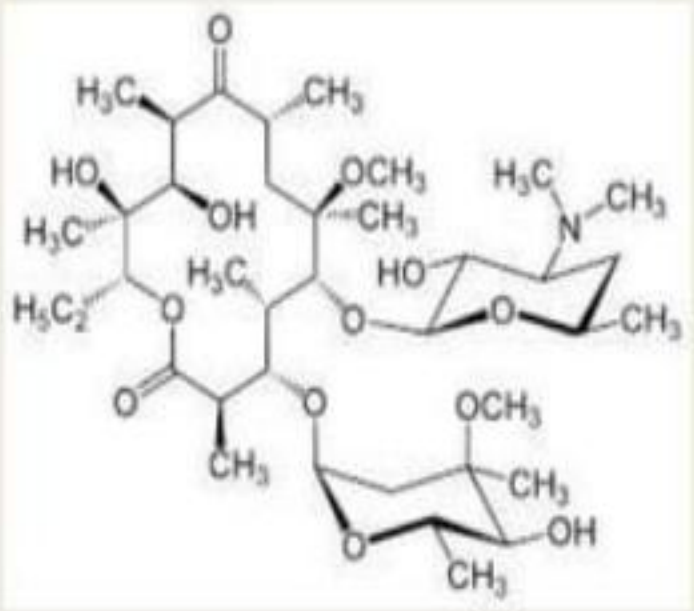

- Uses:1. To treat bacterial infections affecting skin and respiratory tract.

2.Clarithromycin is combined with other drugs to treat stomach ulcers caused by H.pylori

# MECHANISM OF ACTION

- Macrolides inhibits protein synthesis by binding to the 50s ribosomal subunit.
- Suppression of RNA dependant protein synthesis by inhibition of translocation of mRNA.
- Macrolides are bactericidal at high concentrations against very susceptible microorganisms.

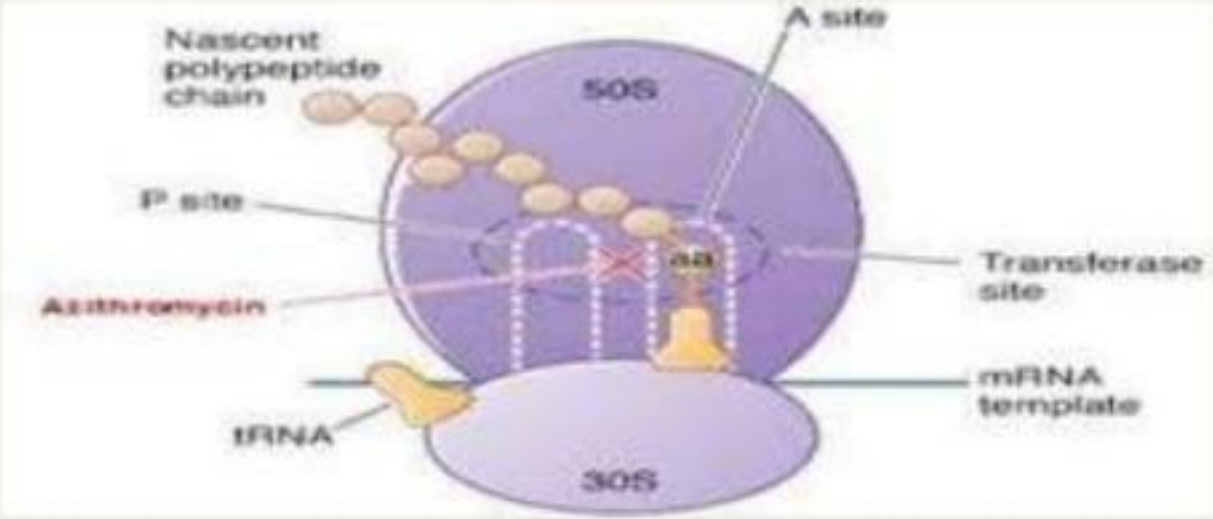

# SIDE EFFECTS

- Nausea
- Vomiting
- Abdominal pain
- Chest pain
- Dyspepsia(burning sensation)
- Flatulance
- Vaginitis
- Nephritis
- Dizziness
- Headache
- Photosensitivity
- Rashes and pruritis

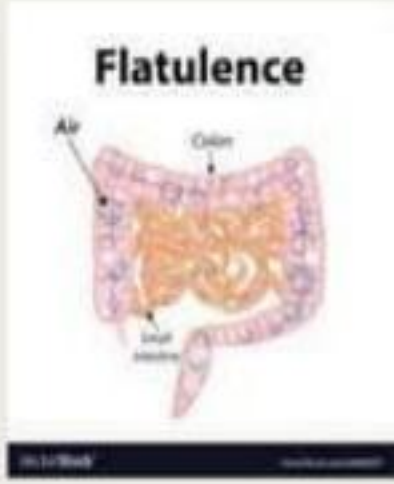


Dyspepsia

# MISCELLANEOUS ANTIBIOTICS

- The antibiotics which shows bactericidal property but not included under any class of antibiotics like beta-lactam, aminoglycoside and tetracyclines are considered as miscellaneous category of antibiotics.
- This class of drugs shows the antibiotic action by chance.

Eg: Chloramphenicol

Vancomycin

Novobiocin

Clindamycin

# CHLORAMPHENICOL


Structure:

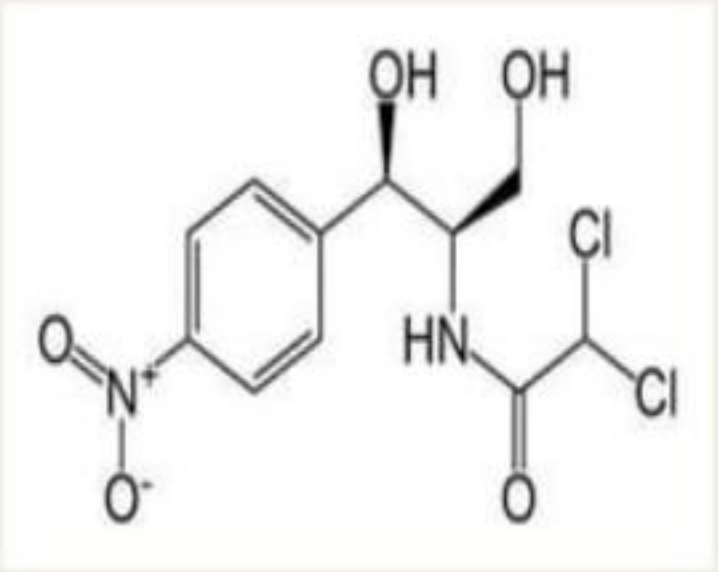


Uses: 1.To treat typhoid fever,meningitis,rocky mountain spotted fever.

2.To treat Enteric fever

3.Chloramphenicol is alternative drug in place of cephalosporins.

4.To treat anaerobic infections and intraocular infections.

# CLINDAMYCIN

- Structure:

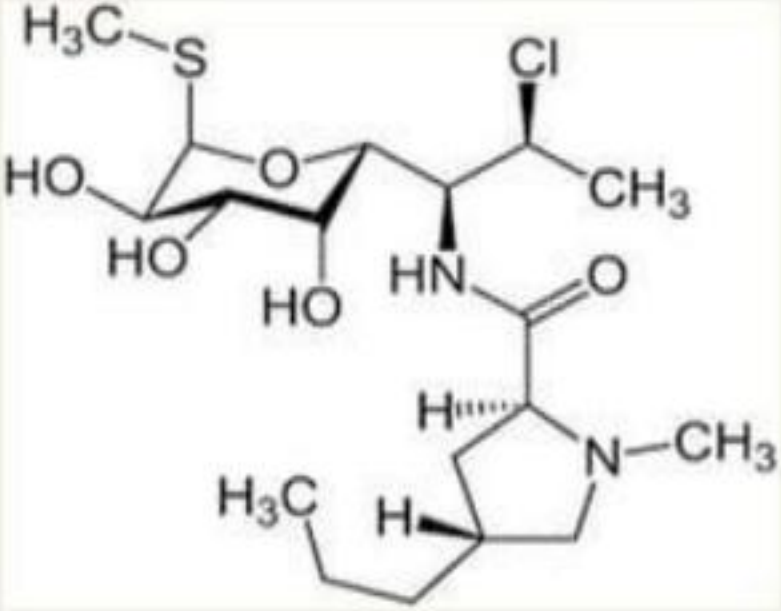



- Uses: 1.Clindamycin is a semisynthetic derivative of lincomycin

  2.It is rarely used today and reserved for patients allergic to penicillins.

# Mechanism of action

- Chloramphenicol is a bacteriostatic drug by inhibiting protein synthesis.It prevents protein chain elongation by inhibiting the peptidyl transferase activity of the bacterial ribosome .It specifically binds to the 50s ribosomal subunit and prevents the peptide bond formation.
- Clindamycin inhibits protein synthesis by binding with the 50s ribosomal subunit of the bacteria.Topical clindamycin reduces free fatty acid concentrations on the skin and suppresses the growth of bacteria,found in sebaceous glands and follicles.

# Synthesis of Chloramphenicol

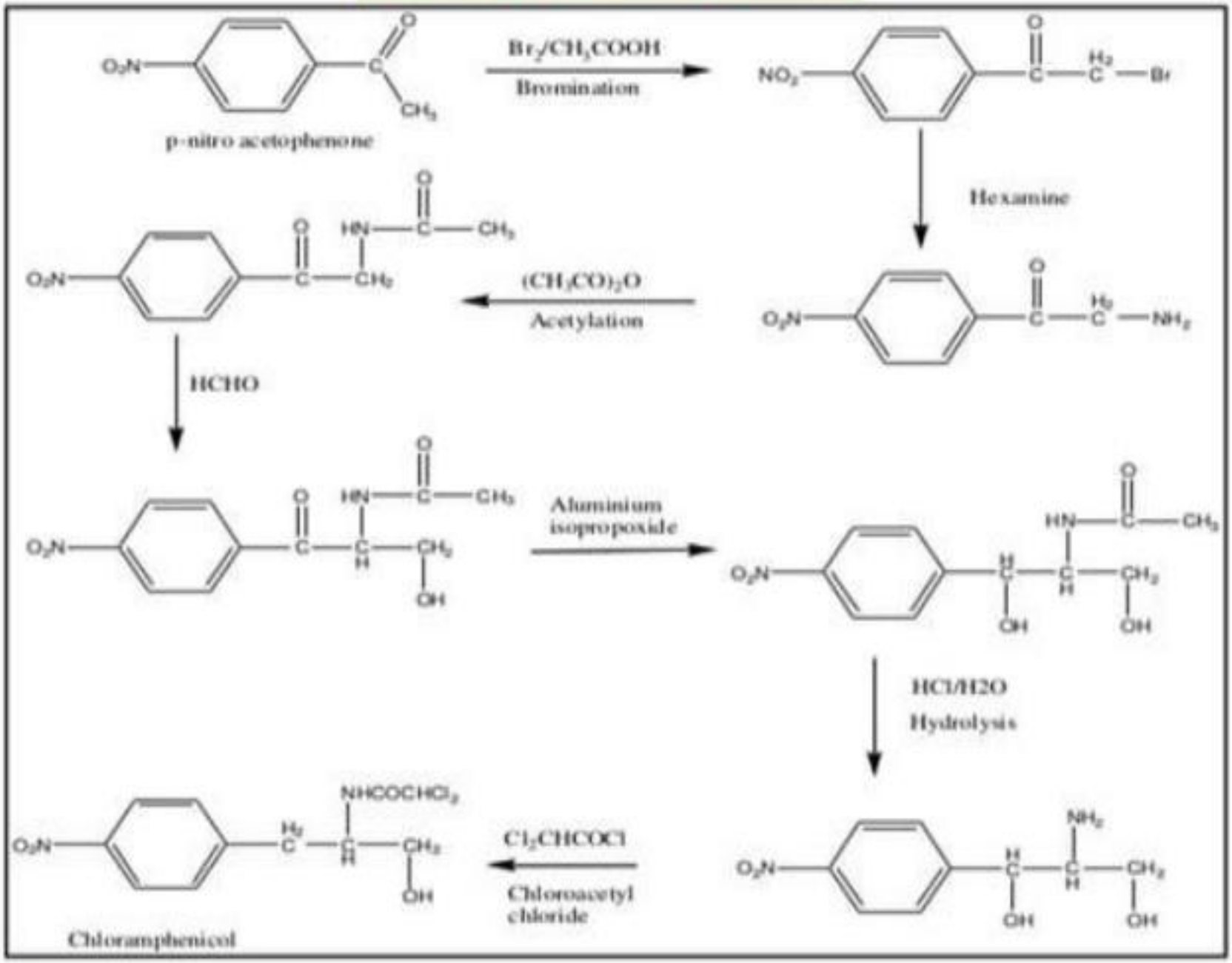

# REFERENCES


- Wilson and Gisvold's textbook of organic ,medicinal and pharmaceutical chemistry
- A textbook of medicinal chemistry by V.Alagarswamy
- Medicinal chemistry by Ashutosh kar
- Principles of organic medicinal chemistry by Rama rao Nadendla
- Foye's principles of medicinal chemistry
- Textbook of medicinal chemistry by Valentine .Ilango
- Medicinal chemistry by Graham Patrick
- www.nlm.nih.gov.pubmed
- Pharmafactz.com – online library for medicinal chemistry
- United states national library of medicine – A research centre

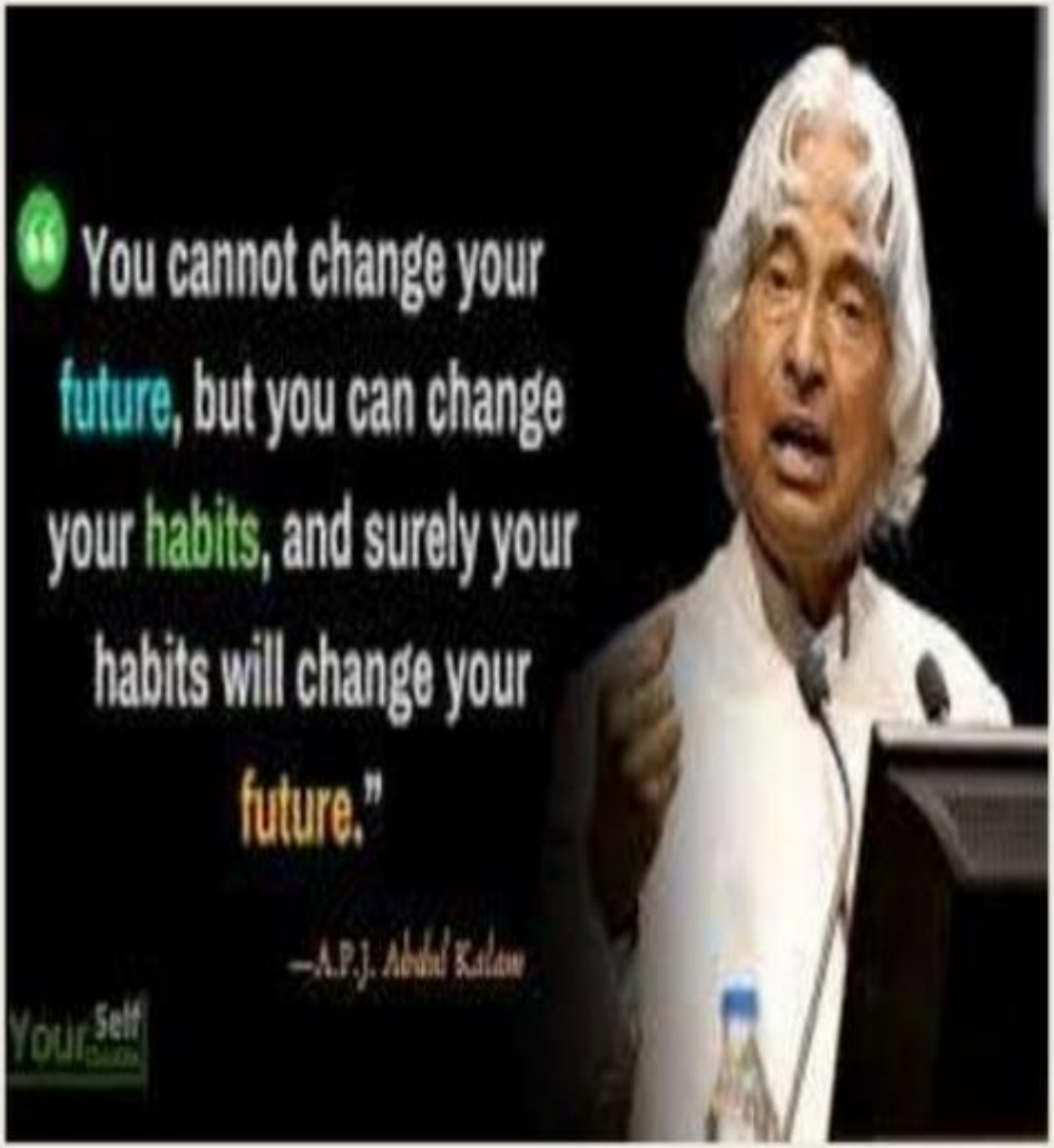
"You cannot change your future, but you can change your habits, and surely your habits will change your future."
—A.P.J. Abdul Kalam
Your Self


GET
WELL
SOON
WITHOUT
ANTIBIOTICS


THANK YOU
THANK YOU!
THANK YOU


# Antimalarial Drugs

Arief Kusuma Wardani, S.Si.,M.Pharm.Sci
Universitas Muhammadiyah Magelang

# Medicinal Chemistry of Antimalarial Drugs

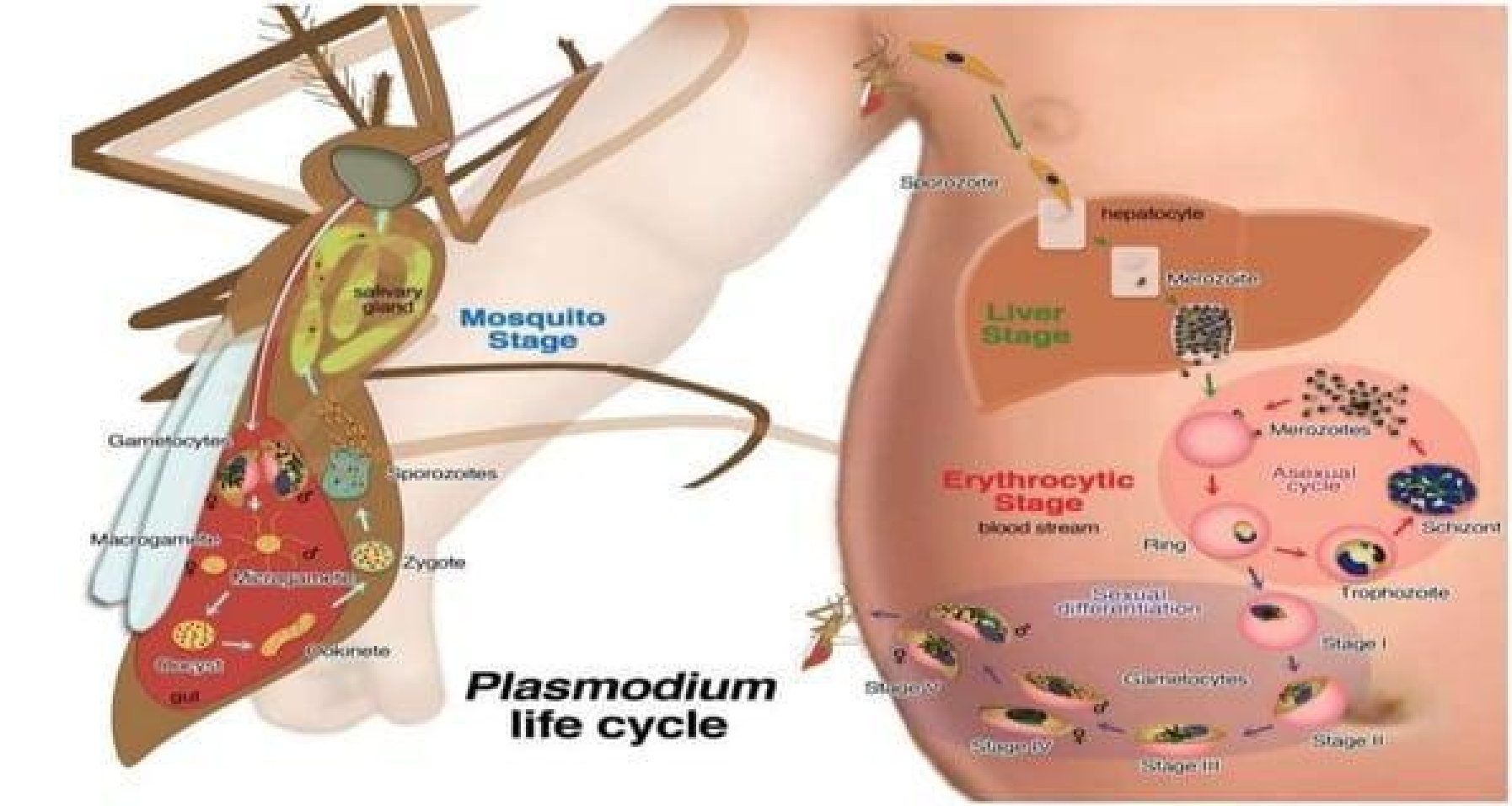

# Malaria

- Malaria is an infectious disease known since ancient times.
- The name comes from the words '*mala aria*' meaning 'bad air'.
- Malaria was associated with regions that are badly drained, swamps, and marshes.
- The disease is caused by a protozoal parasite (genus *plasmodium*), which is carried by female mosquitos (genus *Anopheles*).
- Species of genus *plasmodium* associated with malaria include *vivax*, *malariae*, *falciparum*, and *ovale*.
- Transmission between infected mosquitos and humans occur through mosquito bites.

# MALARIA

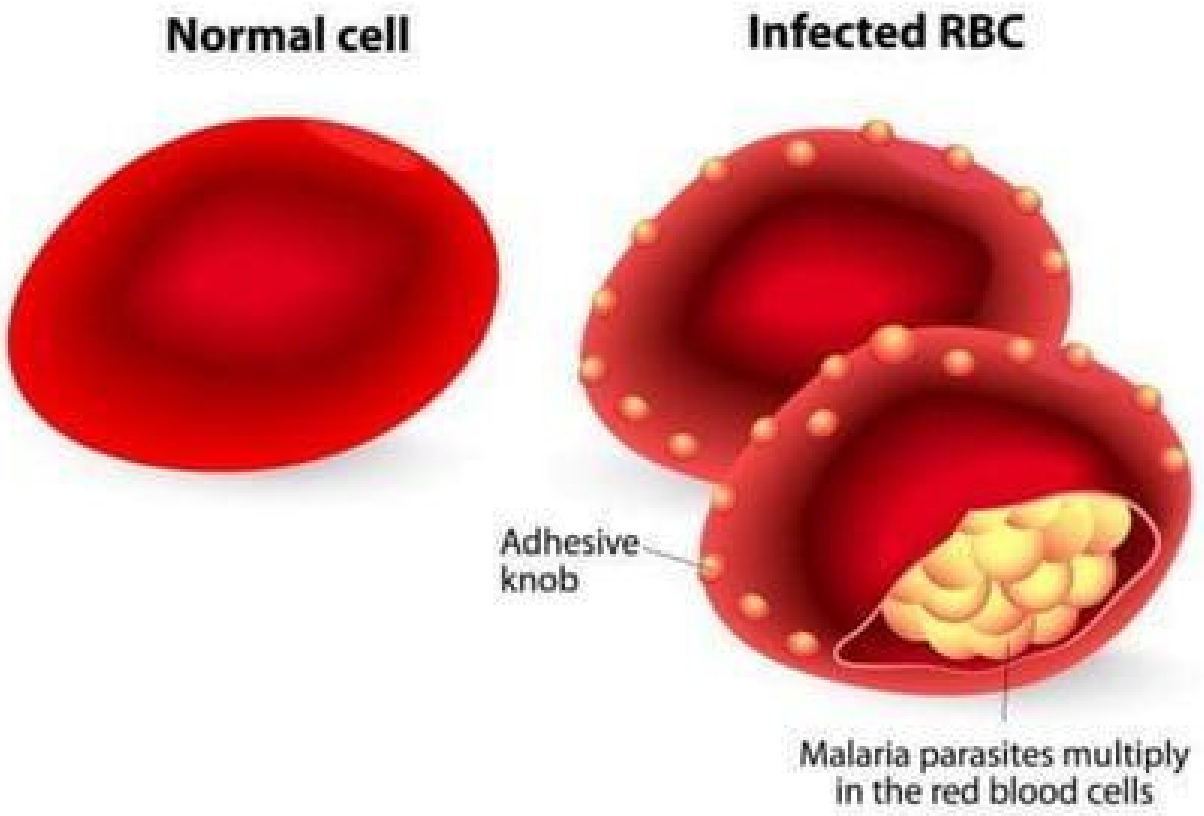

# Malaria Life Cycle

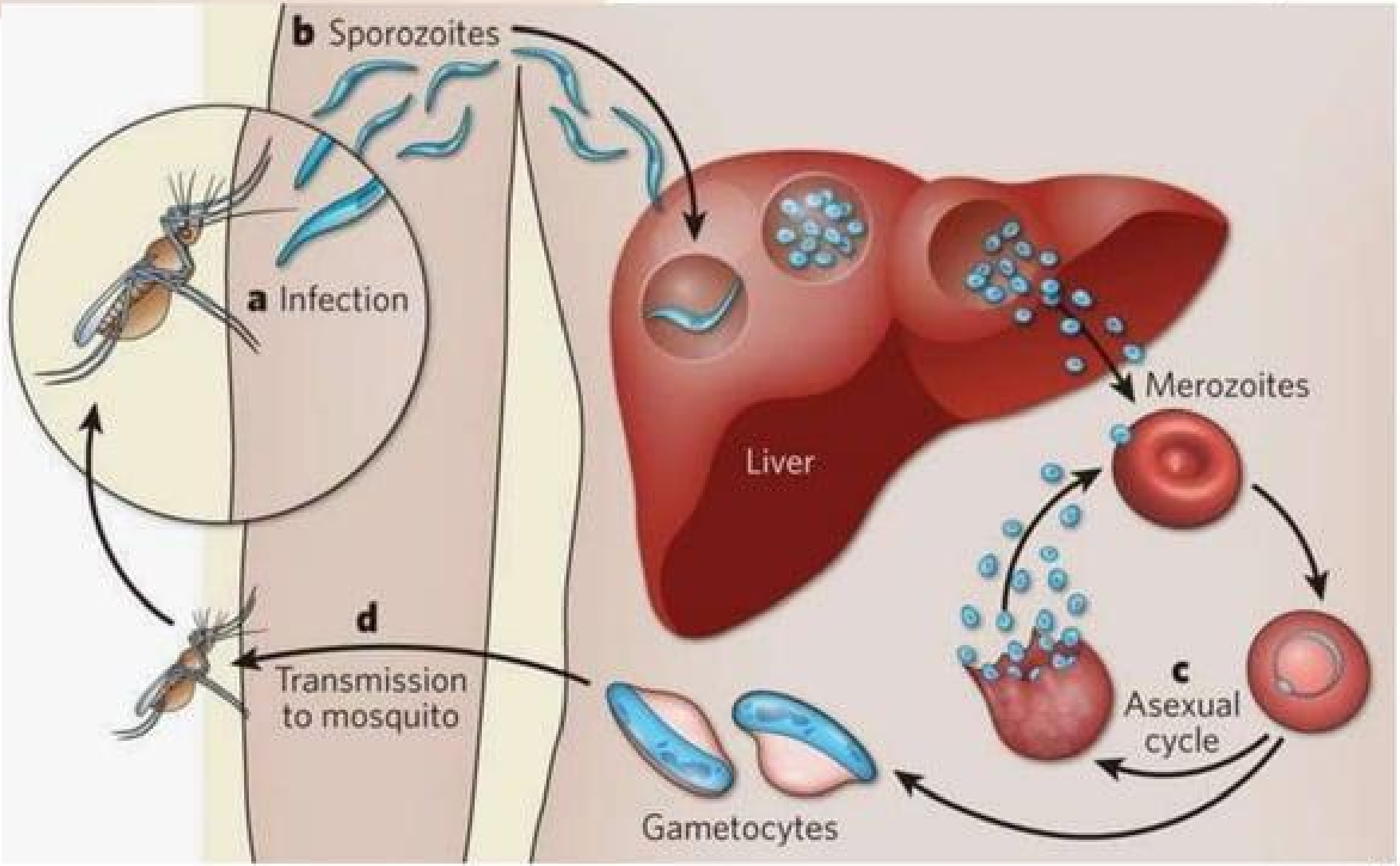

# Symptoms

- Fever
- Shivering
- Pain in joints
- Headache
- Repeated vomiting
- Severe → convulsions, coma

# Controlling Malaria

- Controlling the mosquito is one way of controlling malaria.
- Using screens on windows
- Using mosquito netting in bedrooms
- Impregnating netting systems with insecticidal compounds
- Application of insect repellent on one's skin or clothing
- DEET (N,N-Diethyl-meta-toluamide) is an active ingredient commonly found in insect repellents.
- Mosquitos have strong aversion to the odour of DEET.

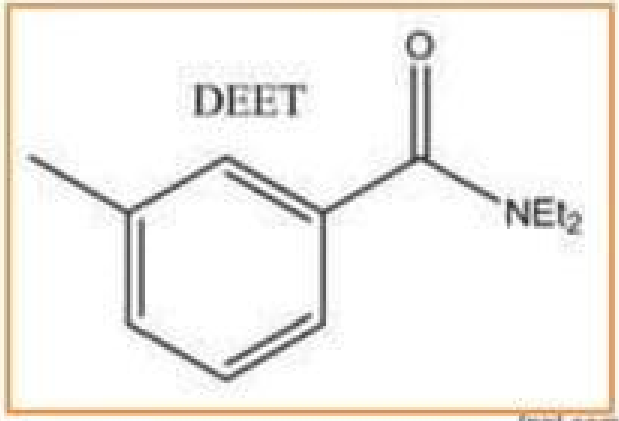

# Treating Malaria

- Natural compounds from the bark of the cinchona tree, most notably quinine was observed to exhibit antimalarial activity.
- Until the development of synthetic derivatives (ie. 4-aminoquinoline antimalarials), quinine continued to be the first choice to treat malaria.
- Quinine is associated with side effects such as diarrhœa.
- 4-aminoquinoline antimalarials such as amodiaquine and chloroquine largely replaced quinine because of reduced unpleasant side effects.

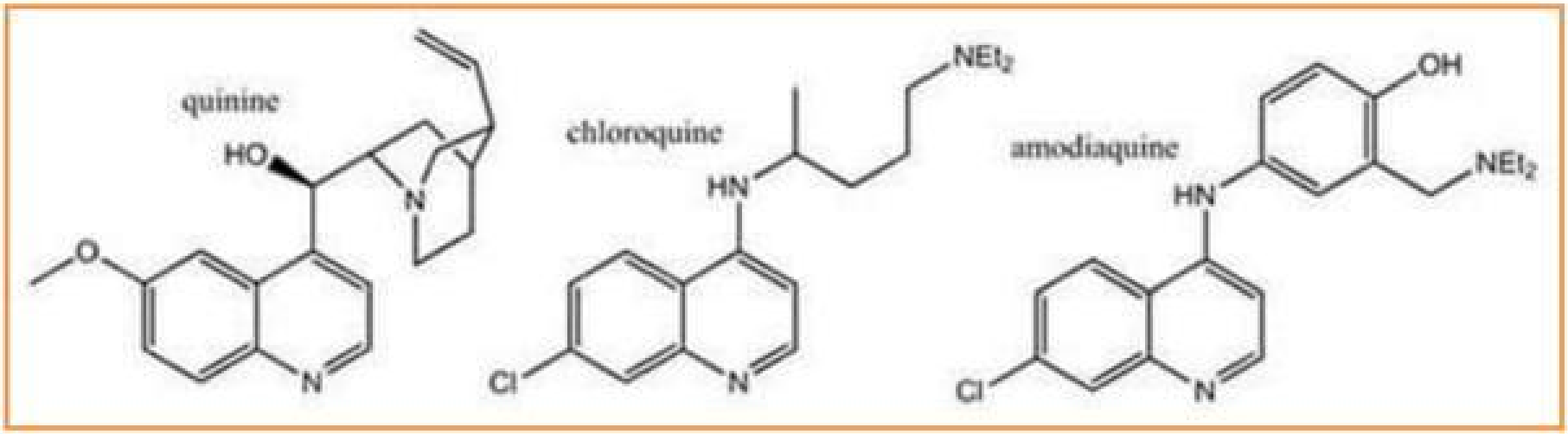
quinine
HO
N
O
N
chloroquine
NEt2
HN
Cl
N
amodiaquine
OH
NEt2
HN
Cl
N

# Treating Malaria

- The life cycle of the parasite and the immunological defence mechanisms against the parasite are complex.
- Part of the parasite's life cycle involves invasion of red blood cells (erythrocytes).
- The haemoglobin within the red blood cell is broken down by the parasite and is used as a source of amino acids.
- The 4-aminoquinolines act at the erythrocytic stage of the parasite.
- Doxycycline is a compound used in prophylaxis against plasmodial parasites.
- Other compounds associated with treating malaria include halofantrine and lumefantrine, often used in combination with other drugs.

# Classification

1. According to anti malarial activity
2. According to the structure

# According to anti malarial activity:

1. **Tissue schizonticides for causal prophylaxis:** These drugs act on the primary tissue forms of the plasmodia which after growth within the liver, initiate the erythrocytic stage. By blocking this stage, further development of the infection can be theoretically prevented. Pyrimethamine and Primaquine have this activity. However since it is impossible to predict the infection before clinical symptoms begin, this mode of therapy is more theoretical than practical.
2. **Tissue schizonticides for preventing relapse:** These drugs act on the hypnozoites of P. vivax and P. ovale in the liver that cause relapse of symptoms on reactivation. Primaquine is the prototype drug; pyrimethamine also has such activity.

# According to anti malarial activity:

3. **Blood schizonticides:** These drugs act on the blood forms of the parasite and thereby terminate clinical attacks of malaria. These are the most important drugs in anti malarial chemotherapy. These include chloroquine, quinine, mefloquine, halofantrine, pyrimethamine, sulfadoxine, sulfones, tetracyclines etc.
4. **Gametocytocides:** These drugs destroy the sexual forms of the parasite in the blood and thereby prevent transmission of the infection to the mosquito. Chloroquine and quinine have gametocytocidal activity against P. vivax and P. malariae, but not against P. falciparum. Primaquine has gametocytocidal activity against all plasmodia, including P. falciparum.

# According to anti malarial activity:

5. **Sporontocides:** These drugs prevent the development of oocysts in the mosquito and thus ablate the transmission. Primaquine and chloroguanide have this action.

- Thus in effect, treatment of malaria would include a blood schizonticide, a gametocytocide and a tissue schizonticide (in case of *P. vivax* and *P. ovale*).
- A combination of chloroquine and primaquine is thus needed in ALL cases of malaria.

# According to the structure:

1. **Aryl amino alcohols:** Quinine, quinidine (cinchona alkaloids), mefloquine, halofantrine.
2. **4-aminoquinolines:** Chloroquine, amodiaquine.
3. **Folate synthesis inhibitors:** Type 1 – competitive inhibitors of dihydropteroate synthase – sulphones, sulphonamides; Type 2 – inhibit dihydrofolate reductase – biguanides like proguanil and chloroproguanil; diaminopyrimidine like pyrimethamine
4. **8-aminoquinolines:** Primaquine
5. **Antimicrobials:** Tetracycline, doxycycline, clindamycin, azithromycin, fluoroquinolones
6. **Peroxides:** Artemisinin derivatives and analogues – artemether, arteether, artesunate, artelinic acid
7. **Naphthoquinones:** Atovaquone
8. **Iron chelating agents:** Desferrioxamine

# Artemisinin

- Artemisinin is a natural product that can be extracted from the leaves of *artemisia annua*
- Formula : $C_{15}H_{22}O_5$
- Molar mass : 282.332 g/mol
- Density : $1.24 \pm 0.1$ g/cm$^3$
- M.P : 152 to 157 °C (306 to 315 °F )

# Artemisinin

The therapeutic utility of the lead itself is limited by poor physicochemical properties such as poor oil & water solubility

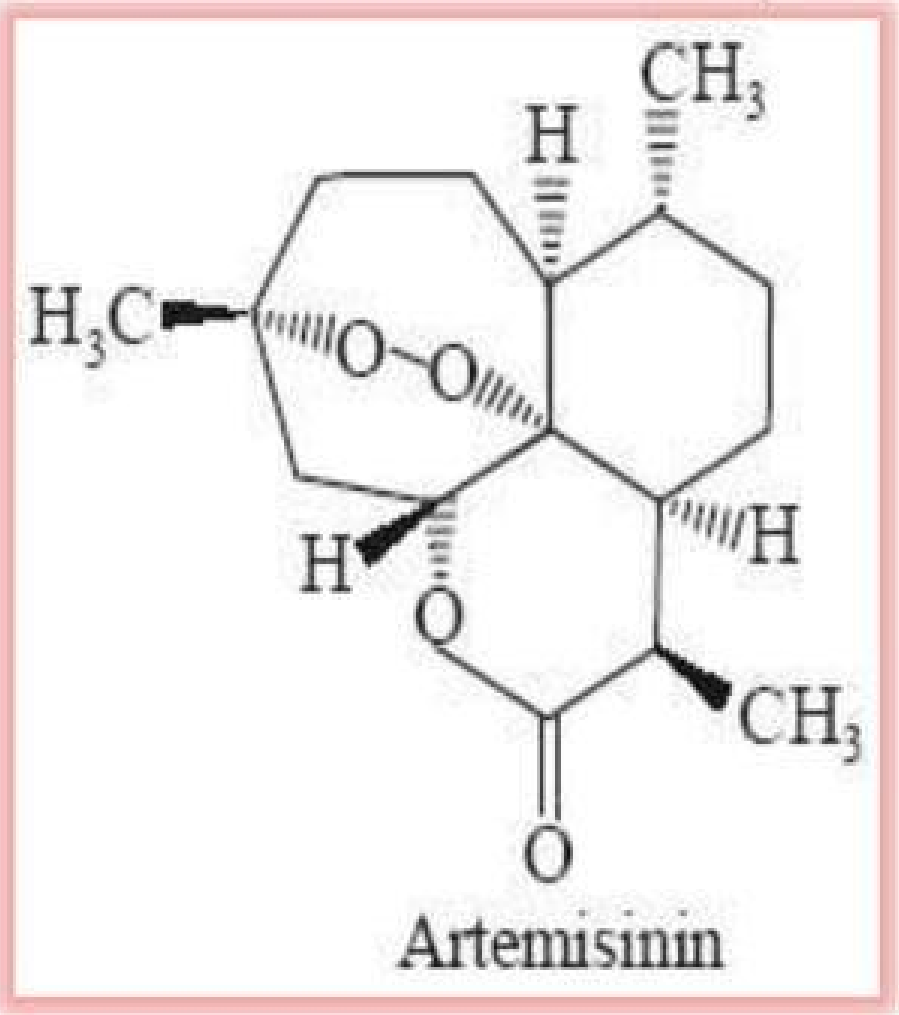

# Artemisinin

## Artemisinin derivatives

**Qinghaosu**
("ching-how-soo")

- Artemisinin derivatives
  - Dihydroartemisin
    - Ethyl Ether
      - Arteether
    - Methyl Ether
      - Artemether
    - Hemisuccinate
      - Artesunate

# SAR Of Artemisinin

Artemisinin serve as a lead compound for the development of new antimalarials with improved properties

- The lactone group can be reduced & form dihydroartemisinin which is used to prepare semi synthetic prodrug that are more water & oil soluble

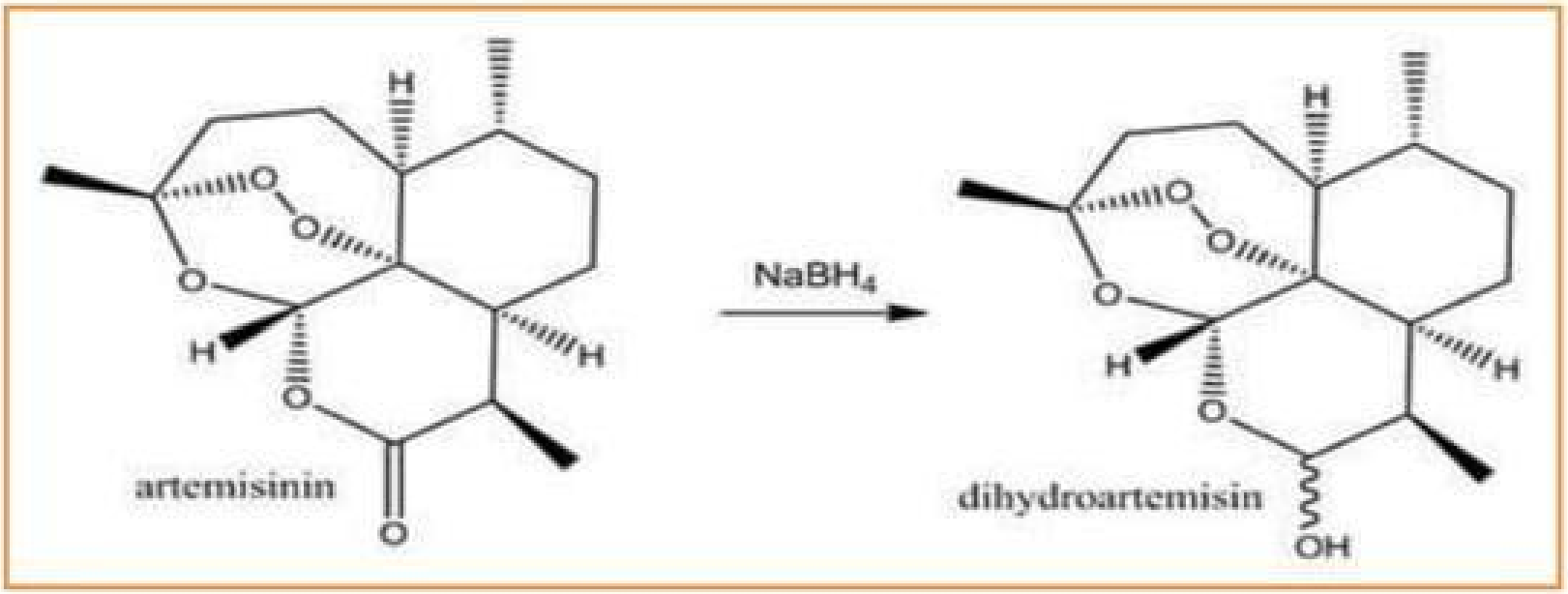

# SAR Of Artemisinin

- The hydroxyl group can be alkylated to give oil soluble ether derivatives such as artemether & arteether
- Esterification of the hydrooxyl with succinic acid gives the water soluble derivative , artesunate

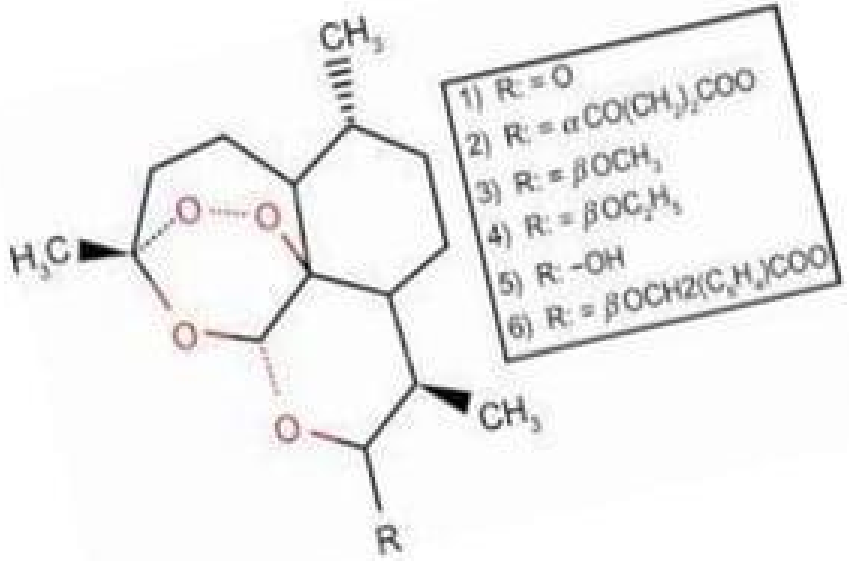

# SAR Of Artemisinin

*Artemisia annua*


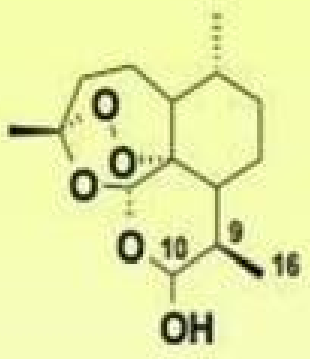


Dihydroartemisinin
(DHA) (Artenimol)

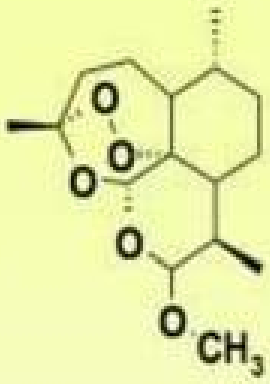


Artemether
(Artemos)

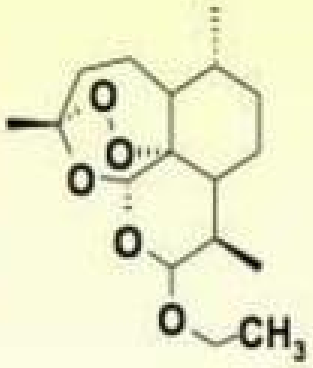


Arteether
(Artemotil)

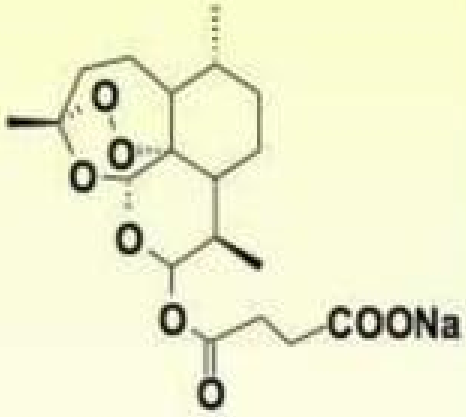


Sodium artesunate

# SAR Of Artemisinin


- Studies of artemisinin analogues such as **deoxyartemisinin** which do not contain the endoperoxide bridge, showed vastly reduced biological activity.
- Moreover, derivatisation at the carbonyl lactone demonstrated that it is a possible region of modification that can be manipulated in order to improve pharmacokinetic properties.
- This was demonstrated by the semisynthetic prodrugs. Compared to artemisinin itself, artemether, artesunate and dihydroartemisinin are more active.

# Artemisinin total synthesis

- The structure of artemisinin is quite complex. The compound is a tetracycle with seven asymmetric centres.
- One example of **artemisinin total synthesis** is shown using 1-cyclohex-2-enone as the main starting material.

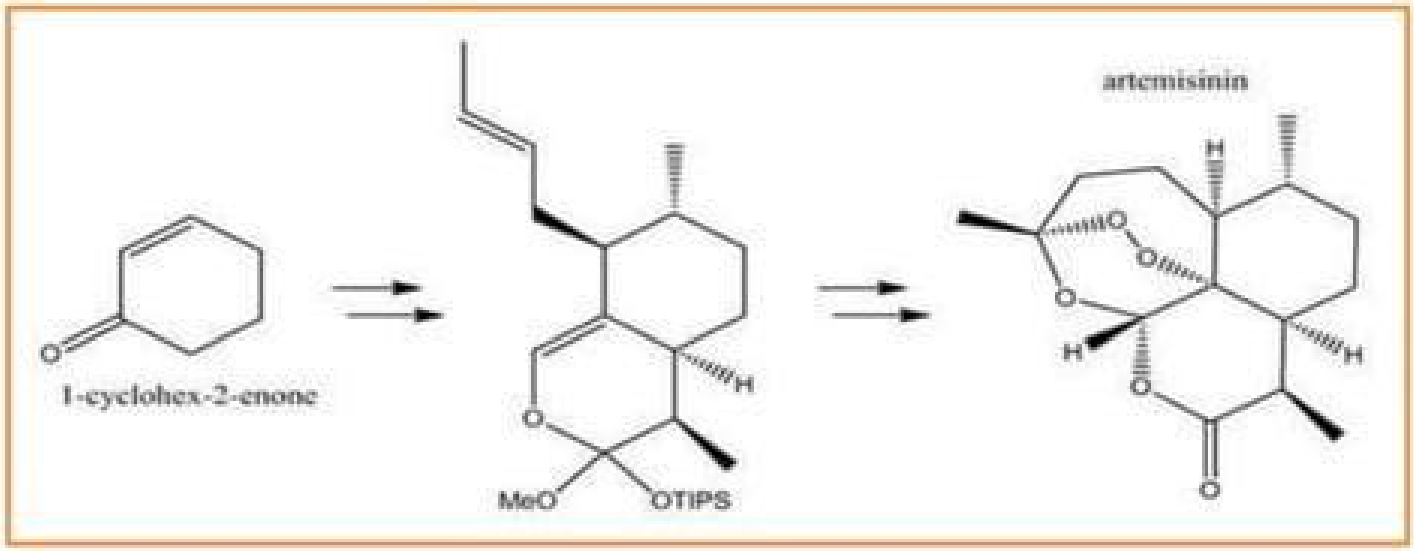

# Development of simplified artemisinin analogues

- Antimalarial cyclic peroxy ketals exhibited greater activity compared to artemisinin. However, these cyclic peroxy ketals faced problems such as short plasma half-life and poor chemical stability.
- Dispiro-1,2,4,5 tetraoxanes synthesised by Vennerstrom and co-workers exhibited good antimalarial behaviour during *in vitro* and *in vivo* studies.

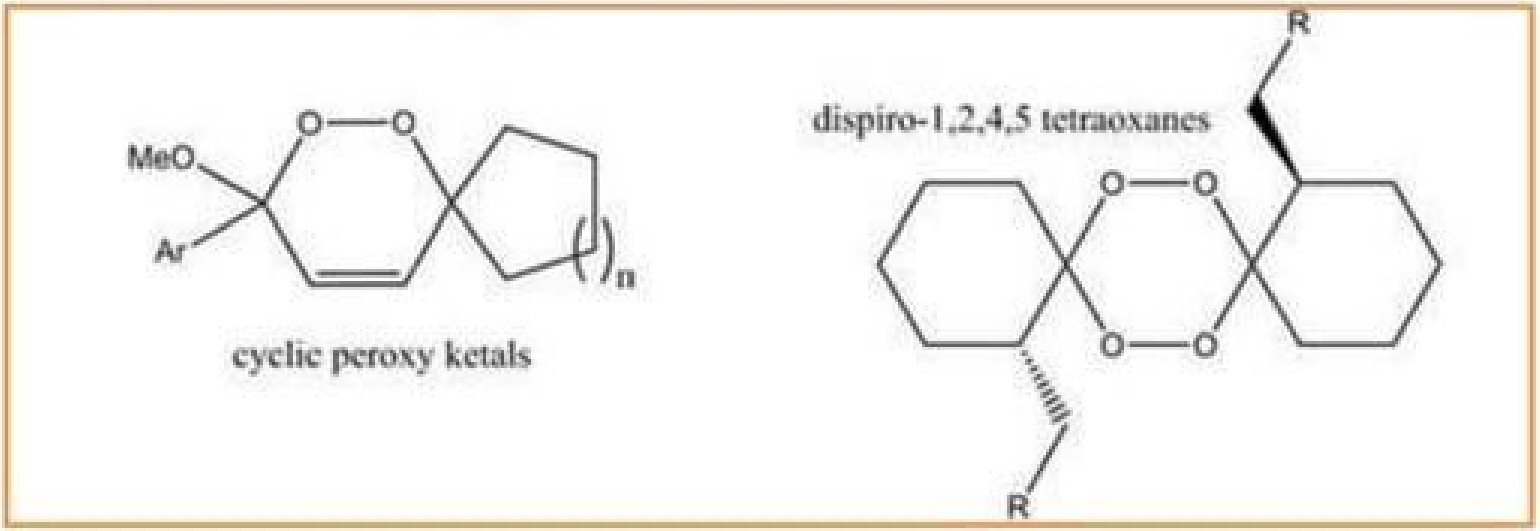

# Artemisinin
# Arteflene & Arterolane

- Arteflene, which is based on another endoperoxide-containing compound exhibited antimalarial activity about half of artemisinin.
- Arterolane, a synthetic trioxolane with better pharmacokinetic properties than semisynthetic artemisinins, is currently in clinical trials. To date, clinical use of simplified derivatives of artemisinin has not reached widespread use.

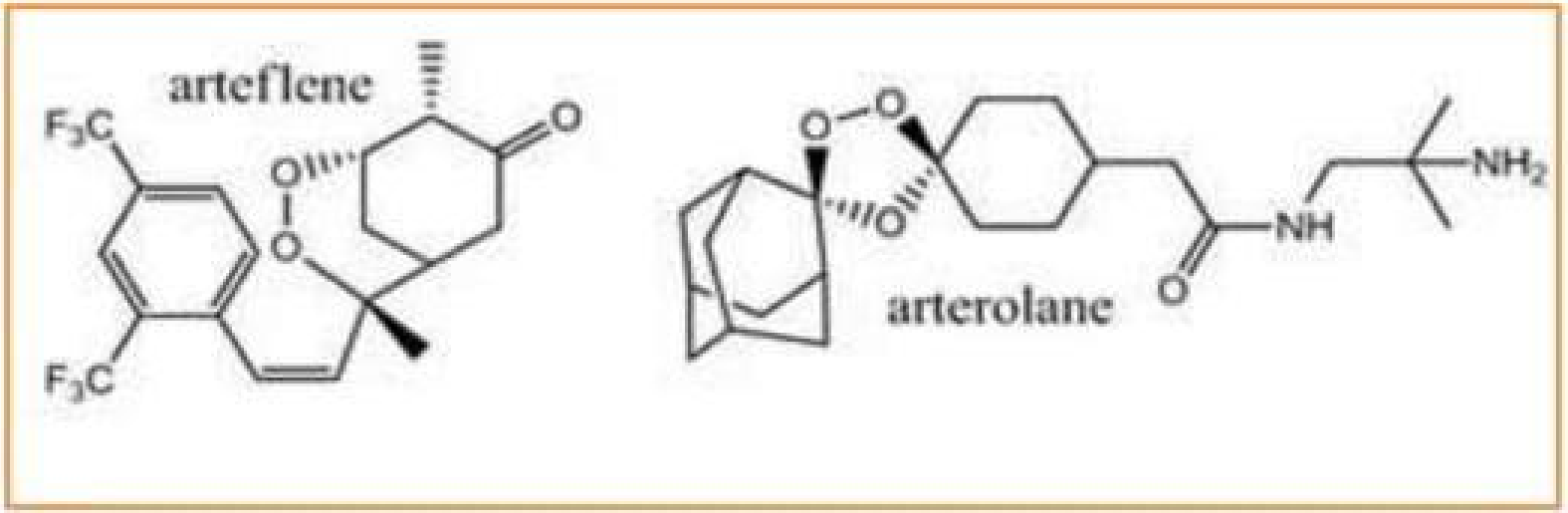

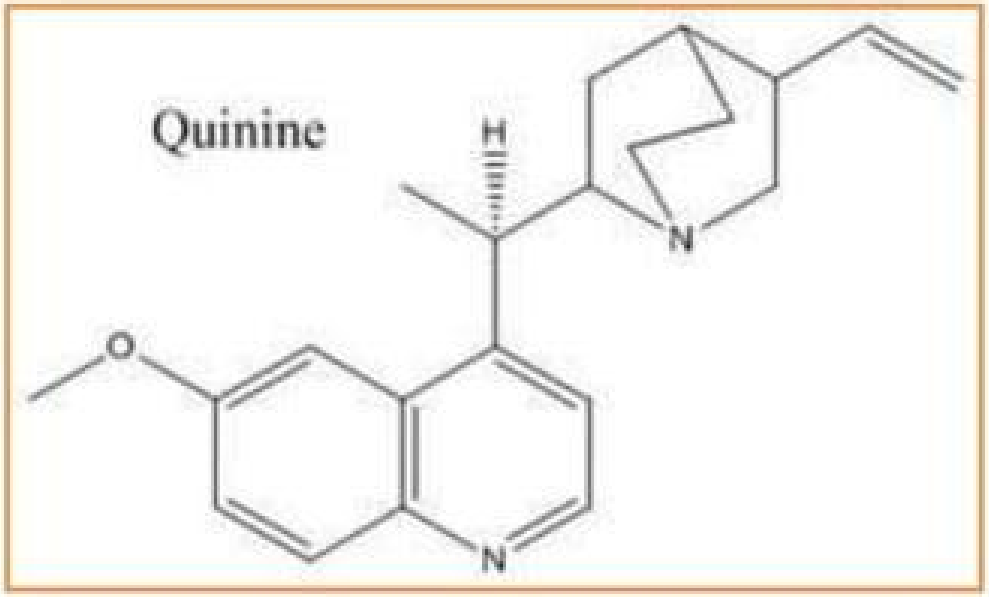



# Quinine & Related Compounds

# Quinine

- The bark of the cinchona tree contains antimalarial compounds, most notably the highly fluorescent compound, **quinine**.
- The bark of the cinchona tree, if made into an aqueous solution was able to treat most cases of malaria.
- The active principle quinine was first isolated from the bark during the early 19$^{th}$ century.
- Quinine is the compound that contributes to the bitter taste of tonic water.

# 4-aminoquinolines

- Increasing concern about cinchona supplies and the desire to find quinine alternatives with reduced side effects led to a massive search for novel antimalarials.
- **Chloroquine** was one of the drugs successfully developed. The drug was first used during the 1950s.
- Chloroquine is effective against erythrocytic forms of the *Plasmodium* parasite. Like chloroquine, the drugs **amodiaquine** and **hydroxychloroquine** belong to a class of quinine analogues called **4-aminoquinolines**.

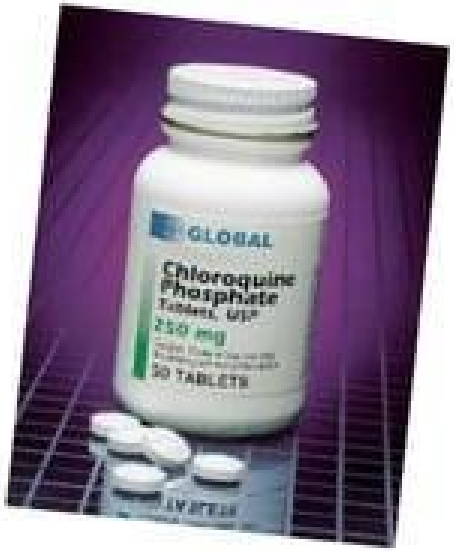

# 4-aminoquinolines

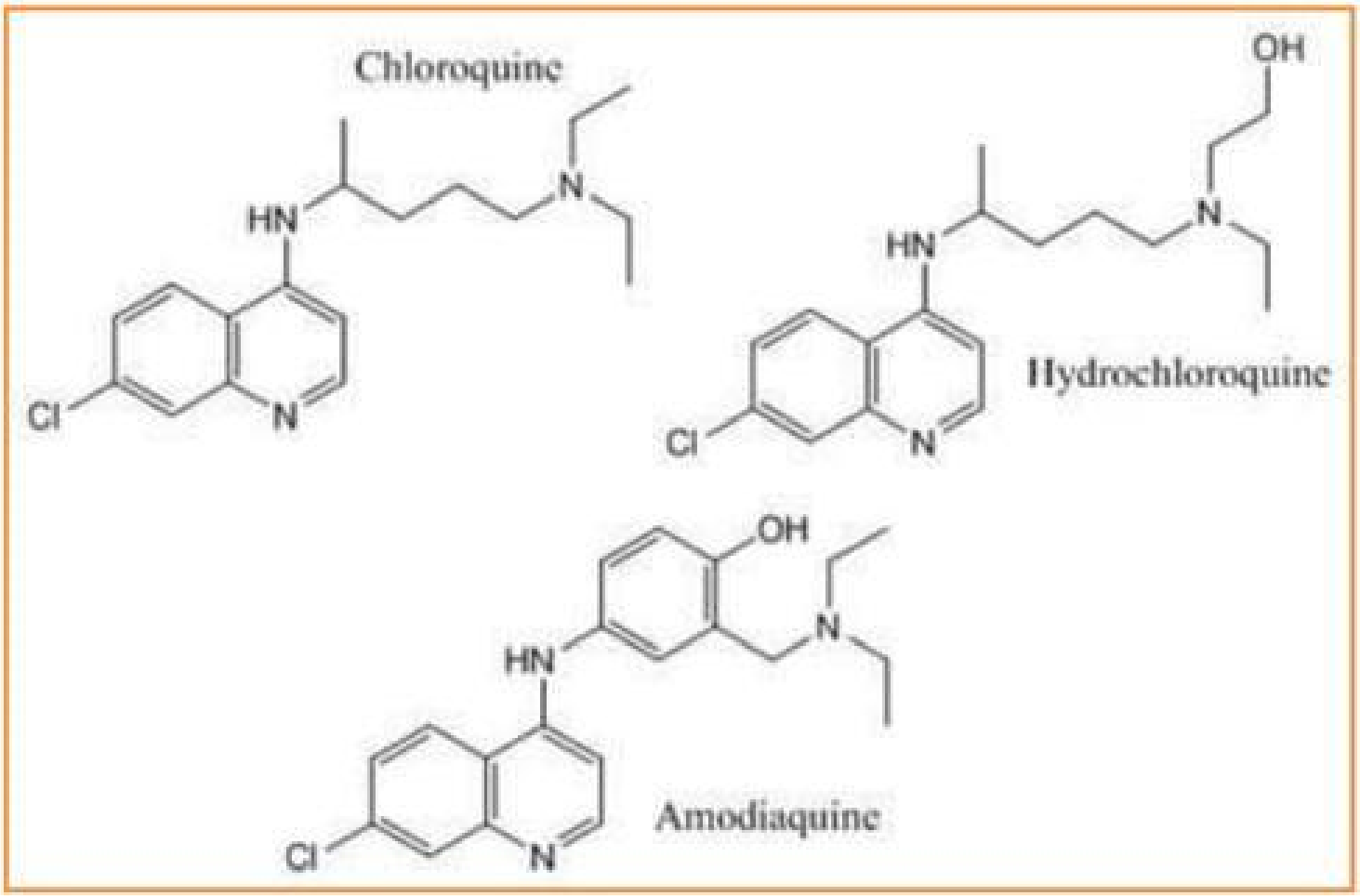

# Drug designed of **Chloroquine** as prototype drug

- It consists of 4-aminoquinoline pharmacophore.
- The structural analogues of chloroquine have been designed in such a way that it will show more drug likeness score than the prototype molecule but having the same pharmacophore essential for the antimalarial activity.

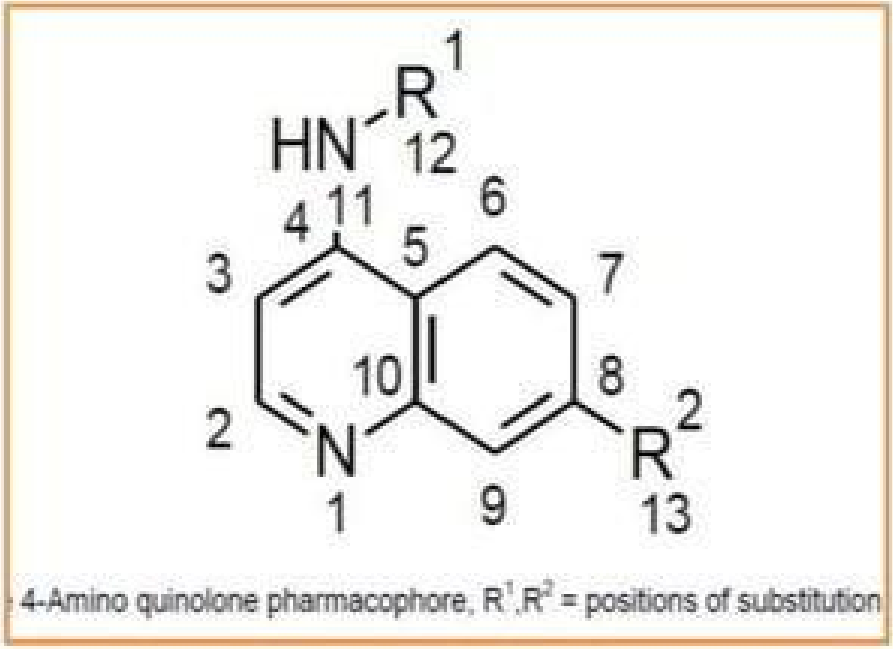


4-Amino quinolone pharmacophore, $R^1$,$R^2$ = positions of substitution

The side chain present at 4 position of chloroquine have been modified with alteration of halogen atom in some cases at position 8 to get increased drug likeness score.

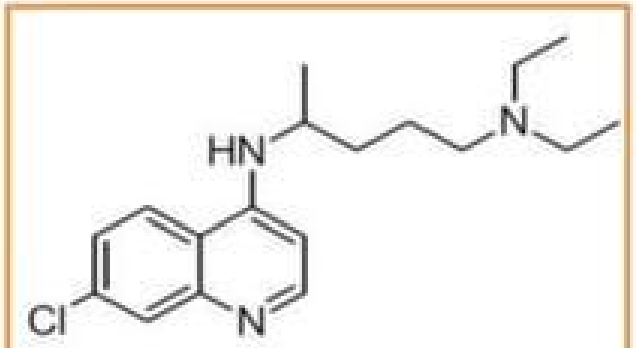


**Figure 6.** Prototype molecule chloroquine having MolSoft drug likeness score of 1.17

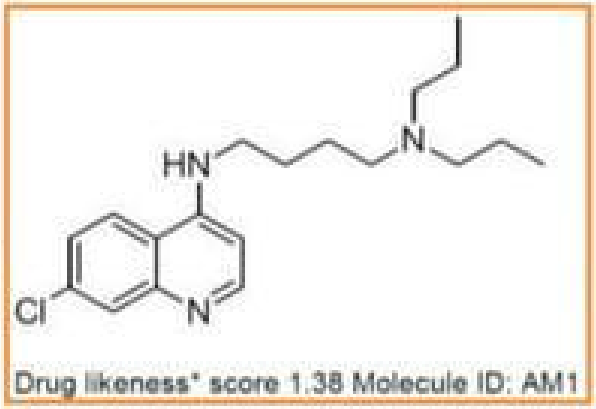


Drug likeness* score 1.38 Molecule ID: AM1

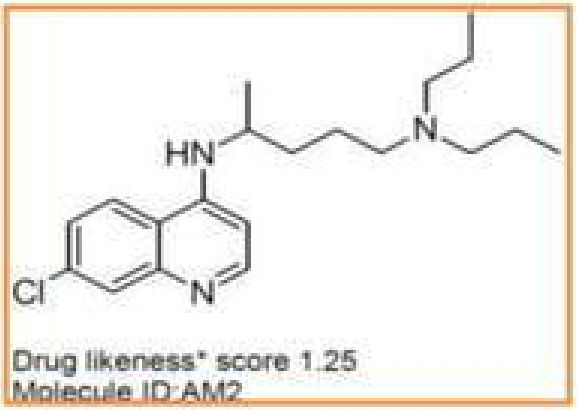


Drug likeness* score 1.25
Molecule ID:AM2

- In case of designed molecules the chlorine molecule at position 8 have been replaced by –F atom to increase the drug likeness score than the prototype molecule chloroquine.
- The position of R1 and R2 in the 4- aminoquinolone ring are modified in these designed molecules to get increased drug likeness score

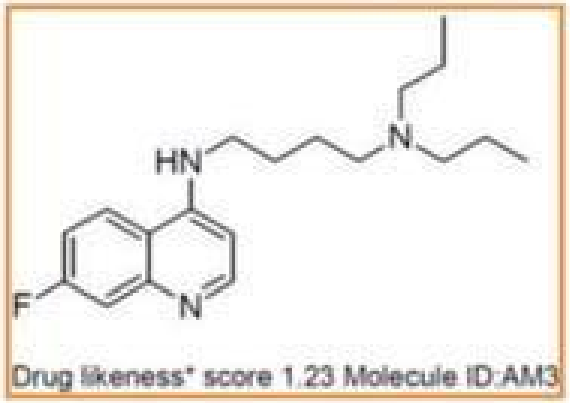

Drug likeness* score 1.23 Molecule ID:AM3

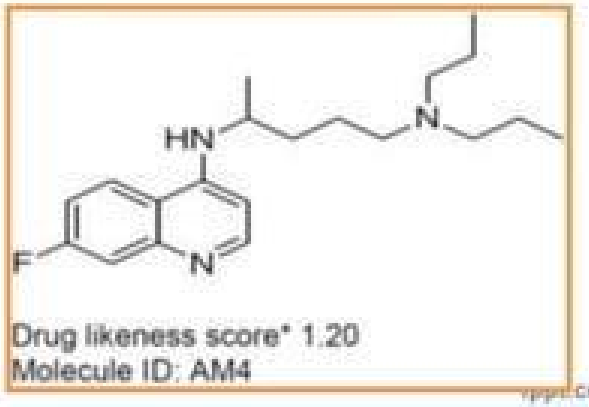

Drug likeness score* 1.20
Molecule ID: AM4

# 8-aminoquinolines

- Drugs in this group have amino group at position 8 of quinoline ring
- Such drugs have $OCH_3$ group at position 6
- Pamaquine, **primaquine**, and **tafenoquine** are antimalarial drugs that belong to a family named **8-aminoquinolines**.
- Pamaquine is closely related to primaquine.
- Compared to primaquine, pamaquine is more toxic and less effacacious.
- Tafenoquine is currently in late clinical trials.

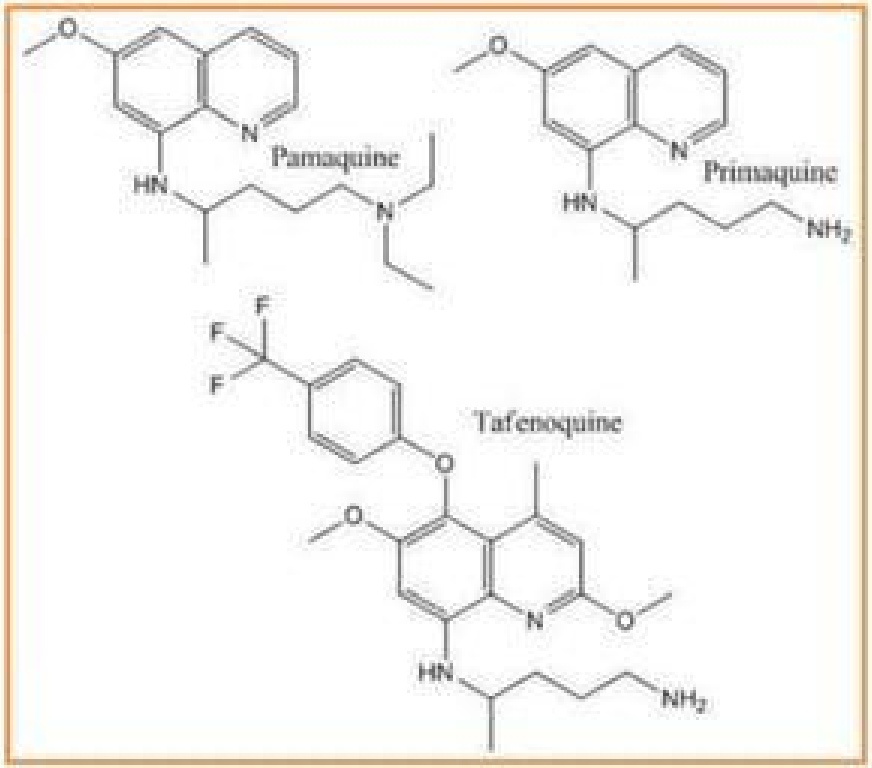

# Pamaquine

- When side chain

  is introduced at amino group antimalarial activity is intensified
- It causes hemolysis of RBCs

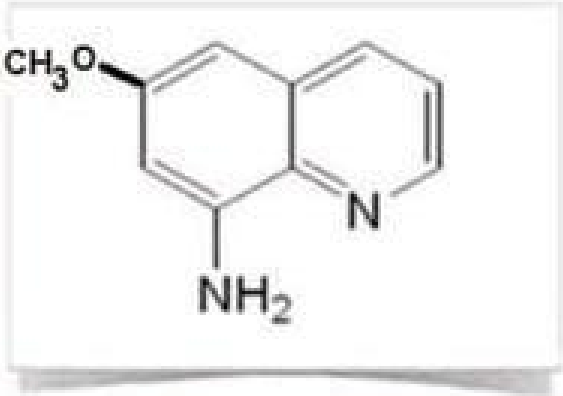


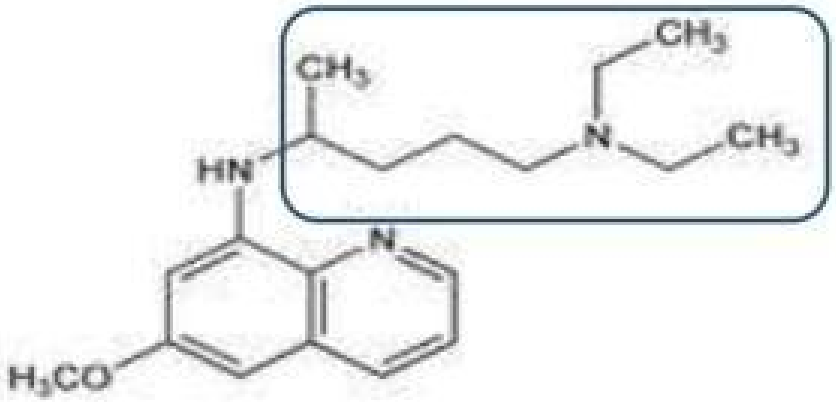


Diethyl amino pentyl side chain

# Primaquine

- It contains tertiary amino group and when it is converted into primary amino group the compound is called primaquine, which is
  - Less toxic
  - Well tolerated


It is the most commonly used agent in this group in the treatment of malaria

- $OCH_3$ is not necessary for antimalarial activity but when replaced by $OC_2H_5$ the compound became
  - less active
  - Toxic in nature
- $OCH_3$ when replaced by $CH_3$ the compound become inactive
- Introduction of halogens increases toxicity
- Presence of quinoline ring is necessary for antimalarial activity. When pyridine ring is converted to piperidine (saturated) the compound became inactive

- Pentyl side chain gives maximum activity, increase or decrease of chain result is reduction of activity.
- The branched side chain when converted into straight chain pentaquine is obtained

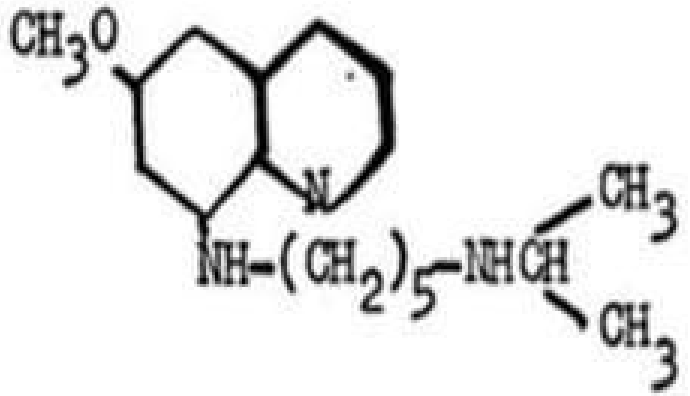


- It has less antimalarial activity as compared to both pamaquine and primaquine

# Other Quinine Analogues

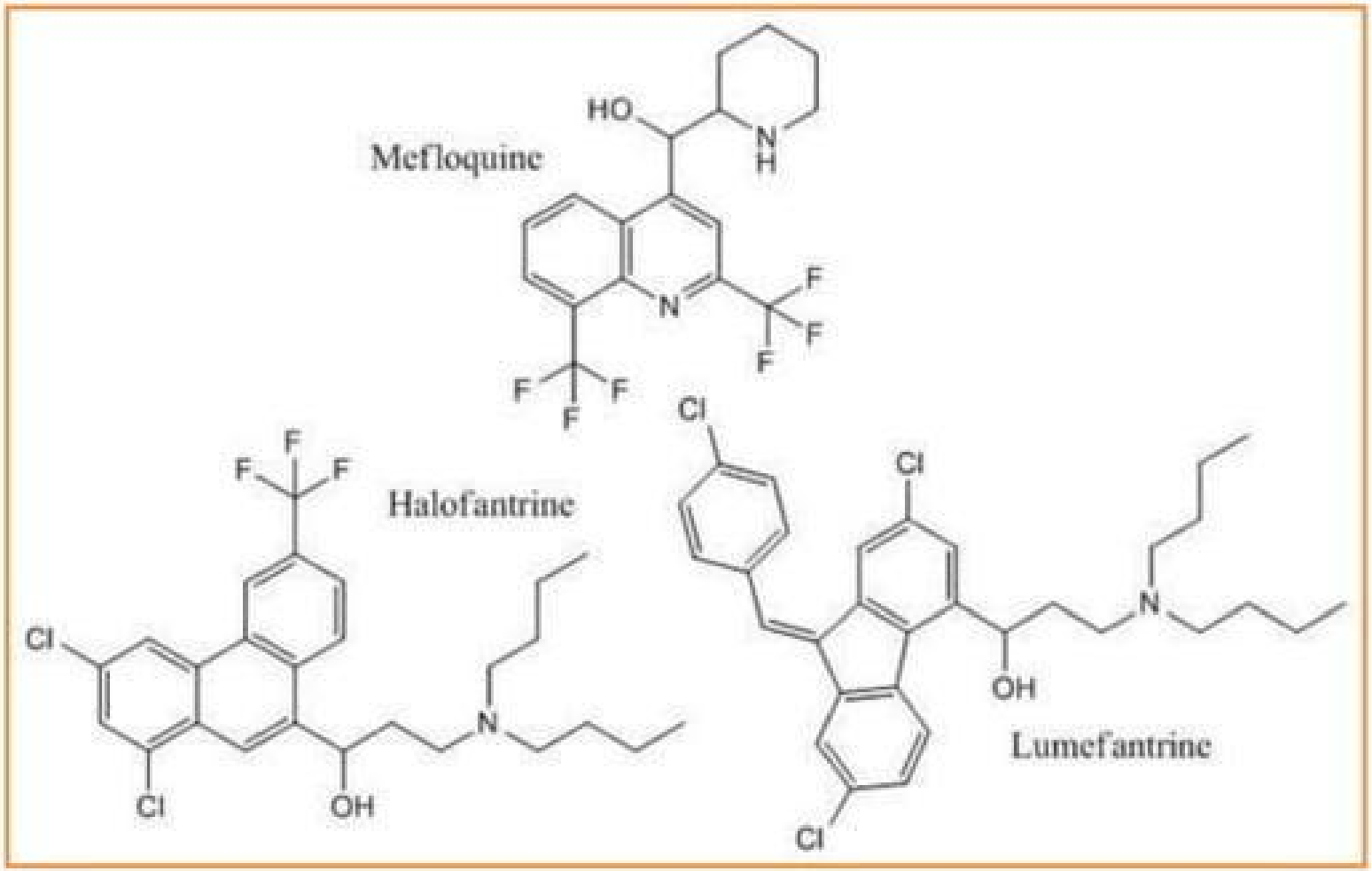

# Other Quinine Analogues

- **Mefloquine** is an orally administered 4-methanolquinoline drug used to prevent and treat malaria.Like the other drugs, the halo substituents deter Phase I metabolism (hydroxylation) of the rings and also contribute to enhanced lipophilicity.
- **Halofantrine** contains a phenanthrene ring. The absorption of halofantrine is enhanced when taken with fatty food.
- **Lumefantrine** is usually taken in combination with the artemisinin based drug, artemether.

# Piperaquine

- Resistance to chloroquine is a major problem which continues to drive the need for new antimalarials structurally similar to chloroquine.
- Resistance to the drug was first documented during the 1950s. During the 1960s, the bisquinoline antimalarial, piperaquine was synthesised. The compound has two of the bicyclic 4-aminoquinoline group.
- Piperaquine showed excellent activity against resistant parasites. However, the use of piperaquine declined during the 1980s as a result of the emergence of resistant strains of P. falciparum.

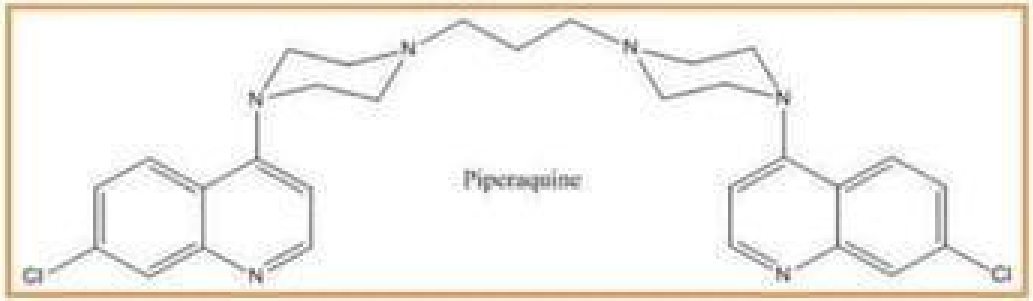

# Isoquine

- One disadvantage of amodiaquine is the formation of toxic amodiaquine quinone imine (AQQI) metabolites.
- Isoquine as a less toxic variant of amodiaquine.
- In fact isoquine is an isomer of amodiaquine, differing only in the positions of the hydroxyl and the diethylamine.
- Isoquine's hydroxyl group is located in the meta position rather than the para position.
- When OH is in the meta-position, AQQI does not form. Isoquine has been described as a new lead compound for less toxic 4-aminoquinolines.


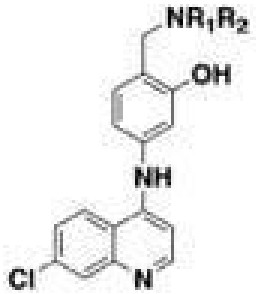


- Phosphate salt of Isoquine superior to Amodiaquine dihydrochloride
- Not metabolised to toxic metabolites
- No excessive accumulation in animal models
- Analogues in Class are Cheap to Prepare

# Fluoroamodiaquine (FAQ)

- Fluorine is commonly used in drug design. Substitution with fluorine also contributes to increased lipophilicity.
- In terms of metabolism, fluorine is used to block parts of the drug that are susceptible to metabolism such as the *para*-position of benzene rings.
- Due to the formation of the toxic amodiaquine metabolite, a series of fluoro-substituted variants of amodiaquine designed and found the desired metabolic stability.

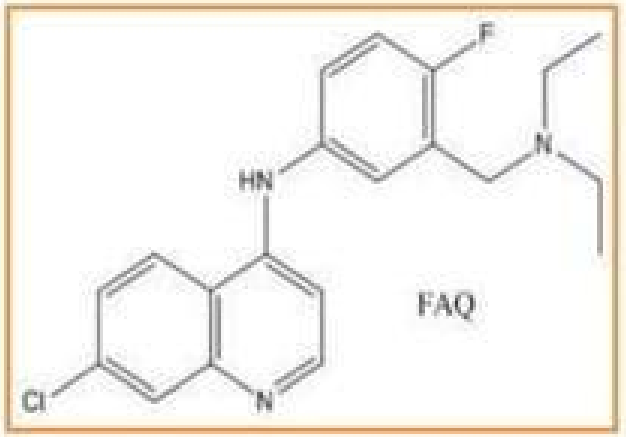

# Medicinal Chemistry of Other Antimalarial Drugs

# Pyronaridine

Pyronaridine is an antimalarial compound exhibits high potency towards P. falciparum and some chloroquine-resistant strains.

Studies of mouse models showed that pyronaridine is active against the erythrocytic stages of malaria.

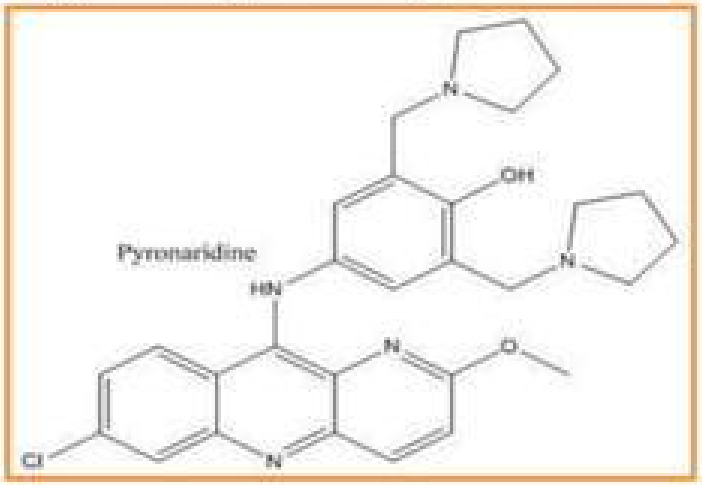


When used in combination with other antimalarials such as artesunate, the emergence of resistance appears to be slowed down considerably.

Current studies suggest that pyronaridine is an ideal candidate for combination therapy with artemisinins.

Pyronaridine's core structure is similar to mepacrine (quinacrine). The drug is typically administered orally as pyronaridine tetraphosphate which appears yellowish and has a bitter taste. The drug can also be administered via the intramuscular or intravenous route.

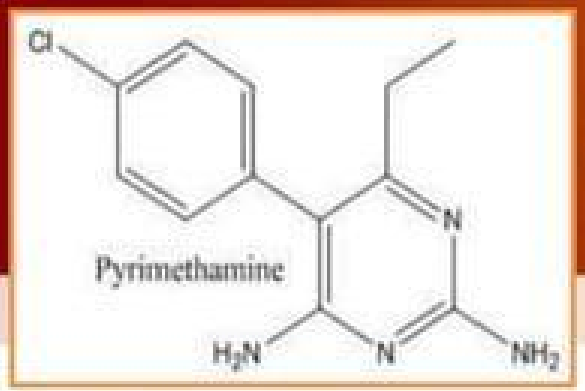


# Pyrimethamine

Often used in combination with other sulfonamide antimalarial drugs, **pyrimethamine** is also an antifolate drug.

Pyrimethamine acts on the **dihydrofolate reductase** enzyme.

Pyrimethamine is administered through the oral route and is well-absorbed.

This drug is also used in the treatment of *Toxoplasma gondii* infections in immunocompromised patients.

Pyrimethamine is also currently being investigated as a treatment for Amyotrophic Lateral Sclerosis (ALS), also known as Lou Gehrig's disease.

# Sulfadoxine

**Sulfadoxine** (or sulphadoxine) is a sulfonamide drug that was used in combination with pyrimethamine to treat or prevent malaria.

However, due to the emergence of resistance, its use has been reduced. Sulfadoxine acts by competitively inhibiting plasmodial **dihydropteroate synthase**, an enzyme not biosynthesised by most eukaryotes including humans.

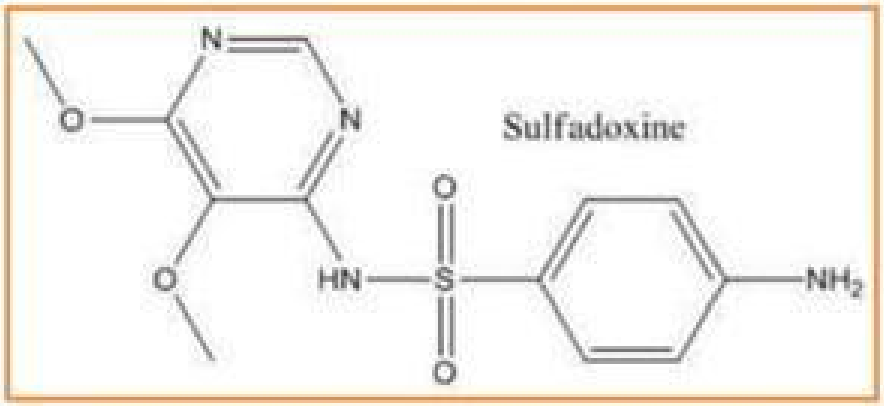

# End note:

Growing resistance to current antimalarials poses a grave threat to human health. There is a great need to discover and design new antimalarial compounds - ones that show a greater safety and efficacy profile. This endeavour ensures not only a more sound pharmacology but also a significantly improved knowledge of the medicinal chemistry of antimalarial drugs themselves, and how they operate at the fundamental level.

Hopefully this presentation has sparked some degree of understanding into this highly pertinent topic.

# Structure Activity Relationship Adrenergic & Cholinergic Drugs

Arief Kusuma Wardani, S.Si., M.Pharm.Sci

UNIVERSITAS MUHAMMADIYAH MAGELANG

# INTRODUCTION TO NERVOUS SYSTEM

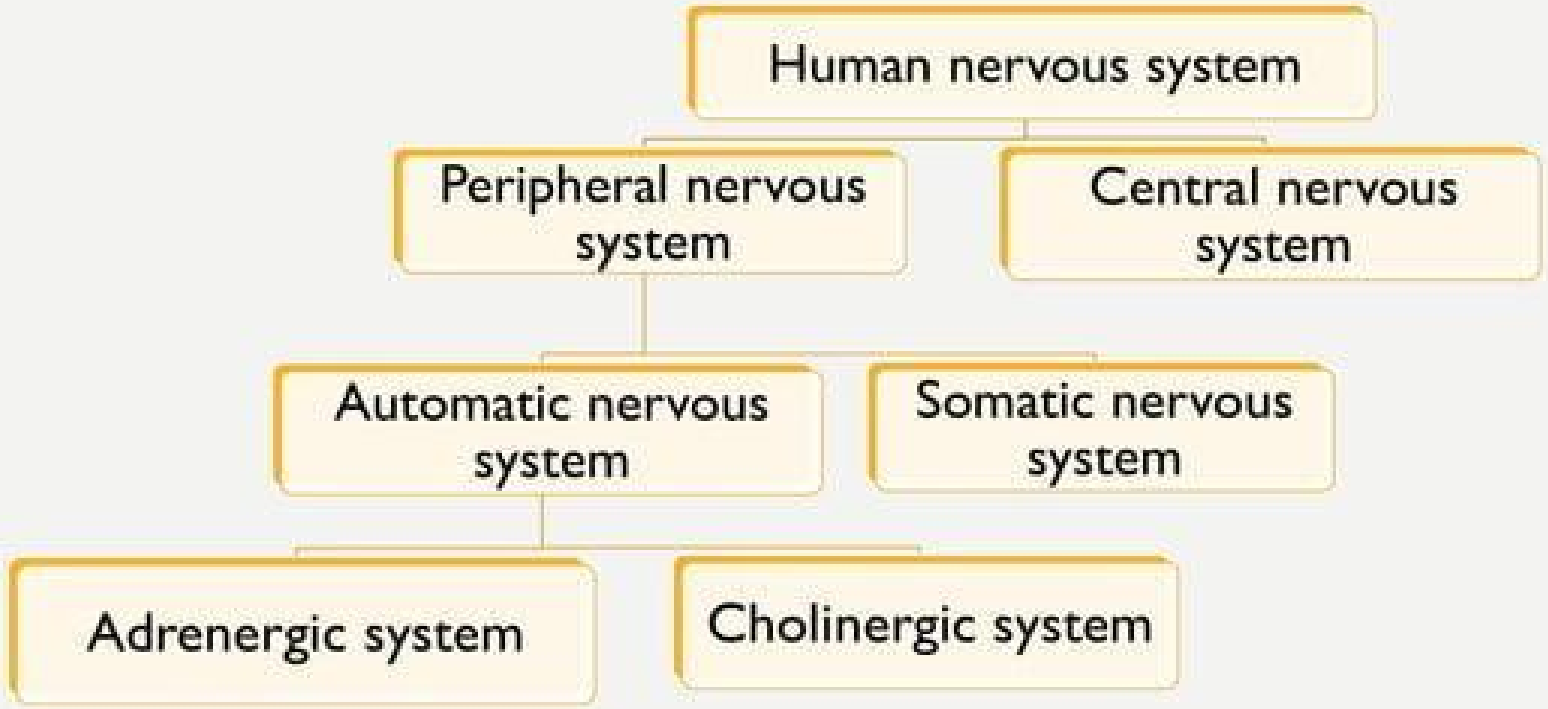

# ADRENERGIC (SYMPATHETIC) SYSTEM

- Adrenergic drugs exert their principal pharmacological and therapeutic effects by either enhancing or reducing the activity of the various components of the sympathetic division of the autonomic nervous system.
- Neurotransmitters of adrenergic system are :-

i. Epinephrine
ii. Norepinephrine
iii. Dopamine

# MECHANISM OF ADRENERGIC SYSTEM

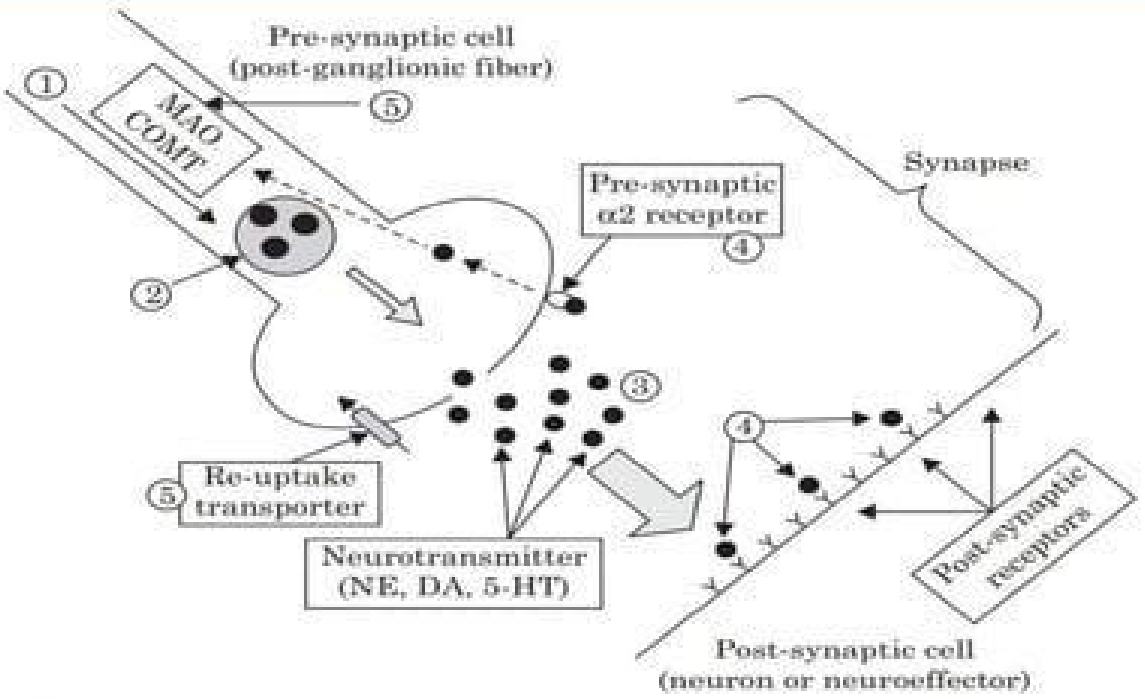


Synthesis and release of neurotransmitters from adrenergic nerves

# ADRENERGIC RECEPTORS

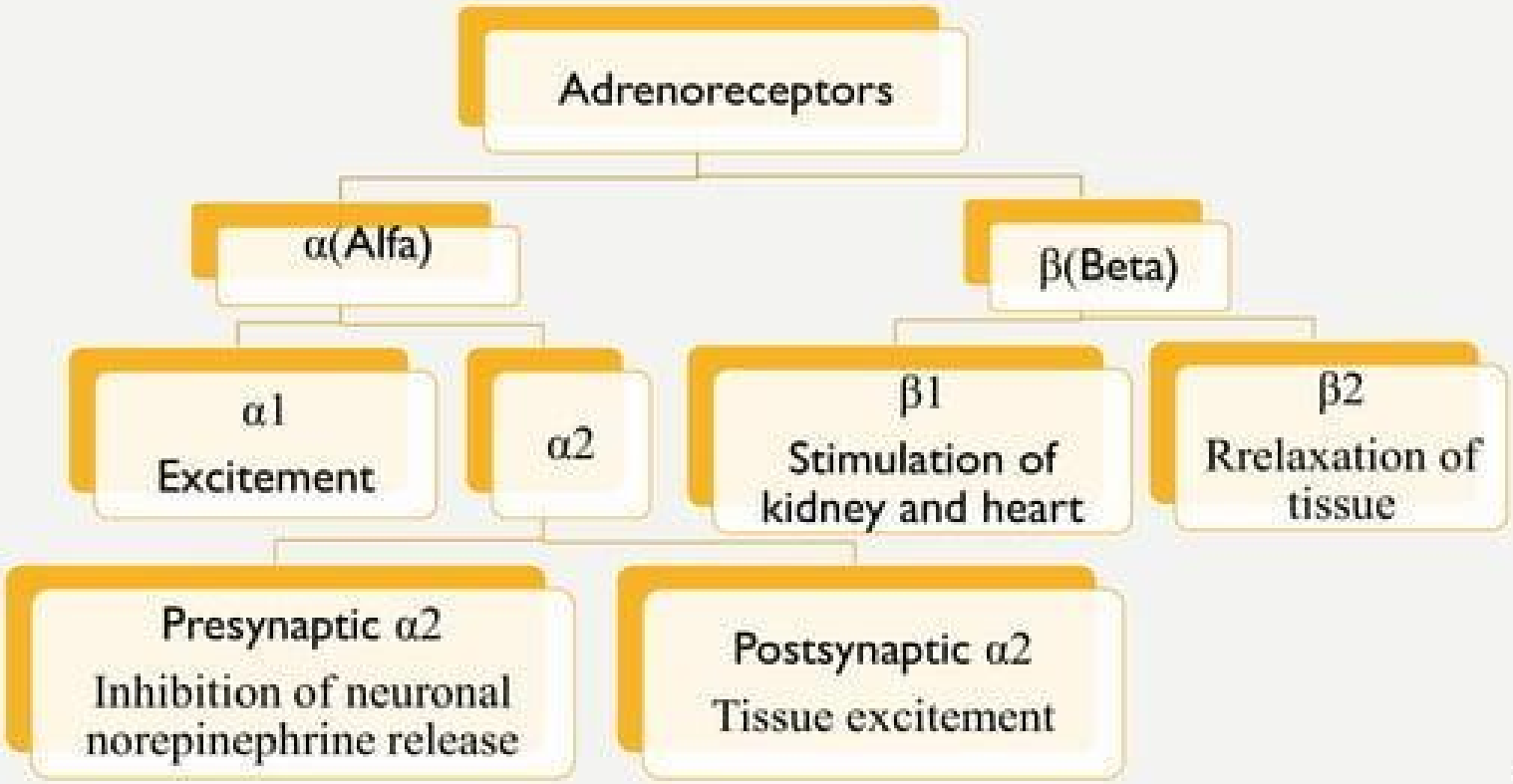

# CLASSIFICATION OF ADRENERGIC AGENTS

## Adrenergic (Sympathomimetic) Agonists

A) Selectiveα- Adrenergic Agonists

A.1) α1- agonists (imidazolines)


Xylometazoline


Oxymetazoline

# CLASSIFICATION OF ADRENERGIC AGENTS

A.2) α2- agonists (imidazolines)


Clonidine


Apraclonidine

# CLASSIFICATION OF ADRENERGIC AGENTS

B) Selective β- Adrenergic Agonists

B.1) β1- agonists

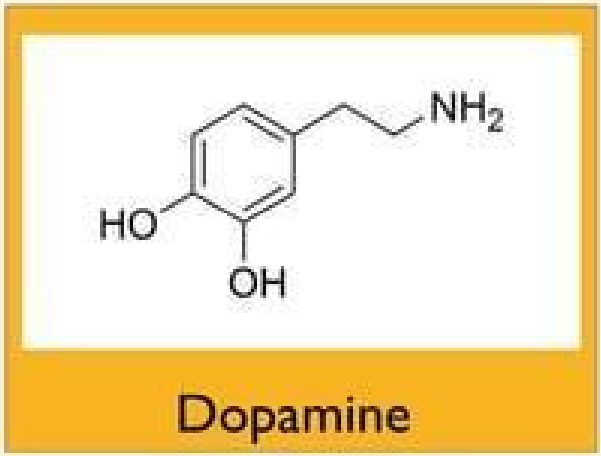


Dopamine

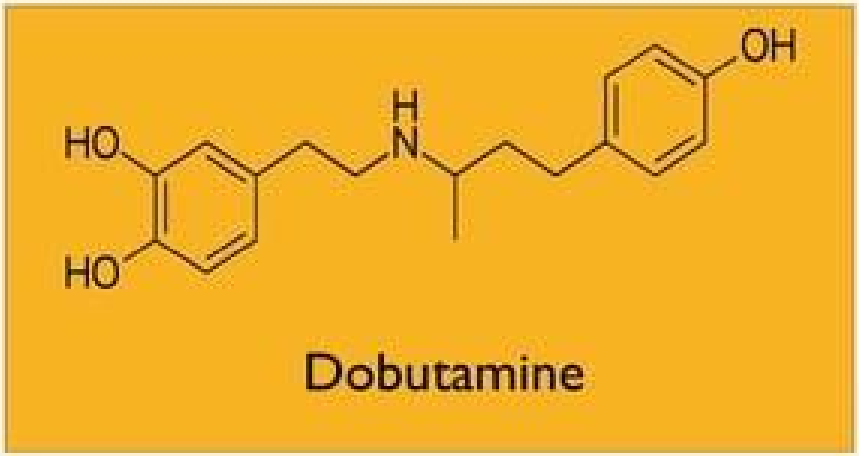


Dobutamine

# CLASSIFICATION OF ADRENERGIC AGENTS

B.2) β2- agonists

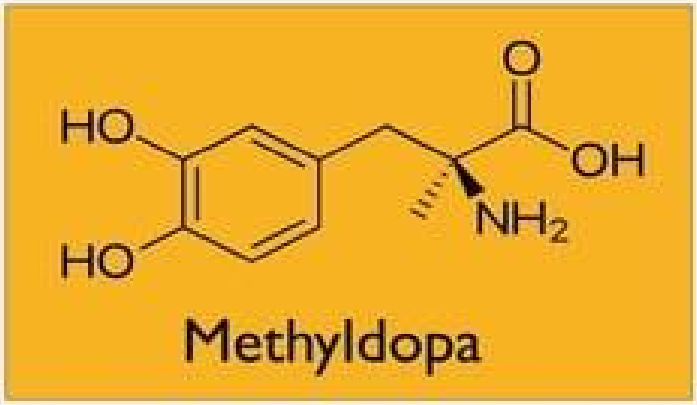

Methyldopa

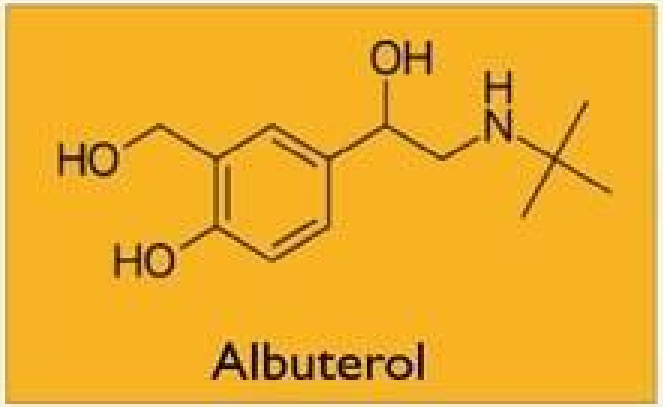

Albuterol

# CLASSIFICATION OF ADRENERGIC AGENTS

C) Mixed acting sympathomimetics

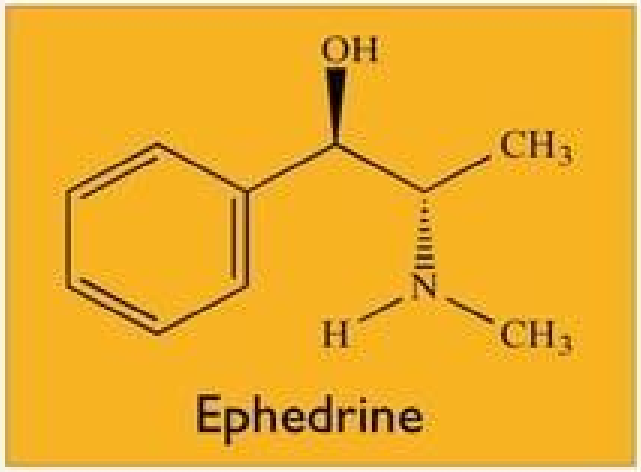


Ephedrine

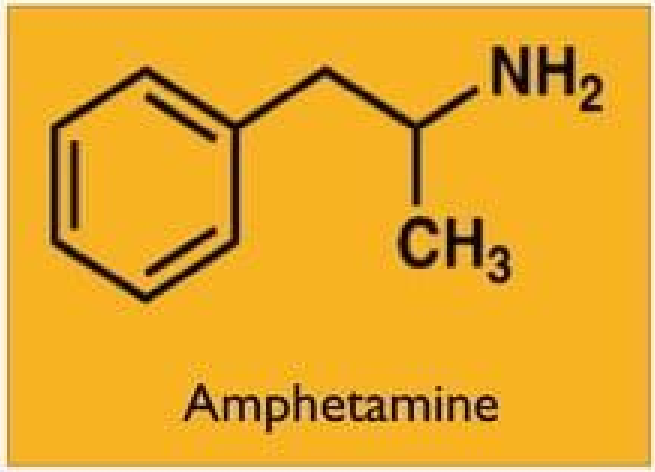


Amphetamine

# CLASSIFICATION OF ADRENERGIC AGENTS

## Adrenergic (Sympatholytic) Antagonists

A) Selective α- Adrenergic Antagonists

A.1) α1- antagonists


Prazocine


Terazocine

# CLASSIFICATION OF ADRENERGIC AGENTS

A.2) α2- antagonists

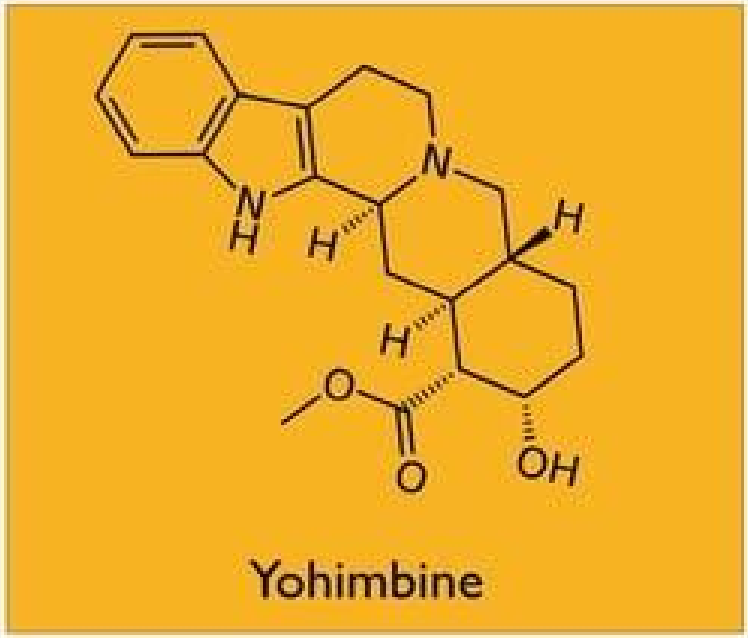


Yohimbine

# CLASSIFICATION OF ADRENERGIC AGENTS

B) Selective β1- antagonists


Metoprolol

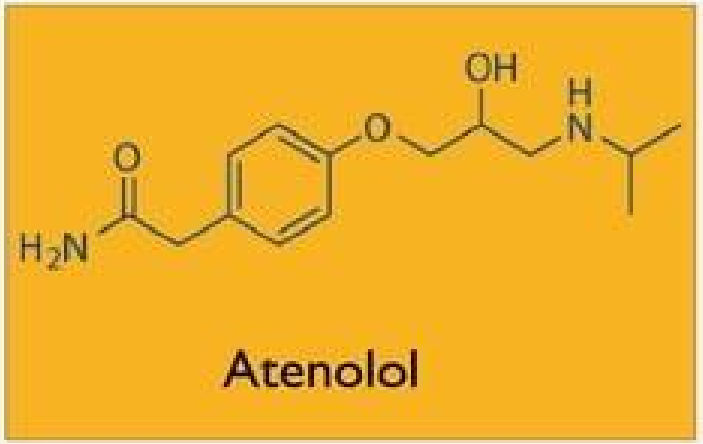


Atenolol

# CLASSIFICATION OF ADRENERGIC AGENTS

C) Nonselective β antagonists

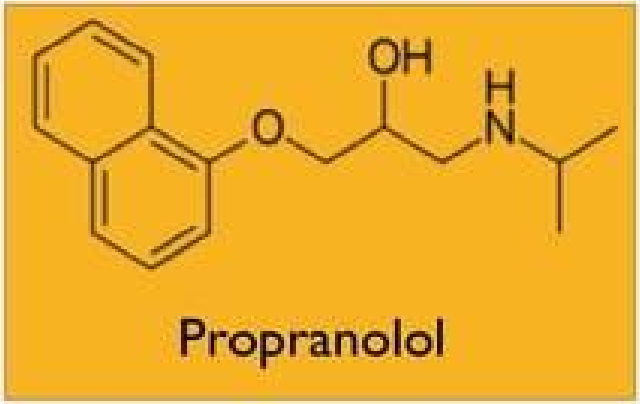


Propranolol

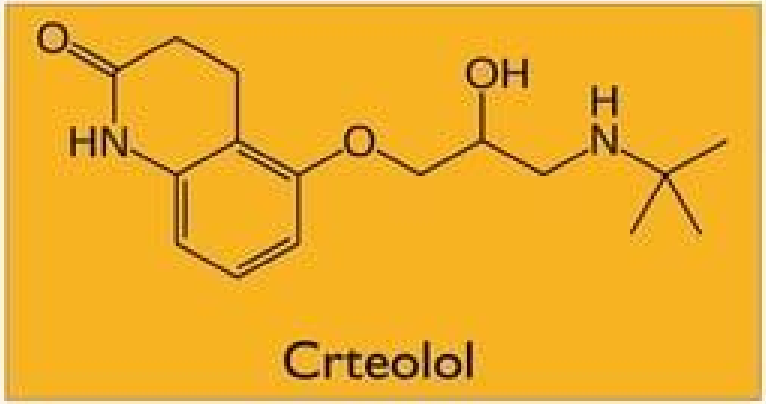


Crteolol

# CLASSIFICATION OF ADRENERGIC AGENTS

D) Mixed α/β antagonists

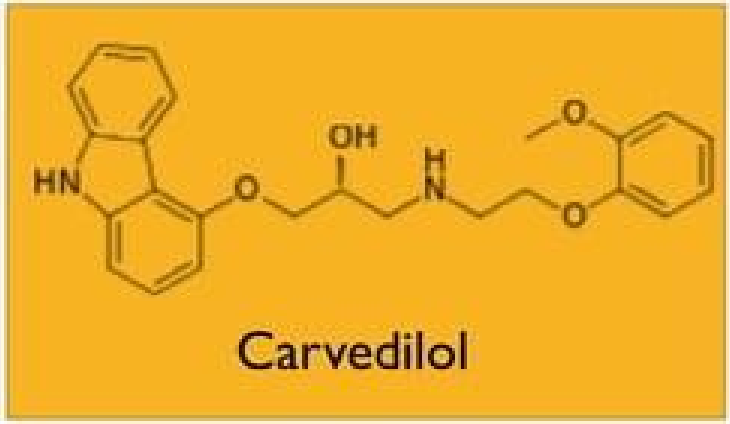


Carvedilol


Labetalol

# STRUCTURE ACTIVITY RELATIONSHIPS

A) Catecholamines:- ((o-dihydroxybenzene)

- Distance between aromatic ring and amine
- Alkyl substitution of amino group- Isoproterenol(β-receptor)
- 3,5-dihydroxy with large amino group confers β2 selectivity
- Substitution with groups other than —OH, reduce activity


Catechol

# STRUCTURE ACTIVITY RELATIONSHIPS

B) Noncatecholamines:- (β-phenylethylamine)

- Distance between aromatic ring and amine
- Substitution on the β-C generally decreases central stimulant action
- Degradation resistant by COMT due to absence of hydroxyl group
- Absence of hydroxyl group reduces overall potency

β-phenylethylamine

Ephedrine

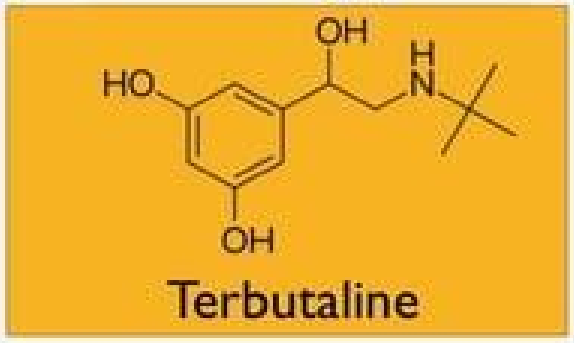

Terbutaline

# THERAPEUTIC USES OF SYMPATHETICS

- Treatment of Acute Hypotension
- Chronic Orthostatic Hypotension
- Treatment therapy of bronchial asthma
- Phenylephrine is an effective mydriatic agent
- Lower intraocular pressure and are approved for use in glaucoma
- β 2-selective agents relax the pregnant uterus
- Clonidine- α 2 -agonist treatment of diarrhea in diabetics with autonomic neuropathy
- Tizanidine- α 2- agonist that is used as a muscle relaxant

# CHOLINERGIC (PARA-SYMPATHETIC) SYSTEM

- The main nerves of the parasympathetic system are the tenth cranial nerve, the vagus nerve, which originate in the medulla oblongata.
- Parasympathetic stimulation causes:-

- slowing down of the heart beat,
- lowering of blood pressure,
- constriction of the pupils,
- increased blood flow to the skin and viscera,
- peristalsis of the GI tract

# NEUROTRANSMITTERS OF CHOLINERGIC SYSTEM

Chemically there are four classes:-

1) Acetylcholine
2) Biogenic amines : Indolamines (serotonin and tryptamine are synthesized from tryptophan), and the catecholamines (dopamine, norepinephrine and epinephrine are synthesized from tyrosine).
3) Excitatory amino acids : There are three major amino acid neurotransmitters in the nervous system ; γ-Amino butyric acid (GABA), glycine, glutamic acid and aspartate.
4) Neuropeptides, over 50 are known.

# MECHANISM OF CHOLINERGIC SYSTEM

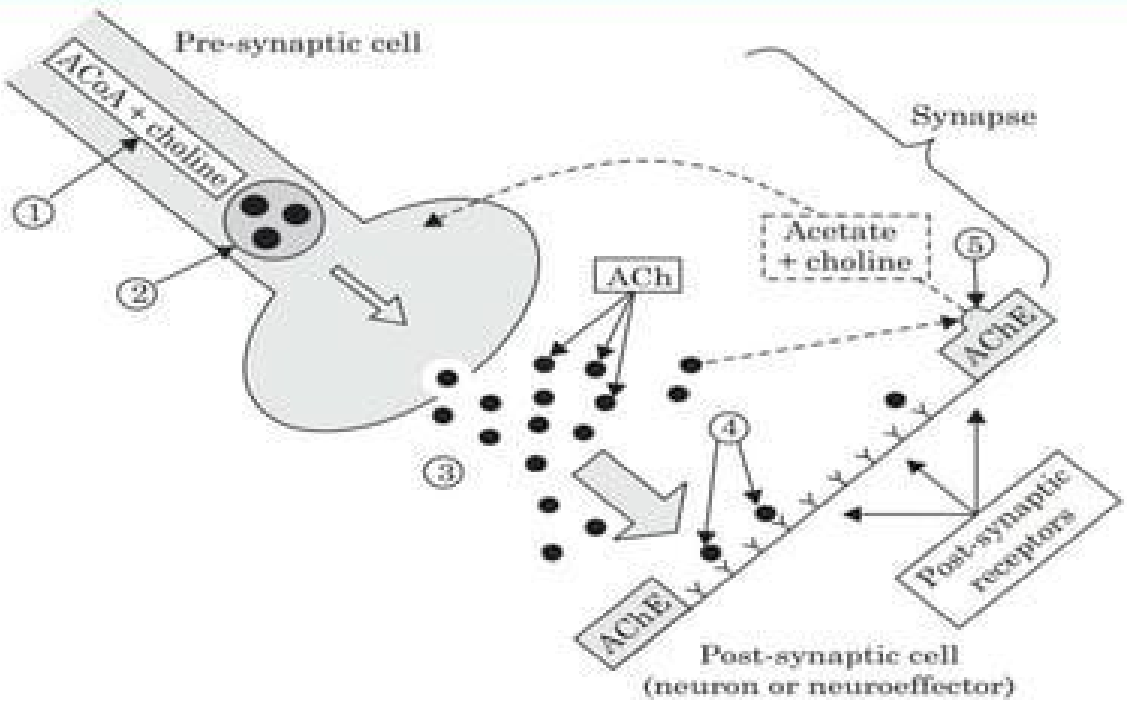


Synthesis and release of acetylcholine

# RECEPTORS OF CHOLINERGIC SYSTEM

| Cholinergic Receptors | | |
|---|---|---|
| **M1** | **Secretory glands** | salivation, stomach acid, sweating, lacrimation |
| **M2** | **Heart** | Decreases heart rate → bradycardia |
| **M3** | **Smooth muscle (GI/GU/Resp)** | Contraction of smooth muscles (some) → diarrhea, bronchospasm, urination |
| **M3** | **Pupil and ciliary muscle** | Contracts → Miosis<br>Increased flow of aqueous humor |
| **Nm** | **Skeletal muscle end plate** | Contraction of skeletal muscle |
| **Nn** | **Autonomic ganglia, Adrenal Medulla** | Secretion of Epinephrine<br>Controls ANS |

# CLASSIFICATION OF CHOLINERGIC AGENTS

**Cholinergic (**Para-Sympathomimetic**) agonists**

A)DIRECT-ACTING CHOLINOMIMETICS

A.1) Choline esters

Acetylcholine

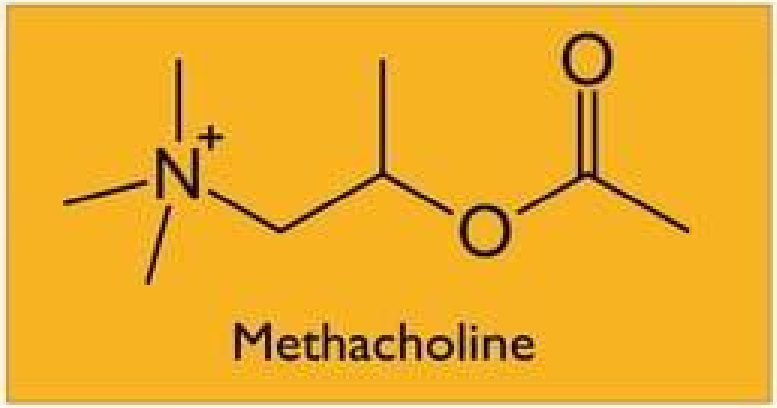

Methacholine

# CLASSIFICATION OF CHOLINERGIC AGENTS

A) DIRECT-ACTING CHOLINOMIMETICS

A.2) Natural alkaloids

A.2.1) Natural muscarinic alkaloids

Muscarine

Pilocarpine

# CLASSIFICATION OF CHOLINERGIC AGENTS

A) DIRECT-ACTING CHOLINOMIMETICS

A.2) Natural alkaloids

A.2.2) Natural nicotinic alkaloids


Nicotine

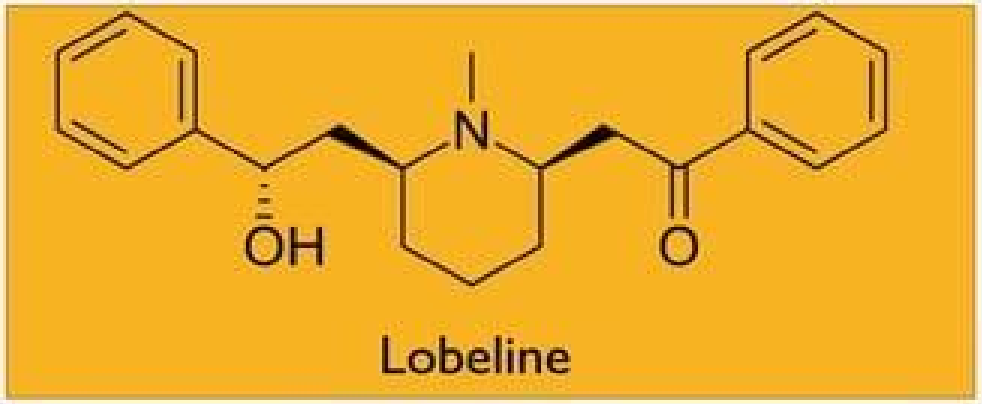


Lobeline

# CLASSIFICATION OF CHOLINERGIC AGENTS

B) INDIRECT-ACTING CHOLINOMIMETICS

B.1) Reversible cholinesterase inhibitors

B .1.1) Carbamates


Physostigmine


Neostigmine

# CLASSIFICATION OF CHOLINERGIC AGENTS

B) INDIRECT-ACTING CHOLINOMIMETICS

B.1) Reversible cholinesterase inhibitors

B.1.1) Quaternary amines


Edrophonium

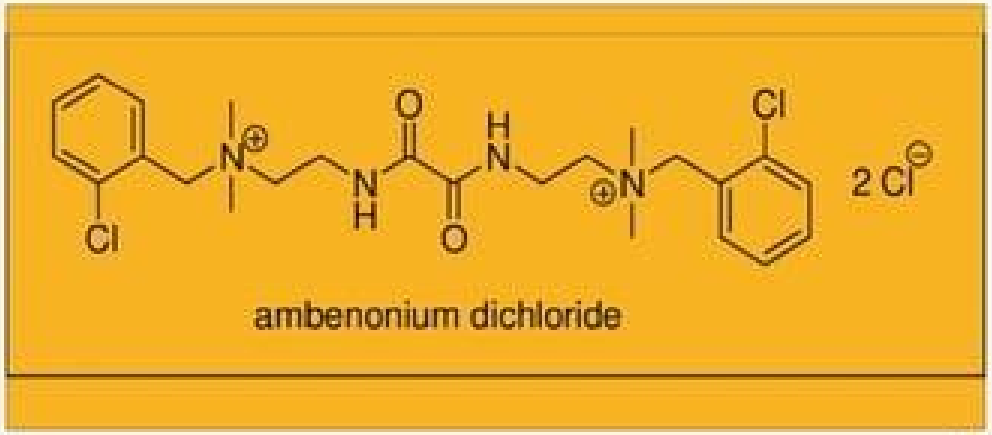


ambenonium dichloride

# CLASSIFICATION OF CHOLINERGIC AGENTS

B) INDIRECT-ACTING CHOLINOMIMETICS

B.2) Reversible cholinesterase inhibitors

Organophosphates

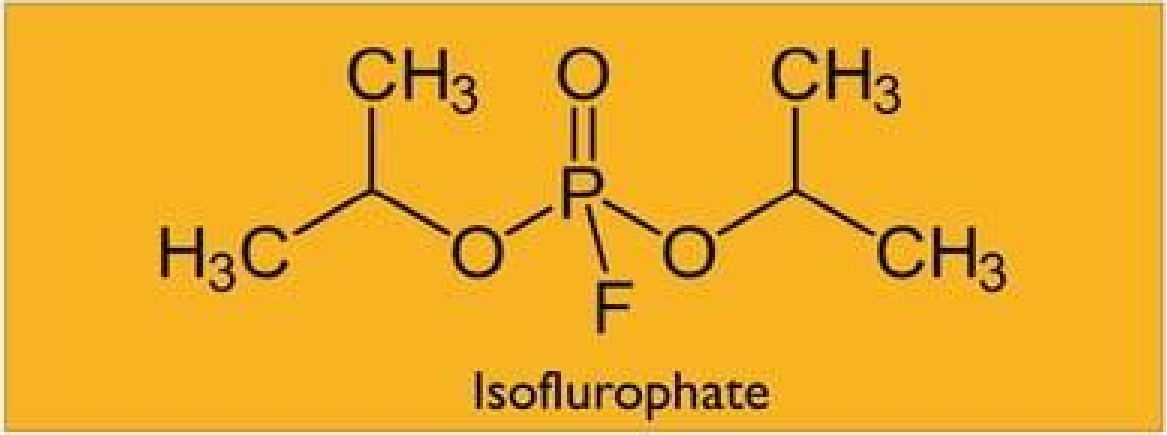


Isoflurophate

# CLASSIFICATION OF CHOLINERGIC AGENTS

**Cholinergic (**Para-Sympatholytic**) Antagonists**

A) ANTIMUSCARINIC DRUGS

A.1) Alkaloids

Atropine

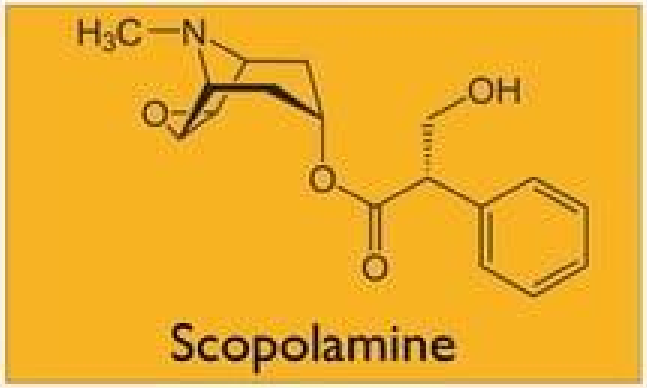

Scopolamine

# CLASSIFICATION OF CHOLINERGIC AGENTS

A) ANTIMUSCARINIC DRUGS

A.2) Anticholinergics of the quaternary amine series


Methscopolamine

# CLASSIFICATION OF CHOLINERGIC AGENTS

A) ANTIMUSCARINIC DRUGS

A.3) Antiparkinsonian drugs of the quaternary amine series

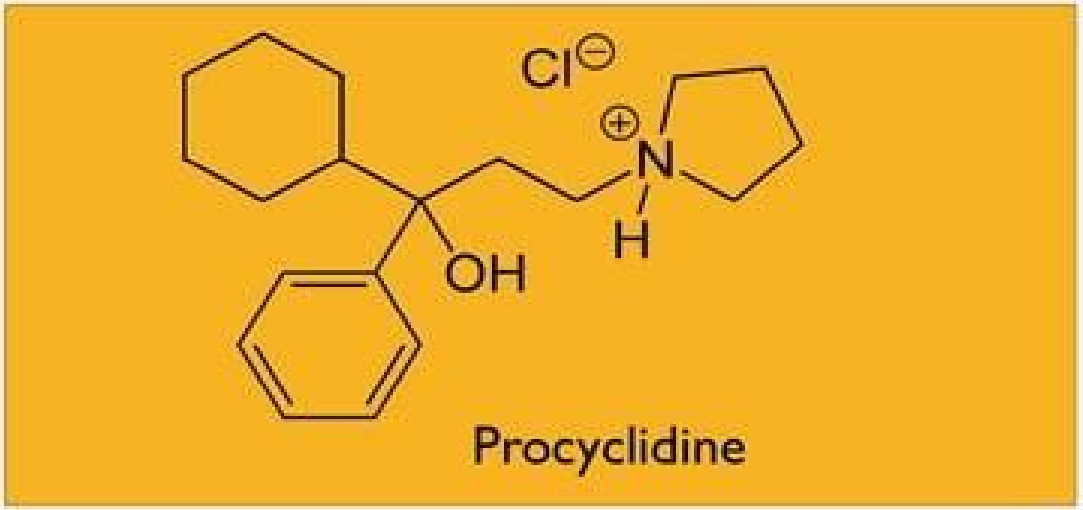


Procyclidine

# CLASSIFICATION OF CHOLINERGIC AGENTS

A) ANTIMUSCARINIC DRUGS

A.4) Antispasmodics of the tertiary amine series


Dicycloamine

# CLASSIFICATION OF CHOLINERGIC AGENTS

A) ANTIMUSCARINIC DRUGS

A.5) Mydriatics of the tertiary amine series

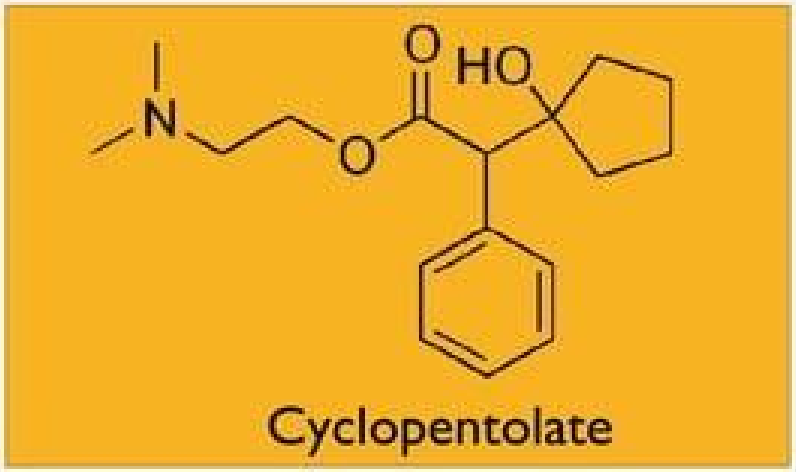


Cyclopentolate

# STRUCTURE ACTIVITY RELATIONSHIPS

- Positively charged quaternary ammonium compound
- Replacement of acetyl group, muscarinic activity decreases
- Acetyl group is replaced by a carbamyl, resistant to hydrolysis by AChE or BuChE, eg. Carbachol
- β-methyl substitution (Bethanechol), mainly muscarinic activity

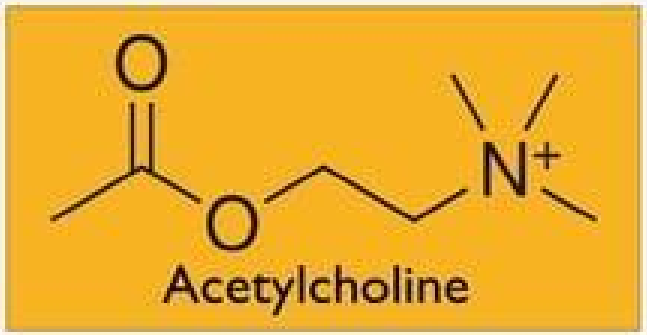

Acetylcholine

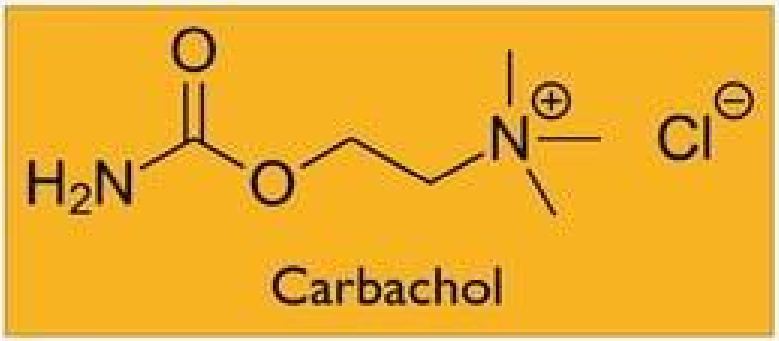

Carbachol

# THANK YOU .

International Journal of
*Molecular Sciences*

MDPI

*Article*

# Structure–Activity Relationship (SAR) Study of Spautin-1 to Entail the Discovery of Novel NEK4 Inhibitors

**Mathias Elsocht [1], Philippe Giron [2,3], Laila Maes [4,5], Wim Versées [4,5], Gustavo J. Gutierrez [3], Jacques De Grève [2] and Steven Ballet [1,*]**

1 Research Group of Organic Chemistry, Faculty of Sciences and Bioengineering Sciences, Vrije Universiteit Brussel, Pleinlaan 2, 1050 Brussels, Belgium; Mathias.Elsocht@vub.be
2 Laboratory of Medical and Molecular Oncology and Center of Medical Genetics, Faculty of Medicine and Pharmacy, Vrije Universiteit Brussel, Laarbeeklaan 103, 1090 Brussels, Belgium; Philippe.Giron@vub.be (P.G.); Jacques.DeGreve@uzbrussel.be (J.D.G.)
3 Laboratory of Pathophysiological Cell Signalling (PACS), Department of Biology, Faculty of Sciences and Bioengineering Sciences, Vrije Universiteit Brussel, Pleinlaan 2, 1050 Brussels, Belgium; Gustavo.Gutierrez.Gonzalez@vub.be
4 VIB-VUB Center for Structural Biology, Pleinlaan 2, 1050 Brussels, Belgium; Laila.Maes@vub.be (L.M.); Wim.Versees@vub.be (W.V.)
5 Structural Biology Brussels, Vrije Universiteit Brussel, Pleinlaan 2, 1050 Brussels, Belgium
* Correspondence: Steven.Ballet@vub.be; Tel.: +32-2-6293292

**Abstract:** Lung cancer is one of the most frequently diagnosed cancers accounting for the highest number of cancer-related deaths in the world. Despite significant progress including targeted therapies and immunotherapy, the treatment of advanced lung cancer remains challenging. Targeted therapies are highly efficacious at prolonging life, but not curative. In prior work we have identified Ubiquitin Specific Protease 13 (USP13) as a potential target to significantly enhance the efficacy of mutant EGFR inhibition. The current study aimed to develop lead molecules for the treatment of epidermal growth factor receptor (EGFR)-mutant non-small cell lung cancer (NSCLC) by developing potent USP13 inhibitors initially starting from Spautin-1, the only available USP13 inhibitor. A SAR study was performed which revealed that increasing the chain length between the secondary amine and phenyl group and introducing a halogen capable of inducing a halogen bond at position 4′ of the phenyl group, dramatically increased the activity. However, we could not confirm the binding between Spautin-1 (or its analogues) and USP13 using isothermal titration calorimetry (ITC) or thermal shift assay (TSA) but do not exclude binding under physiological conditions. Nevertheless, we found that the anti-proliferative activity displayed by Spautin-1 towards EGFR-mutant NSCLC cells in vitro was at least partially associated with kinase inhibition. In this work, we present *N*-[2-(substituted-phenyl)ethyl]-6-fluoro-4-quinazolinamines as promising lead compounds for the treatment of NSCLC. These analogues are significantly more effective towards EGFR-mutant NSCLC cells than Spautin-1 and act as potent never in mitosis A related kinase 4 (NEK4) inhibitors ($IC_{50}$~1 μM) with moderate selectivity over other kinases.

**Keywords:** non-small cell lung cancer; USP13; NEK4; EGFR; quinazolinamines



**Citation:** Elsocht, M.; Giron, P.; Maes, L.; Versées, W.; Gutierrez, G.J.; De Grève, J.; Ballet, S. Structure–Activity Relationship (SAR) Study of Spautin-1 to Entail the Discovery of Novel NEK4 Inhibitors. *Int. J. Mol. Sci.* **2021**, *22*, 635. https://doi.org/10.3390/ijms22020635

Received: 28 November 2020
Accepted: 7 January 2021
Published: 10 January 2021



## 1. Introduction

The World Health Organization estimated that 1.76 million people died of lung cancer in 2018, which represents almost 20% of all cancer-related deaths [1]. The predominant subtype of lung cancer is NSCLC, which accounts for 80–85% of all lung cancer patients [2]. In NSCLC patients with little or no smoking history, mutations in the EGFR, a major regulator of cell proliferation and apoptosis, are frequently observed [3]. The exon 19 in frame deletion (EGFR del E746-A750) and the exon 21 point mutation (L858R) represent together 90% of all activating mutations [4]. Despite the promising initial response of EGFR-mutant NSCLC patients towards first (reversible), second (irreversible), and third

(EGFR mutant specific) generations of EGFR tyrosine kinase inhibitors (examples depicted in Figure 1), patients generally developed acquired resistance (by a secondary mutation or activation of alternative pathways within the cancer cells) which illustrates the need for improved treatment strategies in this subset of lung cancers [4,5].

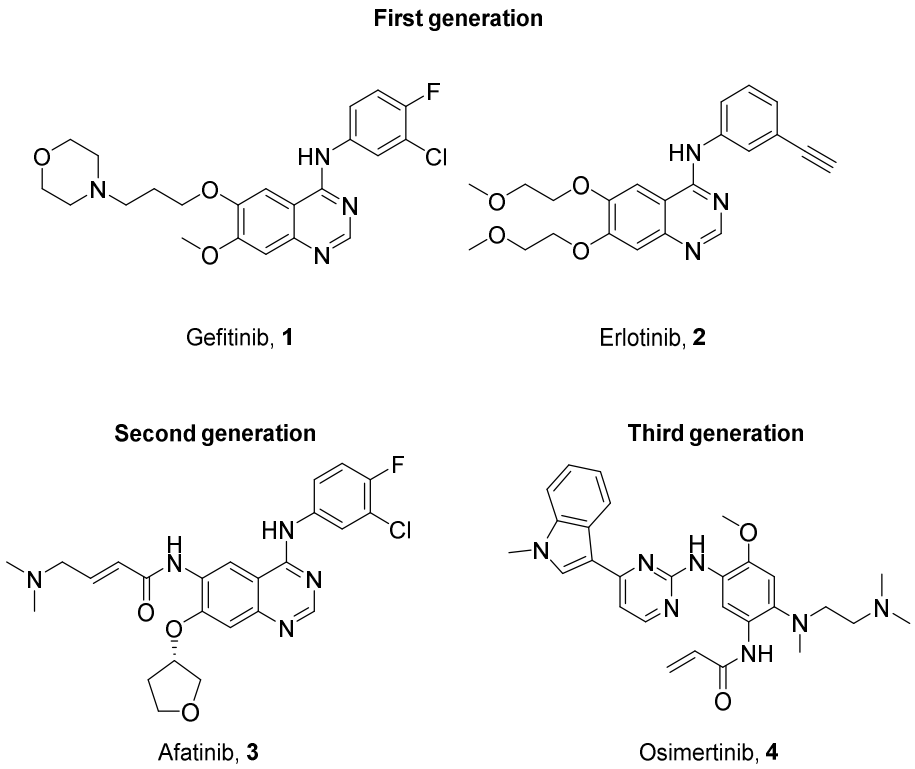


**Figure 1.** Examples of first, second and third generations epidermal growth factor receptor tyrosine kinase inhibitors.

The importance of posttranslational modifications in tumorigenesis is widely accepted [6–8]. Insight in these processes can lead to new therapeutic strategies to improve current treatments [8]. Ubiquitination is, besides phosphorylation, an important posttranslational modification linked to cancer. It consists of the reversible attachment of one or multiple ubiquitin moieties to target proteins, altering their stability, activity, interactors and/or localization [9,10]. It is a three-step process catalyzed by the consecutive action of the E1 activating enzyme, the E2 conjugating enzyme and the E3 ligase [9,11]. Conversely, deubiquitinating enzymes (DUBs) reverse this process by selectively cleaving ubiquitin or poly-ubiquitin chains from ubiquitinated proteins [12].

USP13, a DUB enzyme part of the USP-family, has been linked to multiple cancers. This enzyme acts as a tumor suppressor in breast cancer, human bladder cancer, and oral squamous cell carcinoma [13–15]. However, it also acts as a tumor promotor in glioblastoma (brain tumor), ovarian cancer, melanoma (skin cancer), and prostate cancer [16–23]. In NSCLC, USP13 has been frequently found to be amplified. Moreover NSCLC cell proliferation (in vitro) and tumor growth (in vivo) is inhibited by downregulating USP13 [24].

Despite the differential role of USP13 in tumorigenesis, this enzyme is considered as a potential therapeutic target. Recently, we have reported that inhibition of USP13 destabilizes EGFR and that co-inhibition of USP13 and EGFR suppresses oncogenic signaling in NSCLC cells [25]. These findings motivated us to initiate the development of more potent USP13 inhibitors, starting from the only USP13 inhibitor described in the literature to date (Spautin-1, **5aa**, Figure 2) [26], by exploring the chemical space around Spautin-1 and determining the importance of the quinazoline core by performing a "*N*-screening". The quino-

line [27–30], isoquinoline [31,32], cinnoline [33–35], and quinoxaline [36] cores were considered, all privileged scaffolds which have shown their effectiveness as kinase inhibitors.

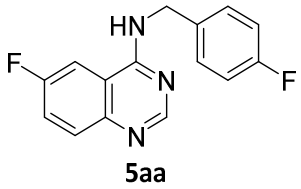


**Figure 2.** Chemical structure of Spautin-1 (**5aa**).

Herein, we elaborate upon *N*-[2-(substituted-phenyl)ethyl]-6-fluoro-4-quinazolinamines as promising lead compounds for the treatment of NSCLC. Based on an EGFR-mutant NSCLC cell viability screening, these analogues were found to be significantly more potent when compared to Spautin-1. We attempted to demonstrate binding of the spautin-1 analogues to USP13 using isothermal titration calorimetry (ITC) or thermal shift assay (TSA) but were unsuccessful. Nevertheless, the *N*-[2-(substituted-phenyl)ethyl]-6-fluoro-4-quinazolinamines showed good activity and moderate selectivity towards NEK4, a kinase previously linked to NSCLC. Park and co-workers reported, for instance, the overexpression of NEK4 in lung cancer and suggested that NEK 4 suppresses Tumor necrosis factor-Related Apoptosis Inducing Ligand (TRAIL)-induced apoptosis, which in turn results into tumor resistance. In contrast, downregulation of NEK4 sensitizes tumor cells to TRIAL-induced apoptosis via decreased levels of survivin, an anti-apoptotic protein [37]. In 2018, along the same lines, Ding and co-workers published that NEK4 is a positive regulator of epithelial-to-mesenchymal transition (EMT) which plays an important role in lung cancer metastasis [38]. To our best knowledge, there are no potent and selective NEK4 inhibitors described in the literature. Some previously reported kinase inhibitors showed good off-target activity for NEK4 but lacked selectivity. Some examples are: BAY 61-3606 (**6**, SYK inhibitor), Abbott compound 17 (**7**, MAP3K8 inhibitor), and Abbott 1141 (**8**, multikinase inhibitor) (structures depicted in Figure 3) [39–42].

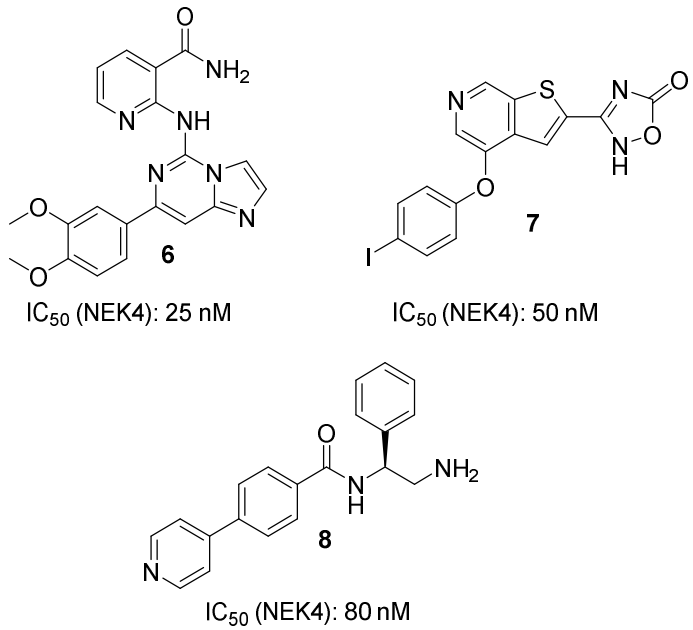


**Figure 3.** Non-selective NEK4 inhibitors reported in the literature so far.

In light of the above, we hypothesize that the activity of our analogues towards EGFR-mutant NSCLC cells is at least in part related to inhibition of NEK4. As far as we know,

these are the first inhibitors described in the literature targeting NEK4, which also show promising single agent anticancer activity towards EGFR-mutant NSCLC cells.

## 2. Results

### *2.1. Chemistry*

The chemical space around Spautin-1 was explored by synthesizing analogues based on the 4-aminoquinazoline core. An efficient three-step protocol was developed (Scheme 1), which only required one purification at the end of the synthesis. The substituted quinazolin-4(3*H*)-ones **11** were synthesized starting from substituted 2-aminobenzamides **9** using trimethyl orthoformate or substituted 2-aminobenzoic acids **10** using formamide [43,44]. Subsequently, the 4-chloroquinazoline core **12** was obtained using thionyl chloride and a catalytic amount of *N*,*N*-dimethylformamide (DMF) [45]. Finally, a microwave-assisted nucleophilic aromatic substitution was performed to obtain the desired analogues **5** in yields varying between 31 and 84% [46].

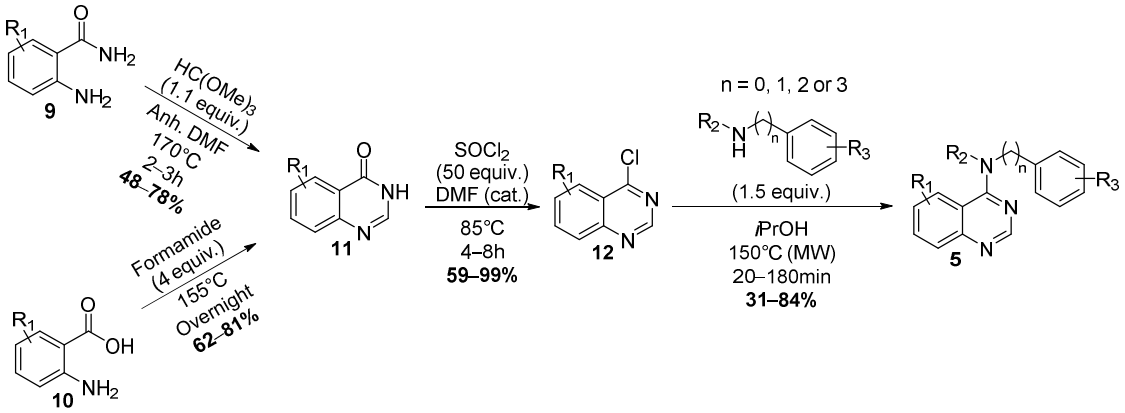


**Scheme 1.** Synthesis of Spautin-1 analogues **5** starting from substituted 2-aminobenzamides **9** or 2-aminobenzoic acids **10**.

Further exploratory diversification was introduced using palladium-catalyzed cross-coupling reactions. In literature described strategies were applied to introduce a phenyl group as in **13**, using the Suzuki reaction, and an alkyne substituent to reach compounds of type **14**, via the Sonogashira reaction (Scheme 2) [47,48]. These larger substituents provided insight in the available chemical space around the quinazoline core. These conversions made use of the I>>F selectivity during Pd-catalyzed transformations.

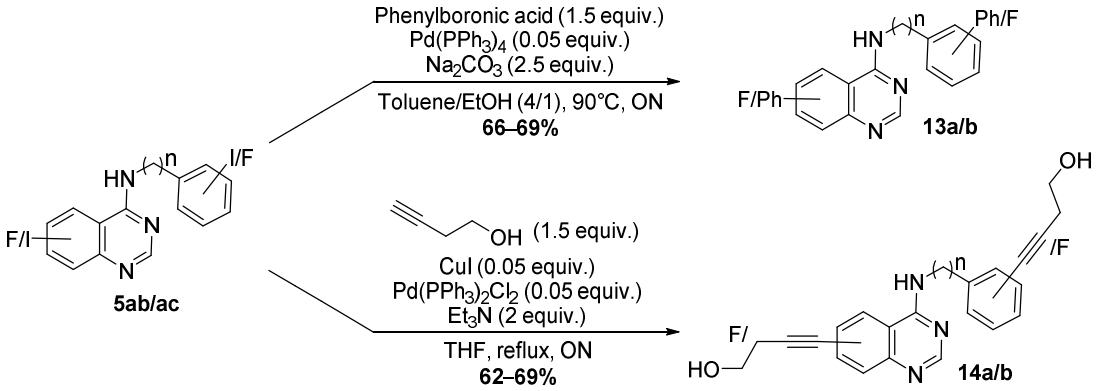


**Scheme 2.** Palladium-catalyzed cross coupling reactions: Suzuki and Sonogashira reactions.

As a ring-contracted analogue, the synthesis of a Spautin-1 analogue bearing the benzimidazole core **17**, was pursued (Scheme 3). The benzimidazole system is a well-established scaffold in medicinal chemistry, but in the current study, it can be regarded as a quinazoline

analogue in which one of both rings is compacted. In consequence, the substituents will be oriented differently as compared to the topological orientation in its homologue. The substituted benzimidazole was synthesized starting from 5-fluoro-2-nitroaniline **15**. In our hands, the highest isolated yield for the nucleophilic substitution reaction towards **16** was obtained in DMF using $Cs_2CO_3$ as a base. Finally, the benzimidazole core was obtained after reduction of the nitro-group using an excess of iron in acetic acid, followed by the cyclisation using trimethyl orthoformate and a catalytic amount of *p*-toluene sulfonic acid yielding **17** [49,50].

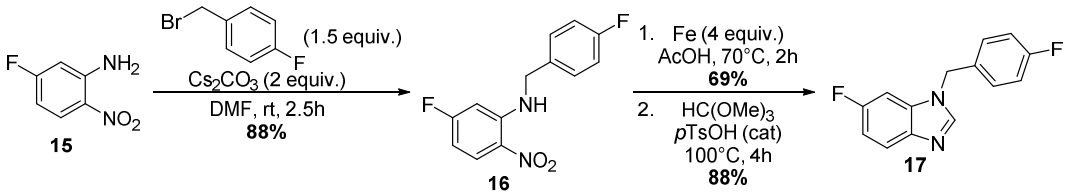


**Scheme 3.** Synthesis of a ring contracted spautin-1 analogue bearing the benzimidazole core.

Thereafter, a "*N*-screening" was performed to determine how important the quinazoline scaffold is for the biological activity. First, the quinazoline core was replaced by the quinoline and isoquinoline core to determine the importance of each individual nitrogen. In one step, compound **19** was obtained from the commercially available 4-chloro-6-fluoroquinoline **18** through a microwave-assisted nucleophilic aromatic substitution (Scheme 4). The previously described conditions of Felts et al. were not efficient in this case, because of which we opted for a solvolytic reaction [51].

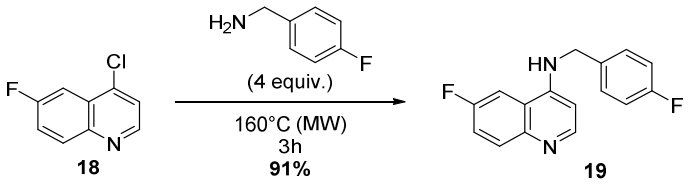


**Scheme 4.** Synthesis of a spautin-1 analogue bearing the quinoline core.

The isoquinoline core was obtained following the procedure reported by Zhao and coworkers (Scheme 5) [52]. Starting from 5-fluoro-2-methylbenzamide **20**, 7-fluoro-isoquinolinone **22** was obtained in two steps. First **20** was allowed to react with *N*,*N*-dimethylformamide dimethyl acetal yielding intermediate **21**, which was subsequently cyclized under basic conditions. Next, 1-chloro-7-fluoroisoquinoline **23** was synthesized using phosphorus oxychloride, which was subsequently converted to the Spautin-1 analogue **24** via a nucleophilic aromatic substitution.

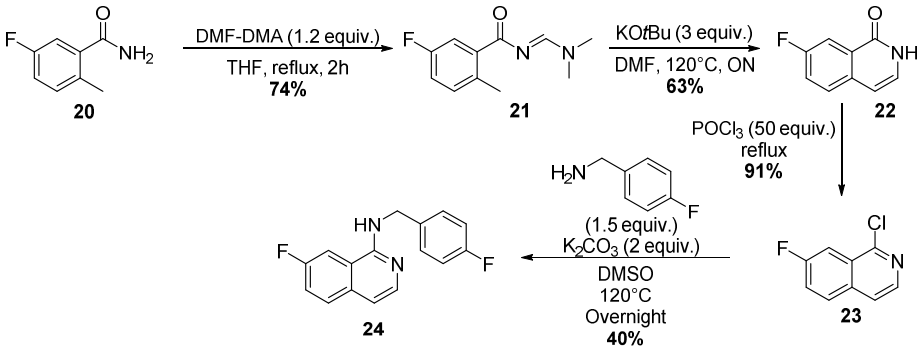


**Scheme 5.** Synthesis of a spautin-1 analogue bearing the isoquinoline core.

Alternatively, the two nitrogens in the central scaffold were preserved but positioned differently. The cinnoline core was accessed via a Sonogashira coupling, followed by a cyclisation through in situ formation of nitrous acid (Scheme 6) [53]. The obtained 6-fluorocinnoline-4-ol **27** was then converted to 4-chloro-6-fluorocinnoline **28** using thionyl chloride in the presence of a catalytic amount of DMF. Finally, a nucleophilic aromatic substitution was performed yielding the desired product **29** in moderate yield.

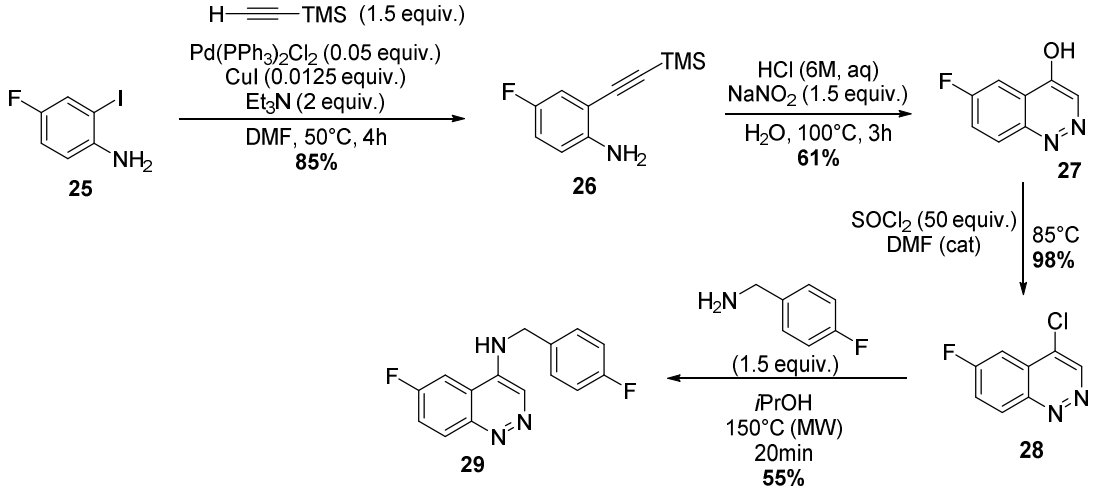


**Scheme 6.** Synthesis of a Spautin-1 analogue bearing the cinnoline core.

An alternative to the cinnoline core is the quinoxaline scaffold. 7-Fluoro-3,4-dihydro-1*H*-quinoxalin-2-one **32** was obtained from 4-fluoro-2-nitroaniline **30**, which was allowed to react with ethyl bromoacetate, yielding **31** (Scheme 7). Afterwards the nitro group was reduced, which immediately resulted in the formation of the cyclized product. After stirring the mixture for another 48 h in the absence of hydrogen gas, the desired core structure **32** was obtained. Similarly to abovementioned schemes, an analogous two-step strategy was used to couple the 4-fluorobenzylamine yielding **34**.

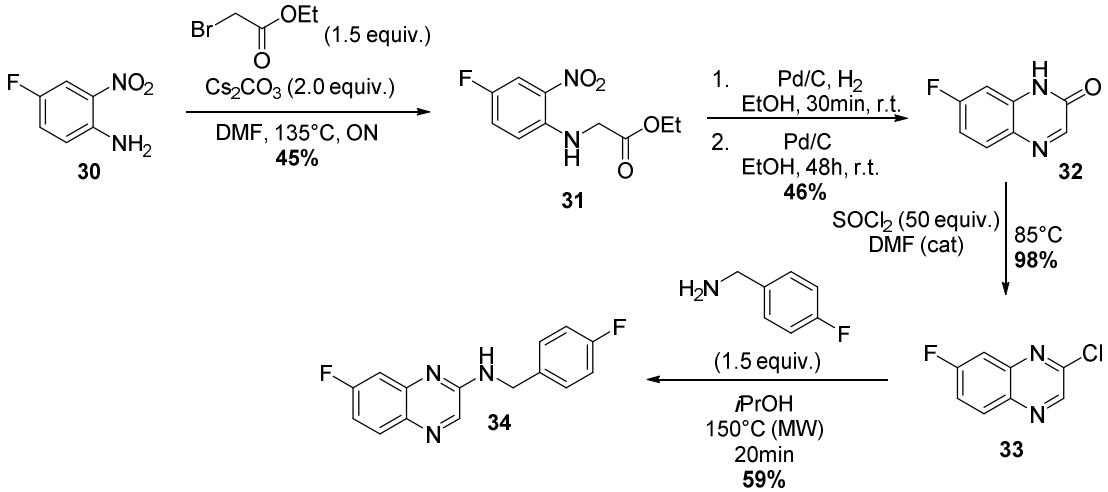


**Scheme 7.** Synthesis of a Spautin-1 analogue bearing the quinoxaline core.

## *2.2. Biological Evaluation*

### 2.2.1. NSCLC Cell Viability Screening

First, the synthesized Spautin-1 analogues were subjected to an EGFR-mutant NSCLC cell viability screening to determine which compounds were the most promising in terms of reducing the viability of EGFR-mutant NSCLC cells in vitro. A reduction of cell viability in the presence of the analogues indicates induction of apoptosis and/or an inhibition of proliferation. The viability assay also helped to get insights in the structure–activity relationships (SARs) of the prepared analogues. As shown below, the analogues were subdivided in nine series in order to efficiently discover SAR trends.

At first, a "*F*-screening" was performed to determine the importance of the fluorine substituent positioning (Figure 4). Remarkably, two compounds showed a significant decrease in tumor cell numbers compared to Spautin-1 (**5aa**), namely the analogue with a fluorine at the ortho position of the benzyl group **5ae** and the analogue with a fluorine at position 8 of the quinazoline core **5ah**. The other analogues were equally **5ag** or less potent **5ad** and **5af** as compared to Spautin-1.

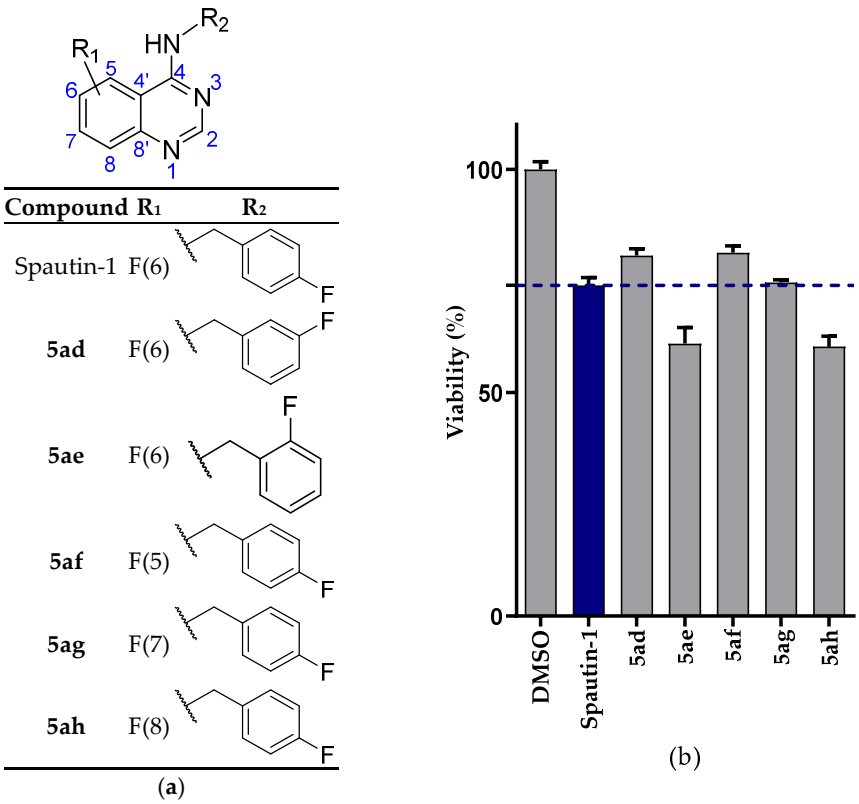


**Figure 4.** (**a**) Spautin-1 analogues synthesized for the "F-screening"; (**b**) viability assay (5 μM) with Spautin-1 as reference.

In the second series, multiple substituents, which differ in lipophilicity and electronic properties, were introduced at position 6 of the quinazoline core (Figure 5). It was observed that electron-donating substituents **5aj, 5ak** had a positive effect on the activity, compared to Spautin-1 **5aa,** while the effect of electron withdrawing groups **5ai, 5al**, **5am** was less consistent. A large hydrophobic phenyl group **13b** slightly improved the activity and confirmed that large substituents are probably allowed at this site of the central scaffold. Interestingly, a 4-hydroxybutynyl substituent at this position **14b**, previously described in EGFR TKIs [48], led to the strongest growth inhibition of the EGFR-mutant NSCLC cells.

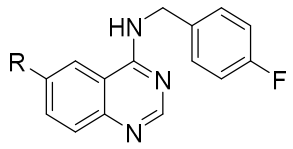


| Compound | R |
|---|---|
| Spautin-1 | F |
| **5ai** | Cl |
| **5aj** | OMe |
| **5ak** | Me |
| **5al** | $CF_3$ |
| **5am** | $NO_2$ |
| **13b** | Ph |
| **14b** | 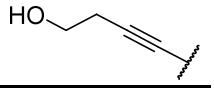 |



(**a**)

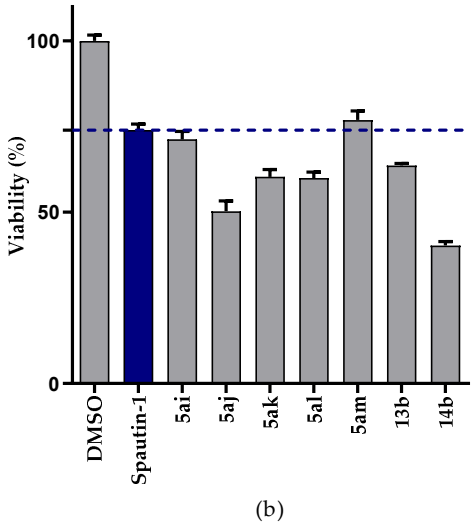


(b)

**Figure 5.** (**a**) Substituents at the 6-position of the quinazoline core were altered; (**b**) viability assay (5μM) with Spautin-1 as reference.

The fluorine at the para position of the benzyl group was replaced by a variety of groups (Cl, OMe, $CF_3$, H) (Figure 6). Notably, a methoxy **5ao**, trifluoromethyl **5ap** group and H atom **5aq** significantly improved the activity while the chlorinated analogue **5an** was equally potent to Spautin-1 (**5aa**). Nevertheless, the electron donating methoxy group resulted in the strongest reduction in the viability of the lung cancer cells in vitro.

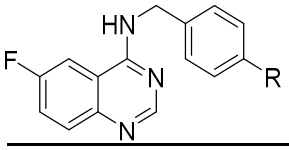


| Compound | R |
|---|---|
| Spautin-1 | F |
| **5an** | Cl |
| **5ao** | OMe |
| **5ap** | $CF_3$ |
| **5aq** | H |

(**a**)

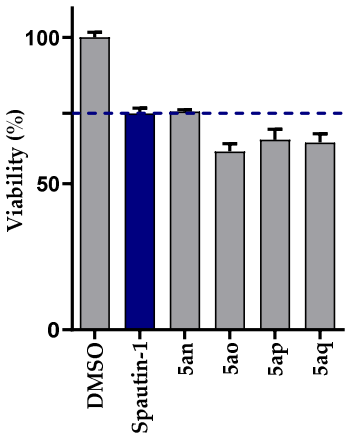


(b)

**Figure 6.** (**a**) Substituent effect on the para position of the phenyl group; (**b**) viability assay (5 μM) with Spautin-1 as reference.

To further improve the activity, the aliphatic chain length was shortened or extended, by altering the number of methylene groups (-$CH_2$-) between the secondary amine and the phenyl group (Figure 7). Remarkably, both a reduction **5ar** and extension **5as-5au** resulted in slightly and significantly more potent analogues, respectively. The extended chain length clearly resulted in an improved activity, while the increased activity of the reduced chain length can be potentially linked to inhibition of EGFR (cfr. examples in Figure 1) [54,55]. We hypothesize that the additional methylene groups increase the flexibility and in this way improve the activity.

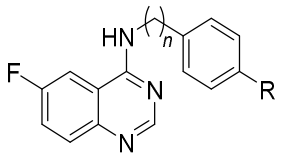


| Compound | R | *n* |
|---|---|---|
| Spautin-1 | F | 1 |
| **5ar** | F | 0 |
| **5as** | F | 2 |
| **5at** | Cl | 2 |
| **5au** | Cl | 3 |

(**a**)

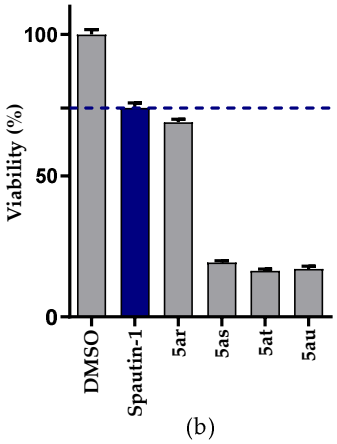


(b)

**Figure 7.** (**a**) Influence of the chain length; (**b**) viability assay (5μM) with Spautin-1 as reference.

Despite the fact that analogues with $n$ = 0 might act as EGFR TKIs, a small series of analogues was tested (Figure 8). Remarkably, a fluorine at the 3′ or 2′ position (**5av**, **5aw**) of the phenyl group significantly improved the activity as compared to the fluorine at the 4′ position **5ar**. Moreover, for $n$ = 1, a fluorine substituent at the 2′ position also gave the best result (Figure 4, **5ae**). However, in the $n$ = 1 series, a fluorine at the 3′ position resulted in a less active compound, as compared to Spautin-1, which indicates that a fluorine in proximity of the quinazoline core is beneficial. An electron-donating group at position $R_1$, on the other hand, providing **5ay**, resulted in a weaker reduction in tumor cell viability as compared to **5av**. Remarkably, a phenyl group at the 3′ position of the phenyl group **13a** was allowed while the 1-hydroxy-3-butynyl group **14a** completely abolished the activity.

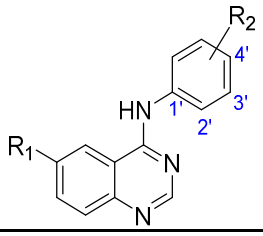


| Compound | $R_1$ | $R_2$ |
|---|---|---|
| **5ar** | F | F(4′) |
| **5av** | F | F(3′) |
| **5aw** | F | F(2′) |
| **5ax** | Cl | F(3′) |
| **5ay** | OMe | F(3′) |
| **13a** | F | Ph(3′) |
| **14a** | F | 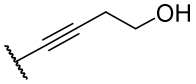 (3′) |



(**a**)

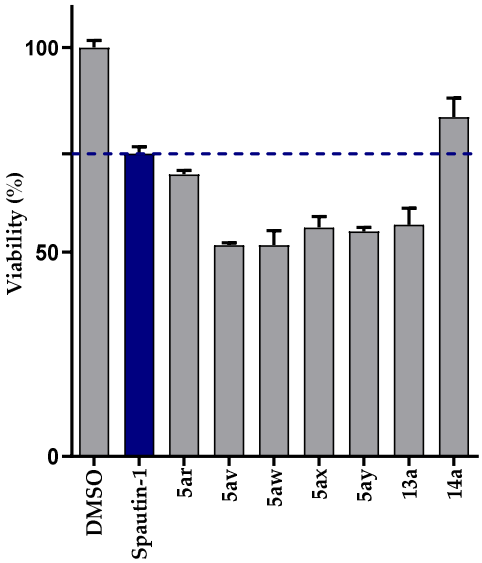


(b)

**Figure 8.** (**a**) Spautin-1 analogues with a reduced chain length; (**b**) viability assay (5 μM) with Spautin-1 as reference.

Nonetheless, the most promising compounds have an extended chain between the secondary amine and the phenyl group. Highly comparable results were obtained for all analogues, except for analogue **5bd**, which was significantly less potent at a test concentration of 5 μM (Figure 9).

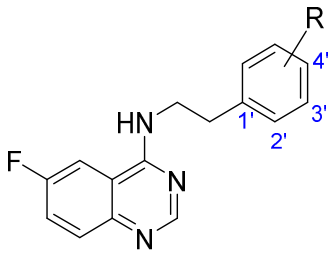


| Compound | R |
|---|---|
| **5as** | F(4′) |
| **5at** | Cl(4′) |
| **5az** | Cl(3′) |
| **5ba** | Cl(2′) |
| **5bb** | Cl(3′,4′) |
| **5bc** | OMe(4′) |
| **5bd** | H(4′) |
| **5be** | Me(4′) |
| **5bf** | Br(4′) |

(**a**)

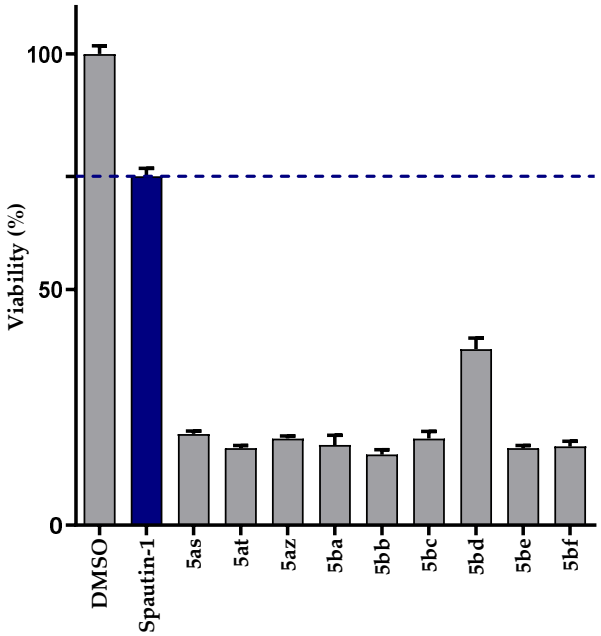


(b)

**Figure 9.** (**a**) Spautin-1 analogues with an extended chain length; (**b**) viability assay (5 μM) with Spautin-1 as reference.

To distinguish these analogues more precisely, $IC_{50}$ values were determined to unravel differences in activity (see Figure S1). These data confirmed that the phenethylamine bearing analogues were definitely more potent than Spautin-1 **5aa** (Figure 10). Additionally, a chlorine **5at** at the para position of the phenyl group of the phenethylamine seemed beneficial for the potency compared to the fluorinated counterpart **5as** but further extension of the chain length, as in **5au**, lowered the potency by a factor of seven. Subsequently, the influence of the substitution pattern of the phenyl group on the activity was evaluated which revealed that the para substituted analogue **5at** is about 1.3 times more potent as compared to the meta **5az** and disubstituted **5bb**, and about 1.1 times more potent than the ortho substituted analogue **5ba**. Replacing the chlorine **5at** by a methoxy group **5bc** resulted in a slightly more active analogue. Remarkably, a methyl group at the para position was disadvantageous **5be**, while the brominated analogue **5bf** resulted in a further increase in activity as compared to **5at** and **5bc**. The observed trend in the $IC_{50}$ values (F > Cl > Br) makes us belief that the formation of a halogen bond in the active site plays a significant role in the activity [56,57].

Finally, a *N*-screening was performed to determine the importance of the quinazoline core (Figure 11). Interestingly, the nitrogen atom at the 3-position does not seem to be important for the activity, as the Spautin-1 analogue bearing the quinoline core (i.e., **19**) showed a higher potency as compared to the quinazoline core **5aa**. This is in contrast to the nitrogen at the 1-position, which appears to be crucial for the activity since its absence resulted in the inactive analogue **24** while the cinnoline **29** and quinoxaline **34** bearing Spautin-1 analogues showed some activity towards EGFR mutant NSCLC cells; however, they were less active compared to Spautin-1.

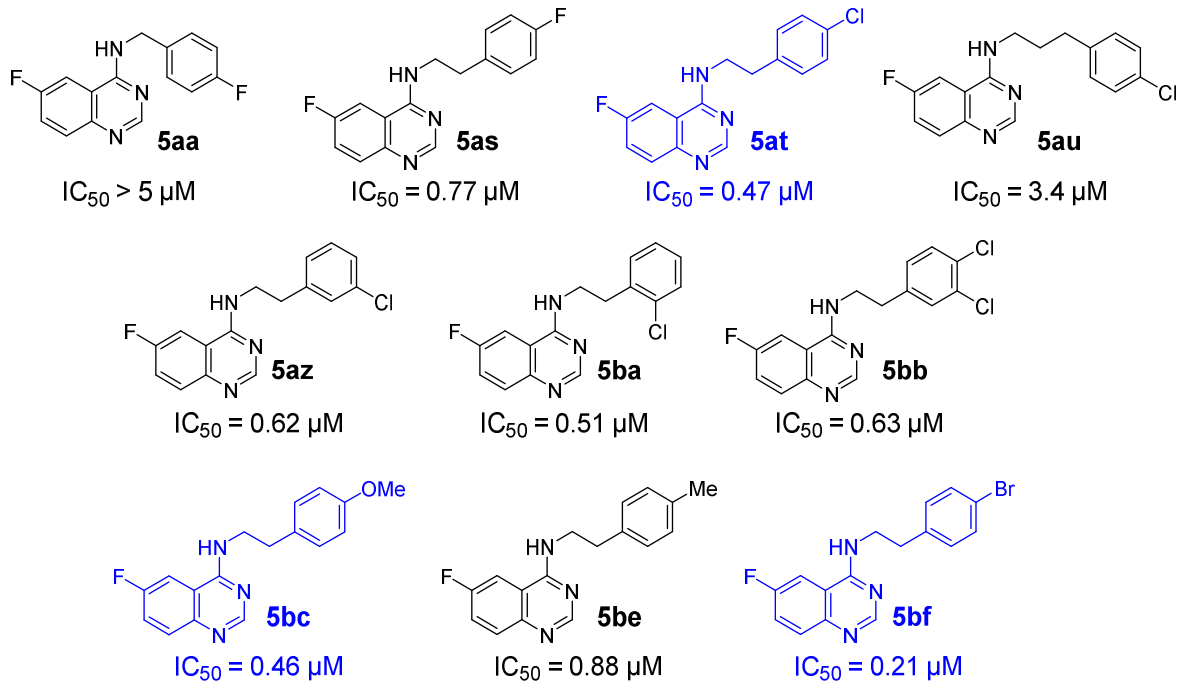


**Figure 10.** $IC_{50}$ values of promising analogues with Spautin-1 as reference (most active compounds ($IC_{50}$ < 0.5 μM) highlighted in blue).

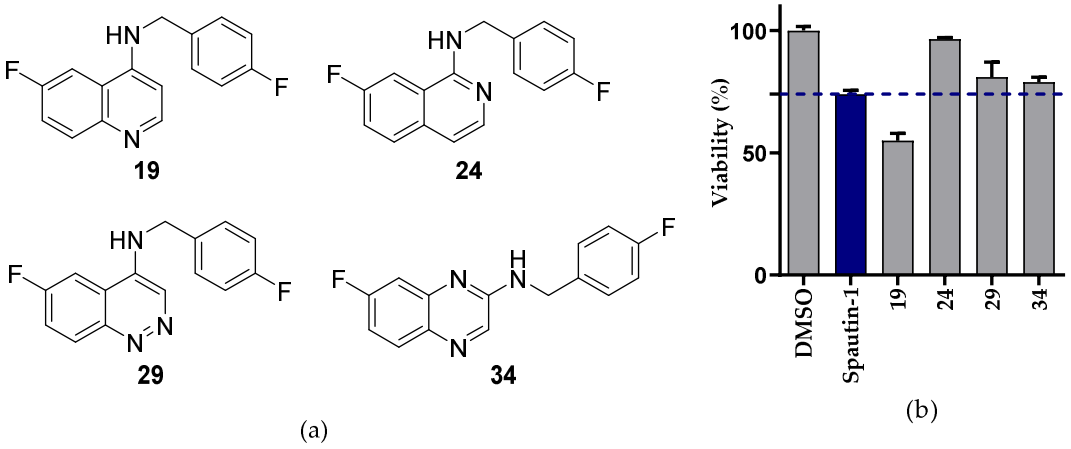


**Figure 11.** (**a**) Spautin-1 analogues for *N*-screening; (**b**) viability assay (5 μM) with Spautin-1 as reference.

Remarkably, the Spautin-1 analogue bearing the benzimidazole core **17** turned out to be less active in the viability screening (Figure 12). We hypothesized that the lack of the secondary amine was responsible for the dramatically decreased activity.

As a control reaction, the secondary amine present in most of the Spautin-1 analogues described above, was alkylated (Figure 13), since it has been reported that this secondary amine is crucial for the activity of EGRF-TKIs, [55] but also kinase inhibitors in general [58–60]. Methylation of the secondary amine dramatically reduced the activity of the analogues (**5aa** vs. **5bg** and **5at** vs. **5bh**) and as such, indicated that this secondary amine was also crucial for the activity in this study.

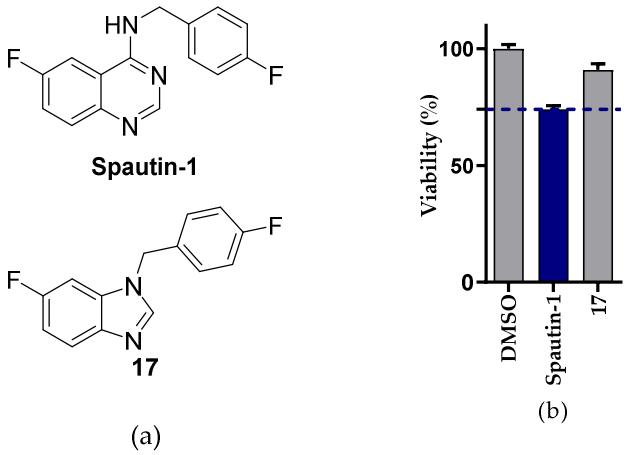


**Figure 12.** (**a**) Spautin-1 analogue **17** bearing the benzimidazole core; (**b**) viability assay (5 μM) with Spautin-1 as reference.

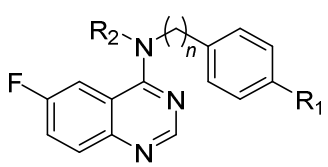


| Compound | *n* | $R_1$ | $R_2$ |
|---|---|---|---|
| Spautin-1 | 1 | F | H |
| **5bg** | 1 | F | Me |
| **5at** | 2 | Cl | H |
| **5bh** | 2 | Cl | Me |

(**a**)

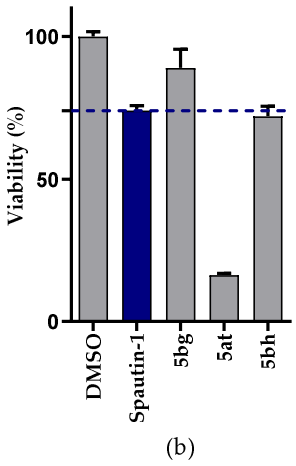


**Figure 13.** (**a**) Alkylation of the secondary amine; (**b**) viability assay (5 μM) with Spautin-1 as reference.

Next, the binding between the spautin-1 analogues and USP13 was evaluated to confirm that the reduced viability of the EGFR mutant NSCLC cells was caused by inhibition of USP13.

2.2.2. ITC/TSA

In order to confirm the binding event between spautin-1 and USP13, an isothermal titration calorimetry (ITC) experiment was performed on recombinant USP13. No binding curve could be fitted on the obtained data (see Figure S2), thus no binding was detected. The addition of DMSO further complicated the experiment, resulting in buffer mismatches and aggregation of the protein. Since the purification yield of protein was low, it was decided to shift to another less consuming method for the analysis of compound binding.

An additional screening was performed by means of a thermal shift assay (TSA). Ligand interactions usually increase protein stability, resulting in a shift of the melting temperature with a few degrees. This assay would thus allow to determine the melting temperature ($T_m$) and to detect a thermal shift upon binding of the ligand to the USP13 protein. Therefore, the protein was incubated with Spautin-1 **5aa** or **5bc** and a melting curve was determined for each sample (see Figure S3). Fitting a Boltzmann–sigmoidal curve to this data allows to determine the corresponding melting temperature, shown in Table 1. To determine a temperature difference, the reference condition was the protein in buffer with the corresponding percentage of DMSO, since addition of DMSO seemed

to increase aggregation during the ITC experiment. However, for both compounds no consistent thermal shift was seen after incubation with the ligands. While binding could not be observed from this dataset, a potential impact on any binding resulting from producing the protein recombinantly in *Escherichia coli* can also not be excluded.

**Table 1.** Melting temperatures, Tm (°C), and the thermal shift, ΔTm (°C), are given for each sample analyzed in a thermal shift assay. The melting temperatures were derived by fitting a Boltzmann–sigmoidal equation to the data. To determine a temperature difference (ΔTm), the reference condition was the protein in buffer with the corresponding percentage of DMSO.

| Sample | $T_m$ (°C) | $\Delta T_m$ (°C) |
|---|---|---|
| USP13 in buffer | 44.56 | N.D. |
| USP13 in 5% DMSO | 45.18 | 0.00 |
| USP13 in 10% DMSO | 44.80 | 0.00 |
| USP13 + 50 µM of **5aa** in 5% DMSO | 45.79 | 0.61 |
| USP13 + 100 µM of **5aa** in 10% DMSO | 45.86 | 1.06 |
| USP13 + 100 µM of **5aa** in 10% DMSO | 44.44 | −0.36 |
| USP13 + 50 µM of **5bc** in 5% DMSO | 46.58 | 1.40 |
| USP13 + 100 µM of **5bc** in 10% DMSO | 43.27 | −1.53 |
| USP13 + 100 µM of **5bc** in 10% DMSO | 44.44 | −0.36 |

#### 2.2.3. Kinase Screening

Since we could not confirm the interaction between Spautin-1 analogues and USP13, a kinase screening was performed using a set of four compounds (Spautin-1 and three analogues) to discover off-targets and identify kinases that are potentially responsible for the reduction in cell viability observed in our screen (Table 2). The KINOMEscan from Eurofins was performed (see Table S1). This screen consists of a competitive binding assay in which the DNA-tagged kinase is incubated with one of the compounds in the presence of immobilized active site binding ligands. Binding of the compounds to the kinase hampers the binding of the kinase to the ligands and this inhibition was quantified by qPCR. The residual kinase activity, which represents the percentage of kinase attached to the immobilized ligands, was determined for 428 kinases at a standard screening concentration of 10 µM of the compounds dissolved in DMSO [61].

Remarkably, Spautin-1 **5aa** showed moderate EGFR TK inhibitory activity at the standard screening concentration (Table 2), however we did not observe a reduction in pEGFR at 10 µM in EGFR mutant NSCLC cells [25]. We reasoned that the concentration used in the kinase screening does not represent the actual intracellular concentration upon treatment with the same concentration on a cellular basis. As expected, reducing the chain length, as in **5ay**, augments the EGFR TK inhibitory activity (Table 2), which probably also induced cell death in the viability screening. Conversely, extending the chain length (e.g., **5as** and **5at**), reduced the EGFR TK inhibitory activity, which implies that the improved activity, observed during the EGFR-mutant NSCLC cell viability screening, was not caused by inhibition of EGFR. Interestingly, the newly synthesized analogues (**5ay**, **5as** and **5at**) inhibited NEK4 more efficiently than Spautin-1 (**5aa**). Moreover, it has been reported that NEK4 is frequently overexpressed in lung cancer [37]. We confirmed the expression of NEK4 in our PC9 cell line model based on the publicly RNA-seq data available through the Cancer Cell Line Encyclopedia (CCLE) [62,63]. The available data represents RNA-seq expression data of a total of 1103 cell lines, including 205 lung cancer cell lines. Based on this data (see Table S2), we conclude that NEK4 is expressed throughout most NSCLC cell lines. Moreover, we found that PC9 expresses 19.3% more mRNA than the A549 NSCLC cell line, in which NEK4 has been functionally characterized and its expression confirmed through western blotting [38]. Collectively, this suggests that NEK4 inhibition possibly causes growth inhibition of EGFR mutant NSCLC cells.

**Table 2.** Kinases which had a residual activity < 60% for at least one of the analogues at a 10 μM concentration (highlighted in red).

| | 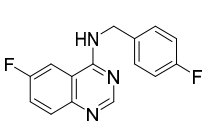 Spautin-1, 5aa | 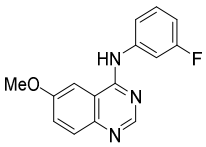 5ay | 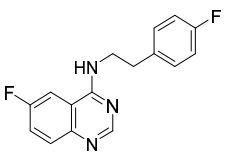 5as | 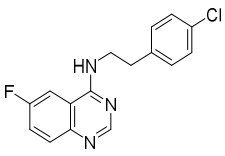 5at |
|---|---|---|---|---|
| **Kinase** | **Residual Activity (%)** | | | |
| AAK1 (h) | 95 | 53 | 81 | 72 |
| Abl (m) | 90 | 56 | 83 | 99 |
| ACK1 (h) | 85 | 56 | 84 | 71 |
| ALK (h) | 82 | 72 | 59 | 86 |
| ALK2 (h) | 60 | 50 | 45 | 58 |
| Aurora-B (h) | 85 | 59 | 69 | 48 |
| BrSK1 (h) | 85 | 30 | 89 | 112 |
| BrSK2 (h) | 79 | 42 | 65 | 71 |
| CaMKIIα (h) | 94 | 58 | 88 | 89 |
| CaMKIIγ (h) | 83 | 41 | 74 | 75 |
| CaMKIIδ (h) | 90 | 41 | 79 | 77 |
| CDK2/cyclinE (h) | 69 | 89 | 103 | 54 |
| CDK7/cyclinH/ MAT1 (h) | 62 | 58 | 49 | 59 |
| CDK13/cyclinK(h) | 75 | 105 | 35 | 114 |
| CDKL3 (h) | 77 | 29 | 65 | 71 |
| CDKL4 (h) | 73 | 38 | 94 | 92 |
| CLK1 (h) | 23 | 14 | 28 | 28 |
| CLK2 (h) | 47 | 43 | 53 | 60 |
| CLK4 (h) | 19 | 6 | 12 | 16 |
| DCAMKL2 (h) | 81 | 80 | 64 | 57 |
| DDR1 (h) | 65 | 7 | 29 | 39 |
| DRAK1 (h) | 98 | 57 | 79 | 85 |
| DYRK1A (h) | 74 | 29 | 68 | 63 |
| DYRK1B (h) | 88 | 53 | 82 | 92 |
| DYRK3 (h) | 117 | 57 | 98 | 98 |
| EGFR (h) | 27 | 1 | 46 | 72 |
| EGFR (L858R) (h) | 23 | 3 | 37 | 60 |
| EGFR (L861Q) (h) | 36 | 1 | 51 | 73 |
| EphB4 (h) | 68 | 63 | 59 | 68 |
| ErbB2 (h) | 74 | 20 | 79 | 65 |
| Flt3 (D835Y) (h) | 91 | 49 | 87 | 80 |
| Haspin (h) | 71 | 36 | 72 | 78 |
| Hck (h) activated | 85 | 46 | 85 | 108 |
| HIPK4 (h) | 103 | 42 | 92 | 93 |
| LOK (h) | 91 | 35 | 81 | 87 |
| LRRK2 (h) | 91 | 44 | 91 | 101 |
| Met (h) | 82 | 72 | 57 | 112 |
| Mnk2 (h) | 93 | 19 | 83 | 80 |
| MST4 (h) | 58 | 64 | 81 | 72 |
| NEK4 (h) | 71 | 30 | 27 | 12 |
| NEK11 (h) | 41 | 53 | 71 | 45 |
| PASK (h) | 66 | 65 | 44 | 30 |
| PDGFRα (D842V) (h) | 114 | 50 | 92 | 86 |
| Pim-1 (h) | 66 | 39 | 73 | 70 |
| Ret (h) | 69 | 43 | 99 | 62 |
| RIPK2 (h) | 82 | 22 | 86 | 86 |
| TAF1L (h) | 80 | 32 | 66 | 70 |
| TRB2 (h) | 69 | 31 | 65 | 60 |
| PI3KC2g (h) | 70 | 40 | 57 | 34 |

For the above stated reasons, we decided to determine the $IC_{50}$ (NEK4) values for Spautin-1 and 5 diverse analogues (NEK4 Human Other Protein Kinase Enzymatic Radiometric Assay by Eurofins) (see Figure S4) [64]. Interestingly, a reduced (**5ay**) and extended (**5at**, **5au**) chain length between the secondary amine and the phenyl group improved the inhibitory activity for NEK4 (Figure 14), which is in line with the viability data. However, only for $n \geq 2$ a dramatic decrease in NSCLC cell viability was observed and the activity of **5au** ($n = 3$) was significantly better as compared to **5ay** ($n = 0$) (Figures 7 and 8) which is contrary to the $IC_{50}$ values. Therefore, we postulate that inhibition of NEK4 only, does not fully explain the results of the viability screening. The introduction of a 1-hydroxy-3-butynyl group at position 6 of the quinazoline core **14b** resulted in a two-fold improved NEK4 inhibitory activity compared to Spautin-1, which suggests that the reduced cell viability was potentially caused by inhibition of NEK4. Remarkably, the Spautin-1 analogue bearing the quinoline core **19** was clearly less potent for NEK4 which is also in contrast to the viability data.

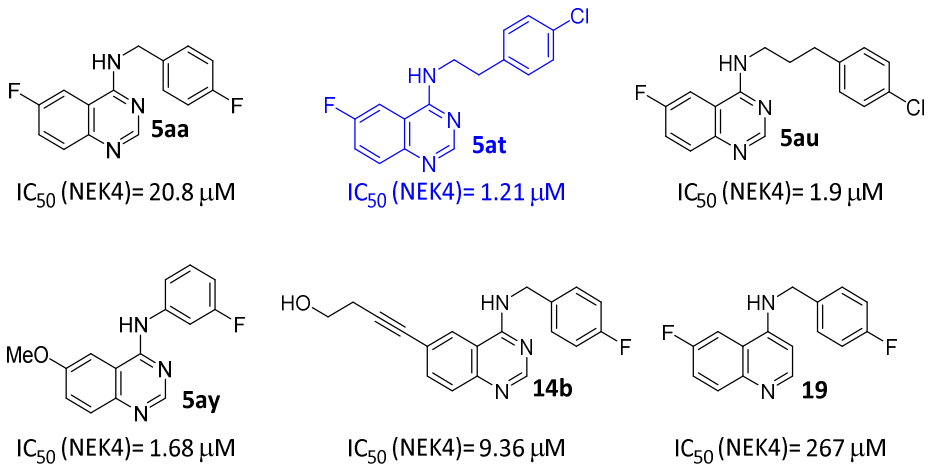


**Figure 14.** $IC_{50}$ values NEK4 for Spautin-1 and 5 diverse analogues (most active compound highlighted in blue).

Even though the $IC_{50}$ (NEK4) values are not fully in line with the viability data, we have strong indications that our compounds bear great potential for the treatment of EGFR mutant NSCLC. The reduced viability is presumably a multifactorial effect of which USP13 and EGFR inhibition cannot be excluded. Further research is needed due to the lack of experimental data on NEK4 and EGFR inhibition at the doses used on a cellular level. The kinase screening also revealed a low remaining activity for CLK1 and CLK4 (Table 2), to our best knowledge, two kinases which have not been linked to lung cancer. However, these can probably be considered as moderate off-targets at the relatively high concentration of inhibitors used (10 μM).

## 3. Discussion

In this work, a SAR-study of spautin-1 was performed to discover lead compounds for the treatment of EGFR mutant NSCLC. The most important SAR trends can be summarized as follow: The secondary amine is crucial for the activity, which has been previously reported for kinase inhibitors in general [55,58–60]; an increased chain length ($n \geq 2$) between the secondary amine and phenyl group dramatically increases the activity, in contrast to EGFR-TKIs [55]; however, the highest potency was observed for $n = 2$; a halogen capable of inducing an halogen bond at position 4' of the phenyl group is beneficial for the activity. A *N*-screening was performed to determine the importance of the quinazoline core, which lead to the conclusion that the nitrogen atom at the 3-position does not seem to be important for the activity, as the analogue bearing the quinoline core showed a high potency. On the contrary, the nitrogen at the 1-position appears to be crucial for the activity, while the cinnoline and quinoxaline bearing Spautin-1 analogues showed limited activity

towards EGFR mutant NSCLC cells. In line with these results, quinoline containing kinase inhibitors have been widely reported and some of these inhibitors were even approved by the FDA [27–30]. Altogether, the extensive SAR study provided compounds with $IC_{50}$ values as low as 210 nM, as determined in the applied cell viability assay, opening up a gateway towards more potent lead structures.

Surprisingly, we were unable to confirm binding between spautin-1, or the analogues, and USP13. Inability to detect binding using TSA or ITC does not exclude a binding under physiological conditions. Previously published assays did not show direct binding either and it might be that Spautin-1 inhibits USP13 via an indirect way [26]. On the other hand, these assays used USP13 purified from eukaryotic cells, while our experiments were performed with recombinant human USP13 [26]. Possible differences in post-translational modifications, protein folding, protein stability and solubility of recombinant USP13 may create a bias which cannot be controlled for, as spautin-1 is the only known small molecule that may bind USP13. In search of off-targets of the investigated analogues, a broad kinase screening unraveled NEK4 as a potential target. The latter kinase is often overexpressed in lung cancer and the expression in our PC9 cell line model was confirmed [37]. The highest activity towards NEK4 was observed for the *N*-[2-(substituted-phenyl)ethyl]-4-quinazolinamines, which were also responsible for the lowest EGFR-mutant NSCLC cell viability. For this reason, we hypothesize that the decreased viability of NSCLC cells was at least partially caused by the inhibition of NEK4. As far as we know, *N*-[2-(substituted-phenyl)ethyl]-4-quinazolinamines have been reported as acetyl- and butyrylcholinesterase inhibitors (AChE $IC_{50}$ = 6.2 μM; BuChE $IC_{50}$ = 14.1 μM) for the treatment of Parkinson disease and inhibitors of NFκB [65,66]. These compounds showed moderate potency towards EGFR as compared to the anilino- and benzylamino derivatives [55], but were never related to NEK4.

In summary, we report *N*-[2-(substituted-phenyl)ethyl]-6-fluoro-4-quinazolinamines as promising single agent lead compounds for the future treatment of EGFR mutant NSCLC. To the best of our knowledge, the *N*-[2-(substituted-phenyl)ethyl]-6-fluoro-4-quinazolinamines are the first potent and relatively selective NEK4 inhibitors reported in literature to date. More research is ongoing to further increase the potency and selectivity of these lead compounds (e.g., replacing the quinazoline core by the quinoline core) and get insight in the mechanism of action. Such optimized inhibitors may eventually be combined with FDA approved EGFR-TKIs to obtain a stronger initial response, increase the progression-free survival and improve the quality of life in EGFR-mutant NSCLC patients [26].

## 4. Materials and Methods

### *4.1. Chemistry*

Unless stated otherwise, all commercial materials were used without further purification and were purchased from fluorochem Ltd. (14 Graphite Way, Hadfield, Derbyshire SK13 1QH United Kingdom) or Merck (2000 Galloping Hill Road, Kenilworth, NJ 07033 U.S.A.). Anhydrous *N*,*N*-dimethylformamide was obtained by storing under argon atmosphere on activated 4Å molecular sieves for 24 h prior to use. Non-commercial starting materials were prepared based on literature procedures and are described below. $^{1}H$ and $^{13}C$ NMR spectra were recorded using different spectrometers. A Bruker Avance II 500 spectrometer (Bruker Scientific LLC, 40 Manning Road, Manning Park, Billerica, MA 01821, USA) was used at 500 MHz ($^{1}H$ NMR) and 126 MHz ($^{13}C$ NMR) at ambient temperature. To obtain spectra at 250 MHz and 63 MHz, the Bruker Avance DRX 250 was used. The chemical shifts were reported in delta (δ) units in parts per million (ppm) relative to the signal of the deuterated solvent. For the $CDCl_3$, the singlet in $^{1}H$ NMR was calibrated at 7.26 ppm and the $^{13}C$ NMR at the central line of the triplet at 77.16 ppm. For DMSO-$d_6$, the calibration was performed at 2.50 ppm for the $^{1}H$ NMR and 39.52 ppm for the $^{13}C$ NMR, respectively. The assignments were made using one dimensional (1D) $^{1}H$ and $^{13}C$ spectra and two-dimensional (2D) HSQC, HMBC and COSY spectra. Multiplicities were

described as singlet (s), doublet (d), triplet (t), quartet (q), multiplet (m), broad (br), or a combination thereof. The corresponding coupling constants (*J* values) were reported in Hertz (Hz). Analytical RP-HPLC analyses were carried out on a Chromaster system (VWR Hitachi, Researchpark Haasrode 2020, Geldenaaksebaan 464, 3001 Leuven) equipped with a Hitachi 5430 DAD, 5310 column oven, 5260 autosampler, and 5160 pump. Chromolith High Resolution RP-18e from Merck (150 Å, 1.1 µm, 50 × 4.6 mm, 3 mL/min flow rate) columns were used for analysis using UV detection at 214 nm. Solvents A and B are 0.1% TFA in water and 0.1% TFA in acetonitrile, respectively. Gradients are 1 to 100% B/A over 4 min. Mass spectra were recorded with a LC-MS triplequadrupole system. HPLC unit was a Waters 600 system combined to a Waters 2487 UV detector at 215 nm (Waters Corporation, 34 Maple Street, Milford, MA 01757, USA) and as stationary phase a Vydac MS RP C18-column (150 mm × 2.1 mm, 3 µm, 300 Å). The solvent system was 0.1% formic acid in water (A) and 0.1% formic acid in acetonitrile (B) with a gradient going from 3% to 100% B over 20 min with a flow rate of 0.3 mL/min. The MS unit, coupled to the HPLC system, was a Micromass QTOF-micro system. For the high resolution mass spectroscopy, the same MS system was used with reserpine (2.10–3 mg/mL) solution in $H_2O$:$CH_3CN$ (1:1) as reference. Automated flash chromatography was performed using Grace® Reveleris X2 system equipped with ELSD and UV detector (254 nm or 280 nm). The used normal phase column for the systems were Interchim® Puriflash® Silica HC 25 µM Flash Cartridges of 40 g or 80 g and Interchim® Puriflash® C18-HP 30 µM flash column of 40 g with a flow rate of 40 mL/min unless stated otherwise. Preparative RP-HPLC was performed on a Knauer system (Wuppertal, Germany) equipped with a RP-18C ReproSil-Pur ODS-3 column (150 mm × 16 mm, 5 mm) with a UV detector set at 214 nm. The same solvent system is used as for the analytical RP-HPLC with a flow rate of 10 mL/min. A Biotage® Initiator + SPWave (Biotage Sweden AB, Box 8, 751 03 Uppsala Sweden) in organic synthesis mode was used for the microwave-assisted reactions. The microwave runs at a frequency of 2.45 GHz and the maximal pressure and temperature are respectively 20–30 bar and 250–300 °C. Upon completion of the reaction and cooling down to 40–50 °C, the cavity lid opens. The reactions were performed in microwave vials with a volume capacity ranging between 0.5–2.0 mL and 2.0–5.0 mL.

#### 4.1.1. General Procedure for the Synthesis of Substituted-Quinazolin-4-One **11**

Method 1: The synthesis was performed according to a literature procedure [43]. Into a flame-dried 10 mL microwave vial, the substituted-2-aminobenzamide **9** (3.0 mmol, 1.0 equiv.) was dissolved in anhydrous DMF (1.5 mL). Subsequently trimethyl orthoformate (3.3 mmol, 1.1 equiv.) was added and the mixture was heated for 2–3 h at 170 °C.

Then the mixture was allowed to cool to room temperature. The precipitate was collected by filtration, washed with $CH_2Cl_2$ and dried in vacuo yielding the desired compound in good purity. The product was used in the next step without further purification.

Method 2: The synthesis was performed according to a slightly adapted literature procedure [44]. Into a flame-dried 10 mL microwave vial, a mixture of substituted-2-aminobenzoic acid **10** (6.0 mmol, 1.0 equiv.) and formamide (0.95 mL, 24 mmol, 4.0 equiv.) was overnight stirred at 155 °C.

Then the mixture was allowed to cool to room temperature. The precipitate was collected by filtration, washed with $CH_2Cl_2$ and dried in vacuo yielding the desired compound in good purity. The product was used in the next step without further purification.

Synthesis of 6-Fluoro-Quinazolin-4-One **11a**

The title compound was prepared following general procedure Section 4.1.1. Method 1, from 2-amino-5-fluorobenzamide **9a** (0.500 g, 3.24 mmol, 1.00 equiv.) and $HC(OMe)_3$ (0.390 mL, 3.57 mmol, 1.10 equiv.) in anhydrous DMF (1.62 mL). This yielded, after work-up, the desired compound as a white solid with 55% (324 mg, 1.79 mmol) yield. $^1$H NMR (500 MHz, DMSO): δ 8.09 (s, 1H), 7.79 (dd, *J* = 8.7, 2.9 Hz, 1H), 7.77–7.73 (m, 1H), 7.70 (dt, *J* = 8.7, 2.9 Hz, 1H). HPLC: 1.34 min. MS(ES+): $[M+H]^+$ = 165.

Synthesis of 5-Fluoro-Quinazolin-4-One **11b**

The title compound was prepared following general procedure Section 4.1.1. Method 1, from 2-amino-4-fluorobenzamide **9b** (0.500 g, 3.24 mmol, 1.00 equiv.) and $HC(OMe)_3$ (0.390 mL, 3.57 mmol, 1.10 equiv.) in anhydrous DMF (1.62 mL). This yielded, after work-up, the desired compound as a white solid with 52% (275 mg, 1.67 mmol) yield. $^1$H NMR (500 MHz, DMSO): δ 8.18 (dd, *J* = 8.8, 6.4 Hz, 1H), 8.15–8.12 (m, 1H), 7.45 (dd, *J* = 10.10, 2.5 Hz, 1H), 7.39 (dt, *J* = 8.8, 2.5 Hz, 1H). HPLC: 1.40 min. MS(ES+): $[M+H]^+$ = 165.

Synthesis of 7-Fluoro-Quinazolin-4-One **11c**

The title compound was prepared following general procedure Section 4.1.1. Method 1, from 2-amino-6-fluorobenzamide **9c** (1.00 g, 6.49 mmol, 1.00 equiv.) and $HC(OMe)_3$ (0.78 mL, 7.14 mmol, 1.10 equiv.) in anhydrous DMF (3.24 mL). This yielded, after work-up, the desired compound as a white solid with 48% (515 mg, 3.14 mmol) yield. $^1$H NMR (500 MHz, DMSO): δ 8.11 (s, 1H), 7.79 (dt, *J* = 8.3, 5.6 Hz, 1H), 7.48 (d, 8.3 Hz, 1H), 7.27 (dd, *J* = 11.2, 8.3 Hz, 1H). HPLC: 1.29 min. MS(ES+): $[M+H]^+$ = 165.

Synthesis of 8-Fluoro-Quinazolin-4-One **11d**

The title compound was prepared following general procedure Section 4.1.1. Method 2, from 2-amino-3-fluorobenzoic acid **10a** (1.00 g, 6.45 mmol, 1.00 equiv.) and formamide (1.05 mL, 26.5 mmol, 4.00 equiv.). This yielded, after work-up, the desired compound as a white solid with 77% (809 mg, 4.93 mmol) yield. $^1$H NMR (500 MHz, DMSO): δ 8.14 (d, *J* = 3.5 Hz, 1H), 7.95–7.91 (m, 1H), 7.69 (ddd, *J* = 10.9, 8.0, 1.4 Hz, 1H), 7.51 (dt, *J* = 8.0, 4.8 Hz, 1H). HPLC: 1.40 min. MS(ES+): $[M+H]^+$ = 165.

Synthesis of 6-Chloro-Quinazolin-4-One **11e**

The title compound was prepared following general procedure Section 4.1.1. Method 1, from 2-amino-5-Chlorobenzamide **9d** (0.600 g, 3.52 mmol, 1.00 equiv.) and $HC(OMe)_3$ (0.42 mL, 3.87 mmol, 1.10 equiv.) in anhydrous DMF (1.76 mL). This yielded, after work-up, the desired compound as a white solid with 59% (374 mg, 2.07 mmol) yield. $^1$H NMR (500 MHz, DMSO): δ 8.14–8.11 (m, 1H), 8.06 (d, *J* = 2.5 Hz, 1H), 7.85 (dd, *J* = 8.7, 2.5 Hz, 1H), 7.70 (d, *J* = 8.7 Hz, 1H). HPLC: 1.67 min. MS(ES+): $[M+H]^+$ = 181 and 183.

Synthesis of 6-Methoxy-Quinazolin-4-One **11f**

The title compound was prepared following general procedure Section 4.1.1. Method 1, from 2-amino-5-methoxybenzamide **9e** (0.500 g, 3.01 mmol, 1.00 equiv.) and $HC(OMe)_3$ (0.360 mL, 3.31 mmol, 1.10 equiv.) in anhydrous DMF (1.50 mL). This yielded, after work-up, the desired compound as a white solid with 78% (413 mg, 2.34 mmol) yield. $^1$H NMR (500 MHz, DMSO): δ 8.18 (s, 1H), 7.64 (d, *J* = 8.9 Hz, 1H), 7.52 (d, *J* = 3.0 Hz, 1H), 7.45 (dd, *J* = 8.9, 3.0 Hz, 1H), 3.88 (s, 3H). HPLC: 1.40 min. MS(ES+): $[M+H]^+$ = 177.

Synthesis of 6-Methyl-Quinazolin-4-One **11g**

The title compound was prepared following general procedure Section 4.1.1. Method 2, from 2-amino-5-Methylbenzoic acid **10b** (1.00 g, 6.62 mmol, 1.00 equiv.) and formamide (1.05 mL, 26.5 mmol, 4.00 equiv.). This yielded, after work-up, the desired compound as a white solid with 81% (858 mg, 5.36 mmol) yield. $^1$H NMR (500 MHz, DMSO): δ 8.28 (s, 1H), 7.95–7.92 (m, 1H), 7.67 (dd, *J* = 8.3, 1.9 Hz, 1H), 7.59 (d, *J* = 8.3 Hz, 1H), 2.45 (s, 3H). HPLC: 1.39 min. MS(ES+): $[M+H]^+$ = 161.

Synthesis of 6-Trifluoromethyl-Quinazolin-4-One **11h**

The title compound was prepared following general procedure Section 4.1.1. Method 2, from 2-amino-5-(trifluoromethyl)benzoic acid **10c** (0.500 g, 2.44 mmol, 1.00 equiv.) and formamide (0.390 mL, 9.75 mmol, 4.00 equiv.). This yielded, after work-up, the desired compound as a white solid with 64% (334 mg, 1.56 mmol) yield. $^1$H NMR (500 MHz,

DMSO): δ 8.39–8.35 (m, 1H), 8.28–8.23 (m, 1H), 8.12 (dd, *J* = 8.5, 2.3 Hz, 1H), 7.87 (d, *J* = 8.5 Hz, 1H). HPLC: 1.87 min. MS(ES+): $[M+H]^+$ = 215.

Synthesis of 6-Nitro-Quinazolin-4-One **11i**

The title compound was prepared following general procedure Section 4.1.1. Method 2, from 2-amino-5-Nitrobenzoic acid **10d** (1.00 g, 5.49 mmol, 1.00 equiv.) and formamide (0.870 mL, 22.0 mmol, 4.00 equiv.). This yielded, after work-up, the desired compound as a yellow solid with 77% (809 mg, 4.23 mmol) yield. $^1$H NMR (500 MHz, DMSO): δ 8.81 (d, *J* = 2.7 Hz, 1H), 8.55 (dd, *J* = 8.9, 2.7 Hz, 1H), 8.32 (s, 1H), 7.87 (d, *J* = 8.9 Hz, 1H). HPLC: 1.52 min. MS(ES+): $[M+H]^+$ = 192.

Synthesis of 6-Iodo-Quinazolin-4-One **11j**

The title compound was prepared following general procedure Section 4.1.1. Method 2, from 2-amino-5-Iodobenzoic acid **10e** (1.00 g, 3.80 mmol, 1.00 equiv.) and formamide (0.600 mL, 15.2 mmol, 4.00 equiv.). This yielded, after work-up, the desired compound as a white solid with 62% (641 mg, 2.36 mmol) yield. $^1$H NMR (500 MHz, DMSO): δ 8.39 (d, *J* = 2.1 Hz, 1H), 8.13 (s, 1H), 8.10 (dd, *J* = 8.6, 2.1 Hz, 1H), 7.46 (d, *J* = 8.6 Hz, 1H). HPLC: 1.81 min. MS(ES+): $[M+H]^+$ = 273.

4.1.2. General Procedure for the Synthesis of Substituted-4-Chloro-Quinazoline **12**

For the synthesis of substituted-4-Chloro-quinazolines, the procedure described by Zhang et al. was followed [45]. Into a flame dried round bottom flask equipped with an oven-dried reflux condenser, a mixture of substituted-quinazolin-4-one (1 equiv.) in $SOCl_2$ (50 equiv.), containing DMF (2 drops) was prepared. The mixture was refluxed for 4–8 h under argon atmosphere. $SOCl_2$ was removed under reduced pressure. The residue was dissolved in $CH_2Cl_2$ (50 mL) and washed three times with HCl (1M, aq). Subsequently, the organic phase was dried over $Na_2SO_4$, filtered and the solvent removed under reduced pressure.

Synthesis of 4-Chloro-6-Fluoroquinazoline **12a**

The title compound was prepared following general procedure Section 4.1.2, from 6-Fluoroquinazolin-4-one **11a** (0.450 g, 2.74 mmol, 1.00 equiv.) in $SOCl_2$ (10.0 mL). This yielded, after work-up, the desired compound as a pale yellow solid with 99% (496 mg, 2.72 mmol) yield. $^1$H NMR (250 MHz, $CDCl_3$): δ 9.01 (s, 1H), 8.13–8.03 (m, 1H), 7.90–7.81 (m, 1H), 7.77–7.65 (m, 1H). HPLC: 2.01 min. MS(ES+): $[M+H]^+$ = 183 and 185.

Synthesis of 4-Chloro-5-Fluoroquinazoline **12b**

The title compound was prepared following general procedure Section 4.1.2, from 5-Fluoroquinazolin-4-one **11b** (0.450 g, 2.74 mmol, 1.00 equiv.) in $SOCl_2$ (10.0 mL). This yielded, after work-up, the desired compound as a pale yellow solid with 98% (492 mg, 2.69 mmol) yield. $^1$H NMR (250 MHz, $CDCl_3$): δ 9.00 (s, 1H), 7.94–7.85 (m, 2H), 7.42–7.31 (m, 1H). HPLC: 2.04 min. MS(ES+): $[M+H]^+$ = 183 and 185.

Synthesis of 4-Chloro-7-Fluoroquinazoline **12c**

The title compound was prepared following general procedure Section 4.1.2, from 7-Fluoroquinazolin-4-one **11c** (0.225 g, 1.37 mmol, 1.00 equiv.) in $SOCl_2$ (5.00 mL). This yielded, after work-up, the desired compound as a pale yellow solid with 97% (243 mg, 1.33 mmol) yield. $^1$H NMR (250 MHz, $CDCl_3$): δ 9.03 (s, 1H), 8.32 (dd, *J* = 9.3, 5.8 Hz, 1H), 7.69 (dd, *J* = 9.3, 2.2 Hz, 1H), 7.56–7.42 (m, 1H). HPLC: 2.00 min. MS(ES+): $[M+H]^+$ = 183 and 185.

Synthesis of 4-Chloro-8-Fluoroquinazoline **12d**

The title compound was prepared following general procedure Section 4.1.2, from 8-Fluoroquinazolin-4-one **11d** (0.500 g, 3.05 mmol, 1.00 equiv.) in $SOCl_2$ (11.1 mL). This yielded, after work-up, the desired compound as a pale yellow solid with 94% (523 mg, 2.86 mmol)

yield. $^1$H NMR (250 MHz, $CDCl_3$): δ 9.06 (s, 1H), 8.09–8.00 (m, 1H), 7.76–7.60 (m, 2H). HPLC: 1.83 min. MS(ES+): $[M+H]^+$ = 183 and 185.

Synthesis of 4,6-Dichloroquinazoline **12e**

The title compound was prepared following general procedure Section 4.1.2, from 6-Chloroquinazolin-4-one **11e** (0.500 g, 2.77 mmol, 1.00 equiv.) in $SOCl_2$ (10.1 mL). This yielded, after work-up, the desired compound as a pale yellow solid with 99% (546 mg, 2.74 mmol) yield. $^1$H NMR (250 MHz, $CDCl_3$): δ 9.03 (s, 1H), 8.22 (d, *J* = 2.3 Hz, 1H), 8.01 (d, *J* = 9.0 Hz, 1H), 7.87 (dd, *J* = 9.0, 2.3 Hz, 1H). HPLC: 2.37 min. MS(ES+): $[M+H]^+$ = 199, 201 and 203.

Synthesis of 4-Chloro-6-Methoxyquinazoline **12f**

The title compound was prepared following general procedure Section 4.1.2, from 6-Methoxyquinazolin-4-one **11f** (0.250 g, 1.42 mmol, 1.00 equiv.) in $SOCl_2$ (5.20 mL). This yielded, after work-up, the desired compound as a pale yellow solid with 99% (274 mg, 1.41 mmol) yield. $^1$H NMR (250 MHz, $CDCl_3$): δ 8.92 (s, 1H), 7.96 (d, J = 9.2 Hz, 1H), 7.58 (dd, *J* = 9.2, 2.8 Hz, 1H), 7.42 (d, J = 2.8 Hz, 1H), 3.99 (s, 3H). HPLC: 2.12 min. MS(ES+): $[M+H]^+$ = 195 and 197.

Synthesis of 4-Chloro-6-Methylquinazoline **12g**

The title compound was prepared following general procedure Section 4.1.2, from 6-Methylquinazolin-4-one **11g** (0.200 g, 1.11 mmol, 1.00 equiv.) in $SOCl_2$ (4.04 mL). This yielded, after work-up, the desired compound as a pale yellow solid with 77% (152 mg, 0.85 mmol) yield. $^1$H NMR (250 MHz, $CDCl_3$): δ 8.98 (s, 1H), 8.04–8.00 (m, 1H), 7.96 (d, *J* = 8.6 Hz, 1H), 7.78 (dd, *J* = 8.6, 1.8 Hz, 1H), 2.60 (s, 3H). HPLC: 2.18 min. MS(ES+): $[M+H]^+$ = 179 and 181.

Synthesis of 4-Chloro-6-Trifluoromethyl-Quinazoline **12h**

The title compound was prepared following general procedure Section 4.1.2, from 5-Trifluoromethyl-quinazolin-4-one **11h** (0.200 g, 0.930 mmol, 1.00 equiv.) in $SOCl_2$ (3.41 mL). This yielded, after work-up, the desired compound as a pale yellow solid with 59% (128 mg, 0.55 mmol) yield. $^1$H NMR (250 MHz, $CDCl_3$): Too unstable to perform NMR-analysis. HPLC: 2.46 min. MS(ES+): $[M+H]^+$ = 233 and 235.

Synthesis of 4-Chloro-6-Nitroquinazoline **12i**

The title compound was prepared following general procedure Section 4.1.2, from 6-Nitroquinazolin-4-one **11i** (0.500 g, 2.60 mmol, 1.00 equiv.) in $SOCl_2$ (9.50 mL). This yielded, after work-up, the desired compound as a yellow solid with 70% (380 mg, 1.81 mmol) yield. $^1$H NMR (250 MHz, $CDCl_3$): δ 9.22–9.19 (m, 2H), 8.73 (dd, *J* = 9.2, 2.5 Hz, 1H), 8.26 (d, *J* = 9.2 Hz, 1H). HPLC: 1.99 min. MS(ES+): $[M+H]^+$ = 210 and 212.

Synthesis of 4-Chloro-6-Iodoquinazoline **12j**

The title compound was prepared following general procedure Section 4.1.2, from 6-Iodoquinazolin-4-one **11j** (0.500 g, 1.84 mmol, 1.00 equiv.) in $SOCl_2$ (6.70 mL). This yielded, after work-up, the desired compound as a pale yellow solid with 93% (495 mg, 1.71 mmol) yield. $^1$H NMR (250 MHz, $CDCl_3$): δ 9.06 (s, 1H), 8.65 (d, J = 1.9 Hz, 1H), 8.20 (dd, *J* = 8.9, 1.9 Hz, 1H), 7.79 (d, *J* = 8.9 Hz, 1H). HPLC: 2.50 min. MS(ES+**):** $[M+H]^+$ = 291 and 293.

4.1.3. General Procedure for the Synthesis of Spautin-1 and Analogues **5**

The synthesis of 4-amino-6-substituted quinazolines was performed according a literature procedure [46]. Into a 5 mL microwave vial, 4-Chloro-substituted-quinazoline (30 mg, 1.0 equiv.) was dissolved in *i*PrOH (0.30–0.80 mL). Subsequently the corresponding amine (1.5 equiv.) and $Et_3N$ (3.0 equiv.) were added. The mixture was heated for 20–180 min (depending on the amine) at 150 °C using microwave irradiation.

Afterwards the solvent was removed under reduced pressure and the crude mixture was purified using preparative HPLC (AcN + 0.1% TFA/$H_2O$ + 0.1% TFA).

Synthesis of 6-Fluoro-N-(4-fluorobenzyl)-4-Quinazolinamine.TFA **5aa**

The title compound was prepared following general procedure Section 4.1.3, from 4-Chloro-6-fluoroquinazoline **12a** (0.030 g, 0.16 mmol, 1.0 equiv.), 4-fluorobenzylamine (0.028 mL, 0.25 mmol, 1.5 equiv.) and $Et_3N$ (0.069 mL, 0.49 mmol, 3.0 equiv.) in *i*PrOH (0.40 mL). This yielded, after purification, the desired compound as a white solid with 63% (38.9 mg, 0.10 mmol) yield. $^1$H NMR (500 MHz, DMSO): δ 10.51–10.44 (m, 1H), 8.89 (s, 1H), 8.38 (dd, *J* = 9.7, 2.1 Hz, 1H), 7.99–7.90 (m, 2H), 7.49–7.43 (m, 2H), 7.20–7.15 (m, 2H), 4.92 (d, *J* = 5.5 Hz, 2H). $^{13}$C NMR (126 MHz, DMSO): δ 162.49 (C), 161.14 (C), 160.56 (C), 160.25 (C), 159.18 (C), 151.47 (CH), 136.33 (C), 133.33 (C), 129.78 (CH), 129.72 (CH), 124.72 (CH), 124.52 (CH), 123.62 (CH), 123.56 (CH), 115.30 (CH), 115.13 (CH), 114.45 (C), 114.38 (C), 109.19 (CH), 109.00 (CH), 44.07 ($CH_2$). HPLC: 1.95 min. HRMS (ESI$^+$) *m*/*z* calc. for $C_{15}H_{12}F_2N_3$ $[M+H]^+$ = 272.0994, found 272.0997.

Synthesis of 6-fluoro-N-(3-iodophenyl)-4-quinazolinamine.TFA **5ab**

The title compound was prepared following general procedure Section 4.1.3, from 4-Chloro-6-fluoroquinazoline **12a** (0.060 g, 0.33 mmol, 1.0 equiv.), 3-Iodoaniline (0.059 mL, 0.49 mmol, 1.5 equiv.) and $Et_3N$ (0.14 mL, 0.99 mmol, 3.0 equiv.) in *i*PrOH (0.80 mL). This yielded, after purification, the desired compound as pale yellow solid with 45% (70.4 mg, 0.14 mmol) yield. $^1$H NMR (500 MHz, DMSO): δ 10.32 (br s, 1H), 8.79 (s, 1H), 8.49 (dd, J = 10.0, 2.4 Hz, 1H), 8.29–8.26 (m, 1H), 7.95–7.87 (m, 3H), 7.60–7.55 (m, 1H), 7.25 (t, *J* = 8.0 Hz, 1H). $^{13}$C NMR (126 MHz, DMSO): δ 160.83 (C), 158.87 (C), 158.04 (C), 152.81 (CH), 142.84 (C), 139.57 (C), 133.27 (CH), 130.92 (CH), 130.64 (CH), 127.98 (CH), 123.80 (CH), 123.60 (CH), 122.09 (CH), 115.38 (C), 115.31 (C), 108.25 (CH), 108.05 (CH), 94.19 (C). HPLC: 1.92 min. HRMS (ESI$^+$) *m*/*z* calc. for $C_{14}H_{10}FIN_3$ $[M+H]^+$ = 365.9904, found 365.9923.

Synthesis of N-(4-Fluorobenzyl)-6-iodo-4-Quinazolinamine.TFA **5ac**

The title compound was prepared following general procedure Section 4.1.3, from 4-Chloro-6-iodoquinazoline **12j** (0.030 g, 0.10 mmol, 1.0 equiv.), 4-fluorobenzylamine (0.017 mL, 0.15 mmol, 1.5 equiv.) and $Et_3N$ (0.042 mL, 0.30 mmol, 3.0 equiv.) in *i*PrOH (0.33 mL). This yielded, after purification, the desired compound as a pale yellow solid with 66% (32.6 mg, 0.07 mmol) yield. $^1$H NMR (500 MHz, DMSO): δ 10.40–10.26 (m, 1H), 8.91 (s, 1H), 8.87 (s, 1H), 8.30–8.25 (m, 1H), 7.57 (d, *J* = 8.8 Hz, 1H), 7.49–7.42 (m, 2H), 7.22–7.15 (m, 2H), 4.89 (d, *J* = 5.6 Hz, 2H). $^{13}$C NMR (126 MHz, DMSO): δ 162.50 (C), 160.57 (C), 159.14 (C), 152.21 (CH), 143.51 (C), 139.23 (C), 133.45 (C), 132.34 (CH), 129.85 (CH), 129.78 (CH), 122.82 (CH), 115.35 (CH), 115.18 (CH), 115.08 (C), 93.24 (C), 44.05 ($CH_2$). HPLC: 2.17 min. HRMS (ESI$^+$) *m*/*z* calc. for $C_{15}H_{12}FIN_3$ $[M+H]^+$ = 380.0060, found 380.0101.

Synthesis of 6-Fluoro-N-(3-Fluorobenzyl)-4-Quinazolinamine.TFA **5ad**

The title compound was prepared following general procedure Section 4.1.3, from 4-Chloro-6-fluoroquinazoline **12a** (0.030 g, 0.16 mmol, 1.0 equiv.), 3-fluorobenzylamine (0.028 mL, 0.25 mmol, 1.5 equiv.) and $Et_3N$ (0.069 mL, 0.49 mmol, 3.0 equiv.) in *i*PrOH (0.40 mL). This yielded, after purification, the desired compound as a colorless oil with 70% (43.3 mg, 0.11 mmol) yield. $^1$H NMR (500 MHz, DMSO): δ 10.54–10.49 (m, 1H), 8.90 (s, 1H), 8.39 (dd, *J* = 9.6, 2.4 Hz, 1H), 8.00–7.91 (m, 2H), 7.43–7.37 (m, 1H), 7.29–7.23 (m, 2H), 7.14–7.09 (m, 1H), 4.96 (d, *J* = 5.6 Hz, 2H). $^{13}$C NMR (126 MHz, DMSO): δ 163.26 (C), 161.32 (C), 161.19 (C), 160.50 (C), 160.47 (C), 159.22 (C), 151.53 (CH), 140.17 (C), 140.11 (C), 136.29 (C), 130.53 (CH), 130.47 (CH) 124.85 (CH), 124.65 (CH), 123.62 (CH), 123.60 (CH), 123.54 (CH), 114.55 (C), 114.48 (C), 114.45 (CH), 114.30 (CH), 114.27 (CH), 114.14 (CH), 109.32 (CH), 109.12 (CH), 44.25 ($CH_2$). HPLC: 1.93 min. HRMS (ESI$^+$) *m*/*z* calc. for $C_{15}H_{12}F_2N_3$ $[M+H]^+$ = 272.0994, found 272.0986.

Synthesis of 6-Fluoro-N-(2-Fluorobenzyl)-4-Quinazolinamine.TFA **5ae**

The title compound was prepared following general procedure Section 4.1.3, from 4-Chloro-6-fluoroquinazoline **12a** (0.030 g, 0.16 mmol, 1.0 equiv.), 2-fluorobenzylamine (0.028 mL, 0.25 mmol, 1.5 equiv.) and $Et_3N$ (0.069 mL, 0.49 mmol, 3.0 equiv.) in *i*PrOH (0.40 mL). This yielded, after purification, the desired compound as a colorless oil with 63% (39.0 mg, 0.10 mmol) yield. $^1$H NMR (500 MHz, DMSO): δ 10.50–10.43 (m, 1H), 8.91 (s, 1H), 8.43 (dd, *J* = 9.6, 2.4 Hz, 1H), 8.00–7.92 (m, 2H), 7.47 (dt, *J* = 7.7, 1.4 Hz, 1H), 7.40–7.34 (m, 1H), 7.26–7.21 (m, 1H), 7.20–7.15 (m, 1H), 4.97 (d, *J* = 5.3 Hz, 2H). $^{13}$C NMR (126 MHz, DMSO): δ 161.27 (C), 161.23 (C), 160.47 (C), 160.44 (C), 159.32 (C), 159.26 (C), 151.47 (CH), 136.23 (C), 130.01 (CH), 129.98 (CH), 129.72 (CH), 129.65 (CH), 124.92 (CH), 124.72 (CH), 124.54 (CH), 124.51 (CH), 123.86 (C), 123.74 (C), 123.62 (CH), 123.55 (CH), 115.44 (CH), 115.28 (CH), 114.46 (C), 114.39 (C), 109.33 (CH), 109.13 (CH), 39.04 ($CH_2$), 39.00 ($CH_2$). HPLC: 1.92 min. HRMS (ESI$^+$) *m*/*z* calc. for $C_{15}H_{12}F_2N_3$ $[M+H]^+$ = 272.0994, found 272.0985.

Synthesis of 5-Fluoro-N-(4-Fluorobenzyl)-4-Quinazolinamine.TFA **5af**

The title compound was prepared following general procedure Section 4.1.3, from 4-Chloro-5-fluoroquinazoline **12b** (0.035 g, 0.19 mmol, 1.0 equiv.), 4-fluorobenzylamine (0.033 mL, 0.29 mmol, 1.5 equiv.) and $Et_3N$ (0.080 mL, 0.58 mmol, 3.0 equiv.) in *i*PrOH (0.48 mL). This yielded, after purification, the desired compound as a white solid with 69% (50.3 mg, 0.13 mmol) yield. $^1$H NMR (500 MHz, DMSO): δ 9.70–9.59 (m, 1H), 8.82 (s, 1H), 8.03–7.96 (m, 1H), 7.65–7.55 (m, 2H), 7.50–7.44 (m, 2H), 7.20–7.12 (m, 2H), 4.90 (d, *J* = 5.8 Hz, 2H). $^{13}$C NMR (126 MHz, DMSO): δ 162.34 (C), 160.41 (C), 159.28 (C), 158.37 (C), 158.34 (C), 157.25 (C), 152.57 (CH), 142.12 (C), 136.31 (CH), 136.23 (CH), 133.80 (C), 133.78 (C), 129.58 (CH), 129.51 (CH), 117.43 (CH), 115.19 (CH), 115.03 (CH), 113.57 (CH), 113.39 (CH), 104.04 (C), 103.93 (C), 44.39 ($CH_2$). HPLC: 1.92 min. HRMS (ESI$^+$) *m*/*z* calc. for $C_{15}H_{12}F_2N_3$ $[M+H]^+$ = 272.0994, found 272.0975.

Synthesis of 7-Fluoro-N-(4-Fluorobenzyl)-4-Quinazolinamine.TFA **5ag**

The title compound was prepared following general procedure Section 4.1.3, from 4-Chloro-7-fluoroquinazoline **12c** (0.035 g, 0.19 mmol, 1.0 equiv.), 4-fluorobenzylamine (0.033 mL, 0.29 mmol, 1.5 equiv.) and $Et_3N$ (0.080 mL, 0.58 mmol, 3.0 equiv.) in *i*PrOH (0.48 mL). This yielded, after purification, the desired compound as a white solid with 66% (48.0 mg, 0.12 mmol) yield. $^1$H NMR (500 MHz, DMSO): δ 10.70–10.64 (m, 1H), 8.91 (s, 1H), 8.61 (dd, *J* = 9.2, 5.3 Hz, 1H), 7.72 (dt, J = 9.2, 2.4 Hz, 1H), 7.64 (dd, *J* = 9.2, 2.4 Hz, 1H), 7.49–7.43 (m, 2H), 7.21–7.15 (m, 2H), 4.93 (d, *J* = 5.6 Hz, 2H). $^{13}$C NMR (126 MHz, DMSO): δ 166.55 (C), 164.52 (C), 162.53 (C), 160.60 (C), 160.17 (C), 152.50 (CH), 140.86 (C), 140.76 (C), 133.37 (C), 133.35 (C), 129.79 (CH), 129.73 (CH), 127.92 (CH), 127.83 (CH), 117.55 (CH), 117.36 (CH), 115.38 (CH), 115.21 (CH), 110.36 (C), 110.35 (C), 105.78 (CH), 105.58 (CH), 44.08 ($CH_2$). HPLC: 1.92 min. HRMS (ESI$^+$) *m*/*z* calc. for $C_{15}H_{12}F_2N_3$ $[M+H]^+$ = 272.0994, found 272.0977.

Synthesis of 8-Fluoro-N-(4-Fluorobenzyl)-4-Quinazolinamine.TFA **5ah**

The title compound was prepared following general procedure Section 4.1.3, from 4-Chloro-8-fluoroquinazoline **12d** (0.035 g, 0.19 mmol, 1.0 equiv.), 4-fluorobenzylamine (0.033 mL, 0.29 mmol, 1.5 equiv.) and $Et_3N$ (0.080 mL, 0.58 mmol, 3.0 equiv.) in *i*PrOH (0.47 mL). This yielded, after purification, the desired compound as a white solid with 61% (44.3 mg, 0.11 mmol) yield. $^1$H NMR (500 MHz, DMSO): **δ** 10.10–10.01 (m, 1H), 8.73 (s, 1H), 8.24 (d, *J* = 8.4 Hz, 1H), 7.86–7.79 (m, 1H), 7.70–7.63 (m, 1H), 7.47–7.41 (m, 2H), 7.20–7.13 (m, 2H), 4.88 (d, *J* = 5.5 Hz, 2H). $^{13}$C NMR (126 MHz, DMSO): δ 162.40 (C), 160.47 (C), 159.48 (C), 154.79 (C), 153.32 (CH), 152.78 (C), 134.04 (C), 133.09 (C), 132.98 (C), 129.59 (CH), 129.53 (CH), 127.23 (CH), 127.17 (CH), 119.41 (CH), 119.38 (CH), 119.13 (CH), 118.99 (CH), 115.51 (C), 115.29 (CH), 115.12 (CH), 43.69 ($CH_2$). HPLC: 1.84 min. HRMS (ESI$^+$) *m*/*z* calc. for $C_{15}H_{12}F_2N_3$ $[M+H]^+$ = 272.0994, found 272.1015.

Synthesis of 6-Chloro-N-(4-Fluorobenzyl)-4-Quinazolinamine.TFA **5ai**

The title compound was prepared following general procedure Section 4.1.3, from 4,6-dichloroquinazoline **12e** (0.030 g, 0.15 mmol, 1.0 equiv.), 4-fluorobenzylamine (0.026 mL, 0.23 mmol, 1.5 equiv.) and $Et_3N$ (0.063 mL, 0.45 mmol, 3.0 equiv.) in *i*PrOH (0.37 mL). This yielded, after purification, the desired compound as a white solid with 71% (42.5 mg, 0.11 mmol) yield. $^1$H NMR (500 MHz, DMSO): δ 10.65–10.56 (m, 1H), 8.92 (s, 1H), 8.68–8.65 (m, 1H), 8.09–8.05 (m, 1H), 7.86 (d, *J* = 8.9 Hz, 1H), 7.50–7.44 (m, 2H), 7.21–7.15 (m, 2H), 4.92 (d, *J* = 5.6 Hz, 2H). $^{13}$C NMR (126 MHz, DMSO): δ 162.56 (C), 160.62 (C), 159.81 (C), 151.92 (CH), 137.63 (C), 135.87 (CH), 133.21 (C), 133.18 (C), 132.34 (C), 129.92 (CH), 129.85 (CH), 123.60 (CH), 122.43 (CH), 115.38 (CH), 115.21 (CH), 114.38 (C), 44.22 ($CH_2$). **HPLC**: 2.07 min. **HRMS** (ESI$^+$) *m*/*z* calc. for $C_{15}H_{12}ClFN_3$ [M+H; $^{35}$Cl]$^+$ = 288.0698 and [M+H; $^{37}$Cl]$^+$ = 290.0673, found 288.0695 and 290.0682 in the expected 3:1 ratio.

Synthesis of N-(4-Fluorobenzyl)-6-Methoxy-4-Quinazolinamine.TFA **5aj**

The title compound was prepared following general procedure Section 4.1.3, from 4-Chloro-6-methoxyquinazoline **12f** (0.030 g, 0.15 mmol, 1.0 equiv.), 4-fluorobenzylamine (0.026 mL, 0.23 mmol, 1.5 equiv.) and $Et_3N$ (0.065 mL, 0.46 mmol, 3.0 equiv.) in *i*PrOH (0.38 mL). This yielded, after purification, the desired compound as a white solid with 65% (39.8 mg, 0.10 mmol) yield. $^1$H NMR (500 MHz, DMSO): δ 10.33–10.21 (m, 1H), 8.83 (s, 1H), 7.96–7.91 (m, 1H), 7.79–7.74 (m, 1H), 7.70–7.65 (m, 1H), 7.49–7.43 (m, 2H), 7.23–7.16 (m, 2H), 4.95 (d, *J* = 5.6 Hz, 2H) 3.92 (s, 3H). $^{13}$C NMR (126 MHz, DMSO): δ 162.50 (C), 160.57 (C), 160.02 (C), 158.78 (C), 149.60 (CH), 133.60 (C), 133.57 (C), 129.71 (CH), 129.64 (CH), 126.47 (CH), 121.76 (CH), 115.42 (CH), 115.25 (CH), 114.16 (C), 103.77 (CH), 56.29 ($CH_3$), 43.98 ($CH_2$). HPLC: 2.06 min. HRMS (ESI$^+$) *m*/*z* calc. for $C_{16}H_{15}FN_3O$ [M+H]$^+$ = 284.1194, found 284.1193.

Synthesis of N-(4-Fluorobenzyl)-6-Methyl-4-Quinazolinamine.TFA **5ak**

The title compound was prepared following general procedure Section 4.1.3, from 4-Chloro-6-methylquinazoline **12g** (0.035 g, 0.20 mmol, 1.0 equiv.), 4-fluorobenzylamine (0.034 mL, 0.29 mmol, 1.5 equiv.) and $Et_3N$ (0.082 mL, 0.59 mmol, 3.0 equiv.) in *i*PrOH (0.5 mL). This yielded, after purification, the desired compound as a white solid with 50% (38.1 mg, 0.10 mmol) yield. $^1$H NMR (500 MHz, DMSO): δ 10.61–10.50 (m, 1H), 8.90 (s, 1H), 8.34 (s, 1H), 7.90 (d, *J* = 8.6 Hz, 1H), 7.75 (d, *J* = 8.6 Hz, 1H), 7.49–7.43 (m, 2H), 7.22–7.15 (m, 2H), 4.93 (d, *J* = 5.7 Hz, 2H), 2.51 (s, 3H). $^{13}$C NMR (126 MHz, DMSO): δ 162.51 (C), 160.57 (C), 160.30 (C), 150.73 (CH), 138.65 (C), 137.42 (CH), 135.97 (C), 133.42 (C), 129.80 (CH), 129.74 (CH), 123.19 (CH), 119.42 (CH), 115.37 (CH), 115.20 (CH), 112.90 (C), 44.07 ($CH_2$), 21.13 ($CH_3$). HPLC: 2.05 min. HRMS (ESI$^+$) *m*/*z* calc. for $C_{16}H_{15}FN_3$ [M+H]$^+$ = 268.1250, found 268.1226.

Synthesis of N-(4-Fluorobenzyl)-6-Trifluoromethyl-4-Quinazolinamine.TFA **5al**

The title compound was prepared following general procedure Section 4.1.3, from 4-Chloro-6-trifluoromethyl quinazoline **12h** (0.035 g, 0.15 mmol, 1.0 equiv.), 4-fluorobenzylamine (0.026 mL, 0.23 mmol, 1.5 equiv.) and $Et_3N$ (0.063 mL, 0.45 mmol, 3.0 equiv.) in *i*PrOH (0.37 mL). This yielded, after purification, the desired compound as a colorless oil with 37% (24.3 mg, 0.06 mmol) yield. $^1$H NMR (500 MHz, DMSO): δ 10.37 (br s, 1H), 8.96 (s, 1H), 8.88 (s, 1H), 8.25 (dd, *J* = 8.8, 1.5 Hz, 1H), 7.94 (d, *J* = 8.8 Hz, 1H), 7.50–7.45 (m, 2H), 7.22–7.16 (m, 2H), 4.91 (d, *J* = 5.7 Hz, 2H). $^{13}$C NMR (126 MHz, DMSO): δ 162.49 (C), 160.55 (C), 160.33 (C), 154.32 (CH), 133.55 (C), 133.52 (C), 130.58 (CH), 129.82 (CH), 129.76 (CH), 127.19 (q, *J* = 32.8 Hz, $CF_3$), 124.73 (C), 123.80 (CH), 122.56 (C), 122.39 (CH), 122.36 (CH), 115.34 (CH), 115.17 (CH), 113.48 (C), 43.98 ($CH_2$). HPLC: 2.18 min. HRMS (ESI$^+$) *m*/*z* calc. for $C_{16}H_{12}F_4N_3$ [M+H]$^+$ = 322.0967, found 322.0981.

Synthesis of N-(4-Fluorobenzyl)-6-Nitro-4-Quinazolinamine.TFA **5am**

The title compound was prepared following general procedure Section 4.1.3, from 4-Chloro-6-nitroquinazoline **12i** (0.036 g, 0.17 mmol, 1.0 equiv.), 4-fluorobenzylamine (0.029 mL, 0.26 mmol, 1.5 equiv.) and $Et_3N$ (0.072 mL, 0.52 mmol, 3.0 equiv.) in *i*PrOH (0.5 mL). This yielded, after purification, the desired compound as a brown solid with 42% (29.4 mg, 0.07 mmol) yield. $^1$H NMR (500 MHz, DMSO): δ 10.45–10.24 (m, 1H), 9.49 (d, *J* = 2.4 Hz, 1H), 8.83 (s, 1H), 8.62 (dd, *J* = 9.2, 2.4 Hz, 1H), 7.91 (d, *J* = 9.2 Hz, 1H), 7.50–7.44 (m, 2H), 7.22–7.15 (m, 2H), 4.89 (d, *J* = 5.6 Hz, 2H). $^{13}$C NMR (126 MHz, DMSO): δ 162.45 (C), 160.55 (C), 155.83 (CH), 144.92 (C), 133.76 (C), 129.83 (CH), 129.76 (CH), 128.06 (CH), 125.34 (CH), 121.05 (CH), 115.31 (CH), 115.14 (CH), 113.57 (C), 43.89 ($CH_2$). HPLC: 1.95 min. HRMS (ESI$^+$) *m*/*z* calc. for $C_{15}H_{12}FN_4O_2$ $[M+H]^+$ = 299.0944, found 299.0900.

Synthesis of N-(4-Chlorobenzyl)-6-Fluoro-4-Quinazolinamine.TFA **5an**

The title compound was prepared following general procedure Section 4.1.3, from 4-Chloro-6-fluoroquinazoline **12a** (0.030 g, 0.16 mmol, 1.0 equiv.), 4-chlorobenzylamine (0.030 mL, 0.25 mmol, 1.5 equiv.) and $Et_3N$ (0.069 mL, 0.49 mmol, 3.0 equiv.) in *i*PrOH (0.40 mL). This yielded, after purification, the desired compound as a colorless oil with 73% (46.7 mg, 0.12 mmol) yield. $^1$H NMR (500 MHz, DMSO): δ 10.40 (br s, 1H), 8.88 (s, 1H), 8.37 (dd, *J* = 9.7, 2.1 Hz, 1H), 7.99–7.88 (m, 2H), 7.46–7.39 (m, 4H), 4.92 (d, *J* = 5.7 Hz, 2H). $^{13}$C NMR (126 MHz, DMSO): δ 161.12 (C), 160.29 (C), 159.16 (C), 151.67 (CH), 136.73 (C), 136.31 (C), 132.01 (C), 129.49 (CH), 128.46 (CH), 124.74 (CH), 124.54 (CH), 123.90 (CH), 114.52 (C), 114.45 (C), 109.14 (CH), 108.95 (CH), 44.07 ($CH_2$). HPLC: 2.14 min. HRMS (ESI$^+$) *m*/*z* calc. for $C_{15}H_{12}ClFN_3$ $[M+H; ^{35}Cl]^+$ = 288.0698 and $[M+H; ^{37}Cl]^+$ = 290.0673, found 288.0699 and 290.0698 in the expected 3:1 ratio.

Synthesis of 6-Fluoro-N-(4-Methoxybenzyl)-4-Quinazolinamine.TFA **5ao**

The title compound was prepared following general procedure Section 4.1.3, from 4-Chloro-6-fluoroquinazoline **12a** (0.040 g, 0.22 mmol, 1.0 equiv.), 4-methoxybenzylamine (0.043 mL, 0.33 mmol, 1.5 equiv.) and $Et_3N$ (0.092 mL, 0.66 mmol, 3.0 equiv.) in *i*PrOH (0.53 mL). This yielded, after purification, the desired compound as a colorless oil with 48% (42.2 mg, 0.11 mmol) yield. $^1$H NMR (500 MHz, DMSO): δ 10.60–10.54 (m, 1H), 8.91 (s, 1H), 8.42–8.37 (m, 1H), 7.98–7.91 (m, 2H), 7.37–7.32 (m, 2H), 6.92–6.88 (m, 2H), 4.87 (d, *J* = 5.6 Hz, 2H), 3.72 (s, 3H). $^{13}$C NMR (126 MHz, DMSO): δ 161.26 (C), 160.16 (C), 160.13 (C), 159.30 (C), 158.77 (C), 151.27 (CH), 135.60 (C), 129.26 (CH), 128.89 (C), 124.92 (CH), 124.72 (CH), 123.13 (CH), 123.06 (CH), 114.40 (C), 114.33 (C), 113.93 (CH), 109.39 (CH), 109.19 (CH), 55.12 ($CH_3$), 44.44 ($CH_2$). HPLC: 1.53 min. HRMS (ESI$^+$) *m*/*z* calc. for $C_{16}H_{15}FN_3O$ $[M+H]^+$ = 284.1194, found 284.1195.

Synthesis of 6-Fluoro-N-(4-(Trifluoromethyl)Benzyl)-4-Quinazolinamine.TFA **5ap**

The title compound was prepared following general procedure Section 4.1.3, from 4-Chloro-6-fluoroquinazoline **12a** (0.030 g, 0.16 mmol, 1.0 equiv.), 4-(trifluoromethyl)benzylamine (0.035 mL, 0.25 mmol, 1.5 equiv.) and $Et_3N$ (0.069 mL, 0.49 mmol, 3.0 equiv.) in *i*PrOH (0.40 mL). This yielded, after purification, the desired compound as a white solid with 84% (58.5 mg, 0.13 mmol) yield. $^1$H NMR (500 MHz, DMSO): δ 10.45 (br s, 1H), 8.86 (s, 1H), 8.38 (dd, *J* = 9.6, 2.4 Hz, 1H), 7.99–7.91 (m, 2H), 7.71 (d, *J* = 8.2 Hz, 2H), 7.63 (d, *J* = 8.2 Hz, 2H), 5.02 (d, *J* = 5.5 Hz, 2H). $^{13}$C NMR (126 MHz, DMSO): δ 161.13 (C), 160.45 (C), 160.42 (C), 159.17 (C), 151.77 (CH), 142.28 (C), 137.05 (C), 128.24 (CH), 128.00 (q, *J* = 31.8 Hz, $CF_3$), 125.41 (CH), 125.38 (CH), 125.35 (CH), 125.32 (CH), 124.72 (CH), 124.52 (CH), 124.19 (CH), 124.12 (CH), 123.18 (C), 114.59 (C), 114.52 (C), 109.12 (CH), 108.93 (CH), 44.31 ($CH_2$). HPLC: 2.23 min. HRMS (ESI$^+$) *m*/*z* calc. for $C_{16}H_{12}F_4N_3$ $[M+H]^+$ = 322.0962, found 322.0958.

Synthesis of 6-Fluoro-N-(Phenylmethyl)-4-Quinazolinamine.TFA **5aq**

The title compound was prepared following general procedure Section 4.1.3, from 4-Chloro-6-fluoroquinazoline **12a** (0.035 g, 0.19 mmol, 1.0 equiv.), benzylamine (0.031 mL, 0.29 mmol, 1.5 equiv.) and $Et_3N$ (0.080 mL, 0.58 mmol, 3.0 equiv.) in *i*PrOH (0.47 mL). This yielded, after purification, the desired compound as a white solid with 76% (53.1 mg, 0.14 mmol) yield. $^1$H NMR (500 MHz, DMSO): δ 10.60–10.51 (m, 1H), 8.90 (s, 1H), 8.41 (d, *J* = 9.6, 2.3 Hz, 1H), 8.00–7.91 (m, 2H), 7.47–7.26 (m, 5H), 4.95 (d, *J* = 5.7 Hz, 2H). $^{13}$C NMR (126 MHz, DMSO): δ 161.22 (C), 160.35 (C), 160.32 (C), 159.25 (C), 151.43 (CH), 137.12 (C), 136.05 (C), 128.54 (CH), 127.66 (CH), 127.46 (CH), 124.85 (CH), 124.65 (CH), 123.45 (CH), 123.38 (CH), 114.45 (C), 114.37 (C), 109.30 (CH), 109.10 (CH), 44.83 ($CH_2$). HPLC: 1.71 min. HRMS (ESI+) *m*/*z* calc. for $C_{15}H_{13}FN_3$ $[M+H]^+$ = 254.1093, found 254.1082.

Synthesis of 6-Fluoro-N-(4-Fluorophenyl)-4-Quinazolinamine.TFA **5ar**

The title compound was prepared following general procedure Section 4.1.3, from 4-Chloro-6-fluoroquinazoline **12a** (0.030 g, 0.16 mmol, 1.0 equiv), 4-fluoroaniline (0.023 mL, 0.25 mmol, 1.5 equiv) and $Et_3N$ (0.069 mL, 0.49 mmol, 3.0 equiv) in *i*PrOH (0.40 mL). This yielded, after purification, the desired compound as a pale yellow solid with 80% (47.5 mg, 0.13 mmol) yield. $^1$H NMR (500 MHz, DMSO): δ 10.98 (br s, 1H), 8.84 (s, 1H), 8.54 (d, *J* = 9.6 Hz, 1H), 7.96 (d, *J* = 6.5 Hz, 2H), 7.82–7.74 (m, 2H), 7.36–7.29 (m, 2H). $^{13}$C NMR (126 MHz, DMSO): δ 161.14 (C), 160.76 (C), 159.17 (C), 158.97 (C), 158.94 (C), 158.82 (C), 151.92 (CH), 139.15 (C), 133.52 (C), 133.50 (C), 126.05 (CH), 125.98 (CH), 125.42 (CH), 125.35 (CH), 124.60 (CH), 124.40 (CH), 115.64 (CH), 115.46 (CH), 115.01 (C), 114.94 (C), 108.98 (CH), 108.78 (CH). HPLC: 1.71 min. HRMS ($ESI^+$) *m*/*z* calc. for $C_{14}H_{10}F_2N_3$ $[M+H]^+$ = 258.0837, found 258.0826.

Synthesis of 6-Fluoro-N-[2-(4-Fluorophenyl)Ethyl]-4-Quinazolinamine.TFA **5as**

The title compound was prepared following general procedure Section 4.1.3, from 4-Chloro-6-fluoroquinazoline **12a** (0.030 g, 0.16 mmol, 1.0 equiv.), 4-fluorophenethylamine (0.032 mL, 0.25 mmol, 1.5 equiv.) and $Et_3N$ (0.069 mL, 0.49 mmol, 3.0 equiv.) in *i*PrOH (0.40 mL). This yielded, after purification, the desired compound as a white solid with 59% (37.8 mg, 0.10 mmol) yield. $^1$H NMR (500 MHz, DMSO): δ 10.10–10.01 (m, 1H), 8.86 (s, 1H), 8.31 (dd, *J* = 9.7, 2.3 Hz, 1H), 7.98–7.88 (m, 2H), 7.35–7.28 (m, 2H), 7.16–7.08 (m, 2H), 3.96–3.87 (m, 2H), 3.00 (t, *J* = 7.3 Hz, 2H). $^{13}$C NMR (126 MHz, DMSO): δ 161.95 (C), 161.11 (C), 160.16 (C), 160.13 (C), 160.03 (C), 159.14 (C), 151.40 (CH), 136.23 (C), 134.82 (C), 134.80 (C), 130.61 (CH), 130.55 (CH), 124.65 (CH), 124.45 (CH), 123.68 (CH), 123.61 (CH), 115.21 (CH), 115.04 (CH), 114.40 (C), 114.33 (C), 109.05 (CH), 108.85 (CH), 43.15 ($CH_2$), 33.03 ($CH_2$). HPLC: 2.04 min. HRMS ($ESI^+$) *m*/*z* calc. for $C_{16}H_{14}F_2N_3$ $[M+H]^+$ = 286.1150, found 286.1136.

Synthesis of N-[2-(4-Chlorophenyl)Ethyl]-6-Fluoro-4-Quinazolinamine.TFA **5at**

The title compound was prepared following general procedure Section 4.1.3, from 4-Chloro-6-fluoroquinazoline **12a** (0.030 g, 0.16 mmol, 1.0 equiv.), 4-chlorophenethylamine (0.035 mL, 0.25 mmol, 1.5 equiv.) and $Et_3N$ (0.069 mL, 0.49 mmol, 3.0 equiv.) in *i*PrOH (0.40 mL). This yielded, after purification, the desired compound as a white solid with 54% (35.9 mg, 0.09 mmol) yield. $^1$H NMR (500 MHz, DMSO): δ 9.77 (br s, 1H), 8.84 (s, 1H), 8.27 (dd, *J* = 9.6, 2.6 Hz, 1H), 7.95–7.90 (m, 2H), 7.86 (dd, *J* = 9.6, 5.0 Hz, 2H), 3.94–3.87 (m, 2H), 3.00 (t, *J* = 7.2 Hz, 2H). $^{13}$C NMR (126 MHz, DMSO): δ 161.00 (C), 160.08 (C), 160.05 (C), 159.04 (C), 151.74 (CH), 137.78 (C), 131.05 (C), 130.67 (CH), 128.35 (CH), 124.45 (CH), 124.25 (CH), 114.48 (C), 114.41 (C), 108.84 (CH), 108.64 (CH), 42.83 ($CH_2$), 33.18 ($CH_2$). HPLC: 2.21 min. HRMS ($ESI^+$) *m*/*z* calc. for $C_{16}H_{14}ClFN_3$ $[M+H; ^{35}Cl]^+$ = 302.0855 and $[M+H; ^{37}Cl]^+$ = 304.0830, found 302.0843 and 304.0826 in the expected 3:1 ratio.

Synthesis of 6-Fluoro-N-[3-(4-Chlorophenyl)Propyl]-4-Quinazolinamine.TFA **5au**

The title compound was prepared following general procedure Section 4.1.3, from 4-Chloro-6-fluoroquinazoline **12a** (0.040 g, 0.22 mmol, 1.0 equiv.), 3-(4-Chlorophenyl)-1-propanamine (0.048 mL, 0.33 mmol, 1.5 equiv.) and $Et_3N$ (0.092 mL, 0.66 mmol, 3.0 equiv.) in *i*PrOH (0.53 mL). This yielded, after purification, the desired compound as a white solid with 69% (65.1 mg, 0.15 mmol) yield. $^1$H NMR (500 MHz, DMSO): δ 10.09–10.00 (m, 1H), 8.86 (s, 1H), 8.32 (dd, *J* = 9.7, 2.4 Hz, 1H), 7.96–7.88 (m, 2H), 7.31–7.23 (m, 4H), 3.74–3.67 (m, 2H), 2.69 (t, *J* = 7.5 Hz, 2H), 2.00 (p, *J* = 7.5 Hz, 2H). $^{13}$C NMR (126 MHz, DMSO): δ 161.10 (C), 160.15 (C), 160.12 (C), 159.14 (C), 151.18 (CH), 140.32 (C), 135.63 (C), 130.45 (C), 130.16 (CH), 128.16 (CH), 124.64 (CH), 124.44 (CH), 123.18 (CH), 123.11 (CH), 114.39 (C), 114.32 (C), 109.31 (CH), 109.11 (CH), 41.39 ($CH_2$), 31.70 ($CH_2$), 29.28 ($CH_2$), 29.16 ($CH_2$). HPLC: 2.25 min. HRMS (ESI$^+$) *m*/*z* calc. for $C_{17}H_{16}ClFN_3$ [M+H; $^{35}$Cl]$^+$ = 316.1017 and [M+H; $^{37}$Cl]$^+$ = 318.0992, found 316.0995 and 318.0993 in the expected 3:1 ratio.

Synthesis of 6-Fluoro-N-(3-Fluorophenyl)-4-Quinazolinamine.TFA **5av**

The title compound was prepared following general procedure Section 4.1.3, from 4-Chloro-6-fluoroquinazoline **12a** (0.060 g, 0.33 mmol, 1.0 equiv.), 3-Fluoroaniline (0.047 mL, 0.49 mmol, 1.5 equiv.) and $Et_3N$ (0.14 mL, 0.99 mmol, 3.0 equiv.) in *i*PrOH (0.80 mL). This yielded, after purification, the desired compound as pale yellow solid with 45% (70.4 mg, 0.14 mmol) yield. $^1$H NMR (500 MHz, DMSO): δ 10.77 (br s, 1H), 8.88 (s, 1H), 8.58–8.53 (m, 1H), 7.99–7.93 (m, 2H), 7.83 (dt, *J* = 11.3, 2.2 Hz, 1H), 7.64–7.60 (m, 1H), 7.53–7.47 (m, 1H), 7.12–7.07 (m, 1H). $^{13}$C NMR (126 MHz, DMSO): δ 162.88 (C), 161.08 (C), 160.95 (C), 159.12 (C), 158.62 (C), 158.58 (C), 152.24 (CH), 140.69 (C), 139.42 (C), 139.33 (C), 130.39 (CH), 130.32 (CH), 126.54 (CH), 126.47 (CH), 124.44 (CH), 124.24 (CH), 119.07 (CH), 119.05 (CH), 115.26 (C), 115.19 (C), 112.08 (CH), 111.91 (CH), 110.37 (CH), 110.17 (CH), 108.74 (CH), 108.54 (CH). HPLC: 1.81 min. HRMS (ESI$^+$) *m*/*z* calc. for $C_{14}H_{10}F_2N_3$ [M+H]$^+$ = 258.0887, found 258.0833.

Synthesis of 6-Fluoro-N-(2-Fluorophenyl)-4-Quinazolinamine.TFA **5aw**

The title compound was prepared following general procedure Section 4.1.3, from 4-Chloro-6-fluoroquinazoline **12a** (0.030 g, 0.16 mmol, 1.0 equiv.), 2-fluoroaniline (0.024 mL, 0.25 mmol, 1.5 equiv.) and $Et_3N$ (0.069 mL, 0.49 mmol, 3.0 equiv.) in *i*PrOH (0.40 mL). This yielded, after purification, the desired compound as a colorless oil with 65% (38.7 mg, 0.10 mmol) yield. $^1$H NMR (500 MHz, DMSO): δ 10.79 (br s, 1H), 8.75 (s, 1H), 8.48–8.43 (m, 1H), 7.99–7.93 (m, 2H), 7.57 (dt, *J* = 7.8, 2.5 Hz, 1H), 7.46–7.37 (m, 2H), 7.35–7.30 (m, 1H). $^{13}$C NMR (126 MHz, DMSO): δ 161.00 (C), 159.59 (C), 159.03 (C), 157.75 (C), 155.78 (C), 152.52 (CH), 140.91 (C), 128.86 (CH), 128.79 (CH), 128.49 (CH), 126.64 (CH), 124.78 (CH), 124.75 (CH), 124.50 (CH), 124.30 (CH), 116.36 (CH), 116.21 (CH), 114.78 (C), 114.71 (C), 108.61 (CH), 108.42 (CH). HPLC: 1.55 min. HRMS (ESI$^+$) *m*/*z* calc. for $C_{14}H_{10}F_2N_3$ [M+H]$^+$ = 258.0837, found 258.0827.

Synthesis of 6-Chloro-N-(3-Fluorophenyl)-4-Quinazolinamine.TFA **5ax**

The title compound was prepared following general procedure Section 4.1.3, from 4,6-Dichloroquinazoline **12e** (0.030 g, 0.15 mmol, 1.0 equiv.), 3-fluoroaniline (0.016 mL, 0.17 mmol, 1.5 equiv.) and $Et_3N$ (0.063 mL, 0.45 mmol, 3.0 equiv.) in *i*PrOH (0.37 mL). This yielded, after purification, the desired compound as a white solid with 63% (36.9 mg, 0.10 mmol) yield. $^1$H NMR (500 MHz, DMSO): δ 10.78 (br s, 1H), 8.87 (s, 1H), 8.82 (s, 1H), 8.06–8.01 (m, 1H), 7.88 (d, *J* = 8.9 Hz, 1H), 7.85–7.81 (m, 1H), 7.65–7.60 (m, 1H), 7.53–7.46 (m, 1H), 7.09 (t, *J* = 8.3 Hz, 1H). $^{13}$C NMR (126 MHz, DMSO): δ 162.86 (C), 160.93 (C), 157.97 (C), 153.07 (CH), 142.87 (C), 139.48 (C), 139.39 (C), 135.10 (CH), 131.88 (C), 130.36 (CH), 130.29 (CH), 126.07 (CH), 123.11 (CH), 118.98 (CH), 118.95 (CH), 115.34 (C), 111.99 (CH), 111.82 (CH), 110.27 (CH), 110.07 (CH). HPLC: 1.95 min. HRMS (ESI$^+$) *m*/*z* calc. for $C_{14}H_{10}ClFN_3$ [M+H; $^{35}$Cl]$^+$ = 274.0542 and [M+H; $^{37}$Cl]$^+$ = 276.0516, found 274.0533 and 276.0521 in the expected 3:1 ratio.

Synthesis of N-(3-Fluorophenyl)-6-Methoxy-4-Quinazolinamine.TFA **5ay**

The title compound was prepared following general procedure Section 4.1.3, from 4-Chloro-6-methoxyquinazoline **12f** (0.030 g, 0.15 mmol, 1.0 equiv.), 3-fluoroaniline (0.022 mL, 0.23 mmol, 1.5 equiv.) and $Et_3N$ (0.065 mL, 0.46 mmol, 3.0 equiv.) in *i*PrOH (0.38 mL). This yielded, after purification, the desired compound as a pale yellow solid with 55% (31.6 mg, 0.08 mmol) yield. $^1$H NMR (500 MHz, DMSO): δ 10.82 (br s, 1H), 8.83 (s, 1H), 8.09 (d, J = 2.6 Hz, 1H), 7.84 (d, *J* = 9.2 Hz, 1H), 7.77 (dt, *J* = 11.1, 2.1 Hz, 1H), 7.71 (dd, *J* = 9.2, 2.6 Hz, 1H), 7.59–7.50 (m, 2H), 7.16–7.11 (m, 1H), 3.98 (s, 3H). $^{13}$C NMR (126 MHz, DMSO): δ 162.88 (C), 160.95 (C), 158.68 (C), 158.51 (C), 150.00 (CH), 139.19 (C), 139.11 (C), 136.90 (C), 130.41 (CH), 130.34 (CH), 126.38 (CH), 123.97 (CH), 119.75 (CH), 119.73 (CH), 114.95 (C), 112.46 (CH), 112.29 (CH), 111.11 (CH), 110.90 (CH), 103.51 (CH), 56.35 ($CH_3$). HPLC: 1.94 min. HRMS ($ESI^+$) *m*/*z* calc. for $C_{15}H_{13}FN_3O$ $[M+H]^+$ = 270.1037, found 270.1020.

Synthesis of 6-Fluoro-N-(3-Chlorophenethyl)-4-Quinazolinamine.TFA **5az**

The title compound was prepared following general procedure Section 4.1.3, from 4-Chloro-6-fluoroquinazoline **12a** (0.032 g, 0.17 mmol, 1.0 equiv.), 3-Chlorophenethylamine (0.036 mL, 0.26 mmol, 1.5 equiv.) and $Et_3N$ (0.073 mL, 0.53 mmol, 3.0 equiv.) in *i*PrOH (0.43 mL). This yielded, after purification, the desired compound as a white solid with 70% (49.7 mg, 0.12 mmol) yield. $^1$H NMR (500 MHz, DMSO): δ 10.01–9.90 (m, 1H), 8.87 (s, 1H), 8.30 (dd, J = 9.6, 2.6 Hz, 1H), 7.99–7.86 (m, 2H), 7.40–7.22 (m, 4H), 3.99–3.89 (m, 2H), 3.02 (t, J = 7.2 Hz, 2H). $^{13}$C NMR (126 MHz, DMSO): δ 161.55 (C), 160.65 (C), 159.59 (C), 151.97 (CH), 141.77 (C), 136.98 (C), 133.49 (C), 130.72 (CH), 129.13 (CH), 128.03 (CH), 126.87 (CH), 125.08 (CH), 124.88 (CH), 124.36 (CH), 124.29 (CH), 114.92 (C), 114.85 (C), 109.44 (CH), 109.24 (CH), 43.22 ($CH_2$), 33.90 ($CH_2$). HPLC: 2.20 min. HRMS ($ESI^+$) *m*/*z* calc. for $C_{16}H_{14}ClFN_3$ $[M+H; ^{35}Cl]^+$ = 302.0860 and $[M+H; ^{37}Cl]^+$ = 304.0835, found 302.0805 and 304.0861 in the expected 3:1 ratio.

Synthesis of 6-Fluoro-N-(2-Chlorophenethyl)-4-Quinazolinamine.TFA **5ba**

The title compound was prepared following general procedure Section 4.1.3, from 4-Chloro-6-fluoroquinazoline **12a** (0.035 g, 0.19 mmol, 1.0 equiv.), 2-Chlorophenethylamine (0.040 mL, 0.29 mmol, 1.5 equiv.) and $Et_3N$ (0.072 mL, 0.52 mmol, 3.0 equiv.) in *i*PrOH (0.47 mL). This yielded, after purification, the desired compound as a white solid with 49% (38.9 mg, 0.09 mmol) yield. $^1$H NMR (500 MHz, DMSO): δ 10.11–10.02 (m, 1H), 8.89 (s, 1H), 8.29 (dd, J = 9.5, 2.5 Hz, 1H), 7.99–7.93 (m, 1H), 7.89 (dd, *J* = 9.5, 5.0 Hz, 1H), 7.47–7.42 (m, 1H), 7.41–7.36 (m, 1H), 7.30–7.24 (m, 2H), 4.00–3.92 (m, 2H), 3.14 (t, *J* = 7.2 Hz, 2H). $^{13}$C NMR (126 MHz, DMSO): δ 161.13 (C), 160.32 (C), 160.30 (C), 159.16 (C), 151.35 (CH), 136.05 (C), 135.97 (C), 133.23 (C), 131.26 (CH), 129.35 (CH), 128.56 (CH), 127.41 (CH), 124.78 (CH), 124.58 (CH), 123.54 (CH), 123.47 (CH), 114.38 (C), 114.31 (C), 109.08 (CH), 108.89 (CH), 41.44 ($CH_2$), 31.75 ($CH_2$). HPLC: 2.06 min. HRMS ($ESI^+$) *m*/*z* calc. for $C_{16}H_{14}ClFN_3$ $[M+H; ^{35}Cl]^+$ = 302.0860 and $[M+H; ^{37}Cl]^+$ = 304.0835, found 302.0865 and 304.0837 in the expected 3:1 ratio.

Synthesis of 6-Fluoro-N-[2-(3,4-Dichlorophenyl)Ethyl]-4-Quinazolinamine.TFA **5bb**

The title compound was prepared following general procedure Section 4.1.3, from 4-Chloro-6-fluoroquinazoline **12a** (0.035 g, 0.19 mmol, 1.0 equiv.), 3,4-dichlorophenethylamine (0.043 mL, 0.29 mmol, 1.5 equiv.) and $Et_3N$ (0.080 mL, 0.58 mmol, 3.0 equiv.) in *i*PrOH (0.47 mL). This yielded, after purification, the desired compound as a white solid with 52% (44.9 mg, 0.10 mmol) yield. $^1$H NMR (500 MHz, DMSO): δ 9.53 (br s, 1H), 8.80 (s, 1H), 8.23 (dd, *J* = 9.7, 2.6 Hz, 1H), 7.92–7.83 (m, 2H), 7.58 (d, *J* = 2.0 Hz, 1H), 7.55 (d, *J* = 8.3 Hz, 1H), 7.27 (dd, *J* = 8.3, 2.0 Hz, 1H), 3.93-3.87 (m, 2H), 3.01 (t, *J* = 7.0 Hz, 2H). $^{13}$C NMR (126 MHz, DMSO): δ 161.36 (C), 160.48 (C), 159.39 (C), 140.68 (C), 131.36 (CH), 130.93 (CH), 129.82 (CH), 129.45 (C), 124.61 (CH), 124.41 (CH), 115.10 (C), 115.03 (C), 109.06 (CH), 108.87 (CH), 42.87 ($CH_2$), 33.38 ($CH_2$). HPLC: 2.31 min. HRMS ($ESI^+$) *m*/*z* calc. for $C_{16}H_{13}Cl_2FN_3$

[M+H; $^{35}Cl]^+$ = 336.0471 and [M+H; $^{37}Cl]^+$ = 338.0443, found 336.0488 and 338.0482 in the expected 3:1 ratio.

Synthesis of 6-Fluoro-N-[2-(4-Methoxyphenyl)Ethyl]-4-Quinazolinamine.TFA **5bc**

The title compound was prepared following general procedure Section 4.1.3, from 4-Chloro-6-fluoroquinazoline **12a** (0.030 g, 0.16 mmol, 1.0 equiv.), 4-methoxyphenethylamine (0.036 mL, 0.25 mmol, 1.5 equiv.) and $Et_3N$ (0.069 mL, 0.49 mmol, 3.0 equiv.) in *i*PrOH (0.40 mL). This yielded, after purification, the desired compound as a white solid with 42% (27.8 mg, 0.07 mmol) yield. $^1H$ NMR (500 MHz, DMSO): δ 9.84 (br s, 1H), 8.85 (s, 1H), 8.29 (dd, *J* = 9.5, 2.1 Hz, 1H), 7.96–7.90 (m, 1H), 7.86 (dd, *J* = 9.5, 5.0 Hz, 1H), 7.19 (d, *J* = 8.4 Hz, 2H), 6.86 (d, *J* = 8.4 Hz, 2H), 3.91-3.83 (m, 2H), 3.71 (s, 3H), 2.94 (t, *J* = 7.4 Hz, 2H). $^{13}C$ NMR (126 MHz, DMSO): δ 161.01 (C), 160.02 (C), 159.99 (C), 159.05 (C), 157.88 (C), 151.64 (CH), 130.47 (C), 129.70 (CH), 124.46 (CH), 124.26 (CH), 124.11 (CH), 114.44 (C), 114.37 (C), 113.87 (CH), 108.89 (CH), 108.70 (CH), 55.00 ($CH_3$), 43.35 ($CH_2$), 33.07 ($CH_2$). HPLC: 2.05 min. HRMS (ESI$^+$) *m*/*z* calc. for $C_{17}H_{17}F_2N_3O$ $[M+H]^+$ = 298.1350, found 298.1347.

Synthesis of 6-Fluoro-N-(2-Phenylethyl)-4-Quinazolinamine.TFA **5bd**

The title compound was prepared following general procedure Section 4.1.3, from 4-Chloro-6-fluoroquinazoline **12a** (0.035 g, 0.19 mmol, 1.0 equiv.), phenethylamine (0.036 mL, 0.29 mmol, 1.5 equiv.) and $Et_3N$ (0.080 mL, 0.58 mmol, 3.0 equiv.) in *i*PrOH (0.47 mL). This yielded, after purification, the desired compound as a white solid with 61% (44.2 mg, 0.12 mmol) yield. $^1H$ NMR (500 MHz, DMSO): δ 9.98–9.84 (m, 1H), 8.86 (s, 1H), 8.30 (dd, *J* = 9.6, 2.6 Hz, 1H), 7.96–7.91 (m, 1H), 7.88 (dd, *J* = 9.6, 5.1 Hz, 1H), 7.34–7.26 (m, 4H), 7.25–7.20 (m, 1H), 3.95–3.88 (m, 2H), 3.01 (t, *J* = 7.4 Hz, 2H). $^{13}C$ NMR (126 MHz, DMSO): δ 161.04 (C), 160.07 (C), 160.05 (C), 159.08 (C), 151.59 (CH), 138.64 (C), 136.63 (C), 128.72 (CH), 128.46 (CH), 126.40 (CH), 124.53 (CH), 124.33 (CH), 123.92 (CH), 114.44 (C), 114.36 (C), 108.93 (CH), 108.73 (CH), 43.10 ($CH_2$), 33.93 ($CH_2$). HPLC: 1.86 min. HRMS (ESI+) *m*/*z* calc. for $C_{16}H_{15}FN_3$ $[M+H]^+$ = 268.1250, found 268.1213.

Synthesis of 6-Fluoro-N-[2-(4-Methylphenyl)ethyl]-4-Quinazolinamine.TFA **5be**

The title compound was prepared following general procedure Section 4.1.3, from 4-Chloro-6-fluoroquinazoline **12a** (0.035 g, 0.19 mmol, 1.0 equiv.), 4-methylphenethylamine (0.042 mL, 0.29 mmol, 1.5 equiv.) and $Et_3N$ (0.080 mL, 0.58 mmol, 3.0 equiv.) in *i*PrOH (0.47 mL). This yielded, after purification, the desired compound as a white solid with 46% (34.8 mg, 0.09 mmol) yield. $^1H$ NMR (500 MHz, DMSO): δ 9.94 (br s, 1H), 8.88 (s, 1H), 8.30 (dd, *J* = 9.5, 2.6 Hz, 1H), 7.97–7.91 (m, 1H), 7.88 (dd, *J* = 9.5, 5.0 Hz, 1H), 7.18–7.09 (m, 4H), 3.92–3.85 (m, 2H), 2.96 (t, *J* = 7.4 Hz, 2H), 2.26 (s, 3H). $^{13}C$ NMR (126 MHz, DMSO): δ 161.07 (C), 160.07 (C), 159.11 (C), 151.49 (CH), 136.33 (C), 135.49 (C), 135.38 (C), 129.02 (CH), 128.58 (CH), 124.60 (CH), 124.40 (CH), 123.78 (CH), 123.71 (CH), 114.41 (C), 114.34 (C), 108.99 (CH), 108.79 (CH), 43.25 ($CH_2$), 33.49 ($CH_2$), 20.61 ($CH_3$). HPLC: 2.10 min. HRMS (ESI+) *m*/*z* calc. for $C_{17}H_{17}FN_3$ $[M+H]^+$ = 282.1407, found 282.1422.

Synthesis of 6-Fluoro-N-[2-(4-Bromophenyl)ethyl]-4-Quinazolinamine.TFA **5bf**

The title compound was prepared following general procedure Section 4.1.3, from 4-Chloro-6-fluoroquinazoline **12a** (0.035 g, 0.19 mmol, 1.0 equiv.), 4-bromophenethylamine (0.045 mL, 0.29 mmol, 1.5 equiv.) and $Et_3N$ (0.080 mL, 0.58 mmol, 3.0 equiv.) in *i*PrOH (0.47 mL). This yielded, after purification, the desired compound as a white solid with 31% (27.0 mg, 0.06 mmol) yield. $^1H$ NMR (500 MHz, DMSO): δ 9.97–9.85 (m, 1H), 8.88 (s, 1H), 8.28 (dd, *J* = 9.6, 2.6 Hz, 1H), 7.99–7.92 (m, 1H), 7.88 (dd, *J* = 9.6, 5.0 Hz, 1H), 7.54–7.47 (m, 2H), 7.30–7.23 (m, 2H), 3.95–3.88 (m, 2H), 2.99 (t, *J* = 7.2 Hz, 2H). $^{13}C$ NMR (126 MHz, DMSO): δ 161.09 (C), 160.16 (C), 160.13 (C), 159.12 (C), 151.52 (CH), 138.15 (C), 131.29 (CH), 131.09 (CH), 124.65 (CH), 124.45 (CH), 123.81 (CH), 119.55 (C), 114.42 (C), 114.35 (C), 108.98 (CH), 108.78 (CH), 42.84 ($CH_2$), 33.22 ($CH_2$). HPLC: 2.22 min. HRMS (ESI$^+$) *m*/*z* calc. for

$C_{16}H_{14}BrFN_3$ [M+H; $^{79}Br]^+$ = 346.0355 and [M+H; $^{81}Br]^+$ = 348.0336, found 346.0331 and 348.0348 in the expected 1:1 ratio.

Synthesis of 6-Fluoro-N-(4-Fluorobenzyl)-N-Methyl-4-Quinazolinamine.TFA **5bg**

The title compound was prepared following general procedure Section 4.1.3, from 4-Chloro-6-fluoroquinazoline **12a** (0.030 g, 0.16 mmol, 1.0 equiv.), 4-fluoro-*N*-methylbenzylamine (0.033 mL, 0.25 mmol, 1.5 equiv.) and $Et_3N$ (0.069 mL, 0.49 mmol, 3.0 equiv.) in *i*PrOH (0.40 mL). This yielded, after purification, the desired compound as a yellow oil with 57% (36.6 mg, 0.09 mmol) yield. $^1$H NMR (500 MHz, DMSO): δ 8.85 (s, 1H), 8.16 (dd, *J* = 10.4, 2.3 Hz, 1H), 8.01–7.91 (m, 2H), 7.49–7.44 (m, 2H), 7.25–7.18 (m, 2H), 5.23 (s, 2H), 3.59 (s, 3H). $^{13}$C NMR (126 MHz, DMSO): δ 162.70 (C), 161.82 (C), 161.79 (C), 160.76 (C), 159.89 (C), 157.94 (C), 148.99 (CH), 138.32 (C), 131.55 (C), 131.52 (C), 129.84 (CH), 129.77 (CH), 124.57 (CH), 124.37 (CH), 122.78 (CH), 122.71 (CH), 115.62 (CH), 115.45 (CH), 113.91 (C), 113.84 (C), 112.98 (CH), 112.78 (CH), 55.37 ($CH_2$), 40.87 ($CH_3$). HPLC: 2.02 min. HRMS ($ESI^+$) *m*/*z* calc. for $C_{16}H_{14}F_2N_3$ $[M+H]^+$ = 286.1150, found 286.1149.

Synthesis of 6-Fluoro-N-(4-Chlorophenethyl)-N-Methyl-4-Quinazolinamine.TFA **5bh**

The title compound was prepared following general procedure Section 4.1.3, from 4-Chloro-6-fluoroquinazoline **12a** (0.034 g, 0.19 mmol, 1.0 equiv.), *N*-Methyl-4-chlorophenethylamine (0.047 g, 0.28 mmol, 1.5 equiv.) and $Et_3N$ (0.078 mL, 0.56 mmol, 3.0 equiv.) in *i*PrOH (0.45 mL). This yielded, after purification, the desired compound as a white solid with 52% (41.6 mg, 0.10 mmol) yield. $^1$H NMR (500 MHz, DMSO): δ 8.76 (s, 1H), 8.12 (dd, *J* = 9.9, 2.6 Hz, 1H), 7.97–7.91 (m, 1H), 7.88 (dd, *J* = 9.9, 5.3 Hz, 1H), 7.37–7.32 (m, 4H), 4.18–4.13 (m, 2H), 3.62 (s, 3H), 3.07–3.02 (m, 2H). $^{13}$C NMR (126 MHz, DMSO): δ 161.64 (C), 160.22 (C), 158.27 (C), 149.43 (CH), 139.10 (C), 137.78 (C), 131.65 (C), 131.22 (CH), 128.85 (CH), 124.71 (CH), 124.52 (CH), 123.54 (CH), 123.47 (CH), 114.23 (C), 114.16 (C), 113.29 (CH), 113.09 (CH), 55.09 ($CH_2$), 41.65 ($CH_3$), 31.82 ($CH_2$). HPLC: 2.27 min. HRMS ($ESI^+$) *m*/*z* calc. for $C_{17}H_{16}ClFN_3$ [M+H; $^{35}Cl]^+$ = 316.1017 and [M+H; $^{37}Cl]^+$ = 318.0992, found 316.1078 and 318.1075 in the expected 3:1 ratio.

4.1.4. General Procedure for the Suzuki Reaction

The Suzuki reaction was performed according to the procedure of Liu and coworkers [47]. In a 5 mL microwave vial, a mixture of the organo-iodine compound (0.11 mmol, 1.0 equiv.), phenylboronic acid (0.019 g, 0.16 mmol, 1.5 equiv.), and $Na_2CO_3$ (0.029 mL, 0.27 mmol, 2.5 equiv., 2M, aq) was dissolved in a solvent mixture of toluene and ethanol (8/2, 1 mL). The mixture was purged with argon gas prior addition of tetrakis(triphenylphosphine)palladium (6.5 mg, 0.006 mmol, 0.050 equiv.). After overnight heating at 90 °C, the mixture was cooled to room temperature and the solvent removed under reduced pressure. The crude product was dissolved in methanol and filtered over celite. Afterwards, the solvent was removed under reduced pressure and the desired product was isolated via preparative chromatography (AcN + 0.1% TFA/$H_2O$ + 0.1% TFA).

Synthesis of N-(1, 1′-Biphenyl)-3-yl-6-Fluoro-4-Quinazolinamine.TFA **13a**

The title compound was prepared following general procedure Section 4.1.4, from 6-fluoro-*N*-(3-iodophenyl)-4-quinazolinamine.TFA **8ab** (0.051 g, 0.11 mmol, 1.0 equiv.), phenylboronic acid (0.019 g, 0.16 mmol, 1.5 equiv.), tetrakis(triphenylphosphine)palladium (6.5 mg, 0.006 mmol, 0.05 equiv.) and $Na_2CO_3$ (0.014 mL, 0.26 mmol, 2.5 equiv., 2M, aq) in toluene/ethanol (8/2, 1 mL). This yielded, after purification, the desired compound as a pale yellow solid with 66% (31.1 mg, 0.07 mmol) yield. $^1$H NMR (500 MHz, DMSO): δ 10.83 (br s, 1H), 8.86 (s, 1H), 8.59 (dd, *J* = 9.9, 2.1 Hz, 1H), 8.10–8.08 (m, 1H), 8.00–7.93 (m, 2H), 7.84–7.79 (m, 1H), 7.72–7.68 (m, 2H), 7.60–7.55 (m, 2H), 7.53–7.48 (m, 2H), 7.44–7.39 (m, 1H). $^{13}$C NMR (126 MHz, DMSO): δ 161.07 (C), 159.11 (C), 158.80 (C), 158.77 (C), 152.23 (CH), 140.77 (C), 139.65 (C), 138.03 (C), 129.41 (CH), 129.06 (CH), 127.80 (CH), 126.68 (CH), 126.13 (CH), 124.41 (CH), 124.21 (CH), 123.99 (CH), 122.54 (CH), 121.91 (CH), 115.20 (C), 115.13

(C), 108.81 (CH), 108.62 (CH). HPLC: 2.34 min. HRMS ($ESI^+$) $m/z$ calc. for $C_{20}H_{15}FN_3$ $[M+H]^+$ = 316.1245, found 316.1238.

Synthesis of N-(4-Fluorobenzyl)-6-Phenyl-4-Quinazolinamine.TFA **13b**

The title compound was prepared following general procedure Section 4.1.4, from *N*-(4-fluorobenzyl)-6-iodo-4-quinolinamine.TFA **8ac** (0.088 g, 0.18 mmol, 1.0 equiv.), phenylboronic acid (0.033 g, 0.27 mmol, 1.5 equiv.), tetrakis(triphenylphosphine)palladium (10.4 mg, 0.009 mmol, 0.05 equiv.) and $Na_2CO_3$ (0.022 mL, 0.45 mmol, 2.5 equiv., 2M, aq) in a solvent mixture of toluene and ethanol (8/2, 2 mL). This yielded, after purification, the desired compound as a white solid with 69% (55.4 mg, 0.12 mmol) yield. $^1$H NMR (500 MHz, DMSO): δ 10.49 (br s, 1H), 8.89 (s, 1H), 8.84–8.82 (m, 1H), 8.38 (dd, *J* = 8.7, 1.6 Hz, 1H), 7.90–7.83 (m, 3H), 7.59–7.54 (m, 2H), 7.52–7.45 (m, 3H), 7.23–7.17 (m, 2H), 4.97 (d, *J* = 5.8 Hz, 2H). $^{13}$C NMR (126 MHz, DMSO): δ 162.49 (C), 160.54 (C), 139.72 (C), 138.01 (C), 134.03 (CH), 133.57 (C), 129.74 (CH), 129.67 (CH), 129.20 (CH), 128.58 (CH), 127.05 (CH), 121.38 (CH), 115.38 (CH), 115.21 (CH), 113.68 (C), 44.00 ($CH_2$). HPLC: 2.43 min. HRMS ($ESI^+$) $m/z$ calc. for $C_{21}H_{17}FN_3$ $[M+H]^+$ = 330.1407, found 330.1426.

4.1.5. General Procedure Sonogashira Reaction

The procedure of Liu, L. et al. was used to perform the Sonogashira reaction [48]. The organo-iodine compound (0.1 mmol, 1.0 equiv.) was dissolved in THF (1.0 mL) and the solution was purged with argon gas. Subsequently the alkyne (0.15 mmol, 1.5 equiv.), CuI (0.005 mmol, 0.05 equiv., 1 mg), $Pd(PPh_3)_2Cl_2$ (0.005 mmol, 0.05 equiv., 3.5 mg) and triethylamine (0.2 mmol, 2.0 equiv., 27.9 µL) were added. The mixture was refluxed overnight under argon atmosphere. Then the solvent was removed under reduced pressure and the crude product was dissolved in methanol and filtered over celite. Afterwards, the solvent was removed under reduced pressure and the desired product was isolated via preparative chromatography (AcN + 0.1% TFA/$H_2O$ + 0.1% TFA).

Synthesis of 4-[3-[(6-Fluoro-4-Quinazolinyl)Amino]Phenyl]-3-Butyn-1-ol.TFA **14a**

The title compound was prepared following general procedure Section 4.1.5, from 6-fluoro-*N*-(3-iodophenyl)-4-quinazolinamine.TFA **8ab** (0.048 g, 0.10 mmol, 1.0 equiv.), 3-Butyn-1-ol (0.011 mL, 0.15 mmol, 1.5 equiv.), CuI (1.0 mg, 0.005 mmol, 0.05 equiv.), $Pd(PPh_3)_2Cl_2$ (3.5 mg, 0.005 mmol, 0.05 equiv.) and triethylamine (27.9 µL, 0.2 mmol, 2 equiv.) in THF (1.0 mL). This yielded, after purification, the desired compound as a pale yellow solid with 62% (26.1 mg, 0.06 mmol) yield. $^1$H NMR (500 MHz, DMSO): δ 10.52 (br s, 1H), 8.83 (s, 1H), 8.54–8.50 (m, 1H), 7.96–7.90 (m, 3H), 7.78–7.73 (m, 1H), 7.43 (t, *J* = 7.9 Hz, 1H), 7.28–7.24 (m, 1H), 3.60 (t, *J* = 6.8 Hz, 2H), 2.58 (t, *J* = 6.8 Hz, 2H). $^{13}$C NMR (126 MHz, DMSO): δ 160.95 (C), 158.99 (C), 158.42 (C), 152.53 (CH), 137.94 (C), 129.07 (CH), 128.05 (CH), 127.03 (CH), 125.83 (CH), 124.12 (CH), 123.92 (CH), 123.54 (C), 122.77 (CH), 115.28 (C), 115.21 (C), 108.55 (CH), 108.35 (CH), 89.09 (C), 80.65 (C), 59.71 ($CH_2$), 23.52 ($CH_2$). HPLC: 1.72 min. HRMS ($ESI^+$) $m/z$ calc. for $C_{18}H_{15}FN_3O$ $[M+H]^+$ = 308.1199, found 308.1187.

Synthesis of, 4-[4-[(4-Fluorobenzyl)Amino]-6-Quinazolinyl]-3-Butyn-1-ol.TFA **14b**

The title compound was prepared following general procedure Section 4.1.5, from *N*-(4-fluorobenzyl)-6-iodo-4-quinolinamine.TFA **8ac** (0.049 g, 0.1 mmol, 1.0 equiv.), 3-Butyn-1-ol (0.011 mL, 0.15 mmol, 1.5 equiv.), CuI (1.0 mg, 0.005 mmol, 0.05 equiv.), $Pd(PPh_3)_2Cl_2$ (3.5 mg, 0.005 mmol, 0.05 equiv.) and triethylamine (27.9 µL, 0.2 mmol, 2.0 equiv.) in THF (1.0 mL). This yielded, after purification, the desired compound as a pale yellow solid with 69% (30.0 mg, 0.069 mmol) yield. $^1$H NMR (500 MHz, DMSO): δ 10.26 (br s, 1H), 8.82 (s, 1H), 8.59–8.56 (m, 1H), 7.94 (dd, *J* = 8.6, 1.5 Hz, 1H), 7.73 (d, *J* = 8.6 Hz, 1H), 7.48–7.43 (m, 2H), 7.21–7.15 (m, 2H), 4.88 (d, *J* = 5.7 Hz, 2H), 3.62 (t, *J* = 6.7 Hz, 2H), 2.62 (t, *J* = 6.7 Hz, 2H). $^{13}$C NMR (126 MHz, DMSO): δ 162.45 (C), 160.52 (C), 159.69 (C), 152.35 (CH), 137.47 (CH), 133.56 (C), 129.79 (C), 129.72 (CH), 126.68 (CH), 122.55 (C), 115.30 (CH),

115.13 (CH), 113.49 (C), 91.45 (C), 79.68 (C), 59.52 ($CH_2$), 43.98 ($CH_2$), 23.24 ($CH_2$). HPLC: 1.99 min. HRMS ($ESI^+$) $m/z$ calc. for $C_{19}H_{17}FN_3O$ $[M+H]^+$ = 322.1356, found 322.1376.

4.1.6. Three-step Synthesis of 6-Fluoro-1-[(4-Fluorophenyl)Methyl]-1H-Benzimidazole **17**
Synthesis of 4-Fluoro-N-(5-Fluoro-2-Nitrophenyl)-Benzenemethanamine **16**

To a solution of 5-Fluoro-2-nitroaniline **15** (0.573 g, 3.67 mmol, 1.00 equiv.) in DMF (6.3 mL), were added $Cs_2CO_3$ (2.39 g, 7.34 mmol, 2.00 equiv.) and 4-fluorobenzyl bromide (0.686 mL, 5.50 mmol, 1.50 equiv.). The mixture was stirred at room temperature for 2.5 h. Subsequently water (50 mL) was added and the mixture was extracted with EtOAc. The combined organic layers were dried over $MgSO_4$, filtered and the solvent removed under reduced pressure. Afterwards, the crude product was purified via Normal Phase silicagel flash chromatography (40 g column, petroleumether/EtOAc), yielding the desired compound as a white solid with 88% (850 mg, 3.22 mmol) yield. $^1$H NMR (250 MHz, $CDCl_3$): δ 8.51 (br s, 1H), 8.30–8.20 (m, 1H), 7.37–7.27 (m, 2H), 7.13–7.02 (m, 2H), 6.49–6.36 (m, 2H), 4.48 (d, $J$ = 5.3 Hz, 2H). HPLC: 2.95 min. MS(ES+/ES-): Mass not found.

Synthesis of 4-Fluoro-N2-[(4-Fluorophenyl)Methyl]-1,2-Benzenediamine

The benzylated aniline **16** (0.20 g, 0.76 mmol, 1.0 equiv.) was stirred in acetic acid (4.5 mL). The solution was heated at 50 °C prior addition of iron powder (0.17 g, 3.0 mmol, 4.0 equiv.) in one portion. Afterwards, the mixture was heated at 70 °C for 2 h. Acetic acid was removed under reduced pressure. The crude reaction mixture was dissolved in $CH_2Cl_2$ (50 mL) and the organic layer was extracted with 1M HCl (3 × 50 mL). Then the combined aqueous layer was washed with $CH_2Cl_2$, basified to pH 9 using a 1M NaOH solution and extracted with $CH_2Cl_2$. The combined organic phase was washed with brine, dried over $MgSO_4$, filtered and the solvent removed under reduced pressure yielding the desired product as a white solid with 69% (123 mg, 0.53 mmol) yield. $^1$H NMR (250 MHz, $CDCl_3$): δ 7.40–7.29 (m, 2H), 7.10–6.99 (m, 2H), 6.70–6.60 (m, 1H), 6.41–6.29 (m, 2H), 4.25 (s, 2H), 4.03 (br s, 1H), 3.12 (br s, 2H). HPLC: 2.06 min. MS(ES+/ES-): Mass not found.

Synthesis of 6-Fluoro-1-[(4-Fluorophenyl)Methyl]-1H-Benzimidazole **17**

4-Fluoro-*N*2-[(4-fluorophenyl)methyl]-1,2-Benzenediamine (0.050 g, 0.21 mmol, 1.0 equiv.) was stirred with trimethyl orthoformate (0.5 mL) and *p*-toluene sulfonic acid monohydrate (2.0 mg, 0.01 mmol, 0.05 equiv.). The mixture was heated at 100 °C for 4 h. Afterwards, the mixture was concentrated under reduced pressure and purified by preparative chromatography (AcN + 0.1% TFA/$H_2O$ + 0.1% TFA) yielding the desired compound as a white solid with 88% (45.1 mg, 0.18 mmol) yield. $^1$H NMR (500 MHz, DMSO): δ 9.11 (br s, 1H), 7.83–7.77 (m, 1H), 7.71 (dd, $J$ = 9.2, 2.1 Hz, 1H), 7.53–7.48 (m, 2H), 7.29–7.18 (m, 3H), 5.58 (s, 2H). $^{13}$C NMR (126 MHz, DMSO): δ 162.90 (C), 160.96 (C), 160.43 (C), 158.52 (C), 131.71 (C), 131.69 (C), 130.28 (CH), 130.21 (CH), 118.90 (CH), 118.82 (CH), 115.80 (CH), 115.63 (CH), 112.52 (CH), 112.32 (CH), 98.89 (CH), 98.66 (CH), 47.90 ($CH_2$). **HPLC**: 1.91 min. **HRMS** ($ESI^+$) $m/z$ calc. for $C_{14}H_{11}F_2N_2$ $[M+H]^+$ = 245.0885, found 245.0876.

4.1.7. One-step Synthesis of 6-Fluoro-N-(4-Fluorobenzyl)-4-Quinolinamine **19**
Synthesis of 6-Fluoro-N-(4-Fluorobenzyl)-4-Quinolinamine.TFA **19**

Into a microwave vial were added, 4-Chloro-6-fluoroquinoline **16** (0.035 g, 0.19 mmol, 1.0 equiv.) and 4-fluorobenzylamine (0.088 mL, 0.77 mmol, 4.0 equiv.). The mixture was heated for 3 h at 160 °C using microwave irradiation. This yielded, after evaporation and purification using preparative chromatography (AcN + 0.1% TFA/$H_2O$ + 0.1% TFA), the desired compound as a white solid with 64% (46.5 mg, 0.12 mmol) yield. $^1$H NMR (500 MHz, DMSO): δ 9.75–9.69 (m, 1H), 8.55 (d, $J$ = 7.0 Hz, 1H), 8.45 (dd, $J$ = 10.5, 2.6 Hz, 1H), 8.04–8.00 (m, 1H), 7.95–7.89 (m, 1H), 7.51–7.46 (m, 2H), 7.24–7.18 (m, 2H), 6.84 (d, $J$ = 7.0 Hz, 1H), 4.80 (d, $J$ = 5.8 Hz, 2H). $^{13}$C NMR (126 MHz, DMSO): δ 162.54 (C), 160.62 (C), 158.67 (C), 155.19 (C), 155.16 (C), 142.65 (CH), 134.93 (C), 132.73 (C), 132.71 (C), 129.44

(CH), 129.38 (CH), 123.45 (CH), 123.38 (CH), 123.07 (CH), 122.87 (CH), 117.96 (C), 117.89 (C), 115.56 (CH), 115.39 (CH), 108.07 (CH), 107.87 (CH), 98.49 (CH), 45.39 ($CH_2$). HPLC: 1.87 min. HRMS ($ESI^+$) *m*/*z* calc. for $C_{16}H_{13}F_2N_2$ $[M+H]^+$ = 271.1047, found 271.1058.

#### 4.1.8. Four-step Synthesis of 7-Fluoro-N-(4-Fluorobenzyl)-1-Isoquinoline **24**

##### Synthesis of (E)-N-((Dimethylamino)Methyl)-5-Fluoro-2-Methylbenzamide **21**

The title compound was prepared from 5-Fluoro-2-methylbenzamide **20** (0.600 g, 3.92 mmol, 1.00 equiv.), dissolved in anhydrous THF (6.11 mL). Then *N*,*N*-dimethylformamide dimethyl acetal (0.625 mL, 4.70 mmol, 1.20 equiv.) was added and the mixture was refluxed for 2 h. Subsequently the solvent was removed under reduced pressure and the obtained oil was crystallized from n-hexane, yielding the desired compound as a white, crystalline solid with 74% (0.605 g, 2.91 mmol) yield. $^1$H NMR (250 MHz, $CDCl_3$): δ 8.57 (s, 1H), 7.81 (d, *J* = 9.9 Hz, 1H), 7.19–7.11 (m, 1H), 7.06–6.96 (m, 1H), 3.17 (s, 6H), 2.58 (s, 3H). HPLC: 1.28 min. MS(ES+): $[M+H]^+$ = 209.

##### Synthesis of 7-Fluoro-1-Isoquinolonone **22**

Potassium *tert*-butoxide (0.808 g, 7.20 mmol, 3.00 equiv.) was added to a solution of (*E*)-*N*-((Dimethylamino)methyl)-5-fluoro-2-methylbenzamide **21** (0.500 g, 2.40 mmol, 1.00 equiv.) in anhydrous DMF (4.00 mL). The mixture was heated at 120 °C for 30 min after which it was poured into water. The pH was adjusted to 5 by addition of 1M HCl (aq). The solvent and water were removed under reduced pressure and the crude product was purified using reversed phase automated flash chromatography (AcN + 0.1% TFA/$H_2O$ + 0.1% TFA) yielding the desired compound, after lyophilization, as a white solid with 63% (0.245 g, 1.50 mmol) yield. $^1$H NMR (500 MHz, DMSO): δ 11.37 (br s, 1H), 7.83 (dd, *J* = 9.6, 2.7 Hz, 1H), 7.73 (dd, *J* = 8.8, 5.4 Hz, 1H), 7.56 (dt, *J* = 8.8, 2.7 Hz, 1H), 7.15 (d, *J* = 7.1 Hz, 1H), 6.57 (d, *J* = 7.1 Hz, 1H). HPLC: 1.50 min. MS(ES+): $[M+H]^+$ = 164.

##### Synthesis of 1-Chloro-7-Fluoroisoquinoline **23**

Into a round bottom flask, equipped with reflux condenser, were added 7-Fluoro-1-isoquinolonone **22** (0.100 g, 0.61 mmol, 1.00 equiv.) and $POCl_3$ (2.86 mL, 30.6 mmol, 50.0 equiv.). The mixture was refluxed for 2 h after which the mixture was poured into a saturated $NaHCO_3$ solution (aq.). The aqueous layer was extracted using $CH_2Cl_2$ (3 × 50 mL). The combined organic layers were dried over $Na_2SO_4$, filtered and the solvent removed under reduced pressure yielding the desired compound as a pale yellow solid with 91% (101 mg, 0.56 mmol) yield. This compound was used in the next step without further purification. $^1$H NMR (250 MHz, $CDCl_3$): δ 8.27 (d, *J* = 5.7 Hz, 1H), 7.96 (dd, *J* = 9.5, 2.5 Hz, 1H), 7.88 (dd, *J* = 9.5, 5.3 Hz, 1H), 7.61 (d, *J* = 5.7 Hz, 1H), 7.54 (dt, *J* = 8.6, 2.5 Hz, 1H). HPLC: 2.13 min. MS(ES+): $[M+H]^+$ = 182 and 184.

##### Synthesis of 7-Fluoro-N-(4-Fluorobenzyl)-1-Isoquinoline.TFA **24**

To a mixture of 1-Chloro-7-fluoroisoquinoline **23** (0.050 g, 0.27 mmol, 1.0 equiv.) and 4-fluorobenzylamine (0.047 mL, 0.41 mmol, 1.50 equiv.) in anhydrous DMSO (0.67 mL), was added potassium carbonate (0.076 mL, 0.55 mmol, 2.0 equiv.). The mixture was heated overnight at 120 °C. The crude product was purified using preparative HPLC (AcN + 0.1% TFA/$H_2O$ + 0.1% TFA), which yielded the desired compound as a white solid with 40% (41.1 mg, 0.11 mmol) yield. $^1$H NMR (500 MHz, DMSO): δ 9.64 (br s, 1H), 8.51–8.44 (m, 1H), 8.06 (dd, *J* = 9.1, 5.7 Hz, 1H), 7.90–7.83 (m, 1H), 7.71 (d, *J* = 6.7 Hz, 1H), 7.51–7.46 (m, 2H), 7.27 (d, *J* = 6.7 Hz, 1H), 7.24–7.18 (m, 2H), 4.81 (d, *J* = 5.6 Hz, 2H). $^{13}$C NMR (126 MHz, DMSO): δ 162.59 (C), 161.96 (C), 160.66 (C), 160.00 (C), 152.00 (C), 133.66 (C), 132.58 (C), 130.69 (CH), 130.62 (CH), 129.65 (CH), 129.59 (CH), 122.91 (CH), 122.72 (CH), 119.29 (C), 119.22 (C), 115.39 (CH), 115.22 (CH), 110.99 (CH), 109.82 (CH), 109.63 (CH), 44.48 ($CH_2$). HPLC: 1.89 min. HRMS ($ESI^+$) *m*/*z* calc. for $C_{16}H_{13}F_2N_2$ $[M+H]^+$ = 271.1047, found 271.1058.

4.1.9. Four-step Synthesis of 6-Fluoro-N-(4-Fluorobenzyl)-4-Cinnolinamine 29
Synthesis of 4-Fluoro-2-(2-(Trimethylsilyl)Ethynyl)-Aniline **26**

Into a microwave vial were added, 2-Iodo-4-fluoroaniline **25** (0.651 mL, 5.00 mmol, 1.00 equiv.), copper iodide (0.012 g, 0.063 mmol, 0.01 equiv.), triethylamine (1.39 mL, 2.00 mmol, 10.0 equiv.), ethynyltrimethylsilane (1.04 mL, 7.50 mmol, 1.50 equiv.) and DMF (12.7 mL). The mixture was purged using argon gas prior addition of Bis(triphenylphosphine)-palla-dium(II) dichloride (0.175 g, 0.25 mmol, 0.05 equiv.). The mixture was overnight heated at 50 °C. Then the solvent was removed under reduced pressure and the crude product was filtered over celite (MeOH). Finally, after evaporation of the solvent, the desired product was isolated using normal phase automated flash chromatography (40 g column, petroleumether/EtOAc) as a white solid with 85% (881 mg, 4.25 mmol) yield. $^{1}$H NMR (250 MHz, $CDCl_3$): δ 7.01 (d, *J* = 8.8 Hz, 1H), 6.92–6.81 (m, 1H), 6.63 (dd, *J* = 8.8, 4.3 Hz, 1H), 4.11 (s, 2H), 0.28 (s, 9H). HPLC: 2.80 min. MS(ES+): $[M+H]^+$ = 208.

Synthesis of 6-FluoroCinnolin-4-ol **27**

Into a round bottom flask, equipped with reflux condenser, 4-fluoro-2-(2-(trimethylsilyl)-ethynyl)-benzenamine **26** (0.829 g, 4.00 mmol, 1.00 equiv.) was dissolved in distilled water (8.00 mL). Afterwards 6N HCl (7.00 mL, 42.0 mmol, 10.5 equiv., aq.) was added followed by the dropwise addition of sodium nitrite (0.414 g, 6.00 mmol, 1.50 equiv.) dissolved in water (1.9 mL). The mixture was heated at 100 °C for 3 h, cooled to room temperature and quenched into a saturated $NaHCO_3$ solution (aq.). The obtained solid was isolated via filtration, washed with $H_2O$ an $CH_2Cl_2$ and dried under reduced pressure. The desired product was obtained after reversed phase flash column chromatography ($H_2O$ + 0.1% TFA/can + 0.1% TFA) as a white solid with 28% (187 mg, 1.14 mmol) yield. $^{1}$H NMR (500 MHz, DMSO): δ 7.76–7.68 (m, 4H). HPLC: 1.34 min. MS(ES+): $[M+H]^+$ = 165.

Synthesis of 4-Chloro-6-Fluoro-Cinnoline **28**

The title compound was prepared following general procedure Section 4.1.2, from 6-Fluoro-4-cinnolinol **27** (0.070 g, 0.43 mmol, 1.0 equiv.) in $SOCl_2$ (1.6 mL). This yielded, after work-up, the desired compound as a pale yellow solid with 98% (76.3 mg, 0.42 mmol) yield. $^{1}$H NMR (250 MHz, $CDCl_3$): δ 9.25 (s, 1H), 8.56 (dd, *J* = 9.0, 5.1 Hz, 1H), 7.73 (dd, *J* = 9.0, 2.4 Hz, 1H), 7.72–7.63 (m, 1H). HPLC: 1.86 min. MS(ES+): $[M+H;^{35}Cl]^+$ = 183 and $[M+H;^{37}Cl]^+$ = 185.

Synthesis of 6-Fluoro-N-(4-Fluorobenzyl)-4-Cinnolinamine.TFA **29**

The title compound was prepared following general procedure Section 4.1.3, from 4-Chloro-6-fluorocinnoline **28** (0.036 g, 0.20 mmol, 1.0 equiv.), 4-fluorobenzylamine (0.034 mL, 0.30 mmol, 1.5 equiv.) and $Et_3N$ (0.084 mL, 0.60 mmol, 3.0 equiv.) in *i*PrOH (0.49 mL). This yielded, after purification, the desired compound as a pale brown oil with 55% (42.1 mg, 0.11 mmol) yield. $^{1}$H NMR (500 MHz, DMSO): δ 10.36–10.17 (m, 1H), 8.78 (s, 1H), 8.43 (dd, *J* = 9.6, 2.6 Hz, 1H), 8.11 (dd, *J* = 9.6, 5.1 Hz, 1H), 8.06-8.00 (m, 1H), 7.57–7.51 (m, 2H), 7.27–7.21 (m, 2H), 4.95 (d, *J* = 3.9 Hz, 2H). $^{13}$C NMR (126 MHz, DMSO): δ 162.72 (C), 161.54 (C), 160.78 (C), 159.55 (C), 146.74 (C), 137.75 (C), 132.26 (C), 132.23 (C), 129.87 (CH), 129.81 (CH), 128.41 (CH), 125.39 (CH), 125.17 (CH), 123.23 (CH), 123.15 (CH), 116.74 (C), 116.66 (C), 115.65 (CH), 115.48 (CH), 107.18 (CH), 106.98 (CH), 45.51 ($CH_2$). HPLC: 1.81 min. HRMS ($ESI^+$) *m*/*z* calc. for $C_{15}H_{12}F_2N_3$ $[M+H]^+$ = 272.0999, found 272.1003.

4.1.10. Four-Step Synthesis of 7-Fluoro-N-(4-Fluorobenzyl)-2-Quinoxalinamine 34
Synthesis of Ethyl 2-(4-Fluoro-2-Nitrophenylamino)Acetate **31**

Into a flame-dried round bottom flask were added 4-Fluoro-2-nitroaniline **30** (1.00 g, 6.41 mmol, 1.00 equiv.), $Cs_2CO_3$ (3.34 g, 10.2 mmol, 1.60 equiv.) and ethyl bromoacetate (2.81 mL, 32.0 mmol, 5.00 equiv.). The mixture was heated overnight at 135 °C under inert atmosphere. Subsequently the obtained mixture was added to a 1N NaOH solution (aq.). The aqueous phase was extracted using $CH_2Cl_2$ (3 × 50 mL). The combined organic

layers were dried over $Na_2SO_4$, filtered and the solvent removed under reduced pressure. The crude product was subjected to reversed phase flash column chromatography ($H_2O$/AcN) yielding the desired compound as a white solid with 45% (0.70 g, 2.89 mmol) yield. $^1$H NMR (250 MHz, $CDCl_3$): δ 8.29 (br s, 1H), 7.93 (d, *J* = 9.0 Hz, 1H), 7.33–7.22 (m, 1H), 6.69 (dd, *J* = 9.0, 4.4 Hz, 1H), 4.29 (q, *J* = 7.2 Hz, 2H), 4.09 (d, *J* = 5.2 Hz, 2H), 1.33 (t, *J* = 7.2 Hz, 3H). HPLC: 2.39 min. MS(ES+): $[M+H]^+$ = 243.

Synthesis of 7-Fluoro-1H-Quinoxalin-2-One **32**

To a solution of Ethyl 2-(4-fluoro-2-nitrophenylamino)acetate **31** (0.250 g, 1.04 mmol, 1.00 equiv.) in methanol (20.0 mL) was added Pd/C (0.222 g, 0.21 mmol, 0.20 equiv., 10 wt%). Then $H_2$-gas was bubbled for 1 h to the stirred mixture at room temperature. Subsequently Argon gas was bubbled through the mixture and the mixture was stirred for 2 days at room temperature. After filtration of the mixture over celite using methanol, the solvent was removed under reduced pressure. The crude product was triturated with $CH_2Cl_2$ to obtain the desired product with 46% (79.1 mg, 0.48 mmol) yield. The product was used in the next step without further purification. $^1$H NMR (500 MHz, DMSO): δ 8.12 (d, *J* = 2.2 Hz, 1H), 7.84 (dd, *J* = 8.9, 5.8 Hz, 1H), 7.17 (dt, *J* = 8.9, 2.8 Hz, 1H), 7.03 (dd, *J* = 9.5, 2.8 Hz, 1H). HPLC: 1.40 min. HPLC: 1.40 min. MS(ES+): $[M+H]^+$ = 165.

Synthesis of 2-Chloro-7-Fluoro-Quinoxaline **33**

The title compound was prepared following general procedure Section 4.1.2, from 7-Fluoro-1*H*-quinoxalin-2-one **32** (0.050 g, 0.30 mmol, 1.0 equiv.) and $SOCl_2$ (1.1 mL). This yielded, after work-up, the desired compound as a white solid with 98% (53.8 mg, 0.29 mmol) yield. $^1$H NMR (250 MHz, $CDCl_3$): δ 8.76 (s, 1H), 8.13 (dd, *J* = 9.3, 5.9 Hz, 1H), 7.77–7.50 (m, 2H). HPLC: 2.08 min. MS(ES+): $[M+H;^{35}Cl]^+$ = 183 and $[M+H;^{37}Cl]^+$ = 185.

Synthesis of 7-Fluoro-N-(4-Fluorobenzyl)-2-Quinoxalinamine.TFA **34**

The title compound was prepared following general procedure Section 4.1.3, from 2-Chloro-7-fluoroquinoxaline **33** (0.040 g, 0.22 mmol, 1.0 equiv.), 4-fluorobenzylamine (0.038 mL, 0.33 mmol, 1.5 equiv.) and $Et_3N$ (0.092 mL, 0.66 mmol, 3.0 equiv.) in *i*PrOH (0.53 mL). This yielded, after purification, the desired compound as a pale yellow solid with 59% (35.3 mg, 0.13 mmol) yield. $^1$H NMR (500 MHz, DMSO): δ 8.33 (s, 1H), 8.31–8.26 (m, 1H), 7.81 (dd, *J* = 9.1, 6.2 Hz, 1H), 7.47–7.42 (m, 2H), 7.27 (dd, *J* = 10.4, 2.8 Hz, 1H), 7.23–7.13 (m, 3H), 4.60 (d, *J* = 5.5 Hz, 2H). $^{13}$C NMR (126 MHz, DMSO): δ 163.49 (C), 162.26 (C), 161.53 (C), 160.33 (C), 152.36 (C), 142.84 (C), 142.73 (C), 139.37 (CH), 135.15 (C), 133.50 (C), 130.61 (CH), 130.52 (CH) 129.72 (CH), 129.65 (CH), 115.16 (CH), 114.99 (CH), 112.52 (CH), 112.32 (CH), 109.73 (CH), 109.56 (CH), 42.91 ($CH_2$). HPLC: 2.37 min. HRMS ($ESI^+$) *m*/*z* calc. for $C_{15}H_{12}F_2N_3$ $[M+H]^+$ = 272.0999, found 272.1003.

*4.2. NSCLC Cells Viability Assay*

PC9 (CVCL_B260; Merck) cells were cultured in RPMI 1640 (Gibco) supplemented with 10% FBS (Greiner). The cells were cultured according to standard procedures in a humid incubator at 37 °C and 5% $CO_2$.

PC9 cells were seeded at a cell density of 500 cells/well in clear bottom 384 well plates (Greiner Bio-One) in a total volume of 50 µL per well. Compounds were added 24 h post seeding and the viability was measured using the ATP-based luminescence CellTiter-Glo assay (Promega Corporation, 2800 Woods Hollow Road, Madison, WI 53711 USA) upon 72 h incubation with the compounds. Luminescence output was measured using a Spectramax M3 (Molecular Devices, LLC., 3860 N First Street, San Jose, CA 95134 USA). Absolute values were normalized to the mean of the control conditions. An identical setup was used to determine the $IC_{50}$ values. PC9 cells were treated with the indicated compounds at concentrations ranging between 0 and 5 µM (as indicated in the ESI). Cell viability was measured using CellTiter Glo upon 72 h of treatment. Data was plotted and $IC_{50}$ values were calculated based on a sigmoidal, 4PL standard curve interpolation

using Graphpad Prism version 8.4.2 (GraphPad Software, 2365 Northside Dr. Suite 560, San Diego, CA 92108).

### *4.3. Kinase Screening*

Eurofins performed a "Full KP Panel [Km ATP], KinaseProfile" which contains 429 radiometric kinase activity assays. The remaining kinase activity (%) was determined after treatment with the compounds at a concentration of 10 μM (Cfr. supporting information).

### *4.4. ITC*

Pure and untagged USP13 protein was produced for the purpose of analysing ligand binding. The pGEX4T2-USP13 vector encoding for an N-terminal GST tag fused to full-length human USP13 was transformed into *E. coli* BL21(DE3) cells for expression. Cells were grown at 37 °C in Terrific Broth (TB) medium, supplemented with 100 μg/mL Ampicillin, until the OD595 reached 0.7–0.8. Expression was then induced with 1 mM Isopropyl β-D-1-thiogalactopyranoside (IPTG). After 6 h induction at 28 °C, cells were collected by centrifugation and resuspended in PBS buffer. The cells were lysed with a cell disruptor (Constant Systems) and centrifuged to remove cell debris. The cell lysate was added to glutathione sepharose resin beads (17-0756-01, GE healthcare) equilibrated in PBS. Washing steps with PBS were performed to remove all other proteins before proceeding. To cleave the GST-tag, 10U/mL Thrombin was added to the beads and incubated at 4 °C on a shaker at slow rocking speed for 6 h. USP-13 was subsequently eluted in PBS and further purified on size exclusion chromatography, using a Superdex 200 16/900 column (GE Healthcare Life Sciences) in protein buffer (20 mM Tris-HCl (pH = 8), 50 mM NaCl, 0.1 mM EDTA), supplemented with 0.5 mM DTT and 5% glycerol for storage purposes.

An isothermal titration calorimetry (ITC) experiment was performed with the MicroCal iTC200 (GE Healthcare) at 25 °C. Spautin-1 was dissolved in DMSO and diluted in the protein buffer (25 mM Tris pH 7.5; 150 mM NaCl; 0.1 mM EDTA) to an end concentration of 300 μM with 5% DMSO. The compound was added to the syringe. The sample cell was filled with 30 μM of the protein in buffer to which 5% DMSO was added to avoid buffer mismatch. A control titration of buffer-buffer and compound-buffer was performed according to the same protocol. Data analysis was done with the Origin software accompanying the ITC instrument (Origin 7, OriginLab Corporation, Northampton, MA, USA).

### *4.5. TSA*

The melting temperature ($T_m$) of the protein sample can be determined by following the fluorescence of SYPRO orange with a CFX Connect real-time PCR instrument (Bio-Rad, Hercules, CA, USA). Samples contained 0.4 mg/mL USP13 protein in 25 mM Tris Ph 7.5; 150 mM NaCl; 0.1 mM EDTA; 0.5 mM DTT. Compounds were added to the protein and incubated for 30 min before adding 20× SYPRO Orange Protein Gel Stain (Thermo Fisher Scientific, Waltham, MA, USA). Control measurements were done for the protein in the corresponding percentages of DMSO.

Fluorescence was measured while increasing the temperature from 10 °C to 85 °C in 0.5 °C/30 s increments. The melting temperature for each protein sample could be determined from the relative fluorescence versus temperature curve by deleting post-peak quenching data and subsequently fitting the Boltzmann–sigmoidal equation, using Graphpad Prism software version 8.4.2 (GraphPad Software, 2365 Northside Dr. Suite 560, San Diego, CA 92108).

Due to lack of protein material, the measurements were only performed once in a screening setup.

**Supplementary Materials:** Supplementary Materials can be found at https://www.mdpi.com/1422-0067/22/2/635/s1.

**Author Contributions:** Conceptualization, G.J.G., J.D.G. and S.B.; methodology, W.V., G.J.G., J.G.D., and S.B.; software, M.E. and P.G.; validation, M.E. and P.G.; formal analysis, M.E. and P.G.; investi-

gation, M.E., P.G., and L.M.; resources, G.J.G., J.D.G., and S.B.; data curation, M.E., P.G., and L.M.; writing—original draft preparation, M.E.; writing—review and editing, P.G., W.V., G.J.G., J.D.G., and S.B.; visualization, M.E., P.G., and L.M.; supervision, S.B.; project administration, G.J.G., J.D.G., and S.B.; funding acquisition, G.J.G., J.D.G., and S.B. All authors have read and agreed to the published version of the manuscript.

**Funding:** This research was funded by the Interdisciplinary Research Programmes (IRP) of the and the Wetenschappelijk Fonds Willy Gepts (WFWG) (UZ Brussel/VUB). Philippe Giron was funded as a Ph.D. Fellow of the FWO.

**Institutional Review Board Statement:** Not applicable.

**Informed Consent Statement:** Not applicable.

**Data Availability Statement:** All data are available upon reasonable request.

**Acknowledgments:** The authors thank both the Interdisciplinary Research Programmes (IRP) of the Vrije Universiteit Brussel (VUB) and the Wetenschappelijk Fonds Willy Gepts (WFWG) (UZ Brussel/VUB) for financial support and Carolien Eggermont (VUB) for the NEK4 expression data. We also acknowledge the Broad Institute and the Novartis Institutes for Biomedical Research and its Genomics Institute of the Novartis Research Foundation for the Cancer Cell Line Encyclopedia.

**Conflicts of Interest:** The authors declare no conflict of interest. The funders had no role in the design of the study; in the collection, analyses, or interpretation of data; in the writing of the manuscript, or in the decision to publish the results.

## Abbreviations

| | |
|---|---|
| SAR | Structure–activity relationship |
| PACS | Pathophysiological cell signaling |
| USP13 | Ubiquitin Specific Protease 13 |
| EGFR | Epidermal growth factor receptor |
| NSCLC | Non-small cell lung cancer |
| ITC | Isothermal titration calorimetry |
| TSA | Thermal shift assay |
| DUBs | Deubiquitinating enzymes |
| NEK4 | Never in mitosis A related kinase 4 |
| TRAIL | Tumor necrosis factor-Related Apoptosis Inducing Ligand |
| EMT | Epithelial to mesenchymal transition |
| ON | Overnight |
| DMF | *N*,*N*-dimethylformamide |
| $T_m$ | Melting temperature |
| $\Delta T_m$ | Melting temperature difference |
| h | Human |
| TB | Terrific Broth |
| IPTG | Isopropyl β-*D*-1-thiogalactopyranoside |
| EDTA | Ethylenediaminetetraacetic acid |
| DTT | 1,4-dithiothreitol |
| IRP | Interdisciplinary Research Programmes |
| WFWG | Wetenschappelijk Fonds Willy Gepts |
| VUB | Vrije Universiteit Brussel |

## References

1. World Health Organization, International Agency for Research on Cancer. Globocan 2018: Lung Cancer. International Agency for Research on Cancer. Available online: http://gco.iarc.fr/today/data/factsheets/cancers/15-Lung-fact-sheet.pdf (accessed on 25 March 2020).
2. D'Addario, G.; Fruh, M.; Reck, M.; Baumann, P.; Klepetko, W.; Felip, E.; On behalf of the ESMO Guidelines Working Group Metastatic Non-Small-Cell Lung Cancer. ESMO Clinical Practice Guidelines for Diagnosis, Treatment and Follow-Up. *Ann. Oncol.* **2010**, *21*, v116–v119. [CrossRef] [PubMed]

3. Lynch, T.J.; Bell, D.W.; Sordella, R.; Gurubhagavatula, S.; Okimoto, R.A.; Brannigan, B.W.; Harris, P.L.; Haserlat, S.M.; Supko, J.G.; Haluska, F.G.; et al. Activating Mutations in the Epidermal Growth Factor Receptor Underlying Responsiveness of Non–Small-Cell Lung Cancer to Gefitinib. *N. Engl. J. Med.* **2004**, *350*, 2129–2139. [CrossRef] [PubMed]
4. Ahn, M.-J.; Sun, J.-M.; Lee, S.-H.; Ahn, J.S.; Park, K. EGFR TKI Combination with Immunotherapy in Non-Small Cell Lung Cancer. *Expert Opin. Drug Saf.* **2017**, *16*, 465–469. [CrossRef] [PubMed]
5. Leonetti, A.; Sharma, S.; Minari, R.; Perego, P.; Giovannetti, E.; Tiseo, M. Resistance Mechanisms to Osimertinib in EGFR-Mutated Non-Small Cell Lung Cancer. *Br. J. Cancer* **2019**, *121*, 725–737. [CrossRef]
6. Martín-Bernabé, A.; Balcells, C.; Tarragó-Celada, J.; Foguet, C.; Bourgoin-Voillard, S.; Seve, M.; Cascante, M. The Importance of Post-Translational Modifications in Systems Biology Approaches to Identify Therapeutic Targets in Cancer Metabolism. *Curr. Opin. Syst. Biol.* **2017**, *3*, 161–169. [CrossRef]
7. Hsu, J.-M.; Li, C.-W.; Lai, Y.-J.; Hung, M.-C. Posttranslational Modifications of PD-L1 and Their Applications in Cancer Therapy. *Cancer Res.* **2018**, *78*, 6349–6353. [CrossRef]
8. Sharma, B.S.; Prabhakaran, V.; Desai, A.P.; Bajpai, J.; Verma, R.J.; Swain, P.K. Post-Translational Modifications (PTMs), from a Cancer Perspective: An Overview. *Oncogen* **2019**, *2*, 12. [CrossRef]
9. Pickart, C.M.; Eddins, M.J. Ubiquitin: Structures, Functions, Mechanisms. *Biochim. Biophys. Acta BBA Mol. Cell Res.* **2004**, *1695*, 55–72. [CrossRef]
10. Clague, M.J.; Heride, C.; Urbé, S. The Demographics of the Ubiquitin System. *Trends Cell Biol.* **2015**, *25*, 417–426. [CrossRef]
11. Castagnoli, L.; Mandaliti, W.; Nepravishta, R.; Valentini, E.; Mattioni, A.; Procopio, R.; Iannuccelli, M.; Polo, S.; Paci, M.; Cesareni, G.; et al. Selectivity of the CUBAN Domain in the Recognition of Ubiquitin and NEDD8. *FEBS J.* **2019**, *286*, 653–677. [CrossRef]
12. Mevissen, T.E.T.; Komander, D. Mechanisms of Deubiquitinase Specificity and Regulation. *Annu. Rev. Biochem.* **2017**, *86*, 159–192. [CrossRef] [PubMed]
13. Zhang, J.; Zhang, P.; Wei, Y.; Piao, H.; Wang, W.; Maddika, S.; Wang, M.; Chen, D.; Sun, Y.; Hung, M.-C.; et al. Deubiquitylation and Stabilization of PTEN by USP13. *Nat. Cell Biol.* **2013**, *15*, 1486–1494. [CrossRef] [PubMed]
14. Man, X.; Piao, C.; Lin, X.; Kong, C.; Cui, X.; Jiang, Y. USP13 Functions as a Tumor Suppressor by Blocking the NF-KB-Mediated PTEN Downregulation in Human Bladder Cancer. *J. Exp. Clin. Cancer Res.* **2019**, *38*, 259. [CrossRef] [PubMed]
15. Qu, Z.; Zhang, R.; Su, M.; Liu, W. USP13 Serves as a Tumor Suppressor via the PTEN/AKT Pathway in Oral Squamous Cell Carcinoma. *Cancer Manag. Res.* **2019**, *11*, 9175–9183. [CrossRef]
16. Fang, X.; Zhou, W.; Wu, Q.; Huang, Z.; Shi, Y.; Yang, K.; Chen, C.; Xie, Q.; Mack, S.C.; Wang, X.; et al. Deubiquitinase USP13 Maintains Glioblastoma Stem Cells by Antagonizing FBXL14-Mediated Myc Ubiquitination. *J. Exp. Med.* **2017**, *214*, 245–267. [CrossRef]
17. Han, C.; Yang, L.; Choi, H.H.; Baddour, J.; Achreja, A.; Liu, Y.; Li, Y.; Li, J.; Wan, G.; Huang, C.; et al. Amplification of USP13 Drives Ovarian Cancer Metabolism. *Nat. Commun.* **2016**, *7*, 13525. [CrossRef]
18. Han, C.; Lu, X.; Nagrath, D. Regulation of Protein Metabolism in Cancer. *Mol. Cell. Oncol.* **2018**, *5*, e1285384. [CrossRef]
19. Li, Y.; Luo, K.; Yin, Y.; Wu, C.; Deng, M.; Li, L.; Chen, Y.; Nowsheen, S.; Lou, Z.; Yuan, J. USP13 Regulates the RAP80-BRCA1 Complex Dependent DNA Damage Response. *Nat. Commun.* **2017**, *8*, 15752. [CrossRef]
20. Zhang, S.; Zhang, M.; Jing, Y.; Yin, X.; Ma, P.; Zhang, Z.; Wang, X.; Di, W.; Zhuang, G. Deubiquitinase USP13 Dictates MCL1 Stability and Sensitivity to BH3 Mimetic Inhibitors. *Nat. Commun.* **2018**, *9*, 215. [CrossRef]
21. Zhao, X.; Fiske, B.; Kawakami, A.; Li, J.; Fisher, D.E. Regulation of MITF Stability by the USP13 Deubiquitinase. *Nat. Commun.* **2011**, *2*, 414. [CrossRef]
22. Wang, Y.; Ou, Z.; Sun, Y.; Yeh, S.; Wang, X.; Long, J.; Chang, C. Androgen Receptor Promotes Melanoma Metastasis via Altering the MiRNA-539-3p/USP13/MITF/AXL Signals. *Oncogene* **2017**, *36*, 1644–1654. [CrossRef] [PubMed]
23. Liao, Y.; Guo, Z.; Xia, X.; Liu, Y.; Huang, C.; Jiang, L.; Wang, X.; Liu, J.; Huang, H. Inhibition of EGFR Signaling with Spautin-1 Represents a Novel Therapeutics for Prostate Cancer. *J. Exp. Clin. Cancer Res.* **2019**, *38*, 157. [CrossRef] [PubMed]
24. Wu, Y.; Zhang, Y.; Liu, C.; Zhang, Y.; Wang, D.; Wang, S.; Wu, Y.; Liu, F.; Li, Q.; Liu, X.; et al. Amplification of USP13 Drives Non-Small Cell Lung Cancer Progression Mediated by AKT/MAPK Signaling. *Biomed. Pharmacother.* **2019**, *114*, 108831. [CrossRef] [PubMed]
25. Giron, P.; Eggermont, C.; Noeparast, A.; Vandenplas, H.; Teugels, E.; Forsyth, R.; De Wever, O.; Aza-Blanc, P.; Gutierrez, G.J.; De Grève, J. Targeting USP13 Mediated Drug Tolerance Increases the Efficacy of EGFR Inhibition of Mutant EGFR in NON-SMALL Cell Lung Cancer. *Int. J. Cancer* **2020**. [CrossRef]
26. Liu, J.; Xia, H.; Kim, M.; Xu, L.; Li, Y.; Zhang, L.; Cai, Y.; Norberg, H.V.; Zhang, T.; Furuya, T.; et al. Beclin1 Controls the Levels of P53 by Regulating the Deubiquitination Activity of USP10 and USP13. *Cell* **2011**, *147*, 223–234. [CrossRef]
27. Aly, R.M.; Serya, R.A.; Amira, M.; Al-Ansary, G.H.; Abou El Ella, D.A. Quinoline-Based Small Molecules as Effective Protein Kinases Inhibitors. *J. Am. Sci.* **2016**, *12*, 10–32.
28. Cortes, J.E.; Kantarjian, H.M.; Brümmendorf, T.H.; Kim, D.-W.; Turkina, A.G.; Shen, Z.-X.; Pasquini, R.; Khoury, H.J.; Arkin, S.; Volkert, A.; et al. Safety and Efficacy of Bosutinib (SKI-606) in Chronic Phase Philadelphia Chromosome–Positive Chronic Myeloid Leukemia Patients with Resistance or Intolerance to Imatinib. *Blood* **2011**, *118*, 4567–4576. [CrossRef]
29. Elisei, R.; Schlumberger, M.J.; Müller, S.P.; Schöffski, P.; Brose, M.S.; Shah, M.H.; Licitra, L.; Jarzab, B.; Medvedev, V.; Kreissl, M.C.; et al. Cabozantinib in Progressive Medullary Thyroid Cancer. *J. Clin. Oncol.* **2013**, *31*, 3639–3646. [CrossRef]

30. Rabindran, S.K.; Discafani, C.M.; Rosfjord, E.C.; Baxter, M.; Floyd, M.B.; Golas, J.; Hallett, W.A.; Johnson, B.D.; Nilakantan, R.; Overbeek, E.; et al. Antitumor Activity of HKI-272, an Orally Active, Irreversible Inhibitor of the HER-2 Tyrosine Kinase. *Cancer Res.* **2004**, *64*, 3958–3965. [CrossRef]
31. Collins, I.; Caldwell, J.; Fonseca, T.; Donald, A.; Bavetsias, V.; Hunter, L.-J.K.; Garrett, M.D.; Rowlands, M.G.; Aherne, G.W.; Davies, T.G.; et al. Structure-Based Design of Isoquinoline-5-Sulfonamide Inhibitors of Protein Kinase B. *Bioorg. Med. Chem.* **2006**, *14*, 1255–1273. [CrossRef]
32. Larocque, E.; Naganna, N.; Ma, X.; Opoku-Temeng, C.; Carter-Cooper, B.; Chopra, G.; Lapidus, R.G.; Sintim, H.O. Aminoisoquinoline Benzamides, FLT3 and Src-Family Kinase Inhibitors, Potently Inhibit Proliferation of Acute Myeloid Leukemia Cell Lines. *Future Med. Chem.* **2017**, *9*, 1213–1225. [CrossRef] [PubMed]
33. Garofalo, A.W.; Adler, M.; Aubele, D.L.; Bowers, S.; Franzini, M.; Goldbach, E.; Lorentzen, C.; Neitz, R.J.; Probst, G.D.; Quinn, K.P.; et al. Novel Cinnoline-Based Inhibitors of LRRK2 Kinase Activity. *Bioorg. Med. Chem. Lett.* **2013**, *23*, 71–74. [CrossRef] [PubMed]
34. Barlaam, B.; Cadogan, E.; Campbell, A.; Colclough, N.; Dishington, A.; Durant, S.; Goldberg, K.; Hassall, L.A.; Hughes, G.D.; MacFaul, P.A.; et al. Discovery of a Series of 3-Cinnoline Carboxamides as Orally Bioavailable, Highly Potent, and Selective ATM Inhibitors. *ACS Med. Chem. Lett.* **2018**, *9*, 809–814. [CrossRef] [PubMed]
35. Szumilak, M.; Stanczak, A. Cinnoline Scaffold—A Molecular Heart of Medicinal Chemistry? *Molecules* **2019**, *24*, 2271. [CrossRef]
36. El Newahie, A.M.S.; Ismail, N.S.M.; Abou El Ella, D.A.; Abouzid, K.A.M. Quinoxaline-Based Scaffolds Targeting Tyrosine Kinases and Their Potential Anticancer Activity: Quinoxaline-Based Scaffolds Targeting Tyrosine Kinases. *Arch. Pharm. (Weinheim)* **2016**, *349*, 309–326. [CrossRef]
37. Park, S.J.; Jo, D.S.; Jo, S.-Y.; Shin, D.W.; Shim, S.; Jo, Y.K.; Shin, J.H.; Ha, Y.J.; Jeong, S.-Y.; Hwang, J.J.; et al. Inhibition of Never in Mitosis A (NIMA)-Related Kinase-4 Reduces Survivin Expression and Sensitizes Cancer Cells to TRAIL-Induced Cell Death. *Oncotarget* **2016**, *7*, 65957–65967. [CrossRef]
38. Ding, N.-H.; Zhang, L.; Xiao, Z.; Rong, Z.-X.; Li, Z.; He, J.; Chen, L.; Ou, D.-M.; Liao, W.-H.; Sun, L.-Q. NEK4 Kinase Regulates EMT to Promote Lung Cancer Metastasis. *J. Cell. Mol. Med.* **2018**, *22*, 5877–5887. [CrossRef]
39. Wells, C.I.; Kapadia, N.R.; Couñago, R.M.; Drewry, D.H. In Depth Analysis of Kinase Cross Screening Data to Identify Chemical Starting Points for Inhibition of the Nek Family of Kinases. *MedChemComm* **2018**, *9*, 44–66. [CrossRef]
40. Yamamoto, N.; Takeshita, K.; Shichijo, M.; Kokubo, T.; Sato, M.; Nakashima, K.; Ishimori, M.; Nagai, H.; Li, Y.-F.; Yura, T.; et al. The Orally Available Spleen Tyrosine Kinase Inhibitor 2-[7-(3,4-Dimethoxyphenyl)-Imidazo[1,2-*c*]Pyrimidin-5-Ylamino]Nicotinamide Dihydrochloride (BAY 61-3606) Blocks Antigen-Induced Airway Inflammation in Rodents. *J. Pharmacol. Exp. Ther.* **2003**, *306*, 1174–1181. [CrossRef]
41. George, D.; Friedman, M.; Allen, H.; Argiriadi, M.; Barberis, C.; Bischoff, A.; Clabbers, A.; Cusack, K.; Dixon, R.; Fix-Stenzel, S.; et al. Discovery of Thieno[2,3-c]Pyridines as Potent COT Inhibitors. *Bioorg. Med. Chem. Lett.* **2008**, *18*, 4952–4955. [CrossRef]
42. Mack, H.; Teusch, N.; Mueller, B.K.; Hornberger, W.; Jarvis, M.F.; Sauer, D. Preparation of 4-(4-Pyridyl)-Benzamides as Rho Kinases Inhibitors. WO2009027392, 5 March 2009.
43. Zayed, M.; Ihmaid, S.; Ahmed, H.; El-Adl, K.; Asiri, A.; Omar, A. Synthesis, Modelling, and Anticonvulsant Studies of New Quinazolines Showing Three Highly Active Compounds with Low Toxicity and High Affinity to the GABA-A Receptor. *Molecules* **2017**, *22*, 188. [CrossRef] [PubMed]
44. Asadi, P.; Khodarahmi, G.; Jahanian-Najafabadi, A.; Saghaie, L.; Hassanzadeh, F. Biologically Active Heterocyclic Hybrids Based on Quinazolinone, Benzofuran and Imidazolium Moieties: Synthesis, Characterization, Cytotoxic and Antibacterial Evaluation. *Chem. Biodivers.* **2017**, *14*, e1600411. [CrossRef] [PubMed]
45. Zhang, Q.; Li, Y.; Zhang, B.; Lu, B.; Li, J. Design, Synthesis and Biological Evaluation of Novel Histone Deacetylase Inhibitors Incorporating 4-Aminoquinazolinyl Systems as Capping Groups. *Bioorg. Med. Chem. Lett.* **2017**, *27*, 4885–4888. [CrossRef]
46. Felts, A.S.; Saleh, S.A.; Le, U.; Rodriguez, A.L.; Weaver, C.D.; Conn, P.J.; Lindsley, C.W.; Emmitte, K.A. Discovery and SAR of 6-Substituted-4-Anilinoquinazolines as Non-Competitive Antagonists of MGlu5. *Bioorg. Med. Chem. Lett.* **2009**, *19*, 6623–6626. [CrossRef]
47. Liu, Q.; Douglas, D.G.; Delucca, G.V.; George, V.; Shi, Q.; Tebben, A.J. Preparation of Carbazole Carboxamide Compounds Useful as Kinase Inhibitors. U.S. Patent Application Publication No. 20100160303A1, 24 June 2010.
48. Liu, L.T.; Yuan, T.-T.; Liu, H.-H.; Chen, S.-F.; Wu, Y.-T. Synthesis and Biological Evaluation of Substituted 6-Alkynyl-4-Anilinoquinazoline Derivatives as Potent EGFR Inhibitors. *Bioorg. Med. Chem. Lett.* **2007**, *17*, 6373–6377. [CrossRef] [PubMed]
49. Guo, Z.; Zhuang, C.; Zhu, L.; Zhang, Y.; Yao, J.; Dong, G.; Wang, S.; Liu, Y.; Chen, H.; Sheng, C.; et al. Structure–Activity Relationship and Antitumor Activity of Thio-Benzodiazepines as P53–MDM2 Protein–Protein Interaction Inhibitors. *Eur. J. Med. Chem.* **2012**, *56*, 10–16. [CrossRef] [PubMed]
50. Duncan, K.W.; Chesworth, R.; Boriack-Sjodin, P.A.; Munchhof, M.J.; Jin, L.; Penebre, E.; Barbash, O.L. Prmt5 Inhibitors and Uses Thereof. WO2016022605A1, 11 February 2016.
51. Berger, M.; Albrecht, B.; Berces, A.; Ettmayer, P.; Neruda, W.; Woisetschläger, M. S(+)-4-(1-Phenylethylamino)Quinazolines as Inhibitors of Human Immunoglobuline E Synthesis: Potency Is Dictated by Stereochemistry and Atomic Point Charges at N-1. *J. Med. Chem.* **2001**, *44*, 3031–3038. [CrossRef] [PubMed]
52. Zhao, X.; Xu, W.; Xu, W. Method for Synthesizing 4-Bromo-7-Fluoroisoquinoline. CN108314648, 24 July 2018.

53. Fisher, B.; Johnson, M.G.; Brian, L.; Shin, Y.; Kaizerman, J. Preparation of 5-Cyano-4,6-Diaminopyrimidine or 6-Aminopurine Derivatives as PI3K-Delta Inhibitors. WO 2012061696, 10 May 2012.
54. Ismail, R.S.M.; Ismail, N.S.M.; Abuserii, S.; Abou El Ella, D.A. Recent Advances in 4-Aminoquinazoline Based Scaffold Derivatives Targeting EGFR Kinases as Anticancer Agents. *Future J. Pharm. Sci.* **2016**, *2*, 9–19. [CrossRef]
55. Rewcastle, G.W.; Denny, W.A.; Bridges, A.J.; Zhou, H.; Cody, D.R.; McMichael, A.; Fry, D.W. Tyrosine Kinase Inhibitors. 5. Synthesis and Structure-Activity Relationships for 4-[(Phenylmethyl)Amino]- and 4-(Phenylamino)Quinazolines as Potent Adenosine 5′-Triphosphate Binding Site Inhibitors of the Tyrosine Kinase Domain of the Epidermal Growth Factor Receptor. *J. Med. Chem.* **1995**, *38*, 3482–3487. [CrossRef]
56. Politzer, P.; Lane, P.; Concha, M.C.; Ma, Y.; Murray, J.S. An Overview of Halogen Bonding. *J. Mol. Model.* **2007**, *13*, 305–311. [CrossRef]
57. Wilcken, R.; Zimmermann, M.O.; Lange, A.; Joerger, A.C.; Boeckler, F.M. Principles and Applications of Halogen Bonding in Medicinal Chemistry and Chemical Biology. *J. Med. Chem.* **2013**, *56*, 1363–1388. [CrossRef] [PubMed]
58. Mérour, J.-Y.; Buron, F.; Plé, K.; Bonnet, P.; Routier, S. The Azaindole Framework in the Design of Kinase Inhibitors. *Molecules* **2014**, *19*, 19935–19979. [CrossRef] [PubMed]
59. Liu, J.; Yang, C.; Simpson, C.; DeRyckere, D.; Van Deusen, A.; Miley, M.J.; Kireev, D.; Norris-Drouin, J.; Sather, S.; Hunter, D.; et al. Discovery of Small Molecule Mer Kinase Inhibitors for the Treatment of Pediatric Acute Lymphoblastic Leukemia. *ACS Med. Chem. Lett.* **2012**, *3*, 129–134. [CrossRef] [PubMed]
60. Gucký, T.; Řezníčková, E.; Radošová Muchová, T.; Jorda, R.; Klejová, Z.; Malínková, V.; Berka, K.; Bazgier, V.; Ajani, H.; Lepšík, M.; et al. Discovery of $N^2$-(4-Amino-Cyclohexyl)-9-Cyclopentyl-$N^6$-(4-Morpholin-4-Ylmethyl-Phenyl)-9*H*-Purine-2,6-Diamine as a Potent FLT3 Kinase Inhibitor for Acute Myeloid Leukemia with FLT3 Mutations. *J. Med. Chem.* **2018**, *61*, 3855–3869. [CrossRef]
61. Eurofins DiscoverX. KINOMEscan®Assay. Available online: https://www.discoverx.com/services/drug-discovery-development-services/kinase-profiling/kinomescan (accessed on 10 April 2020).
62. Barretina, J.; Caponigro, G.; Stransky, N.; Venkatesan, K.; Margolin, A.A.; Kim, S.; Wilson, C.J.; Lehár, J.; Kryukov, G.V.; Sonkin, D.; et al. The Cancer Cell Line Encyclopedia Enables Predictive Modelling of Anticancer Drug Sensitivity. *Nature* **2012**, *483*, 603–607. [CrossRef]
63. The Cancer Cell Line Encyclopedia. Available online: www.broadinstitute.org/ccle. (accessed on 17 December 2020).
64. Eurofins, KinaseProfiler, NEK4 Human Other Protein Kinase Enzymatic Radiometric Assay [Km ATP]. Available online: https://www.eurofinsdiscoveryservices.com/catalogmanagement/viewitem/NEK4-Human-Other-Protein-Kinase-Enzymatic-Radiometric-Assay-Km-ATP-KinaseProfiler/15-033KP (accessed on 10 April 2020).
65. Mohamed, T.; Rao, P.P.N. 2,4-Disubstituted Quinazolines as Amyloid-β Aggregation Inhibitors with Dual Cholinesterase Inhibition and Antioxidant Properties: Development and Structure-Activity Relationship (SAR) Studies. *Eur. J. Med. Chem.* **2017**, *126*, 823–843. [CrossRef]
66. Tobe, M.; Isobe, Y.; Tomizawa, H.; Nagasaki, T.; Takahashi, H.; Fukazawa, T.; Hayashi, H. Discovery of Quinazolines as a Novel Structural Class of Potent Inhibitors of NF-KB Activation. *Bioorg. Med. Chem.* **2003**, *11*, 383–391. [CrossRef]

European Journal of Medicinal Chemistry 56 (2012) 10–16

Contents lists available at SciVerse ScienceDirect

European Journal of Medicinal Chemistry

journal homepage: http://www.elsevier.com/locate/ejmech

Original article

# Structure–activity relationship and antitumor activity of thio-benzodiazepines as p53–MDM2 protein–protein interaction inhibitors

Zizhao Guo [1], Chunlin Zhuang [1], Lingjian Zhu, Yongqiang Zhang, Jianzhong Yao, Guoqiang Dong, Shengzheng Wang, Yang Liu, Hai Chen, Chunquan Sheng***, Zhenyuan Miao*, Wannian Zhang**

*School of Pharmacy, Second Military Medical University, 325 Guohe Road, Shanghai 200433, People's Republic of China*

ARTICLE INFO

*Article history:*
Received 22 April 2012
Received in revised form
19 July 2012
Accepted 1 August 2012
Available online 10 August 2012

*Keywords:*
p53–MDM2
Thio-benzodiazepine
SAR
Antitumor activity

ABSTRACT

In order to discuss the structure–activity relationship (SAR) of the thio-benzodiazepine compounds which showed excellent activity against p53–MDM2 protein–protein interaction, we designed and synthesized twenty compounds with electrophilic and nucleophilic groups on the benzene ring. Among them, compounds **8i** ($K_i$ = 91 nM) and **8n** ($K_i$ = 89 nM) showed better binding activity than that of the reference drug Nutlin-3a ($K_i$ = 121 nM). In addition, *in vitro* antitumor activity against Saos-2, U-2 OS, A549 and NCI-H1299 cell-lines were assayed by the MTT method. Especially, compounds **8i** and **8n** possessed excellent biological activity and good selectivity comparable to Nutlin-3a, which were promising candidates for further evaluation.



## 1. Introduction

The tumor suppressor p53 is one of the most important proteins in human cancers [1,2]. Its main functions are cell-cycle arrest, DNA repair, and apoptosis [3]. The p53 mutations are very common in human tumors, however it remains wild-type in approximately 50% of human cancers [4]. Although 50% of all human tumors express wild-type p53, many are thought to have inadequate p53 function due to abnormalities in p53 regulation or defective signaling in the p53 pathway [2]. Murine double minute 2 (MDM2) is a protein which can inhibit p53's ability to bind to DNA, activate transcription and promote rapid degradation of p53. In turn, p53 activates the expression of the MDM2 protein in an autoregulatory negative feedback loop [5].

Due to the crucial role of p53 in tumor suppression, reactivation of the p53 function by disruption of the p53–MDM2 interaction using non-peptide small-molecule inhibitors is now recognized as a new and promising strategy for anticancer drug design [6]. So far, many series of small-molecule inhibitors were described, including benzodiazepinediones, nutlins, spiro-oxindoles, quinolinols, isoindolinones, chlorofusin, norbornanes, sulfonamides, chalcones, terphenyls, and piperazine-4-phenyl derivatives [3,7–15], many of which showed relatively weak bioactivity, only the nutlins, the spiro-oxindoles and the benzodiazepinediones are particularly valuable [3,7]. Nultins were the first potent and selective p53–MDM2 interaction inhibitors developed by Roche, and promising candidates RG7112 [16] and RO5503781 [17] entered phase I clinical trials, but their detailed structures were not reported [18]. The spiro-oxindoles developed by Wang's group possessed good pharmacokinetic properties as well as a high binding affinity to MDM2. Among them, one representative candidate MI-219 with a $K_i$ value of 5 nM was a potent and orally active small-molecule inhibitor [19].

In 2005, Grasberger and his co-workers firstly reported 1,4-benzodiazepine-2,5-dione compounds as the small molecule inhibitors of the p53–MDM2 protein–protein interaction [7]. The benzodiazepine was thought to be a "privileged structure" in medicinal chemistry [20]. In our previous work, we first reported and synthesized a series of thio-benzodiazepines with the principle of bioisosterism and found that many compounds had nanomolar affinity toward MDM2 and exhibited potent antitumor activities against the U-2 OS human osteosarcoma cell line (Fig. 1) [21], which is worthy of further structural optimization. Herein, we designed and synthesized a series of thio-benzodiazepines with electrophilic

* Corresponding author. Tel./fax: +86 21 81871241.
** Corresponding author. Tel./fax: +86 21 81871243.
*** Corresponding author. Tel./fax: +86 21 81871239.
*E-mail addresses:* shengcq@hotmail.com (C. Sheng), miaozhenyuan@hotmail.com (Z. Miao), zhangwnk@hotmail.com (W. Zhang).
[1] These two authors contributed equally to this work.

0223-5234/$ – see front matter © 2012 Elsevier Masson SAS. All rights reserved.
http://dx.doi.org/10.1016/j.ejmech.2012.08.003

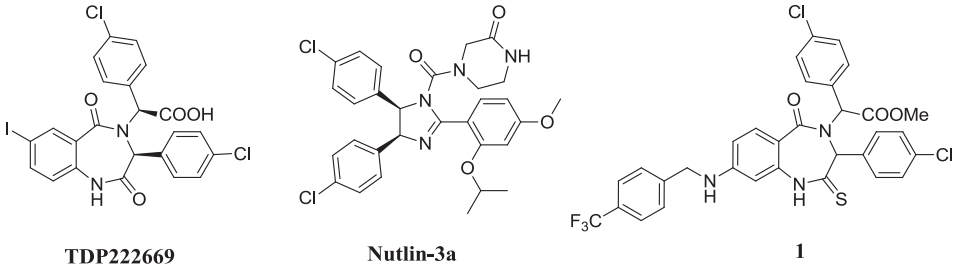


**Fig. 1.** The structures of TDP222669, Nutlin-3a and **1**.

and nucleophilic groups on the benzene ring to extend the SAR and find promising lead compounds with excellent biological properties.

## 2. Chemistry

A general pathway for the synthesis of target compounds **8a**–**t** (Table 2) was outlined in Scheme 1. The skeleton of thio-benzodiazepines was synthesized utilizing the highly efficient and versatile Ugi four-component condensation (Ugi 4CC reaction) [22]. We used substituted benzaldehydes (**5**) as the aldehyde, methyl amino(4-chlorophenyl)acetate hydrochloride or methyl 2-amino-2-(4-fluorophenyl) acetate hydrochloride (**3**) as the amine, substituted nitrobenzoic acids (**2**) as the carboxylic acid and 1-isocyanocyclohexene (**4**) as the isocyanide to perform the Ugi reaction. In this synthetic process, the purity of the starting material **4** had significant influence on the yield of Ugi reaction. The obtained key intermediate **7** was treated with the Lawesson's reagent to afford the compounds **8a**–**r** with the yield of 50–87%. In order to increase the structural diversity, two compounds **8s** and **8t** with substituents on sulfur atom were synthesized by the nucleophilic substitution reaction in presence of 1,8-diazabicyclo[5.4.0] undec-7-ene (DBU) at room temperature. Owing to the stronger nucleophilic activity of sulfur atom, the substitution reaction took place on sulfur instead of nitrogen atom.

**Table 1**
Binding constants ($K_i$) of the MDM2 ligands and $IC_{50}$ values of *in vitro* antitumor activity.

| Compounds | $K_i$[a](μM) | $IC_{50}$[b] (μM) | | | |
|---|---|---|---|---|---|
| | | Saos-2 (p53 null) | U-2 OS (wt-p53) | A549 (wt-p53) | NCI-H1299 (p53 null) |
| **8a** | 1.37 | 11.1 | 12.1 | 37.2 | 16.5 |
| **8b** | >100 | 61.8 | 88.5 | >100 | >100 |
| **8c** | 0.721 | 8.91 | 3.50 | 18.7 | 24.7 |
| **8d** | 0.707 | 6.59 | 12.0 | 8.44 | 16.5 |
| **8e** | >100 | 3.84 | 2.61 | 11.3 | 5.73 |
| **8f** | 1.72 | 12.7 | 44.3 | 25.6 | >100 |
| **8g** | 0.315 | 6.48 | 7.23 | 19.7 | 29.7 |
| **8h** | 8.18 | >100 | >100 | >100 | >100 |
| **8i** | 0.0910 | 6.78 | 5.69 | 26.9 | 11.1 |
| **8j** | 3.02 | 13.7 | 11.8 | 9.44 | 14.0 |
| **8k** | >100 | 20.0 | 35.3 | >100 | >100 |
| **8l** | >100 | 19.1 | 27.8 | >100 | 73.3 |
| **8m** | 37.7 | 25.5 | 32.7 | >100 | 73.6 |
| **8n** | 0.0890 | 11.9 | 7.53 | 12.9 | 14.5 |
| **8o** | 1.05 | 32.1 | 28.0 | 19.4 | 25.0 |
| **8p** | 3.98 | 11.0 | 35.7 | >100 | 35.4 |
| **8q** | 0.518 | 9.23 | 27.4 | 23.7 | 39.5 |
| **8r** | 11.9 | >100 | 33.9 | >100 | >100 |
| **8s** | >100 | >100 | 67.6 | >100 | >100 |
| **8t** | 21.1 | >100 | >100 | >100 | >100 |
| **Nutlin-3a** | 0.121 | 12.1 | 19.6 | 15.0 | 20.4 |
| **1** | 6.70 | 25.3 | 15.9 | 25.7 | 42.6 |

[a] Values were determined by fluorescence polarization assay.
[b] Values were measured with MTT method.

## 3. Results and discussion

### 3.1. p53–MDM2 binding assays

The binding $K_i$ constants of small molecule ligands were measured by fluorescence polarization (FP) binding assay. Nutlin-3a, one of the most active small molecule p53–MDM2 inhibitors, was used as the reference drug. The results were listed in Table 1. Most of the targeted thio-benzodiazepines had nanomolar to micromolar affinity toward MDM2. The detailed SAR analysis demonstrated that the proper substituents on the position 7 and 8 were beneficial to the binding activity. In particular, most fluorine-containing compounds on the position 7 or 8 exhibited moderate to excellent affinity. For example, compounds **8i** ($K_i$ = 91 nM) and **8n** ($K_i$ = 89 nM) with trifluoromethyl group and fluorine atom on position 8 showed excellent binding activity superior to the reference compound ($K_i$ = 121 nM). In addition, compounds **8d**, **8f**, **8g**, **8j**, **8o** and **8q** also displayed good binding affinity comparable to Nutlin-3a. However, the difluorinated compound **8e** had relatively weak activity. Interestingly, compound **8c** with three chlorine atoms also showed good binding affinity with a $K_i$ value of 721 nM.

The results also revealed that the substituents on the position 9 generated negative influence on the activity. For instance, compounds **8b**, **8h** and **8l** exhibited weak binding activity. Furthermore, we found that the substituents on sulfur atom led to significant decrease of activity, such as compounds **8s** and **8t**. According to the previously reported structures of the inhibitors binding to MDM2 and our docking model, we presented

**Table 2**
The structures of thio-benzodiazepines compounds **8a**–**8r**.

| compounds | $R_1$ | $R_2$ | $R_3$ | $R_4$ | R | R′ |
|---|---|---|---|---|---|---|
| **8a** | H | H | Cl | H | Cl | Cl |
| **8b** | H | H | H | Cl | Cl | Cl |
| **8c** | H | Cl | H | H | Cl | Cl |
| **8d** | H | H | F | H | Cl | Cl |
| **8e** | H | F | F | H | Cl | Cl |
| **8f** | H | H | Cl | H | F | F |
| **8g** | H | Cl | H | H | F | Cl |
| **8h** | H | H | H | $OCH_3$ | Cl | Cl |
| **8i** | H | H | $CF_3$ | H | Cl | Cl |
| **8j** | H | H | $CF_3$ | H | F | Cl |
| **8k** | H | H | $OCH_3$ | H | Cl | Cl |
| **8l** | H | H | H | $CH_3$ | Cl | Cl |
| **8m** | H | $CH_3$ | H | H | Cl | Cl |
| **8n** | H | F | H | H | Cl | Cl |
| **8o** | H | H | F | H | F | Cl |
| **8p** | H | H | Br | H | Cl | Cl |
| **8q** | H | H | Cl | H | Cl | $CF_3$ |
| **8r** | H | H | Cl | H | Cl | $OCH_3$ |

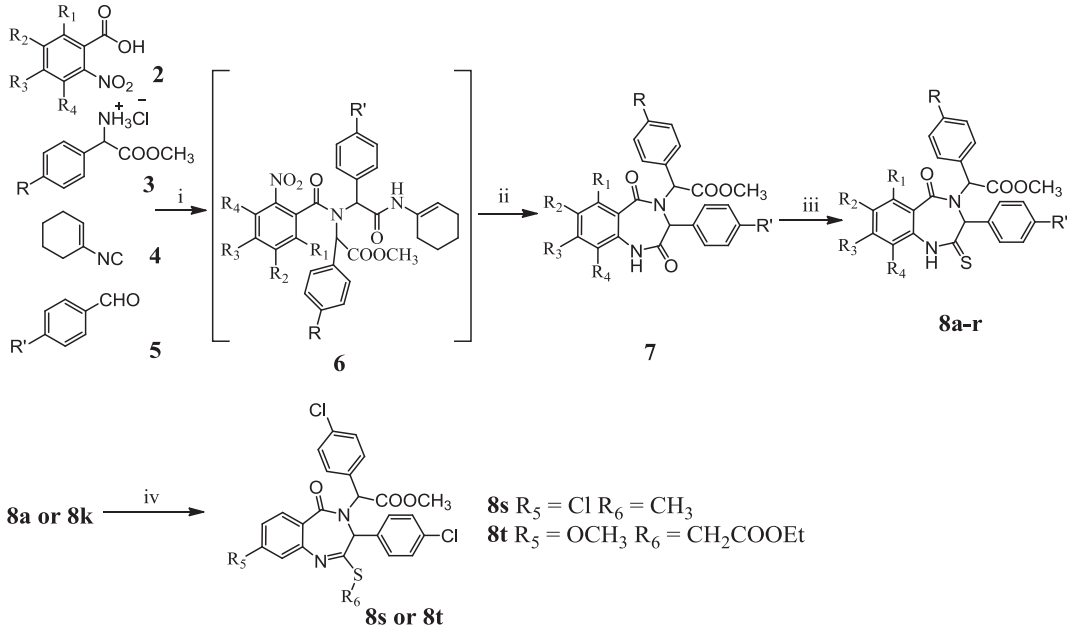


**Scheme 1.** Reagents and conditions: (i) MeOH, KOH, r.t., 24 h; (ii) Fe powder, AcOH, 70 °C, 1 h; (iii) Lawesson's reagent, toluene, 70 °C, 4 h (iv) MeI or $BrCH_2COOEt$, DBU, DCM, r.t., 0.5–1 h.

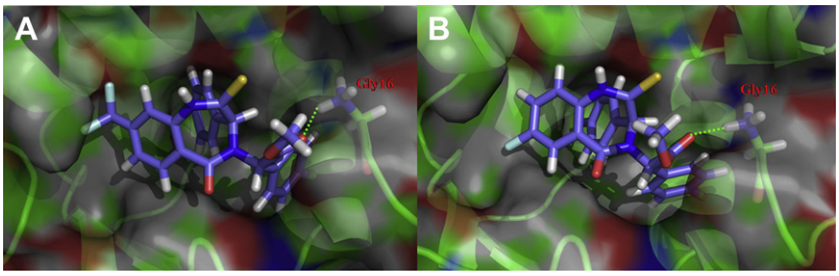


**Fig. 2.** The docking models of thio-benzodiazepines inhibitors with MDM2. The inhibitors are shown in stick models with carbon atoms light purple, nitrogen blue, oxygen red, fluorine light green and sulfur yellow. Hydrogen bonds are depicted as green dashed lines. The amino acid residues which were formatted H-bonds are labeled. (A) Compound **8i**; (B) Compound **8n**. The figures were prepared from PDB ID: 1T4E, using PyMol (http://pymol.souceforge.net/).

a hypothetical binding model for the thio-benzodiazepine-MDM2 complex (Fig. 2). The binding interactions involved three hydrophobic pockets that were filled by three aromatic rings of the thio-benzodiazepine. This binding model also predicted that the ester group was well positioned as hydrogen bond acceptor with Gly16, which may account for the enhancement of binding activity.

### 3.2. *In vitro* antitumor activity

All the compounds were further evaluated in MTT assays for ascertaining whether their *in vitro* antitumor activity showed good relevance with the inhibitory activity of p53–MDM2 binding. In order to demonstrate the rationality of this class of thio-benzodiazepines, they were compared with the most potent thio-compound **1** reported by our group [21]. The results (Table 1) revealed that most compounds showed moderate to excellent *in vitro* antitumor activity. With regard to the human osteosarcoma U-2 OS cell line (wild-type p53), many compounds, such as **8a**, **8c**, **8d**, **8e**, **8g**, **8i**, **8j** and **8n**, showed better biological activity than Nutlin-3a and **1**. For the lung cancer A549 cell line (wild-type p53), compounds **8d**, **8e**, **8j** and **8n** displayed higher *in vitro* anti-proliferative activity than Nutlin-3a. At the same time, eight compounds, namely **8a**, **8c**, **8e**, **8g**, **8i**, **8n**, **8p** and **8q**, also exhibited better antitumor activity than the most potent compound **1**. Meaningfully, most compounds revealed good selectivity against the U-2 OS cell line with wild type p53 and the Saos-2 cell line with p53 deficiency. Several compounds also had good inhibitory selectivity against the A549 cell line (wild type p53) and the NCI-H1299 cell line (p53 null). Importantly, based on the data in Table 1, we found that most compounds showed good *in vitro* antitumor activity, which were consistent with the results in the p53–MDM2 binding assays. Two promising compounds, **8i** and **8n** showed excellent p53–MDM2 binding affinity and excellent *in vitro* antitumor activity, which were promising candidates for further evaluation.

## 4. Conclusion

In conclusion, we designed and synthesized a series of novel thio-benzodiazepines by Ugi reaction with the purpose to explore its SAR. In the p53–MDM2 binding assay, most of targeted compounds have good binding affinity comparable to the reference drug. Moreover, many compounds displayed good activity in *in vitro* antitumor activity assay compared with Nutlin-3a. Interestingly, several compounds exhibited good correlation between the binding activity and *in vitro* antitumor activity. In particular,

two representative compounds, namely **8i** and **8n**, showed excellent biological activity in both p53–MDM2 binding affinity and *in vitro* antitumor activity. A better understanding of this SAR could provide meaningful insights for further optimization.

## 5. Experimental protocols

### 5.1. General methods

All reagents and solvents were purchased from commercial suppliers and used as received unless otherwise stated. Melting points were measured on an uncorrected X-5 digital melting point apparatus (Gongyi City Yuhua Instrument Co., Ltd.; China).$^1$H NMR and $^{13}$C NMR spectra were recorded on a BRUKER AVANCE 600 spectrometer (Bruker Company, Germany), using TMS as an internal standard and $CDCl_3$ or DMSO-$d_6$ as solvents. Chemical shifts ($\delta$ values) and coupling constants ($J$ values) are given in ppm and Hz, respectively. TLC analysis was carried out on silica gel plates GF254 (Qindao Haiyang Chemical, China). Flash column chromatography (Biotage, LCD 2073 A) was carried out on silica gel 300–400 mesh. Anhydrous solvent and reagents were all analytical pure and dried through routine protocols.

### 5.2. General procedure for the synthesis of benzodiazepines (**7**) [23]

Powdered substituted 2-nitrobenzoic acid (10 mmol) was added to a well stirred solution of KOH (10 mmol) in $CH_3OH$ (10 mL). The resulting suspension was stirred at room temperature for 10 min and then cooled to 0 °C and treated with methyl 2-amino-2-(4-chlorophenyl)acetate hydrochloride (10 mmol) or 2-amino-2-(4-fluorophenyl)acetate hydrochloride (10 mmol) (**3**), a solution of 1-isocyanocyclohexene (**4**) (11 mmol) in $CH_3OH$ (2 mL) and a solution of *p*-chlorobenzaldehyde or 4-fluorobenzaldehyde (**5**) (10 mmol) in $CH_3OH$ (2 mL), in the order given. The cooling bath was removed and the reaction mixture was stirred at room temperature for 1 day. Removal of the solvent under reduced pressure left a residue which was stirred with $H_2O$ (10 mL) and $CH_2Cl_2$ (80 mL). The organic layer was dried ($Na_2SO_4$) and evaporated to dryness. The residue was stirred with boiling hexanes (50 mL) for 5 min. The supernatant liquid was discarded while still warm. An analogous treatment was performed with boiling $H_2O$ (50 mL × 2). The resulting solid product was stirred with AcOH (60 mL). The resulting solution was heated at 50 °C and treated under vigorous stirring with iron powder (40 mmol) in one portion. When the exothermic reaction had subsided, the reaction mixture was heated at 70 °C for 1 h and then allowed to cool and stirred with $CH_2Cl_2$ (50 mL) and $H_2O$ (50 mL). The resulting suspension was filtered to remove the unreacted iron and the filtrate transferred to a separating funnel. The organic layer was washed with $H_2O$ (50 mL), $NaHCO_3$ (aq. 2%, 50 mL), $H_2O$ (50 mL) and then separated, dried ($Na_2SO_4$), and evaporated to dryness. The residue was purified by column chromatography (*n*-hexane–ethyl acetate, 5:1) to give **7a**–**r**, yield: 45–52%.

The $^1$H NMR data of the partly representative benzodiazepines.

#### 5.2.1. Methyl 2-(8-chloro-3-(4-chlorophenyl)-2,5-dioxo-2,3-dihydro-1H-benzo [e][1,4]diazepin-4(5H)-yl)-2-(4-chlorophenyl) acetate (**7a**)

$^1$H NMR (DMSO-$d_6$, 600 MHz): $\delta$ 10.89 (s, 1H, N–H), 7.52–7.47 (m, 5H, C–H), 7.23–7.06 (m, 5H, Ar–H), 6.92 (s, 1H, Ar–H), 6.29 (s, 1H, C–H), 5.33 (s, 1H, C–H), 3.76 (s, 3H, C–H). $^{13}$C NMR (150 MHz, $CDCl_3$) $\delta$: 171.35, 170.02, 166.94, 138.40, 135.76, 135.69, 133.87, 132.46, 131.38, 131.24, 129.66, 128.68, 125.77, 125.15, 124.90, 119.82, 62.62, 61.77, 52.91; HRMS (ESI): $m/z$ [M + H]$^+$ calcd for $C_{24}H_{17}Cl_3N_2O_4$: 503.0332; found: 503.0327.

#### 5.2.2. Methyl 2-(9-chloro-3-(4-chlorophenyl)-2,5-dioxo-2,3-dihydro-1H-benzo[e] [1,4]diazepin-4(5H)-yl)-2-(4-chlorophenyl) acetate (**7b**)

$^1$H NMR (DMSO-$d_6$, 500 MHz): $\delta$ 10.39 (s, 1H, N–H), 7.55–7.53 (d, 2H, $J$ = 8.55 Hz, Ar–H), 7.48–7.46 (d, 2H, $J$ = 8.55 Hz, Ar–H), 7.43–7.38 (m, 2H, Ar–H), 7.20–7.04 (m, 5H, Ar–H), 6.19 (s, 1H, C–H), 5.38 (s, 1H, C–H), 3.77 (s, 3H, C–H). $^{13}$C NMR (150 MHz, $CDCl_3$) $\delta$: 169.69, 169.46, 166.67, 135.78, 133.80, 132.45, 131.45, 131.32, 131.19, 131.17, 129.65, 129.61, 128.61, 128.49, 125.49, 125.23, 123.59, 62.80, 61.69, 52.91; HRMS (ESI): $m/z$ [M + H]$^+$ calcd for $C_{24}H_{17}Cl_3N_2O_4$: 503.0332; found: 503.0333.

#### 5.2.3. Methyl 2-(7-chloro-3-(4-chlorophenyl)-2,5-dioxo-2,3-dihydro-1H-benzo [e][1,4]diazepin-4(5H)-yl)-2-(4-chlorophenyl) acetate (**7c**)

$^1$H NMR (DMSO-$d_6$, 500 MHz): $\delta$ 10.91 (s, 1H, N–H), 7.51–7.35 (m, 6H, Ar–H), 7.24–7.22 (d, 2H, $J$ = 9.9 Hz, Ar–H), 7.10–7.09 (d, 2H, $J$ = 8.05 Hz, Ar–H), 6.88–6.86 (d, 2H, $J$ = 8.6 Hz, Ar–H), 6.28 (s, 1H, C–H), 5.33(s, 1H, C–H), 3.76 (s, 3H, C–H). $^{13}$C NMR (150 MHz, $CDCl_3$) $\delta$: 170.92, 169.87, 166.38, 135.76, 133.93, 133.16, 132.77, 131.30, 131.21, 130.59, 130.26, 129.62, 128.70, 127.62, 125.71, 121.41, 62.66, 61.94, 52.88; HRMS (ESI): $m/z$ [M + H]$^+$ calcd for $C_{24}H_{17}Cl_3N_2O_4$: 503.0332; found: 503.0336.

### 5.3. General procedure for the synthesis of thio-benzodiazepines (**8a**–**r**)

A dry toluene solution of **7a**–**r** (10 mmol) under an atmosphere of nitrogen was treated with Lawesson's reagent (2,4-bis(4-methoxyphenyl)-2,4-disulfide, 5.5 mmol) under 70 °C for 4 h, cooled to room temperature, concentrated under vacuum and purified by column chromatography(*n*-hexane–ethyl acetate, 10:1) to give compounds **8a**–**r**, yield: 50–80%.

#### 5.3.1. Methyl 2-(8-chloro-3-(4-chlorophenyl)-5-oxo-2-thioxo-2,3-dihydro-1H-benzo[e][1,4]diazepin-4(5H)-yl)-2-(4-chlorophenyl) acetate (**8a**)

According to the general procedure, compound **7a** (5 mmol), Lawesson's reagent (3 mmol) gave compound **8a** as a light-yellow solid (1.619 g, yield: 62%), m.p. 156–158 °C. $^1$H NMR (DMSO-$d_6$, 600 MHz): $\delta$ 12.79 (s, 1H, N–H), 7.56–7.46 (m, 5H, C–H), 7.26–7.22 (m, 4H, Ar–H), 7.16 (dd, 1H, $J$ = 10.1, 1.7 Hz, Ar–H), 7.07 (d, 1H, $J$ = 1.4 Hz, Ar–H), 6.21 (s, 1H, C–H), 5.85 (s, 1H, C–H), 3.74 (s, 3H, C–H). $^{13}$C NMR (150 MHz, DMSO-$d_6$) $\delta$: 200.03, 169.35, 165.45, 137.49, 136.75, 134.17, 133.52, 132.90, 132.70, 132.61, 132.37, 128.98, 128.95, 127.26, 126.64, 125.96, 120.10, 70.63, 66.03, 52.86; ESI-MS ($m/z$): 517.25 (M − H).

#### 5.3.2. Methyl 2-(9-chloro-3-(4-chlorophenyl)-5-oxo-2-thioxo-2,3-dihydro-1H-benzo[e][1,4]diazepin-4(5H)-yl)-2-(4-chlorophenyl) acetate (**8b**)

A light-yellow solid. Yield: 70%. M.p. 151–153 °C. $^1$H NMR (DMSO-$d_6$, 600 MHz): $\delta$ 12.17 (s, 1H, N–H), 7.59 (d, 2H, $J$ = 8.55 Hz, Ar–H), 7.47–7.42 (m, 4H, Ar–H), 7.23–7.12 (m, 5H, Ar–H), 6.16 (s, 1H, C–H), 5.92 (s, 1H, C–H), 3.77 (s, 3H, C–H). $^{13}$C NMR (150 MHz, DMSO-$d_6$) $\delta$: 204.20, 173.19, 169.29, 138.06, 137.55, 137.34, 137.19, 136.97, 136.80, 136.50, 135.67, 132.94, 132.82, 132.77, 131.86, 130.66, 129.48, 75.48, 70.41, 56.85; ESI-MS ($m/z$): 517.26 (M − H).

#### 5.3.3. Methyl 2-(7-chloro-3-(4-chlorophenyl)-5-oxo-2-thioxo-2,3-dihydro-1H-benzo[e][1,4]diazepin-4(5H)-yl)-2-(4-chlorophenyl) acetate (**8c**)

A yellow solid. Yield: 59%. M.p. 260–262 °C. $^1$H NMR (DMSO-$d_6$, 600 MHz): $\delta$ 12.84 (s, 1H, N–H), 7.55 (d, 2H, $J$ = 8.55 Hz, Ar–H), 7.48–7.45 (m, 3H, Ar–H), 7.42 (dd, 1H, $J$ = 8.7, 2.6 Hz, Ar–H),

7.26–7.22 (m, 4H, Ar–H), 7.02 (d, 1H, $J$ = 8.7 Hz, Ar–H), 6.22 (s, 1H, C–H), 5.87 (s, 1H, C–H), 3.76 (s, 3H, C–H). $^{13}$C NMR (150 MHz, $CDCl_3$) $\delta$: 199.93, 169.21, 165.67, 135.92, 133.92, 133.82, 132.68, 131.84, 131.59, 130.91, 130.44, 129.50, 128.88, 128.72, 126.21, 120.59, 67.13, 64.27, 52.77; ESI-MS ($m/z$): 517.36 (M − H).

*5.3.4. Methyl 2-(4-chlorophenyl)-2-(3-(4-chlorophenyl)-8-fluoro-5-oxo-2- thioxo-2,3-dihydro-1H-benzo[e][1,4]diazepin-4(5H)-yl) acetate (**8d**)*

A light-yellow solid. Yield: 58%. M.p. 140–142 °C. $^1$H NMR (DMSO-$d_6$, 600 MHz): $\delta$ 12.79 (s, 1H, NH), 7.57–7.55 (m, 3H, Ar–H), 7.46 (d, 2H, $J$ = 8.52 Hz, Ar–H), 7.23 (s, 4H, Ar–H), 6.98–6.95 (m, 1H, Ar–H), 6.82 (dd, 1H, $J$ = 9.9, 2.4 Hz, Ar–H), 6.21 (s, 1H, CH), 5.85 (s, 1H, CH), 3.74 (s, 3H, $CH_3$). $^{13}$C NMR (150 MHz, $CDCl_3$) $\delta$: 200.48, 169.51, 166.40, 165.04, 163.35, 137.20, 137.13, 135.93, 133.89, 133.82, 133.78, 131.99, 131.88, 130.40, 129.53, 128.64, 126.23, 124.14, 124.12, 113.75, 113.60, 106.43, 106.26, 67.15, 64.30, 52.79; ESI-MS ($m/z$): 501.35 (M − H).

*5.3.5. Methyl 2-(4-chlorophenyl)-2-(3-(4-chlorophenyl)-7,8-difluoro-5-oxo-2- thioxo-2,3-dihydro-1H-benzo[e][1,4]diazepin-4(5H)-yl) acetate (**8e**)*

A yellow solid. Yield: 69%. M.p. 94–95 °C. $^1$H NMR (DMSO-$d_6$, 600 MHz): $\delta$ 12.77 (s, 1H, NH), 7.52 (d, 2H, $J$ = 8.52 Hz, Ar–H), 7.48 (dd, 1H, $J$ = 8.58, 10.62 Hz, Ar–H), 7.44 (d, 2H, $J$ = 8.64 Hz, Ar–H), 7.25 (d, 2H, $J$ = 8.82 Hz, Ar–H), 7.21 (d, 2H, $J$ = 7.98 Hz, Ar–H), 7.04 (dd, 1H, $J$ = 11.2, 7.00 Hz, Ar–H), 6.20 (s, 1H, CH), 5.86 (s, 1H, CH), 3.73 (s, 3H, $CH_3$). $^{13}$C NMR (150 MHz, $CDCl_3$) $\delta$: 200.05, 169.42, 165.29, 164.28, 164.26, 164.14, 136.06, 134.53, 134.42, 134.07, 134.02, 133.96, 131.87, 131.80, 130.14, 129.58, 128.84, 126.13, 67.08, 64.43, 52.89; ESI-MS ($m/z$): 519.53 (M − H).

*5.3.6. Methyl 2-(8-chloro-3-(4-fluorophenyl)-5-oxo-2-thioxo-2,3-dihydro-1H-benzo[e][1,4]diazepin-4(5H)-yl)-2-(4-fluorophenyl) acetate (**8f**)*

A yellow solid. Yield: 70%. M.p. 143–144 °C. $^1$H NMR (DMSO-$d_6$, 600 MHz): $\delta$ 12.75 (s, 1H, NH), 7.59 (d, 1H, $J$ = 5.52 Hz, Ar–H), 7.58 (d, 1H, $J$ = 5.46 Hz, Ar–H), 7.47 (d, 1H, $J$ = 8.58 Hz, Ar–H), 7.24–7.19 (m, 4H, Ar–H), 7.13 (dd, 1H, $J$ = 2.10, 8.52 Hz, Ar–H), 7.06 (d, 1H, $J$ = 1.98 Hz, Ar–H), 6.98 (t, 2H, $J$ = 8.82 Hz, Ar–H), 6.23 (s, 1H, CH), 5.78 (s, 1H, CH), 3.29 (s, 3H, $CH_3$); $^{13}$C NMR (150 MHz, DMSO-$d_6$) $\delta$: 200.43, 169.64, 165.49, (163.71, 162.60), (161.75, 160.66), 137.52, 136.63, 132.91, 132.84, 130.64, 130.03, 127.50, 126.77, 125.83, 120.02, 116.01, 115.89, 70.01, 65.72, 52.80; ESI-MS ($m/z$): 487.43 (M + H).

*5.3.7. Methyl 2-(7-chloro-3-(4-chlorophenyl)-5-oxo-2-thioxo-2,3-dihydro-1H-benzo[e][1,4]diazepin-4(5H)-yl)-2-(4-fluorophenyl) acetate (**8g**)*

A light-yellow solid. Yield: 73%. M.p. 120–123 °C. $^1$H NMR (DMSO-$d_6$, 600 MHz): $\delta$ 12.70 (s, 1H, NH), 7.53 (d, 1H, $J$ = 5.52 Hz, Ar–H), 7.52 (d, 1H, $J$ = 5.28 Hz, Ar–H), 7.49 (d, 1H, $J$ = 2.52 Hz, Ar–H), 7.38 (dd, 1H, $J$ = 2.58, 8.70 Hz, Ar–H), 7.25–7.17 (m, 6H, Ar–H), 6.97 (d, 1H, $J$ = 8.7 Hz, Ar–H), 6.16 (s, 1H, CH), 5.76 (s, 1H, CH), 3.71 (s, 3H, $CH_3$). $^{13}$C NMR (150 MHz, $CDCl_3$) $\delta$: 199.70, 169.59, 165.92, 164.13, 162.47, 139.19, 134.17, 133.84, 132.61, 132.55, 132.50, 131.97, 131.45, 130.73, 129.84, 128.80, 128.69, 126.23, 124.45, 123.95, 120.98, 67.10, 64.33, 52.78; ESI-MS ($m/z$): 503.64 (M + H).

*5.3.8. Methyl 2-(4-chlorophenyl)-2-(3-(4-chlorophenyl)-9-methoxy-5-oxo-2-thioxo-2,3-dihydro-1H-benzo[e][1,4]diazepin-4(5H)-yl)acetate (**8h**)*

A light-yellow solid. Yield: 62%. M.p. 123–125 °C. $^1$H NMR (DMSO-$d_6$, 600 MHz): $\delta$ 11.70 (s, 1H, NH), 7.59 (d, 2H, $J$ = 5.52 Hz, Ar–H), 7.42 (d, 2H, $J$ = 8.58 Hz, Ar–H), 7.17 (s, 4H, Ar–H), 7.06–7.01 (m, 2H, Ar–H), 6.98 (dd, 1H, $J$ = 1.50, 7.92 Hz, Ar–H), 6.12 (s, 1H, CH), 5.86 (s, 1H, CH), 3.73 (s, 6H, $CH_3$). $^{13}$C NMR (150 MHz, DMSO-$d_6$) $\delta$: 198.88, 169.33, 165.91, 149.60, 133.96, 133.86, 133.37, 132.45, 132.39, 129.63, 128.79, 128.66, 127.26, 126.81, 126.27, 121.33, 114.93, 71.42, 66.33, 57.09, 52.78; ESI-MS ($m/z$): 515.52 (M + H).

*5.3.9. Methyl 2-(4-chlorophenyl)-2-(3-(4-chlorophenyl)-5-oxo-2-thioxo-8-(trifluoromethyl)-2,3-dihydro-1H-benzo[e][1,4]diazepin-4(5H)-yl)acetate (**8i**)*

A light-yellow solid. Yield: 53%. M.p. 151–152 °C. $^1$H NMR (DMSO-$d_6$, 600 MHz): $\delta$ 12.89 (s, 1H, N–H), 7.68 (d, 1H, $J$ = 8.15 Hz, Ar–H), 7.56 (d, 2H, $J$ = 8.5 Hz, Ar–H), 7.48–7.43 (m, 3H, Ar–H), 7.36 (s, 1H, Ar–H), 7.26–7.21 (m, 4H, Ar–H), 6.24 (s, 1H, C–H), 5.90 (s, 1H, C–H), 3.76 (s, 3H, C–H). $^{13}$C NMR (150 MHz, DMSO-$d_6$) $\delta$: 200.19, 169.26, 165.23, 136.84, 134.21, 133.31, 132.76, 132.73, 132.26, 132.20, 131.08, 130.54, 129.70, 129.00, 128.92, 127.28, 126.61, 124.25, 122.44, 122.14, 117.60, 70.58, 66.08, 52.92; ESI-MS ($m/z$): 553.24 (M + H).

*5.3.10. Methyl 2-(3-(4-chlorophenyl)-5-oxo-2-thioxo-8-(trifluoromethyl)-2,3-dihydro-1H-benzo[e][1,4]diazepin-4(5H)-yl)-2-(4-fluorophenyl)acetate (**8j**)*

A light-yellow solid. Yield: 59%. M.p. 132–135 °C. $^1$H NMR (DMSO-$d_6$, 600 MHz): $\delta$ 12.89 (s, 1H, N–H), 7.68 (d, 1H, $J$ = 8.25 Hz, Ar–H), 7.62–7.60 (m, 2H, Ar–H), 7.44 (d, 1H, $J$ = 7.45 Hz, Ar–H), 7.36 (s, 1H, Ar–H), 7.26–7.21 (m, 6H, Ar–H), 6.27 (s, 1H, C–H), 5.84 (s, 1H, C–H), 3.75 (s, 3H, C–H). $^{13}$C NMR (150 MHz, $CDCl_3$) $\delta$: 200.50, 169.69, 166.14, 164.20, 162.54, 135.76, 134.23, 134.00, 133.95, 132.56, 132.51, 132.25, 131.91, 130.28, 128.73, 127.46, 126.22, 122.16, 116.56, 116.42, 66.91, 64.40, 52.82; ESI-MS ($m/z$): 537.13 (M + H).

*5.3.11. Methyl 2-(4-chlorophenyl)-2-(3-(4-chlorophenyl)-8-methoxy-5-oxo-2-thioxo- 2,3-dihydro-1H-benzo[e][1,4]diazepin-4(5H)-yl)acetate (**8k**)*

A light-yellow solid. Yield: 56%. M.p. 135–136 °C. $^1$H NMR (DMSO-$d_6$, 600 MHz): $\delta$ 12.64 (s, 1H, N–H), 7.54 (d, 2H, $J$ = 8.40 Hz, Ar–H), 7.54–7.45 (m, 3H, Ar–H), 7.23 (s, 4H, Ar–H), 6.69 (dd, 1H, $J$ = 2.00, 6.65 Hz, Ar–H), 6.54 (d, 1H, $J$ = 1.6 Hz, Ar–H), 6.18 (s, 1H, C–H), 5.82 (s, 1H, C–H), 3.73 (s, 3H, C–H), 3.69 (s, 3H, C–H); $^{13}$C NMR (150 MHz, DMSO-$d_6$) $\delta$: 199.57, 169.57, 166.00, 162.11, 138.05, 134.03, 133.93, 133.24, 132.75, 132.47, 132.33, 128.91, 128.78, 127.20, 120.48, 112.23, 105.25, 70.75, 65.92, 55.94, 52.74; ESI-MS ($m/z$): 513 (M − H).

*5.3.12. Methyl 2-(4-chlorophenyl)-2-(3-(4-chlorophenyl)-9-methyl-5-oxo-2-thioxo-2,3-dihydro-1H-benzo[e][1,4]diazepin-4(5H)-yl)acetate (**8l**)*

A light-yellow solid. Yield: 50%. M.p. 240–241 °C. $^1$H NMR (DMSO-$d_6$, 600 MHz): $\delta$ 11.97 (s, 1H, C–H), 7.58 (d, 2H, $J$ = 8.5 Hz, Ar–H), 7.44 (d, 2H, $J$ = 8.55 Hz, Ar–H), 7.30 (d, 1H, $J$ = 7.65 Hz, Ar–H), 7.21–7.12 (m, 5H, Ar–H), 7.01 (t, 1H, $J$ = 7.7 Hz, Ar–H), 6.12 (s, 1H, C–H), 5.88 (s, 1H, C–H), 3.76 (s, 3H, C–H), 2.18 (s, 3H, C–H); $^{13}$C NMR (150 MHz, DMSO-$d_6$) $\delta$: 199.92, 169.38, 166.52, 135.09, 133.93, 133.83, 133.47, 132.50, 132.28, 130.11, 128.77, 128.65, 127.86, 126.71, 126.64, 71.51, 66.42, 52.81, 17.94; ESI-MS ($m/z$): 499.28 (M + H).

*5.3.13. Methyl 2-(4-chlorophenyl)-2-(3-(4-chlorophenyl)-7-methyl-5-oxo-2-thioxo-2,3-dihydro-1H-benzo[e][1,4]diazepin-4(5H)-yl)acetate (**8m**)*

A light-yellow solid. Yield: 71%. M.p. 220–222 °C. $^1$H NMR (DMSO-$d_6$, 600 MHz): $\delta$ 12.67 (s, 1H, N–H), 7.54 (d, 2H, $J$ = 8.5 Hz, Ar–H), 7.45 (d, 2H, $J$ = 8.55 Hz, Ar–H), 7.32 (d, 1H, $J$ = 1.25 Hz, Ar–H), 7.24–7.20 (m, 4H, Ar–H), 7.14 (dd, 1H, $J$ = 1.55, 8.35 Hz, Ar–H), 6.88 (d, 1H, $J$ = 8.3 Hz, Ar–H), 6.17 (s, 1H, C–H), 5.87 (s, 1H, C–H), 3.74 (s, 3H, C–H), 2.16 (s, 3H, C–H); $^{13}$C NMR (150 MHz,

DMSO-$d_6$) $\delta$: 198.84, 169.41, 166.23, 135.38, 134.39, 133.96, 133.81, 133.57, 133.31, 132.46, 132.31, 130.44, 128.85, 128.78, 127.48, 127.21, 120.81, 71.10, 66.20, 52.78, 20.59; ESI-MS ($m/z$): 499.54 (M + H).

#### 5.3.14. Methyl 2-(4-chlorophenyl)-2-(3-(4-chlorophenyl)-7-fluoro-5-oxo-2-thioxo-2,3-dihydro-1H-benzo[e][1,4]diazepin-4(5H)-yl) acetate(**8n**)

A light-yellow solid. Yield: 66%. M.p. 146–148 °C. $^1$H NMR (DMSO-$d_6$, 600 MHz): $\delta$ 12.76 (s, 1H, N–H), 7.55 (d, 2H, $J$ = 8.55 Hz, Ar–H), 7.45 (d, 2H, $J$ = 8.55 Hz, Ar–H), 7.24–7.20 (m, 6H, Ar–H), 7.06–7.02 (m, 1H, Ar–H), 6.20 (s, 1H, C–H), 5.85 (s, 1H, C–H), 3.74 (s, 3H, C–H); $^{13}$C NMR (150 MHz, DMSO-$d_6$) $\delta$: 199.19, 169.31, 165.07, (159.83, 158.21), 134.18, 133.54, 133.35, 132.89, 132.66, 132.40, (129.65, 129.60), 128.98, 128.93, 127.24, (123.52, 123.46), (120.40, 120.25), (116.28, 116.11), 70.76, 66.12, 52.90; ESI-MS ($m/z$): 503.28 (M + H).

#### 5.3.15. Methyl 2-(3-(4-chlorophenyl)-8-fluoro-5-oxo-2-thioxo-2,3-dihydro-1H-benzo[e][1,4]diazepin-4(5H)-yl)-2-(4-fluorophenyl) acetate (**8o**)

A light-yellow solid. Yield: 80%. M.p. 106–107 °C. $^1$H NMR (DMSO-$d_6$, 600 MHz): $\delta$ 12.79 (s, 1H, N–H), 7.56 (d, 2H, $J$ = 8.5 Hz, Ar–H), 7.46 (d, 2H, $J$ = 8.5 Hz, Ar–H), 7.26–7.23 (m, 6H, Ar–H), 7.06–7.04 (m, 1H, Ar–H), 6.22 (s, 1H, C–H), 5.87 (s, 1H, C–H), 3.75 (s, 3H, C–H); $^{13}$C NMR (150 MHz, DMSO-$d_6$) $\delta$: 199.18, 169.28, 165.04, (159.98, 158.04), 134.15, 133.52, 133.33, 132.89, 132.63, 132.38, (129.65, 129.59), 128.96, 128.90, 127.22, (123.51, 123.45), (120.39, 120.20), (116.27, 116.08), 70.77, 66.11, 52.87; ESI-MS ($m/z$): 487.69 (M + H).

#### 5.3.16. Methyl 2-(8-bromo-3-(4-chlorophenyl)-5-oxo-2-thioxo-2,3-dihydro-1H-benzo[e][1,4]diazepin-4(5H)-yl)-2-(4-chlorophenyl) acetate (**8p**)

A yellow solid. Yield: 73%. M.p. 139–141 °C. $^1$H NMR (DMSO-$d_6$, 600 MHz): $\delta$ 12.76 (s, 1H, N–H), 7.55 (d, 2H, $J$ = 8.58 Hz, Ar–H), 7.46 (d, 2H, $J$ = 8.58 Hz, Ar–H), 7.42 (d, 1H, $J$ = 8.46 Hz, Ar–H), 7.29 (dd, 1H, $J$ = 1.86, 8.46 Hz, Ar–H), 7.26–7.24 (m, 4H, Ar–H), 7.21 (d, 1H, $J$ = 1.86 Hz, Ar–H), 6.21 (s, 1H, C–H), 5.75 (s, 1H, C–H), 3.74 (s, 3H, C–H); $^{13}$C NMR (150 MHz, DMSO-$d_6$) $\delta$: 200.00, 169.35, 165.57, 137.47, 134.17, 133.51, 132.89, 132.71, 132.60, 132.36, 128.97, 128.83, 127.26, 126.93, 125.47, 122.98, 70.63, 66.03, 52.86; ESI-MS ($m/z$): 560.89 (M − H).

#### 5.3.17. Methyl 2-(8-chloro-5-oxo-2-thioxo-3-(4-(trifluoromethyl) phenyl)-2,3-dihydro-1H-benzo[e][1,4]diazepin-4(5H)-yl)-2-(4-chlorophenyl)acetate (**8q**)

A light-yellow solid. Yield: 68%. M.p. 160–162 °C. $^1$H NMR (DMSO-$d_6$, 600 MHz): $\delta$ 12.83 (s, 1H, N–H), 7.56 (d, 4H, $J$ = 8.52 Hz, Ar–H), 7.50 (d, 1H, $J$ = 8.58 Hz, Ar–H), 7.46 (d, 4H, $J$ = 8.52 Hz, Ar–H), 7.14 (dd, 1H, $J$ = 2.04, 7.38 Hz, Ar–H), 7.06 (d, 1H, $J$ = 2.04 Hz, Ar–H), 6.23 (s, 1H, C–H), 5.97 (s, 1H, C–H), 3.76 (s, 3H, C–H). $^{13}$C NMR (150 MHz, $CDCl_3$) $\delta$: 199.84, 169.54, 166.46, 138.47, 137.58, 136.38, 136.09, 132.65, 131.91, 130.26, 130.14, 130.04, 129.63, 126.33, 125.91, 125.51, 125.48, 125.29, 124.37, 122.57, 119.37, 67.25, 64.45, 52.89; ESI-MS ($m/z$): 551.37 (M − H).

#### 5.3.18. Methyl 2-(8-chloro-3-(4-methoxyphenyl)-5-oxo-2-thioxo-2,3-dihydro-1H-benzo[e][1,4]diazepin-4(5H)-yl)-2-(4-chlorophenyl)acetate (**8r**)

A yellow solid. Yield: 75%. M.p. 137–138 °C. $^1$H NMR (DMSO-$d_6$, 600 MHz): $\delta$ 12.72 (s, 1H, N–H), 7.57–7.47 (m, 5H, Ar–H), 7.15–7.08 (m, 4H, Ar–H), 6.70 (d, 2H, $J$ = 8.8 Hz, Ar–H), 6.23 (s, 1H, C–H), 5.78 (s, 1H, C–H), 3.74 (s, 3H, C–H), 3.61 (s, 3H, C–H); $^{13}$C NMR (150 MHz, DMSO-$d_6$) $\delta$: 201.03, 169.45, 165.60, 158.85, 137.54, 136.52, 134.12, 132.97, 132.56, 132.41, 128.95, 126.74, 126.61, 125.99, 125.69, 119.93, 114.26, 70.54, 65.87, 55.42, 52.77; ESI-MS ($m/z$): 515.83 (M + H).

### 5.4. General procedure for the synthesis of **8s** and **8t**

To a dry $CH_2Cl_2$ solution of **8a** or **8k** (5 mmol) was added MeI (5 mmol) or ethyl bromoacetate (5 mmol), then DBU (5 mmol) was added to the resulting solution and stirred at room temperature for 30–60 min. After that, the reaction mixture was concentrated under vacuum and purified by column chromatography ($n$-hexane–ethyl acetate, 10:1) to give **8s** or **8t**, yield: 90–95%.

#### 5.4.1. Methyl 2-(8-chloro-3-(4-chlorophenyl)-2-(methylthio)-5-oxo-3H-benzo[e] [1,4]diazepin-4(5H)-yl)-2-(4-chlorophenyl)acetate (**8s**)

A light-yellow solid. Yield: 95%. M.p. 185–187 °C. $^1$H NMR (DMSO-$d_6$, 600 MHz): $\delta$ 7.53 (d, 1H, $J$ = 8.46 Hz, Ar–H), 7.49 (d, 2H, $J$ = 8.58 Hz, Ar–H), 7.46 (d, 2H, $J$ = 8.76 Hz, Ar–H), 7.21 (d, 2H, $J$ = 8.58 Hz, Ar–H), 7.17 (d, 2H, $J$ = 8.46 Hz, Ar–H), 7.11 (dd, 1H, $J$ = 2.16, 8.58 Hz, Ar–H), 7.03 (d, 1H, $J$ = 2.10 Hz, Ar–H), 6.02 (s, 1H, CH), 5.44 (s, 1H, CH), 3.75 (s, 3H, $CH_3$), 2.52 (s, 3H, $CH_3$). $^{13}$C NMR (150 MHz, $CDCl_3$) $\delta$: 170.10, 169.58, 167.38, 145.98, 137.63, 135.83, 133.48, 132.97, 131.57, 131.50, 130.74, 129.52, 128.34, 126.25, 125.71, 125.33, 125.29, 64.31, 60.60, 52.76, 14.38; ESI-MS ($m/z$): 533.52 (M + H).

#### 5.4.2. Methyl 2-(4-chlorophenyl)-2-(3-(4-chlorophenyl)-2-((2-ethoxy-2-oxoethyl) thio)-8-methoxy-5-oxo-3H-benzo[e][1,4] diazepin-4(5H)-yl)acetate (**8t**)

A light-yellow solid. Yield: 90%. M.p. 130–131 °C. $^1$H NMR (DMSO-$d_6$, 600 MHz): $\delta$ 7.49–7.44 (m, 5H, Ar–H), 7.25–7.19 (m, 4H, Ar–H), 6.66 (dd, 1H, $J$ = 2.45, 8.85 Hz, Ar–H), 6.28 (d, 1H, $J$ = 2.4 Hz, Ar–H), 5.98 (s, 1H, C–H), 5.49 (s, 1H, C–H), 4.20–4.16 (m, 2H, C–H), 4.01 (s, 2H, C–H), 3.75 (s, 3H, C–H), 3.69 (s, 3H, C–H), 1.21 (t, 3H, $J$ = 7.1 Hz, C–H). $^{13}$C NMR (150 MHz, $CDCl_3$) $\delta$: 170.36, 167.96, 167.82, 167.29, 162.16, 145.86, 135.72, 133.19, 133.07, 132.15, 131.92, 131.16, 129.54, 127.93, 127.21, 119.95, 112.53, 109.40, 62.09, 61.71, 60.01, 55.23, 52.54, 33.37, 14.21; ESI-MS ($m/z$): 601.59 (M + H).

### 5.5. Computational protocol

Molecular docking was used to predict the binding mode of the synthesized thio-benzodiazepine derivatives. The crystal structure [7] of MDM2 (PDB code: 1T4E) was prepared by removing the benzodiazepine and adding hydrogen atoms in MVD 4.3.0. We used two known potent inhibitors of the p53–MDM2 interaction with different chemical structures (TDP222669 and nutlin-3a) as positive controls. The docking parameters of MVD were similar to the literatures [24]. The active site was defined to encompass all MDM2 atoms within a 12 Å radius sphere from the center of the Trp23 of the p53 peptide ligand. Other parameters were set by default.

### 5.6. p53–MDM2 binding assay

The dose-dependent binding experiments were carried out with serial dilution in DMSO of compounds. A 5 μL sample of the tested sample and preincubated (for 30 min) MDM2 binding domain (1–118) (10 nM) and PMDM-F peptide (Anaspec) (10 nM) in the assay buffer (100 mM potassium phosphate, pH 7.5; 100 μg/mL bovine gamma globulin; 0.02% sodium azide was added into black 96-well microplates with F-bottom and chimney wells (Corning) to produce a final volume of 115 μl. For each assay, the controls included the MDM2 binding domain and PMDM-F. The polarization values were measured after 1 h of incubation at room temperature using Biotek Synergy H2 with a 485 nm excitation filter, a 528 nm static and

polarized filter. The $K_i$ values were determined from a plot using nonlinear least-squares analysis. And curve fitting was performed using GraphPad Prism software. Nutlin-3a (Sigma–Aldrich), the first potent and specific non-peptide small-molecule MDM2 inhibitor was used as reference compound for validating the assay in each plate.

### 5.7. In vitro antitumor activity

The cellular growth inhibitory activity was determined using two human osteosarcoma cell lines [U-2 OS (wild type p53), Saos-2 (p53 null)]. $5–6 \times 10^4$ cells per well were plated in 96-well plates. After culturing for 24 h, test compounds were added onto triplicate wells with different concentrations and 0.1% DMSO for control. After 72 h of incubation, 20 μL of MTT (3-[4,5-dimethylthiazol-2-yl]-2,5-di phenyltetrazoliumbromide) solution (5 mg/mL) was added to each well, and after the samples were shaken for 1 min the plate was incubated further for 4 h at 37 °C. Thio-benzodiazepines were dissolved with 100 μL of DMSO. The absorbance (OD) was quantitated with microplate using Biotek Synergy H2 at 570 nm. Wells containing no drugs were used as blanks. Concentration of the compounds that inhibited cell growth by 50% ($IC_{50}$) was calculated.

## Acknowledgments

This research was supported in part by the Key Project of Science and Technology of Shanghai (No. 09431901700), Major Special Project for the Creation of New Drugs (Grant No. 2009ZX09301-011), the 863 Hi-Tech Program of China (No. 2012AA020302), Shanghai Rising-Star Program (No. 12QH1402600), Shanghai Municipal Health Bureau (No. XYQ2011038).

## References

[1] A.J. Levine, Cell 88 (1997) 323–331.
[2] B. Vogelstein, D. Lane, A.J. Levine, Nature 408 (2000) 307–310.
[3] L.T. Vassilev, B.T. Vu, B. Graves, D. Carvajal, F. Podlaski, Z. Filipovic, N. Kong, U. Kammlott, C. Lukacs, C. Klein, N. Fotouhi, E.A. Liu, Science 303 (2004) 844–848.
[4] P. Hainaut, M. Hollstein, Adv. Cancer Res. 77 (2000) 81–137.
[5] M.S. Greenblatt, W.P. Bennett, M. Hollstein, C.C. Harris, Cancer Res. 54 (1994) 4855–4878.
[6] D.P. Lane, P.A. Hall, Trends Biochem. Sci. 22 (1997) 372–374.
[7] B.L. Grasberger, T. Lu, C. Schubert, D.J. Parks, T.E. Carver, H.K. Koblish, M.D. Cummings, L.V. LaFrance, K.L. Milkiewicz, R.R. Calvo, D. Maguire, J. Lattanze, C.F. Franks, S. Zhao, K. Ramachandren, G.R. Bylebyl, M. Zhang, C.L. Manthey, E.C. Petrella, M.W. Pantoliano, I.C. Deckman, J.C. Spurlino, A.C. Maroney, B.E. Tomczuk, C.J. Molloy, R.F. Bone, J. Med. Chem. 48 (2005) 909–912.
[8] K. Ding, Y. Lu, Z. Nikolovska-Coleska, S. Qiu, Y. Ding, W. Gao, J. Stuckey, K. Krajewski, P.P. Roller, Y. Tomita, D.A. Parrish, J.R. Deschamps, S. Wang, J. Am. Chem. Soc. 127 (2005) 10130–10131.
[9] Y. Lu, Z. Nikolovska-Coleska, X. Fang, W. Gao, S. Shangary, S. Qiu, D. Qin, S. Wang, J. Med. Chem. 49 (2006) 3759–3762.
[10] P.S. Galatin, D.J. Abraham, J. Med. Chem. 47 (2004) 4163–4165.
[11] S.J. Duncan, S. Gruschow, D.H. Williams, C. McNicholas, R. Purewal, M. Hajek, M. Gerlitz, S. Martin, S.K. Wrigley, M. Moore, J. Am. Chem. Soc. 123 (2001) 554–560.
[12] A.G. Cochran, Curr. Opin. Chem. Biol. 5 (2001) 654–659.
[13] R. Stoll, C. Renner, S. Hansen, S. Palme, C. Klein, A. Belling, W. Zeslawski, M. Kamionka, T. Rehm, P. Muhlhahn, R. Schumacher, F. Hesse, B. Kaluza, W. Voelter, R.A. Engh, T.A. Holak, Biochemistry 40 (2001) 336–344.
[14] H. Yin, G.I. Lee, H.S. Park, G.A. Payne, J.M. Rodriguez, S.M. Sebti, A.D. Hamilton, Angew. Chem., Int. Ed. Engl. 44 (2005) 2704–2707.
[15] R.W.A. Luke, P.J. Jewsbury, R. Cotton, EP 1,112,284 B1, 2001.
[16] M. Millard, D. Pathania, F. Grande, S. Xu, N. Neamati, Curr. Pharm. Des. 17 (2011) 536–559.
[17] http://clinicaltrials.gov/ct2/show/NCT01462175?term=RO5503781&rank=1.
[18] W. Wang, Y. Hu, Med. Res. Rev. (2011). http://dx.doi.org/10.1002/med.20236.
[19] A.S. Azmi, P.A. Philip, A. Aboukameel, Z. Wang, S. Banerjee, S.F. Zafar, A.S. Goustin, K. Almhanna, D. Yang, F.H. Sarkar, R.M. Mohammad, Curr. Cancer Drug Targets 10 (2010) 319–331.
[20] M.E. Welsch, S.A. Snyder, B.R. Stockwell, Curr. Opin. Chem. Biol. 14 (2010) 347–361.
[21] C. Zhuang, Z. Miao, L. Zhu, Y. Zhang, Z. Guo, J. Yao, G. Dong, S. Wang, Y. Liu, H. Chen, C. Sheng, W. Zhang, Eur. J. Med. Chem. 46 (2011) 5654–5661.
[22] G. Gokel, G. Ludke, I. Ugi, Isonitrile Chemistry, Academic, New York, 1971, 145–199.
[23] C. Faggi, S. Marcaccini, R. Pepino, M.C. Pozo, Synthesis (2002) 2756–2760.
[24] H.K. Koblish, S. Zhao, C.F. Franks, R.R. Donatelli, R.M. Tominovich, L.V. LaFrance, K.A. Leonard, J.M. Gushue, D.J. Parks, R.R. Calvo, K.L. Milkiewicz, J.J. Marugan, P. Raboisson, M.D. Cummings, B.L. Grasberger, D.L. Johnson, T. Lu, C.J. Molloy, A.C. Maroney, Mol. Cancer Ther. 5 (2006) 160–169.

# Accepted Manuscript


2,4-Disubstituted Quinazolines as amyloid-β aggregation inhibitors with dual cholinesterase inhibition and antioxidant properties: Development and structure-activity relationship (SAR) studies

Tarek Mohamed, Praveen P.N. Rao

PII: S0223-5234(16)31011-X

DOI: 10.1016/j.ejmech.2016.12.005

Reference: EJMECH 9096

To appear in: *European Journal of Medicinal Chemistry*

Received Date: 22 September 2016

Revised Date: 30 November 2016

Accepted Date: 2 December 2016

Please cite this article as: T. Mohamed, P.P.N. Rao, 2,4-Disubstituted Quinazolines as amyloid-β aggregation inhibitors with dual cholinesterase inhibition and antioxidant properties: Development and structure-activity relationship (SAR) studies, *European Journal of Medicinal Chemistry* (2017), doi: 10.1016/j.ejmech.2016.12.005.

# 2,4-Disubstituted Quinazolines as Amyloid-*β* Aggregation Inhibitors with Dual Cholinesterase Inhibition and Antioxidant Properties: Development and Structure-Activity Relationship (SAR) Studies

Tarek Mohamed [a, b] and Praveen P. N. Rao [a,*]

**Graphical Abstract**

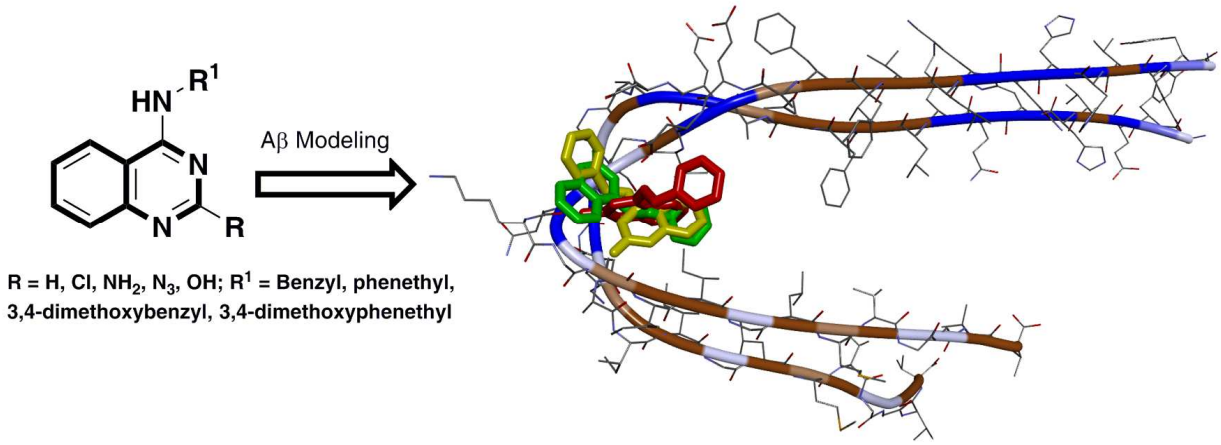


**Quinazolines as multi-targeting agents in Alzheimer's disease**

*Corresponding author: Tel: +1 519 888 4567 ext: 21317; e-mail: praopera@uwaterloo.ca

[a]School of Pharmacy, Health Sciences Campus, University of Waterloo, 200 University Avenue West, Waterloo, Ontario, Canada N2L 3G1

# 2,4-Disubstituted Quinazolines as Amyloid-*β* Aggregation Inhibitors with Dual Cholinesterase Inhibition and Antioxidant Properties: Development and Structure-Activity Relationship (SAR) Studies

Tarek Mohamed [a, b] and Praveen P. N. Rao [a,*]

[a] *School of Pharmacy, Health Sciences Campus, University of Waterloo, 200 University Ave. West., Waterloo, Ontario, Canada, N2L 3G1*

[b] *Department of Chemistry, University of Waterloo, 200 University Ave. West., Waterloo, Ontario, Canada, N2L 3G1*

---

**Abstract:** A library of fifty-seven 2,4-disubstituted quinazoline derivatives were designed, synthesized and evaluated as a novel class of multi-targeting agents to treat Alzheimer's disease (AD). The biological assay results demonstrate the ability of several quinazoline derivatives to inhibit both acetyl and butyrylcholinesterase (AChE and BuChE) enzymes ($IC_{50}$ range = 1.6–30.5 µM), prevent beta-amyloid (Aβ) aggregation ($IC_{50}$ range 270 nM–16.7 µM) and exhibit antioxidant properties (34–63.4% inhibition at 50 µM). Compound **9** ($N^2$-(1-benzylpiperidin-4-yl)-$N^4$-(3,4-dimethoxybenzyl)quinazoline-2,4-diamine) was identified as a dual inhibitor of cholinesterases (AChE $IC_{50}$ = 2.1 µM; BuChE $IC_{50}$ = 8.3 µM) and exhibited good inhibition of Aβ aggregation (Aβ40 $IC_{50}$ = 2.3 µM). Compound **15b** (4-(benzylamino)quinazolin-2-ol) was the most potent Aβ aggregation inhibitor (Aβ40 $IC_{50}$ = 270 nM) and was ~4 and 1.4-fold more potent compared to the reference agents curcumin and resveratrol. These comprehensive structure activity-relationship (SAR) studies demonstrate the application of a 2,4-disubstituted quinazoline ring as a suitable template to develop multi-targeting agents to treat AD.

*Keywords:* Alzheimer's disease, Amyloid-beta, Cholinesterase, Quinazoline, Molecular Modeling

Abbreviations: AD – Alzheimer's disease; ChE – cholinesterase; AChE – acetylcholinesterase; BuChE – butyrylcholinesterase; Aβ – amyloid-beta; NaH – sodium hydride; DMSO – dimethylsulfoxide; DMA – dimethylacetamide; DIPEA – diisopropylethylamine; DBU – 1,8-diazabicyclo[5.4.0]undec-7-ene; $POCl_3$ – phosphoryl chloride; TLC – thin layer chromatography; ThT – Thioflavin T; DTNB – 5,5'-dithiobis-(2-nitrobenzoic acid); DPR – disubstituted pyrimidine ring; DQR – disubstituted quinazoline ring.

---

## 1. Introduction

Neurodegenerative disorders elicit substantial socioeconomic impacts atop the mounting burdens on the healthcare and caregiver networks [1]. In the case of Alzheimer's disease (AD), its progressive nature, coupled with an undefined origin adds a complex dimension to its pathology. Initial research efforts that made way to first-generation therapies were based on cholinesterase (ChE) inhibition such as tacrine and the currently prescribed regimens, donepezil and rivastigmine, (Figure 1) [2–4]. Another marketed cholinesterase inhibitor galantamine (Figure 1) is also known to act as a nicotinic acetylcholine receptor (nAChR) agonist [5–7]. However, these dual acetyl (AChE) and butyrylcholinesterase (BuChE) inhibitors provide only symptomatic relief and are not effective as a long term AD therapy. These inadequacies mandate the need to develop novel therapeutics to treat AD.

Current literature strongly points toward the amyloid cascade (Aβ) and tau pathology as the primary targets for AD research. In this regard, the naturally occurring compounds curcumin and resveratrol (Figure 1) represent some examples of small molecules with good inhibitory activity

toward both beta-amyloid (Aβ) aggregation [8–13]. The neurotoxic forms of amyloid peptides (Aβ oligomers) play various roles in AD pathology including, but not limited to, self-regulation, oxidative stress, cellular metabolism and beyond [14–23]. The current approach to discover novel anti-AD therapies aims to use a multi-targeted approach where hybrid small molecules exhibit ability to target multiple pathological factors involved in AD. While this is not a new concept in its entirety, it is a more rational approach, especially when the disease in question is as complex and multifaceted as AD [24–28].

In this regard, the quinazoline ring scaffold represents a privileged structure that has been utilized to design therapeutic agents for a wide number of diseases including, but not limited to, cancer, anti-microbial therapy and neurodegeneration [29–31]. In the latter platform, quinazoline based compounds were reported as potential anti-AD agents (**1–3**, Figure 2). In this context, our earlier work on a 2,4-disubstituted pyrimidine ring scaffold (**DPR-1**, Figure 2), [32] and 2,4-disubstituted quinazolines [33] provided novel agents with dual cholinesterase and Aβ aggregation inhibition respectively. In this study, we report the design, synthesis and a comprehensive structure-activity relationship (SAR) studies of a 2,4-disubstituted quinazoline (**DQR**, Figure 2) derivatives that exhibit multi-targeting ability aimed at the cholinergic, amyloid and oxidative stress hypothesis of AD. Our results show that DQR based compounds exhibit excellent Aβ-aggregation inhibition; provide dual cholinesterase inhibition and antioxidant properties. These small molecules represent a new class of compounds to treat AD.

## 2. Chemistry

The common precursor 2,4-dichloroquinazoline (**7**, Scheme 1) required to synthesize the quinazoline target library (**8a**–**d**, **9**, **10a**–**d**, **12a**, **12b**, **13a**–**d**, **14a**–**d**, **15a**–**d**, **17a**, **17b**, **18a**–**d**,

**19a**–**d**, **20a**–**d** and **21a**–**t**) was prepared starting from either 2-nitrobenzoic acid (**4a**) or methyl 2-nitrobenzoate (**4b**) to afford the bicyclic 2,4-dichloroquinazoline intermediate **7** (Scheme 1) using a well-documented, three-step synthetic route (80–85% yield) [34–36]. The 2-chloro-*N*-substituted-quinazolin-4-amines (**8a**–**d**) were synthesized by coupling the benzyl amines (3,4-dimethoxybenzyl, benzyl, 3,4-dimethoxyphenethyl or phenethylamines respectively) to the C4-position of **7** using *N*,*N*'-diisopropylethylamine (DIPEA) as shown in Scheme 2 (yield range = 78–86%) [32, 37]. Heating **8a** with 4-amino-1-benzylpiperidine at 160–165 °C in the presence of DIPEA provided the quinazoline derivative **9** (Scheme 2) [32]. The C2 dechlorinated quinazoline derivatives **10a**–**d** were synthesized by reducing the respective C2 chloro derivatives **8a**–**d** using Pd/C and hydrazine hydrate under gentle reflux in dry ethanol for 2 hours as shown in Scheme 2 (yield range = 40–47%) [38–40]. The corresponding regioisomers of compounds **10c** and **10b** were synthesized starting from 2-chloroquinazoline **11** (Scheme 3) which was reacted with either 3,4-dimethoxybenzylamine or phenethylamine in the presence of DIPEA under pressure vial conditions to afford compounds **12a** (52%) and **12b** (47%) respectively (Scheme 3) [32].

The SAR was further explored by synthesizing quinazoline derivatives **13a**–**d** with a C2 azido ($N_3$) substituent starting from the C2 chloro derivatives **8a**–**d** (Scheme 4). This was accomplished by using sodium azide with **8a–d**, in ethanol: acetic acid (4:1 ratio) and under reflux at 95 °C for 2 hours (Scheme 4) [41–44]. Our previous attempts at direct amination of C2 chloro substituted quinazoline derivatives using ammonia or combination of copper (I) oxide/*N*,*N*'-dimethylethylenediamine (DMEDA) with ammonia provided poor yields. This limitation was overcome by reducing the C2 azido derivatives **13a**–**d** to amines **14a–d** with Pd/C and hydrazine hydrate which proved to be a more efficient alternative (yield = 80–85%, Scheme

4). On another note, we were able to obtain the C2 azido derivatives **13a**–**d**, via the corresponding C2 amino derivatives **14a**–**d**, by using the conventional method (hydrochloric acid and sodium nitrite) via the diazo intermediate. However, the yield obtained was not promising (~ 15–20%). The SAR was further expanded by incorporating a C2 hydroxy group. This was accomplished by refluxing C2-chloro derivatives (**8a–d**) in formic acid with potassium formate at 120 °C for 14–16 hours to obtain quinazoline derivatives **15a**–**d** (yield ~ 58–70%, Scheme 4). During the course of this project, we also discovered an alternative route to synthesize either C2 or C4 amino regioisomers of quinazolines (Scheme 5). Selective amination of 2,4-diaminoquinazoline **16** to obtain the C2 amino isomer (**14b** and **14d**) was accomplished using sodium hydride and benzyl bromide at r.t, whereas C4 amino isomer (**17a** and **17b**) was obtained by reacting **16** with potassium carbonate and benzyl bromide under reflux (Scheme 5). However, the drawback of this method was poor yields (~14–31%) [33]. Additional SAR expansion was completed by preparing quinazoline derivatives possessing a C2 urea or glycinamido or acetamido substituents (Scheme 6). Compound **18a**–**d** (C2 urea) was prepared by heating **8a**–**d** with urea under pressure (yield ~45–55%) [43]. It should be noted that during this reaction we also obtained the C2 amino derivatives **14a**–**d** (yield ~40–45%) due to C2 urea (**18a**–**d**) hydrolysis (Scheme 6). The C2 glycinamido derivatives **19a–d**, were synthesized by heating the corresponding C2 chloro derivatives **8a**–**d** with glycinamide in 1,4-dioxane in the presence of DBU under pressure (Scheme 6). The acetylation of the C2 amino derivatives **14a–d** using acetyl chloride under reflux afforded C2 acetamido derivatives **20a**–**d** (yield ~35–42%, Scheme 6) [45]. The C2 alkylamino derivatives **21a**–**t** ($R^1$ = Me, Et, *n*-Pr, *i*-Pr and *c*-Pr) were prepared by heating **8a**–**d** (Scheme 7) with respective amines at 150 °C for 2 hours in the presence of DIPEA under pressure to afford quinazoline derivatives **21a–t**. The yields ranged from 55–70%.

## 3. Biological results and discussion

### *3.1. Cholinesterase inhibition*

The ability of the 2,4-disubstituted quinazoline library to inhibit the ChE enzymes (AChE/BuChE) was assessed using the Ellman's method [46]. Inhibition was expressed as $IC_{50}$ values (Tables 1–3) along with ClogP values and molecular volumes ($Å^3$). Known cholinesterase inhibitors; donepezil, tacrine, galantamine and rivastigmine were used for comparison. In this study, we synthesized a library of 57 quinazoline-based derivatives with varying substituents at the C2-position along with substituted benzylamines (3,4-dimethoxybenzylamine, benzylamine, 3,4-dimethoxyphenethylamine or phenethylamine respectively) at the C4 position. It was hypothesized that the additional methylene (-$CH_2$-) group present in 3,4-dimethoxyphenethylamine and phenethylamine would enhance the C4 group's flexibility and allow for more favorable binding within the ChE enzymes and amyloid structures.
On the other hand, the nature of the substituents present at the C2 position (H, Cl, $N_3$, $NH_2$, OH, secondary amines, urea, glycinamide and acetamides) that vary in size, steric and electrostatic properties were also incorporated as it was hypothesized that these substituents will influence ChE inhibition and the degree of Aβ-aggregation. In addition, compounds with C2 OH substituents were assessed for potential antioxidant properties. The SAR data was further explored by synthesizing C2 and C4 regioisomers.

Initial assessments with the C2 chlorine derivatives (**8a–d**, Table 1) indicated good to moderate activity toward AChE with no activity toward BuChE. The presence of the C4 3,4-dimethoxybenzyl or phenethylamine moiety in **8a** and **8c** enhanced AChE-inhibition by ~ 2.5-fold (AChE $IC_{50}$ ~ 2.8–3.0 μM) compared to **8b** and **8d** (AChE $IC_{50}$ ~ 7.6 μM). The presence of the C2 aminobenzylpiperidine in **9** provided dual cholinesterase inhibition (AChE $IC_{50}$ = 2.1 μM;

BuChE $IC_{50}$ = 8.3 μM). In compound **9**, we observed ~ 4.7-fold improvement in AChE potency and ~ 1.4-fold improvement in BuChE potency compared to pyrimidine derivative reported earlier (DPR-1 AChE $IC_{50}$ = 9.90 μM; BuChE $IC_{50}$ = 11.40 μM, Fig.2) [32]. This highlighted the improved ChE-binding profile seen with the quinazoline (DQR) scaffold compared to the pyrimidine template.

Removal of the C2 chloro in compounds **10a**–**d**, Table 1, generally retained AChE activity but were ineffective toward BuChE except for the phenethylamine derivative **10d** (AChE $IC_{50}$ = 6.2 μM; BuChE $IC_{50}$ = 14.1 μM), which exhibited dual ChE inhibition. In contrast, the corresponding C2 3,4-dimethoxyphenethylamine and phenethylamine regioisomers **12a** (AChE $IC_{50}$ = 8.4 μM; BuChE $IC_{50}$ > 50 μM) and **12b** (AChE $IC_{50}$ = 7.6 μM; BuChE $IC_{50}$ > 50 μM) were less potent toward AChE and were not inhibiting BuChE. Introducing the azide functionality at the C2 position in **13a–d** retained AChE inhibition, but did not improve inhibitory potency. The C2 azido derivatives were also ineffective toward BuChE similar to C2 chloro derivatives **8a**–**d**.

The conversion of the C2 azido to an amino substituent (**14a–d**) was beneficial with all the compounds except **14a** exhibiting dual inhibition of AChE and BuChE. Compound **14d** was identified as a good nonselective inhibitor of both AChE ($IC_{50}$ = 5.7 μM) and BuChE ($IC_{50}$ = 4.9 μM, Table 1). Replacing the C2 amino with a C2 hydroxy group in compounds **15a**–**d**, retained AChE inhibition. However, these compounds were ~1–3 fold less potent compared to their corresponding amino derivatives **14a–d** and did not exhibit any BuChE inhibition. In other SAR modification, C4 amino regioisomers of **17a** and **17b** exhibited dual ChE inhibition while exhibiting reduced AChE inhibitory potency compared to C2 amino isomers **14b** and **14d**.

Interestingly, the C4 amino regioisomer **17b** possessing a C2 phenethylamine substituent was a potent BuChE inhibitor ($IC_{50}$ = 2.4 μM, Table 1) and was ~1.5-fold more potent compared to the marketed agent donepezil (BuChE $IC_{50}$ = 3.6 μM).

Modifying the C2 amino to urea and glycinamido substituents (**18a–d** and **19a–d**, Table 2) led to a loss of BuChE activity, while retaining AChE inhibition although these compounds were less potent (AChE $IC_{50}$ ~ 7.3–12.5 μM) compared to the C2 amino derivatives **14a–d** (Table 1). Interestingly, the glycinamido derivative **19d**, exhibited BuChE inhibition ($IC_{50}$ = 3.5 μM) and was comparable to donepezil (BuChE $IC_{50}$ = 3.6 μM). The acetylation of the C2 amines gave acetamido compounds **20a–d** and this modification reduced AChE inhibition potency compared to **14a**–**d**. These compounds exhibited similar AChE inhibition potency as C2 urea derivatives **18a**–**d.** As these derivatives did not exhibit BuChE inhibition, the SAR studies suggest that small polar entities at the C2 position were not favorable for BuChE inhibition.

In order to develop dual inhibitors of ChE, we screened C2 alkylamino derivatives **21a–t** ($R^1$ = Me, Et, *n*-Pr, *i*-Pr and *c*-Pr; Table 3) possessing various C4 substituents (3,4-dimethoxybenzylamine, benzyl, 3,4-dimethoxyphenethylamine and phenethylamine). The C4 3,4-dimethoxybenzylamino group of compounds (**21a**–**e**) exhibited dual inhibition of ChE (Table 3). The AChE inhibition was in the range of ~ 5.6–8.7 μM with the C2 *n*-propylamine (**21c**) being best, followed by C2 ethyl- and isopropyl being equipotent AChE inhibitors (compounds **21b** and **21d** respectively). Interestingly all these compounds exhibited BuChE inhibition ($IC_{50}$ ~ 1.6–30 μM, Table 3). Replacing the C4 3,4-dimethoxybenzylamino substituent with an unsubstituted C4 benzylamino substituent in compounds **21f–j** led to better BuChE inhibition potency (BuChE $IC_{50}$ ~11.7–22 μM), whereas AChE inhibition activity ranged between $IC_{50}$ ~

6.4–8.1 μM. Interestingly, the addition of a methylene group at the C4 position in **21k–o** (C4 3,4-dimethoxyphenethyl) improved BuChE activity in varying degrees (BuChE $IC_{50}$ ~4.5–25 μM), while generally retaining AChE inhibitory activity (AChE $IC_{50}$ ~ 7.0–8.5 μM). In the C4 phenethyl series of compounds (**21p**–**s**), potency toward BuChE continued to improve, for the most part, while AChE inhibitory activity remained static with $IC_{50}$ values ranging between 7.2–8.7 μM. The C2 ethyl-, *n*-propyl- and isopropylamino based derivatives in the phenethylamine series (**21q–s**, Table 3) were more potent toward BuChE compared to their 3,4-dimethoxyphenethylamino counterparts (**21l–n**, Table 3). Among this series of C2 and C4 substituted quinazolines, the C2 isopropylamino derivative **21s**, was identified as the most potent BuChE inhibitor ($IC_{50}$ = 1.6 μM) and was ~ 2.3-fold more potent compared to donepezil (BuChE $IC_{50}$ = 3.6 μM).

Overall, most of these quinazoline derivatives displayed moderate to good activity toward AChE ranging between $IC_{50}$ ~ 2.1 and < 10 μM. The most potent AChE inhibitor was compound **9** ($N^2$-(1-benzylpiperidin-4-yl)-$N^4$-(3,4-dimethoxybenzyl)quinazoline-2,4-diamine; AChE $IC_{50}$ = 2.1 μM), featuring the aminobenzylpiperidine C2 group, which surpassed the activity of rivastigmine (AChE $IC_{50}$ = 6.5 μM) and galantamine (AChE $IC_{50}$ = 2.6 μM) followed by compound **14c** ($N^4$-(3,4-dimethoxphenethyl) quinazoline-2,4-diamine; AChE $IC_{50}$ = 2.5 μM). With respect to BuChE, activity was more widespread as it ranged from $IC_{50}$ ~ 1.6 to no inhibition at 50 μM. Compound **21s** ($N^2$-isopropyl-$N^4$-(phenethyl)quinazoline-2,4-diamine) was the most potent BuChE inhibitor ($IC_{50}$ = 1.6 μM) and exhibited better potency compared to donepezil.

*3.2. Beta amyloid (Aβ) aggregation inhibition studies*

The 2,4-disubstituted quinazoline library was evaluated for anti-Aβ activity by monitoring the aggregation kinetics of both Aβ40 and Aβ42 using the thioflavin T (ThT) binding fluorescence assay [44, 47]. Initially, quinazolines with promising anti-aggregation activity were identified by screening the compounds at a concentration of 25 μM using Aβ40 (5 μM). The data obtained is presented as percent inhibition (Figure 3) along with curcumin and resveratrol as the reference compounds. These initial screening assisted us in identifying quinazoline derivatives that were able to exhibit ≥50% inhibition of Aβ40 aggregation. Among the library of 57 quinazoline derivatives synthesized, we were pleased to note that 39 compounds exhibited ≥50% inhibition of Aβ40 aggregation when tested at a concentration of 25 μM. Interestingly, this initial screen also identified few compounds (**13d**, **19a**–**d** and **21d**) which were promoting Aβ40 aggregation. It appears that the presence of a C2 glycinamido substitutent in compounds **19a**–**d** was detrimental to Aβ aggregation inhibition property. This observation needs additional studies to understand the mechanisms involved.

Based on these results, we proceeded to conduct a systematic study by monitoring the Aβ40 aggregation kinetics using various concentrations of quinazoline inhibitors (1–25 μM range) to assess the Aβ aggregation inhibitory potency ($IC_{50}$ values are given in Table 4). In addition, these compounds were also evaluated against Aβ42. It was gratifying to see that 13 of 39 quinazolines (~33%) with various C4/C2 group combinations, displayed potent inhibition of Aβ40 that surpassed the inhibitory activity shown by the known inhibitor curcumin ($IC_{50}$ = 3.3 μM, Table 4). On the other hand, tested quinazoline compounds did not exhibit similar inhibition profile toward Aβ42 and the activity ranged from inactive to ≥50% inhibition (Table 4). However, three quinazoline derivatives **8c**, **17a** and **21k** (Aβ42 $IC_{50}$ = 8.4–23.1 μM range)

showed good inhibition, with compound **8c** and **17a** exhibiting better inhibition potency compared to the reference agent resveratrol ($IC_{50}$ = 15.3 μM) against Aβ42.

Among the C2 chloro-based derivatives **8b**–**d**, the benzylamine moiety in **8b** provided weak inhibition of Aβ40 aggregation ($IC_{50}$ ~ 17 μM), while the addition of the methylene group in **8d** enhanced Aβ40 activity by ~ 3.5-fold ($IC_{50}$ ~ 5 μM) and slightly increased the Aβ42 activity from 22% inhibition (**8b**) to 36% at 25 μM. Compared to **8d**, the 3,4-dimethoxybenzylamine derivative (**8c**) was ~ 1.6-fold less potent toward Aβ40 aggregation and more significantly exhibited superior Aβ42 aggregation ($IC_{50}$ ~ 13 μM, Table 4). Compound **9** (C2 aminobenzylpiperidine), while being the most potent AChE inhibitor, was almost 1.3-fold more potent toward Aβ40 aggregation ($IC_{50}$ ~ 2.3 μM) compared to curcumin ($IC_{50}$ ~ 3.3 μM) but was not effective toward Aβ42 (27% inhibition at 25 μM, Table 4).

Removal of the C2 chloro substituent led to a decrease in the Aβ40 anti-aggregation properties of compounds **10c** and **10d** ($IC_{50}$ ~ 12 μM) which were not as potent as either **8c** or **8d**. They were also weak inhibitors of Aβ42 (32–36% inhibition, Table 4). The presence of a C2 azido substituent enhanced the activity toward Aβ40 aggregation inhibition (compounds **13a** and **13b**). Compound **13b** with a C4 benzylamine was ~ 2.8-fold more potent toward Aβ40 compared to **13a** which had a C4 3,4-dimethoxybenzylamino substituent ($IC_{50}$ ~ 2.6 μM vs. 7.3 μM, Table 4). Furthermore, **13b** was a much more potent inhibitor of Aβ40 compared to the reference agent curcumin. In addition, **13b** also exhibited better Aβ42 aggregation inhibition compared to **13a** (37% vs < 10% at 25 μM). Among the C2 amino derivatives **14a**–**d**, the presence of a C4-3,4-dimethoxybenzylamino substituent in **14c** provided good inhibition of Aβ40 aggregation ($IC_{50}$ = 2.7 μM) and exhibited ~ 45% inhibition of Aβ42 aggregation at 25 μM (Table 4). The corresponding C4 amino regioisomers **17a** and **17b** exhibited Aβ40 aggregation inhibition with

compound **17a** identified as good inhibitor ($IC_{50}$ = 2.2 μM) and was ~1.4-fold more potent compared to the reference agent curcumin. In addition, **17a** exhibited superior inhibition of Aβ42 ($IC_{50}$ ~ 8 μM) compared to the corresponding C2 amino regioisomer **14b** and was ~ 1.8-fold more potent compared to resveratrol ($IC_{50}$ = 15.3 μM) and ~ 1.2-fold more potent compared to curcumin ($IC_{50}$ = 3.3 μM). It should be noted that anti-Aβ activity of quinazoline derivatives **14b**, **14d**, **17a** and **17b** were previously reported by us [33].

Investigating the replacement of C2 amines with C2 hydroxy substituents (**15a–d**) showed interesting SAR. Compound **15a** (C4 3,4-dimethoxybenzylamine) was equipotent to the C2 azido compound **13a** with respect to Aβ40/42 inhibition (Aβ40 $IC_{50}$ ~ 7 μM and Aβ42 < 10% inhibition at 25 μM). In contrast, replacing the C4 3,4-dimethoxyphenethylamino with a C4 benzylamino substituent led to a drastic increase in its anti-Aβ40 activity with compound **15b** identified as a potent inhibitor of Aβ40 aggregation ($IC_{50}$ = 270 nM). It was ~12-fold and ~4-fold more potent compared to the reference agents curcumin (Aβ40 $IC_{50}$ = 3.3 μM) and resveratrol (Aβ40 $IC_{50}$ = 1.1 μM, Table 4). All the C2 hydroxy compounds exhibited weak inhibition of Aβ42 aggregation (<10% to 32% inhibition at 25 μM).

The modification of C2 amino to urea or acetamido substituent (compounds **18a**–**d**, **20a** and **20b**) did retain Aβ40 aggregation inhibition. Within the C2 urea derivatives, compound **18d**, possessing a C4 phenethylamino substituent exhibited potent inhibition of Aβ40 ($IC_{50}$ ~ 1 μM) and was equivalent to the reference agent resveratrol ($IC_{50}$ ~1.1 μM, Table 4). The C2 urea based compounds exhibited ~33–48% inhibition of Aβ42 when tested at 25 μM. Replacing the C2 urea with an acetamido (compounds **20a** and **20b**) generally exhibited better Aβ40 inhibition ($IC_{50}$ =

1.9 and 3.1 µM respectively). However, they exhibited weak inhibition of Aβ42 (<10% and 31% inhibition respectively) compared to **18a**–**d** (Table 4).

Within the C2-alkylamino series of compounds (**21c**, **21e**, **21g**–**m** and **21o**–**t**, Table 4), presence of a C2 *n*-propylamino and a C4 3,4-dimethoxybenzylamino in compound **21c** provided good Aβ40 aggregation inhibition ($IC_{50}$ ~ 1.7 µM, Table 4) and was superior to the reference agent curcumin ($IC_{50}$ = 3.3 µM). In contrast, within the C4 benzylamino series **21g**–**j**, the best compound was **21i** with a C2 isopropylamino substituent (Aβ40 $IC_{50}$ = 4.4 µM, Table 4); however, they exhibited weak inhibition of Aβ42 aggregation. Introducing a C4 3,4-dimethoxyphenethylamino substituent, identified compound **21l** with a C2 ethyl substituent as a good inhibitor of Aβ40 aggregation ($IC_{50}$ = 2.9 µM, Table 4) with equivalent inhibition compared to reference agent curcumin and with better Aβ42 inhibition profile (41% inhibition at 25 µM) within this series. Interestingly, the C4 phenethylamino series of compounds (**21p–t**), yielded the most active compounds (Aβ40 $IC_{50}$ ~0.8–4.4 µM) with the C2 cyclopropylamine **21t** exhibiting excellent inhibition ($IC_{50}$ = 790 nM, Table 4). It was ~4.1-fold and ~1.4-fold more potent compared to the reference agents curcumin ($IC_{50}$ = 3.3 µM) resveratrol ($IC_{50}$ = 1.1 µM) respectively. The activity order based on the C2 substituent present was of the order, cyclopropylamine (**21t**) >> ethylamine (**21q**) ~ methylamine (**21p**) > isopropylamine (**21s**) ~ *n*-propylamine (**21r**). With respect to Aβ42 aggregation inhibition, these C2 alkylamino derivatives exhibited 22–47% aggregation inhibition at 25 µM except **21s** which was inactive (Table 4).

Among this quinazoline library, compound **15b** (C4 benzylamino and C2 hydroxyl) was identified as the most potent Aβ40 aggregation inhibitor with an $IC_{50}$ ~ 270 nM, which was significantly more potent compared to reference agents curcumin and resveratrol. On the other

hand, compound **17a** (C4 amino and C2 benzylamino) was identified as the most potent Aβ42 aggregation inhibitor with an $IC_{50}$ ~ 8.4 μM, which was more potent compared to either curcumin or resveratrol.

*3.3. Aβ Aggregation kinetics and transmission electron microscopy (TEM) studies*

In order to understand the mode of anti-Aβ aggregation mechanisms of lead compounds **15b**, **18d**, **21q** and **21t**, we analyzed the aggregation kinetics based on the ThT fluorescence assay over a period of 24 h to monitor the effect of these compounds on the lag phase, growth phase and saturation phase in the aggregation kinetics pathway of Aβ40. As seen in Figure 4 (Panels A–D), compounds **15b**, **18d**, **21q** and **21t** showed concentration-dependent inhibition and modulation of Aβ40 aggregation kinetics, when the concentration of test compounds was increased from 1 μM to 25 μM. The kinetic curves observed suggests that these compounds can stabilize the amyloid monomers, as seen by the extended lag phase time, which were roughly double that observed with the Aβ40 alone control. Moreover, the considerable decline in the fluorescence intensity observed in the presence of test compounds indicates their ability to prevent Aβ fibrillogenesis. It can be seen from the kinetics plot (Figure 4, Panels A–D) that at the end of the 24 h incubation period, there was a significant reduction in the overall Aβ fibril load. Most notably, compound **15b** (C2 hydroxy and C4 benzylamino) was identified as a potent inhibitor of Aβ40 aggregation and it exhibited complete inhibition of aggregation at 25 μM (Figure 4, Panel A). Significantly, these studies suggest that compounds **15b**, **18d**, **21q** and **21t** exhibit multimodal inhibition mechanisms toward Aβ40 aggregation with an ability to interact both with the lower order and higher order Aβ aggregates. This was further confirmed by carrying out TEM studies during the course of 24 h incubation period to determine the aggregation morphology (Figure 4, Panels A–D). The Aβ40 alone TEM shows the formation of

distinct Aβ fibrils whereas in the presence of 25 μM of test compounds (**15b**, **18d**, **21q** and **21t**) a significant decline in the Aβ-fibrillogenesis was observed (Figure 4, Panels A–D).

The aggregation kinetics of Aβ42 in the presence of quinazoline derivatives **8c**, **17a**, **17b** and **21k** exhibited superior anti-aggregation properties based on the ThT fluorescence assay (Figure 5, Panels A–D). They generally showed a concentration-dependent inhibition and moderate modulation of Aβ42 aggregation kinetics. With the exception of **17a** (Figure 5, Panel B), these derivatives did not extend the lag phase suggesting that they were not effective at interacting and stabilizing the Aβ42 monomers. However, at higher concentrations, the kinetic curves showed a decline in the fluorescence intensity indicating that these compounds can interfere in the fibrillogenesis and reduce fibril load (Figure 5, Panels A–D) although they were less effective as Aβ aggregation inhibitors compared to compounds **15b**, **18d**, **21q** and **21t** (Figure 4, Panels A–D). Furthermore, confirmation of compounds **8c**, **17a**, **17b** and **21k** to prevent Aβ42 aggregation was obtained by conducting TEM studies to determine the aggregation morphology (Figure 5, Panels A–D) [44, 48]. The TEM image of Aβ42 alone shows fibril structures whereas in the presence of 25 μM of either **8c**, **17a**, **17b** or **21k** the fibril load reduced considerably (Figure 5, Panels A–D). Both compounds **8c** (C2 chloro and C4 3,4-dimethoxyphenethylamino) and 1**7a** (C2 phenethylamino and C4 amino) exhibited almost similar reduction in fibril load (Figure 5, Panels A and B respectively) whereas compound **21k** (C2 Me and C4 3,4-dimethoxyphenethylamino) was less effective (Figure 5, Panel D).

*3.4. Evaluation of antioxidant properties*

The core quinazoline-2-ol scaffold, present in **15a–d** (C2 hydroxy, Table 5) was anticipated to elicit antioxidant activity. This was evaluated by UV spectrophotometry using the stable radical 2,2-diphenyl-1-picrylhydrazyl (DPPH) [49, 50]. The known antioxidants resveratrol and trolox

were used as reference compounds (Table 5). These studies indicate that compounds **15a–d** exhibit moderate to good ability to scavenge DPPH radical (~34–63% at 50 μM, Table 5). Maximum antioxidant activity was observed with **15a** (% DPPH scavenging ~ 63%), which was ~1.5-fold more potent compared to resveratrol (~42%). The antioxidant activity order based on the C4 substituent was **15a** (3,4-dimethoxybenzylamine) > **15d** (phenethyl) > **15b** (benzyl) > **15c** (3,4-dimethoxyphenethylamine).

*3.5. Molecular docking studies*

The binding interactions of cholinesterase inhibitors with good activity identified from the quinazoline library (Compounds **9** and **14c** AChE $IC_{50}$ = 2.1 and 2.5 μM respectively; compounds **21q** and **21s** BuChE $IC_{50}$ = 3.2 and 1.6 μM respectively) were investigated by conducting molecular docking studies using the crystal structures of either human AChE or BuChE [50]. In *h*AChE compounds **9** ($N^2$-(1-benzylpiperidin-4-yl)-$N^4$-(3,4-dimethoxybenzyl)quinazoline-2,4-diamine) and **14c** ($N^4$-(3,4-dimethoxyphenethyl)quinazoine-2,4-diamine) showed unique binding modes (Figure 6, Panel A) which corroborate their similar inhibitory potency. The presence of the $N^2$-1-benzylpiperidine pharmacophore in **9**, showed a similar binding mode in the catalytic site as seen with donepezil [51], however, the $N^2$-1-benzylpiperidine moiety was not extending deep into the catalytic site. Instead, the major interaction of compound **9** was at the mouth of the active site known as the peripheral anionic site (PAS), where the C4 N*H* was undergoing hydrogen-bonding interactions with the backbone carbonyl of Tyr341 (distance ~ 2.9 Å) and the piperidine ring was stacked parallel to the phenol ring of Tyr341. On the other hand, **14c** displayed more favorable interactions, where the quinazoline ring scaffold was predominately interacting, with the anionic site closer to Trp86 (distance ~ 4–5 Å). The C4 3,4-dimethoxyphenethylamino was oriented toward the PAS residues

(Trp286 and Tyr341) and was stacked parallel to Trp286's indole ring (distance ~ 4 Å). One of the key contributing factors to this compound's potency is the multiple hydrogen bonding contacts of C2 $NH_2$ substituent with the hydroxyl group of Ser198 and the imidazole ring of His447 (distance ~ 2.5–3.5 Å) closer to the catalytic site.

In *h*BuChE, compounds **21q** ($N^2$-ethylquinazoline-$N^4$-(phenethyl)-2,4-diamine) and **21s** ($N^2$-isopropylquinazoline-$N^4$-(phenethyl)-2,4-diamine) (Figure 6, Panel B) exhibited contrasting binding modes that supports the 2-fold difference in inhibition potencies (**21q** and **21s** BuChE $IC_{50}$ = 3.2 and 1.6 µM respectively). The smaller ethylamino substituent at the C2 position enabled the quinazoline ring in **21q** to stack parallel to Trp82 (distance ~ 3–4 Å), interaction commonly seen with BuChE inhibitors. The ethylamino moiety was oriented toward His438 and was undergoing hydrogen-bonding interactions with its backbone carbonyl (distance ~ 3 Å), while the C4 phenethylamino substituent was oriented toward the hydrophobic acyl pocket (Leu286–Val288, distance ~ 5–6 Å). Increasing the steric bulk at the C2 position with the isopropyl group in **21s**, completely reversed the binding orientation compared to **21q**. The quinazoline ring scaffold was oriented perpendicular to the hydrophobic acyl pocket (Leu286–Val288, distance ~ 3–7 Å), and was stacked over the catalytic triad. The C4 phenethylamino substituent was oriented toward the mouth. The C2 isopropylamino N*H* was in contact with His438 and Ser198 via hydrogen bonding whereas the quinazoline *N*1 also underwent hydrogen bonding interaction with Ser198 (Figure 6, Panel B).

The binding interactions of the most potent Aβ aggregation inhibitors **15b** (Aβ40 $IC_{50}$ = 270 nM) and **21t** (Aβ40 $IC_{50}$ = 790 nM) was investigated using the NMR solution structure of Aβ protein (Aβ9–40) [52]. We used both Aβ dimer and fibril models in order to understand the binding interactions of quinazoline derivatives with both lower and higher order Aβ aggregates. In the

Aβ dimer assembly, both compounds **15b** (4-(benzylamino)quinazolin-2-ol) and **21t** ($N^2$-cyclopropylquinazoline-$N^4$-(phenethyl)-2,4-diamine) were interacting within the turn/loop region consisting of Asp23–Gly29 (Figure 7, Panel A). The ability of misfolded monomers to dimerize and aggregate is dependent on their ability to form the loop conformation [53]. This can be prevented by small molecules that can bind in this loop region which can delay and or prevent further self-assembly to form higher order structures such as oligomers and fibrils. The quinazoline ring scaffold of **15b**, was closely interacting with the backbone structures of Asn27-Gly29 (distance ~ 3–4 Å), while the C4 benzylamino moiety was oriented in a perpendicular manner toward the backbones of Asp23-Gly25 (distance ~ 4 Å). Of greater interest, was the proximity of the C2 hydroxy group to the backbones of Asn27 and Gly29 respectively (distance ~ 2.7–3.5 Å). On the other hand, compound **21t** was primarily acting via hydrophobic contacts in the turn region of the dimer structure. The C4 phenethylamino substituent was oriented toward the Asn27–Gly29 (distance ~ 3–5 Å) and underwent vander Waal's contact with the backbone of Asp27. The quinazoline ring scaffold was between the turn/loop region, closer to Asp23 side chain (distance ~ 4–5 Å), whereas the C2 hydrophobic cyclopropyl substituent was interacting with the backbones of Ala21 and Glu22 (Figure 7, Panel A).

When investigating the binding modes in the fibril model (Figure 7, Panel B), the quinazoline ring scaffold of **15b** was extended outward from the hydrophobic fibril core, while the C4 benzylamine substituent was interlocked between the two pairs of Met35 residues (distance ~ 4–5 Å). This conformation allowed the C2 OH and the C4-N*H* to undergo hydrogen bonding interactions with the backbone amides of Gly33–Met35 (distance ~ 3–3.5 Å). Interestingly, the conformation of **21t** was more interesting in the fibril model as its quinazoline ring scaffold was stacked in parallel between the fibril core region distance to Met35 pairs (~ 4–5 Å). Both its C4

and C2 groups were extended outward from the fibril core region, giving an overall Y-shaped conformation that was intercalated within the fibril core (Figure 7, Panel B). This conformation also enabled both C4 and C2 amines to undergo hydrogen bonding interactions with backbone of Gly33-Met35 (distance ~ 3–5 Å). The C4 phenethylamine was above Ile32-Leu34 backbones and underwent van der Waal's contact, while the C2 cyclopropyl ring was closer to side chains of Leu34 and Val36 (distance ~ 5–7 Å) as shown in Figure 7 (Panel A). These studies indicate that a 2,4-disubstituted quinazoline serves as a suitable template to design Aβ aggregation inhibitors.

In summary, molecular docking studies show that the presence of a C4 3,4-dimethoxyphenethylamine substituent (**14c**) provides peripheral anionic site (PAS) binding in the AChE active site. Binding modes of quinazolines (**15b** and **21t**) with potent anti-Aβ activity shows their ability to bind in the loop region (Asp23–Gly29) which can prevent further self-assembly, whereas in the fibril assembly quinazolines were capable of intercalating in the fibril core to perturb the β-sheet assembly.

**4. Conclusions**

In this study, we report the development of a novel library of 2,4-disubstituted quinazoline ring scaffold as multi-targeting agents that exhibit cholinesterase inhibition as well as anti-amyloid and antioxidant properties. A total of 28 quinazoline derivatives exhibited varying levels of dual ChE inhibition while 36 derivatives exhibited varying levels of Aβ aggregation inhibition. The AChE inhibition was in the range of 2.1–14 μM ($IC_{50}$ values) and BuChE inhibition was in the range of 1.6–30 μM ($IC_{50}$ values), Aβ40 aggregation inhibition was in the range of 0.27-16 μM ($IC_{50}$ values) and antioxidant activity ranged from 34–63% inhibition. TEM studies revealed the

ability of quinazoline derivatives to prevent the formation of both lower and higher order Aβ aggregates.

Compound **9** (C4 3,4-dimethoxybenzylamino and C2 benzylpiperidine) exhibited dual ChE inhibition (AChE $IC_{50}$ = 2.1 µM; BuChE $IC_{50}$ = 8.3) and good inhibition of Aβ40 aggregation (Aβ40 $IC_{50}$ = 2.3 µM); compound **15b** (C4 benzylamino and C2 hydroxyl) was identified as the most potent Aβ40 aggregation inhibitor ($IC_{50}$ ~ 270 nM) which possessed selective AChE inhibition ($IC_{50}$ = 9.8 µM) and antioxidant activity (47% inhibition at 50 µM) whereas compound **17a** (C4 $NH_2$ and C2 benzylamino) exhibited dual cholinesterase (AChE $IC_{50}$ = 7.5 µM; BuChE $IC_{50}$ = 11.6 µM) and Aβ aggregation inhibition (Aβ40 $IC_{50}$ = 2.2 µM; Aβ42 $IC_{50}$ = 8.4 µM). These comprehensive structure activity-relationship (SAR) studies demonstrate the application of a 2,4-disubstituted quinazoline ring as a suitable template to develop multi-targeting agents to treat AD.

## 5. Experimental methods

### *5.1. Chemistry*

#### *5.1.1. Materials and methods*

All the reagents and solvents were reagent grade purchased from various vendors (Acros Organics, Sigma-Aldrich, and Alfa Aesar, USA) with a minimum purity of 95% and were used without further purification. The quinazoline derivative **11** was obtained from Sigma-Aldrich and the other quinazoline derivatives **8a**–**d**, **14a**–**d**, **17a** and **17b** were synthesized and characterized as per our previously reported methods [33, 36, 43]. Melting points (mp) were determined using a Fisher-Johns apparatus and are uncorrected. Reaction progress was monitored by UV using thin-layer chromatography (TLC) using Merck 60F254 silica gel plates. Column chromatography was performed with Merck silica gel 60 (230−400 mesh) with 5:1

EtOAc:MeOH as the solvent system unless otherwise specified. Proton ($^{1}$H NMR) and carbon ($^{13}$C NMR) spectra were performed on a Bruker Avance (at 300 and 100 MHz respectively) spectrometer using DMSO-$d_6$. Coupling constants (*J* values) were recorded in hertz (Hz) and the following abbreviations were used to represent multiplets of NMR signals: s = singlet, d = doublet, t = triplet, m = multiplet, br = broad. Carbon multiplicities (C, CH, $CH_2$ and $CH_3$) were assigned by DEPT 90/135 experiments. High-resolution mass spectrometry (HRMS) was determined using a Thermo Scientific Q-Exactive Orbitrap mass spectrometer (positive mode, ESI), Department of Chemistry, University of Waterloo. Compound purity (~95% or over) was determined using an Agilent 1100 series HPLC equipped with an analytical column (Agilent Zorbax Eclipse XDB-C8 column, 4.6 x 150 mm, 5 μm particle size) running 50:50 Water:ACN with 0.1% TFA at a flow rate of 1.0-1.5 mL/min or an Agilent 6100 series single quad LCMS equipped with an Agilent 1.8 μm Zorbax Eclipse Plus C18 (2.1 x 50 mm) running 50:50 Water:ACN with 0.1% FA with a flow rate of 0.5mL/min. All the final compounds exhibited ≥ 95% purity.

*5.1.2. Procedure for the synthesis of compound **9** [32].*

In a 50 mL pressure vial (PV), 0.25 g of **8a** (0.76 mmol) was dissolved in 5 mL of 1,4-dioxane followed by the addition of 4 eq. (3.03 mmol) of 4-amino-1-benzylpiperidine and 5 eq. of DIPEA (3.78 mmol). Pressure vial was sealed and stirred in an oil bath at 160–165 °C for 6 h. Upon completion and cooling to room temperature, the reaction mixture was diluted with ~ 40 mL of EtOAc and washed 2-3 times with equal volumes of brine solution. The combined aqueous layers were washed with ~ 25 mL of EtOAc. The combined EtOAc layers were dried

over $MgSO_4$ and the organic solvent was removed in vacuo to yield a solid product which was purified by silica gel column chromatography using 9:1 acetone:MeOH solvent system.

*5.1.2.1. $N^2$-(1-Benzylpiperidin-4-yl)-$N^4$-(3,4-dimethoxybenzyl)quinazoline-2,4-diamine (**9**).* Yield: 42% (0.15 g, 0.32 mmol); mp 127–129 °C. $^1$H NMR (300 MHz, DMSO-$d_6$): δ 7.96 (d, *J* = 8.2 Hz, 1H), δ 7.42 (t, *J* = 7.8 Hz, 1H), δ 7.28–7.20 (m, 7H), δ 7.02–6.98 (m, 2H), δ 6.85-6.80 (m, 2H), 6.65 (br s, 1H), δ 4.58 (d, *J* = 5.0 Hz, 2H), δ 3.70–3.66 (m, 6H), δ 3.46 (s, 2H), δ 2.77–2.70 (m, 3H), δ 2.04–2.00 (m, 2H), δ 1.78–1.73 (m, 2H), δ 1.47–1.44 (m, 2H). HRMS (ESI) m/z calcd for $C_{29}H_{34}N_5O_2$ $[M + H]^+$ 485.2634, found 485.2705. Purity: 98.7%

*5.1.3. General procedure for the synthesis of compounds **10a–d.***

In a 50 mL round bottom flask (RBF), 0.5 g of **8a–d** (1.45-1.85 mmol) was dissolved in 20 mL of anhydrous ethanol. While stirring on ice, 10 mol. % of 10% Pd/C was added to reaction mixture followed by the drop-wise addition of 1.3 eq. of hydrazine hydrate. Solution was stirred on ice for 5 min before refluxing for 2 h at 80–85 °C. Upon completion and cooling to room temperature, the reaction mixture was passed through a tightly-packed cotton-filled syringe that has been pre-rinsed with ethanol, to remove the Pd/C catalyst. A 30 mL aliquot of ethanol was used to rinse the syringe. The combined ethanol solutions were evaporated in vacuo, diluted in EtOAc (20 mL) and washed 25 mL x 2 with equal volumes of brine solution. The combined aqueous layers were washed with 15 mL of EtOAc. The combined EtOAc layers were dried over $MgSO_4$, before removing the EtOAc in vacuo to yield a solid or semi-solid crude product that was purified by silica gel column chromatography using 5:1 EtOAc:MeOH solvent system. Final compounds were white to pale yellow solids with yields ranging from 40–47%.

*5.1.3.1. N-(3,4-Dimethoxybenzyl)quinazolin-4-amine (**10a**).* Yield 47% (0.21 g, 0.71 mmol); mp 187–189 °C. $^{1}$H NMR (300 MHz, DMSO-$d_6$): δ 8.69 (br s, 1H), δ 8.42 (s, 1H), δ 8.25 (d, *J* = 6.0 Hz, 1H), δ 7.71 (t, *J* = 9.0 Hz, 1H), δ 7.64 (d, *J* = 6.0 Hz, 1H), δ 7.45 (t, *J* = 9.0 Hz, 1H), δ 6.99 (s, 1H), δ 6.84 (s, 2H), δ 4.67 (d, *J* = 6.0 Hz, 2H), δ 3.68 (s, 3H), δ 3.67 (s, 3H). HRMS (ESI) m/z calcd for $C_{17}H_{18}N_3O_2$ $[M + H]^+$ 296.1321, found 296.1392. Purity: 97.3%

*5.1.3.2. N-Benzylquinazolin-4-amine (**10b**).* Yield 45% (0.20 g, 0.85 mmol); mp 142–145 °C. $^{1}$H NMR (300 MHz, DMSO-$d_6$): δ 8.84 (t, *J* = 9.0 Hz, 1H), δ 8.42 (s, 1H), δ 8.26 (d, *J* = 6.0 Hz, 1H), δ 7.72 (t, *J* = 6.0 Hz, 1H), δ 7.64 (d, *J* = 6.0 Hz, 1H), δ 7.47 (t, *J* = 9.0 Hz, 1H), δ 7.31–7.19 (m, 5H), δ 4.71 (d, *J* = 6.0 Hz, 2H). HRMS (ESI) m/z calcd for $C_{15}H_{14}N_3$ $[M + H]^+$ 236.1109, found 236.1181. Purity: 97.9%

*5.1.3.3. N-(3,4-Dimethoxyphenethyl)quinazolin-4-amine (**10c**).* Yield 40% (0.18 g, 0.58 mmol); mp 155–157 °C. $^{1}$H NMR (300 MHz, DMSO-$d_6$): δ 8.44 (s, 1H), δ 8.28 (br s, 1H), δ 8.16 (d, *J* = 6.0 Hz, 1H), δ 7.71–7.62 (m, 2H), δ 7.46 (t, *J* = 9.0 Hz, 1H), δ 6.83-6.72 (m, 3H), δ 3.70 (d, *J* = 6.0 Hz, 2H), δ 3.67 (s, 3H), δ 3.66 (s, 3H), δ 2.84 (t, *J* = 9.0 Hz, 2H). HRMS (ESI) m/z calcd for $C_{18}H_{20}N_3O_2$ $[M + H]^+$ 310.1477, found 310.1549. Purity: 98.6%

*5.1.3.4. N-Phenethylquinazolin-4-amine (**10d**).* Yield 42% (0.19 g, 0.76 mmol); mp 137–139 °C. $^{1}$H NMR (300 MHz, DMSO-$d_6$): δ 8.44 (s, 1H), δ 8.33 (t, *J* = 9.0 Hz, 1H), δ 8.16 (d, *J* = 6.0 Hz, 1H), δ 7.71-7.62 (m, 2H), δ 7.43 (t, *J* = 9.0 Hz, 1H), δ 7.26-7.16 (m, 5H), δ 3.69 (d, *J* = 6.0 Hz, 2H), δ 2.91 (t, *J* = 9.0 Hz, 2H). $^{13}$C NMR (100 MHz, DMSO-$d_6$): δ 159.25, δ 155.12, δ 149.05, δ

139.52, δ 132.42, δ 128.65, δ 128.33, δ 127.47, δ 126.07, δ 125.51, δ 122.54, δ 114.94, δ 42.06, δ 34.46. HRMS (ESI) m/z calcd for $C_{16}H_{16}N_3$ $[M + H]^+$ 250.1266, found 250.1338. Purity: 96.6%

*5.1.4. General procedure for the synthesis of compounds **12a** and **12b**.*

In a 50 mL PV, 0.25 g of **11** (1.52 mmol) was dissolved in 5 mL of 1,4-dioxane followed by the addition of 3 eq. (4.56 mmol) of 3,4-dimethoxyphenethlyamine or phenethylamine and 5 eq. of DIPEA (7.60 mmol). Pressure vial was sealed and stirred in an oil bath at 155–160 °C for 5 h. Upon completion and cooling to room temperature, the reaction mixture was diluted with ~ 40 mL of EtOAc and washed 25 mL x 3 times with equal volumes of brine solution. The combined aqueous layers were washed with ~ 25 mL of EtOAc. The combined EtOAc layers were dried over $MgSO_4$ before removing the EtOAc in vacuo to yield a solid crude product that was purified by silica gel column chromatography using 5:1 EtOAc:MeOH as the solvent system. Final compounds were pale yellow to pale brown solids with yields ranging from 47–52%.

*5.1.4.1. N-(3,4-Dimethoxyphenethyl)quinazolin-2-amine (**12a**).* Yield 52% (0.18 g, 0.58 mmol); mp 144–146 °C. $^1$H NMR (300 MHz, DMSO-$d_6$): δ 9.09 (s, 1H), δ 7.72 (d, $J$ = 8.0 Hz, 1H), δ 7.72–7.63 (m, 2H), δ 7.45–7.33 (m, 1H), δ 7.32–7.20 (m, 2H), δ 6.84–6.69 (m, 3H), δ 3.70 (s, 3H), δ 3.67 (s, 3H), δ 3.62 (q, $J$ = 8.2 Hz, 2H), δ 2.75 (t, $J$ = 7.6 Hz, 2H). HRMS (ESI) m/z calcd for $C_{18}H_{20}N_3O_2$ $[M + H]^+$ 310.1477, found 310.1549. Purity: 99.6%

*5.1.4.2. N-Phenethylquinazolin-2-amine (**12b.*** Yield 47% (0.19 g, 0.76 mmol); mp 133–135 °C. $^1$H NMR (300 MHz, DMSO-$d_6$): δ 9.06 (s, 1H), δ 7.74 (dd, $J$ = 0.9, 8.0 Hz, 1H), δ 7.70–7.62 (m,

1H), δ 7.47–7.32 (m, 2H), δ 7.27–7.16 (m, 6H), δ 3.54 (q, *J* = 8.2 Hz, 2H), δ 2.88 (t, *J* = 7.6 Hz, 2H). HRMS (ESI) m/z calcd for $C_{16}H_{16}N_3$ $[M + H]^+$ 250.1266, found 250.1338. Purity: 98.0%

*5.1.5. General procedure for the synthesis of compounds **13a**–**d**.*

These compounds were synthesized as per our previously reported method [43]. Briefly, quinazoline derivatives **8a**–**d** (~1.86 mmol), 1.1 eq. $NaN_3$ (2.05 mmol), 4:1 EtOH (20 mL) and glacial acetic acid (5 mL) were taken in a 50 mL RBF and refluxed at 90–95 °C for 2 h with stirring. After cooling, 10 mol. % of Pd/C was added followed by slow addition of hydrazine hydrate (~2.79 mmol) and then stirred under reflux at 90–95 °C for an additional 2 h. The warm solution was washed with EtOH (2 x 20 mL) by passing through tightly packed cotton syringe. The ethanolic mixture was evaporated in vacuo to afford **13a**–**d** as white solids (yield = 80–85%).

*5.1.5.1. 2-Azido-N-(3,4-dimethoxybenzyl)quinazolin-4-amine (**13a**).* Yield 80% (0.41 g, 1.21 mmol); mp 253–255 °C. $^1$H NMR (300 MHz, DMSO-$d_6$): δ 9.34 (br s, 1H), δ 8.52 (d, *J* = 8.2 Hz, 1H), δ 8.32 (d, *J* = 8.3 Hz, 1H), δ 7.99 (t, *J* = 8.0 Hz, 1H), δ 7.73 (t, *J* = 8.0 Hz, 1H), δ 7.05 (s, 1H), δ 6.93–6.85 (m, 2H), δ 4.74 (d, *J* = 3.0 Hz, 2H), δ 3.71 (s, 3H), δ 3.67 (s, 3H). HRMS (ESI) m/z calcd for $C_{17}H_{16}N_6O_2$ $[M + H]^+$ 337.1335, found 337.1407. Purity: 98.5%

*5.1.5.2. 2-Azido-N-benzylquinazolin-4-amine (**13b**).* Yield 85% (0.43 g, 1.57 mmol); mp 224–226 °C. $^1$H NMR (300 MHz, DMSO-$d_6$): δ 9.40 (br s, 1H), δ 8.48 (d, *J* = 8.2 Hz, 1H), δ 8.29 (d, *J* = 8.3 Hz, 1H), δ 7.97 (t, *J* = 8.0 Hz, 1H), δ 7.72 (t, *J* = 8.0 Hz, 1H), δ 7.40–7.21 (m, 5H), δ

4.81 (d, *J* = 3.0 Hz, 2H). HRMS (ESI) m/z calcd for $C_{15}H_{13}N_6$ $[M + H]^+$ 277.1123, found 277.1195. Purity: 96.3%

*5.1.5.3. 2-Azido-N-(3,4-dimethoxyphenethyl)quinazolin-4-amine (**13c**).* Yield 82% (0.42 g, 1.20 mmol); mp 259–261 °C. $^1$H NMR (300 MHz, DMSO-$d_6$): δ 8.91 (br s, 1H), δ 8.42 (d, *J* = 8.2 Hz, 1H), δ 8.31 (d, *J* = 8.3 Hz, 1H), δ 7.96 (t, *J* = 8.0 Hz, 1H), δ 7.71 (t, *J* = 8.0 Hz, 1H), δ 6.86–6.78 (m, 3H), δ 3.78–3.76 (m, 2H), δ 3.67 (s, 6H), δ 2.91 (t, *J* = 7.2 Hz, 2H). $^{13}$C NMR (100 MHz, DMSO-$d_6$): δ 157.43, δ 153.90, δ 148.61, δ 147.28, δ 134.48, δ 132.33, δ 131.74, δ 127.72, δ 124.87, δ 120.54, δ 115.88, δ 112.61, δ 112.22, δ 111.90, δ 55.48, δ 55.32, δ 42.85, δ 33.46. HRMS (ESI) m/z calcd for $C_{18}H_{19}N_6O_2$ $[M + H]^+$ 351.1491, found 351.1564. Purity: 94.9%

*5.1.5.4. 2-Azido-N-phenethylquinazolin-4-amine (**13d**).* Yield 83% (0.42 g, 1.46 mmol); mp 233–235 °C. $^1$H NMR (300 MHz, DMSO-$d_6$): δ 8.96 (br s, 1H), δ 8.40 (d, *J* = 8.2 Hz, 1H), δ 8.30 (d, *J* = 8.3 Hz, 1H), δ 7.97 (t, *J* = 8.0 Hz, 1H), δ 7.71 (t, *J* = 8.0 Hz, 1H), δ 7.27–7.16 (m, 5H), δ 3.76 (q, *J* = 6.6 Hz, 2H), δ 2.97 (t, *J* = 7.3 Hz, 2H). HRMS (ESI) m/z calcd for $C_{16}H_{15}N_6$ $[M + H]^+$ 291.1280, found 291.1351. Purity: 97.8%

*5.1.6. General procedure for the synthesis of compounds* **15a–d**.

In a 50 mL RBF, 0.5 g of **8a–d** (1.45-1.85 mmol) was combined with 1.3 eq. of potassium formate (1.89–2.41 mmol) then was dissolved in 20 mL of formic acid. Solution was refluxed for 14–16 h at 120–125 °C. Upon completion and cooling to room temperature, the reaction mixture was diluted with ~ 30 mL of brine solution, ~ 50 mL of saturated $NaHCO_3$ solution before

extracting with ~ 25 mL (x3) of EtOAc and washed with 25 mL (x3) parts of brine solution. The combined aqueous layers were washed twice with 15 mL of EtOAc. The combined EtOAc layers were dried over $MgSO_4$ before removing the EtOAc in vacuo to yield a solid product that generally did not require additional purification. Additional purification as required, was accomplished by silica gel column chromatography using 5:1 EtOAc:MeOH as the eluent. The compounds were obtained as white solids with yields ranging from 58–70%.

*5.1.6.1. 4-((3,4-Dimethoxybenzyl)amino)quinazolin-2-ol (**15a**).* Yield 70% (0.33 g, 1.06 mmol); mp 202–204 °C. $^1$H NMR (300 MHz, DMSO-$d_6$): δ 10.61 (br s, 1H), δ 8.65 (t, $J$ = 5.7 Hz, 1H), δ 8.02 (d, $J$ = 8.1 Hz, 1H), δ 7.49 (t, $J$ = 7.5 Hz, 1H), δ 7.11–7.05 (m, 1H), δ 6.98 (s, 1H), δ 6.88–6.85 (m, 2H), δ 4.58 (d, $J$ = 5.6 Hz, 2H), δ 3.70 (s, 3H), δ 3.68 (s, 3H). HRMS (ESI) m/z calcd for $C_{17}H_{18}N_3O_3$ $[M + H]^+$ 312.1270, found 312.1342. Purity: 99.9%

*5.1.6.2. 4-(Benzylamino)quinazolin-2-ol* (***15b***). Yield 65% (0.30 g, 1.20 mmol); mp 198–200 °C. $^1$H-NMR (300 MHz, DMSO-$d_6$): δ 10.60 (br s, 1H), δ 8.67 (t, $J$ = 5.7 Hz, 1H), δ 8.47 (d, $J$ = 8.1 Hz, 1H), δ 8.35 (t, $J$ = 7.5 Hz, 1H), δ 7.31–7.09 (m, 7H), δ 4.66 (d, $J$ = 5.6 Hz, 2H). HRMS (ESI) m/z calcd for $C_{15}H_{14}N_3O$ $[M + H]^+$ 252.1059, found 252.1130. Purity: 99.7%

*5.1.6.3. 4-((3,4-Dimethoxyphenethyl)amino)quinazolin-2-ol* (***15c***). Yield 62% (0.29 g, 0.90 mmol); mp 210–212 °C. $^1$H NMR (300 MHz, DMSO-$d_6$): δ 10.60 (br s, 1H), δ 8.40 (br s, 1H), δ 8.02 (d, $J$ = 8.1 Hz, 1H), δ 7.47 (t, $J$ = 7.5 Hz, 1H), δ 7.12–7.02 (m, 2H), δ 6.83–6.71 (m, 3H), δ 3.70–3.60 (m, 8H), δ 2.82 (t, $J$ = 7.1 Hz, 2H). HRMS (ESI) m/z calcd for $C_{18}H_{20}N_3O_3$ $[M + H]^+$ 326.1426, found 326.1499. Purity: 97.3%

*5.1.6.4. 4-(Phenethylamino)quinazolin-2-ol (**15d**).* Yield 58% (0.27 g, 1.02 mmol); mp 189–191 °C. $^1$H NMR (300 MHz, DMSO-$d_6$): δ 10.60 (br s, 1H), δ 8.57 (br s, 1H), δ 8.06 (d, *J* = 8.1 Hz, 1H), δ 7.47 (t, *J* = 7.5 Hz, 1H), δ 7.29–7.02 (m, 7H), δ 3.60 (q, *J* = 7.6 Hz, 2H), δ 2.89 (t, *J* = 7.4 Hz, 2H). HRMS (ESI) m/z calcd for $C_{16}H_{16}N_3O$ $[M + H]^+$ 266.1215, found 266.1287. Purity: 96.9%

*5.1.7. General procedure for the synthesis of compounds* **18a–d**

These compounds were synthesized as per our previously reported method [43]. Briefly **8a**–**d** (~1.85 mmol) was mixed with 6 eq. urea (~11.2 mmol) and 10 mL of anhydrous 1,4-dioxane in a pressure vial, sealed tightly and heated at 160–165 °C in an oil bath for 24 h. After cooling to room temperature, the solution was diluted with 20 mL EtOAc, washed with 20 mL x 3 times brine solution; the aqueous layers were extracted twice with 20 mL EtOAc. The combined organic layers were dried over $MgSO_4$, evaporated in vacuo and purified using silica gel column chromatography using a combination of 5:1 EtOAc:MeOH and 5:1 EtOAc:MeOH w/ 1% TEA (triethylamine) to afford **18a**–**d** as white solids with yields ranging from 45–55%.

*5.1.7.1. 1-(4-((3,4-Dimethoxybenzyl)amino)quinazolin-2-yl)urea (**18a**).* Yield 45% (0.24 g, 0.68 mmol); mp 263–265 °C. $^1$H NMR (300 MHz, DMSO-$d_6$): δ 9.06 (br s, 1H), δ 8.80 (br s, 2H), δ 8.11 (d, *J* = 8.2 Hz, 1H), δ 7.59 (t, *J* = 7.5 Hz, 1H), δ 7.44 (d, *J* = 8.2 Hz, 1H), δ 7.23 (t, *J* = 7.3 Hz, 1H), δ 7.06 (br s, 1H), δ 6.95-6.82 (m, 3H), δ 4.60 (d, *J* = 5.7 Hz, 2H), δ 3.71 (s, 3H), δ 3.67 (s, 3H). HRMS (ESI) m/z calcd for $C_{18}H_{20}N_5O_3$ $[M + H]^+$ 354.1488, found 354.1560. Purity: 95.5%

*5.1.7.2. 1-(4-(Benzylamino)quinazolin-2-yl)urea (**18b**).* Yield 55% (0.30 g, 1.02 mmol); mp 214–216 °C. $^1$H NMR (300 MHz, DMSO-$d_6$): δ 9.11 (br s, 1H), δ 8.88 (br s, 1H), δ 8.76 (br s, 1H), δ 8.12 (d, *J* = 8.2 Hz, 1H), δ 7.42 (d, *J* = 8.2 Hz, 1H), δ 7.31–7.26 (m, 2H), δ 7.24–7.20 (m, 5H), δ 6.80 (br s, 1H), δ 4.70 (d, *J* = 5.7 Hz, 2H). HRMS (ESI) m/z calcd for $C_{16}H_{16}N_5O$ $[M + H]^+$ 294.1277, found 294.1348. Purity: 95.5%

*5.1.7.3. 1-(4-((3,4-Dimethoxyphenethyl)amino)quinazolin-2-yl)urea (**18c**).* Yield 47% (0.25 g, 0.68 mmol); mp 246–248 °C. $^1$H NMR (300 MHz, DMSO-$d_6$): δ 9.10 (br s, 1H), δ 8.76 (br s, 1H), δ 8.35 (br s, 1H), δ 8.03 (d, *J* = 8.2 Hz, 1H), δ 7.46 (t, *J* = 7.6 Hz, 1H), δ 7.44 (d, *J* = 8.2 Hz, 1H), δ 7.28 (t, *J* = 7.6 Hz, 1H), δ 6.90–6.78 (m, 4H), δ 3.70–3.67 (m, 8H), δ 2.86 (t, *J* = 7.5 Hz, 2H). HRMS (ESI) m/z calcd for $C_{19}H_{22}N_5O_3$ $[M + H]^+$ 368.1644, found 368.1718. Purity: 95.7%

*5.1.7.4. 1-(4-(Phenethylamino)quinazolin-2-yl)urea (**18d**).* Yield 51% (0.27 g, 0.90 mmol); mp 197–199 °C. $^1$H NMR (300 MHz, DMSO-$d_6$): δ 9.08 (br s, 1H), δ 8.83 (br s, 1H), δ 8.45 (br s, 1H), δ 8.05 (d, *J* = 8.2 Hz, 1H), δ 7.58 (t, *J* = 7.6 Hz, 1H), δ 7.44 (d, *J* = 8.2 Hz, 1H), δ 7.32–7.17 (m, 6H), δ 6.87 (br s, 1H), δ 3.67–3.62 (m, 2H), δ 2.90 (t, *J* = 7.5 Hz, 2H). HRMS (ESI) m/z calcd for $C_{17}H_{18}N_5O$ $[M + H]^+$ 308.1433, found 308.1505. Purity: 95.9%

*5.1.8. General procedure for the synthesis of compounds **19a–d** [32]*

In a 50 mL PV, 0.25 g of **8a–d** (0.73-0.93 mmol) was combined with 3 eq. (2.19-2.79 mmol) of glycinamide.HCl, dissolved in 5 mL of 1,4-dioxane followed by the addition of 5 eq. of DBU (3.65-4.65 mmol). Pressure vial was sealed and stirred in an oil bath at 150–155 °C for 4 h. Upon completion and cooling to room temperature, the reaction mixture was diluted with ~ 40 mL of EtOAc and washed with 25 mL (x3) brine solution. The combined aqueous layers were washed with ~ 25 mL of EtOAc, dried over $MgSO_4$ and EtOAc was removed in vacuo to yield a solid product that was purified by silica gel column chromatography using 5:1 EtOAc:MeOH as the eluent to afford target compounds as pale yellow to brown solids (yield = 52–58%).

*5.1.8.1. 2-((4-((3,4-Dimethoxybenzyl)amino)quinazolin-2-yl)amino)acetamide (**19a**).* Yield 54% (0.15 g, 0.41 mmol); mp 164–166 °C. $^1$H NMR (300 MHz, DMSO-$d_6$) δ 8.33 (br s, 1H), δ 8.02 (d, $J$ = 8.2 Hz, 1H), δ 7.47 (t, $J$ = 7.5 Hz, 1H), δ 7.23 (d, $J$ = 8.4 Hz, 2H), δ 7.09–7.03 (m, 2H), δ 6.96 (br s, 1H), δ 6.91–6.82 (m, 2H), δ 6.65 (br s, 1H), δ 4.60 (d, $J$ = 5.6 Hz, 2H), δ 3.98 (d, $J$ = 7.1 Hz, 2H), δ 3.70 (s, 3H), δ 3.68 (s, 3H). HRMS (ESI) m/z calcd for $C_{19}H_{22}N_5O_3$ $[M + H]^+$ 368.1644, found 368.1719. Purity: 99.4%

*5.1.8.2. 2-((4-(Benzylamino)quinazolin-2-yl)amino)acetamide (**19b**).* Yield 58% (0.16 g, 0.54 mmol); mp 161–163 °C. $^1$H NMR (300 MHz, DMSO-$d_6$): δ 8.23 (br s, 1H), δ 8.02 (d, $J$ = 8.2 Hz, 1H), δ 7.47 (t, $J$ = 7.5 Hz, 1H), δ 7.38–7.17 (m, 7H), δ 7.04 (t, $J$ = 7.5 Hz, 1H), δ 6.95 (br s, 1H), δ 6.45 (br s, 1H), δ 4.68 (d, $J$ = 5.5 Hz, 2H), δ 3.81 (d, $J$ = 5.2 Hz, 2H). HRMS (ESI) m/z calcd for $C_{17}H_{18}N_5O$ $[M + H]^+$ 308.1433, found 308.1506. Purity: 98.8%

*5.1.8.3 2-((4-((3,4-Dimethoxyphenethyl)amino)quinazolin-2-yl)amino)acetamide (**19c**).* Yield 52% (0.14 g, 0.38 mmol); mp 159–161 °C. $^1$H NMR (300 MHz, DMSO-$d_6$): δ 8.13 (br s, 1H), δ 7.93 (d, *J* = 8.2 Hz, 1H), δ 7.45 (t, *J* = 7.5 Hz, 1H), δ 7.21 (d, *J* = 8.4 Hz, 2H), δ 7.01 (t, *J* = 7.5 Hz, 1H), δ 6.97 (br s, 1H), δ 6.84–6.74 (m, 3H), δ 6.42 (br s, 1H), δ 3.86 (d, *J* = 7.1 Hz, 2H), δ 3.68 (s, 3H), δ 3.67 (s, 3H), δ 3.64–3.59 (m, 2H), δ 2.82 (t, *J* = 7.1 Hz, 2H). HRMS (ESI) m/z calcd for $C_{20}H_{24}N_5O_3$ $[M + H]^+$ 382.1801, found 382.1873. Purity: 99.6%

*5.1.8.4. 2-((4-(Phenethylamino)quinazolin-2-yl)amino)acetamide (**19d**).* Yield 55% (0.16 g, 0.48 mmol); mp 149–151 °C. $^1$H NMR (300 MHz, DMSO-$d_6$): δ 8.06 (br s, 1H), δ 7.92 (d, *J* = 8.2 Hz, 1H), δ 7.45 (t, *J* = 7.5 Hz, 1H), δ 7.28–7.16 (m, 7H), δ 7.01 (t, *J* = 7.5 Hz, 1H), δ 6.97 (br s, 1H), δ 6.37 (br s, 1H), δ 3.86 (d, *J* = 7.1 Hz, 2H), δ 3.61 (q, *J* = 5.9 Hz, 2H), δ 2.89 (t, *J* = 7.1 Hz, 2H). HRMS (ESI) m/z calcd for $C_{18}H_{20}N_5O$ $[M + H]^+$ 322.1590, found 322.1662. Purity: 99.2%

*5.1.9. General procedure for the synthesis of compounds **20a–d***

In a 50 mL RBF, 0.5 g of **14a–d** (1.54-2.00 mmol) was dissolved in 15 mL of 1,4-dioxane and 10 mL of glacial acetic acid/acetyl chloride combination (4:1 ratio). Solution was refluxed for 24 h at 90–95 °C. Upon completion and cooling to room temperature, the reaction mixture was diluted with ~ 30 mL of brine solution, ~ 30 mL of concentrated $NaHCO_3$ solution before extracting with ~ 25 mL (x3) of EtOAc. The combined EtOAc layers were dried over $MgSO_4$ and the organic solvent was removed in vacuo to yield a solid product that generally did not require additional purification. Purification was carried out as required, by silica gel column

chromatography using 5:1 EtOAc:MeOH as the eluent to afford target compounds as white solids with yields ranging from 35–42%.

*5.1.9.1. N-(4-((3,4-Dimethoxybenzyl)amino)quinazolin-2-yl)acetamide (**20a**).* Yield 55% (0.31 g, 0.88 mmol); mp 263–265 °C. $^1$H NMR (300 MHz, DMSO-$d_6$): δ 9.88 (br s, 1H), δ 8.67 (br s, 1H), δ 8.24 (d, *J* = 8.0 Hz, 1H), δ 7.64 (t, *J* = 7.2 Hz, 1H), δ 7.58 (d, *J* = 9.0 Hz, 1H), δ 7.26 (t, *J* = 6.0 Hz, 1H), δ 6.87–6.78 (m, 3H), δ 4.63 (d, *J* = 6.0 Hz, 2H), δ 3.69 (s, 3H), δ 3.67 (s, 3H), δ 2.24 (s, 3H). ESI-MS m/z calcd for $C_{19}H_{21}N_4O_3$ $[M + H]^+$ 353.15, found 353.17. Purity: 99.1%

*5.1.9.2. N-(4-(Benzylamino)quinazolin-2-yl)acetamide (**20b**).* Yield 50% (0.29 g, 0.99 mmol); mp 219–221 °C. $^1$H NMR (300 MHz, DMSO-$d_6$): δ 9.68 (br s, 1H), δ 8.18 (t, *J* = 6.0 Hz, 1H), δ 7.95 (d, *J* = 6.0 Hz, 1H), δ 7.42 (t, *J* = 8.4 Hz, 1H), δ 7.34–7.24 (m, 5H), δ 7.18 (d, *J* = 6.0 Hz, 1H), δ 6.95 (t, *J* = 6.0 Hz, 1H), δ 4.69 (d, *J* = 6.0 Hz, 2H), δ 2.22 (s, 3H). HRMS (ESI) m/z calcd for $C_{17}H_{17}N_4O$ $[M + H]^+$ 293.1324, found 293.1396. Purity: 99.9%

*5.1.9.3. N-(4-((3,4-Dimethoxyphenethyl)amino)quinazolin-2-yl)acetamide (**20c**).* Yield 57% (0.33 g, 0.90 mmol); mp 241–243 °C. $^1$H NMR (300 MHz, DMSO-$d_6$): δ 9.83 (br s, 1H), δ 8.47 (br s, 1H), δ 8.07 (d, *J* = 8.0 Hz, 1H), δ 7.60 (t, *J* = 7.2 Hz, 1H), δ 7.43 (d, *J* = 8.2 Hz, 1H), δ 7.26 (t, *J* = 6.0 Hz, 1H), δ 6.87-6.76 (m, 3H), δ 3.66–3.63 (m, 8H), δ 2.84 (t, *J* = 7.5 Hz, 2H), δ 2.52 (s, 3H). HRMS (ESI) m/z calcd for $C_{20}H_{23}N_4O_3$ $[M + H]^+$ 367.1692, found 367.1766. Purity: 96.8%

*5.1.9.4. N-(4-(Phenethylamino)quinazolin-2-yl)acetamide (**20d**)*: Yield 49% (0.28 g, 0.92 mmol); mp 187–189 °C. $^1$H NMR (300 MHz, DMSO-$d_6$): δ 9.45 (br s, 1H), δ 7.86 (m, 2H), δ 7.39 (t, *J* =

9.0 Hz, 1H), δ 7.27–7.16 (m, 6H), δ 6.93 (t, *J* = 6.0 Hz, 1H), δ 3.63 (q, *J* = 6.0 Hz, 2H), δ 2.92 (t, *J* = 7.5 Hz, 2H), δ 2.26 (s, 3H). HRMS (ESI) m/z calcd for $C_{18}H_{19}N_4O$ $[M + H]^+$ 307.1481, found 307.1553. Purity: 99.9%

*5.1.10. General procedure for the synthesis of compounds **21a–t** [32]*

In a 50 mL pressure vial (PV), 0.25 g of **8a–d** (0.73-0.93 mmol) was combined with 2 eq. (1.46-1.86 mmol) of primary amine (methyl-, ethyl-, *n*-propyl-, isopropyl- or cyclopropylamine), dissolved in 5 mL of 1,4-dioxane followed by the addition of 3 eq. of DIPEA (2.19–2.79 mmol). The pressure vial was sealed and stirred in an oil bath at 150–155 °C for 2 h. Upon completion and cooling to room temperature, the reaction mixture was diluted with ~ 40 mL of EtOAc and washed with brine solution (25 mL x 2). The combined aqueous layer was washed with ~ 25 mL of EtOAc, dried over $MgSO_4$ before removing EtOAc in vacuo to yield a solid product that was purified by silica gel column chromatography using 5:1 EtOAc:MeOH as the eluent to afford pale yellow to brown solids (yield range = 55–70%).

*5.1.10.1. $N^4$-(3,4-Dimethoxybenzyl)-$N^2$-methylquinazoline-2,4-diamine (**21a**).* Yield 68% (0.33 g, 1.02 mmol); mp 199–201 °C. $^1$H NMR (300 MHz, DMSO-$d_6$): δ 8.23 (br s, 1H), δ 8.01 (d, *J* = 8.0 Hz, 1H), δ 7.41 (t, *J* = 7.2 Hz, 1H), δ 7.21 (m, 2H), δ 6.95 (t, *J* = 6.0 Hz, 1H), δ 6.84–6.80 (m, 2H), δ 6.50 (br s, 1H), δ 4.58 (d, *J* = 6.0 Hz, 2H), δ 3.68 (s, 3H), δ 3.66 (s, 3H), δ 2.77 (d, *J* = 4.5 Hz, 3H). HRMS (ESI) m/z calcd for $C_{18}H_{21}N_4O_2$ $[M + H]^+$ 325.1586, found 325.1659. Purity: 97.6%

*5.1.10.2. $N^4$-(3,4-Dimethoxybenzyl)-$N^2$-ethylquinazoline-2,4-diamine (**21b**).* Yield 67% (0.36 g, 1.06 mmol); mp 186–188 °C. $^1$H NMR (300 MHz, DMSO-$d_6$): δ 8.25 (br s, 1H), δ 7.95 (d, *J* =

8.0 Hz, 1H), δ 7.41 (t, *J* = 7.2 Hz, 1H), δ 7.20–7.18 (m, 1H), δ 7.00–6.95 (m, 2H), δ 6.84–6.72 (m, 2H), δ 6.40 (br s, 1H), δ 4.59 (d, *J* = 6.0 Hz, 2H), δ 3.68 (s, 3H), δ 3.66 (s, 3H), δ 3.24–3.19 (m, 2H), δ 1.06 (t, *J* = 7.0 Hz, 3H). HRMS (ESI) m/z calcd for $C_{19}H_{23}N_4O_2$ $[M + H]^+$ 339.1743, found 339.1817. Purity: 98.8%

*5.1.10.3. $N^4$-(3,4-Dimethoxybenzyl)-$N^2$-propylquinazoline-2,4-diamine (**21c**).* Yield 65% (0.34 g, 0.97 mmol); mp 156–158 °C. $^1$H NMR (300 MHz, DMSO-$d_6$): δ 8.20 (br s, 1H), δ 7.90 (d, *J* = 8.0 Hz, 1H), δ 7.40 (t, *J* = 7.2 Hz, 1H), δ 7.15 (d, *J* = 9.0 Hz, 1H), δ 7.05–6.95 (m, 2H), δ 6.82-6.74 (m, 2H), δ 6.50 (br s, 1H), δ 4.58 (d, *J* = 6.0 Hz, 2H), δ 3.68 (s, 3H), δ 3.66 (s, 3H), δ 3.24–3.19 (m, 2H), δ 1.46 (q, *J* = 7.0 Hz, 2H), δ 0.80 (t, *J* = 7.0 Hz, 3H). HRMS (ESI) m/z calcd for $C_{20}H_{25}N_4O_2$ $[M + H]^+$ 353.1899, found 353.1927. Purity: 98.9%

*5.1.10.4. $N^4$-(3,4-Dimethoxybenzyl)-$N^2$-isopropylquinazoline-2,4-diamine (**21d**).* Yield 68% (0.36 g, 1.02 mmol); mp 177–179 °C. $^1$H NMR (300 MHz, DMSO-$d_6$): δ 8.21 (br s, 1H), δ 7.95 (d, *J* = 8.0 Hz, 1H), δ 7.39 (t, *J* = 7.2 Hz, 1H), δ 7.20 (d, *J* = 9.0 Hz, 1H), δ 7.02–6.95 (m, 2H), δ 6.84–6.72 (m, 2H), δ 6.20 (br s, 1H), δ 4.58 (d, *J* = 6.0 Hz, 2H), δ 4.10–4.05 (m, 1H), δ 3.68 (s, 3H), δ 3.66 (s, 3H), δ 1.07 (d, *J* = 6.0 Hz, 6H). HRMS (ESI) m/z calcd for $C_{20}H_{25}N_4O_2$ $[M + H]^+$ 353.1899, found 353.1926. Purity: 98.6%

*5.1.10.5. $N^2$-Cyclopropyl-$N^4$-(3,4-dimethoxybenzyl)quinazoline-2,4-diamine (**21e**).* Yield 70% (0.37 g, 1.06 mmol); mp 201–203 °C. $^1$H NMR (300 MHz, DMSO-$d_6$): δ 8.20 (br s, 1H), δ 7.85 (d, *J* = 8.0 Hz, 1H), δ 7.40 (t, *J* = 7.2 Hz, 1H), δ 7.20 (d, *J* = 9.0 Hz, 1H), δ 7.00–6.97 (m, 2H), δ 6.84-6.70 (m, 2H), δ 6.60 (br s, 1H), δ 4.59 (d, *J* = 6.0 Hz, 2H), δ 3.67 (s, 3H), δ 3.66 (s, 3H), δ

2.46–2.42 (m, 1H), δ 0.63-0.58 (m, 2H), δ 0.48–0.41 (m, 2H). HRMS (ESI) m/z calcd for $C_{20}H_{23}N_4O_2$ $[M + H]^+$ 351.1743, found 351.1816. Purity: 98.2%

*5.1.10.6. $N^4$-(Benzyl)-$N^2$-methylquinazoline-2,4-diamine (**21f**).* Yield 68% (0.33 g, 1.25 mmol); mp 139–141 °C. $^1$H NMR (300 MHz, DMSO-$d_6$): δ 8.23 (t, *J* = 6.0 Hz, 1H), δ 7.95 (d, *J* = 6.0 Hz, 1H), δ 7.55 (t, *J* = 9.0 Hz, 1H), δ 7.34–7.20 (m, 6H), δ 6.99 (t, *J* = 6.0 Hz, 1H), δ 6.53 (br s, 1H), δ 4.66 (d, *J* = 6.0 Hz, 2H), δ 2.74 (d, *J* = 4.7 Hz, 3H). HRMS (ESI) m/z calcd for $C_{16}H_{17}N_4$ $[M + H]^+$ 265.1375, found 265.1446. Purity: 100.0%

*5.1.10.7. $N^4$-(Benzyl)-$N^2$-ethylquinazoline-2,4-diamine (**21g**).* Yield 70% (0.36 g, 1.29 mmol); mp 130–132 °C. $^1$H NMR (300 MHz, DMSO-$d_6$): δ 8.25 (t, *J* = 6.0 Hz, 1H), δ 7.96 (d, *J* = 6.0 Hz, 1H), δ 7.45 (t, *J* = 9.0 Hz, 1H), δ 7.36–7.18 (m, 6H), δ 6.99 (t, *J* = 6.0 Hz, 1H), δ 6.40 (br s, 1H), δ 4.67 (d, *J* = 6.0 Hz, 2H), δ 3.27–3.22 (m, 2H), δ 1.03 (t, *J* = 6.0 Hz, 3H). $^{13}$C NMR (100 MHz, DMSO-$d_6$) δ 159.78, δ 159.57, δ 158.96, δ 151.63, δ 139.94, δ 132.33, δ 128.16, δ 127.98, δ 127.34, δ 127.26, δ 126.58, δ 126.23, δ 122.68, δ 119.90, δ 43.26, δ 35.25, δ 15.08. HRMS (ESI) m/z calcd for $C_{17}H_{19}N_4$ $[M + H]^+$ 279.1531, found 279.1602. Purity: 98.0%

*5.1.10.8. $N^4$-(Benzyl)-$N^2$-propylquinazoline-2,4-diamine (**21h**).* Yield 58% (0.31 g, 1.06 mmol); mp 114–116 °C. $^1$H NMR (300 MHz, DMSO-$d_6$): δ 8.21 (t, *J* = 6.0 Hz, 1H), δ 7.94 (d, *J* = 6.0 Hz, 1H), δ 7.42 (t, *J* = 9.0 Hz, 1H), δ 7.35–7.23 (m, 4H), δ 7.18 (m, 2H), δ 6.95 (t, *J* = 6.0 Hz, 1H), δ 6.40 (br s, 1H), δ 4.66 (d, *J* = 6.0 Hz, 2H), δ 3.14 (q, *J* = 6.0 Hz, 2H), δ 1.45–1.40 (m, *2*H), δ 0.78 (t, *J* = 7.5 Hz, 3H). HRMS (ESI) m/z calcd for $C_{18}H_{21}N_4$ $[M + H]^+$ 293.1688, found 293.1759. Purity: 98.9%

*5.1.10.9. $N^4$-(Benzyl)-$N^2$-isopropylquinazoline-2,4-diamine (**21i**).* Yield 67% (0.37 g, 1.27 mmol); mp 135–137 °C. $^1$H NMR (300 MHz, DMSO-$d_6$): δ 8.30 (t, *J* = 6.0 Hz, 1H), δ 7.90 (d, *J* = 6.0 Hz, 1H), δ 7.42 (t, *J* = 9.0 Hz, 1H), δ 7.35–7.23 (m, 4H), δ 7.20–7.18 (m, 2H), δ 6.90 (t, *J* = 6.0 Hz, 1H), δ 6.28 (br s, 1H), δ 4.67 (d, *J* = 6.0 Hz, 2H), δ 4.13–3.99 (m, 1H), δ 1.05 (d, *J* = 6.0 Hz, 6H). HRMS (ESI) m/z calcd for $C_{18}H_{21}N_4$ $[M + H]^+$ 293.1688, found 293.1759. Purity: 98.1%

*5.1.10.10. $N^4$-(Benzyl)-$N^2$-cyclopropylquinazoline-2,4-diamine (**21j**).* Yield 56% (0.30 g, 1.03 mmol); mp 145–147 °C. $^1$H NMR (300 MHz, DMSO-$d_6$): δ 8.25 (t, *J* = 6.0 Hz, 1H), δ 7.98 (d, *J* = 6.0 Hz, 1H), δ 7.40 (t, *J* = 9.0 Hz, 1H), δ 7.30–7.20 (m, 5H), δ 7.18 (d, *J* = 6.0 Hz, 1H), δ 6.95 (t, *J* = 6.0 Hz, 1H), δ 6.45 (br s, 1H), δ 4.68 (d, *J* = 6.0 Hz, 2H), δ 2.78–2.66 (m, 1H), δ 0.60 (d, *J* = 4.8 Hz, 2H), δ 0.45 (d, *J* = 4.8 Hz, 2H). HRMS (ESI) m/z calcd for $C_{18}H_{19}N_4$ $[M + H]^+$ 291.1531, found 291.1603. Purity: 99.6%

*5.1.10.11. $N^4$-(3,4-Dimethoxyphenethyl)-$N^2$-methylquinazoline-2,4-diamine (**21k**).* Yield 70% (0.34 g, 1.01 mmol); mp 153–155 °C. $^1$H NMR (300 MHz, DMSO-$d_6$): δ 7.87 (d, *J* = 8.0 Hz, 2H), δ 7.40 (t, *J* = 7.2 Hz, 1H), δ 7.19 (d, *J* = 9.0 Hz, 1H), δ 6.94 (t, *J* = 6.0 Hz, 1H), δ 6.83–6.72 (m, 3H), δ 6.42 (br s, 1H), δ 3.66 (s, 6H), δ 3.63–3.60 (m, 2H), δ 2.86–2.79 (m, 2H), δ 2.80 (d, *J* = 4.5 Hz, 3H). HRMS (ESI) m/z calcd for $C_{19}H_{23}N_4O_2$ $[M + H]^+$ 339.1743, found 339.1816. Purity: 97.8%

*5.1.10.12. $N^4$-(3,4-Dimethoxyphenethyl)-$N^2$-ethylquinazoline-2,4-diamine (**21l**).* Yield 70% (0.33 g, 0.94 mmol); mp 157–159 °C. $^1$H NMR (300 MHz, DMSO-$d_6$): δ 7.86 (d, *J* = 8.0 Hz, 2H), δ 7.41 (t, *J* = 7.2 Hz, 1H), δ 7.19 (d, *J* = 9.0 Hz, 1H), δ 6.96 (t, *J* = 6.0 Hz, 1H), δ 6.84-6.75 (m,

3H), δ 6.40 (br s, 1H), δ 3.67 (s, 6H), δ 3.63–3.60 (m, 2H), δ 3.34–3.32 (m, 2H), δ 2.82 (t, *J* = 7.2 Hz, 2H), δ 1.08 (t, *J* = 7.0 Hz, 3H). HRMS (ESI) m/z calcd for $C_{20}H_{24}N_4O_2$ $[M + H]^+$ 353.1899, found 353.1971. Purity: 98.6%

*5.1.10.13. $N^4$-(3,4-Dimethoxyphenethyl)-$N^2$-propylquinazoline-2,4-diamine (**21m**).* Yield 68% (0.36 g, 0.98 mmol); mp 127–129 °C. $^1$H NMR (300 MHz, DMSO-$d_6$): δ 7.87 (d, *J* = 8.0 Hz, 2H), δ 7.39 (t, *J* = 7.2 Hz, 1H), δ 7.16 (d, *J* = 9.0 Hz, 1H), δ 6.94 (t, *J* = 6.0 Hz, 1H), δ 6.83-6.72 (m, 3H), δ 6.52 (br s, 1H), δ 3.63 (s, 6H), δ 3.63–3.60 (m, 2H), δ 3.34–3.32 (m, 2H), δ 2.82 (t, *J* = 7.2 Hz, 2H), δ 1.59–1.46 (m, 2H), 0.83 (t, *J* = 7.0 Hz, 3H). HRMS (ESI) m/z calcd for $C_{21}H_{27}N_4O_2$ $[M + H]^+$ 367.2056, found 367.2132. Purity: 99.0%

*5.1.10.14. $N^4$-(3,4-Dimethoxyphenethyl)-$N^2$-isopropylquinazoline-2,4-diamine (**21n**).* Yield 67% (0.35 g, 0.96 mmol); mp 134–136 °C. $^1$H NMR (300 MHz, DMSO-$d_6$): δ 7.90 (d, *J* = 8.0 Hz, 2H), δ 7.45 (t, *J* = 7.2 Hz, 1H), δ 7.18 (d, *J* = 9.0 Hz, 1H), δ 7.00 (t, *J* = 6.0 Hz, 1H), δ 6.84–6.72 (m, 3H), δ 6.55 (br s, 1H), δ 4.02–3.95 (m, 1H), δ 3.66 (s, 6H), δ 3.63–3.60 (m, 2H), δ 2.82 (t, *J* = 7.2 Hz, 2H), δ 1.13 (d, *J* = 6.0 Hz, 6H). HRMS (ESI) m/z calcd for $C_{21}H_{27}N_4O_2$ $[M + H]^+$ 367.2056, found 367.2131. Purity: 97.5%

*5.1.10.15. $N^2$-Cyclopropyl-$N^4$-(3,4-dimethoxyphenethyl)quinazoline-2,4-diamine (**21o**).* Yield 67% (0.35 g, 0.96 mmol); mp 166–168 °C. $^1$H NMR (300 MHz, DMSO-$d_6$): δ 7.90 (d, *J* = 8.0 Hz, 2H), δ 7.40 (t, *J* = 7.2 Hz, 1H), δ 7.20 (d, *J* = 9.0 Hz, 1H), δ 7.00 (t, *J* = 6.0 Hz, 1H), δ 6.85–6.72 (m, 3H), δ 6.48 (br s, 1H), δ 3.68–3.65 (m, 8H), δ 2.85–2.80 (m, 3H), δ 0.63–0.55 (m, 2H), δ 0.48-0.40 (m, 2H). HRMS (ESI) m/z calcd for $C_{21}H_{25}N_4O_2$ $[M + H]^+$ 365.1899, found 365.1975. Purity: 95.8%

*5.1.10.16. $N^2$-Methyl-$N^4$-(phenethyl)quinazoline-2,4-diamine (**21p**).* Yield 65% (0.32 g, 1.15 mmol); mp 121–123 °C. $^1$H NMR (300 MHz, DMSO-$d_6$): δ 7.97 (m, 2H), δ 7.42 (t, $J$ = 9.0 Hz, 1H), δ 7.29–7.16 (m, 6H), δ 6.93 (t, $J$ = 6.0 Hz, 1H), δ 6.35 (br s, 1H), δ 3.60 (q, $J$ = 6.0 Hz, 2H), δ 2.80 (t, $J$ = 9.0 Hz, 2H), δ 2.70 (d, $J$ = 3.0 Hz, 3H). HRMS (ESI) m/z calcd for $C_{17}H_{19}N_4$ [M + H]$^+$ 279.1531, found 279.1603. Purity: 98.6%

*5.1.10.17. $N^2$-Ethyl-$N^4$-(phenethyl)quinazoline-2,4-diamine (**21q**).* Yield 61% (0.31 g, 1.06 mmol); mp 117–119 °C. $^1$H NMR (300 MHz, DMSO-$d_6$): δ 7.86 (m, 2H), δ 7.43 (t, $J$ = 9.0 Hz, 1H), δ 7.30–7.16 (m, 6H), δ 6.97 (t, $J$ = 6.0 Hz, 1H), δ 6.50 (br s, 1H), δ 3.61 (q, $J$ = 6.0 Hz, 2H), δ 3.32 (d, $J$ = 9.0 Hz, 2H), δ 2.92 (t, $J$ = 9.0 Hz, 2H), δ 1.09 (t, $J$ = 6.0 Hz, 3H). HRMS (ESI) m/z calcd for $C_{18}H_{21}N_4$ [M + H]$^+$ 293.1688, found 293.1795. Purity: 98.0%

*5.1.10.18. $N^4$-(Phenethyl)-$N^2$-propylquinazoline-2,4-diamine (**21r**).* Yield 55% (0.30 g, 0.98 mmol); mp 102–104 °C. $^1$H NMR (300 MHz, DMSO-$d_6$): δ 7.86 (m, 2H), δ 7.39 (t, $J$ = 9.0 Hz, 1H), δ 7.27–7.16 (m, 6H), δ 6.93 (t, $J$ = 6.0 Hz, 1H), δ 6.40 (br s, 1H), δ 3.60 (q, $J$ = 6.0 Hz, 2H), δ 3.30–3.24 (m, 2H), δ 2.89 (t, $J$ = 7.5 Hz, 2H), δ 1.56–1.49 (sextet, $J$ = 6.0 Hz, 2H), δ 0.84 (t, $J$ = 7.5 Hz, 3H). HRMS (ESI) m/z calcd for $C_{19}H_{23}N_4$ [M + H]$^+$ 307.1844, found 307.1916. Purity: 100.0%

*5.1.10.19. $N^2$-Isopropyl-$N^4$-(phenethyl)quinazoline-2,4-diamine (**21s**).* Yield 58% (0.32 g, 1.06 mmol); mp 112–114 °C. $^1$H NMR (300 MHz, DMSO-$d_6$): δ 7.89 (m, 2H), δ 7.40 (t, $J$ = 9.0 Hz, 1H), δ 7.27–7.17 (m, 6H), δ 6.98 (t, $J$ = 6.0 Hz, 1H), δ 6.30 (br s, 1H), δ 4.12 (m, 1H), δ 3.60 (q, $J$ = 6.0 Hz, 2H), δ 2.91 (t, $J$ = 7.5 Hz, 2H), δ 1.12 (d, $J$ = 6.0 Hz, 6H). HRMS (ESI) m/z calcd for $C_{19}H_{23}N_4$ [M + H]$^+$ 307.1844, found 307.1916. Purity: 98.5%

*5.1.10.20. $N^2$-Cyclopropyl-$N^4$-(phenethyl)quinazoline-2,4-diamine (**21t**).* Yield 58% (0.32 g, 1.05 mmol); mp 116–118 °C. $^1$H NMR (300 MHz, DMSO-$d_6$): δ 7.87 (m, 2H), δ 7.40 (t, *J* = 9.0 Hz, 1H), δ 7.30–7.12 (m, 6H), δ 6.90 (t, *J* = 6.0 Hz, 1H), δ 6.60 (br s, 1H), δ 3.63 (q, *J* = 6.0 Hz, 2H), δ 2.92 (t, *J* = 7.5 Hz, 2H), δ 2.82 (m, 1H), δ 0.59 (d, *J* = 4.8 Hz, 2H), δ 0.44 (d, *J* = 4.8 Hz, 2H). HRMS (ESI) m/z calcd for $C_{19}H_{21}N_4$ $[M + H]^+$ 305.1688, found 305.1759. Purity: 100.0%

*5.1.11. Cholinesterase inhibition assay*

The inhibition profile of quinazoline derivatives was evaluated using Ellman's reagent [46]. Human AChE and BuChE enzymes were obtained from Sigma-Aldrich, St. Louis, MO, USA (AChE product number C0663 and BuChE product number B4186 respectively). The cholinesterase inhibitors tacrine (item number 70240, Cayman Chemical Company, Ann Arbor, MI), donepezil (product number D6821, Sigma-Aldrich, St. Louis, MO), galantamine (product number G1660, Sigma-Aldrich, St. Louis, MO) and rivastigmine (product number SML0881, Sigma-Aldrich, St. Louis, MO) were used as reference agents. Quinazoline derivative stock solutions were prepared in DMSO (maximum 1% v/v in final wells) and diluted in buffer solution (50 mM Tris.HCl, pH 8.0, 0.1 M NaCl, 0.02 M $MgCl_2.6H_2O$). Then 160 µL of 5,5'-dithiobis(2-nitrobenzoic acid) (1.5 mm DTNB), 50 µL of *h*AChE (0.22 U/mL in 50 mm Tris.HCl, pH 8.0, 0.1% w/v bovine serum albumin, BSA) or 50 µL of *h*BuChE (0.12 U/mL in 50 mM Tris.HCl, pH 8.0, 0.1% w/v BSA) were added to 96-well plates after which 10 µL each of quinazoline derivatives (final concentration range 0.1–50 µM) were added and incubated for 5 min. Then 30 µL of either acetylthiocholine iodide (15 mM ATCl prepared in ultra-pure water) or *S*-butyrylthiocholine iodide (15 mM BTCI prepared in ultra-pure water) were added. The absorbance was measured at different time intervals (0, 60, 120, 180, 240 and 300 s) using a

wavelength of 412 nm. The inhibitory concentration ($IC_{50}$ values) was calculated from the concentration–inhibition dose response curve on a logarithmic scale. The results were expressed as average values based on two to three independent experiments run in triplicate measurements.

*5.1.12. Aβ-aggregation kinetics by thioflavin T (ThT) fluorescence studies*

The ability of quinazoline-based derivatives to inhibit Aβ-aggregation kinetics was determined using a thioflavin T (ThT)-based fluorescence assay [47]. These assays were conducted in Costar, black-surround, clear-bottom 384-well plates with frequent shaking (30 sec. of linear shaking at 730 cpm every 5 minutes) and constant heating at 37 °C for 24 h. The ThT excitation/emission was measured at 440 nm/490 nm and readings were taken every 5 minutes using a BioTek Synergy H1 microplate reader. Quinazoline stock solutions were prepared in DMSO and diluted to 10x in 215 mM phosphate buffer at pH 7.4. Abeta.HFIP samples (Aβ40 or Aβ42, rPeptide, Bogart, USA) were dissolved in 1% ammonium hydroxide, sonicated at room temperature for 5 minutes then diluted to 50 μM in 215 mM phosphate buffer (pH 7.4). A 15 μM ThT stock solution was prepared with 50 mM glycine and adjusted to pH 7.4. The assay was carried out by adding 44 μL of ThT, 20–35 μL buffer, 1 μL DMSO (for background and controls only) followed by the addition of 8 μL of 10x compound dilutions (1–25 μM concentration range). An end point reading was conducted to evaluate potential test compound interference with ThT-fluorescence before adding 8 μL of Aβ40 or Aβ42 stock solutions (5 μM final concentration). Plates were sealed with a transparent plate film before initiating the assay. RFU values were corrected for ThT-interference before calculating end point percent inhibitions or $IC_{50}$ values to obtain the aggregation kinetic plots. Data presented was an average of triplicate reading for two-three independent experiments.

*5.1.13. Transmission electron microscopy (TEM)*

In Costar 96-well, round-bottom plates were added 80 μL of 215 mM phosphate buffer, 20 μL of 10x test compound dilutions (250 μM – prepared in the same way as for the ThT assay) and 100 μL of Aβ40 or Aβ42 respectively (50 μM each). For the control wells, 2 μL of DMSO and 18 μL of phosphate buffer was added. Final Aβ: test compound ratio was 1:1 (25 μM:25 μM). Plates were incubated on a Fisher plate incubator set to 37 °C and the contents were shaken at 730 cpm for 24 h. To prepare the TEM grids, ~ 20 μL droplet was added using a disposable Pasteur pipette over the formvar-coated copper grids (400 mesh). Grids were air-dried for about 3 h before adding two droplets (~ 40 μL, using a disposable Pasteur pipette) of ultra-pure water and using small pieces of filter paper to wash out precipitated buffer salts. After air-drying for ~ 15-20 min, the grids were negatively stained by adding a droplet (~ 20 μL, using a disposable Pasteur pipette) of 2% phosphotungstic acid (PTA) and immediately after the grids were dried using small pieces of filter paper. Grids were further air-dried overnight. The scanning was carried out using a Philips CM 10 transmission electron microscope at 60 kV (Department of Biology, University of Waterloo) and micrographs were obtained using a 14-megapixel AMT camera [48].

*5.1.14. Antioxidant capacity (DPPH scavenging)*

The ability of $N^4$-substituted quinazoline-2-ols to scavenge the DPPH radical was utilized as a measure of antioxidant capacity [50]. Quinazoline derivatives (500 μM) and DPPH (56 μM) stock solutions were prepared in anhydrous methanol. The addition sequence was carried out in a 96-well clear, flat bottom plate as follows: 90 μL DPPH, 10 μL test compound solution (50 μM) final concentration. Control solutions contained 90 μL anhydrous methanol and 10 μL test

compound whereas DPPH control contained 90 μL of DPPH, and 10 μL anhydrous methanol. The readings were taken initially at 517 nm with 30 sec. shaking (double orbital at 530 cpm) prior to the 1 h, light restrictive, incubation period at room temperature after which readings were taken again at 517 nm after another round of 30 sec shaking (double orbital at 530 cpm) using a BioTek Synergy H1 microplate reader. The results were expressed as percentage inhibition and the data presented was average of triplicate reading (for two independent experiments).

*5.1.15. Molecular docking studies*

The molecular docking experiments were conducted using the computational software Discovery Studio (DS), Structure-Based-Design program (version 4.0) from BIOVIA Inc. San Diego, USA. The quinazolines derivatives **9**, **14c**, **15b**, **21q**, **21s** and **21t** were built using the *small molecules* module in DS. The x-ray coordinates of cholinesterases were obtained from protein data bank (AChE PDB id: 1B41 and BuChE PDB id: 1P0I) [54, 55], to dock quinazolines **9**, **14c**, **21q** and **21s**. The protein structures were prepared using the *macromolecules* module in DS. Ligand binding site was defined by selecting a 12 Å radius sphere for AChE and 15 Å radius sphere for BuChE. The molecular docking was performed using the *receptor-ligand interactions* module in DS. The LibDock algorithm was used to find the most appropriate binding modes of quinazoline derivatives using CHARMm force field. The docked poses obtained were ranked based on the LibDock scores and the binding modes were analyzed by evaluating all the polar and nonpolar interactions. For Aβ docking studies, the NMR solution structure of both Aβ fibrils were obtained from protein data bank (PDB id: 2LMN) [52]. The Aβ dimer and Aβ fibril assemblies were built using the *macromolecules* module in DS [56]. Ligand binding site was defined by

selecting a 15 Å radius sphere for both Aβ dimer and fibril assembly. Then molecular docking was performed using the *receptor-ligand interactions* module in DS. The LibDock algorithm was used to find the most appropriate binding modes of quinazoline derivatives (**15b** and **21t**) using CHARMm force field. The docked poses obtained were ranked based on the LibDock scores and the binding modes were analyzed by evaluating all the polar and nonpolar interactions.

**Acknowledgments**

The authors would like to thank the Faculty of Science, the School of Pharmacy, University of Waterloo, the Ontario Mental Health Foundation (TM), NSERC-Discovery (RGPIN: 03830-2014), Canada Foundation of Innovation, CFI-JELF; Ontario Research Fund (ORF) and Early Researcher Award, Ministry of Research and Innovation, Government of Ontario, Canada (PR) for financial support of this research project.

**Supplementary data**

Supplementary data related to this article can be found at

**References**

[1] C. Takizawa, P. L. Thompson, A. van Walsem, C. Faure, W. C. Maier, Epidemiological and economic burden of Alzheimer's disease: a systematic literature data across Europe and United States of America, J. Alzheimers Dis. 43 (2015) 1271–1284.
[2] W. H. Suh, K. S. Suslick, Y. H. Suh, Therapeutic agents for Alzheimer's disease, Curr. Med. Chem. 5 (2005) 259–269.
[3] J. Birks, Cholinesterase inhibitors for Alzheimer's disease, Cochrane Database Syst. Rev. (2006) CD005593.

[4] Y. Takada-Takatori, T. Kume, M. Sugimoto, H. Katsuki, H. Sugimoto, A. Akaike, Acetylcholinesterase inhibitors used in treatment of Alzheimer's disease prevent glutamate neurotoxicity via nicotinic acetylcholine receptors and phosphatidylinositol 3-kinase cascade, Neuropharmacology 51 (2006) 474–486.

[5] I. E. Orhan, G. Orhan, E. Gurkas, An overview on natural cholinesterase inhibitors-a multitargeted drug class-and their mass production. Mini Rev. Med. Chem. 11 (2011) 836–842.

[6] X. Zhao, W. Marszalec, P. T. Toth, J. Huang, J. Z. Yeh, T. Narahashi, In vitro galantamine-memantine co-application: mechanism of beneficial action, Neuropharmacology 51 (2006) 1181–1191.

[7] H. Geerts, P. O. Guillaumat, C. Grantham, W. Bode, K. Anciaux, S. Sachak, Brain levels and acetylcholinesterase inhibition with galantamine and donepezil in rats, mice, and rabbits, Brain Res. 1033 (2005) 186–193.

[8] I. Caesar, M. Jonson, K. P. Nilsson, S. Thor, P. Hammarstrom, Curcumin promotes Abeta fibrillation and reduces neurotoxicity in transgenic Drosophila, PLoS One 7 (2012) e31424.

[9] S. Dolai, W. Shi, C. Corbo, C. Sun, S. Averick, D. Obeysekera, M. Farid, A. Alonso, P. Banerjee, K. Raja, "Clicked" sugar-curcumin conjugate: modulator of amyloid-beta and tau peptide aggregation at ultralow concentrations, ACS Chem. Neurosci. 2 (2011) 694–699.

[10] J. Kim, H. J. Lee, K. W. Lee, Naturally occurring phytochemicals for the prevention of Alzheimer's disease, J. Neurochem. 112 (2010) 1415–1430.

[11] F. Yang, G. P. Lim, A. N. Begum, O. J. Ubeda, M. R. Simmons, S. S. Ambegaokar, P. P. Chen, R. Kayed, C. G. Glabe, S. A. Frautschy, G. M. Cole, Curcumin inhibits formation of amyloid beta oligomers and fibrils, binds plaques, and reduces amyloid in vivo, J. Biol. Chem. 280 (2005) 5892–5901.

[12] Y. Feng, X. P. Wang, S. G. Yang, Y. J. Wang, X. Zhang, X. T. Du, X. X. Sun, M. Zhao, L. Huang, R. T. Liu, Resveratrol inhibits beta-amyloid oligomeric cytotoxicity but does not prevent oligomer formation, Neurotoxicology 30 (2009) 986–995.

[13] X. L. Bu, P. P. N. Rao, Y. J. Wang, Anti-amyloid aggregation activity of natural compounds: implications for Alzheimer's drug discovery, Mol. Neurobiol. 53 (2015) 3565–3575.

[14] D. J. Selkoe, Alzheimer's disease genes, proteins, and therapy, Physiol. Rev. 81 (2001) 741–766.

[15] D. J. Selkoe, Cell biology of protein misfolding: The examples of Alzheimer's and Parkinson's diseases, Nat. Cell Biol. 6 (2004) 1054–1061.
[16] M. Landau, M. R. Sawaya, K. F. Faull, A. Laganowsky, H. Jiang, S. A. Sievers, J. Liu, J. R. Barrio, D. Eisenberg, Towards a pharmacophore for amyloid, PLoS Biol. (2011) e1001080.
[17] H. Zheng, E. H. Koo, The amyloid precursor protein: beyond amyloid, Mol. Neurodegener. 1 (2006), 5.
[18] J. Ávila, F. Lim, F. Moreno, C. Belmonte, C. Cuello, Tau function and dysfunction in neurons, Mol. Neurobiol. 25 (2002) 213–231.
[19] L. Buée, T. Bussière, V. Buée-Scherrer, A. Delacourte, P. R. Hof, Tau protein isoforms, phosphorylation and role in neurodegenerative disorders, Brain Res.Rev. 33 (2000) 95–130.
[20] S. C. Correia, R. Resende, P. I. Moreira, C. M. Pereira, Alzheimer's disease-related misfolded proteins and dysfunctional organelles on autophagy menu, DNA Cell Biol. 34 (2015) 261–273.
[21] X. Hu, X. Li, M. Zhao, A. Gottesdiener, W. Luo, S. Paul, Tau pathogenesis is promoted by Aβ1-42 but not Aβ1-40, Mol. Neurodegener. 9 (2014) 52–62.
[22] V. Rhein, X. Song, A. Wiesner, L. M. Ittner, G. Baysang, F. Meier, L. Ozmen, H. Bluethmann, S. Drose, U. Brandt, E. Savaskan, C. Czech, J. Gotz, A. Eckert, Amyloid-beta and tau synergistically impair the oxidative phosphorylation system in triple transgenic Alzheimer's disease mice, Proc. Natl. Acad. Sci. U S A 106 (2009) 20057–20062.
[23] T. F. Gendron, L. Petrucelli, The role of tau in neurodegeneration, Mol. Neurodegener. 4 (2009) 13.
[24] S. Salloway, J. Mintzer, M. F. Weiner, J. L. Cummings, Disease-modifying therapies in Alzheimer's disease, Alzheimers Dement. 4 (2008) 65–79.
[25] A. Cavalli, M. L. Bolognesi, A. Minarini, M. Rosini, V. Tumiatti, M. Recanatini, M. Carlo, Multi-target-directed ligands to combat neurodegenerative diseases, J. Med. Chem. 51 (2008) 347–372.
[26] N. Guzior, M. Bajda, M. Skrok, K. Kurpiewska, K. Lewinski, B. Brus, A. Pislar, J. Kos, S. Gobec, B. Malawska, Development of multifunctional, heterodimeric isoindoline-1,3-dione derivatives as cholinesterase and beta-amyloid aggregation inhibitors with neuroprotective properties, Eur. J. Med. Chem. 92 (2015) 738–749.

]27] M. Hernandez-Rodriguez, J. Correa-Basurto, F. Martinez-Ramos, M. Padilla, C. G. Benitez-Cardoza, E. Mera-Jimenez, M. C. Rosales-Hernandez, Design of multi-target compounds as AChE, BACE1, and amyloid-beta(1-42) oligomerization inhibitors: in silico and in vitro studies, J. Alzheimers Dis. 41 (2014) 1073–1085.

[28] T. Mohamed, P. P. N. Rao, Alzheimer's disease: emerging trends in small molecule therapies, Curr. Med. Chem. 18 (2011) 4299–4320.

[29] A. Elkamhawy, J. Lee, B. G. Park, I. Park, A. N. Pae, E. J. Roh, Novel quinazoline-urea analogues as modulators for abeta-induced mitochondrial dysfunction: design, synthesis, and molecular docking study, Eur. J. Med. Chem. 84 (2014) 466–475.

[30] B. Smith, F. Medda, V. Gokhale, T. Dunckley, C. Hulme, C. Recent advances in the design, synthesis, and biological evaluation of selective DYRK1A inhibitors: a new avenue for a disease modifying treatment of Alzheimer's? ACS Chem. Neurosci. 3 (2012) 857–872.

[31] Z. Li, B. Wang, J. Q. Hou, S. L. Huang, T. M. Ou, J. H. Tan, L. K. An, D. Li, L. Q. Gu, Z. S. Huang, 2-(2-Indolyl-)-4(3H)-quinazolines derivates as new inhibitors of AChE: design, synthesis, biological evaluation and molecular modelling, J. Enzyme Inhib. Med. Chem. 28 (2013) 583–592.

[32] T. Mohamed, J. C. Yeung, M. S. Vasefi, M. A. Beazely, P. P. N. Rao, Development and evaluation of multifunctional agents for potential treatment of Alzheimer's disease: application to a pyrimidine-2,4-diamine template, Bioorg. Med. Chem. Lett. 22 (2012) 4707–4712.

[33] T. Mohamed, A. Shakeri, G. Tin, P. P. N. Rao, Structure-activity relationship studies of isomeric 2,4-diaminoquinazolines on β-amyloid aggregation kinetics, ACS Med. Chem. Lett. 7 (2016) 502–507

[34] K. Kanuma, K. Omodera, M. Nishiguchi, T. Funakoshi, S. Chaki, Y. Nagase, I. Lida, J. Yamaguchi, G. Semple, A. Tran, Y. Sekiguchi, Identification of 4-amino-2-cyclohexylaminoquinazolines as metabolically stable melanin-concentrating hormone receptor 1 antagonists, Bioorg. Med. Chem. 14 (2006) 3307–3319.

[35] M. Font, A. Gonzalez, J. A. Palop, C. Sanmartin, New insights into the structural requirements for pro-apoptotic agents based on 2,4-diaminoquinazoline, 2,4-diaminopyrido[2,3-d]pyrimidine and 2,4-diaminopyrimidine derivatives, Eur. J. Med. Chem. 46 (2011) 3887–38899.

[36] E. A. Arnott, L. C. Chan, B. G. Cox, B. Meyrick, A. Phillips, $POCl_3$ chlorination of 4-quinazolones, J. Org. Chem. 76 (2011) 1653–1661.
[37] T. Mohamed, A. Assoud, P. P. N. Rao, N-Benzyl-2-chloro-quinazolin-4-amine, Acta. Crystallogr. Sect E Struct Rep. Online 70 (2014) o554.
[38] P. P. Cellier, J. F. Spindler, M. Taillefer, H. J. Cristau, Pd/C-catalyzed room-temperature hydrodehalogenation of aryl halides with hydrazine hydrochloride, Tetrahedron Lett. 44 (2003) 7191–7195.
[39] M. Lauwiner, J. Wissmann, Reduction of aromatic nitro compounds with hydrazine hydrate in the presence of an iron oxide hydroxide catalyst. I. The reduction of monosubstituted nitrobenzenes with hydrazine hydrate in the presence of ferrihydrite, J. Appl. Cat. A 172 (1998) 141–148.
[40] A. Furst, R. C. Berlo, S. Hooton, Hydrazine as a reducing agent for organic compounds (catalytic hydrazine reductions), Chem. Rev. 65 (1965) 51–68.
[41] E. F. V. Scriven, K. Turnbull, Azides: Their preparation and synthetic uses, Chem. Rev. 88 (1988) 297–368.
[42] S. Brase, C. Gil, K. Knepper, V. Zimmermann, Organic azides: an exploding diversity of a unique class of compounds, Angew. Chem. Int. Ed. Engl. 44 (2005) 5188–5240.
[43] A. A. Malik, S. B. Preston, T. G. Archibald, M. P. Cohen, K. A. Baum, Facile reduction of azides to amines using hydrazine, Synthesis 6 (1989) 450–451.
[44] T. Mohamed, P. P. N. Rao, Facile approaches toward the synthesis of N4-monosubstituted quinazolin-2,4-diamines, Tetrahedron Lett. 56 (2015) 6882–6885.
[45] C. Helgen, C. G. Bochet, Pyridine-derived heterocycles as potential photoacylating reagents, Heterocycles 67 (2006) 797–805.
[46] G. L. Ellman, K. D. Courtney, V. Andres, R. M. Featherstone, A new and rapid colormetric determination of acetylcholinesterase activity. Biochem. Pharmacol. 7 (1961) 88–95.
[47] H. Levine, Thioflavine T interaction with synthetic Alzheimer's disease beta-amyloid peptide: detection of amyloid aggregation in solution, Protein Sci. 20 (1993) 404–410.
[48] V. L. Anderson, T. F. Ramlal, C. C. Rospigliosi, W. W. Webb, D. Eliezer, Identification of a helical intermediate in trifluorethanol-induced alpha-synuclein aggregation, Proc. Natl. Acad. Sci. USA. 107 (2010) 18850-18855.

[49] S. B. Kedare, R. P. Singh, Genesis and development of DPPH method of antioxidant assay, J. Food Sci. Technol. 48 (2011) 412–422.
[50] G. Tin, T. Mohamed, N. Gondora, M. B. Beazely, P. P. N. Rao, Tricyclic phenothiazine and phenoselenazine derivatives as potential multi-targeting agents to treat Alzheimer's disease, MedChemComm. 6 (2015) 1907–2044.
[51] G. Kryget, I. Silman, J. L. Sussman, Structure of acetylcholinesterase complexed with E2020 (Aricept®): implications for the design of new anti-Alzheimer drugs, Structure 7 (1999) 297–307.
[52] A. T. Petkova, W. M. Yau, R. Tycko, Experimental constraints on quaternary structure in Alzheimer's beta amyloid fibrils, Biochemistry 45 (2006) 498–512.
[53] A. Melquiond, X. Dong, N. Mousseau, P. Derreumaux, Role of the region 23–28 in Aβ fibril formation: insights from simulations of the monomers and dimers of Alzheimer's peptides Aβ40 and Aβ42, Curr. Alzheimer Res. 5 (2008) 244–250.
[54] G. Kryger, M. Harel, K. Giles, L. Toker, B. Velan, A. Lazar, C. Kronman, D. Barak, N. Ariel, A. Shafferman, I. Silman, J. L. Sussman, Structures of recombinant native and E202Q mutant human acetylcholinesterase complexed with the snake-venom toxin fasciculin-II, Acta. Crystallogr. D. Biol. Crystallogr. 56 (2000) 1385–1394.
[55] Y. Nicolet, O. Lockridge, P. Masson, J. C. Fontecilla-Camps, F. Nachon, Crystal structure of human butyrylcholinesterase and of its complexes with substrate and products, J. Biol. Chem. 278 (2003) 41141–41147.
[56] P. P. N. Rao, T. Mohamed, K. Teckwani, G. Tin, Curcumin binding to beta amyloid: a computational study, Chem. Biol. Drug Des. 86 (2015) 813–820.

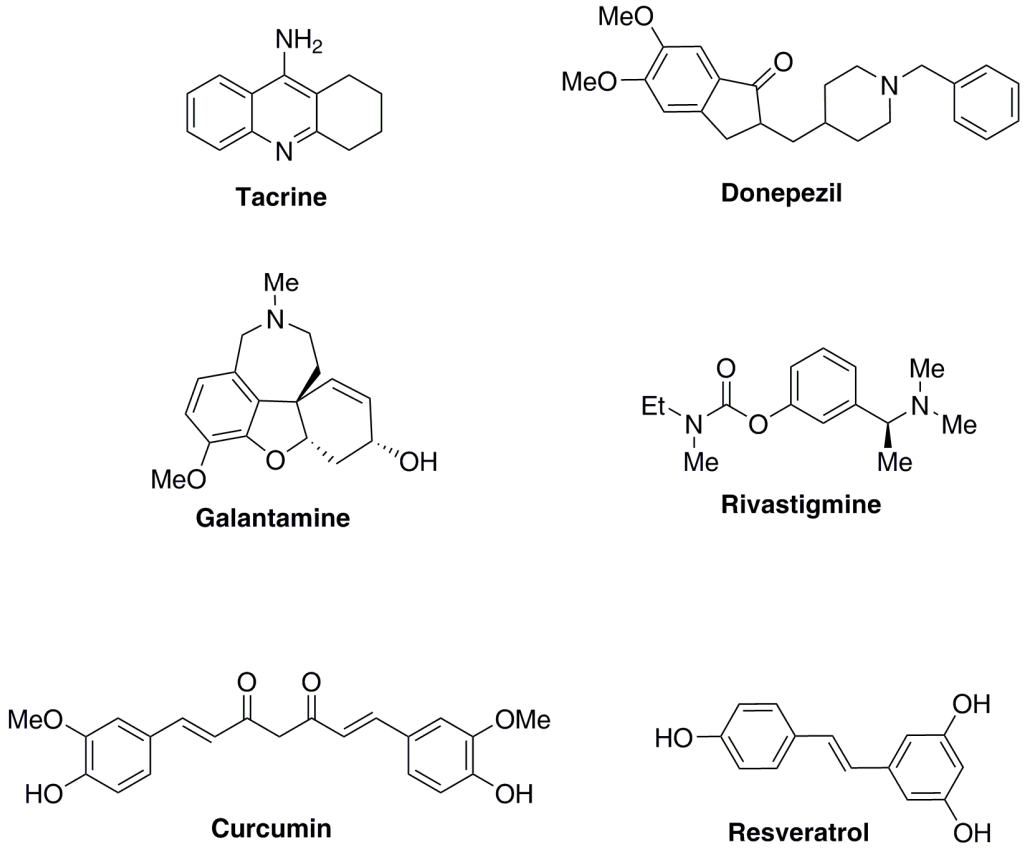


**Fig.1.** Chemical structures of some compounds with anti-AD activity

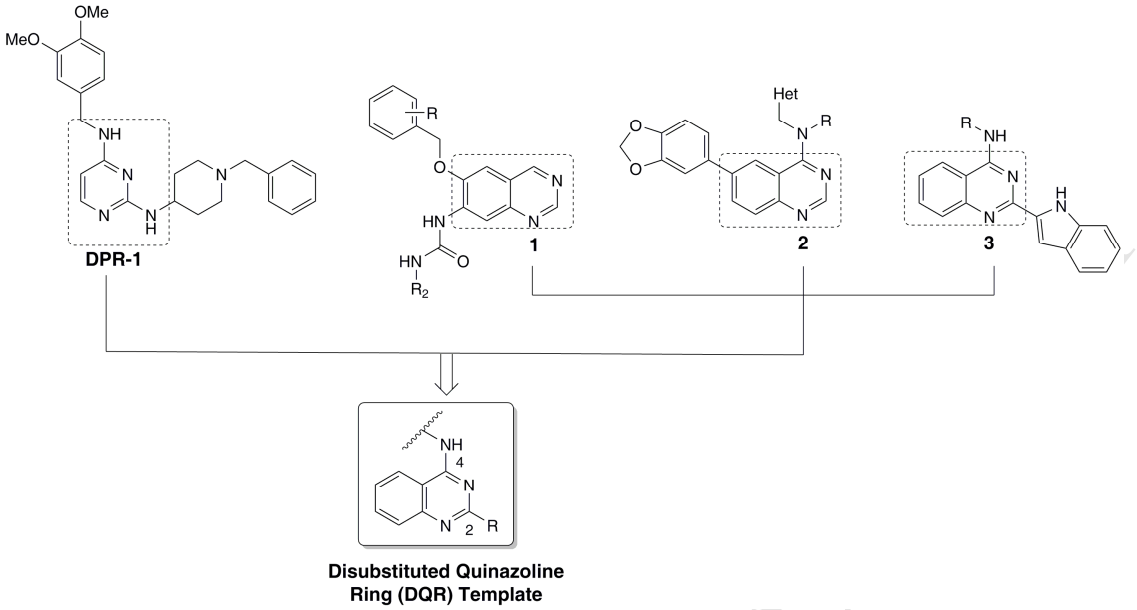


**Fig.2.** Design strategy summary toward developing a disubstituted quinazoline ring (**DQR**) scaffold based on a 2,4-disubstituted pyrimidine (**DPR-1**) and quinazolines (**1**–**3**) as multi-targeting agents to treat Alzheimer's disease.

**Scheme 1.** Synthesis of 2,4-dichloroquinazoline (**7**).

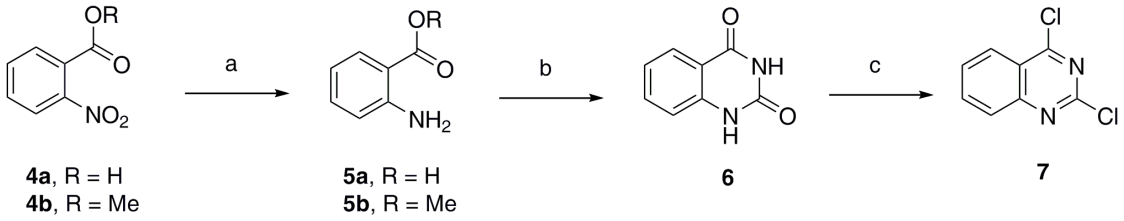


**4a**, R = H
**4b**, R = Me

**5a**, R = H
**5b**, R = Me

**6**

**7**

Reagents and conditions: (a) Pd/C, hydrazine hydrate, EtOH, 80–85 °C, 2 h; (b) Urea, 150–155 °C, pressure vial, oil bath, 2 h; (c) $POCl_3$, toluene, *N*,*N*-diethylaniline, 0–105 °C, reflux, 14–16 h.

**Scheme 2.** Synthetic route toward quinazoline derivatives **8a–d**, **9** and **10a**–**d**.

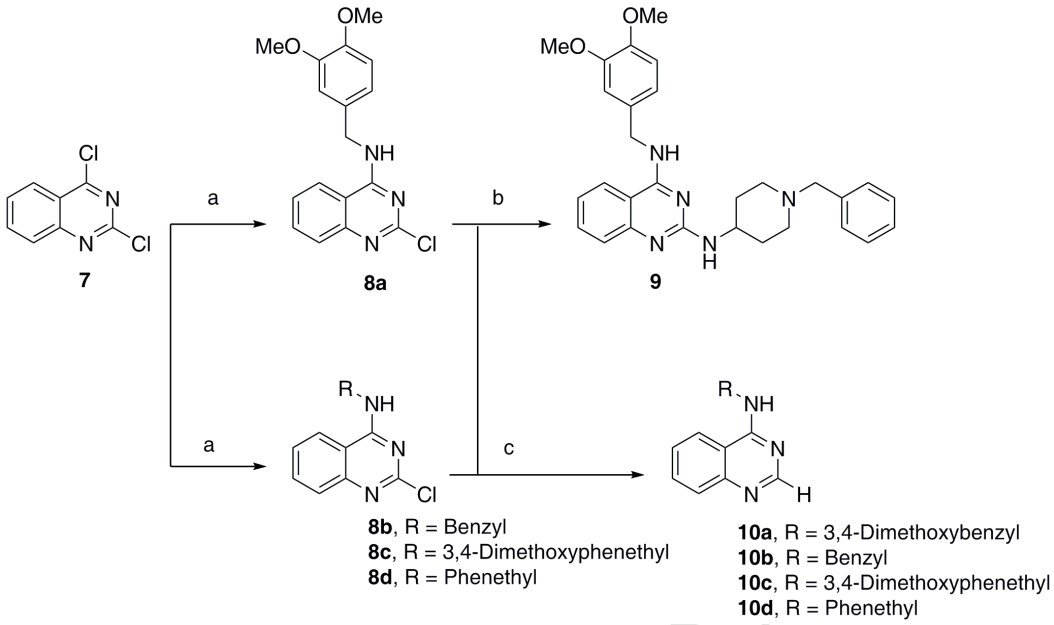


Reagents and conditions: (a) Primary amine, DIPEA, EtOH, reflux, 4 h; (b) 4-amino-1-benzylpiperidine, DIPEA, 1,4-dioxane, 160–165 °C, pressure vial, oil bath, 6 h; (c) Pd/C, hydrazine hydrate, EtOH, reflux, 2 h.

**Scheme 3.** Synthesis of **12a** and **12b**.

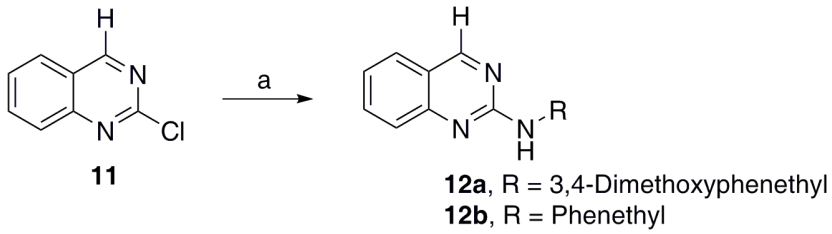


**11**

**12a**, R = 3,4-Dimethoxyphenethyl
**12b**, R = Phenethyl

Reagents and conditions: (a) Primary amine, DIPEA, 1,4-dioxane, pressure vial, oil bath, 155–160 °C, 5 h.

**Scheme 4.** Synthesis of C2-azide (**13a–d**), C2-amino (**14a–d**) and C2-hydroxy (**15a–d**) derivatives.

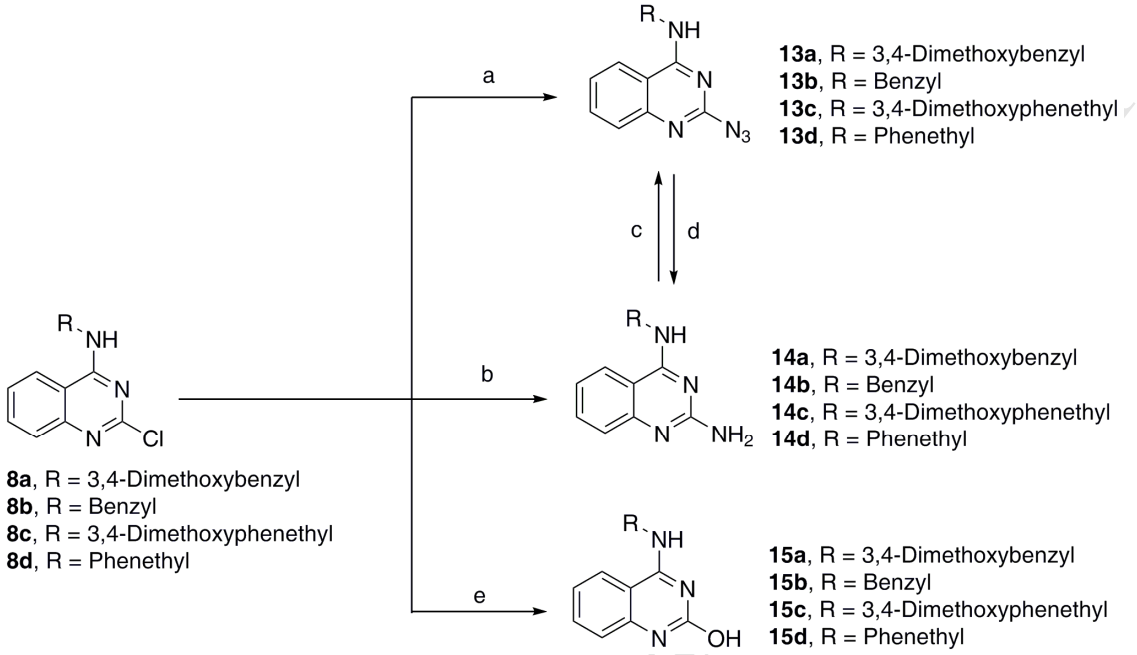


Reagents and conditions: (a) Sodium azide, EtOH, acetic acid, 90–95 °C, 2 h; (b) $Cu_2O$, potassium carbonate, DMEDA, ethylene glycol, $NH_4OH$, pressure vial, oil bath, 105 °C, 24 h; (c) Hydrochloric acid, sodium nitrite, sodium azide, 0 °C – r.t., 1 h; (d) Pd/C, hydrazine hydrate, EtOH, reflux, 2 h; (e) $HCO_2K$, formic acid, 120–125 °C, 14–16 h.

**Scheme 5.** Synthesis of quinazoline derivatives **14b, 14d** and **17a, 17b**.

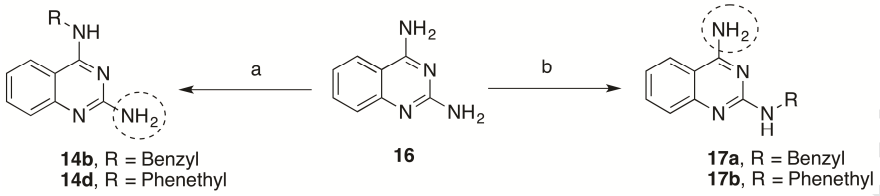


Reagents and conditions: (a) Benzyl bromide or 2-bromoethyl benzene, NaH, DMSO, 0 °C – r.t., 14–16 h.; (b) benzyl bromide or 2-bromoethyl benzene, *N*,*N*-dimethylacetamide, $K_2CO_3$, reflux, 85 °C, 5 h.

**Scheme 6.** Synthesis of quinazoline derivatives **18a–d**, **19a–d** and **20a–d**.

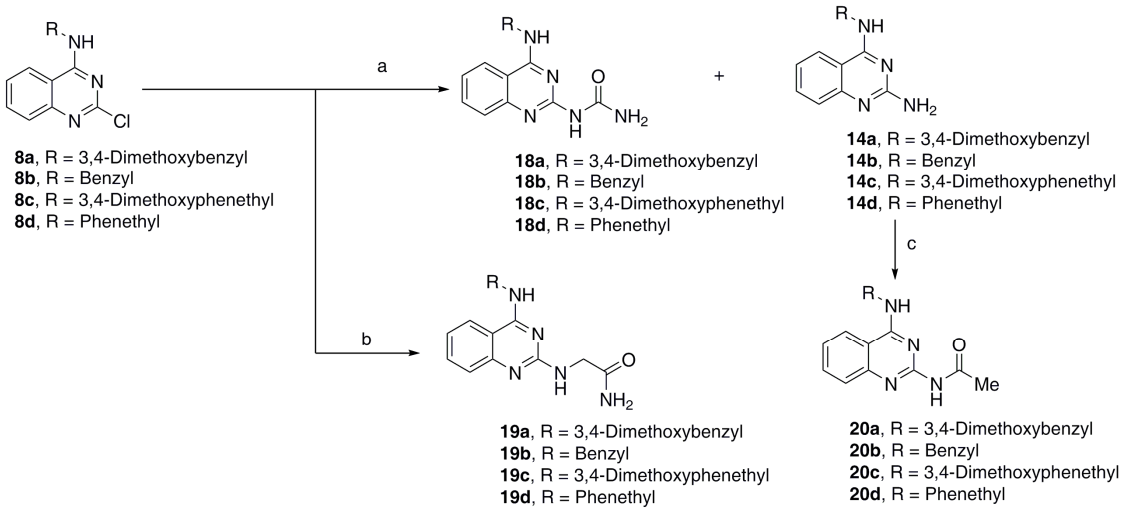


Reagents and conditions: (a) Urea, 1,4-dioxane, pressure vial, 160–165 °C, 24 h.; (b) glycinamide, DBU, 1,4-dioxane, pressure vial, 150–155 °C, 4 h.; (c) acetyl chloride, acetic acid, 1,4-dioxane, 120 °C, 24 h.

**Scheme 7.** Synthesis of quinazoline derivatives **21a–t**.

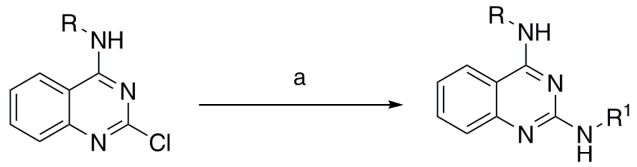


**8a**, R = 3,4-Dimethoxybenzyl
**8b**, R = Benzyl
**8c**, R = 3,4-Dimethoxyphenethyl
**8d**, R = Phenethyl

**21a–e**, R = 3,4-Dimethoxybenzyl; $R^1$ = Me, Et, *n*-Pr, *i*-Pr, *c*-Pr
**21f–j**, R = Benzyl; $R^1$ = Me, Et, *n*-Pr, *i*-Pr, *c*-Pr
**21k–o**, R = 3,4-Dimethoxyphenethy; $R^1$ = Me, Et, *n*-Pr, *i*-Pr, *c*-Pr
**21p–t**, R = Phenethyl; $R^1$ = Me, Et, *n*-Pr, *i*-Pr, *c*-Pr

Reagents and conditions: (a) Primary amine ($R^1$ = Me, Et, *n*-Pr, *i*-Pr or *c*-Pr), DIPEA, dioxane, 150–155 °C, 2 h.

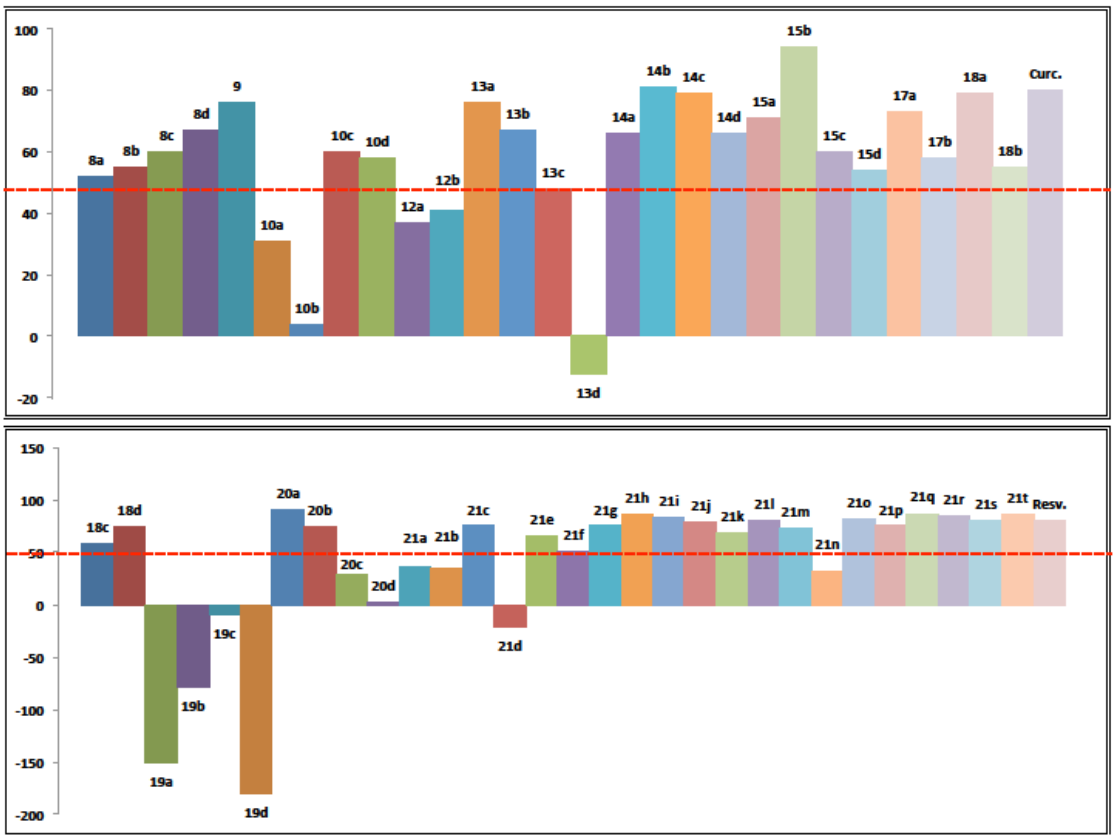


**Fig.3.** Percent inhibition of amyloid (Aβ40, 5 μM) aggregation by quinazoline compound library (**8**–**10**, **12**–**15** and **17**–**21**) evaluated by ThT-based fluorescence spectroscopy (excitation = 440 nm; emission = 490 nm) at 37 °C, pH 7.4 phosphate buffer. Positive values indicate inhibition of Aβ aggregation and negative values indicate promotion of aggregation. The red dotted line indicates 50% inhibition. Values are an average of triplicate readings for two independent experiments.

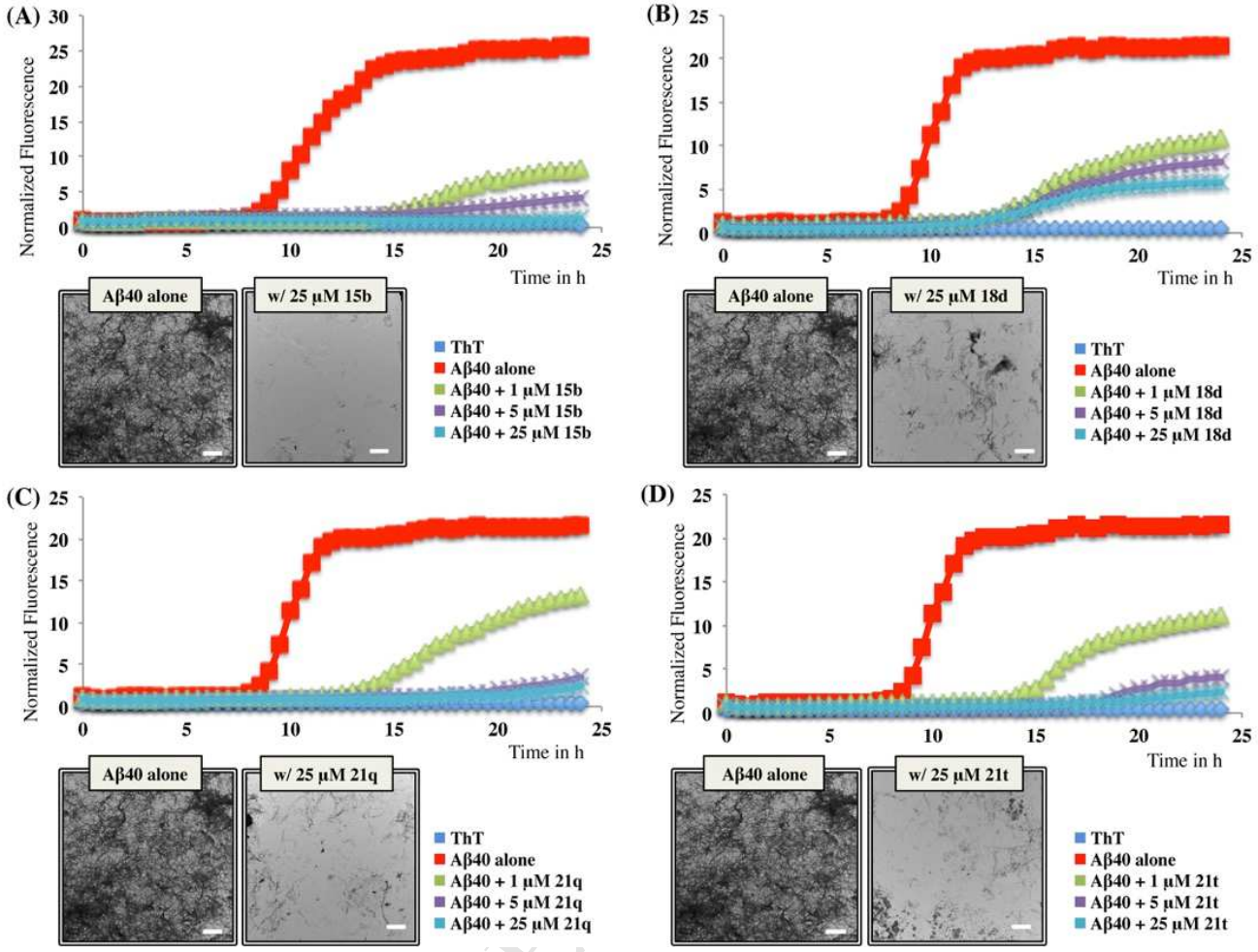


**Fig.4.** ThT-monitored kinetics of Aβ40 aggregation with quinazoline derivatives **15b**, **18d, 21q** and **21t** at 37 °C in phosphate buffer pH 7.4, 24 h period along with the transmission electron microscopy (TEM) images assessing Aβ morphology. Panels A–D: Kinetic plots of Aβ40-alone (5 μM) and in the presence of 1, 5 or 25 μM of **15b**, **18d**, **21q** and **21t** respectively. All the samples (Aβ alone and Aβ + compound samples) contain ThT. The TEM images are based on a 1:1 ratio of Aβ and compound (25 μM each) at 37 °C, 24 h incubation. White scale bars in TEM images represent 500 nm.

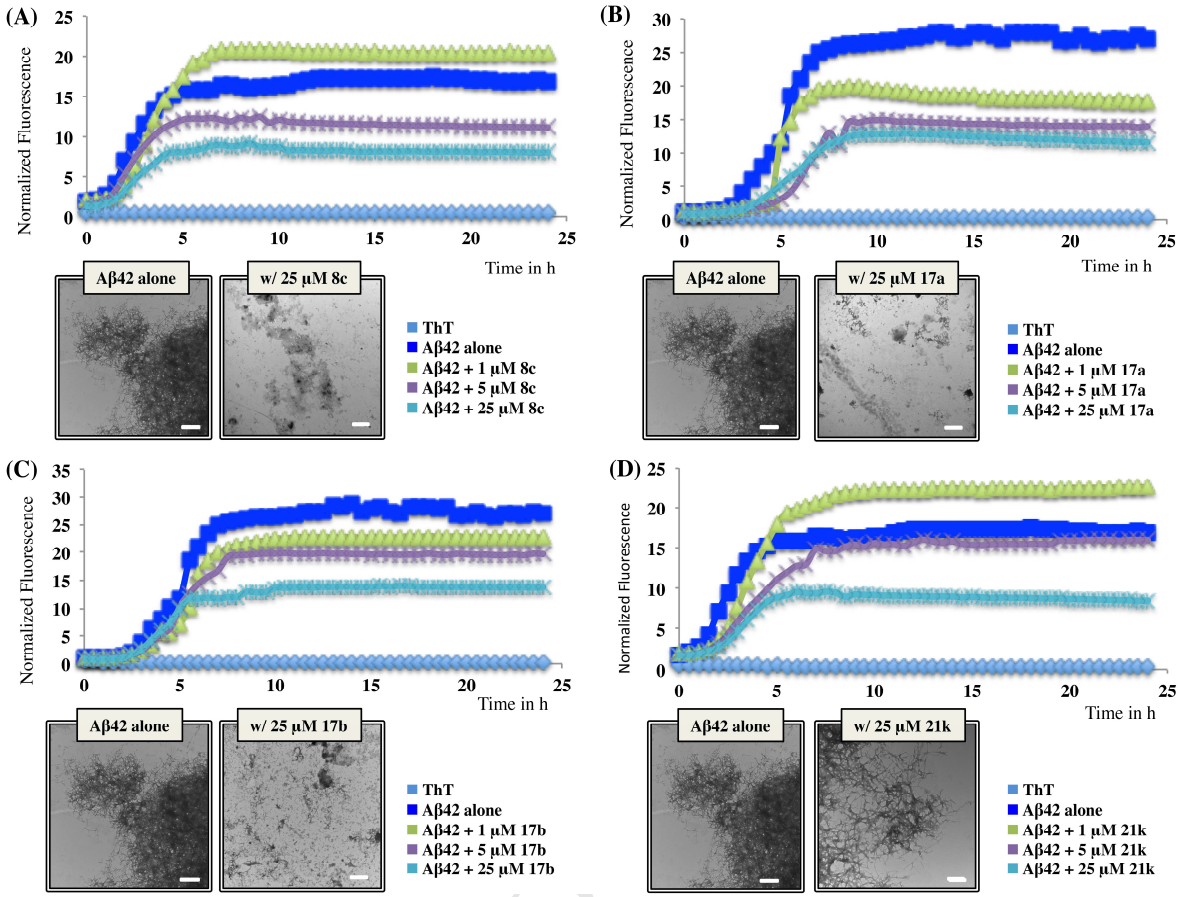


**Fig.5.** ThT-monitored kinetics of Aβ42 aggregation with quinazoline derivatives **8c**, **17a**, **17b** and **21k** at 37 °C in phosphate buffer pH 7.4, 24 h period along with the transmission electron microscopy (TEM) images assessing Aβ morphology. Panels A–D: Kinetic plots of Aβ42-alone (5 μM) and in the presence of 1, 5 or 25 μM of **8c**, **17a**, **17b** and **21k** respectively. All the samples (Aβ alone and Aβ + compound samples) contain ThT. The TEM images are based on a 1:1 ratio of Aβ and compound (25 μM each) at 37 °C, 24 h incubation. White scale bars in TEM images represent 500 nm.

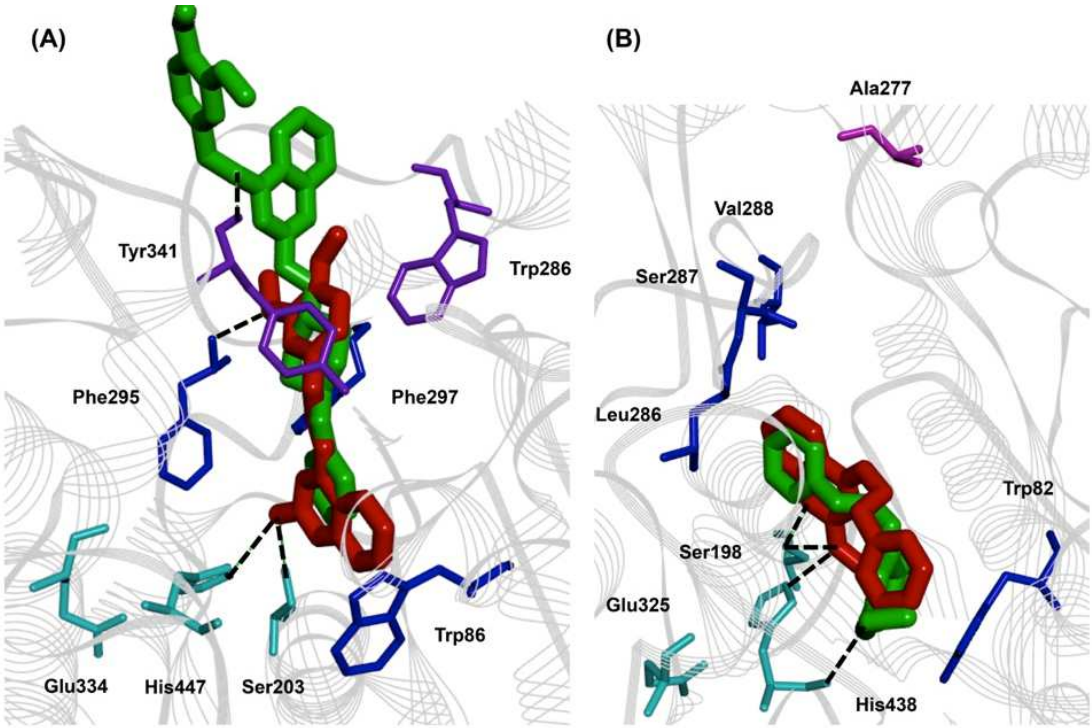


**Fig.6.** Binding modes of quinazoline derivatives in human cholinesterases. Panel (A) Compound **9** (green) and compound **14c** (red) docked in *h*AChE. Panel (B) Compound **21q** (green) and compound **21s** (red) docked in *h*BuChE. Hydrogen atoms were removed for clarity. Black-dotted lines represent hydrogen-bonding interactions. Residues in turquoise represent the catalytic triad, blue represents the anionic and acyl pockets and purple represents the active-site entry (or PAS).

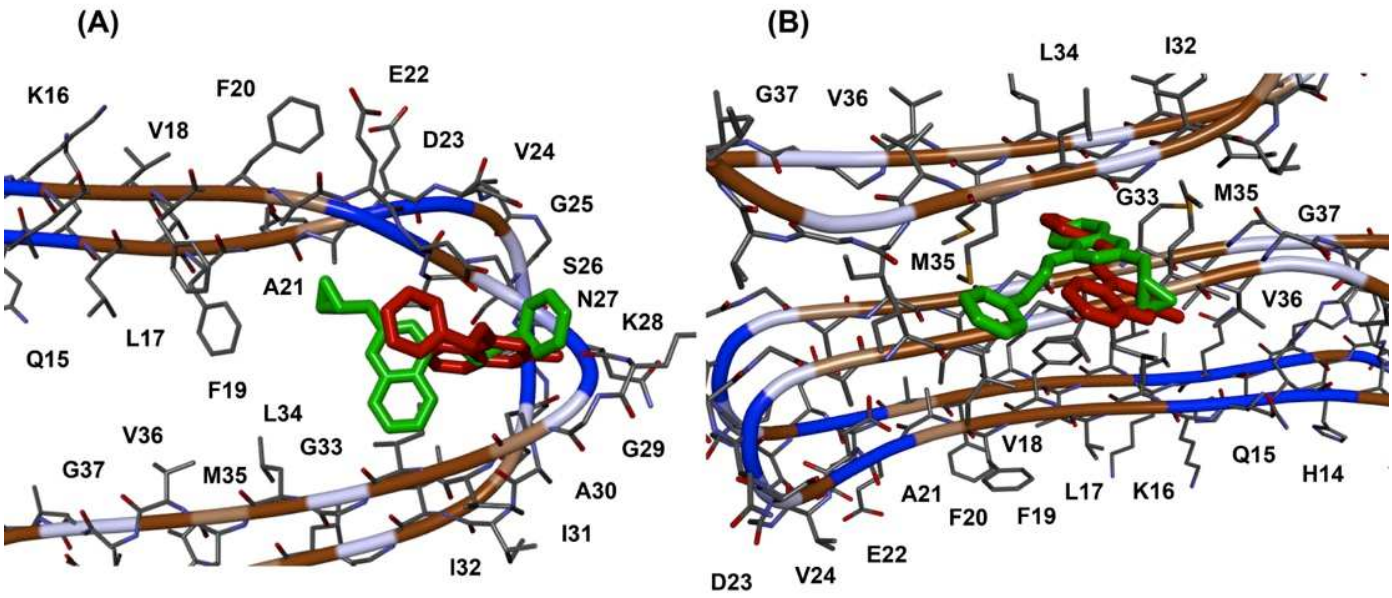


**Fig.7.** Binding modes of quinazoline derivatives in Aβ dimer and fibril models. Compound **15b** (red) and compound **21t** (green) docked in Aβ dimer-model (Panel A) and Aβ fibril-model (Panel B). Hydrogen atoms were removed for clarity.

**Table 1**

Cholinesterase inhibition $IC_{50}$ values for quinazoline derivatives **8**–**10**, **12**–**15**, and **17**, along with ClogP and molecular volumes (Å$^3$).

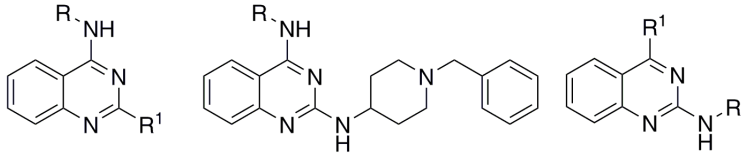

**8a-d**
**10a-d**
**13a-d**
**14a-d**
**15a-d**



**9**



**12a-b**
**17a-b**

| Compd | R | $R^1$ | ChE $IC_{50}$ (μM) | | ClogP | Mol. Vol. (Å$^3$) |
|---|---|---|---|---|---|---|
| | | | AChE | BuChE | | |
| **8a** | 3,4-Dimethoxybenzyl | Cl | 3.0 ± 0.2 | > 50 | 3.75 | 213.6 |
| **8b** | Benzyl | Cl | 7.5 ± 0.8 | > 50 | 4.09 | 174.5 |
| **8c** | 3,4-Dimethoxyphenethyl | Cl | 2.8 ± 0.3 | > 50 | 4.40 | 225.3 |
| **8d** | Phenethyl | Cl | 7.7 ± 0.5 | > 50 | 4.74 | 182.1 |
| **9** | 3,4-Dimethoxybenzyl | – | 2.1 ± 0.09 | 8.3 ± 0.9 | 5.65 | 400.2 |
| **10a** | 3,4-Dimethoxybenzyl | H | 2.8 ± 0.2 | > 50 | 1.84 | 199.6 |
| **10b** | Benzyl | H | 5.8 ± 0.4 | > 50 | 3.33 | 158.1 |
| **10c** | 3,4-Dimethoxyphenethyl | H | 2.8 ± 0.3 | > 50 | 3.64 | 210.9 |
| **10d** | Phenethyl | H | 6.2 ± 0.7 | 14.1 ± 1.2 | 3.98 | 168.7 |
| **12a** | 3,4-Dimethoxyphenethyl | H | 8.4 ± 0.9 | > 50 | 3.64 | 252.1 |
| **12b** | Phenethyl | H | 7.6 ± 0.5 | > 50 | 3.98 | 197.7 |
| **13a** | 3,4-Dimethoxybenzyl | $N_3$ | 8.3 ± 0.7 | > 50 | 4.41 | 262.7 |

| | | | | | | |
|---|---|---|---|---|---|---|
| **13b** | Benzyl | $N_3$ | 14.0 ± 1.1 | > 50 | 4.75 | 210.6 |
| **13c** | 3,4-Dimethoxyphenethyl | $N_3$ | 9.5 ± 1.0 | > 50 | 5.05 | 271.3 |
| **13d** | Phenethyl | $N_3$ | 9.7 ± 0.09 | > 50 | 5.39 | 221.5 |
| **14a** | 3,4-Dimethoxybenzyl | $NH_2$ | 2.6 ± 0.2 | > 50 | 2.98 | 209.5 |
| **14b** | Benzyl | $NH_2$ | 5.0 ± 0.7 | 30.1 ± 4.0 | 3.32 | 163.9 |
| **14c** | 3,4-Dimethoxyphenethyl | $NH_2$ | 2.5 ± 0.3 | 14.5 ± 1.8 | 3.63 | 217.4 |
| **14d** | Phenethyl | $NH_2$ | 5.7 ± 0.7 | 4.9 ± 0.6 | 3.97 | 176.6 |
| **15a** | 3,4-Dimethoxybenzyl | OH | 7.7 ± 0.9 | > 50 | 3.61 | 248.3 |
| **15b** | Benzyl | OH | 9.8 ± 0.6 | > 50 | 3.95 | 199.6 |
| **15c** | 3,4-Dimethoxyphenethyl | OH | 7.6 ± 0.5 | > 50 | 4.26 | 259.9 |
| **15d** | Phenethyl | OH | 8.1 ± 0.6 | > 50 | 4.61 | 208.5 |
| **17a** | Benzyl | $NH_2$ | 7.5 ± 0.8 | 11.6 ± 1.3 | 3.32 | 195.5 |
| **17b** | Phenethyl | $NH_2$ | 7.1 ± 0.7 | 2.4 ± 0.1 | 3.97 | 209.2 |
| **Donepezil hydrochloride monohydrate** | | | 0.03 ± 0.002 | 3.6 ± 0.4 | 4.59 | 321.7 |
| **Tacrine hydrochloride** | | | 0.16 ± 0.01 | 0.04 ± 0.001 | 3.27 | 165.6 |
| **Galantamine hydrobromide** | | | 2.6 ± 0.6 | > 50 | 1.18 | 239.4 |
| **Rivastigmine tartrate** | | | 6.5 ± 0.5 | > 10 | 2.10 | 226.3 |

$IC_{50}$ values are an average ± SD of triplicate readings based on two to three independent experiments. ClogP values were determined using ChemDraw Professional 15.0 while molecular volumes in $Å^3$ units were determined using Discovery Studio, Structure-Based Design software, BIOVIA Inc., USA.

**Table 2**

Cholinesterase inhibition $IC_{50}$ values for quinazoline derivatives **18**–**20** along with ClogP and molecular volumes ($Å^3$)

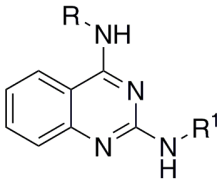

**18a-d**
**19a-d**
**20a-d**

| Compd | R | $R^1$ | ChE $IC_{50}$ (μM) | | ClogP | Mol. Vol. ($Å^3$) |
|---|---|---|---|---|---|---|
| | | | AChE | BuChE | | |
| **18a** | 3,4-Dimethoxybenzyl | $CONH_2$ | 8.6 ± 0.6 | > 50 | 3.01 | 269.2 |
| **18b** | Benzyl | $CONH_2$ | 8.3 ± 0.9 | > 50 | 3.35 | 221.2 |
| **18c** | 3,4-Dimethoxyphenethyl | $CONH_2$ | 8.7 ± 0.7 | > 50 | 3.65 | 287.0 |
| **18d** | Phenethyl | $CONH_2$ | 7.9 ± 0.6 | > 50 | 3.99 | 232.8 |
| **19a** | 3,4-Dimethoxybenzyl | $CH_2CONH_2$ | 7.4 ± 0.8 | > 50 | 2.59 | 289.1 |

| | | | | | | |
|---|---|---|---|---|---|---|
| **19b** | Benzyl | $CH_2CONH_2$ | 7.2 ± 0.7 | > 50 | 2.78 | 241.1 |
| **19c** | 3,4-Dimethoxyphenethyl | $CH_2CONH_2$ | 12.5 ± 1.5 | > 50 | 3.08 | 304.2 |
| **19d** | Phenethyl | $CH_2CONH_2$ | 7.3 ± 0.9 | 3.5 ± 0.2 | 3.59 | 247.9 |
| **20a** | 3,4-Dimethoxybenzyl | COMe | 8.5 ± 0.6 | > 50 | 2.53 | 277.8 |
| **20b** | Benzyl | COMe | 7.5 ± 0.5 | > 50 | 2.87 | 228.4 |
| **20c** | 3,4-Dimethoxyphenethyl | COMe | 7.4 ± 0.6 | > 50 | 3.18 | 294.6 |
| **20d** | Phenethyl | COMe | 7.0 ± 0.5 | > 50 | 3.52 | 245.5 |
| **Donepezil hydrochloride monohydrate** | | | 0.03 ± 0.002 | 3.6 ± 0.4 | 4.59 | 321.7 |
| **Tacrine hydrochloride** | | | 0.16 ± 0.01 | 0.04 ± 0.001 | 3.27 | 165.6 |
| **Galantamine hydrobromide** | | | 2.60 ± 0.6 | > 50 | 1.18 | 239.4 |
| **Rivastigmine tartrate** | | | 6.5 ± 0.5 | > 10 | 2.10 | 226.3 |

$IC_{50}$ values are an average ± SD of triplicate readings based on two to three independent experiments. ClogP values were determined using ChemDraw Professional 15.0 while molecular volumes in $Å^3$ units were determined using Discovery Studio, Structure-Based Design software, BIOVIA Inc., USA.

**Table 3**

Cholinesterase inhibition $IC_{50}$ values for quinazoline derivatives **21a–t** along with ClogP and molecular volumes ($Å^3$)

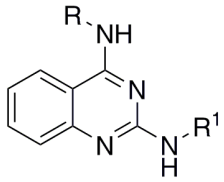


**21a-t**

| Compd | R | $R^1$ | ChE $IC_{50}$ (μM) | | ClogP | Mol. Vol. ($Å^3$) |
|---|---|---|---|---|---|---|
| | | | AChE | BuChE | | |
| **21a** | 3,4-Dimethoxybenzyl | Me | 7.3 ± 0.5 | 30.5 ± 4.0 | 3.80 | 218.8 |
| **21b** | 3,4-Dimethoxybenzyl | Et | 6.3 ± 0.4 | 25.0 ± 1.2 | 4.33 | 232.8 |
| **21c** | 3,4-Dimethoxybenzyl | *n*-Pr | 5.6 ± 0.4 | 30.4 ± 1.7 | 4.86 | 245.5 |
| **21d** | 3,4-Dimethoxybenzyl | *i*-Pr | 6.8 ± 0.5 | 29.8 ± 2.0 | 4.64 | 243.8 |
| **21e** | 3,4-Dimethoxybenzyl | *c*-Pr | 7.2 ± 0.6 | 29.8 ± 2.5 | 4.38 | 241.8 |
| **21f** | Benzyl | Me | 8.0 ± 0.5 | 18.8 ± 1.5 | 4.14 | 176.9 |
| **21g** | Benzyl | Et | 7.5 ± 0.6 | 15.2 ± 1.0 | 4.67 | 186.5 |
| **21h** | Benzyl | *n*-Pr | 7.8 ± 0.9 | 14.4 ± 0.9 | 5.20 | 205.1 |
| **21i** | Benzyl | *i*-Pr | 6.4 ± 0.5 | 11.7 ± 0.8 | 4.98 | 198.5 |
| **21j** | Benzyl | *c*-Pr | 6.6 ± 0.4 | 22.0 ± 1.6 | 4.73 | 200.9 |
| **21k** | 3,4-Dimethoxyphenethyl | Me | 8.5 ± 0.5 | 4.5 ± 0.3 | 4.45 | 229.4 |
| **21l** | 3,4-Dimethoxyphenethyl | Et | 7.5 ± 0.4 | 14.0 ± 1.8 | 4.98 | 245.9 |
| **21m** | 3,4-Dimethoxyphenethyl | *n*-Pr | 7.0 ± 0.6 | 24.9 ± 3.0 | 5.51 | 258.6 |
| **21n** | 3,4-Dimethoxyphenethyl | *i*-Pr | 7.6 ± 0.7 | 7.8 ± 0.0 | 5.29 | 259.9 |

| | | | | | | |
|---|---|---|---|---|---|---|
| **21o** | 3,4-Dimethoxyphenethyl | *c*-Pr | 7.2 ± 0.8 | 5.6 ± 0.4 | 5.03 | 252.7 |
| **21p** | Phenethyl | Me | 8.7 ± 1.0 | 5.0 ± 0.3 | 4.79 | 187.6 |
| **21q** | Phenethyl | Et | 7.6 ± 0.5 | 3.2 ± 0.3 | 5.32 | 199.2 |
| **21r** | Phenethyl | *n*-Pr | 7.2 ± 0.6 | 5.0 ± 0.4 | 5.85 | 212.3 |
| **21s** | Phenethyl | *i*-Pr | 7.2 ± 0.4 | 1.6 ± 0.05 | 5.63 | 214.3 |
| **21t** | Phenethyl | *c*-Pr | 8.6 ± 0.6 | 11.4 ± 0.9 | 5.38 | 208.5 |
| **Donepezil hydrochloride monohydrate** | | | 0.03 ± 0.002 | 3.6 ± 0.4 | 4.59 | 321.7 |
| **Tacrine hydrochloride** | | | 0.16 ± 0.01 | 0.04 ± 0.001 | 3.27 | 165.6 |
| **Galantamine hydrobromide** | | | 2.6 ± 0.6 | > 50 | 1.18 | 239.4 |
| **Rivastigmine tartrate** | | | 6.5 ± 0.5 | > 10 | 2.10 | 226.3 |

$IC_{50}$ values are an average ± SD of triplicate readings based on two to three independent experiments. ClogP values were determined using ChemDraw Professional 15.0 while molecular volumes in $Å^3$ units were determined using Discovery Studio, Structure-Based Design software, BIOVIA Inc., USA.

**Table 4**

Inhibition of Aβ40 and Aβ42 aggregation by quinazoline derivatives [33].

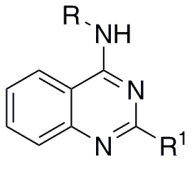

**8b-d**
**10c-d**
**13a-b**
**14a-d**
**15a-d**

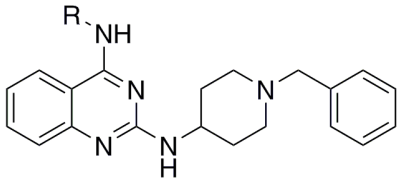

**9**

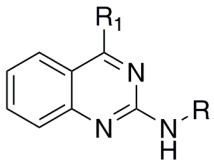

**17a-b**

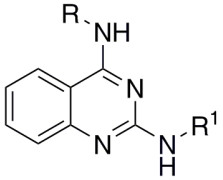

**18a-d**
**20a,b**
**21c,e,g-m, o-t**

| Compd | R | $R^1$ | Aβ40 $IC_{50}$ (μM) | Aβ42 $IC_{50}$ or % Inhibition |
|---|---|---|---|---|
| **8b** | Benzyl | Cl | 16.7 ± 2.5 | 22% |
| **8c** | 3,4-Dimethoxyphenethyl | Cl | 8.2 ± 1.5 | 13.0 ± 1.9 |
| **8d** | Phenethyl | Cl | 5.0 ± 0.8 | 36% |
| **9** | 3,4-Dimethoxybenzyl | – | 2.3 ± 0.5 | 27% |
| **10c** | 3,4-Dimethoxyphenethyl | H | 12.0 ± 2.4 | 36% |
| **10d** | Phenethyl | H | 11.9 ± 2.5 | 32% |
| **13a** | 3,4-Dimethoxybenzyl | $N_3$ | 7.2 ± 1.5 | < 10% |
| **13b** | Benzyl | $N_3$ | 2.6 ± 0.7 | 37% |
| **14a** | 3,4-Dimethoxybenzyl | $NH_2$ | 8.4 ± 2.0 | 34% |
| **14b** | Benzyl | $NH_2$ | 4.8 ± 1.0 | < 10% |
| **14c** | 3,4-Dimethoxyphenethyl | $NH_2$ | 2.7 ± 0.8 | 45% |
| **14d** | Phenethyl | $NH_2$ | 7.8 ± 2.0 | 37% |

| | | | | |
|---|---|---|---|---|
| **15a** | 3,4-Dimethoxybenzyl | OH | 7.8 ± 1.2 | < 10% |
| **15b** | Benzyl | OH | 0.27 ± 0.03 | 24% |
| **15c** | 3,4-Dimethoxyphenethyl | OH | 10.4 ± 1.2 | 32% |
| **15d** | Phenethyl | OH | 11.2 ± 1.4 | NA |
| **17a** | Benzyl | $NH_2$ | 2.2 ± 0.2 | 8.4 ± 1.0 |
| **17b** | Phenethyl | $NH_2$ | 14.9 ± 1.9 | 50% |
| **18a** | 3,4-Dimethoxybenzyl | $CONH_2$ | 8.3 ± 1.2 | 40% |
| **18b** | Benzyl | $CONH_2$ | 13.3 ± 2.5 | 48% |
| **18c** | 3,4-Dimethoxyphenethyl | $CONH_2$ | 14.4 ± 2.9 | 33% |
| **18d** | Phenethyl | $CONH_2$ | 1.0 ± 0.1 | 46% |
| **20a** | 3,4-Dimethoxybenzyl | COMe | 3.1 ± 0.4 | < 10% |
| **20b** | Benzyl | COMe | 1.9 ± 0.3 | 31% |
| **21c** | 3,4-Dimethoxybenzyl | *n*-Pr | 1.7 ± 0.3 | NA |
| **21e** | 3,4-Dimethoxybenzyl | *c*-Pr | 8.3 ± 1.6 | 20% |
| **21g** | Benzyl | Et | 7.0 ± 1.4 | 24% |
| **21h** | Benzyl | *n*-Pr | 5.0 ± 1.0 | 26% |
| **21i** | Benzyl | *i*-Pr | 4.4 ± 0.8 | 13% |
| **21j** | Benzyl | *c*-Pr | 5.7 ± 1.1 | 31% |
| **21k** | 3,4-Dimethoxyphenethyl | Me | 6.6 ± 1.3 | 23.1 |
| **21l** | 3,4-Dimethoxyphenethyl | Et | 2.9 ± 0.5 | 41% |
| **21m** | 3,4-Dimethoxyphenethyl | *n*-Pr | 4.3 ± 0.9 | 14% |
| **21o** | 3,4-Dimethoxyphenethyl | *c*-Pr | 4.9 ± 1.0 | 25% |
| **21p** | Phenethyl | Me | 2.0 ± 0.4 | 40% |

| | | | | |
|---|---|---|---|---|
| **21q** | Phenethyl | Et | 1.4 ± 0.3 | 47% |
| **21r** | Phenethyl | *n*-Pr | 4.4 ± 0.6 | 33% |
| **21s** | Phenethyl | *i*-Pr | 3.8 ± 0.7 | NA |
| **21t** | Phenethyl | *c*-Pr | 0.79 ± 0.01 | 22% |
| **Curcumin** | | | 3.3 ± 0.4 | 9.9 ± 1.4 |
| **Resveratrol** | | | 1.1 ± 0.1 | 15.3 ±1.9 |

$IC_{50}$ values are an average ± SD of triplicate readings for three independent experiments using a ThT-based fluorescence spectroscopy (440 nm, emission and 490 nm, excitation) at pH 7.4 phosphate buffer using either 5 µM each of Aβ40 or Aβ42. Percent inhibitions (%) represent activity at 25 µM of quinazoline derivatives against 5 µM of Aβ42. NA = Not active.

**Table 5**

Percent scavenging of DPPH radical by quinazoline derivatives **15a–d.**


**15a-d**

| **Compd** | **R** | **% DPPH Scavenging at 50 µM** |
|---|---|---|
| **15a** | 3,4-Dimethoxybenzyl | 63.4 ± 5.6 |
| **15b** | Benzyl | 47.0 ± 5.0 |
| **15c** | 3,4-Dimethoxyphenethyl | 33.9 ± 3.6 |
| **15d** | Phenethyl | 51.5 ± 4.6 |
| **Resveratrol** | | 41.9 ± 7.9 |
| **Trolox** | | 99.6 ± 3.7 |

% DPPH scavenging values are an average ± SD of triplicate readings for two independent experiments

**Highlights**

- Describes the design & synthesis of a novel class of quinazoline compound libraries
- SAR studies demonstrate their anti-Aβ, anti-cholinesterase and antioxidant properties
- They represent a new class of multi-targeting agents to treat Alzheimer's disease

*Corresponding author: Tel: +1 519 888 4567 ext: 21317; e-mail: praopera@uwaterloo.ca

[a]School of Pharmacy, Health Sciences Campus, University of Waterloo, 200 University Avenue West, Waterloo, Ontario, Canada N2L 3G1